

mw

①

NASA CONTRACTOR REPORT



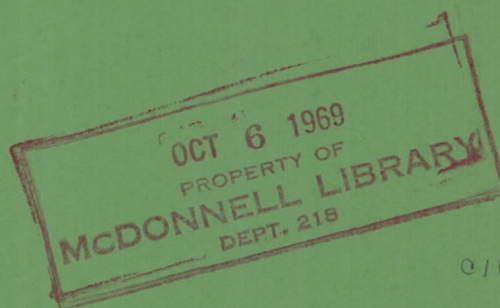
NASA CR-1402

NASA CR-1402
COPY ON MICROFICHE
169-37964
REFERENCE COPY
NOT CHARGED

MAN'S CAPABILITY FOR SELF-LOCOMOTION ON THE MOON

Volume I - Detailed Report

by E. C. Wortz, W. G. Robertson,
L. E. Browne, and W. G. Sanborn



Prepared by
GARRETT CORPORATION
Los Angeles, Calif.
for Langley Research Center

NATIONAL AERONAUTICS AND SPACE ADMINISTRATION • WASHINGTON, D. C. • SEPTEMBER 1969

MAN'S CAPABILITY FOR SELF-LOCOMOTION ON THE MOON

Volume I - Detailed Report

By E. C. Wortz, W. G. Robertson,
L. E. Browne, and W. G. Sanborn

Distribution of this report is provided in the interest of information exchange. Responsibility for the contents resides in the author or organization that prepared it.

Issued by Originator as AiResearch Report 68-3986, Rev. 1 ✓ CIR

Prepared under Contract No. NAS 1-7053 by
AIRESEARCH MANUFACTURING COMPANY
A Division of The Garrett Corporation
Los Angeles, Calif.

for Langley Research Center

NATIONAL AERONAUTICS AND SPACE ADMINISTRATION

For sale by the Clearinghouse for Federal Scientific and Technical Information
Springfield, Virginia 22151 - CFSTI price \$3.00

ANALYSIS OF THE PROBABILITIES FOR THE OCCURRENCE OF THE MOON

Figure 1 - Detailed Diagram

BY D. C. FORT, W. G. ROBERTSON,
J. I. HIGGINS, AND W. G. RAYMOND

The probability of the occurrence of the moon is analyzed in the interest of
the national economy. Responsibility for the occurrence
is placed in the hands of organizations that produce it.

Issued by the Government of the United States, Report 48-3888, Rev. 1

Prepared by the Government of the United States, Report 48-3888, Rev. 1
AEROSPACE MANUFACTURING COMPANY
A Division of the General Corporation
Los Angeles, Calif.

for the Research Center

NATIONAL AERONAUTICS AND SPACE ADMINISTRATION

ABSTRACT

This document presents the results of a comprehensive study of man's self-locomotive capabilities in simulated lunar gravity. An inclined-plane and a gimbal-vertical simulator equipped with treadmills were used to simulate lunar gravity. Man's locomotive characteristics and the metabolic costs of walking, running, and loping at velocities from 2 to 12.8 km/hr were determined for subjects in pressurized Gemini-4C suits. The results showed that the energy cost of locomotion in simulated lunar gravity is considerably less than that in earth gravity. Ascending grades caused large increases in metabolic cost over that of level walking where the magnitude of the cost depends on the simulation technique used. Increasing the load carried from 75 to 400 earth-pounds had a small and inconsistent effect on metabolic costs. Changing the smooth, hard walking surface to sandy soil caused a large increase in the metabolic cost at the higher locomotion rates.

Page Intentionally Left Blank

FOREWORD

This report was prepared by the Department of Life Sciences, AiResearch Manufacturing Company, Los Angeles, California. The technical assistance of M. Gafvert, N.J. Belton, A. Camacho, S. Salzberg, W. Price, R.A. Diaz, W. Pepper, and G. Raynes is gratefully acknowledged. The dedicated efforts of the test subjects that performed throughout this program are also gratefully acknowledged.

1940-1941

The following is a summary of the work done during the year 1940-1941. The work was done in the laboratory of the Department of Biology, University of California, Berkeley, California. The work was done under the supervision of Professor J. H. R. Taylor, and the results are reported in the following paper.

PREFACE

This research on man's capability for self-locomotion on the moon is part of the Human Factors Systems Program, Walton L. Jones, M.D., Director. In this contractor report, the investigators describe a comprehensive data gathering study to provide predictive information on the ability of man to walk on level and sloped terrain, utilizing a one-sixth gravity simulator. This study is included in the Man-Systems Integration research program. It was performed under the technical monitorship of Mr. William Letko, Langley Research Center.

Page Intentionally Left Blank

CONTENTS

<u>Section</u>	<u>Page</u>
1 INTRODUCTION	1
2 EXPERIMENTAL DESIGN AND STATISTICAL TECHNIQUES	3
3 FACILITIES AND APPARATUS	9
General Facilities	9
Lunar Gravity Simulators	9
Inclined-Plane Simulator	14
Vertical Suspension	18
Treadmill Systems	61
Lunar Surface Simulation	69
Criteria for Material Selection	69
Material Composition for Smooth Surface Simulation	69
Material Composition for Rough Surface Simulation	71
Pressure Suits	74
Physiological and Metabolic Apparatus	99
Instrumentation	99
Metabolic Rate Apparatus	102
Respiratory System	104
Gas Analysis	104
Minute Volume Measurement	104
Miscellaneous Equipment and Apparatus	106
Environmental Control System	106
Mounting Shell	110
Basic Backpacks and Respirometer	110
Liquid Air Backpack	114
Weighing Equipment	118
Treadmill Speedometer	118
Ambient Pressure and Temperature Measurement	118
Air Supply	118

CONTENTS (Continued)

<u>Section</u>	<u>Page</u>
General Procedures	118
Preparation of Subjects	118
Inclined-Plane Simulator Procedure	120
TOSS Simulator Procedure	122
Test Procedure	122
Calibration of Gas Analyzers	124
4 SUBJECTS AND TRAINING	125
Subject Selection	125
Tests for Selection	125
Basal Metabolic Rates	125
Modified Harvard Step Test	125
Modified Balke Test	128
Preliminary Metabolic Rate Tests (One G) Without Pressure Suit	128
Preliminary Metabolic Rate Tests (One G) With Pressure Suit	134
Suit Training	134
Training for Locomotion in Lunar Gravity Simulators	134
Inclined-Plane Simulator	134
Six-Degrees-of-Freedom Vertical Suspension Simulator	139
5 RESULTS AND DISCUSSIONS	145
Physiological Results	145
Metabolic Rate Data	146
Steady-State Metabolic Rates	168
Heart Rate Data	202
Respiratory Rates	204
Oxygen Consumption, Carbon Dioxide Production, and Minute Expired Ventilation	212
Special Considerations of the Physiological Data	217

CONTENTS (Continued)

<u>Section</u>	<u>Page</u>
Interactions of Gait Characteristics and Metabolic Rates	232
Summary of Observations on the Physiological Parameters	240
Kinematics	246
Discussion of Kinematic Data	251
Locomotive Index, Step Rate, and Stride Length	252
Summary of Observations on Stride Length, Step Rate, and Locomotive Index	269
Body Position Data	276
Summary of Observations on Body Angles	300
Comparison of Kinematics Data with Previous Studies	305
Range Computation	315
6 CONCLUSIONS	319
 <u>Appendix</u>	
A METABOLIC RATE TIME COURSES	321
B CRITIQUE OF LITERATURE COMPARING LOCOMOTION ON A TREADMILL TO LOCOMOTION ON A STATIONARY SURFACE	363
Parameters	364
Training	364
Velocity	364
Environmental Conditions	364
Surface	364
Clothing	364
Analysis of Data	365

CONTENTS (Continued)

<u>Appendix</u>		<u>Page</u>
C	PILOT STUDY: EFFECT OF STEP RATE ON METABOLIC COST OF LOCOMOTION ON AN INCLINED-PLANE TREADMILL AT 1/6 G	367
	Methods and Apparatus	367
	Procedures	367
	Results	368
	Discussion	368
D	SYSTEM ERROR ANALYSIS	373
E	LOAD CELL TRACES	387
F	TIME CONSTANT FOR GAS ANALYSIS	393
G	REFERENCES	395

MAN'S CAPABILITY FOR SELF-LOCOMOTION ON THE MOON

VOLUME I - DETAILED REPORT

By E. C. Wortz, Ph.D.,

W. G. Robertson, Ph.D.,

L. E. Browne, and W. G. Sanborn

Department of Life Sciences

AiResearch Manufacturing Company, Los Angeles

A Division of The Garrett Corporation

SECTION I

INTRODUCTION

This report contains the results, methods, procedures, and apparatus of an extensive study conducted to evaluate man's capability for self-locomotion on the surface of the moon. These data are summarized in NASA CR-14013. This program was conducted for the Langley Research Center of the National Aeronautics and Space Administration under Contract NAS 1-7053.

The objectives of this program were to investigate systematically the effects of space suits, pack weights, slope grades, lunar surface conditions, gaits used in locomotion, velocity of traverse, and methods of simulating lunar gravity on self-locomotive performance. The effects of these independent variables were primarily evaluated by physiological and kinematic measurements.

Prior investigation at Langley Research Center concerning the effects of lunar gravity on a wide range of activities had indicated that walking, running, climbing, and other activities on the lunar surface would be substantially improved over that which we are accustomed to on Earth (References 5-2, 5-27, 5-28, 5-33, and 5-34). The lunar gravity conditions have indicated a high probability of a corresponding substantial decrease in the metabolic cost of walking compared to rates for Earth gravity conditions (References 5-11, 5-12, and 5-13).

The amount of research conducted on energy levels prior to the program reported in this document has been quite limited and the level of confidence for generalization to the actual lunar surface has been uncertain. Among the reasons for this were the uncertainty regarding adequacy of the various simulation techniques, the lack of data with space suits, and the uncertainty concerning lunar surface conditions. The primary reason, however, for the lack of sufficient confidence for predictive purposes has simply been the paucity of data. This program represents a major step toward correcting these deficiencies.

This report consists of six major sections and seven appendixes. Section 2 describes the experimental designs employed in the investigations and the statistical procedures utilized to evaluate the data. The experimental conditions (independent variables) for all of the tests conducted are listed in Table 2-1. This section also defines the statistical terminology used in

the body of the report. Familiarity with limited statistical terminology, such as "statistically significant," is necessary to properly evaluate the results of this program.

Section 3 describes the facilities, apparatus, and general procedures utilized in the experiments. Included in this section are the methods for controlling the independent variables and measuring the dependent variables. The design of the various test apparatus and the results from tests of their characteristics are also provided.

Section 4 describes the relevant characteristics of the test subjects and discusses the methods employed in their selection and training.

Section 5 contains the results of the experiments conducted in this program. The results are divided into two major subsections on physiological and kinematic data. The data for each dependent variable are tabulated in terms of mean values and standard deviations. These data are also presented graphically to illustrate the relationships that were found. General summaries of the results are presented at appropriate points within the section. The two major subsections are concluded with projections of the data to limitations on distances achievable by self-locomotion on the lunar surface.

Section 6 lists the major conclusions, and supplements the summaries in Section 5 with additional conclusions and observations.

The appendixes contain relevant data for this program, including an error analysis on the metabolic apparatus and the data reduction system.

SECTION 2

EXPERIMENTAL DESIGN AND STATISTICAL TECHNIQUES

The test conditions for the experiments conducted in this program are presented in Table 2-1. The table lists all the independent variables tested, including subjects, simulators, locomotion velocities, locomotion gaits, walking surface characteristics, the weights of packs carried, the inclination of the slope traversed, and suiting. The experimental program tested the effects of these independent variables on dependent variables such as metabolic rate, total energy expenditure, heart rate, respiratory rate, and kinematic characteristics of gait. The combinations of experimental conditions selected for testing resulted in a program of 836 tests. In addition, training and baseline testing were conducted under this program on the inclined walkway at Langley Research Center.

A series of statistical treatments were made on the data collected (dependent variables) to define more precisely the effects of the independent variables. These statistical calculations included both descriptive and inferential techniques. The descriptive techniques were limited to the determination of the mean (average) value \bar{X} and the standard deviation of σ grouped data

$$\bar{X} = \frac{\sum X}{n}$$

where Σ = sum of

X = each individual measurement

n = number of measurements

and
$$\sigma = \sqrt{\sum x^2 / n - 1}$$

where x^2 = the square of a deviation from the mean

$$\sum x^2 = \sum (X - \bar{X})^2$$

In employing σ to evaluate the data, a normal or Gaussian distribution is assumed, in which event 34.13 percent of the data will have a value $\leq \bar{X} + 1\sigma$, and 34.13 percent will have a value $\geq \bar{X} - 1\sigma$. Consequently, 68.26 percent of the data will be expected to occur within the range $\bar{X} \pm 1\sigma$ and 84.13 percent will be $< \bar{X} + 1\sigma$. All of the dependent variables will be reported in terms of \bar{X} and σ .

The inferential statistical techniques employed were primarily the product moment coefficient of correlation r and the analysis of variance. The product moment coefficient of correlation is used to ascertain how one variable X can be predicted from a second variable Y . When $r = 1$ or $r = -1$, X is

TABLE 2-1
EXPERIMENTAL DESIGN

Experimental conditions						
Simulator and suit mode	Slope, deg	Surface condition	Pack	Number of velocities	Number of subjects	Total tests
Inclined plane, pressurized (press.) suit	0 (horiz)	Hard	I, 75 lb	4 each; walk, lope and run	6, with 2 repeating once	96
Inclined plane, pressurized suit	0	Hard	I	1 each; walk, lope, and run	6, with all repeating twice	36
Inclined plane, subject in mufti (without press. suit)	0	Hard	I	4 each; walk, lope, and run	2	24
Incl plane, mufti	0	Hard	I	Fatigue test	6	24
Inclined plane, pressurized suit	0	Hard	I	Fatigue test	2	8
Inclined plane, pressurized suit	0	Hard	II, 240 lb	4 each; walk, lope, and run	6	72
Inclined plane, pressurized suit	0	Hard	III, 400 lb	4 each; walk, lope, and run	2	24
TOSS (6-deg-of-freedom), pressurized suit	0	Hard	I	4 each; walk, lope, and run	6	72
TOSS, press. suit	0	Smooth lunar	I	4	6	24
TOSS, press. suit	0	Coarse lunar	I	4	6	24
TOSS, pressurized suit	7.5	Hard	I	4	6	48
TOSS, pressurized suit	7.5	Smooth lunar	I	4	6	48
TOSS, pressurized suit	15	Hard	I	4	6	48
TOSS, pressurized suit	15	Smooth lunar	I	4	6	48
TOSS, pressurized suit	30	Hard	I	4	6	48
Inclined plane, pressurized suit	7.5	Hard	I	4	6	48
Inclined plane, pressurized suit	7.5	Hard	II	4	6	48
Inclined plane, pressurized suit	15	Hard	I	4	6	48
Inclined plane, pressurized suit	30	Hard	I	4	6	48

perfectly predicted from Y and the regression of Y on X is equal to the regression of X on Y. When $r = 0$ there is no predictability. Normally r is some intermediate value.

$$r = \frac{\Sigma XY - \frac{(\Sigma X)(\Sigma Y)}{n}}{\sqrt{\left(\Sigma X^2 - \frac{(\Sigma X)^2}{n}\right) \left(\Sigma Y^2 - \frac{(\Sigma Y)^2}{n}\right)}}$$

The primary use of inferential statistics is in decision-making. The problem is to determine from the values of the dependent variables whether condition A is different from condition B. This is accomplished by assuming that the data from condition A and condition B are samples from the same population (i.e., there is no real difference between A and B). The hypothesis of no difference is termed to null hypothesis. The validity of the null hypothesis is tested by comparing the means or variances of the samples and ascertaining the probability that means or variances as different as those observed could have been obtained by chance factors alone. If two means were sufficiently different to have occurred by chance sampling of the same population only one time in a hundred, the hypothesis of no difference would be rejected. This decision is written as a statement such as the following: "statistically significant difference $p < 0.01$."

The most important inferential statistic utilized in evaluation of the data is the technique of analysis of variance. In analysis of variance, a comparison is made between the variance of the observed means with the expected chance variation of these means (variance = σ^2). The rationale of the analysis of variance is that the sum of squares Σx_T^2 can be analyzed in two parts: a Σx_W^2 within groups and a $\Sigma x_{\bar{X}}^2$ based on the variation between group means.

The sum of squares for a simple two-dimensional analysis of variance is:

$$\sum_{i=1}^r \sum_{j=1}^c n_{ij} (X - \bar{X})^2 = \sum_{i=1}^r \sum_{j=1}^c n_{ij} (X - \bar{X}_{ij})^2 +$$

$$\sum_{i=1}^r n_i (\bar{X}_i - \bar{X}_T)^2 +$$

$$\sum_{j=1}^c n_j (\bar{X}_j - \bar{X}_T)^2 +$$

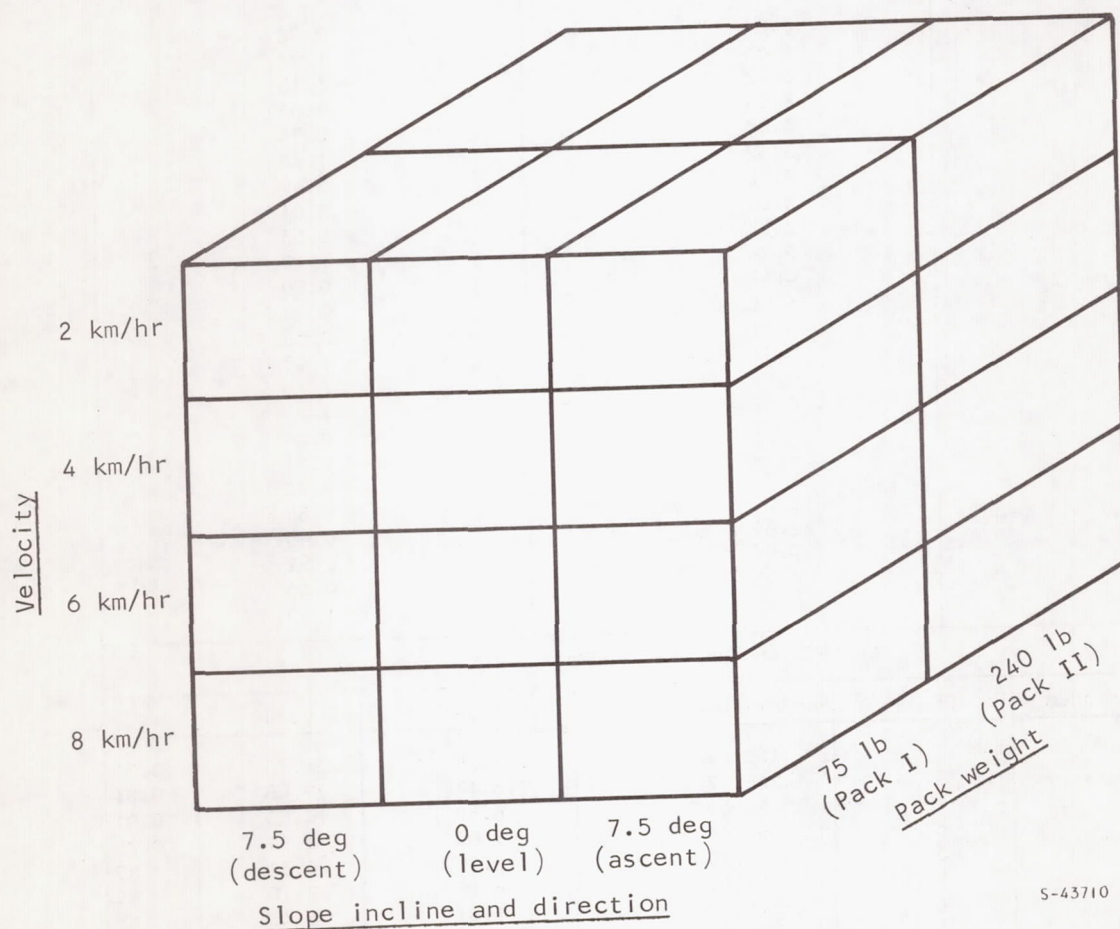
$$\sum_{i=1}^r \sum_{j=1}^c n_{ij} (\bar{X}_{ij} - \bar{X}_i - \bar{X}_j + \bar{X}_T)^2$$

where	X	= any measure
	r	= number of rows or number of sampling points along the continuum of one independent variable
	c	= number of columns
	n_{ij}	= numbers of measures in i^{th} cell of j^{th} column
	$\sum_{i=1}^r n_{ij}$	= numbers of measures in row i
	$\sum_{j=1}^c n_{ij}$	= number of measures in column j
	\sum_{ij}	= sum of all measures in cell ij
	\bar{X}_{ij}	= mean of cell $ij = \frac{1}{n_{ij}} \sum_{ij} X$
	\bar{X}_j	= mean of all measures in column $j = \frac{1}{n_j} \sum_{i=1}^r n_{ij} \bar{X}_{ij}$
	\bar{X}_T	= general mean = $\frac{1}{n} \sum_{j=1}^c \sum_{i=1}^r n_{ij} \bar{X}_{ij}$ and
	n	= total number of measures

The sums of squares are divided by the degrees of freedom $(r-1)$, $(c-1)$, $(r-1)(c-1)$, and $N - 1$ for rows, column, row-column interaction, and total sum of square, respectively, to achieve the variance for rows, columns, the row-column interaction, and the total variance. Ratios are computed for the variance of rows, columns, and row-column interaction to the within-cells variance. This ratio, termed F ratio, is then compared to the distribution of F for samples taken from a normal population. If F differs substantially from the expected value, it may be assumed that the ratio could not have occurred by chance and that the variable in question has a true effect on the dependent variable.

A typical example of the application of analysis of variance to the data is the analysis of the combination of experimental conditions shown in Figure 2-1. Table 2-2 tabulates the statistical analysis. Means and standard deviations for the cells shown in Figure 2-1 are listed. The analysis of variance summary shows the source of variation, the degrees-of-freedom (DF), the sum of squares, the mean squares value, the value of the F ratios, and the probability of the chance occurrence of each F ratio. Probability values of $p < 0.01$

for the variables of locomotion, velocity, angle and direction of incline, and pack weight indicate that each of these variables has a statistically significant effect on metabolic rate. A $p < 0.05$ for the AB interaction (velocity and incline) indicates that there is an effect of the combination of these variables on metabolic rate that is over and above that produced individually by these variables. "Not significant" (NS) indicates that occurrence of the tabulated value of F has a probability of $p > 0.05$.



S-43710

Figure 2-1. Typical Combination of Conditions for Statistical Analysis

TABLE 2-2
TYPICAL STATISTICAL ANALYSIS

Variables tested:			Dependent variable: metabolic rate		
A is <u>velocity</u> in km/hr (2,4,6,8 km/hr)			Independent variables held constant:		
B is <u>angle</u> in deg (0, 7.5 ascend, 7.5 descend)			(1) Simulator, inclined plane		
C is <u>pack</u> (75 lb, 240 lb)			(2) Suit, pressurized G-4C		
			(3) Subjects, 6		
			(4) Surface, hard		

Cell definition	Mean, kcal/min	Standard deviation, kcal/min
A,B,C		
1,1,1	3.51	0.92
2,1,1	4.63	1.91
3,1,1	6.42	3.15
4,1,1	8.04	2.03
1,2,1	3.06	0.74
2,2,1	5.42	1.73
3,2,1	7.12	3.49
4,2,1	8.84	3.01
1,3,1	2.52	0.53
2,3,1	3.74	1.10
3,3,1	4.42	0.90
4,3,1	4.58	0.98
1,1,2	5.11	2.33
2,1,2	5.51	1.02
3,1,2	6.86	2.15
4,1,2	8.48	1.39
1,2,2	4.18	0.54
2,2,2	7.04	1.47
3,2,2	9.94	1.92
4,2,2	12.09	2.85
1,3,2	2.89	0.45
2,3,2	4.11	0.97
3,3,2	4.93	0.66
4,3,2	6.19	1.40

ANALYSIS OF VARIANCE SUMMARY					
Source of variance	DF	Sum of squares	Mean square	F value	p
A	3	405.89	135.29	34.78	<0.01
B	2	226.27	113.13	29.08	<0.01
C	1	56.50	56.50	14.53	<0.01
AB	6	66.21	11.03	2.84	<0.05
AC	3	3.58	1.19	0.31	NS
BC	2	16.31	8.15	2.10	NS
ABC	6	11.26	1.87	0.48	NS
Cells	23	786.05	34.17	8.79	<0.01
Within	120	466.79	3.88		
Total	143	1252.84	8.76		

SECTION 3

FACILITIES AND APPARATUS

GENERAL FACILITIES

The facilities and apparatus used in this program can be categorized into simulators, treadmill systems, lunar surface simulators, pressure suits, physiological and metabolic apparatus, and miscellaneous equipment such as digital data systems, weighing equipment, and environmental control systems. These items of equipment are described in this section.

Most of the tests conducted in this program were performed at an outdoor facility especially designed for this purpose. The general layout of the facilities used in this program is depicted by a photograph of the primary test area in Figure 3-1. This aerial photograph shows the relationship of the three basic simulators. The treadmill for the inclined-plane simulator is shown at the base of the tower. The suspension cables for this simulator extended from the cross-beam at the top of the tower to the subject. Figure 3-1 shows a test being conducted with the treadmill in a 15-deg ascending slope condition. The horizontal treadmill used for the TOSS (Turbine Operated Suspension System) is located beneath the center of the tower, but is not visible in the photograph because of the wind-screening on the tower. The variable-surface treadmill/conveyor system is on the left. In addition to these facilities, the inclined-plane simulator at Langley Research Center (Figure 3-2) was used for training two special subjects.

The instrumentation and control room is a small building situated so that the distance from the control room to the point where the subject is being tested is approximately the same for all three simulators. An internal view of the control room is shown in Figure 3-3. The subjects were instrumented and dressed for testing in a dressing room located in the laboratory and support area in the main building. Initial training was conducted on the small inclined-plane simulator (Figure 3-4) in the laboratory area. Tests for basal, resting, sitting, and standing metabolic rates were performed in this area using the Goddard Pulmonet.

LUNAR GRAVITY SIMULATORS

The simulators used in this program were extensions of techniques developed during previous programs. The inclined-plane simulator was built from the data and design provided by Hewes and Spady and reported in NASA TND-2716 (Reference 3-1) with modifications in the method of holding the subjects due to the constraints of the pressure suits and backpacks used in this program. The vertical suspension was originally scheduled to use spring negation of the force required for reduced-gravity simulation. A parallel company-funded research program, however, indicated difficulties with the springs; consequently, the company-funded program was expanded to develop a vertical turbine-operated suspension system (TOSS) which is described in a later subsection.



Figure 3-1. Primary Test Area

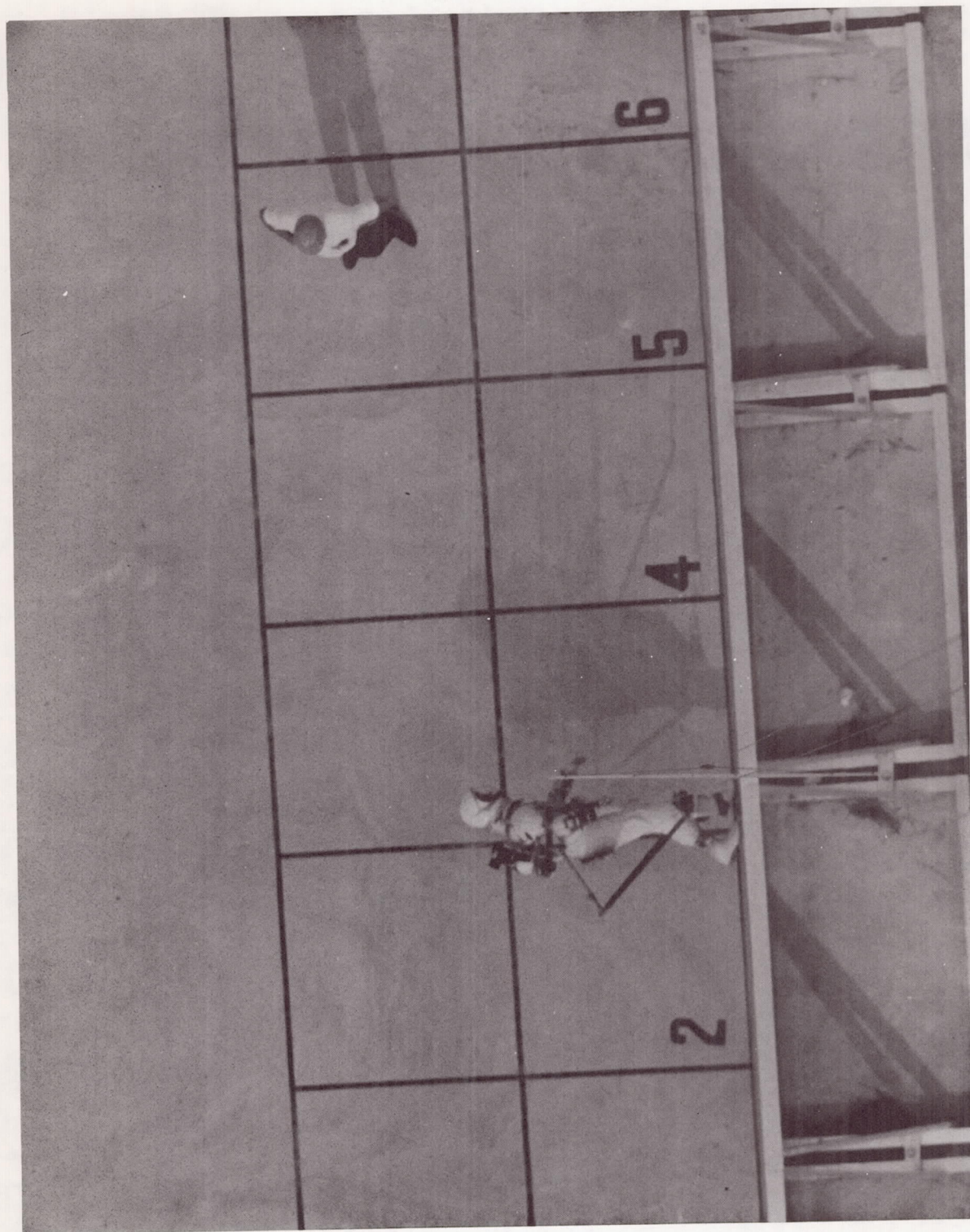


Figure 3-2. Inclined-Plane Simulator at Langley Research Center

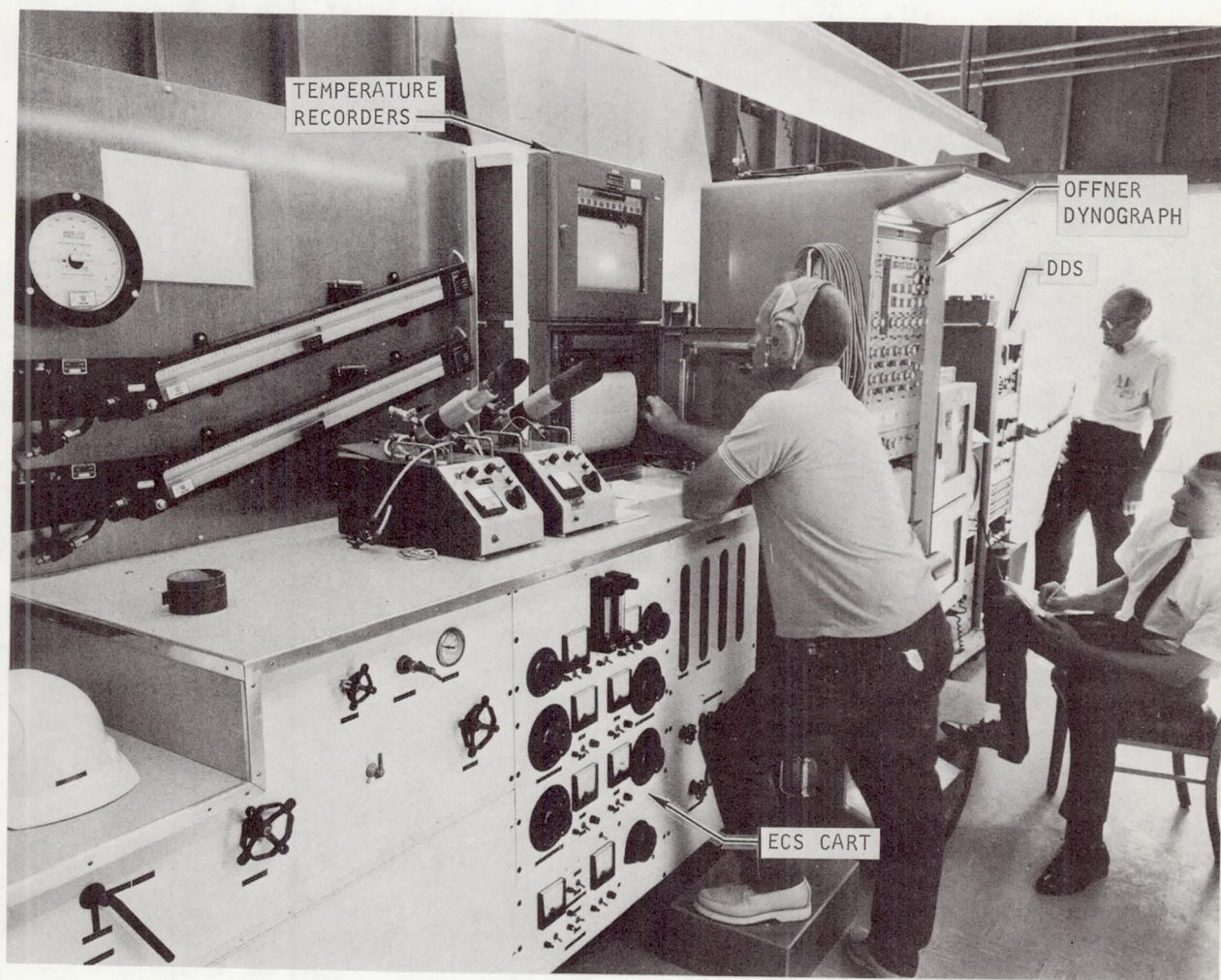


Figure 3-3. Control and Recording Room

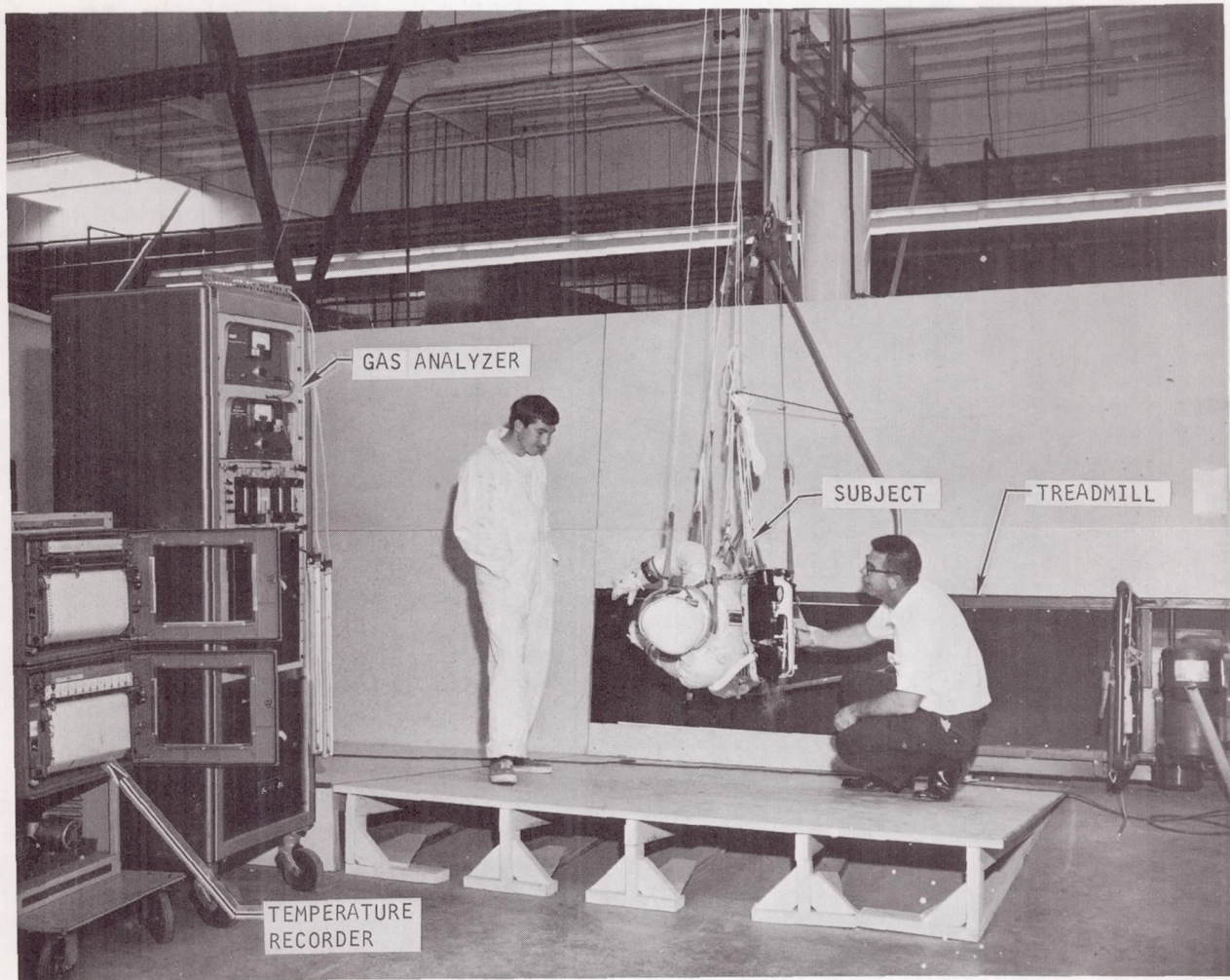


Figure 3-4. Laboratory Inclined-Plane Simulator (Training Configuration) and Integrated Gas Analyzer Console

Inclined-Plane Simulator

The inclined-plane simulator consists of a treadmill, a suspension system, and a tower for the suspension system.

The inclined treadmill is a flat conveyor 60 in. wide and 16 ft long on centers of the head and tail pulleys. The basic treadmill is mounted on a frame holding it at 9-1/2 deg from vertical. The surface is a uniformly tufted rubber surface providing a maximized traction surface.

Some difficulties arose in making this belt track correctly without having the upper portion of the belt sag due to the weight of the belt. This was rectified by removing the crown from the head and tail pulleys and adding three pulleys on the back side of the conveyor belt to take up the slack and provide a uniform tension across the belt. It was also found that all pulleys must be carefully balanced to reduce undesirable vibration at high belt speeds. Although not required, this treadmill can be reversed if care is taken to readjust belt tension.

The treadmill was installed integral with and parallel to the plane upon which the subject stands. This plane is 9-1/2 deg from vertical with respect to the point of suspension, and results in an effective acceleration to the feet of the suspended subject almost equivalent to that on the lunar surface. Extension platforms were attached to the ends of the treadmill for safety and improved visual reference. A stairway and platform were installed on the back of the treadmill to provide a work space for test personnel. An aerostand, used for servicing aircraft, was modified to provide an 8- by 10-ft work platform. A movie camera was installed on the middle platform of the tower, and was controlled by a remote switch in the control room. These items are illustrated in Figure 3-5 which is a photograph taken from the middle platform of the tower, adjacent to the movie camera.

The backpack, gas meter, and associated harnesses required to suspend the subject are illustrated in Figure 3-6.

The test tower (Figure 3-7) provides a suspension height of 136 ft for the inclined-plane simulator. This structure provides double the minimum elevation specified under the contract. This structure is an oil derrick procured from, and erected by, the Macco Corporation. The foundation and erection of the tower was completed after receiving approval of the City and the FAA. The derrick was modified by the addition of a 4- by 12-in. I-beam, 40-ft long, attached to the legs just under the top platform. The middle platform was installed at 75-1/2 ft elevation. This tower provides the structure required for suspension of the inclined-plane simulator.

The suspension cabling is attached at one end to foam-rubber filled slings that hold the subject and at the other end to a trolley on the 40-ft-long horizontal beam 136-ft from the base of the tower. The trolley consists of two sets of high quality rollers to minimize frictional drag. A swiveled eye hook is provided between these rollers for the attachment of the main supporting cable. This cable is a 1/4-in. stainless steel wire cable that extends to the 75-ft level and attaches to the load distribution plate for the cables used for suspending the subject and backpacks. This cable is supplemented by a safety

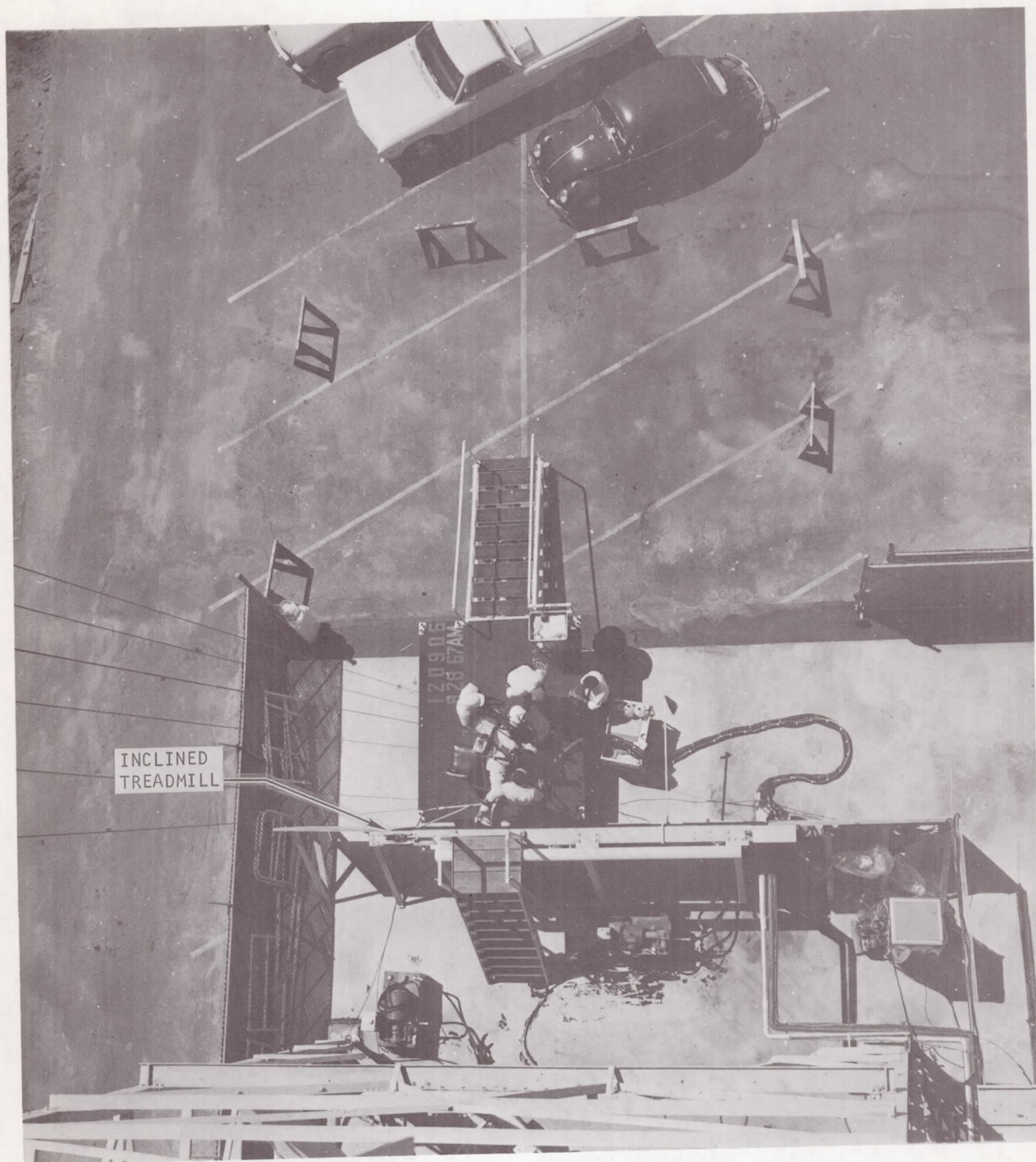


Figure 3-5. Inclined Treadmill Installation (viewed from above)

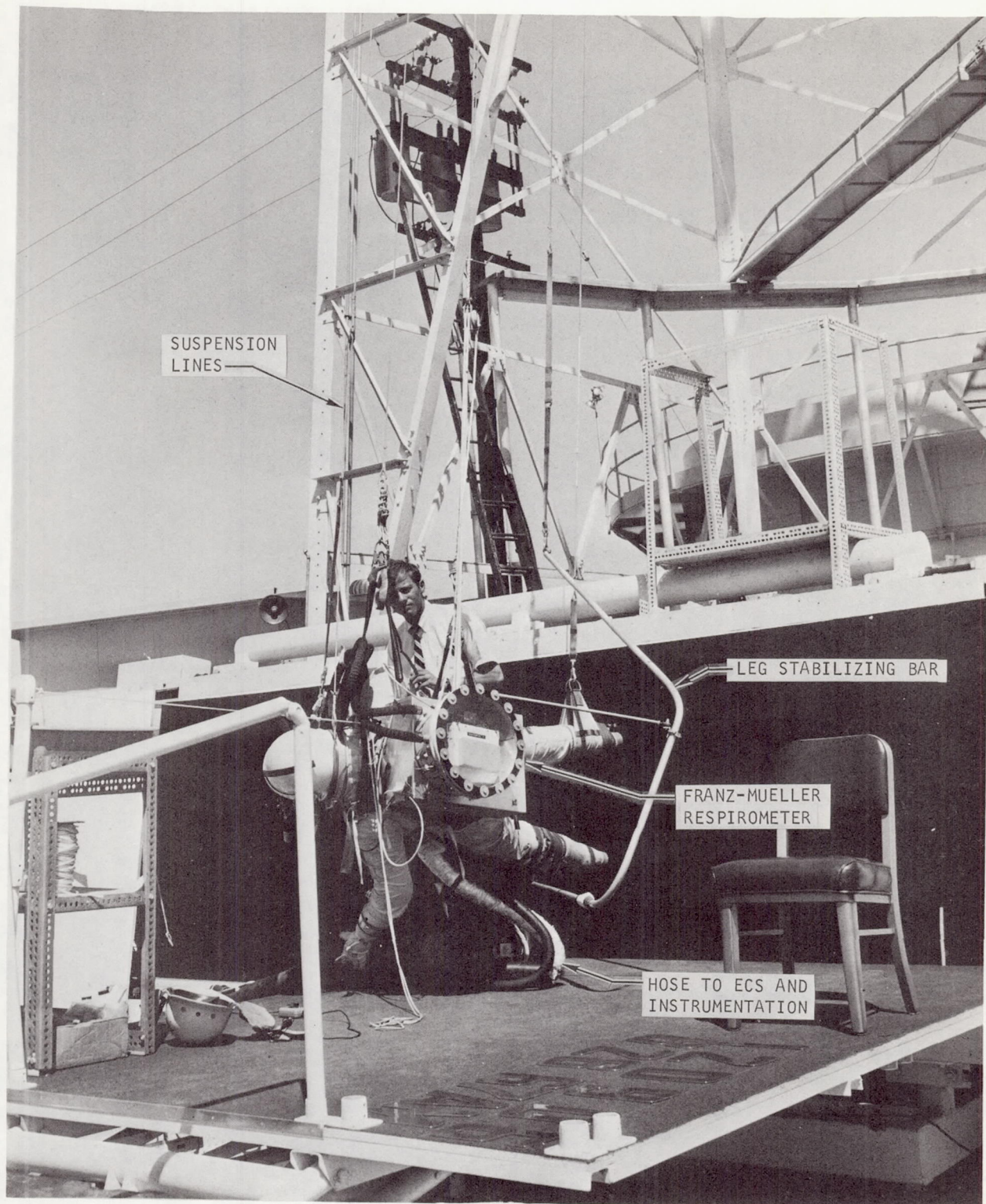


Figure 3-6. Inclined-Plane Test Configuration Showing Backpack, Gas Meter, and Harness Assembly

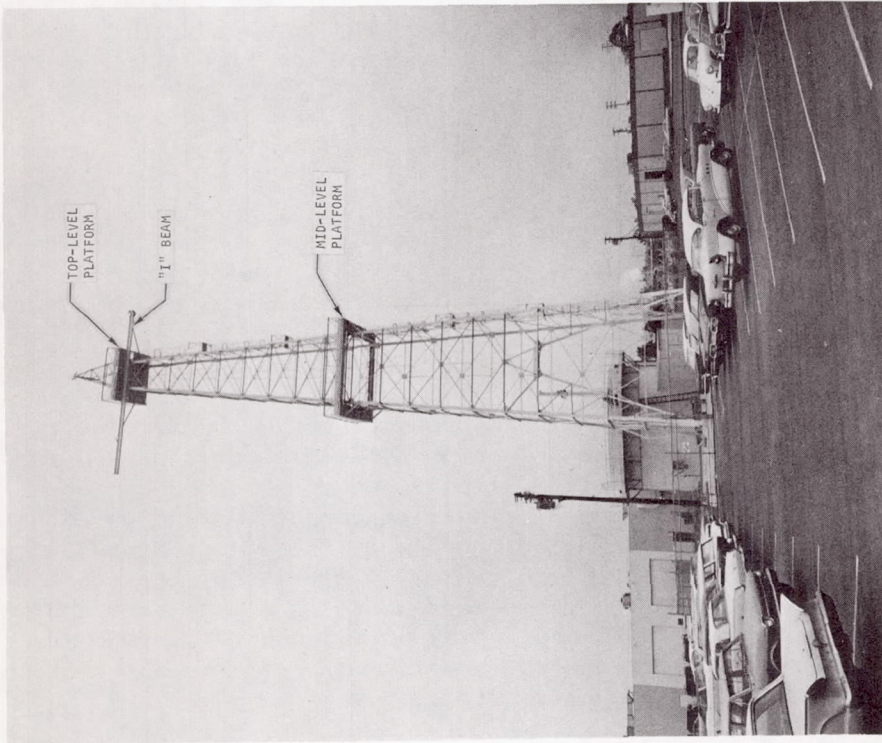
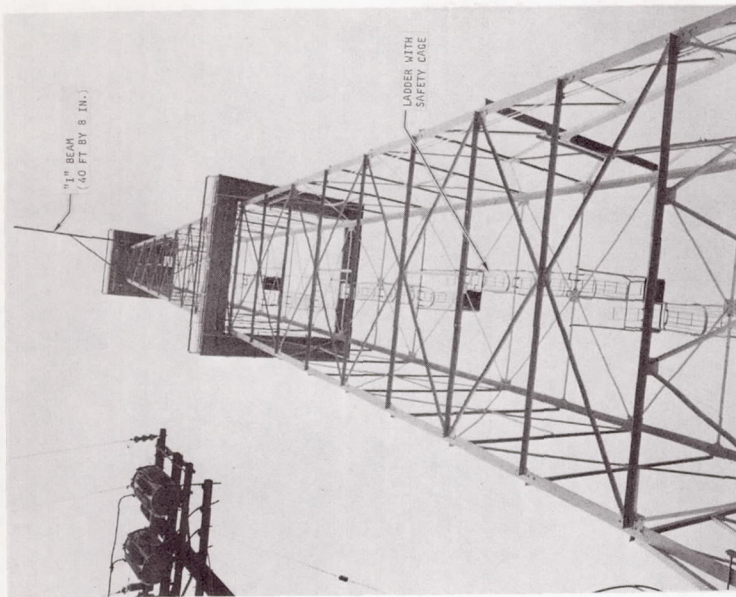


Figure 3-7. Test Tower

cable made of 5/16-in. Dacron braided rope in the event of support cable failure. This cable was proof-tested to 1500 lb. A spreader bar maintains the distance between take-up cables, and is placed approximately 10 ft from the distribution plate. This bar is constructed of two lightweight tubes bolted together to hold smooth ferrule-type guides for each rope. These guides also provide spreading adjustment if required. The length of the individual support cable from the spreader bar to the subject is approximately 70 ft. The principal load cables and the torso cables attach directly to clips on a mounting shell molded to the shape of the pressure suits, thus eliminating torso slings.

Weights were suspended, and the simulated acceleration was checked by the use of a ring load cell to verify proper placement of the treadmill and backpack position.

Vertical Suspension

The vertical simulators in this program used a horizontal treadmill with a walking surface material similar to that of the inclined-plane simulator. An additional treadmill system was designed for varying the walking surface by depositing soil material on that surface. These simulators required a vertical support system to provide the simulation of lunar gravity. This vertical support system was used for both horizontal treadmill systems.

Lunar gravity simulation was provided by the turbine-operated suspension system (TOSS) designed and developed by AiResearch to improve dynamic response over that observed for negator spring systems used for the simulation of reduced gravity in manned testing. The prime objectives in the development of this system were the development of a method for supplying a constant vertical force and the reduction of external inertial forces while the system is in operation.

The basic system, illustrated schematically in Figure 3-8, consists of a "C" brace gimbal, a swivel, a yoke with air pad bearing, a cable and pulleys, a lightweight beam, and a turbine/take-up pulley. This provides the six degrees-of-freedom desired for reduced gravity simulation. The sources of the degrees-of-freedom with reference to the subject's center of gravity are listed in Table 3-1.

The "C" brace consists of three major support pieces. The first piece is a U-shaped closed channel structure to which the fiber-glass rigid body mounting shell is firmly attached. This piece is attached to a second U-shaped piece at the ends of the "U" through a ball bearing connection and an adjustable plate. This attachment provides the pitch degree-of-freedom and an adjustment for aligning the lifting force through the center of gravity of the suspended subject vertically and fore and aft. The second piece is attached to the main C-shaped support piece through a ball-bearing-supported shaft. This connection provides the roll degree-of-freedom, which is adjusted by moving the rigid body support laterally to obtain the balance required.

The main C-shaped piece containing the gimbal assembly can be suspended vertically by any attachment or suspension method. The point of attachment

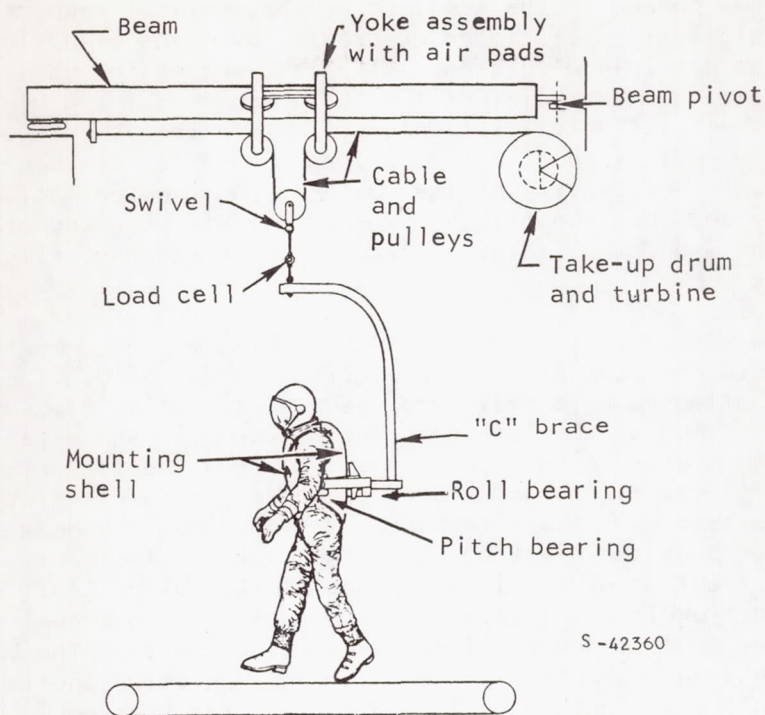


Figure 3-8. Turbine-Operated Suspension System (TOSS)

TABLE 3-1
TOSS DEGREES-OF-FREEDOM

Component	Degrees-of-Freedom
"C" Brace Gimbal - pitch and roll	2
Swivel - yaw	1
Turbine Take-up - vertical	1
Yoke (with air pads) - fore and aft	1
Beam (pivot and air pads) - lateral	1
Total degrees-of-freedom	6

for lifting allows a change in the location of the vertical support with respect to the overall assembly center of gravity by means of a slotted attachment mechanism that provides a fore-and-aft adjustment of the main pickup point. The pickup attachment point of the "C" brace contains a high quality swivel that allows a relatively frictionless pivot in the yaw direction. The "C" brace was designed to support a 500-lb load mounted at the approximate location of the center of gravity of the subject. Unlike the incline plane, the TOSS simulator does not support the subject's feet. Leg and arm motions cause shifts in the subject's center of gravity which may have slight effects on his performance.

In the following description of the TOSS mechanism, the numbers in parentheses correspond to the item numbers in Figures 3-9 and 3-10. The subject and "C" frame are attached by a cable and a swivel to pulley (1) supported by cable (2) which is fixed at the left-hand end of beam (3) and extends through pulleys attached to spacer (4) and yoke (5). This continuous cable extends around the pulley on the right-hand end of the beam and feeds directly into the take-up drum (6) driven by the air turbine. Motion along the beam, right, left, or laterally about the pivot point on the right of the beam, requires no extension or retraction of the load applied at the pulley (1). This means that only the force required for movement is necessary to overcome the friction of the air pads and pulleys and the inertia of moving parts. The beam (3) is pivoted at the right end through a pinned bearing connection and is supported at the left end on the air cushions (7) riding on a track assembly (8). The yokes (5) with spacer (4) and pulleys are rigidly assembled and are suspended on four air cushions (9). This allows free travel from left to right on the beam (3) assembly. The take-up drum (6) is attached to the mount (10) which is attached to a shaft and then to the air turbine (11). The mount is adjustable to allow alignment of each size take-up drum so that the support cable feeds directly into the drum regardless of the lateral rotation of the beam.

The air cushions used for this system are procured from Vega Enterprises, Decatur, Illinois. These cushions are a formed vinyl material attached to a steel backing plate. These pads are relatively inexpensive and perform well with proper application and use. The air required to operate these pads is a function of surface roughness, load alignment, and load variation.

The air turbine used in this application is AiResearch Model ATS 100-189, developed for the ground starting of jet engines on the Boeing 727 airplane.

Air is supplied to the air pads through 1/4-in.-dia flow lines which are routed up the support post and along the top of the beam. Loops of adequate length to provide fore-and-aft excursions are left in the lines feeding the yoke air pads.

The TOSS system at the hard-surface treadmill installation provides a clearance of approximately 21 ft from the base to the pulleys on the yoke.

Structural test of suspension boom assembly. - The suspension boom assembly was tested independently of all other factors to determine the natural frequency of the assembly to allow a better interpretation of data on the dynamics of this simulator.

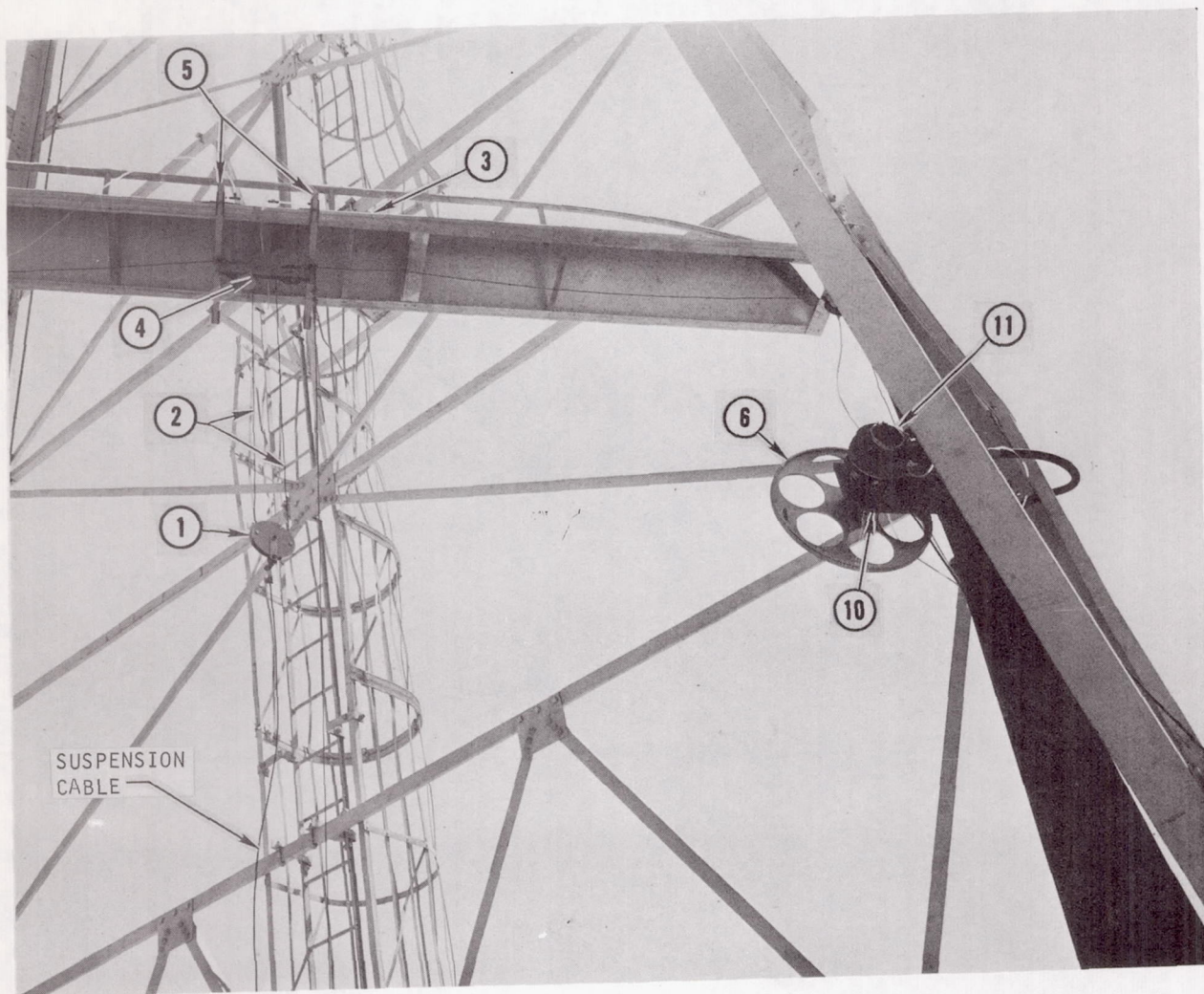


Figure 3-9. Yoke and Cable Assembly with Air Turbine

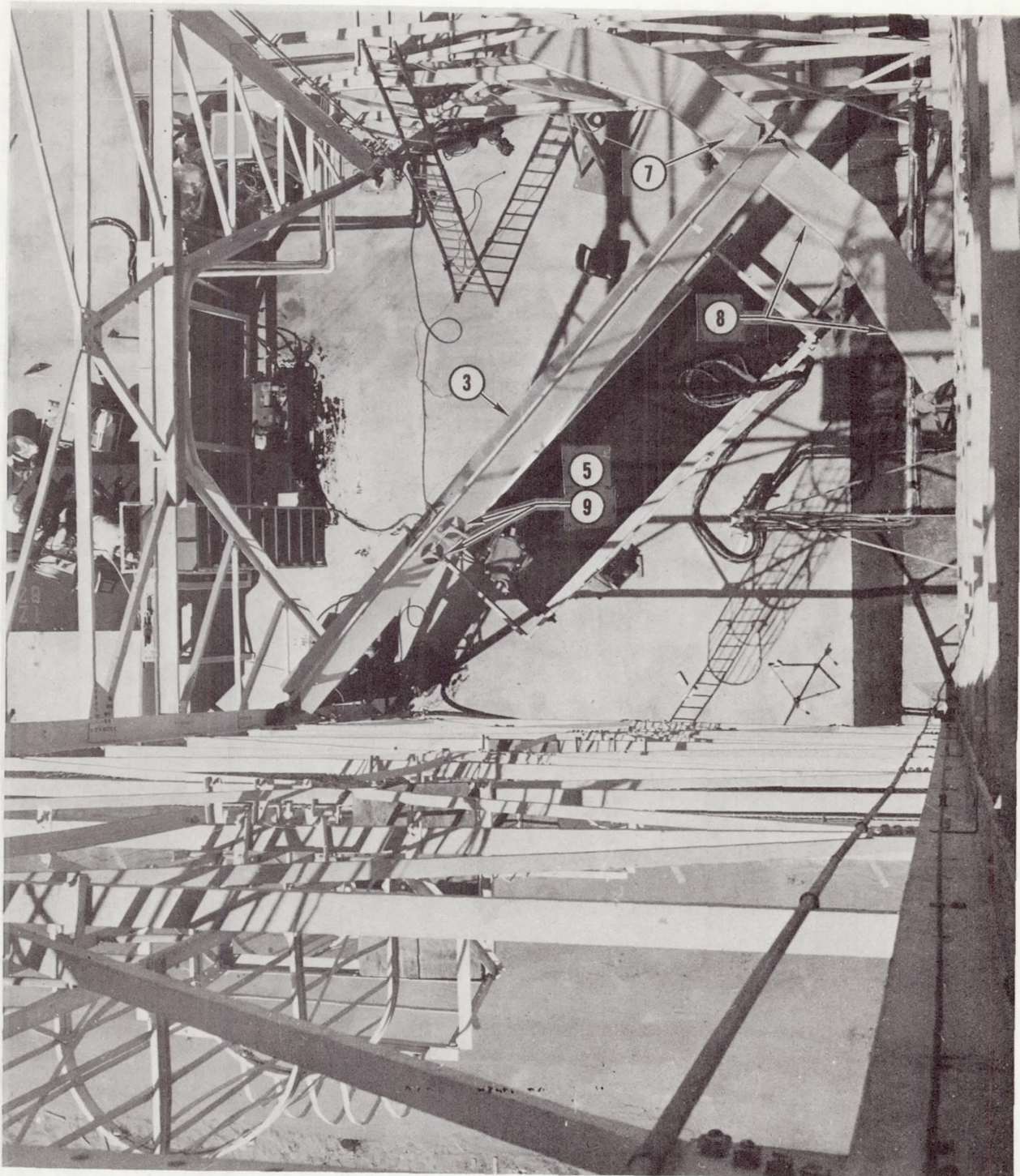


Figure 3-10. Lunar Gravity Simulation System (viewed from above)

The suspension assembly consisting of the boom, the suspension cable, the yoke assembly, and air pads was mounted on two concrete pipes as shown in Figure 3-11. The concrete pipes were used to provide a rigid base that would not influence the characteristics of the assembly.

The yoke assembly was tested independently of the beam by shoring up a short section of the beam as shown in Figure 3-12. Air was supplied to the yoke air pads. The suspension cable was fixed at the turbine end of the beam. The weight of the mass suspended was 244 lb which is approximately 5/6 of the nominal weight of a pressure-suited subject with a 75-lb pack. A load-cell was placed between the suspended mass and the suspension system similar to the actual test configuration. The output from this cell was recorded on a Dynograph strip recorder.

The test conditions were devised to isolate each contributing resonating component to the overall system. The effect of the air pads was determined in each configuration by testing with and without air. The effect of the suspension cable was determined by attaching the suspended mass directly to the yoke assembly as shown in Figure 3-12. The method used for isolating the yoke is also illustrated in Figure 3-12.

The tests conducted are listed in Table 3-2. The exciting forces in tests 1 through 12 were accomplished manually by pushing or striking. The exciting force for the balance of the tests was a given input of 22.25 lb which was suspended from the mass by a cord and then cut off.

In tests 18 and 19, the load cell was placed in the main suspension cable at the fixed end shown on the left in Figure 3-11.

The load cell traces for test configurations 1 through 4 are presented in Figure 3-13. The trace for the remaining configurations are presented in Appendix E. The span set for tests 18 and 19 is 300 lb (approximately). The chart speed for each test was 2.5 cm/sec. The zero time for each test starts at the top and moves down.

Figure 3-14 is the deflection curve of the beam. The deflection was obtained by placing the beam on rigid supports and placing the load at the center of the beam. A dial indicator was used to measure the deflection. These deflection/load data show that the effective area moment of inertia is 63.5 in.⁴, and the maximum stress associated with a 300-lb load is 1860 psi. The beam is capable of suspending 650 lb safely at the center. The ultimate load could be as high as 3000 lb, but there would be local buckling of the panels used as a bearing surface for the air pads.

The natural frequency of each configuration is listed in Table 3-2. The traces also illustrate the vibration damping of each configuration, and since the time periods are much larger than the actual forcing function (i.e., a man walking or running), this factor has little influence on the system evaluation.

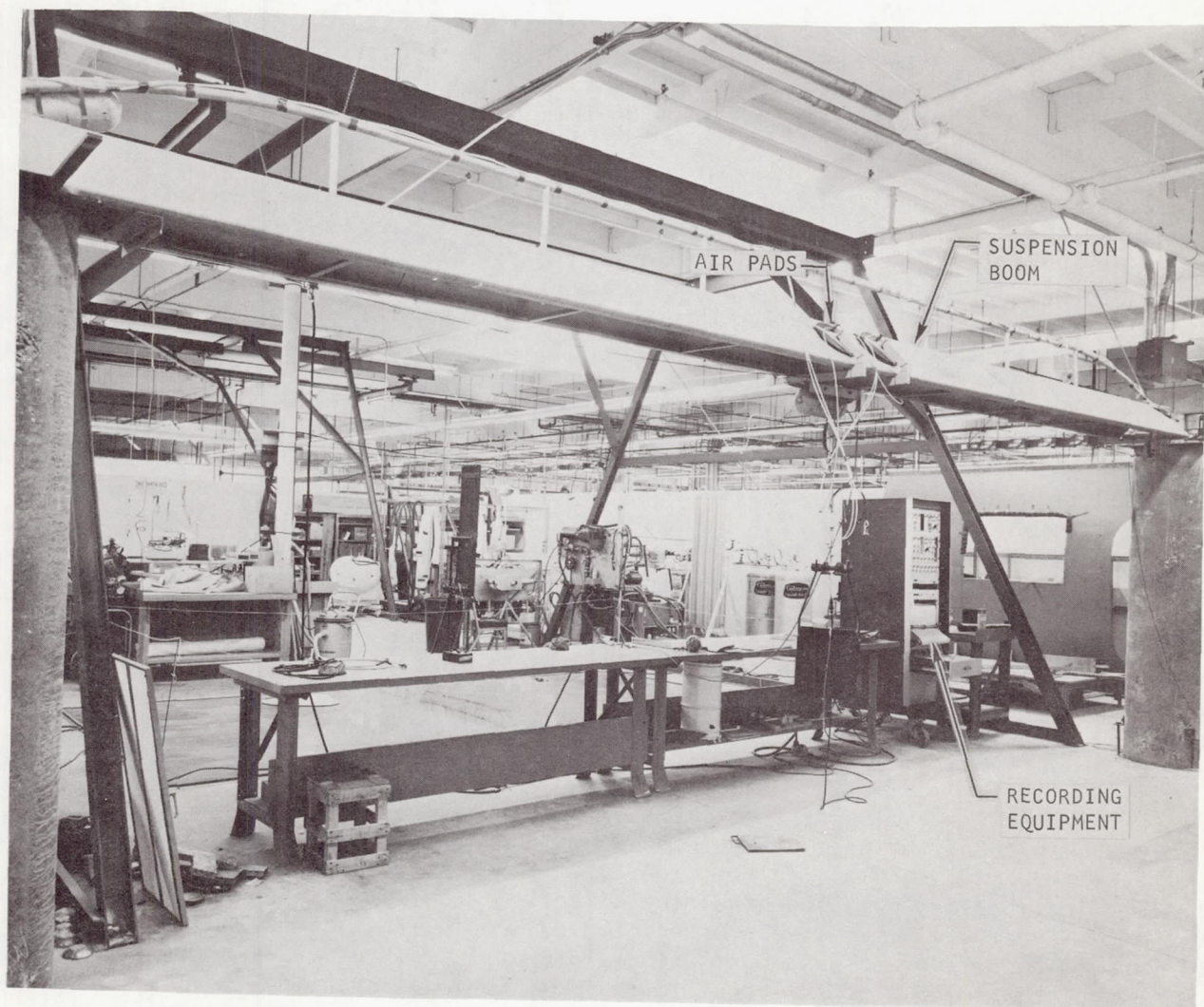


Figure 3-11. Suspension Boom Test Setup

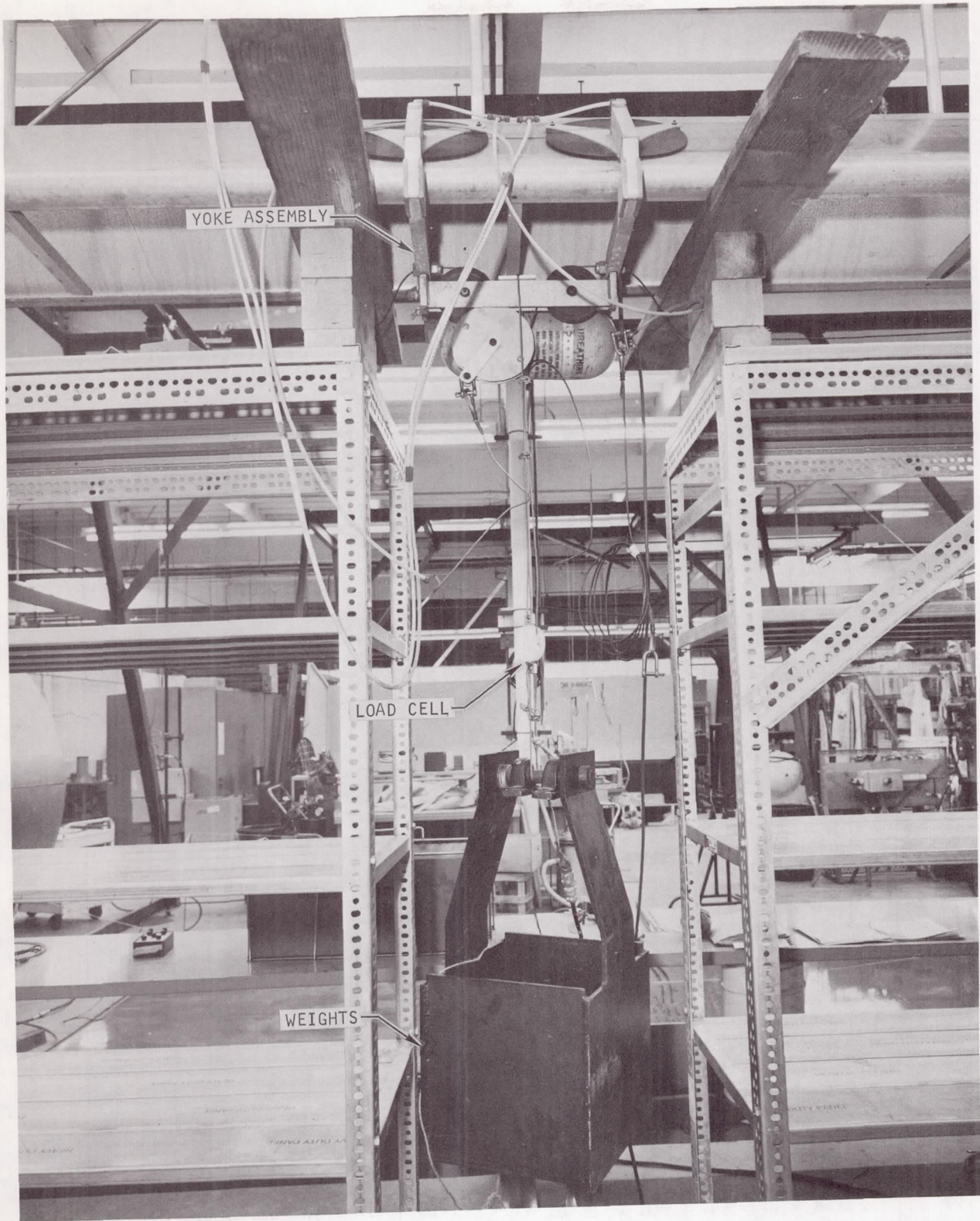


Figure 3-12. Yoke Assembly Testing

TABLE 3-2
SUSPENSION ASSEMBLY TESTS

Test No.	Configuration	Frequency, cps
1	Complete assembly, without air in cushions	4.67
2	Complete assembly, with air in cushions	4.08
3	Same as test 2 (cyclic loading)	16 (approx)
4	Same as test 2 (torsional forcing on end of beam)	5.8
5	Same as test 2 (impact forcing on end of beam)	25 (approx)
6	Same as test 2 (impact loading on panels adjacent to air pads)	15.0
7	Same as test 6 (no air to pads)	15.5
8	Assembly with suspension cable removed (no air to pads)	6.0
9	Same as test 8 (with air to pads)	4.7
10	Short beam section and yoke (no air to pads, no suspension cable)	9.5
11	Same as test 10 (with air to pads)	6.0
12	Same as test 11 (striking panel adjacent to pads)	25 (approx)
13	Same as test 11 (given input)	6.5
14	Full beam (without suspension cable and given input)	4.5
15	Same as test 14 (with suspension cable)	4.0
16	Same as test 15 (with yoke at the extreme right, turbine end)	4.5
17	Same as test 15 (with yoke at the extreme left, air pad end)	5.0
18	Complete beam assy (with load cell at fixed end of suspension cable and yoke assembly at extreme left)	5.0
19	Same as test 18 (with yoke at the center position)	4.0

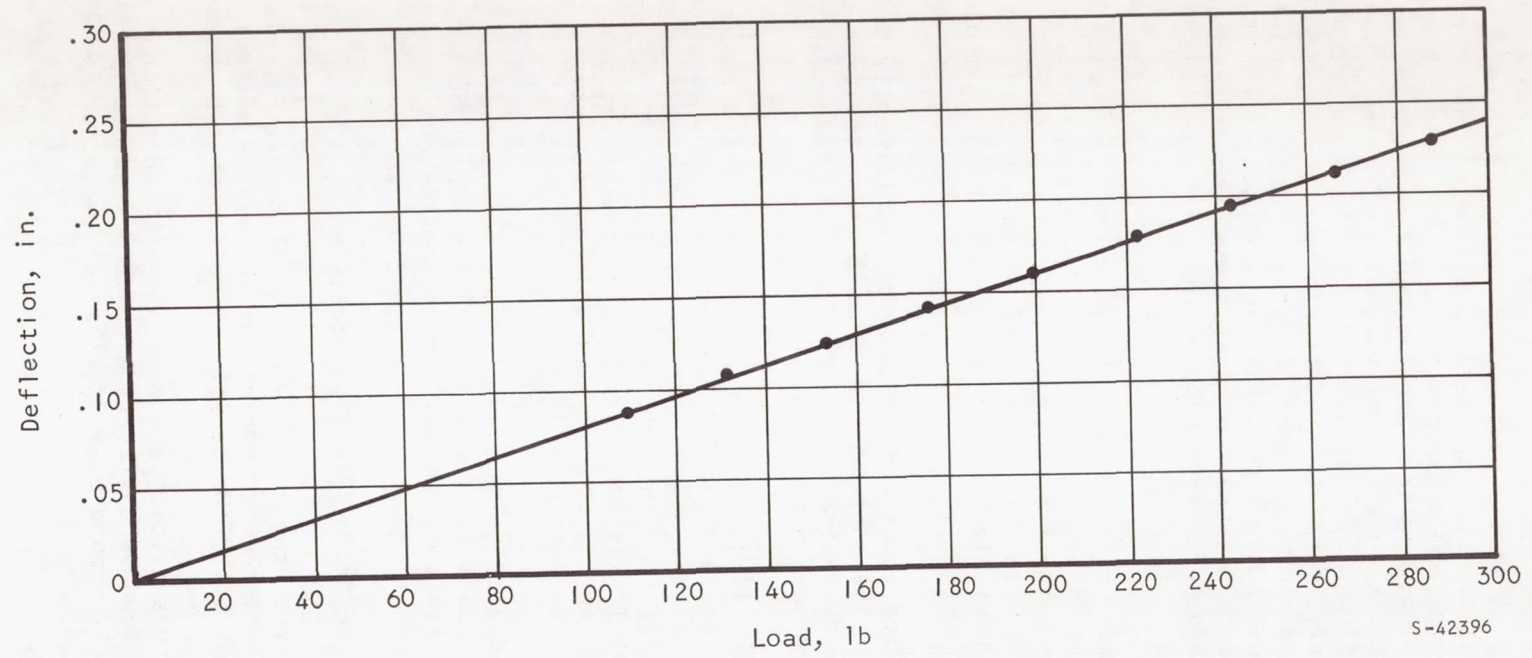


Figure 3-13. Beam Load Deflection

The test 2 data illustrate the general vibrational effect of the total system. The natural frequency of approximately 4 cps is discernable in all traces made during testing. The test 3 data show an interaction of several predominant frequencies. This test was run by impact loading on the suspended mass at the rate of approximately 90 beats per minute. The beam frequency is shown by the principal excursion, and the superimposed frequency of approximately 16 cps is apparently attributable to the panel vibration. The test 4 training, where a torsional force was slowly applied to rotate the beam, apparently is the result of the air pads only. In test 5, the primary frequency of the beam is again apparent with the superimposed panel vibration. Tests 6 and 7 show the vibrations due to the panel surface on which the air pads ride. Tests 8 and 9 show the effects of the main suspension cable when compared to tests 1 and 2. Test 10 indicates the natural frequency of the yoke, which is 9.5 cps under these test conditions.

The effect of the air pads on the natural frequency of the system is best illustrated by comparing tests 10 and 11. The effective spring constant with air to the pads decreases the natural frequency of the overall system. The vibration of the beam assembly with air to the pads is damped within 30 percent of the time required without air to the pads, thus indicating the air pad damping characteristics.

The tests with a controlled input did not provide significantly different data than the previous tests. The amplitude of the vibration in terms of load is demonstrated. These tests demonstrate that the load cell responds to vibrations as though the vibrations were a direct load change.

Comparison of tests 14 and 15 shows again the effects of the suspension cable. Tests 16 and 17 show the results of the effective spring constant of the beam on the resonance of the assembly. With the suspended mass at the right end (test 16), the natural frequency changed to 0.5 cps. This position of the suspended mass for test 17 was very close to the end of the beam, thus giving a much higher effective spring constant and raising the natural frequency.

Tests 18 and 19 were conducted to determine if the location of the load cell would produce a different output. Comparison of the amplitude and natural frequencies to similar tests with the load cell at the mass shows no significant change in data.

The conclusions that may be drawn from these tests are:

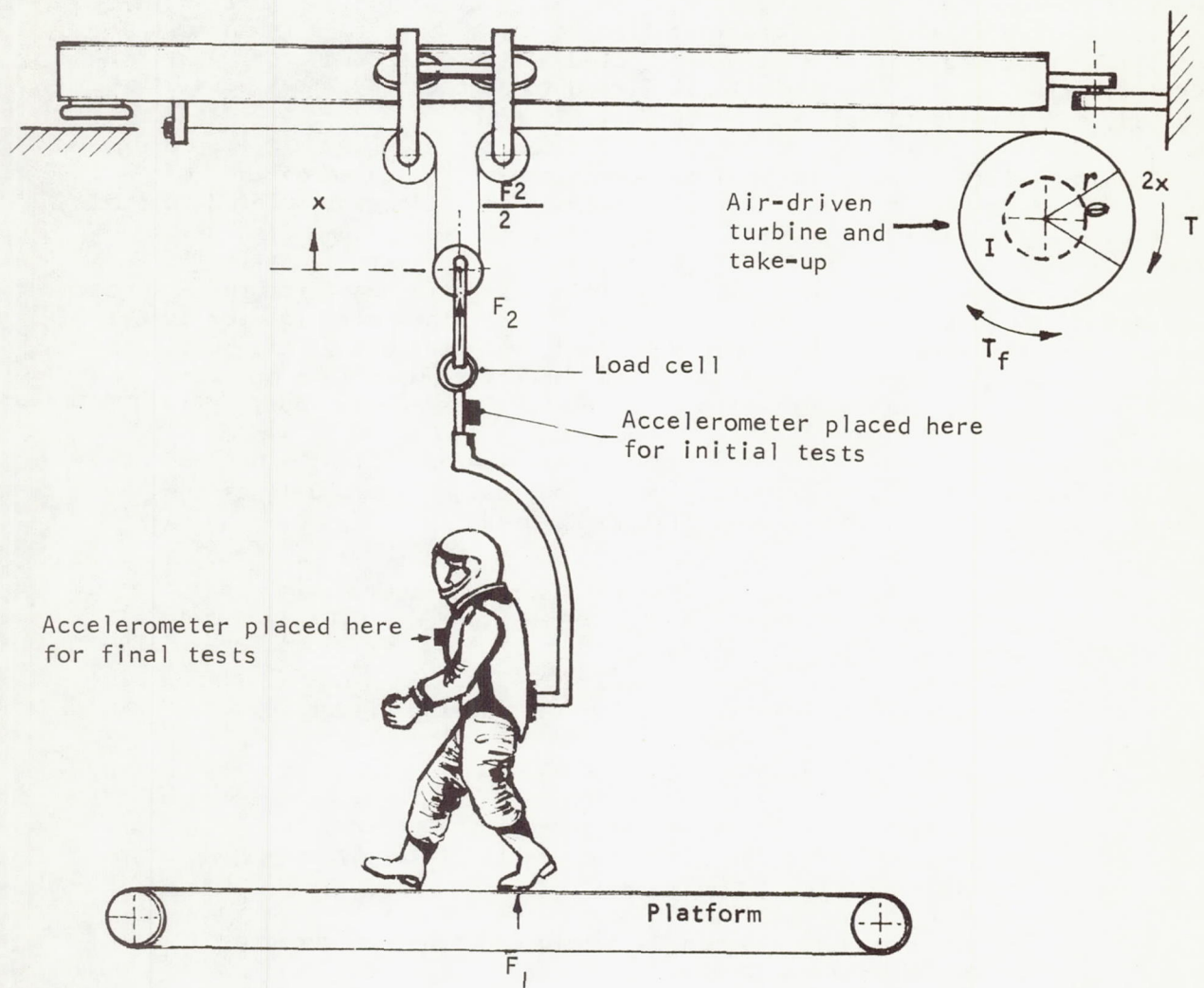
1. The natural frequency of the system would be difficult to raise by stiffening the beam or other components of the system without adding mass which might compromise the overall operation of the system.
2. The load cell is very sensitive and responsive to vibrational loads and shows an impact load as a vibration reading. However, the mean value of the load cell should be very close to the effective load.

Dynamic analysis of turbine-operated suspension system (TOSS). — Dynamic tests were conducted on the turbine-operated suspension system (TOSS) to evaluate the adequacy of the suspension system in simulating reduced gravity. These tests were conducted with the complete operable system used on the horizontal treadmill. Figure 3-14 is a schematic of the physical system. A test subject was dressed in a pressure suit and installed in the simulator as in normal tests. He performed jumping tests as directed by the test conductor. In additional free-fall tests, the subject was lifted to a height by a test assistant, released, and allowed to fall to the treadmill surface.

The initial tests were made using an accelerometer located on the "C" frame as shown in Figure 3-14 with a displacement potentiometer mounted on the air turbine cable take-up drum and a load cell in the main support cable. Because of difficulties in analyzing these results, the instrumentation was changed for the next series of tests. The instrumentation used for these tests consisted of an accelerometer mounted on the subject, the potentiometer on the take-up drum, the load cell, and special conductive materials on the boots and on the aluminum plate on the treadmill. The conductive materials provided more precise data for the computation of airborne times during tests.

Analytical equations (used in TOSS evaluation). — The analytical equations used in the evaluation of this system are given below, using Figure 3-14 as the physical system. The following nomenclature is used:

- F_1 = reactive force at the platform due to the subject's activity; F_1 varies from some maximum value to zero when the subject is airborne.
- $F_1(P)$ = reactive force effective during the jumping effort
- F_2 = force in the main suspension cable
- I = mass moment of inertia of the air-driven turbine, the take-up reel, and the cable components (total system inertia)
- T = torque, which is assumed to remain constant, produced by the air-driven turbine
- T_f = friction torque which always opposes the direction of motion of θ
- W = subject's total weight (force) and his attached harness
- g = gravitational acceleration
- h_1 = distance of the ascent
- h_2 = distance of the descent



S-42359

Figure 3-14. TOSS Simulator Schematic

- h_3 = distance through which the subject exerted F_1 prior to liftoff
 h_4 = calculated distance h_1 assuming perfect simulation, i.e., T_f and $I = 0$
 r = radius of the take-up reel, 12 in.
 t = time
 t_1 = time interval between liftoff from the platform and the subjects apogee
 t_2 = time interval between the subject's apogee and his touchdown on the platform
 t_3 = calculated time t_1 assuming a perfect simulation, i.e., T_f and $I = 0$
 u = denominator of the fractional gravity actually being simulated, i.e., where $g' = g/u$
 x = subject's vertical displacement
 $x(0)$ = reference point for the subject on platform
-
- $x(A)$ = subject's position when he is in his apogee
 \dot{x} = subject's velocity
 $\dot{x}_1(0)$ = subject's velocity just as he leaves the platform
 $\dot{x}_2(0)$ = subject's velocity just as he touches down on the platform
 \ddot{x} = subject's acceleration
 $\ddot{x}_1(0)$ = subject's acceleration at the instant he leaves the platform
 $\ddot{x}_2(0)$ = subject's acceleration at the instant he touches down on the platform
 $\ddot{x}_1(A)$ = subject's negative acceleration during his ascent from the platform
 $\ddot{x}_2(A)$ = subject's negative acceleration during his descent to the platform

θ = angular displacement in radians of the take-up reel due to a change in x ; $\dot{\theta}$ and $\ddot{\theta}$ will designate the velocity and acceleration of the reel

τ = total period of ascent and descent

Using the above symbols and Figure 3-26, the following relationships can be developed:

$F_2/2$ = force in the take-up reel cable due to mechanical advantage

$r\theta$ = $2x$

$\ddot{\theta}$ = $2\ddot{x}/r$

I = Wr_j^2/g

where

r_j = equivalent radius of gyration of the system

I = Σ (moments of inertia of suspension system)

I = $(5.4 + 3.58 + 0.56)$ lb-in.-sec² (turbine + reel + cable + pulley)

I = 9.54 lb-in.-sec²

$$T = F_2 r / 2$$

From inspection of the physical system, the following equations of motion apply:

$$I\ddot{\theta} = T \pm T_f - \frac{F_2 r}{2} \quad (3-1)$$

and

$$\frac{W}{g} \ddot{x} = F_1 + F_2 - W \quad (3-2)$$

so that when $\ddot{x} = 0$,

$$F_1 + F_2 = W \quad (3-3)$$

and when $\ddot{\theta} = 0$, $\dot{\theta} = 0$,

$$T = \frac{F_2 r}{2} \quad (3-4)$$

Substituting $\ddot{\theta} = 2\ddot{x}/r$ into Equation (3-1),

$$\frac{2I\ddot{x}}{r} = T \pm T_f - \frac{F_2 r}{2}$$

and

$$\ddot{x} = \frac{r}{2I} \left(T \pm T_f - \frac{F_2 r}{2} \right) \quad (3-5)$$

Solving Equation (3-2) for \ddot{x} and substituting in Equation (3-4) yields

$$\frac{g}{W} \left(F_1 + F_2 - W \right) = \frac{r}{2I} \left(T \pm T_f - \frac{F_2 r}{2} \right) \quad (3-6)$$

For any specific test, F_2 is determined by

$$F_2 = W - F_1 \quad [\text{transposition of Equation (3-3)}]$$

and u is determined by

$$u = \frac{W}{F_1 (\text{static})}$$

Using these two relationships and substituting into

$$\begin{aligned} T &= \frac{F_2 r}{2} \quad (\text{definition}) \\ T &= \frac{W}{2} \left(1 - \frac{1}{u} \right) r \frac{Wr}{2} \left(1 - \frac{1}{u} \right) \end{aligned} \quad (3-7)$$

or

$$T = \frac{Wr}{2} - \frac{Wr}{2u}$$

Using this value for T and solving Equations (3-2) and (3-5) to eliminate F_2 ,

$$\ddot{x} = \frac{\frac{g}{u} \left[\frac{u}{W} F_1 - 1 \right] \left[1 \pm \frac{2uT_f}{rW \left(\frac{u}{W} F_1 - 1 \right)} \right]}{1 + \frac{4Ig}{Wr^2}} \quad (3-8)$$

This equation is especially useful because it indicates the effect of quantities I and T_f on acceleration. For example, during ascent and descent, $F_1 = 0$, and

$$\ddot{x}_1(A) = \frac{-g}{u} \left[\frac{1 + \frac{2uT_f}{rW}}{1 + \frac{4Ig}{Wr^2}} \right] \quad (3-9)$$

and

$$\ddot{x}_2(A) = \frac{-g}{u} \left[\frac{1 - \frac{2uT_f}{rW}}{1 + \frac{4Ig}{Wr^2}} \right] \quad (3-10)$$

To complete the equations required in the analysis, the platform phase of each event must be developed. The work done by the subject during his lift-off effort is simply

$$\text{Work} = \int F_1 dx$$

At any height during his effort, his total energy is the sum of the kinetic and potential energies. Therefore, after equating work and total energy the expression becomes

$$\int_0^{h_3} F_1 dx = \frac{W}{2g} V_0^2 + \int_0^{h_3} (W - F_2) dh$$

Since W is not a function of h , and V_0^2 is $\dot{x}_1(0)$ (the velocity of W at distance h_3),

then

$$\frac{W}{2g} \dot{x}_2^2(0) = \int_0^{h_3} F_1 dh + \int_0^{h_3} F_2 dh - Wh_3 \quad (3-11)$$

Using Equations (3-2), (3-5), and (3-7), F_2 may be solved in terms of F_1 .

$$F_2 = \frac{2}{ri} \left(\frac{Wr}{2} - \frac{Wr}{2u} - T_f \right) - \frac{4IgF_1}{Wir^2} + \frac{4IgW}{Wir^2} \quad (3-12)$$

where

$$i = \text{the term } 1 + \frac{4Ig}{Wr^2}$$

Substituting this value into Equation (3-11) and combining and simplifying produces

$$\dot{x}_1(0)^2 \frac{W}{2g} = \frac{1}{i} \int_0^{h_3} F_1 dh - \frac{Wh_3}{u} - \frac{2T_f h_3}{r} \quad (3-13)$$

Since F_1 can be the only variable in this equation, certain values can be assigned to it, and a force function C_1 can be determined. Integrating and simplifying Equation (3-13), Equation (3-14) can be obtained.

$$\dot{x}_1(0) = \left\{ \frac{2gh_3}{ui} \left[C_1 \left(\frac{u}{W} F_1(P) - 1 \right) - \frac{2uT_f}{rW} \right] \right\}^{1/2} \quad (3-14)$$

where C_1 has the following values:

Force function or force profile	C_1
Constant force	1
Sine force	$2/\pi$
Ramp force	$1/2$

The maximum velocity obtained by the subject due to a jump effort equals that at the point of liftoff. Equation (3-7) may be solved for initial velocity $\dot{x}_1(0)$, which results in an ascent height of h_1 influenced by an acceleration of $\ddot{x}_1(A)$, i.e.,

$$\dot{x}_1(0) = \left(2h_1 \ddot{x}_1(A) \right)^{1/2}$$

Using the value of $\ddot{x}_1(A)$ from Equation (3-7) yields

$$\dot{x}_1(0) = \left[\frac{2gh_1}{ui} \left(1 + \frac{2uT_f}{rW} \right) \right]^{1/2} \quad (3-15)$$

Equating Equations (3-14) and (3-15) and solving for $F_1(P)$, Equation (3-16) results.

$$F_1(P) = \frac{W}{u} \left[\frac{2uT_f}{C_1 rW} \left(\frac{h_1}{h_3} + 1 \right) + \frac{1}{C_1} \left(\frac{h_1}{h_3} + C_1 \right) \right] \quad (3-16)$$

Assuming that T_f is equal during ascent and descent, but opposite in sign, Equations (3-7) and (3-8) may be solved for T_f and then combined giving

$$T_f = \frac{Wr}{2u} \left[\frac{\ddot{x}_1(A) - \ddot{x}_2(A)}{\ddot{x}_1(A) + \ddot{x}_2(A)} \right] \quad (3-17)$$

This can also be written by transposing as

$$T_f \frac{2u}{Wr} = \left[\frac{\ddot{X}_1(A) - \ddot{X}_2(A)}{\ddot{X}_1(A) + \ddot{X}_2(A)} \right] \quad (3-17a)$$

These equations are referred to by number in the comparative analyses given below.

The data from initial tests using the instrumentation previously described were reduced and are summarized in Table 3-3. The inability to determine accurately the total airborne time affected the quality of the reduced data. This limitation is illustrated by the large variation in the friction torque (T_f column, Table 3-3). Unless the defining parameters for TOSS operate randomly, the friction torque, T_f , would be expected to show less variation. For events 1 to 7, Figure 3-15, the scatter is much less than that shown for events 8 to 15, Figure 3-16. It is explained that events 1 to 7 resulted from the subjects vigorous jumping, while for events 8 through 15 the subject exerted minimal energy. The former test produced data that were more easily resolved than data from the last test. A tentative conclusion was reached, however, speculating that TOSS yielded data that were within 12 percent of data expected from the system. Since further analysis using these data would yield no further improvements, the second test sequence was planned.

The difficulty in determining the total airborne time was rectified by covering the soles and heels of the boots with a conductive material. The subject executing his jumps from an aluminum plate placed on the treadmill provided a method for determining his position — airborne or in contact with the ground. This provision enabled a more precise interpretation of the data and permitted a more analytical approach.

To evaluate system performance, it should be demonstrated whether (1) the system simulates a reduced gravity; (2) this fractional gravity is constant; (3) the acceleration extant during an ascent equals that during the descent. Data from the experiments run initially did not directly answer these questions. This became a primary objective during the final experimental tests conducted.

The first two questions are answered by an analysis of five free-fall events. (Raw data for free-fall test events 4 and 5 are reproduced in Figures 3-17 and 3-18.) For these tests, an assistant held the subject as far off the platform as the pulley/cable assembly would allow; then the subject was released and the data were recorded by an Offner recorder. The acceleration extant during the subject's fall was calculated by five independent methods and are presented in Table 3-4. The calculated mean and standard deviation are $\bar{X} = 26.3 \text{ in./sec}^2$ and $\sigma = 2.95 \text{ in./sec}^2$.

TABLE 3-3

SUMMARY OF TOSS SIMULATOR TEST DATA

Event No.	Airborne Period T , sec	Velocity in./sec		Distance, in.			Ascent Time t_1 , sec	Descent Time t_2 , sec	Friction Torque T_f , in. lbs	Reactive Force F_1 (P), lb	Ascent Time t_3 , sec	Distance h_4 , in.
		$\dot{x}_1(0)$	$\dot{x}_2(0)$	h_1	h_2	h_3						
1	0.840	20.3	14.8	4.20	4.20	2.60	0.354	0.486	88.4	138	0.373	4.88
2	0.800	23.5	19.0	3.60	4.70	2.93	0.306	0.494	96.2	154	0.429	6.45
3	0.800	23.1	18.2	4.13	4.13	3.06	0.369	0.431	45.1	126	0.377	4.97
4	0.720	21.0	19.7	3.40	4.00	3.06	0.319	0.401	42.0	124	0.370	4.82
5	0.813	22.9	16.0	4.26	3.60	3.33	0.368	0.445	77.1	136	0.416	6.09
6	0.880	21.6	18.6	4.00	5.06	3.33	0.354	0.526	76.7	127	0.396	5.51
7	0.854	22.6	15.1	5.06	4.13	2.20	0.391	0.463	80.3	172	0.402	5.67
8	0.530	11.5	8.78	1.53	1.08	0.375	0.274	0.256	23.3	212	0.245	1.67
9	0.526	12.5	6.86	1.81	0.796	0.890	0.291	0.235	44.1	130	0.274	2.09
10	0.546	11.4	8.52	1.59	1.17	0.500	0.276	0.270	31.0	169	0.245	1.67
11	0.560	9.14	4.98	1.53	0.718	0.469	0.313	0.247	42.5	131	0.200	1.11
12	0.560	14.8	6.94	1.83	1.12	0.610	0.244	0.316	108	229	0.327	2.98
13	0.526	11.5	6.70	1.36	1.12	0.281	0.220	0.306	94.2	281	0.250	1.75
14	0.533	13.4	6.18	1.56	0.937	0.437	0.232	0.301	110	255	0.295	2.42
15	0.500	13.9	4.46	1.59	0.703	0.406	0.218	0.282	138	291	0.307	2.63

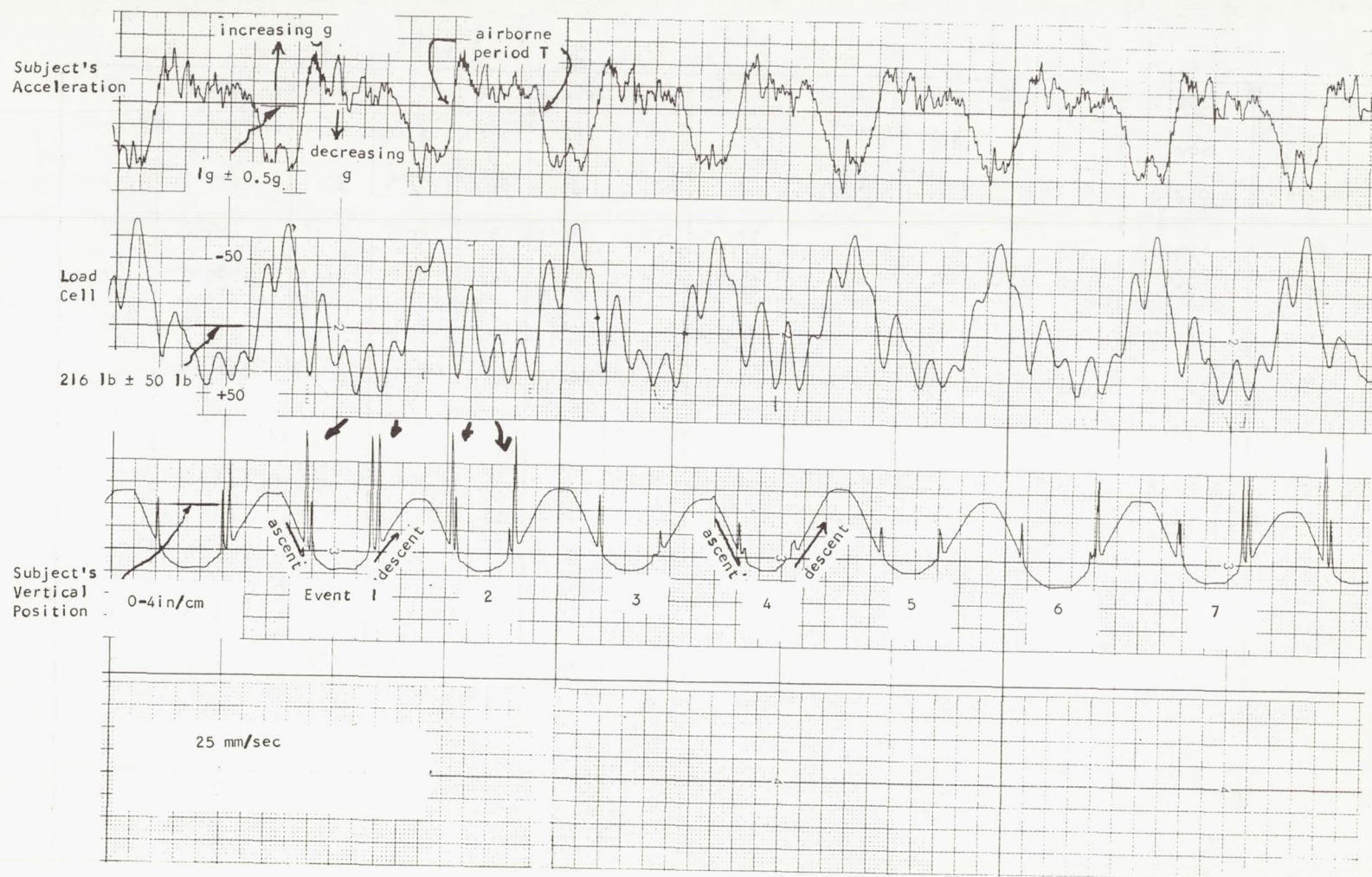


Figure 3-15. Recorded Data for Events 1 Through 7 (from First Day)

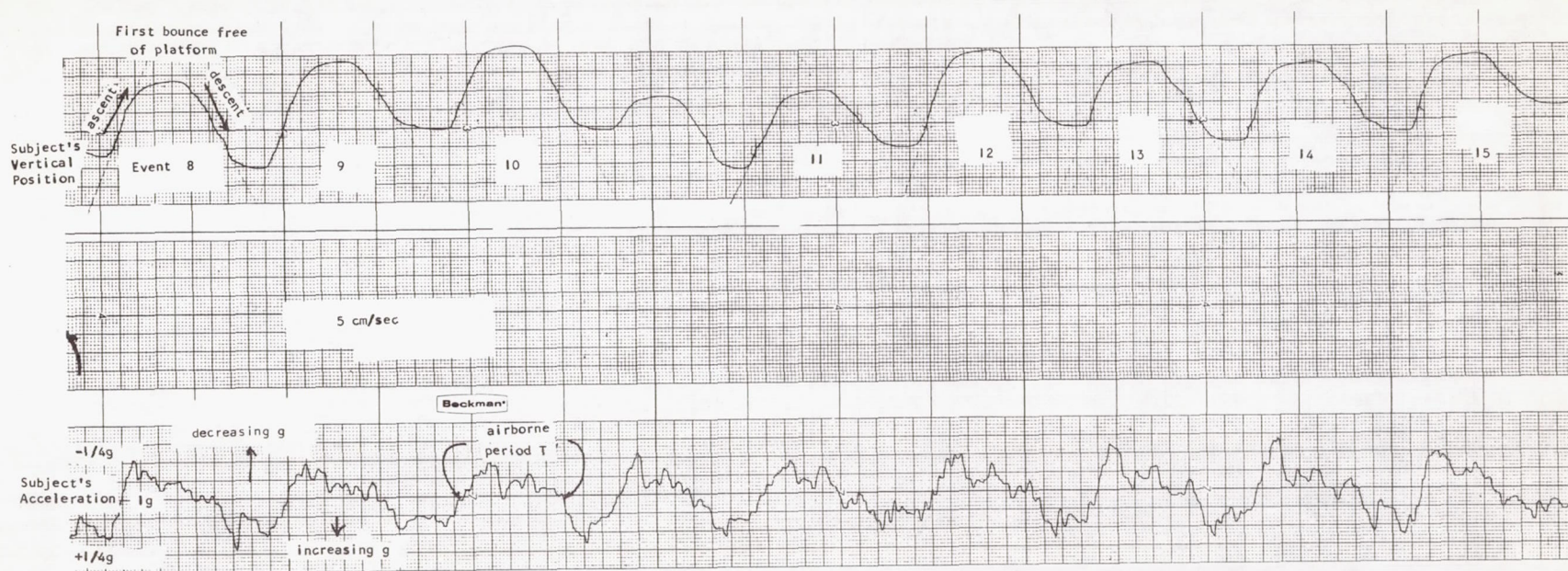


Figure 3-16. Recorded Data for Events 8 Through 15 (from Second Day)

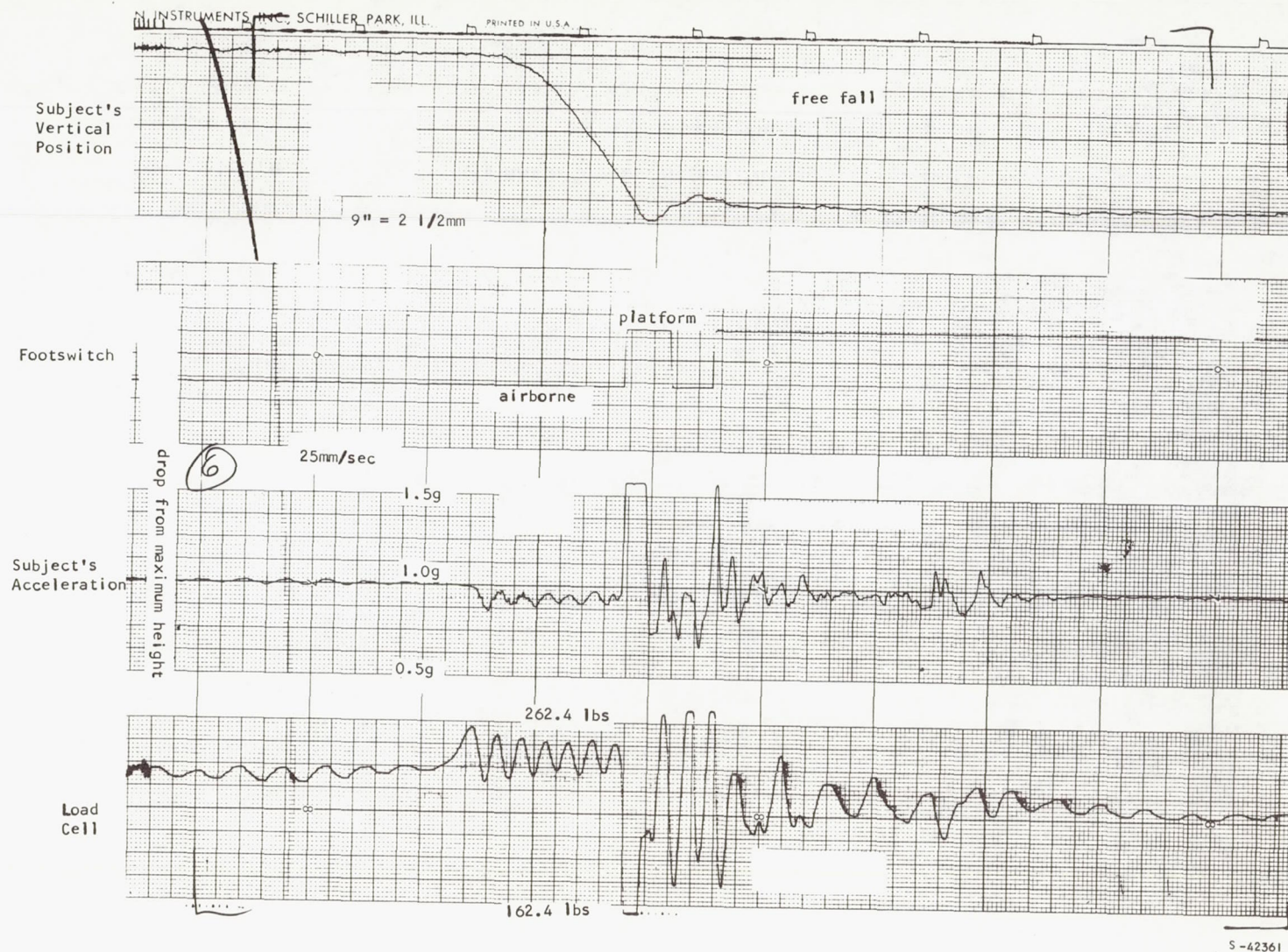


Figure 3-17. Dynamic Test Traces (Free-Fall Event 4)

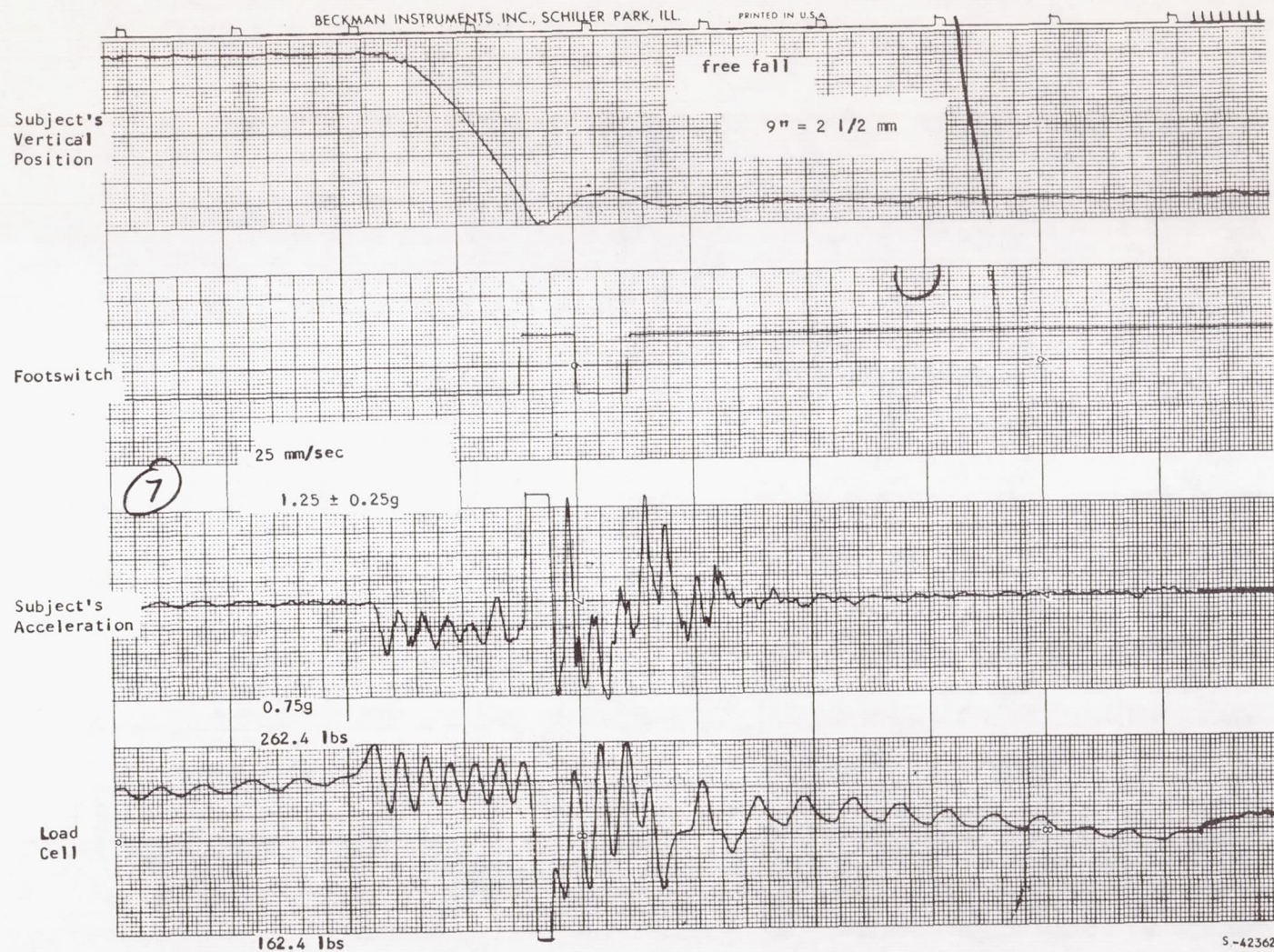


Figure 3-18. Dynamic Test Traces (Free-Fall Event 5)

TABLE 3-4

ACCELERATION DURING FREE FALL

Event	a_1 $a_1 = -\frac{2s}{t^2}$	a_2 $a_2 = -\frac{v}{t}$	a_3 $a_3 = -\frac{v^2}{2s}$	a_4 $a_4 = \frac{g}{w} (0 + F_2 - w)$	a_5 from accelero- meter trace
1	28.2 in/sec ²	26.3 in/sec ²	24.9 in/sec ²	30.4 in/sec ²	27.0 in/sec ²
2	21.1 in/sec ²	22.8 in/sec ²	24.8 in/sec ²	29.4 in/sec ²	24.1 in/sec ²
3	29.1 in/sec ²	25.0 in/sec ²	21.5 in/sec ²	29.4 in/sec ²	27.8 in/sec ²
4	25.4 in/sec ²	24.4 in/sec ²	23.4 in/sec ²	34.1 in/sec ²	26.0 in/sec ²
5	27.2 in/sec ²	25.2 in/sec ²	23.4 in/sec ²	29.4 in/sec ²	27.0 in/sec ²

To test whether the recorded fall actually is modeled by the simple expression, $s = 1/2 at^2$, the trace from free fall event 4 was expanded by plotting it on separate graph paper as shown in Figure 3-19. The simultaneous plotting of recorded and calculated position-time points indicates that the calculated acceleration is constant through the fall. Initially, after the subject is released, there is a discrepancy between recorded and calculated data; however, this may be caused by resonant oscillation set up in the beam at that point in time.

Examination of the jumping traces answers the third question. The acceleration acting during ascent and descent is not equal. This may be calculated simply by assuming that the friction torque is constant but of opposite sign during ascent and descent. For example, assume $u = 6$, $w = 262.4$ lb, and $T_f = 75$ in-lb. After inserting these values into Equations (3-9) and (3-10), they yield

$$\ddot{x}_1(A) = -59.5 \text{ in/sec}^2$$

$$\ddot{x}_2(A) = -33.0 \text{ in/sec}^2$$

Only if I and T_f are equal to zero will $\ddot{x}_1(A)$ and $\ddot{x}_2(A)$ be equal to $-g/u$.

The dynamic analysis of the jumping events performed on the TOSS simulator includes two separate phases. The first and most easily handled involves that portion of the event during which the subject is airborne. During this time the recorded data are readily reducible and verify the model equations within the limits of one's ability to resolve the recorded traces. Quantification of the events occurring during the period when the subject is in contact with the platform requires a different analytical approach.

As the subject effects his touchdown, completing the jump event, and prepares for another jump, the force transducer located in the suspension cable is subjected to two resonant impulses generated by the support beam. Examination of the load cell trace indicates that the resonant frequency of the beam-suspension system, approximately 4.8 cps, persists throughout the jumping event once the jump itself is completed. The transition from touchdown to lift-off interrupts the period of vibration in many of the events. This break in the resonant oscillation of the beam coincides with the subject's thrust from the jump position. This is especially true of run 7 during which the subject exerted his maximum efforts. Attempts to deduce the lift-off force from the load cell trace were abandoned in favor of a more general analysis in which three lift-off force profiles were compared. Their effects on the equivalent $1/6$ -g airborne time were then determined.

The two previous TOSS analyses relied on fitting measurements taken from the recording traces into the analytical expressions developed from the modeling of the system. For example, two essential parameters that must be determined are the acceleration acting during ascent and descent, respectively denoted $\ddot{x}_1(A)$ and $\ddot{x}_2(A)$. Since the airborne period, the ascent height and the descent distance are the most precise measurements available from the traces; these parameters were used with equations that would yield $\ddot{x}_1(A)$ and $\ddot{x}_2(A)$.

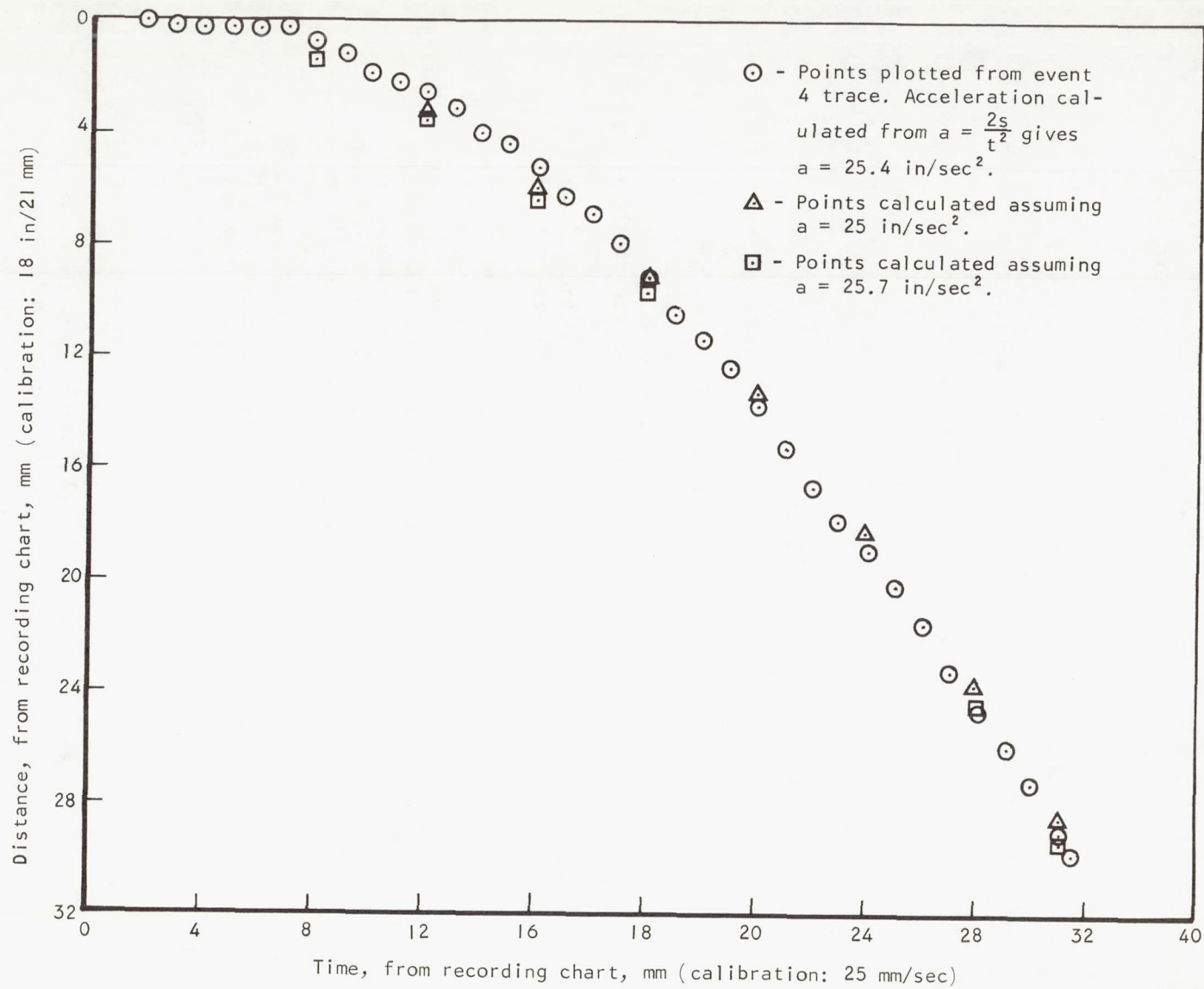


Figure 3-19. Comparison of Recorded and Calculated Position - Time Points

S-42712

If the system acts consistently from event to event, the acceleration values should be identical. Although many of the calculated values for $\ddot{x}_1(A)$ and $\ddot{x}_2(A)$ compared favorably, some did not.

For example, events 1 and 8, run 7 (Figure 3-20), fit these two extremes. Calculated acceleration for event 1, 58.7 in/sec² and 27.0 in/sec², fit the data within the limits of interpretative error. Figure 3-21 presents the trajectories recorded and calculated using these acceleration values for event 1. In contrast to event 1 is event 8 in which the calculated $x_1(A)$ value was 51.3 in/sec². The question to be answered was the following. Were the differences in calculated acceleration values real or were they due to simple resolution errors originating in the data reduction?

To determine whether the accelerations $x_1(A)$ and $x_2(A)$ were consistent from event to event, another approach was applied to run 5 (Figure 3-22) in which the discrepancies among $x_1(A)$ values were greater than those from run 7. Precise enlargement of the four displacement traces for events 1, 2, 4, and 9 were made, and examples of those negatives (as shown in Figure 3-23) were compared with acceleration curves plotted to the same scale (Figures 3-24 and 3-25). Except for discrepancies due to the beam deflections, the four displacement profiles are superimposable. Best fit values for $\ddot{x}_1(A)$ and $\ddot{x}_2(A)$ are 56.0 and 33.5 in/sec², respectively. The $\ddot{x}_1(A)$ values calculated for events 1, 2, 4, and 9 are listed in Table 3-5.

If the acceleration values determined with the aid of photographis enlargement are representative of the true $\ddot{x}_1(A)$ and $\ddot{x}_2(A)$ acting during the entire run, then calculated airborne time should compare favorably with the measured times. Tables 3-6 and 3-7 present these data. The calculated period was obtained from the equation in which h_1 and h_2 are the measured ascent and descent distances. For run 7, Table 3-7 gives the comparison.

$$\tau = \left(\frac{2h_1}{\ddot{x}_1(A)} \right)^{\frac{1}{2}} + \left(\frac{2h_2}{\ddot{x}_2(A)} \right)^{\frac{1}{2}}$$

TABLE 3-5
CALCULATED ACCELERATION VALUES

Event	$\ddot{x}_1(A)$, in/sec ²
1	56.2
2	58.1
4	40.1
9	56.4

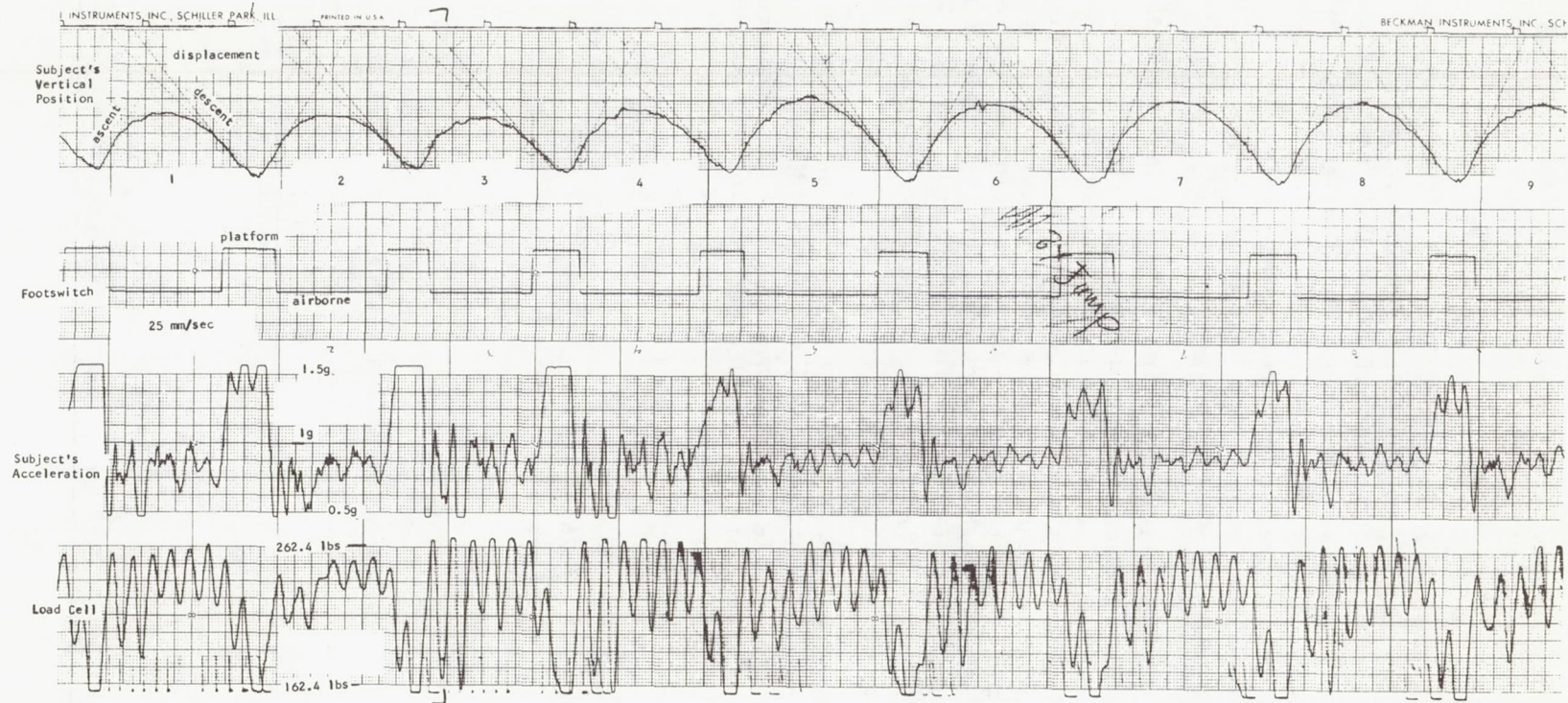


Figure 3-20. Dynamic Test Traces (Run 7)

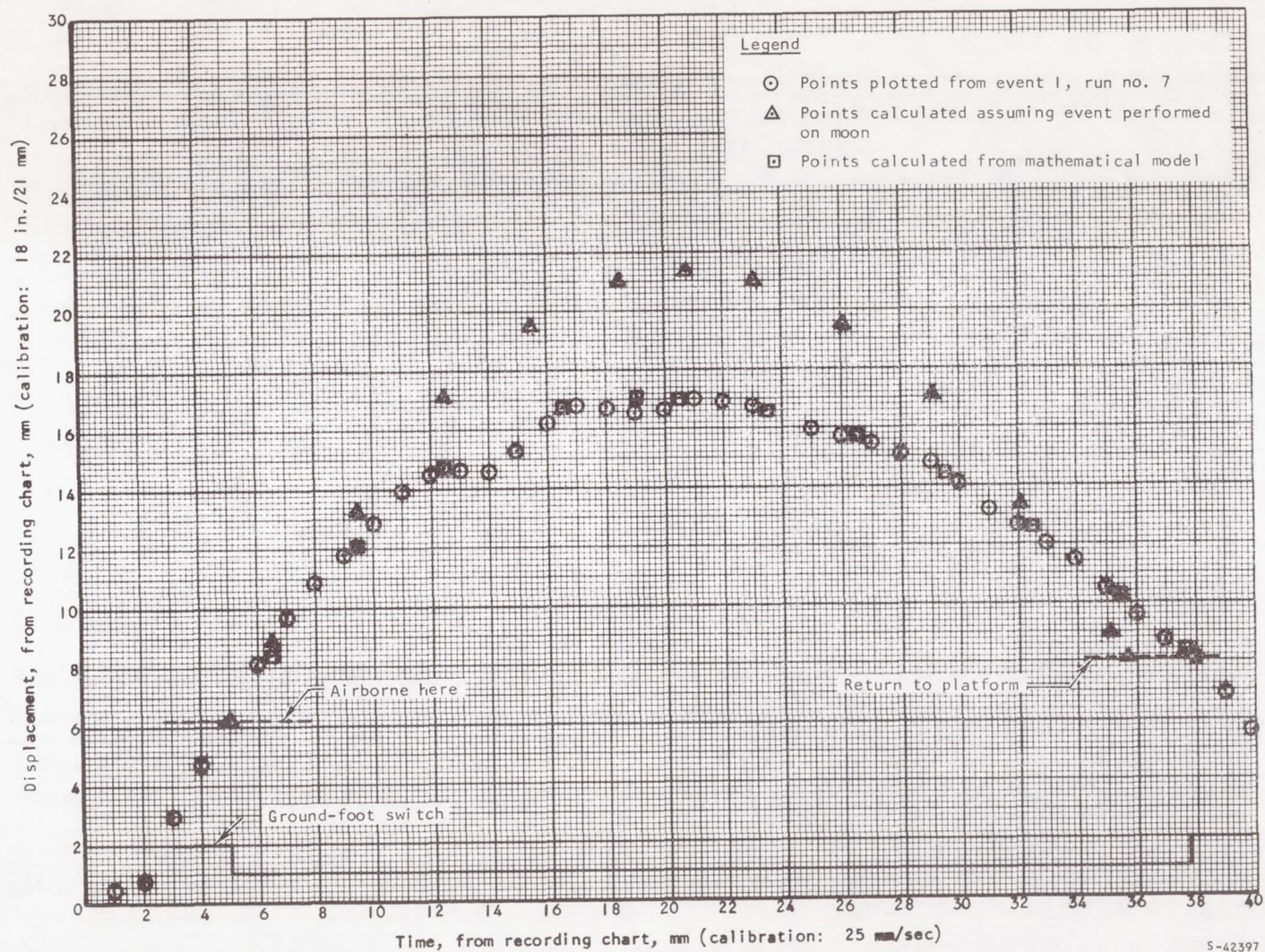


Figure 3-21. Comparison of Computed and Actual Displacements

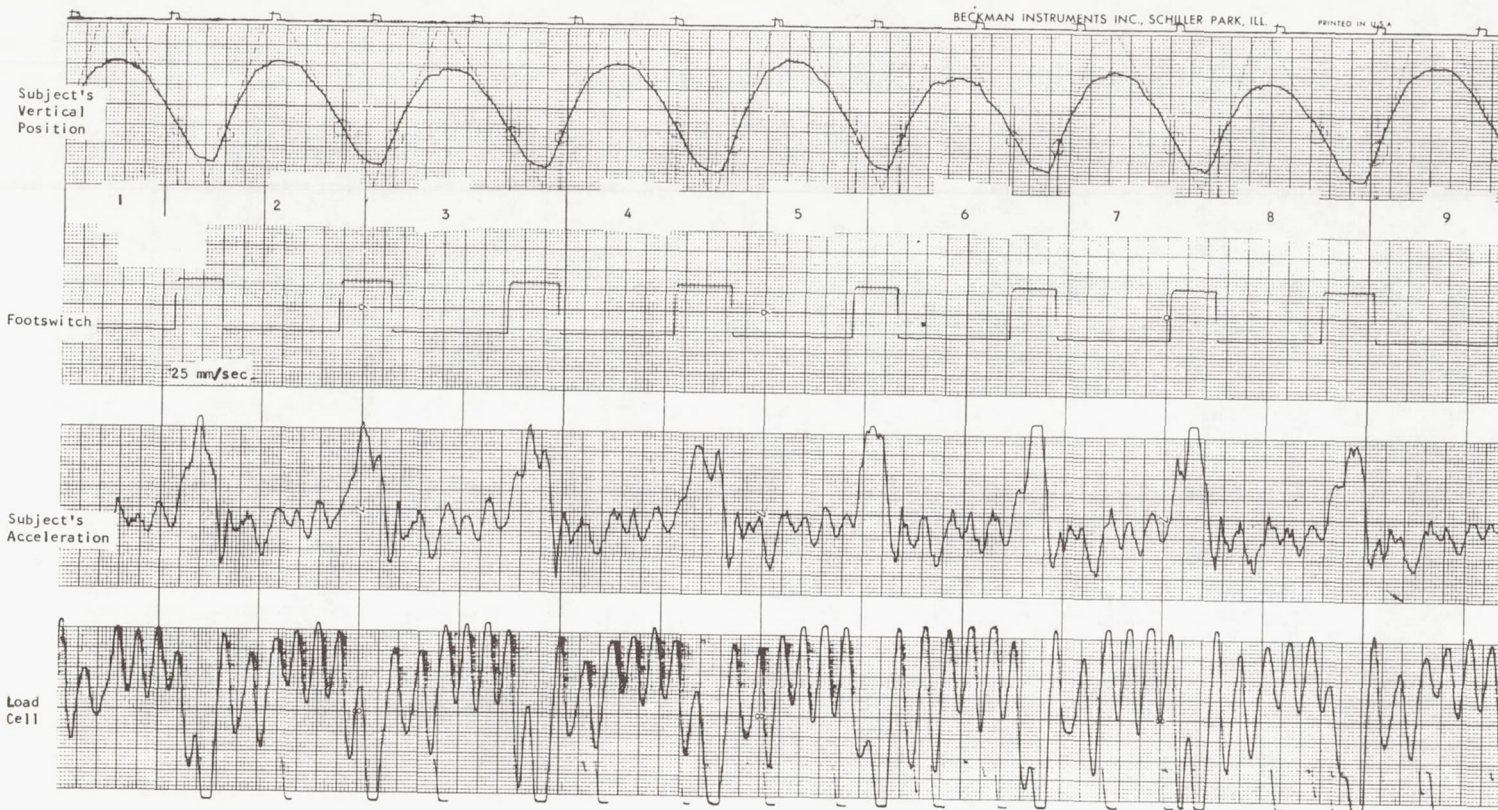


Figure 3-22. Dynamic Test Traces (Run 5)

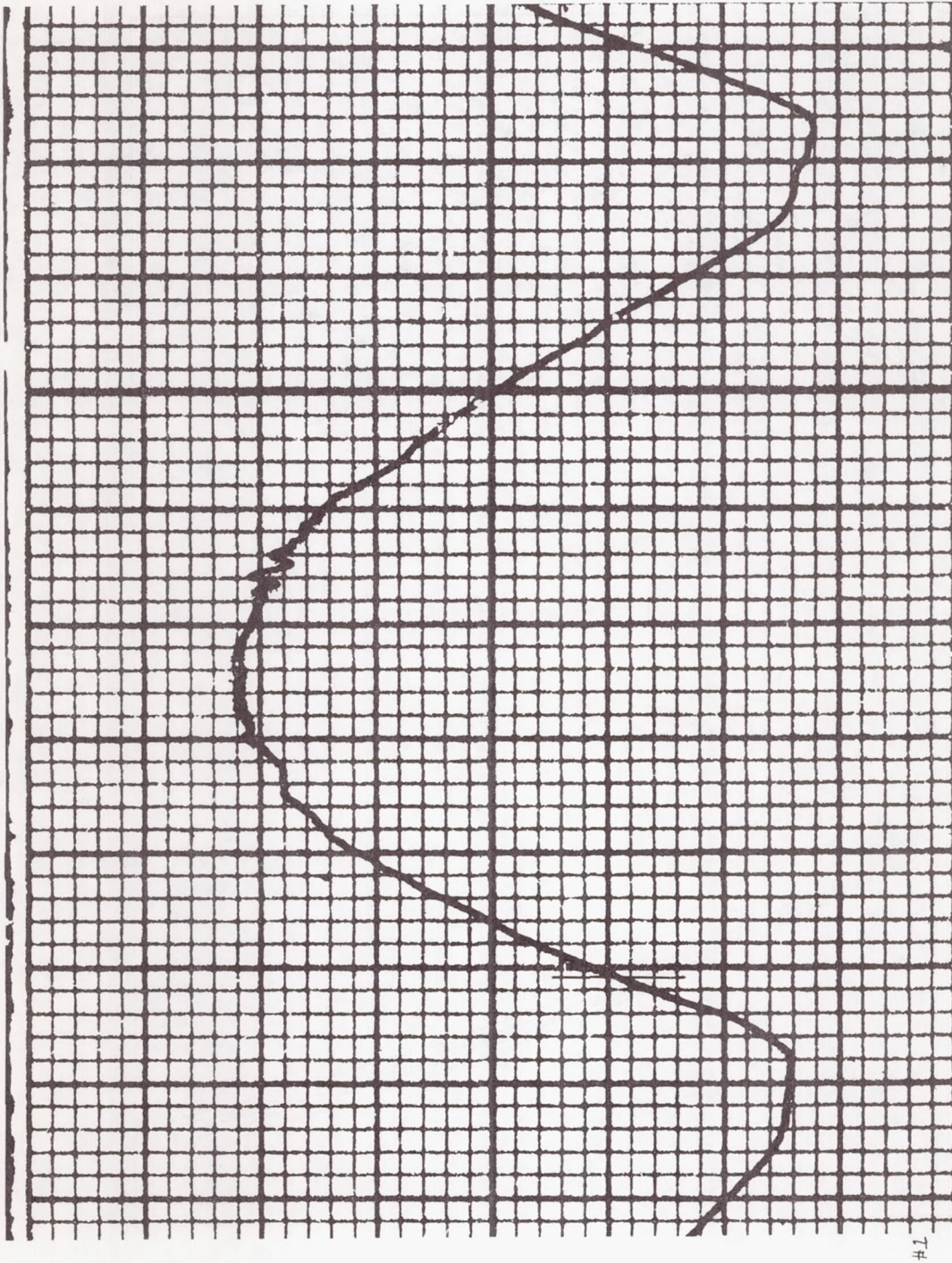
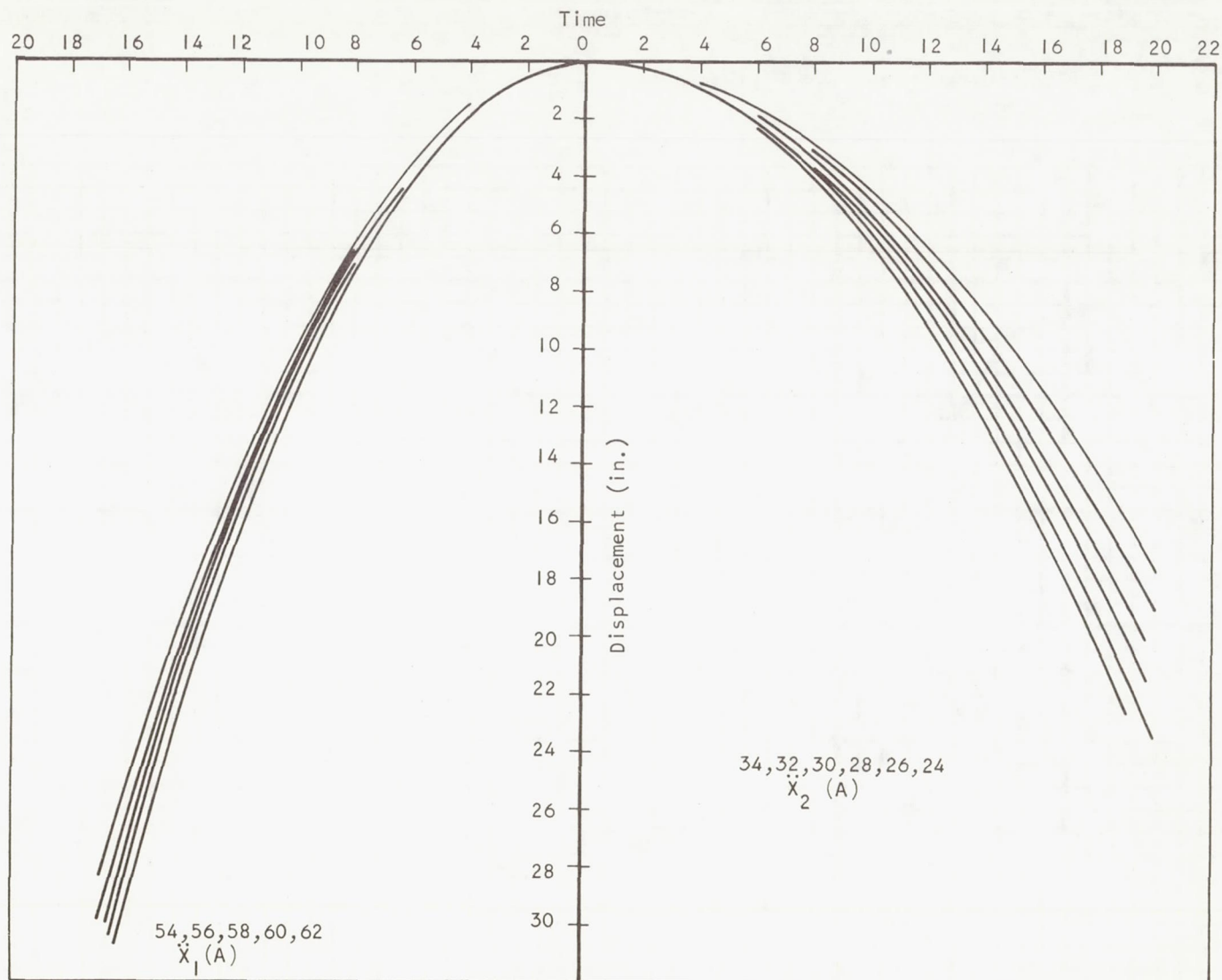
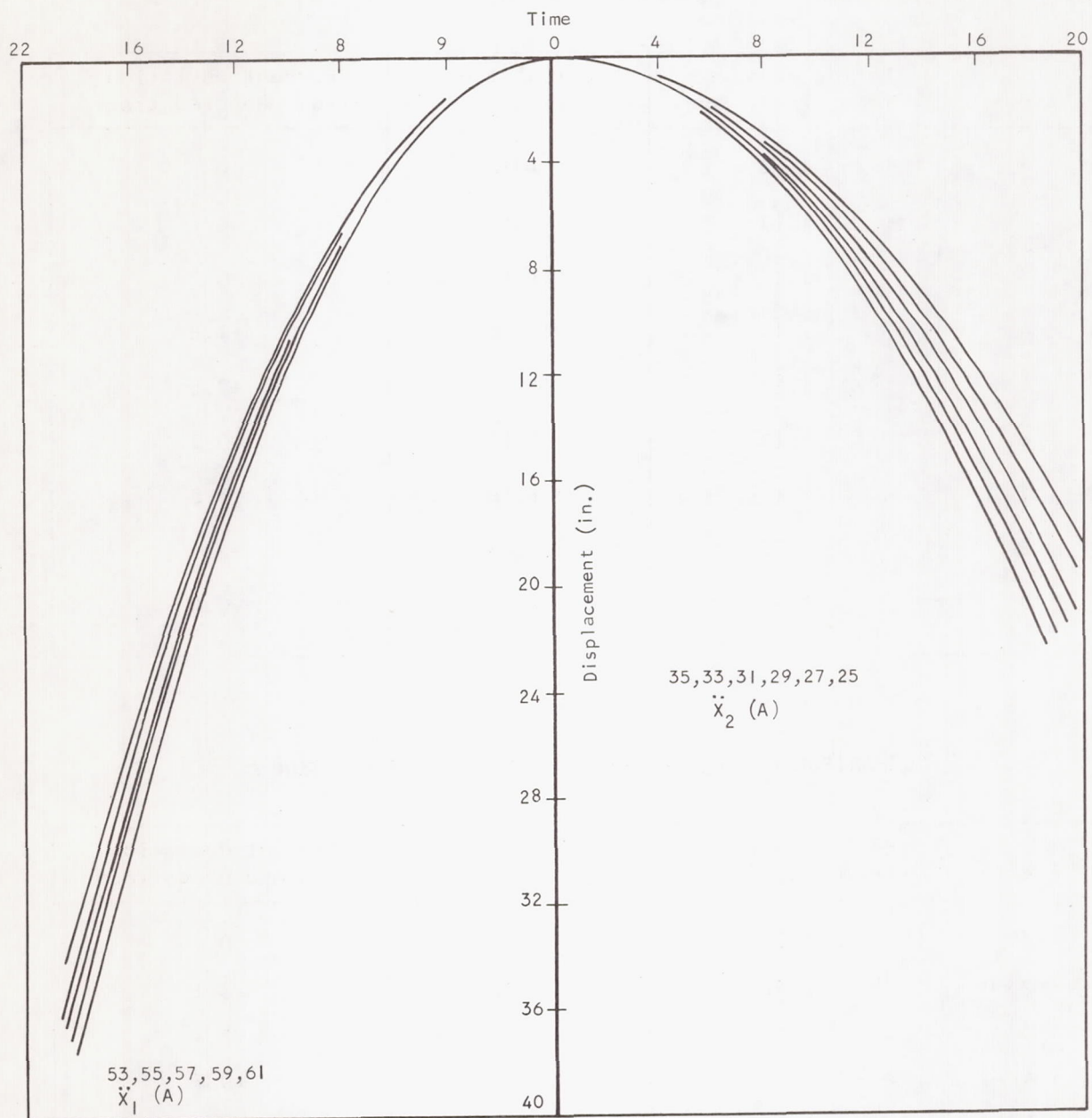


Figure 3-23. Enlargement of One Displacement Recording



S-42709

Figure 3-24. Composite of Plotted Acceleration Curves for Even Values



S-42710

Figure 3-25. Composite of Plotted Acceleration Curves for Odd Values

TABLE 3-6

COMPARISON OF CALCULATED AND MEASURED TIMES, RUN 5

Event	Period measured from trace, sec	Calculated period, sec	Percent deviation from measured trace
1	1.14	1.14	0
2	1.17	1.17	0
3	1.17	1.17	0
4	1.14	1.16	+1.8
5	1.21	1.24	+2.5
6	1.12	1.11	-0.9
7	1.14	1.18	+3.5
8	1.05	1.08	+2.9
9	1.24	1.25	+0.8

TABLE 3-7

COMPARISON OF CALCULATED AND MEASURED TIMES, RUN 7

Event	Period measured from trace, sec	Calculated period, sec	Percent deviation from measured trace
1	1.32	1.32	0
2	1.31	1.27	-3.1
3	1.21	1.24	+2.4
4	1.40	1.41	+0.7
5	1.56	1.61	+3.2
6	1.53	1.54	+0.7
7	1.57	1.60	+1.9
8	1.55	1.62	+4.5
9	1.58	1.57	-0.6

From the foregoing analysis the following is deduced:

1. The system can be described by simple Newtonian mechanics during ascent and descent.
2. Within any one run during which a subject is performing repeated and nearly identical jumps, i.e., the heights attained are approximately equal, the ascent and descent accelerations remain constant.
3. When one run is compared to another, the acceleration values are not necessarily equal.

In regards to item 3 above, Equation 3-8 is repeated below.

$$\ddot{x} = \frac{g}{u} \frac{\left[\frac{u}{W} F_I - I \right] \left[1 \pm \frac{2uT_f}{rW \frac{u}{W} F_I - I} \right]}{1 + \frac{4Ig}{Wr^2}} \quad (3-8)$$

During ascent and descent, F_I is zero and the following equations apply:

$$\ddot{x}_1(A) = -\frac{g}{u} \left[\frac{\frac{2uT_f}{rW}}{1 + \frac{4Ig}{Wr^2}} \right] \quad (3-9)$$

$$\ddot{x}_2(A) = -\frac{g}{u} \left[\frac{1 - \frac{2uT_f}{rW}}{1 + \frac{4Ig}{Wr^2}} \right] \quad (3-10)$$

In the above equations, parameters \ddot{x} , u , T_f , and I must be examined.

The moment of inertia, I , is constant and is accurate only if the value for each system component has been carefully calculated. The values measured for the turbine, reel, and cable plus pulley assembly were 5.4, 3.58, and 0.56 lb-in-sec², respectively. If T_f and u are known then \ddot{x} is fixed. But T_f is not known, and u is extremely sensitive to changes in the torque produced by the turbine. For example, if the subject, harness, and space suit weigh 262.4 lb, the load cell should read 5/6 by 262.4, or 219 lb. During any test period, while the subject is standing erect, the load cell trace will vary by approximately ± 10 lb. This value is predicted by Equation (3-14). If the subject's velocity, \dot{x} , is low enough, it may be taken as equal to zero. For this condition Equation (3-14) yields

$$\frac{u}{W} F_I(p) - I = \frac{2uT_f}{rW}$$

Since T_f takes plus and minus values,

$$F_I(p) = \frac{W}{u} \left(1 \pm \frac{2uT_f}{rW} \right)$$

$$F_I(p) = \frac{W}{u} \pm \frac{2T_f}{r}$$

Assume T_f equals ± 72 in/lb,

$$F_I(p) = \frac{W}{u} \pm 12 \text{ lb}$$

With respect to w/u , the variation is approximately ± 25 percent. The explanation here is that effective torque is the sum of developed torque, T , and friction torque, T_f .

Depending on the take-up reel's direction of rotation, the effective torque is either $T + T_f$ or $T - T_f$. Only if the subject stands quietly and the turbine torque is slowly increased and set from one direction is the reading reliable. With careful attention to this procedure, the value of u will be known within ± 4 percent, i.e., u will lie between 6.0 and 6.5. The variation of T_f during any one event is not known. For the purposes of this analysis, T_f is considered constant during the entire jump and subsequent ascent. Friction torque is considered to be equal but of opposite sign during the descent and energy absorption phase. That the turbine's torque is not constant but rather varies with impeller rpm is known. Hence the more rapid the lift-off event, the less torque developed by the turbine. The effect here is to make the system look like the friction torque increases.

Also to be considered is the ratio of $\ddot{X}_1(A)$ to $\ddot{X}_2(A)$ and values of T_f . Assume T_f is equal but of opposite sign during ascent and descent. Using Equations (3-9) and (3-10) to find the ratio of $\ddot{X}_1(A)$ to $\ddot{X}_2(A)$ yields

$$\frac{\ddot{X}_1(A)}{\ddot{X}_2(A)} = \frac{1 + \frac{2wT_f}{rw}}{1 - \frac{2wT_f}{rw}}$$

Assuming u equals 6.0, and taking the measured values of r and W , 12 in. and 262.4 lb, respectively, a graph of the acceleration ratio as a function of T_f may be plotted. Figure 3-26 presents the resulting curve. The acceleration ratio is seen to be quite sensitive to changes in T_f . Consider the following:

Assumed value of T_f (in. - lb)	Approximate value for $\ddot{X}_1(A)/\ddot{X}_2(A)$	Value deducted from recording traces
64	1.65	1.67 (run 5)
89	2.025	2.15 (run 7)

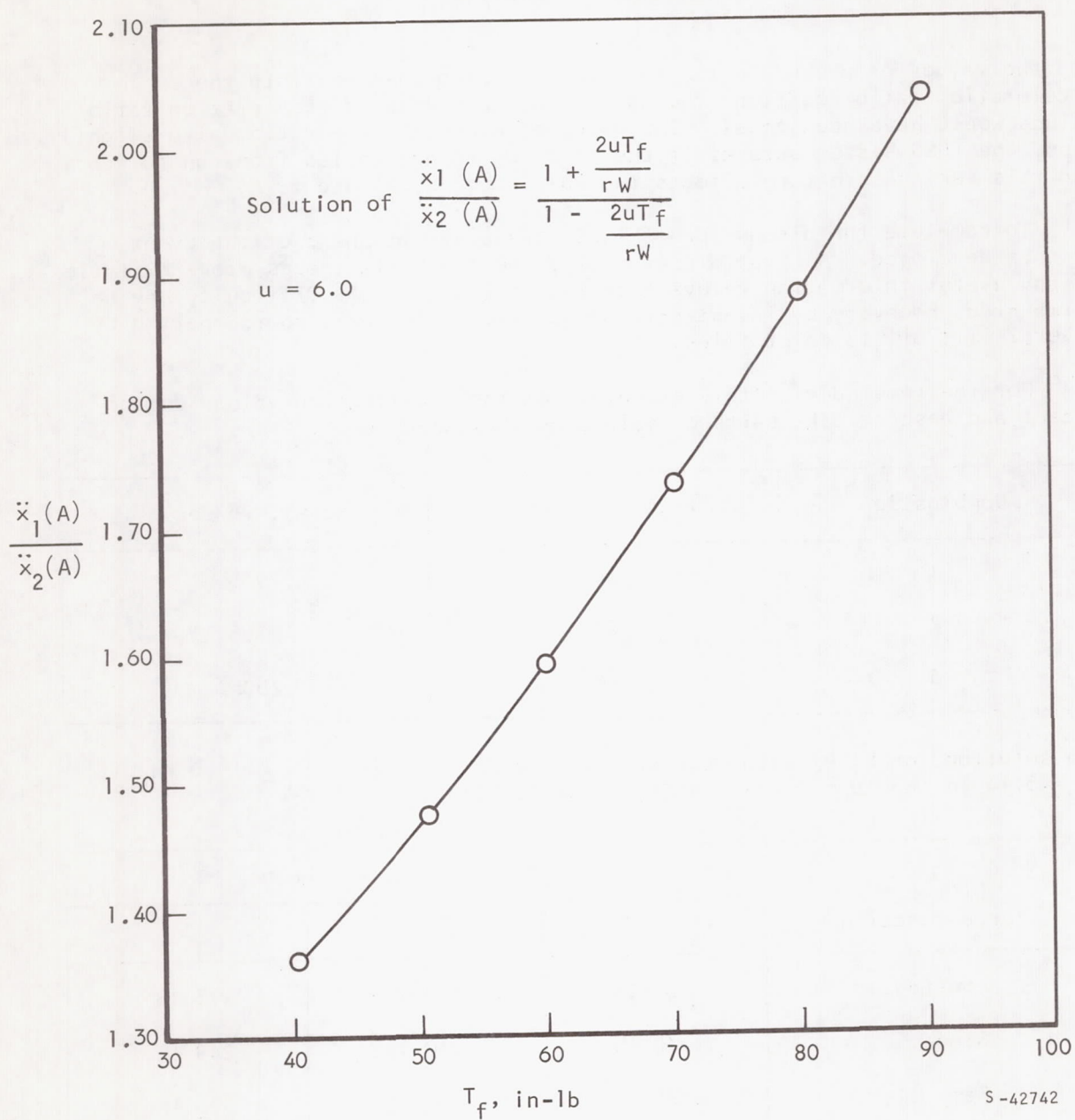


Figure 3-26. Acceleration Ratio as a Function of Friction Torque, T_f

Had the values of u used in the calculations been inserted into the acceleration ratio equation, the approximate and deduced acceleration ratio values would have been equal. The value of u affects the ratio value slightly. Thus, the TOSS system acts as if the friction torque varies from run to run and this variance in turn affects the values for $\ddot{x}_1(A)$ and $\ddot{x}_2(A)$.

To complete the discussion of TOSS, the platform phase of the event must be developed. As stated previously, the load cell traces provide little if any useful information relevant to the analysis. This difficulty may be surmounted, however, by investigating the effects on the airborne period by several lift-off force profiles.

For the remainder of this example, let the acceleration values during ascent and descent take pairs of values as indicated below.

Combination	$\ddot{x}_1(A)$, in/sec ²	$\ddot{x}_2(A)$, in/sec ²
1	56	29.5
2	58	27.5
3	60	25.5

The solution for $F_1(P)$ using the data from event 4, run 7 ($h_1 = 10.5$ in, $h_3 = 5.14$ in, and $u = 6.48$) yields the table below.

Lift-off force function	$F_1(P)$, combination number		
	1	2	3
Constant	161 lb	167 lb	173 lb
Sine	230 lb	240 lb	248 lb
Ramp	282 lb	294 lb	305 lb

When airborne times are calculated using these $F_1(P)$ values, assuming perfect simulation at $1/6$ g and equal ascent and descent distances, the data in the table below results.

Combination	Airborne time on moon			Airborne TOSS time, sec if $h_1 = h_2$	Percent deviation from moon time
	Constant force, sec	Sine force, sec	Ramp force, sec		
1	1.31	1.31	1.32	1.47	12
2	1.34	1.35	1.35	1.48	10
3	1.38	1.38	1.38	1.50	9

Thus, with respect to jumping events, it is expected that the TOSS system will yield airborne times approximately 10 percent greater than those that would result had the simulation been perfect.

Using Equations (3-9) and (3-10), and assuming I remains constant and T_f could be reduced to near zero, the accelerations become

$$\ddot{x}_1(A) = \ddot{x}_2(A) = -\frac{g}{u} \left(\frac{1}{1 + \frac{4Ig}{Wr^2}} \right)$$

Using the appropriate values for runs 5 and 7 ($I = 9.54 \text{ lb-in-sec}^2$, $W = 262.4 \text{ lb}$, $r = 12 \text{ in.}$, and $u = 6$),

$$\ddot{x}_1(A) = \ddot{x}_2(A) = -\frac{386}{6} \text{ in/sec}^2 \left(\frac{1}{1 + 0.390} \right)$$

$$\ddot{x}_1(A) = \ddot{x}_2(A) = -46.3 \text{ in/sec}^2$$

Thus, the limiting acceleration values, when only T_f is eliminated, are 28 percent lower than desired. Significant improvements in airborne simulation will be achieved only by reducing both T_f and I . Assume T_f and I both can be reduced by one-half ($T_f = 40 \text{ in-lb}$, $I = 5 \text{ lb-in-sec}^2$ and $u = 6$).

$$\ddot{x}_1(A) = -62.1 \text{ in/sec}^2$$

$$\ddot{x}_2(A) = -45.6 \text{ in/sec}^2$$

The error in $\ddot{x}_1(A)$ has improved from 9.8 to 3.4 percent while the error in $\ddot{x}_2(A)$ has improved from 53.3 to 29.1 percent.

With respect to the example, event 4, run 7 presented above, the following data would result (considering F_I constant during lift-off):

$F_I(P)$	Airborne time on moon	Predicted TOSS time	Percent deviation from moon time
142 lb	1.15 sec	1.26 sec	9.6 percent

Hence, by assuming the prime error contributing parameters T_f and I could be halved, the total event error would be reduced from 12 to 9.6 percent.

Even if improvements to the TOSS system are not feasible, the present system can be used to better advantage. Assume a subject was to perform a jump from the platform, the goal being to land on a yet higher platform. Let the height of this second platform be h_I . Consider that the subject is capable of producing a constant lift-off force, $F_I(P)$, over a distance h_3 . Where gravity equals g/u , his velocity at the instant he leaves the platform is given by

$$\dot{x}_I(0) = \left[\frac{2gh_3}{u} \left(\frac{u}{W} F_I(P) - 1 \right) \right]^{\frac{1}{2}}$$

If $F_I(P)$ is sufficient to achieve the jump height h_I ,

$$h_I = - \frac{\dot{x}_I(0)^2}{2\ddot{x}_I(A)}$$

Thus, h_I is given by

$$h_I = - \frac{\frac{2gh_3}{u} \left[\frac{u}{W} F_I(P) - 1 \right]}{2 \frac{g}{u}}$$

$$h_I = -h_3 \left[\frac{u}{W} F_I(P) - 1 \right]$$

On the moon,

$$h_I = -h_3 \left[\frac{6}{W} F_I(P) - 1 \right]$$

Performing the same event on the TOSS simulator yields

$$\dot{x}_1(0)^I = \left[\frac{2gh_3}{ui} \left(\frac{u}{W} F_I(P) - 1 - \frac{2uTf}{rW} \right) \right]^{\frac{1}{2}}$$

The subject will be able to jump a height of h_1 , given by,

$$h_1^I = - \frac{\frac{2gh_3}{ui} \left[\frac{u}{W} F_I(P) - 1 - \frac{2uTf}{rW} \right]}{\frac{2g}{u} \left[\frac{1 + \frac{2uTf}{rW}}{i} \right]}$$

$$h_1^I = - h_3 \left[\frac{\frac{u}{W} F_I(P)}{1 + \frac{2uTf}{rW}} - 1 \right]$$

If h_1^I is to equal h_1 ,

$$h_3 = \frac{6}{W} F_I(P) - 1 = h_3 \left[\frac{\frac{u}{W} F_I(P)}{1 + \frac{2uTf}{rW}} - 1 \right]$$

$$u = \frac{6}{1 - \frac{12Tf}{rW}}$$

Again using the data from run 7, the value of u is calculated from

$$u = \frac{6}{1 - \frac{12 \times 89}{12 \times 262.4}}$$

$$u = 9.08$$

The validity of this new u determination directly depends upon the constancy of T_f . In all probability, T_f varies with u . Hence, T_f as a function of u must be known. At the present time, however, this relationship is not known. Further manipulation of the equations yields some insight into how this adjustment in the u setting would affect equivalent jump heights. Equation (3-9), when solved for T_f/rW , gives

$$\frac{Tf}{rW} = \frac{1}{2u} \left[\frac{ui}{g} \ddot{x}_1(A) + 1 \right]$$

The equation for u given above yields

$$\frac{T_f}{rW} = \frac{1}{12} \left(1 - \frac{6}{u} \right)$$

Equating the two values of T_f/rW ,

$$- \frac{1}{2u} \left[\frac{ui}{g} \ddot{x}_I(A) + 1 \right] = \frac{1}{12} \left(1 - \frac{6}{u} \right)$$

$$\frac{ui}{g} \ddot{x}_I(A) + 1 = \frac{u}{6} \left(\frac{6}{u} - 1 \right)$$

$$\frac{ui}{g} \ddot{x}_I(A) = 1 - \frac{u}{6} - 1$$

$$\ddot{x}_I(A) = \frac{g}{6i}$$

$$\ddot{x}_I(A) = 46.3 \text{ in/sec}^2$$

Thus, the simulation is achieved primarily by reducing the deceleration the subject experiences during his ascent. Although the jump height has been simulated, imperfections exist in the quality of the simulation. The equation predicts this imperfection as long as the moment of inertia, I , has a finite value.

In conclusion, as long as I and T_f are finite, the simulation will involve errors. Although a total event may be accurately simulated, such as airborne time following a jump, or jump to a specified height, errors within the simulation will exist. In the equation for $\ddot{x}_I(A)$ above, the ascent acceleration will equal the desired value, $g/6$, only when $i = 1$, i.e., when I in the expression

$$i = 1 + \frac{4Ig}{Wr^2}$$

equals zero. Similarly in the previously developed expression for $F_I(P)$, Equation (3-16),

$$F_I(P) = \frac{W}{u} \left[\frac{2uT_f}{C_I rW} \left(\frac{h_I}{h_3} + 1 \right) + \frac{1}{C_I} \left(\frac{h_I}{h_3} + C_I \right) \right]$$

$F_I(P)$ will equal the force necessary under perfect simulation only when T_f equals zero. If this occurs,

$$F_I(P) = \frac{W}{u} \left(\frac{h_I}{h_3} + C_I \right) \frac{1}{C_I}$$

This is just the expression for the lift-off force when gravity equals g/u .

TREADMILL SYSTEMS

Three different treadmills of somewhat similar design were used. The horizontal treadmill is a flat conveyor 60 in. wide, 16 ft long on centers of the head and tail pulleys. The conveyor is manually adjustable to any prescribed elevation. This adjustment requires location holes for each position and is presently capable of 0, 7-1/2, 15, 20, and 30 deg of elevation. The drive system is reversible so that positive or negative traverses of grades can be tested. The belt speed is variable from 0 to 12 mph through a hydraulic drive system and is continuously adjustable during operation. The belt has a traction type surface and slides on a teflon-covered bed. The TOSS system is used with this treadmill assembly.

The inclined-plane treadmill, described earlier under the heading "Inclined-Plane Simulator," also is hydraulically driven, and belt speed is continuously adjustable. This treadmill is not adjustable in incline. Slope traverse was simulated by pivoting the whole treadmill to the desired incline with respect to its horizontal position.

The variable-surface treadmill system is a system containing four conveyor belts, a flat belt conveyor (the treadmill), a storage hopper, the drives for each belt, and the various structure platform and equipment required to operate this system. This treadmill is an endless flat-belt conveyor, 60 in. wide and 18 ft long on centers of the head and tail pulleys. Soil material is retained on the treadmill surface by vertical 4.5-in.-high fences that run the length of the belt surface. The soil surface contained within these gates is 3 ft wide. Treadmill inclination is manually adjustable from 0 through ± 15 deg from horizontal. Four return conveyors receive the material from the treadmill and return it to a storage hopper for reapplication to the treadmill surface. Each of these conveyors has 48-in.-wide belts riding on trough-shaped rollers for handling the material. Each of these belts runs at a constant speed of 600 fpm, and the system handles 1500 tons of material per hour. The first conveyor is fixed to the treadmill structure below the treadmill and is lowered or elevated with the treadmill. A hopper collects the material from the treadmill and feeds this conveyor. The material is then carried in the opposite direction for emptying into the first long (52 ft long) conveyor, which is inclined 18 deg from horizontal. The material is deposited from this conveyor into a short horizontal cross-feed conveyor (12 ft long). This feeds the final return conveyor (52 ft long) also inclined at 18 deg from horizontal. This conveyor deposits the material into a storage hopper with a capacity of approximately 300 cu ft.

The depth of the soil surface deposited on the belt for any given treadmill speed is determined by the position of a combined spreader and hopper gate. Control of this function is effected through a manually positioned valve that determines the position of the hydraulically operated gate door.

A variable-height platform, 8 ft wide and 10 ft long with a 42-in. guard rail, was constructed adjacent to the treadmill to permit access to the treadmill and provide a work space for the test conductor and his assistants. This system is illustrated in Figures 3-27 through 3-33.

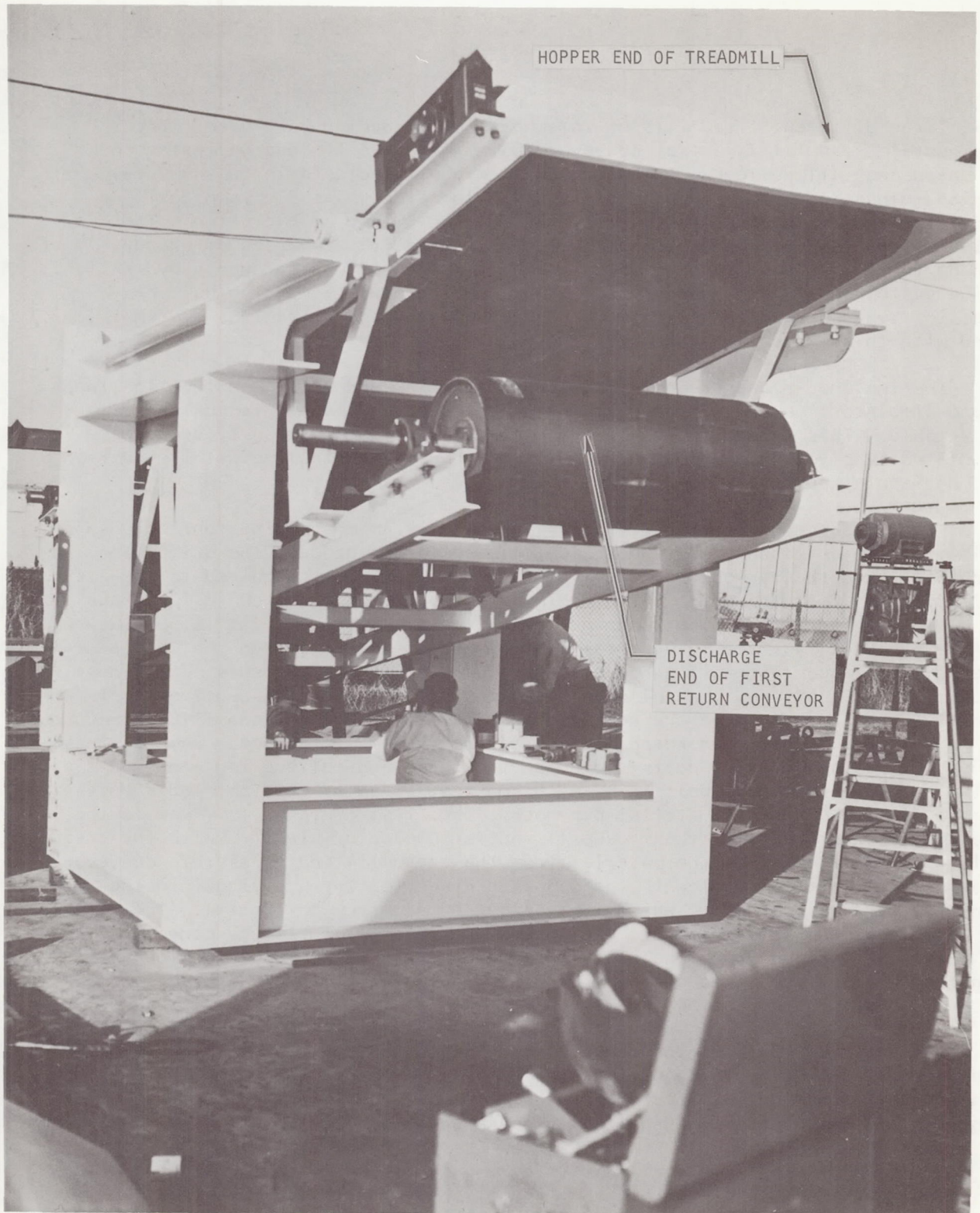


Figure 3-27. Treadmill and First Conveyor Return Assembly



Figure 3-28. Installation of Treadmill and First Return Conveyor



Figure 3-29. Soil Material Return to Hopper

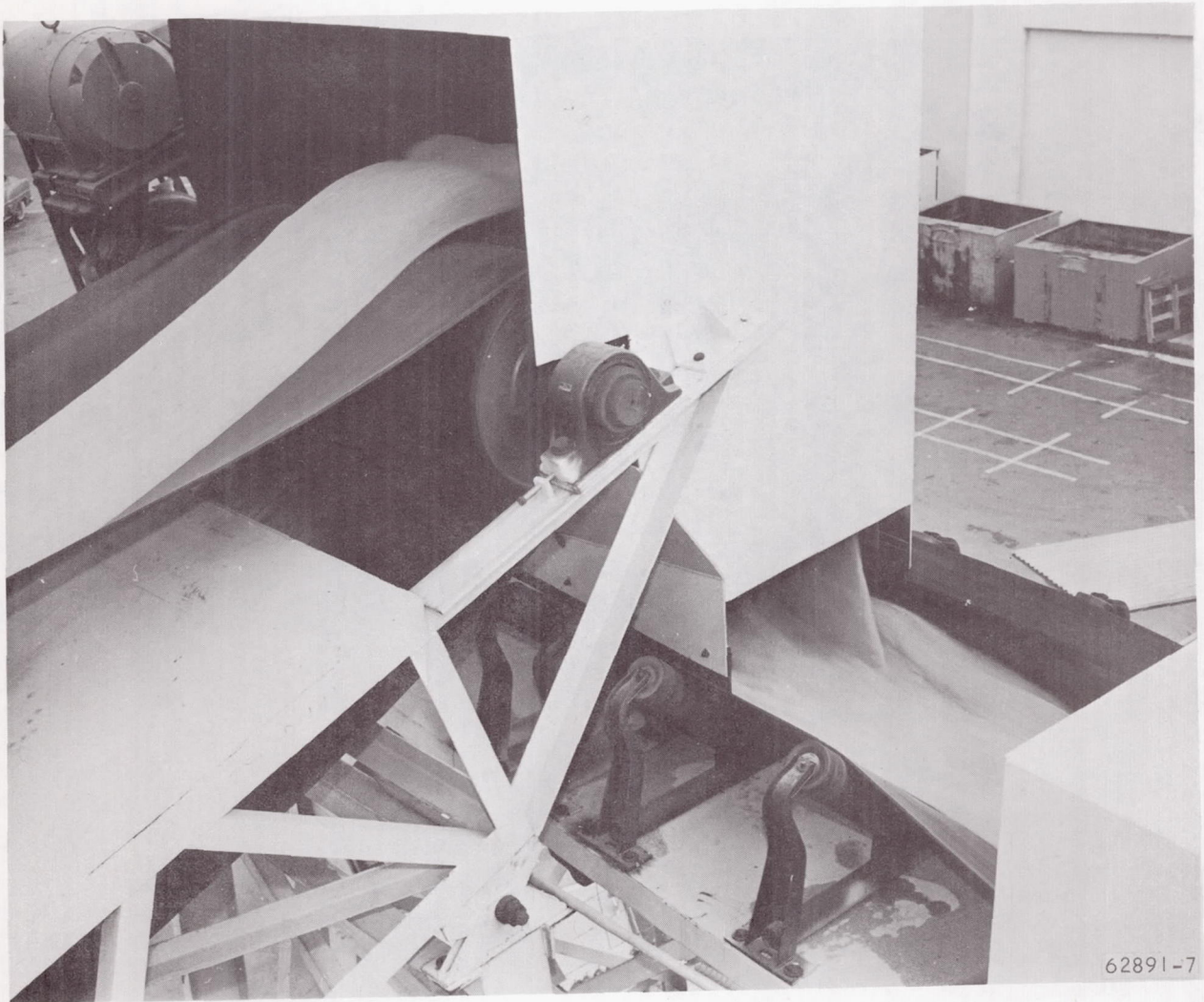


Figure 3-30. Lunar Soil Transport at First Inclined Conveyor Transfer to Cross-Feed Conveyor

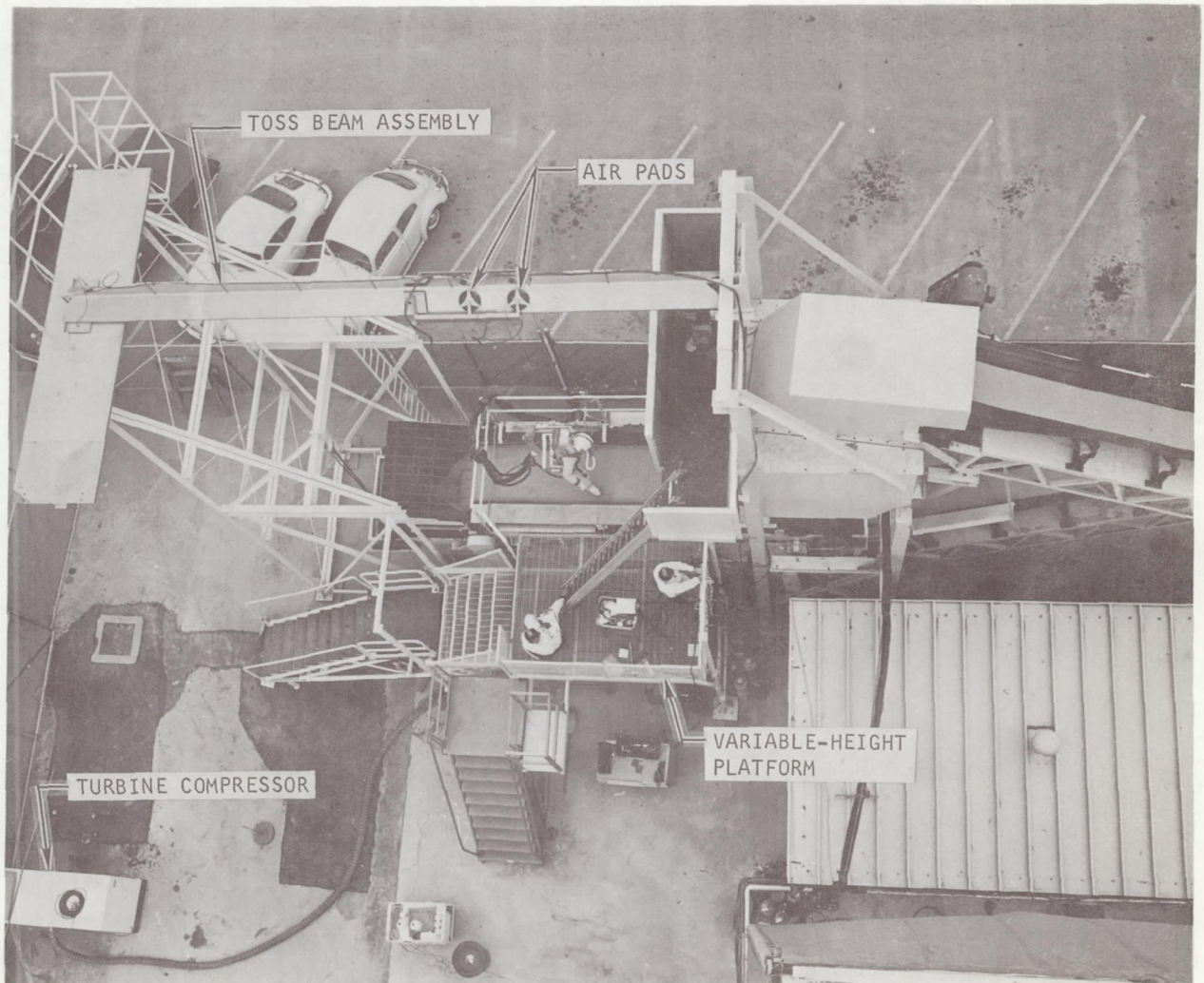


Figure 3-31. TOSS and Lunar Surface Simulating Treadmill System (viewed from above)

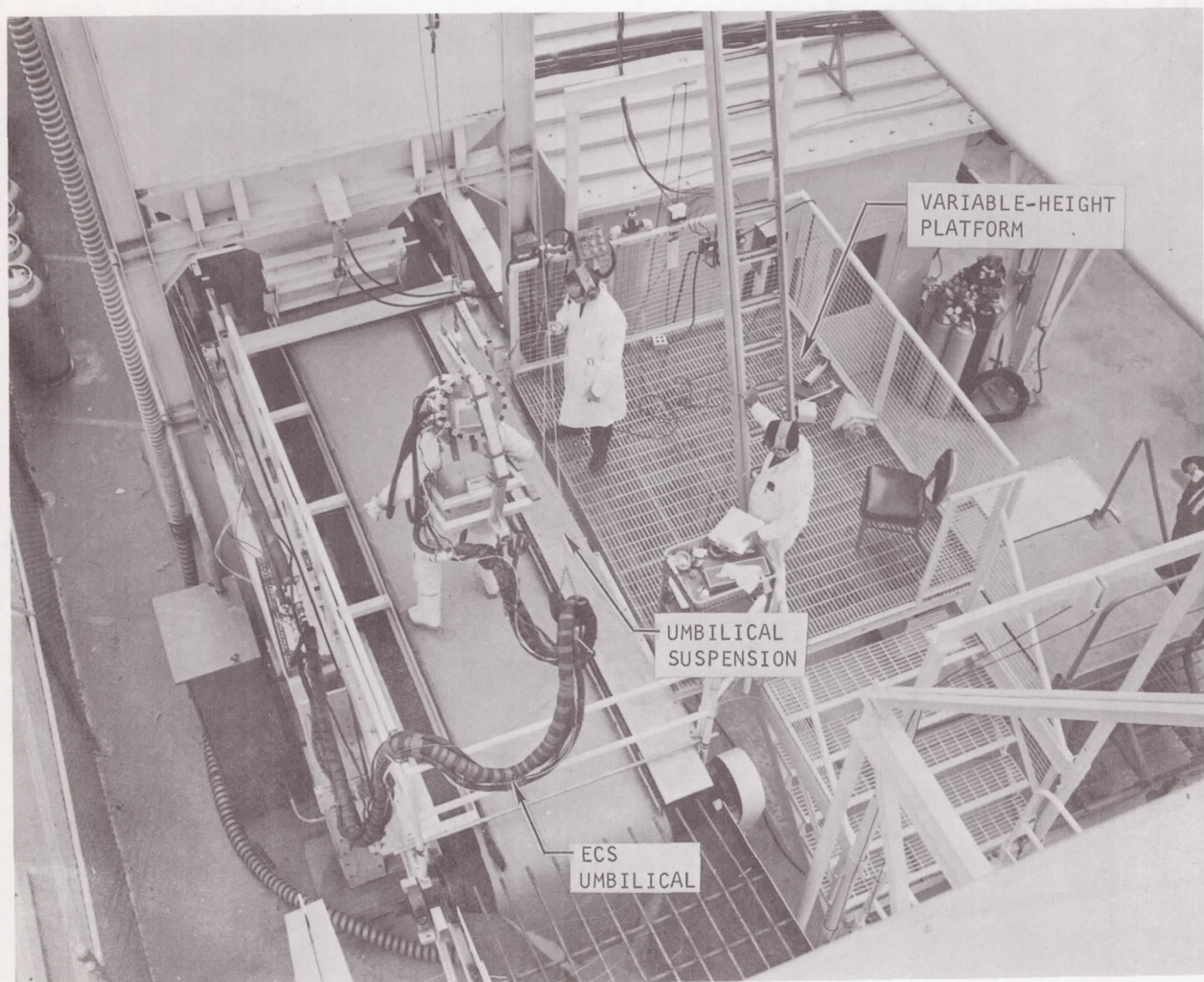


Figure 3-32. Subject Being Tested on Simulated Lunar Soil



Figure 3-33. Subject Walking on Simulated Lunar Surface

LUNAR SURFACE SIMULATION

The materials for simulating the lunar surface were selected based on data from the Surveyor program (References 3-2 and 3-3) and personal communications with personnel of the Jet Propulsion Laboratories.*

The principal factors affecting the trafficability of a soil surface related to a man moving over the surface are not well defined. Whether the most predominant consideration is density or shear strength is not known. However, it is agreed that soil can fail by the push-off of the subject whether the soil fails in bearing or shear.

Criteria for Material Selection

The criteria for selection of the lunar soil simulation material are as follows:

1. Readily available material
2. Reasonably dust-free
3. Reasonably uniform without a large variation in a specific size
4. Angle of repose of greater than 30 deg
5. Density of 1.2 to 1.6 gm/cc (75 to 100 lb/cu ft)
6. Static bearing strength of 3.5×10^5 to 5.0×10^5 dynes/cm² (5 to 7 psi)

Material Composition for Smooth Surface Simulation

A sandblasting-type sand was chosen as one of the most likely candidate soils to simulate a smooth lunar surface. A sample of the material was sent to an independent laboratory for analysis of its physical and mechanical properties. The results of this analysis were as follows:

1. The density of the samples was determined by filling a 0.5-cu-ft container and weighing it. The average of 3 trials indicated a density of 106.2 lb/cu ft at hydroscopic moisture content. (Hydroscopic moisture at the time of testing was 0.2 percent.)
2. Direct shear testing was performed on samples remolded to a density of 106.2 lb/cu ft at 0 to 2 percent moisture. An angle of inertial friction of 44 deg and cohesion of zero was determined under a surcharge of 260, 520, and 1040 lb/sq ft. These data are shown in Figure 3-34.
3. The safe static bearing capacity at this density is 1500 lb/sq ft.

*Communications with R.F. Scott, Professor of Civil Engineering, California Institute of Technology (Surveyor team member), January and February 1968.

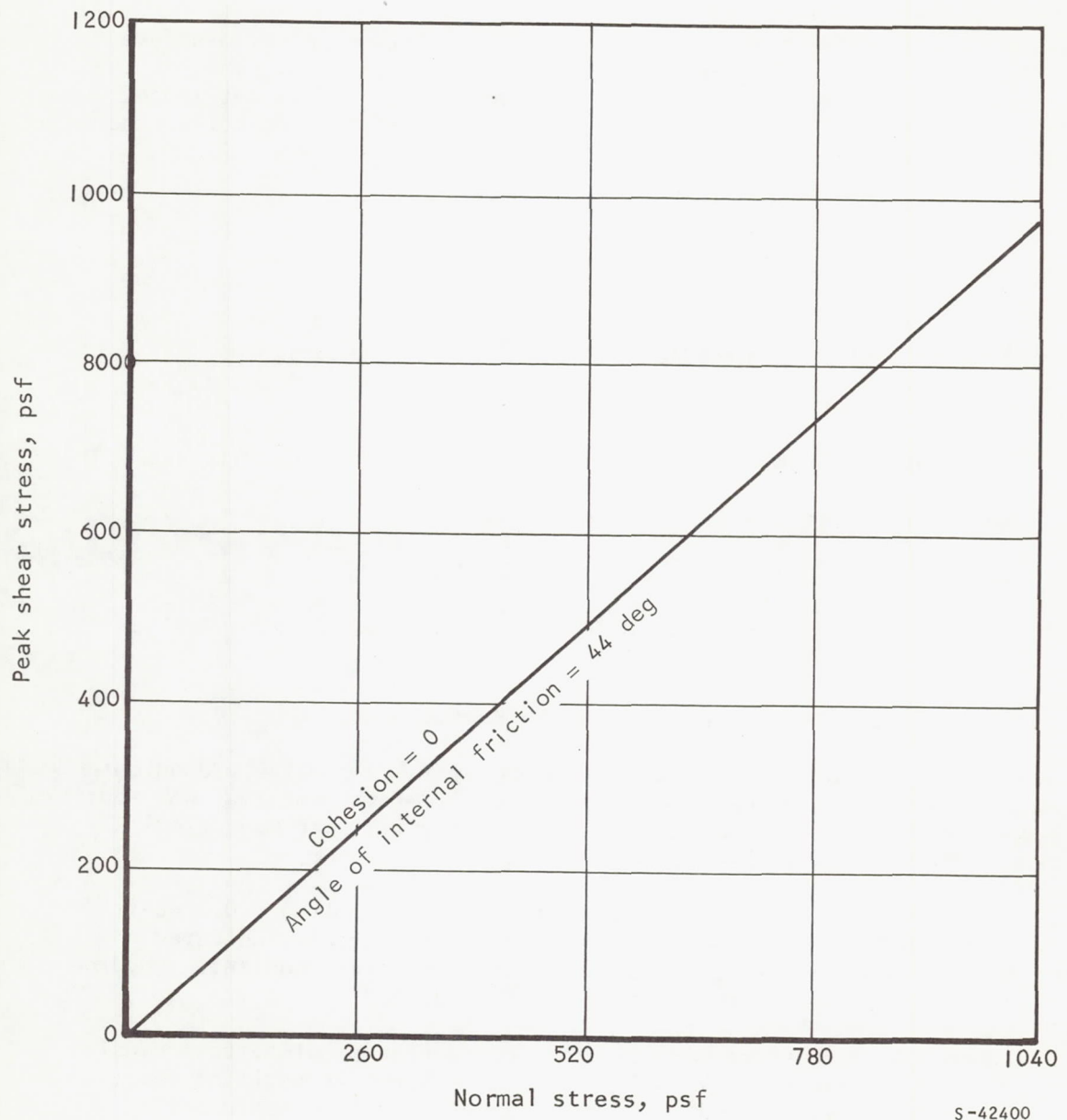


Figure 3-34. Direct Shear Test Data

4. An average angle of repose of 35 deg was determined by dropping a 6-in. high sand sample.
5. Particle size distribution was determined by sieve analysis at the 0.2-percent hygroscopic content. The results are shown below.

<u>Screen size</u>	<u>Weight retained</u>	<u>Percent retained</u>	<u>Percent passing</u>
10 Tyler (12 U.S.)	0	0.0	100.0
16 Tyler	26	13.0	87.0
20 Tyler	112	56.0	44.0
35 Tyler	196	98.0	2.0
100 Tyler	199	99.5	0.5
200 U.S.	200	100.0	0.0

In a comparison of these data with the selection criteria, the material compared favorably with the reported lunar surface properties and was chosen as the simulated lunar soil for the smooth surface condition.

Following selection of the sand, it was loaded into the variable-surface treadmill/conveyor system for a checkout to determine its capacity to handle the material. After minor adjustments and modifications were made to reduce spillage of soil, the system was ready for use.

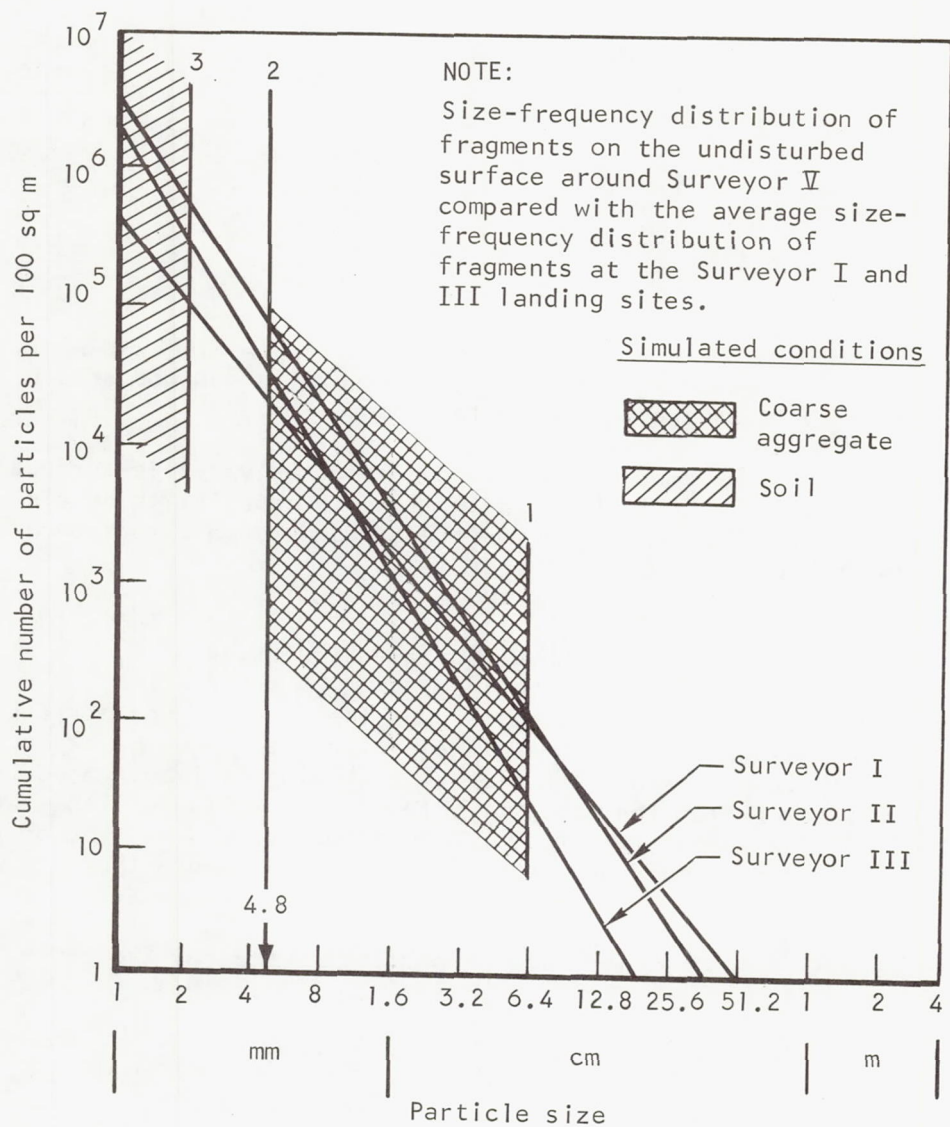
Material Composition for Rough Surface Simulation

The rough or rubble-strewn surface areas around the Surveyor spacecrafts I, III, and V show that a reasonably uniform surface particle size can be expected in the relatively smooth lunar maria. The size distribution is illustrated in Figure 3-35, which was taken from the Surveyor V report. The figure illustrates that the area immediately adjacent to Surveyor V does not contain as many of the larger particles as the areas around Surveyors I and III. However, there is good general agreement.

The criteria used in selecting the size of particles used for the rough lunar surface were as follows:

1. Readily available material
2. Maximum size particle that the conveyor system can readily handle
3. A particle distribution that is approximated by the distribution shown in Figure 3-35

To simulate the rough surface condition, concrete aggregate and crushed granite in sizes ranging from 4.8 mm (0.187 in.) to 62 mm (2.5 in.) were mixed with the surface material used for simulating the smooth surface. The distribution of the particle size is illustrated by the vertical lines shown between



S-42676-A

Figure 3-35. Lunar Surface Particle Size Distribution

lines 1 and 2 in Figure 3-35. The line marked 3 is the upper limit of the particle size used to simulate the smooth surface. The distribution was obtained by adding the coarse aggregate volumetrically to the sand.

The amount of gravel mixed was based on the particle distribution of a 1-in. dia (2.54 cm) expected in accordance with the following equation from Surveyor I report:

$$N = 3 \times 10^5 y^{-1.77}$$

where

N = cumulative number of grains in 100 m^2

y = diameter of grains in mm

if

$$y = 25.4 \text{ mm}$$

then

$$N = \frac{3 \times 10^5}{25.4^{1.77}} = \frac{3 \times 10^5}{309} = 0.972 \times 10^3 \text{ particles}/100 \text{ m}^2$$

or

$$n = \frac{N}{100} = 9.72 \text{ particles}/\text{m}^2$$

The specific gravity of gravel (SiO_2 , no voids) is approximately 2.5. Assuming a 1-in.-dia particle, the weight of that particle would be

$$W = 2.5 \rho_{\text{H}_2\text{O}} V$$

where

$$\rho_{\text{H}_2\text{O}} = \frac{62.4 \text{ lb}}{12^3 \text{ cu in.}}$$

$$W = 2.5 \times \frac{62.4}{12^3} \times \frac{\pi}{3} \times \left(\frac{1}{2}\right)^3 \frac{\text{lb}}{\text{particle}}$$

$$W = 0.047 \text{ lb/particle}$$

If each 9.72 particles is distributed in a 1-in.-thick layer, the number of particles, n_v , to be placed in the volume to assure the particles will appear on the surface is

$$n_v = \frac{\text{particle}}{m^2 - \text{layer}} \times \frac{\text{in.}}{m} \times \frac{\text{layers}}{\text{in.}}$$

$$n_v = 9.72 \times 39.37 \times 1 \text{ particles}/m^3$$

$$n_v = 382 \text{ particles}/m^3$$

or

$$\frac{382}{1.0936^3} = 292 \text{ particles}/yd^3$$

The volume of sand in the hopper system is

$$V_s = \text{volume of sand (assume sand weight} = 10 \text{ tons)}$$

$$V_s = \frac{20,000}{106 \times 27} \text{ cu yd} = 7 \text{ yd}^3$$

Therefore, the number of particles required for the above surface distribution is

$$292 \times 7 = 2044 \text{ particles}$$

$$W_p = 2044 \times 0.047 \text{ lb} = 96 \text{ lb}$$

If 50 percent of the gravel is in the specified size range, the total weight of gravel is $96/0.5$ or 200 lb.

Since the amount of gravel required was so small, several bags of gravel and crushed granite were procured. The gravel was of a well-rounded quality similar to no. 2 grade. The crushed granite was very angular and of a size range from 3/4 in. dia minimum to 2-1/2 in. dia maximum. These particles were added to the sand while the system was running to assure a good mix. The number of particles appearing on the surface and through the total volume was checked until there was statistical assurance of repeatability. During the tests using this material there was no separation or accumulation of the particles in any volume.

PRESSURE SUITS

Six subjects were sent to NASA-Houston where they were given the best possible fit in the available Gemini G-3C and G-4C pressure suits. Each of

these suits, together with gloves and helmet liner, was assigned to an individual test subject for his exclusive use throughout the program. Because of many suit failures, however, the test subjects were forced to exchange or rotate suits. Since the subjects were of similar size and weight, refitting presented no problem.

Damage to the suit was generally confined to the lower torso and to the leg areas that are subject to extreme flexing during the various ambulatory test modes. Several failures of the pressure retention net appeared to be due to abrading.

The more critical wear problems occurring during the program were those related to wear resulting from high usage rates, test conditions, and the type of tasks being performed in the suits. Inasmuch as the G-3C and G-4C suits were not specifically designed to accomplish tasks involving walking, loping, and running, an extensive amount of wear and degradation has occurred with boots and lower torso suit sections. Due to the basic suit inadequacies and the high work loads imposed, a high ratio of suit maintenance and repair activity was required to achieve a reasonable suit failure rate during tests.

Figures 3-36 and 3-37 show some typical boot wear effects and damage that occurred during testing. Figure 3-38 shows the repair method employed for the boot cover layer.

A test program to study the deflection characteristics of pressure suits used in this program was conducted for the following:

1. To provide comparative data for evaluating variations in deflection characteristics between suits of similar types, as well as possible variations within G-3C and G-4C suit configurations
2. To provide data that would allow evaluation of changes in the suits over long working periods, i.e., changes in the suits that might affect the metabolic rate or kinematic data

The six subjects were individually fitted and provided with a David Clark G-3C and G-4C pressure suit and corresponding glove and helmet assemblies. All data were obtained with each subject in his assigned suit and in a pressurized state (3.5 psig). The subject was rigidly held at the torso by a fiber glass, contoured "clam shell" (back half only) used in the primary test program for all measured modes except ankle deflections; for ankle dorsiflexion and plantar flexion, the subject was in an unrestrained supine position. Data were collected for left and right limbs.

Deflections were measured in accordance with the Cave and Roberts method as modified by Batch (Reference 3-4). For shoulder measurements, force was applied at the elbow; for elbow measurements, force was applied at the wrist; for hip measurements, force was applied at the knee; for knee measurements, force was applied at the ankle; and for ankle measurements, force was applied through special hardware.

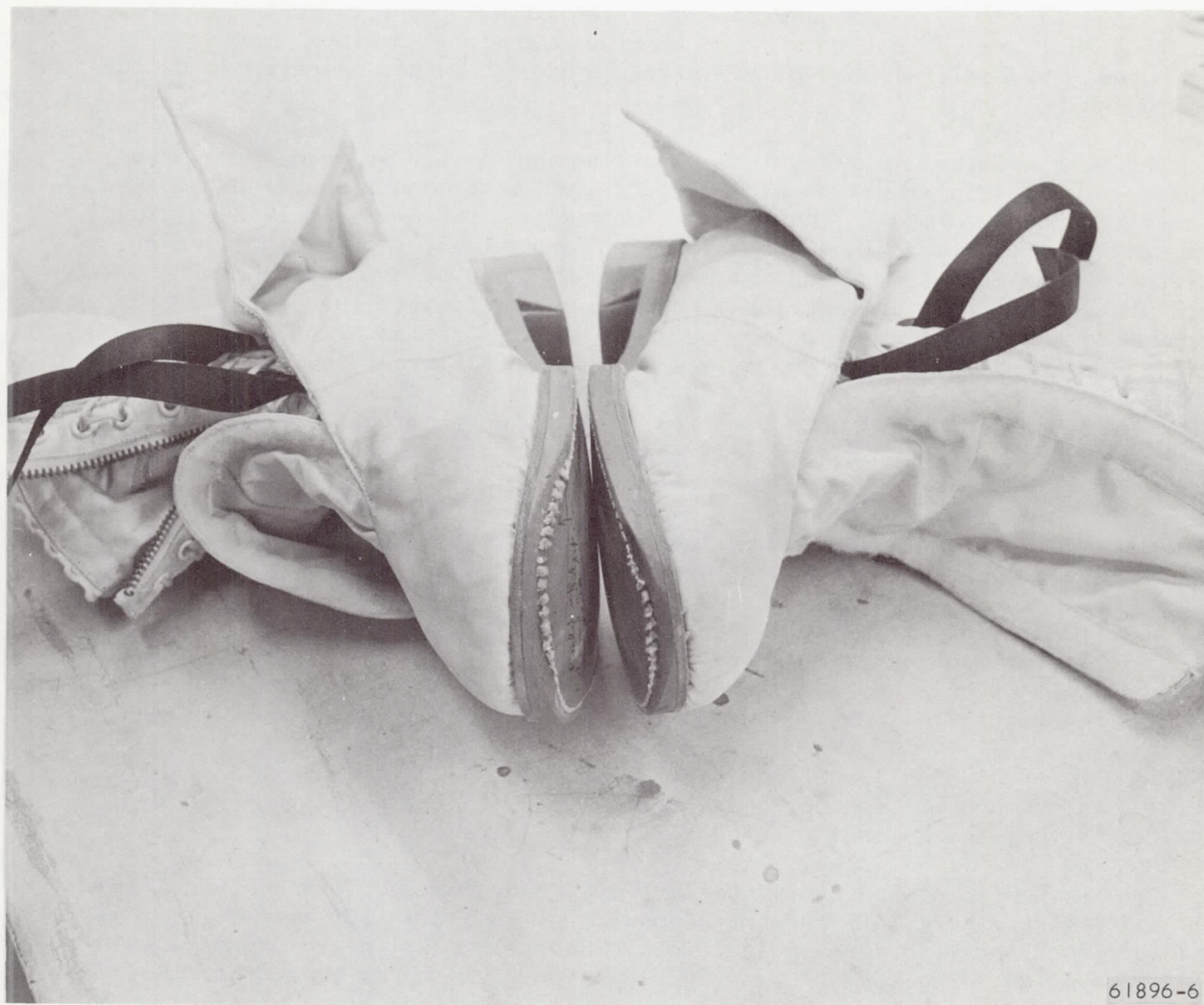


Figure 3-36. Wear Effects on Boots During Testing



Figure 3-37. Damage to Boot Casings During Testing



61896-4

Figure 3-38. Repair Method Used on Boot Cover Layer

Caution was exercised so that the applied force always acted normally to the direction of resistance and in the same plane as deflection. Deflections were measured by a goniometer located in the plane of true limb motion. Forces were measured by a ring load cell and recorder.

Figures 3-39 and 3-40 demonstrate the measuring equipment schematic and the modes measured. Figures 3-41 through 3-47 show actual measurements at various locations. Figure 3-48 shows the ankle bending hardware.

The original modes studied (Figure 3-40) included shoulder abduction and flexion, hip abduction and flexion, elbow flexion, and knee flexion. At each joint, initial values, final deflection, applied forces, and reset angles (deviation from original rest position when unloaded) were recorded. All measurements were performed six times to assure repeatability; all bending moment data are averages of these six values.

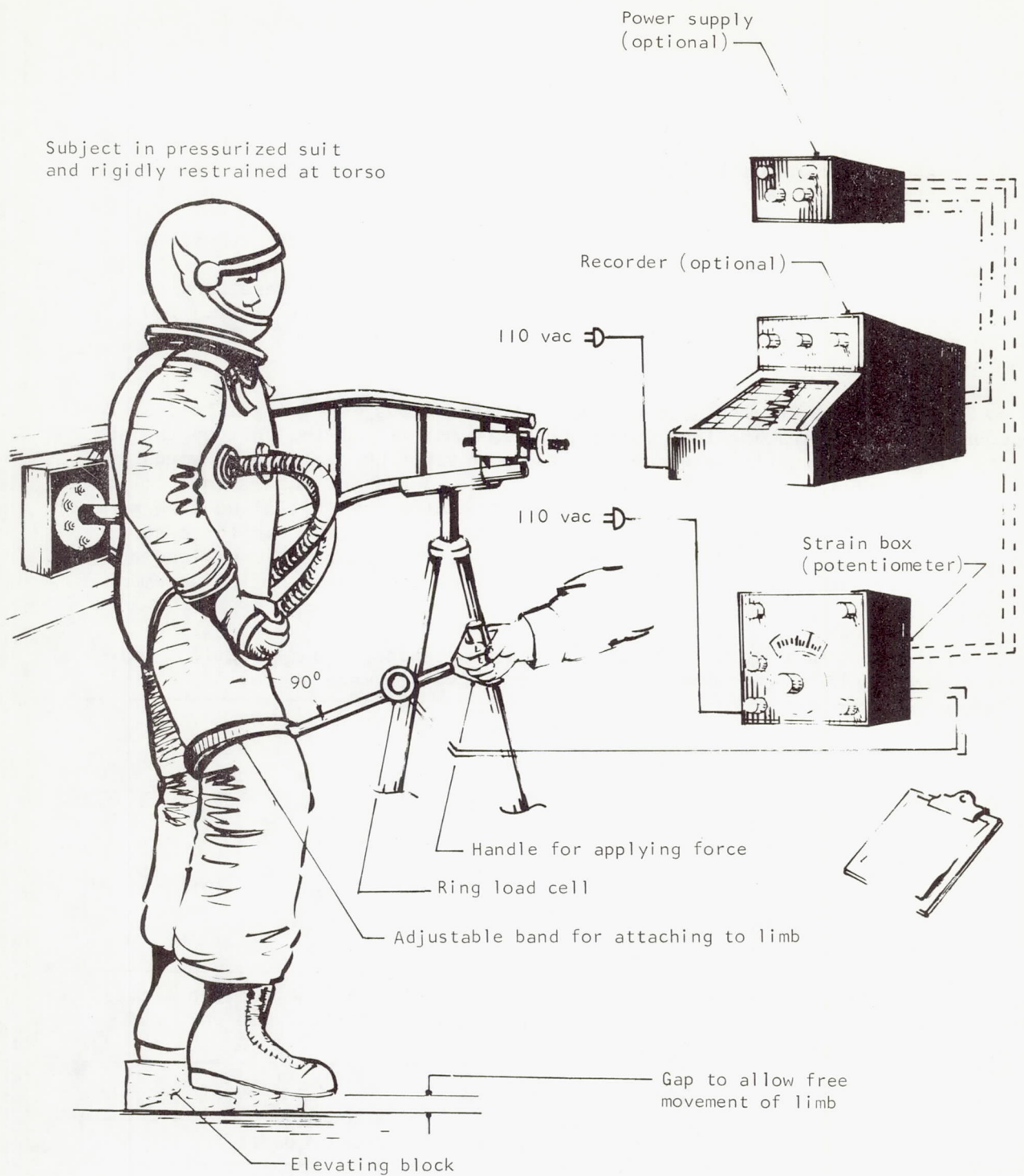
After initial studies were conducted, deflections were set at realistically encountered values rather than using the maximum limit of the suit or the subject. It was originally intended that all six suits be evaluated through the previously described method at three stages of program testing — start, middle, and conclusion of the test program. After completion of initial bending moment measurements, the study was limited to two special subjects. In the case of these two subjects, hip deflections, knee deflections, and ankle deflections were the only required modes; these were measured through specific incremental values.

At the conclusion of the first few tests, standardized deflections were introduced. Unless otherwise specified, these values were as follows:

Original tests (before walking)	
Mode	Deflection, deg
Shoulder abduction	30
Shoulder flexion	20
Hip abduction	20
Hip flexion	10
Elbow flexion	50
Knee flexion	50

All tests performed after the initial tests followed these deflection limits. The initial tests were utilized in establishing these limits, however, and may not be in complete correspondence.

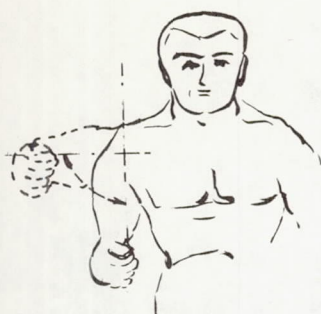
Two special subjects	
Mode	Incremental measurements, deg
Hip flexion	0, 3, 6, 10
Knee flexion	0, 15, 30, 40, 50
Ankle dorsiflexion	0, 5, 10, 15
Ankle plantar flexion	0, 5, 10, 15



S-42401

Figure 3-39. Measuring Equipment Schematic

Shoulder



Abduction



Flexion

Elbow

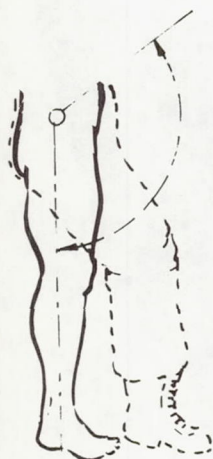


Neutral
extension



Flexion

Hip



Flexion

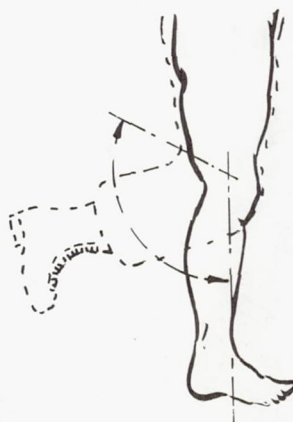


Neutral



Abduction

Knee



Flexion



Neutral

Ankle



Neutral



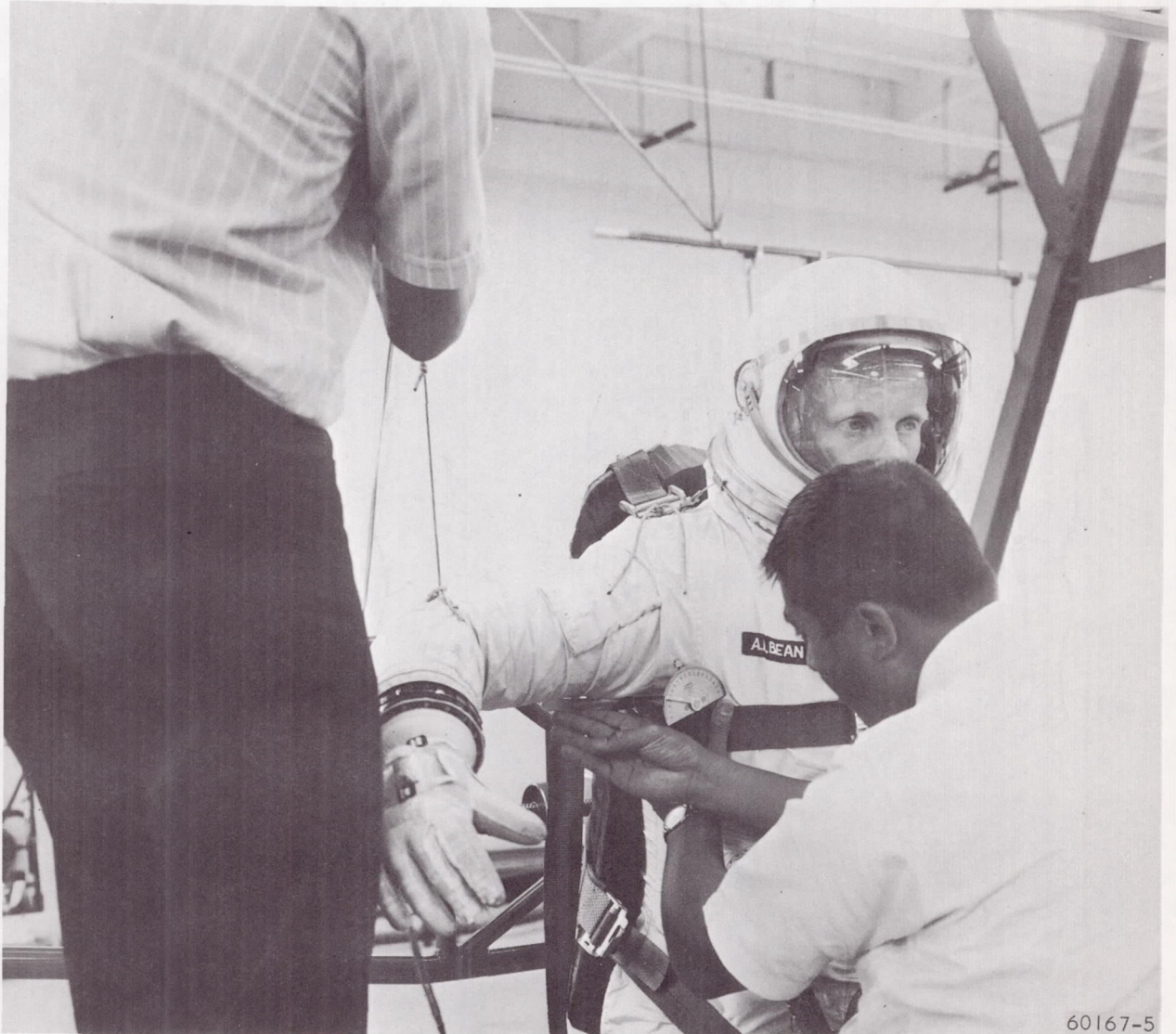
Dorsiflexion

Plantar flexion

Dorsiflexion and
plantar flexion

S-42402

Figure 3-40. Deflection Modes Studied



60167-5

Figure 3-41. Shoulder Abduction Measurement

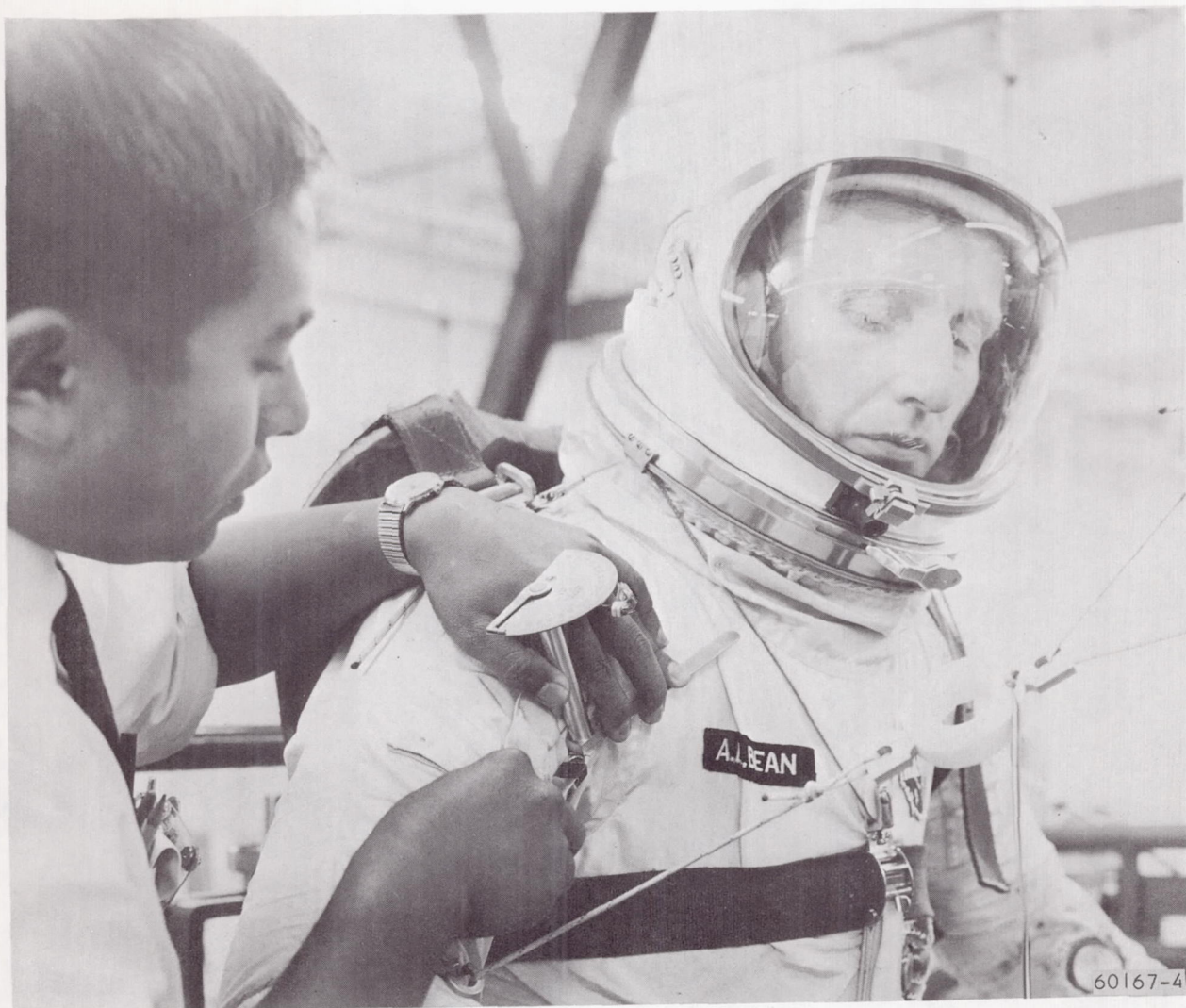


Figure 3-42. Shoulder Flexion Measurement

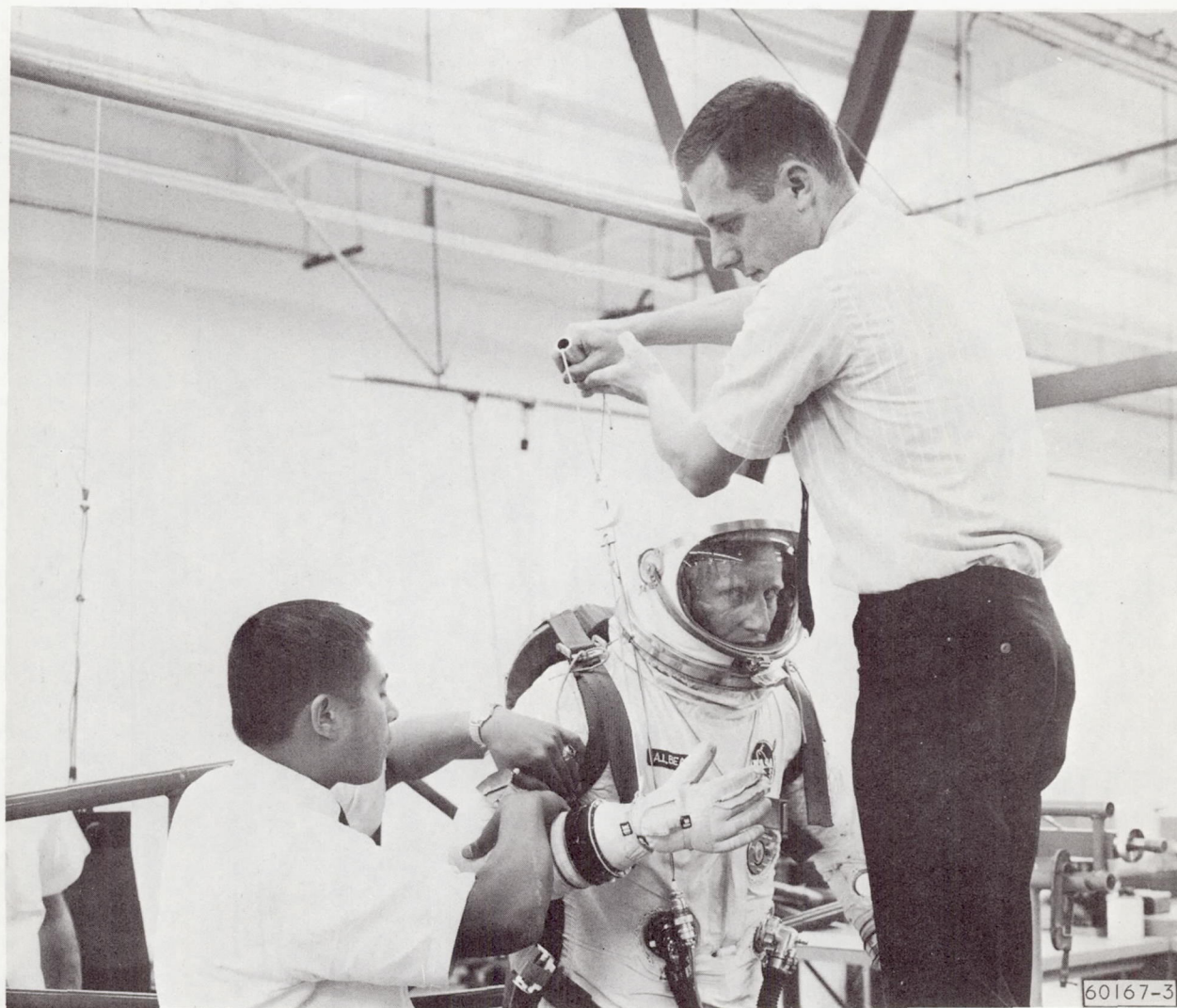


Figure 3-43. Elbow Flexion Measurement

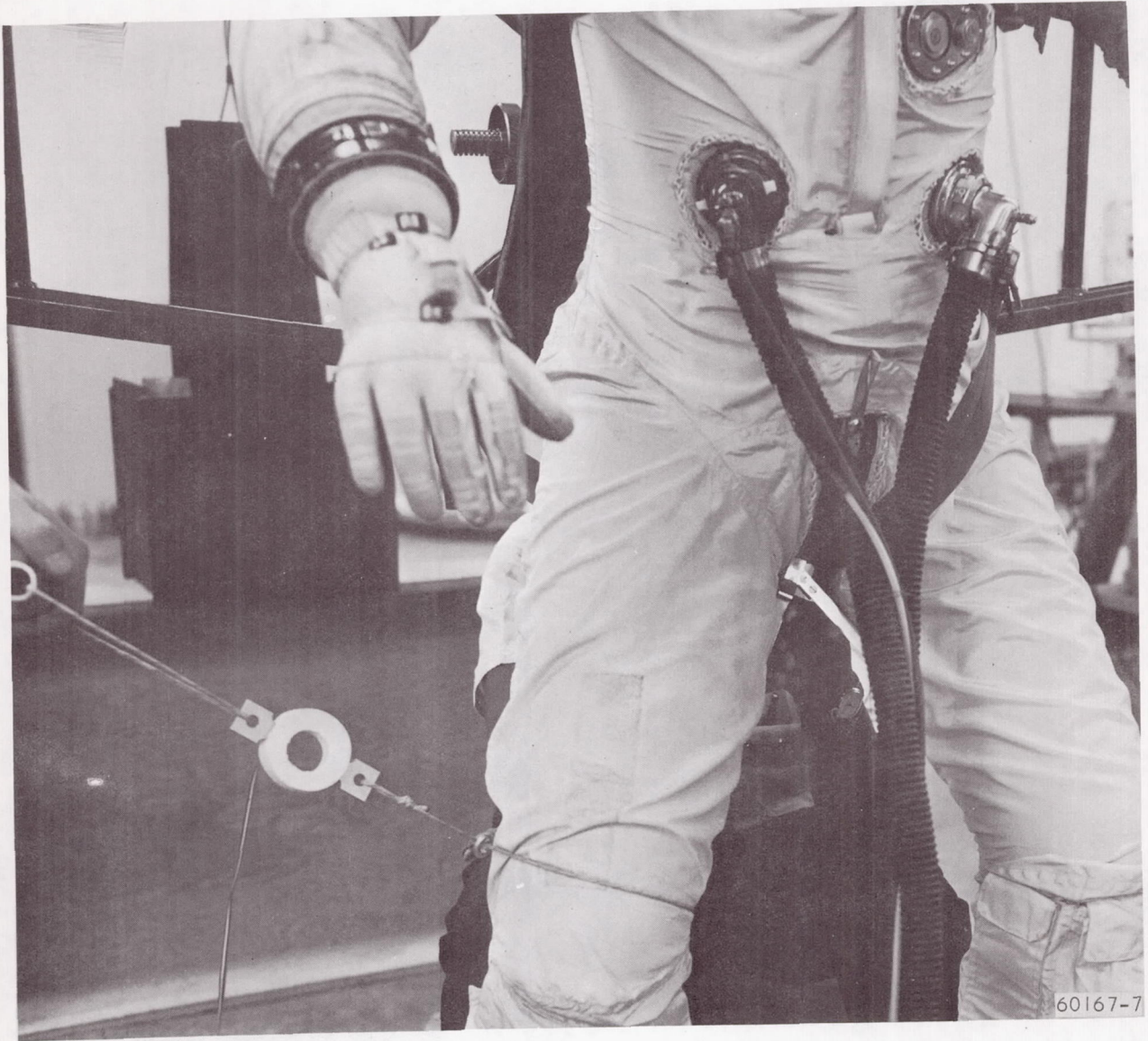


Figure 3-44. Hip Abduction Measurement



60167-6

Figure 3-45. Hip Flexion Measurement

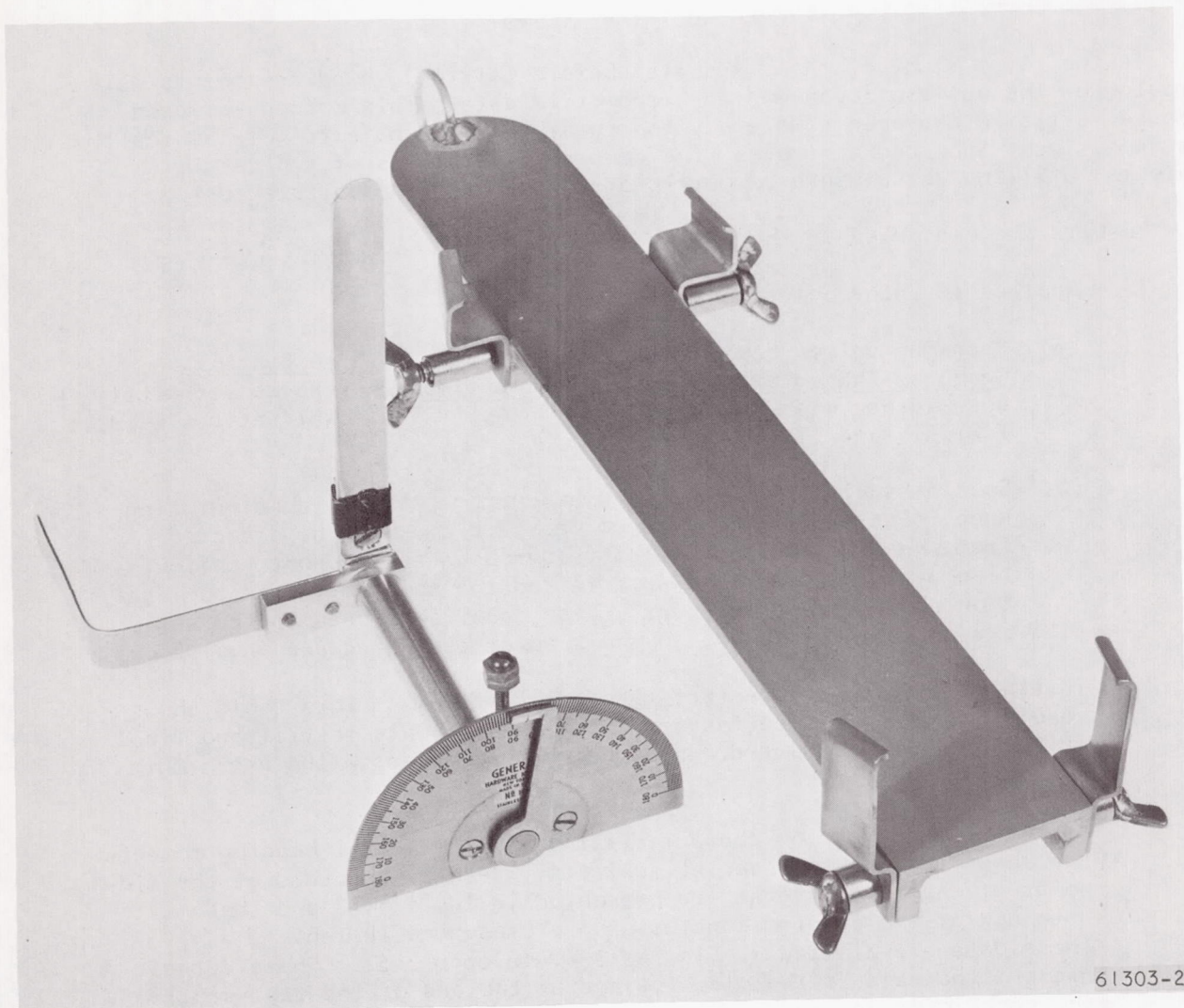


Figure 3-46. Knee Flexion Measurement



61303-1

Figure 3-47. Technique for Evaluating Ankle Deflection Characteristics



61303-2

Figure 3-48. Ankle Deflection Measurement Hardware

All deflection characteristics are presented in the form of bending moments, computed by the following formula:

$$\text{bending moment} = \text{force} \times \text{distance}$$

Distance, in this case, was taken to be the anthropometric data for distances between joints. For example, during the elbow flexion tests, the force was applied at the wrist and the movement was applied at the elbow joint. The distance is thus equal to the anthropometric distance between elbow and wrist joints. The moments presented are in ft-lb or mkg.

In the first study of the six suits (before walking), bending moments were computed on the basis of mean-man anthropometric data. This method was used because initial measurements were developmental and the subjects were basically the same size. Subsequent studies (incremental deflections of two special subjects) utilized actual anthropometric distances for the subjects tested.

Results are presented in the format below.

1. Applicable anthropometric data (Table 3-8).
 - (a) Mean-man values based upon data presented in Some Dynamic Response Characteristics of Weightless Man, Air Force Technical Documentary Report AMRL-TDR-63-18, April 1963; Whitsett, C.E. Jr.; Tables V and VI, pp 10 and 11.
 - (b) Special subject data as measured during tests. In calculating knee joint bending moments, 3 in. (7.6 cm) must be deducted from the published lower leg values because the boot configuration of the pressurized suit raised the point of force application above the ankle joint. Also, published data on the ankle are not applicable due to the special test hardware involved.
2. Initial deflection characteristics (Table 3-9). — This table shows results of the first series of measurements. Only initial and final deflections were measured. Measurements were made with test subjects in the suits.
3. Incremental deflection characteristics. — Incremental bending moments are shown for the two special subjects. Results obtained at the midpoint of the test program are presented in Table 3-10 and those obtained at the program conclusion are presented in Table 3-11. These data are plotted in Figures 3-49 through 3-52. These curves present the data at the midpoint and at the end of the test program for each joint and each subject.

The variation in the bending moments between the midpoint and the end of the test program can be attributed to several factors.

1. Suit fatigue. — This could cause an increase in load required to bend the joints if the restraint fabric stretched or wore allowing slight growth of joint.

TABLE 3-8

APPLICABLE ANTHROPOMETRIC DATA

Mean man (assumed subject for initially evaluating general deflection characteristics of pressure suits)				
Limb		Length between joints in. cm		Mode involved
Upper arm		13.0	33.0	Shoulder abduction and flexion
Lower arm		10.0	25.4	Elbow flexion
Upper leg		15.8	40.1	Hip abduction and flexion
Lower leg		16.0	40.6	Knee flexion
Special subjects (Subject B, Chidsey; Subject C, Gafvert)				
Limb	Subject	Length between joints* in. cm		Mode involved
Upper arm	B	11.5	29.2	Shoulder abduction and flexion
	C	10.5	26.7	
Lower arm	B	10.5	26.7	Elbow flexion
	C	10.5	26.7	
Upper arm	B	16.5	41.9	Hip abduction and flexion
	C	16.5	41.9	
Lower leg	B	18.0	45.7	Knee flexion
	C	17.0	43.2	
Ankle	B	11.0	27.9	Angle dorsiflexion and plantar flexion
	C	11.0	27.9	

*Hardware values

TABLE 3-9

INITIAL DEFLECTION CHARACTERISTICS OF PRESSURE
SUITS PRIOR TO TEST MODES USING SPECIAL SUBJECTS
(ASSUMING MEAN MAN AS SUBJECT)

Mode	Suit	Deflection Angle, deg	Limb				Reset Angle, deg	
			Left		Right			
			ft-lb	mkg	ft-lb	mkg	Left	Right
Shoulder flexion	G-4C-20	10	21.7	3.0	28.2	3.9	-1.3	-0.3
	G-3C-14	20	34.1	4.7	40.1	5.5	+1.3	-0.3
	G-3C-8	20	28.3	3.9	20.6	2.8	0.0	+0.2
	G-4C-6	20	27.6	3.8	26.0	3.6	1.2	+0.3
	G-4C-33	20	27.1	3.7	30.9	4.3	-0.7	+0.7
	G-4C-14	20	10.8	1.5	10.3	1.5	+4.2	+5.2
Shoulder abduction	G-4C-20	40	29.8	4.1	29.2	4.0	+7.5	+8.3
	G-3C-14	30	30.3	4.2	31.9	4.4	+0.7	+1.8
	G-3C-8	50	29.2	4.1	28.7	4.0	+3.7	+2.3
	G-4C-6	30	30.3	4.2	26.0	3.6	+1.3	+1.0
	G-4C-33	30	23.3	3.2	24.9	3.4	+4.8	-0.2
	G-4C-14	30	28.7	4.0	24.4	3.4	-1.3	-2.0
Hip flexion	G-4C-20	10	69.1	9.6	67.8	9.4	+2.2	+0.7
	G-3C-14	10	70.4	11.8	71.8	11.8	-0.5	-0.3
	G-3C-8	10	48.7	6.7	56.9	7.8	-1.7	+0.2
	G-4C-6	10	17.1	2.4	48.7	6.7	+0.8	0.0
	G-4C-33	10	65.1	9.0	61.9	8.5	0.0	-1.7
	G-4C-14	10	40.8	3.8	29.6	4.1	+1.3	+1.3
Hip abduction	G-4C-20	20	53.3	7.4	53.3	7.4	+3.0	+2.0
	G-3C-14	20	52.0	6.8	65.1	9.0	+0.8	+1.5
	G-3C-8	20	62.5	8.6	48.7	6.7	+0.3	+1.5
	G-4C-6	10	68.4	9.4	44.7	6.2	+0.7	+0.5
	G-4C-33	15	57.3	7.9	55.3	7.6	+2.5	+2.3
	G-4C-14	20	55.9	7.7	71.1	9.8	-0.3	+1.0
Elbow flexion	G-4C-20	50	11.2	1.6	11.2	1.6	-1.0	+1.3
	G-3C-14	50	12.9	1.8	10.8	1.5	-1.3	-0.5
	G-3C-8	35	10.8	1.5	8.7	1.2	0.0	-0.3
	G-4C-6	50	10.4	1.4	11.7	1.6	-0.5	+0.5
	G-4C-33	50	9.6	1.3	8.3	1.1	-2.2	-2.3
	G-4C-14	50	15.8	2.2	22.1	3.0	+1.0	+0.3
Knee flexion	G-4C-20	50	21.5	2.4	22.5	3.1	+7.5	+7.5
	G-3C-14	50	28.6	3.5	28.6	3.1	+2.5	+1.0
	G-3C-8	50	20.5	2.9	17.0	2.3	0.0	+4.8
	G-4C-6	50	26.3	3.5	24.8	3.4	-1.0	+1.0
	G-4C-33	50	23.5	3.2	21.5	2.9	+8.8	+8.2
	G-4C-14	50	38.5	5.2	44.4	6.1	+1.0	+10.0

TABLE 3-10

INCREMENTAL DEFLECTION CHARACTERISTICS OF PRESSURE
SUITS, USING SPECIAL SUBJECTS
(MIDPOINT OF TEST MODES)

Mode	Subject* and Suit	Deflection Angle, deg	Limb				Reset Angle, deg	
			Left		Right		Left	Right
			ft-lb	mkg	ft-lb	mkg		
Hip flexion	Subject B G-3C-14	3	49.0	6.8	51.8	7.1	-	-
		6	65.6	9.1	72.5	10.0	-	-
		10	90.4	12.5	90.4	12.5	-0.5	+0.3
	Subject C G-4C-37	3	53.8	7.9	38.1	5.3	-	-
		6	79.8	11.0	59.3	8.2	-	-
		10	95.8	13.2	77.2	10.7	+0.3	0.0
Knee flexion	Subject B G-3C-14	15	17.19	2.37	17.56	2.42	-	-
		30	24.73	3.41	26.46	3.65	-	-
		40	27.59	3.81	25.53	3.52	-	-
		50	32.44	4.48	28.54	3.94	+2.2	+1.0
	Subject C G-4C-37	15	18.47	2.55	20.20	2.79	-	-
		30	26.65	3.68	28.76	3.97	-	-
		40	30.88	4.26	32.71	4.51	-	-
		50	34.15	4.71	35.79	4.94	+1.7	-1.5
Ankle dorsiflexion	Subject B G-3C-14	5	7.3	1.0	7.2	1.0	-	-
		10	11.2	1.6	10.4	1.4	-	-
		15	14.5	2.0	13.6	1.9	0.0	+1.5
	Subject C G-4C-37	5	9.4	1.3	11.1	1.5	-	-
		10	13.5	1.9	14.8	2.1	-	-
		15	16.5	2.3	17.3	2.4	+3.7	+2.5
Ankle plantar flexion	Subject B G-3C-14	5	5.0	0.7	4.4	0.6	-	-
		10	8.5	1.2	7.7	1.1	-	-
		15	11.7	1.6	11.2	1.6	+1.5	+4.2
	Subject C G-4C-37	5	7.6	1.1	7.7	1.1	-	-
		10	12.2	1.7	12.5	1.7	-	-
		15	18.1	2.5	17.3	2.4	+3.2	+4.0

*Dates of measurements:

Subject B (Chidsey), hip and knee, 7 August 1967;
ankle, 20 November 1967

Subject C (Gafvert), 20 November 1967

TABLE 3-11

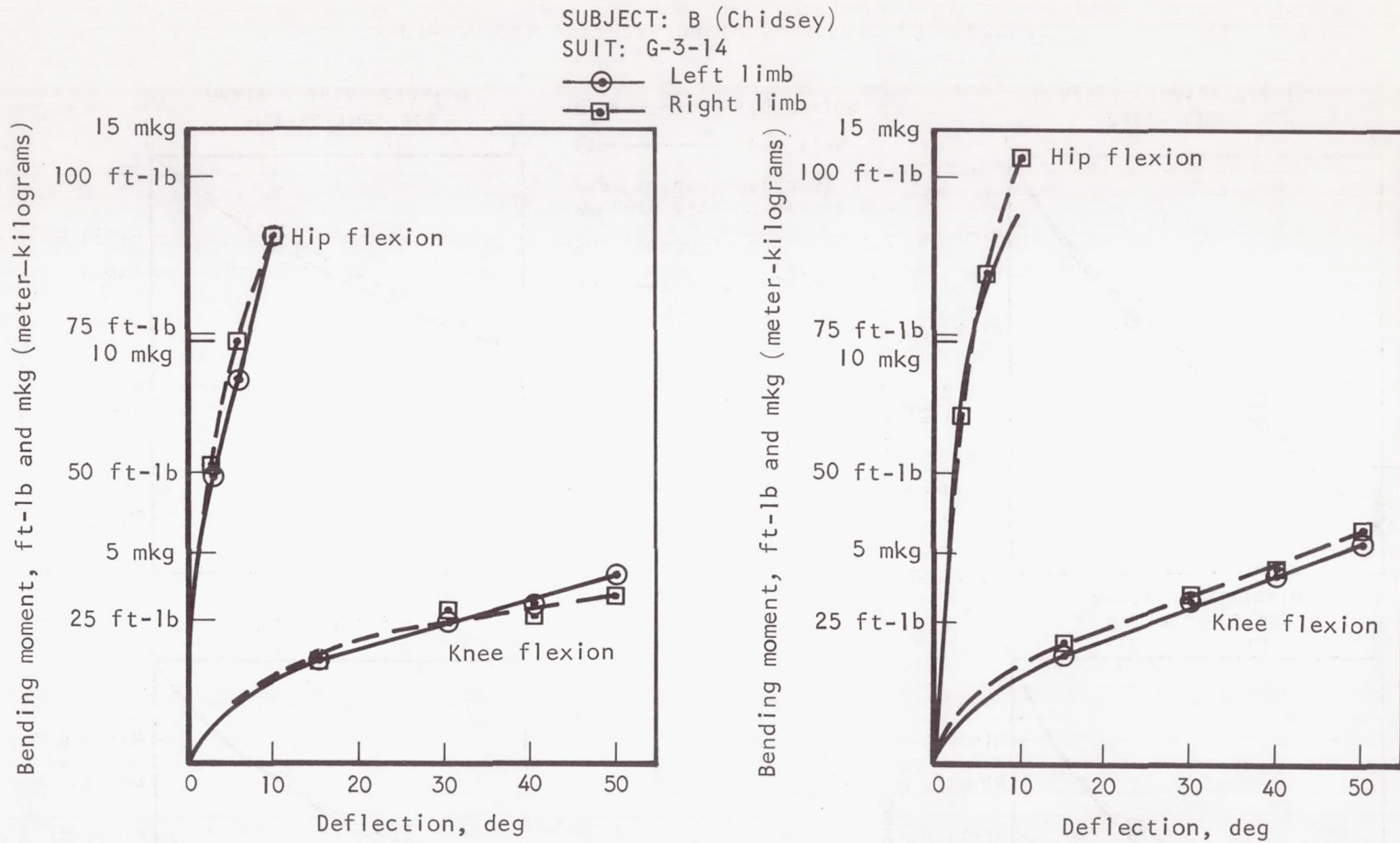
INCREMENTAL DEFLECTION CHARACTERISTICS OF PRESSURE
SUITS, USING SPECIAL SUBJECTS
(COMPLETION OF WALKING MODES)

Mode	Subject* and Suit	Deflection Angle, deg	Limb				Reset Angle, deg	
			Left		Right		Left	Right
			ft-lb	mkg	ft-lb	mkg		
Hip flexion	Subject B G-3C-14	3	62.60	8.64	60.27	8.32	-	-
		6	82.91	11.44	83.42	11.51	-	-
		10	94.19	13.00	104.34	14.40	+0.2	+0.3
	Subject C G-4C-37	3	53.9	7.44	53.63	7.40	-	-
		6	71.78	9.91	74.59	10.29	-	-
		10	88.29	12.18	89.39	12.39	0.0	-0.8
Knee flexion	Subject B G-3C-14	15	18.89	2.60	21.16	2.92	-	-
		30	27.68	3.82	29.30	4.04	-	-
		40	32.47	4.48	32.97	4.59	-	-
	Subject C G-4C-37	15	21.41	2.95	21.07	2.91	-	-
		30	28.76	3.97	28.39	3.92	-	-
Ankle dorsiflexion	Subject B G-3C-14	5	11.03	1.52	10.17	1.40	-	-
		10	15.19	2.10	13.54	1.87	-	-
		15	18.57	2.56	15.22	2.10	+1.0	+0.7
	Subject C G-4C-37	5	13.05	1.80	12.14	1.68	-	-
		10	16.52	2.28	15.82	2.18	-	-
		15	19.29	2.66	17.65	2.44	-0.3	-1.7
Ankle plantar flexion	Subject B G-3C-14	5	10.11	1.40	9.70	1.34	-	-
		10	15.21	2.10	14.52	2.00	-	-
		15	22.44	3.10	21.8	3.01	+0.7	0.0
	Subject C G-4C-37	5	12.36	1.71	9.83	1.36	-	-
		10	17.05	2.35	15.30	2.11	-	-
		15	24.02	3.31	20.68	2.85	-0.2	+0.3

Dates of measurements:

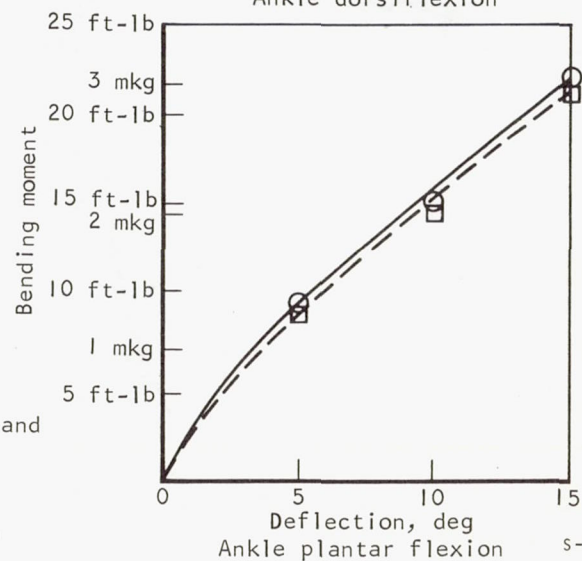
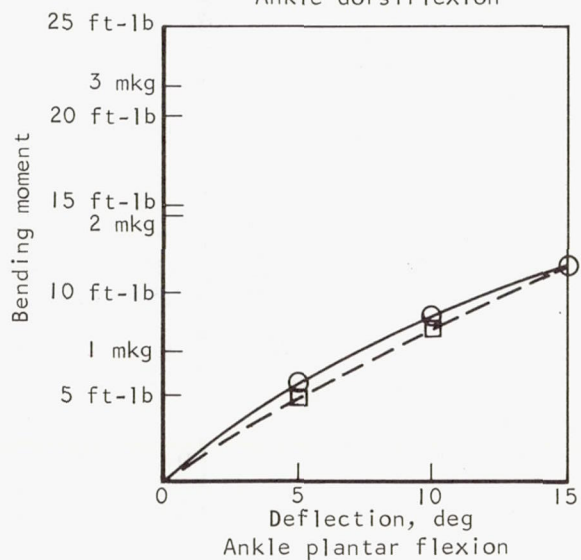
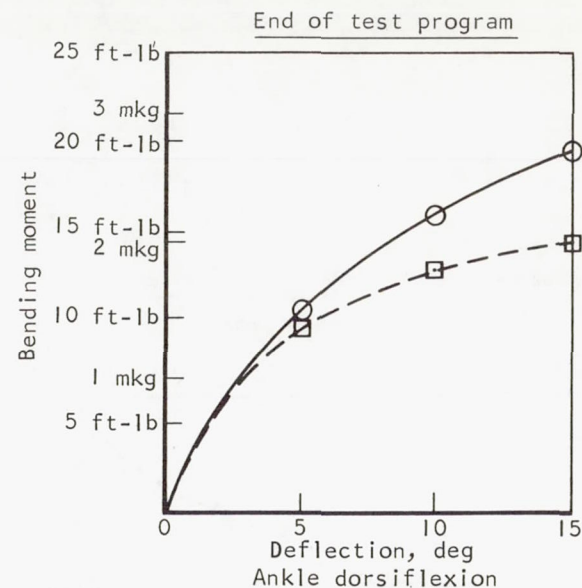
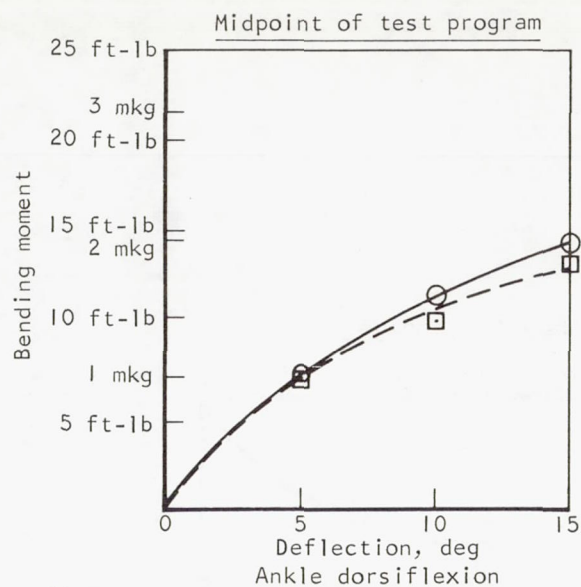
Subject B (Chidsey), 11 April 1968

Subject C (Gafvert), 9 April 1968



S-42634

Figure 3-49. Hip and Knee Deflection Data (Subject B)



Subject: A (Chidsey)

Suit: G-3C-14

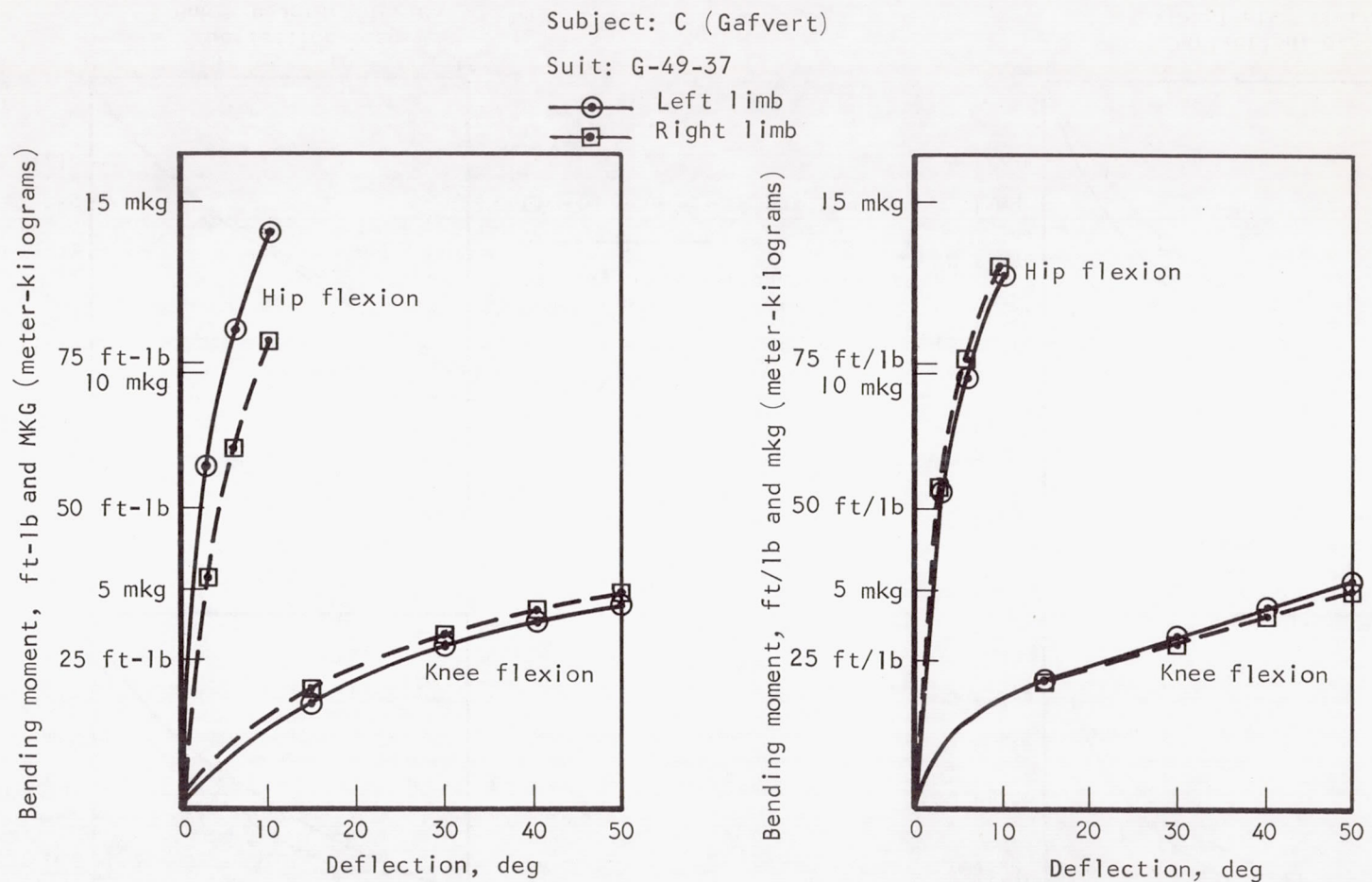
Moments given in ft-lb and
mkg (meter-kilograms)

○ ——— Left limb

□ - - - - Right limb

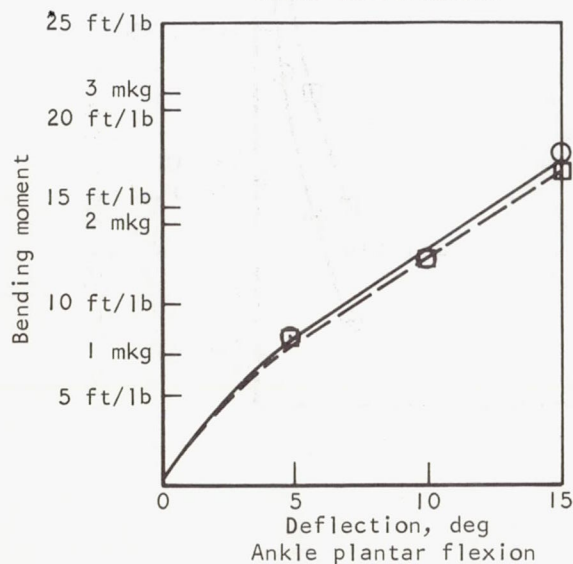
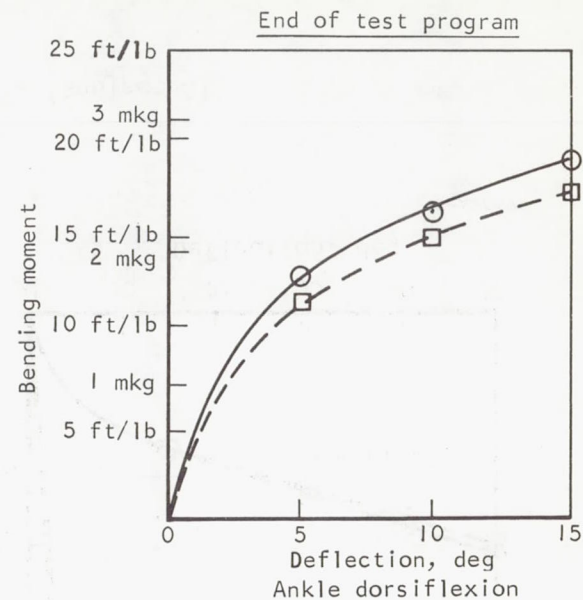
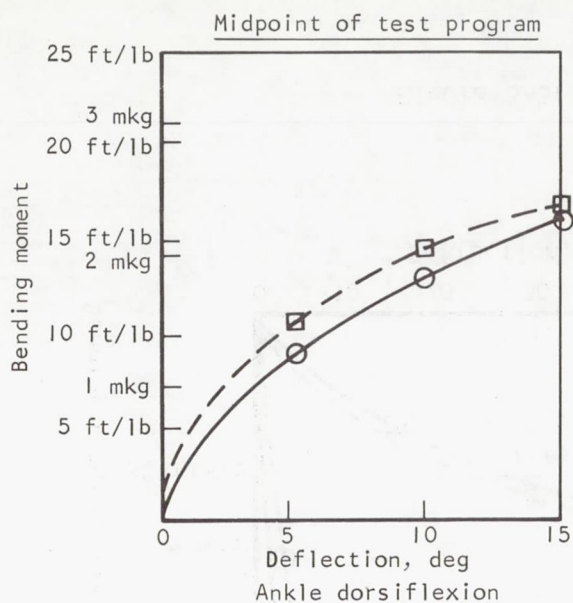
S-42650

Figure 3-50. Ankle Deflection Data (Subject B)



S-42649

Figure 3-51. Hip and Knee Deflection Data (Subject C)



Subject: C (Gafvert)
 Suit: G-4C-37
 Moments given in ft/lb
 and mkg (meter-kilograms)

○ ——— Left limb
 □ - - - Right limb

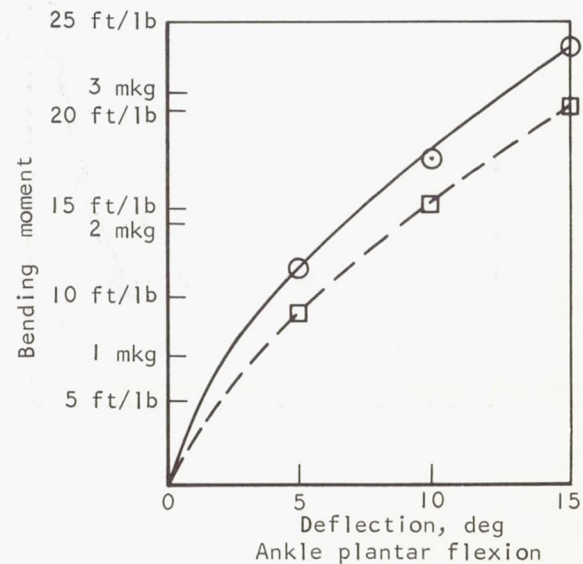


Figure 3-52. Ankle-Deflection Data (Subject C)

2. Suit repairs.— During this test program many repairs were made on the suits, including bladder patching, restraint garment reweaving, and reinforcing of weakened areas, particularly on the boots.
3. Boot lacing and straps.— If the boot lacings or straps were either loose or tight for each test, which could easily result from either item 1 or 2, the ankle bending moment would be either greater or less.
4. Method of measuring.— The method used was investigated for repeatability and found to be repeatable if proper care is taken in locating the goniometer and applying the force. To minimize the error due to methodology, each deflection force was accomplished six times and the mean used. Another possible error is the proper calibration of the load cell and recorder.

Comparison of the bending moments between tests is not recommended because of the above factors. Statistical analysis of the deflection data showed that the degree of suit fatigue encountered was not significant.

The largest source of error was the variation encountered in positioning the goniometer for angular measurement. The location of the goniometer was found to be critical in reading actual deflections. The standard followed was to locate the goniometer at such a point to make it most sensitive to angular deflections. Any deviation from this position caused significantly different readings. This deviation was minimized by moving the joint in the desired measurement direction and relocating the goniometer to read the true (maximum) deflection.

Even though this error is inherent in using this method the data were found to be repeatable if proper care is used to establish the location of the goniometer. This procedure of indexing may be used in all suit testing, even though it requires a visual observation and a manual adjustment.

The suit bending points do not necessarily coincide with the anthropometric location of the subject's joint and presents the possible variations of subject's suit fit since the suits were actually made for specific individuals. This deviation from a perfect fit would also influence the value measured. The mean values initially measured are representative of the Gemini suit configuration.

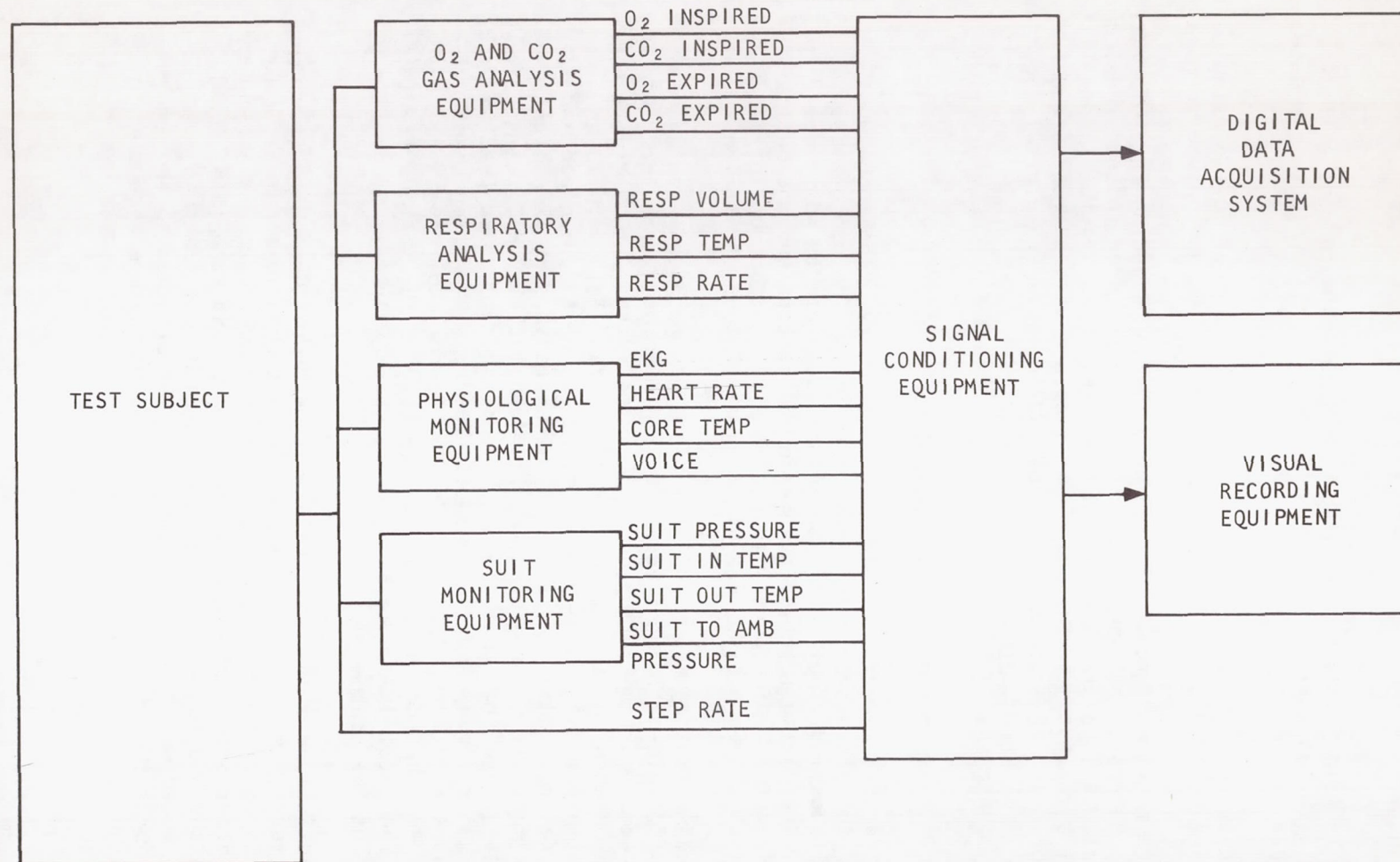
PHYSIOLOGIC AND METABOLIC APPARATUS

Instrumentation

The physiologic instrumentation used to determine the various parameters for these experiments is listed in Table 3-12 and shown schematically in Figure 3-53. In addition to the analog data collection system, provisions were made for an analog-to-digital conversion system with an automatic recording of all the digital data on punched paper tape. The format of this tape was programmed to match the computer link located within the test facility. With the digital

TABLE 3-12
PHYSIOLOGIC INSTRUMENTATION FOR DATA COLLECTION

Parameter	Sensor Accuracy	Recording Device Accuracy
Inspired/expired O ₂ fraction	Beckman F-3 $\pm 1\%$	Brown Recorder - 2 channel $\pm 1\%$
Inspired/expired CO ₂ fraction	Beckman IR-15A $\pm 1\%$	Brown Recorder - 2 channel $\pm 1\%$
Expired volume	Franz-Mueller Respirometer $\pm 1\%$	Special modification for electrical output to offner Dynograph ± 2 liters
Suit gas flow	Meriam Flowmeter $\pm 1\%$	Manual recording
Suit temperature in	Cu-Co Thermocouple $\pm 0.75\%$	Brown Multipoint Recorder $\pm 1\%$
Suit temperature out	Cu-Co Thermocouple $\pm 0.75\%$	Brown Multipoint Recorder $\pm 1\%$
Suit pressure	Sathan Pressure Transducer $\pm 1\%$	Offner Dynograph $\pm 1\%$
ECG - heart rate	ECG/Cardio Tachometer $\pm 1\%$	Offner Dynograph $\pm 1\%$
Core temperature	Thermistor $\pm 1\%$	Offner Dynograph $\pm 1\%$
Respiration rate	Cu-Co Thermocouple $\pm 0.75\%$	Offner Dynograph $\pm 1\%$
Suit dew point in	Cambridge Dewpointer $\pm 1\%$	Brown Multipoint Recorder $\pm 1\%$
Suit dew point out	Cambridge Dewpointer $\pm 1\%$	Brown Multipoint Recorder $\pm 1\%$
Franz-Mueller temperature	Cu-Co Thermocouple $\pm 0.75\%$	Brown Multipoint Recorder $\pm 1\%$
Ambient pressure	Mercury barometer, Wallace and Tiernan Gauge $\pm 0.25\%$	Manual recording
Ambient temperature	Cu-Co Thermocouple $\pm 0.75\%$	Brown Multipoint $\pm 1\%$
Treadmill velocity	Tachometer $\pm 5\%$	Offner Dynograph $\pm 1\%$
Subject weight	Buffalo Scale $\pm 0.25\%$	Manual recording
Subject height	Meter stick $\pm 0.1\%$	Manual recording
Surface area	Dubois Nomogram	Manual recording
Gravity gradient	Load cell $\pm 5\%$	Manual recording



A-34960-A

Figure 3-53. Data Collection System Block Diagram

recording system, it is possible to calculate the data for each mode as it is accumulated or as often as desired. Thus, it is possible to evaluate the data as they are obtained.

The digital data acquisition system comprises a 20-channel multiplexing unit, an amplifier, an analog-to-digital converter, a buffer unit, and a tape perforator.

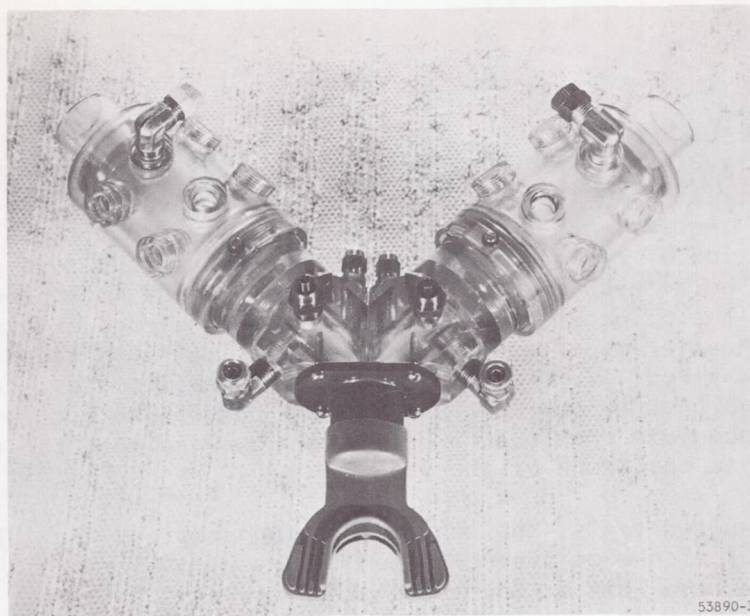
All parameters require signal conditioning prior to recording the information. Power sensitivity, balance, and range adjustments were included in the signal conditioning equipment. All information recorded on the digital system is conditioned for a dc output of 0 to 10.0 mv. Standard system accuracy is $\pm 0.1\%$. Standard system quantization using the successive approximation analog-to-digital converter is three digits (1 part in 1,000).

Metabolic Rate Apparatus

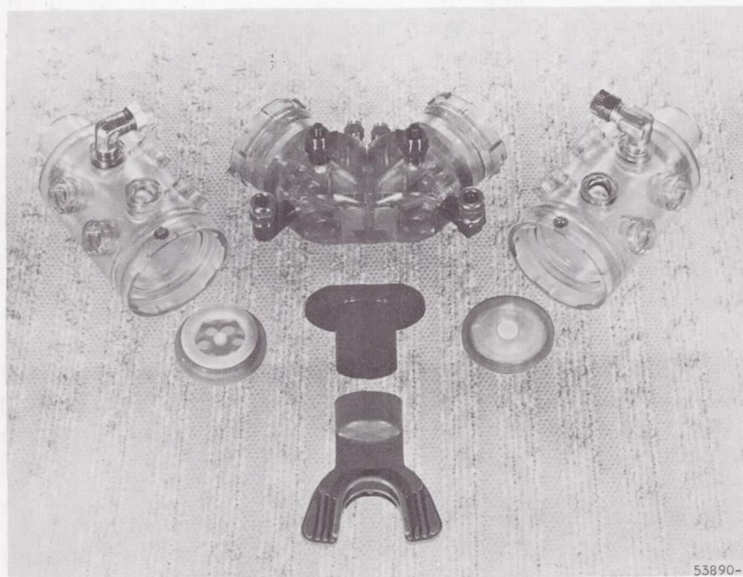
Metabolic rates were measured by indirect calorimetry. The technique employs the use of the AiResearch bifurcated mouthpiece. The use of this mouthpiece necessitates modification of the helmet faceplate to admit access of three 1-in. tubes, one on the right side, one in the center, and one on the left side of the faceplate. The center tube allows easy attachment of the bifurcated mouthpiece by means of a leak-tight quick-disconnect fitting.

The bifurcated mouthpiece shown in Figure 3-54 was machined from an elastomeric compound of double-wall construction to minimize heat transfer. An epoxy septum separates the inspiration and expiration systems, thus minimizing thermal conduction between the two systems at the mouth. This permits an accurate determination of the true physical conditions of the inspired and expired gases, if desired. Upon inspiration, a low-pressure-drop inspiration check valve in the mouthpiece (pressure drop less than 0.5 in. H₂O) opens, allowing the inspiration gas to flow into the mouth on demand. Upon expiration, the inspiration check valve closes and the low-pressure-drop expiration check valve (pressure drop less than 0.5 in. H₂O) opens, allowing the expired gas to flow from the bifurcated mouthpiece through a flexible hose to the various items of instrumentation. The total deadspace between the check valves is 56 cc (i.e., 28 cc on each side of the septum).

A rubber athletic type of mouthpiece is inserted into the subject's mouth. During the suited tests, this rubber mouthpiece is attached to the metal tube in the center of the faceplate to which the bifurcated mouthpiece is attached. The weight of the bifurcated mouthpiece is supported by the faceplate. During the unsuited tests the subject wears an aviation-type helmet. An L-shaped bracket, which can be adjusted in three dimensions, is attached to the top of the helmet and supports the weight of the bifurcated mouthpiece assembly. Thus the bifurcated mouthpiece, with the rubber mouthpiece directly attached to it, moves in relation to the subject's head.



53890-3



53890-7

Figure 3-54. Bifurcated Mouthpiece

Respiratory System

For the suited tests the basic respiratory system is shown in Figure 3-55. The suit is ventilated by the environmental control system which is described earlier in this section, under "Pressure Suits." The inspired air is drawn from the right side of the helmet through a hose connected to a port in the faceplate. The hose leads externally to the bifurcated mouthpiece. The expired gases pass from the bifurcated mouthpiece through a second external hose leading to a Franz-Mueller-type respirometer which is attached to the subject's backpack. The expired volume is measured by the respirometer. A third hose conducts this gas back to the left side of the helmet where it passes through a port in the faceplate and is then deflected downward into the airstream from the helmet to the trunk of the suit.

For the unsuited tests, the subject breathes ambient air. The inspiratory side of the bifurcated mouthpiece is open to the atmosphere. This expired gas is passed to the respirometer mounted on the subject's backpack. After passing through the respirometer, these gases are exhausted to the atmosphere.

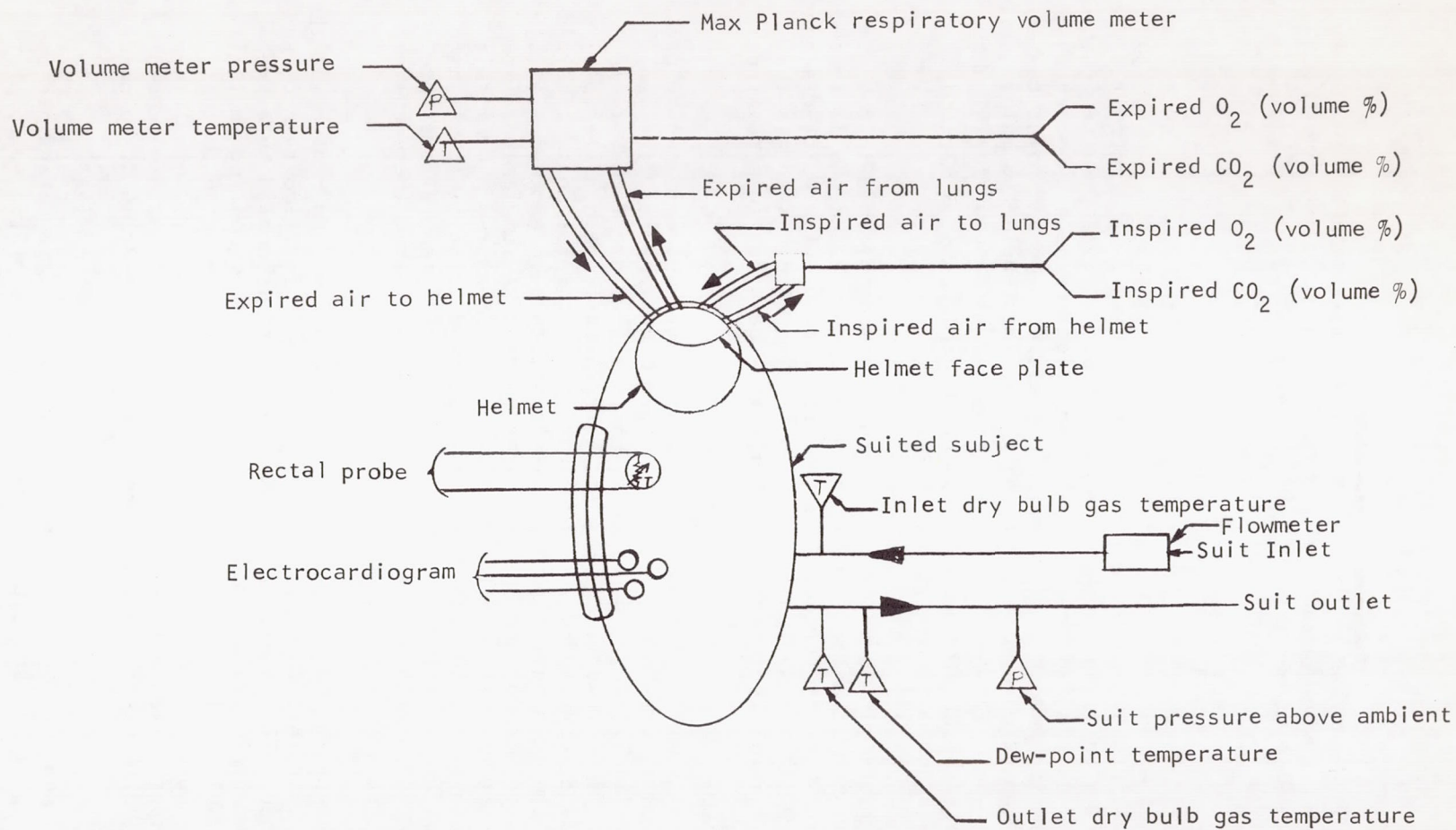
Gas Analysis

Samples of inspired and expired gas were routed to Beckman F-3 and IR-15A instruments for measurement of oxygen and carbon dioxide fractions. The time constants for the sensors are given in Appendix F.

Minute Volume Measurement

The respiratory minute volume is determined by passing the expired gas through a Franz-Mueller modification of the Kofranyl-Michaelis-type dry gas meter (Model 59, Max-Planck Institute for Work Physiology). This instrument, which was developed to determine the minute volume of humans performing various work loads, is ideally suited for these tests. The gas meter was encased in a pressure-tight cylindrical housing with a plexiglass window permitting a constant visual readout. Total pressure and dry-bulb temperature of the gas at the meter were monitored and accounted for in all quantitative measurements. The respiration gas meter was calibrated to insure an accurate and precise volumetric measurement.

For measuring minute volume rate, a magnetic reed-type switch was mounted on the respirometer. The switching signal is fed into a ramping circuit that produces an accumulative breath volume signal. The respirometer has a volume counter mounted on the instrument. The switching signal was also fed into an Offner Dynograph recorder for visual monitoring.



A-28980

Figure 3-55. Basic Respiratory System

MISCELLANEOUS EQUIPMENT AND APPARATUS

This subsection describes and illustrates additional apparatus used in conducting the tests, including the environmental control system, mounting shells, backpacks, and respirometers.

Environmental Control System

The environmental control system (ECS) used in this program was designed as an open loop suit pressurization and ventilation system. It controlled the suit ventilation flow rate, suit inlet dry bulb temperature, and suit-to-ambient differential pressure. In addition, it was used to determine and record the suit outlet ventilation temperature, flow rate pressure, and dew point temperature. The ECS is mounted on a mobile cart which was located in the main instrumentation control room. Insulated copper ducting and insulated flexible hose were used to connect the ECS to the space suit. Figures 3-56, 3-57, and 3-58 are front, back, and end views of the ECS.

Operation of the ECS in the open-loop circuit is accomplished in the following manner: cryogenic oxygen, cryogenic air, or compressed gas is routed through a vaporizer, which is connected to the ECS by means of a quick-disconnect hose, and is supplied to the system in a gaseous state. The gas enters the system at the suit circuit heat exchanger where it is adjusted to a desired dry-bulb temperature.

From the heat exchanger, it flows through a reheater where it can be heated to a desired suit-inlet, dry-bulb temperature. From the reheater, the gas passes through a Meriam laminar-flow element, where the volume flow rate is measured. From the flow element, the gas is then routed through a flexible, temperature-controlled, convoluted hose and into the suit inlet port. The gas then exits through the suit outlet port and is routed through another flexible, temperature-controlled, convoluted hose and into another Meriam laminar-flow element where the suit exhaust ventilation flow rate is measured. From this flow element, the gas passes through a manually operated valve, which is used to regulate the suit back pressure or suit-to-ambient differential pressure. At this point, the gas is exhausted to ambient, thus completing the open-loop circuit.

Excess water vapor in the suit exhaust gas is condensed and removed at the suit heat exchanger; in this manner, the suit inlet dew point temperature can be readily maintained. The gas-to-liquid heat exchanger is cooled by a Freon refrigeration system employing a water-glycol mixture as the cooling medium. The suit inlet and suit outlet laminar flow elements are connected to their respective inclined water manometers for a more accurate measurement of the pressure drop across the flow matrix. All dry-bulb temperatures are sensed by copper-constantan thermocouples and are read on a Honeywell-Brown strip chart recorder.

The suit inlet and suit outlet dew point temperatures are determined by two AiResearch dew point measurement instruments. Samples of the suit inlet and suit outlet gas are picked up independently at the suit inlet and suit outlet quick-disconnect fittings and routed through temperature-controlled flexible

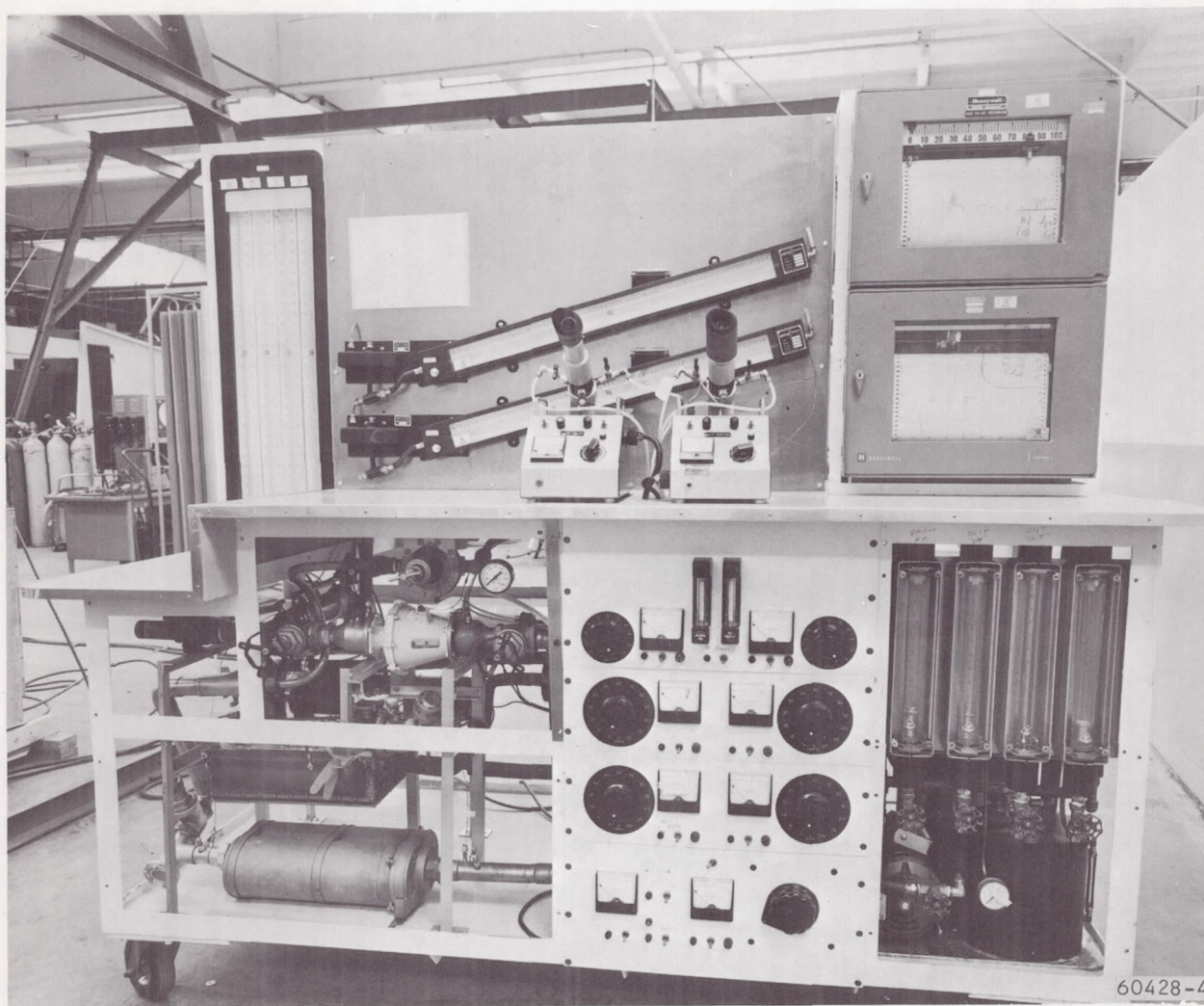


Figure 3-56. Mobile ECS, Front View

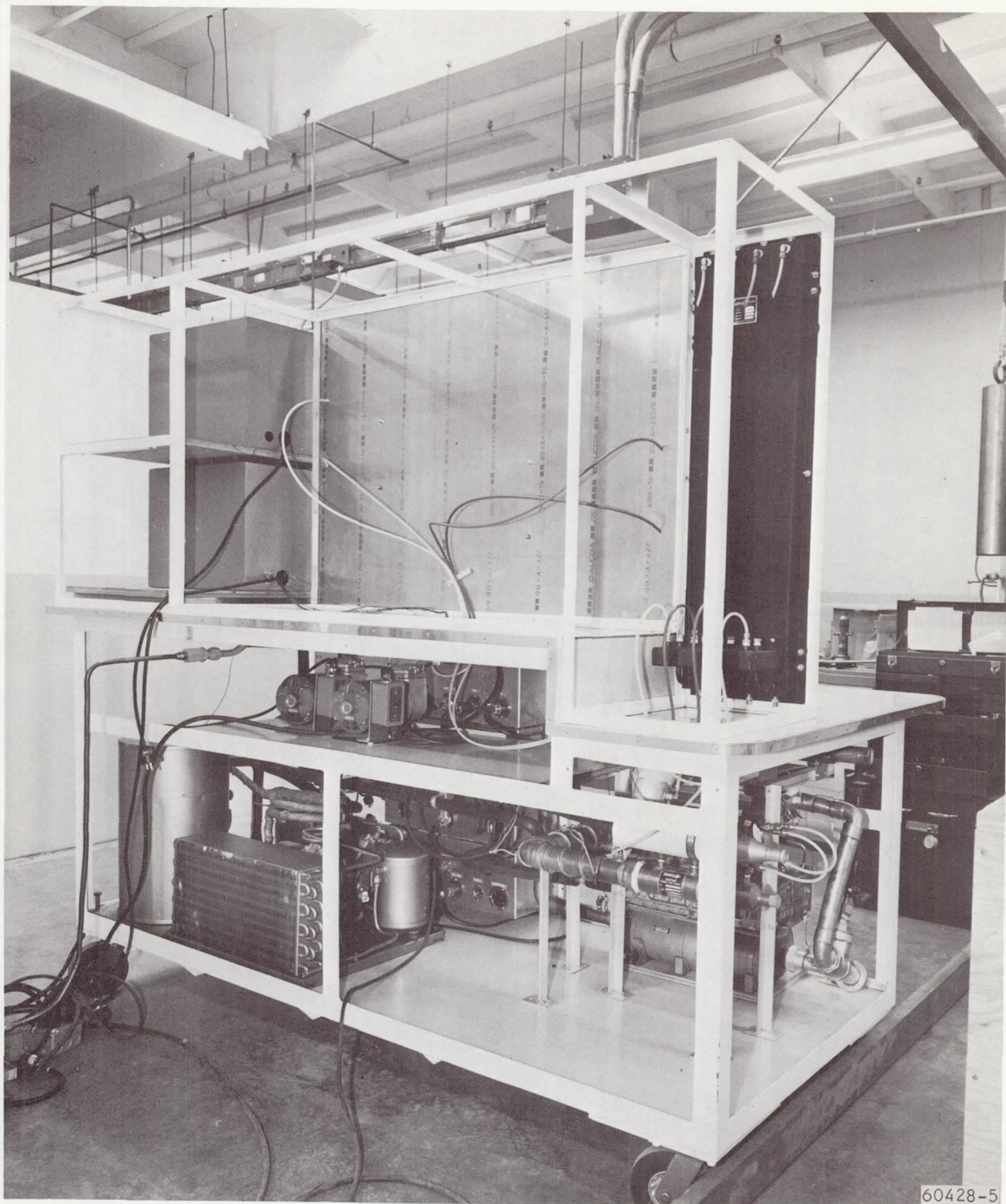


Figure 3-57. Mobile ECS, Back View

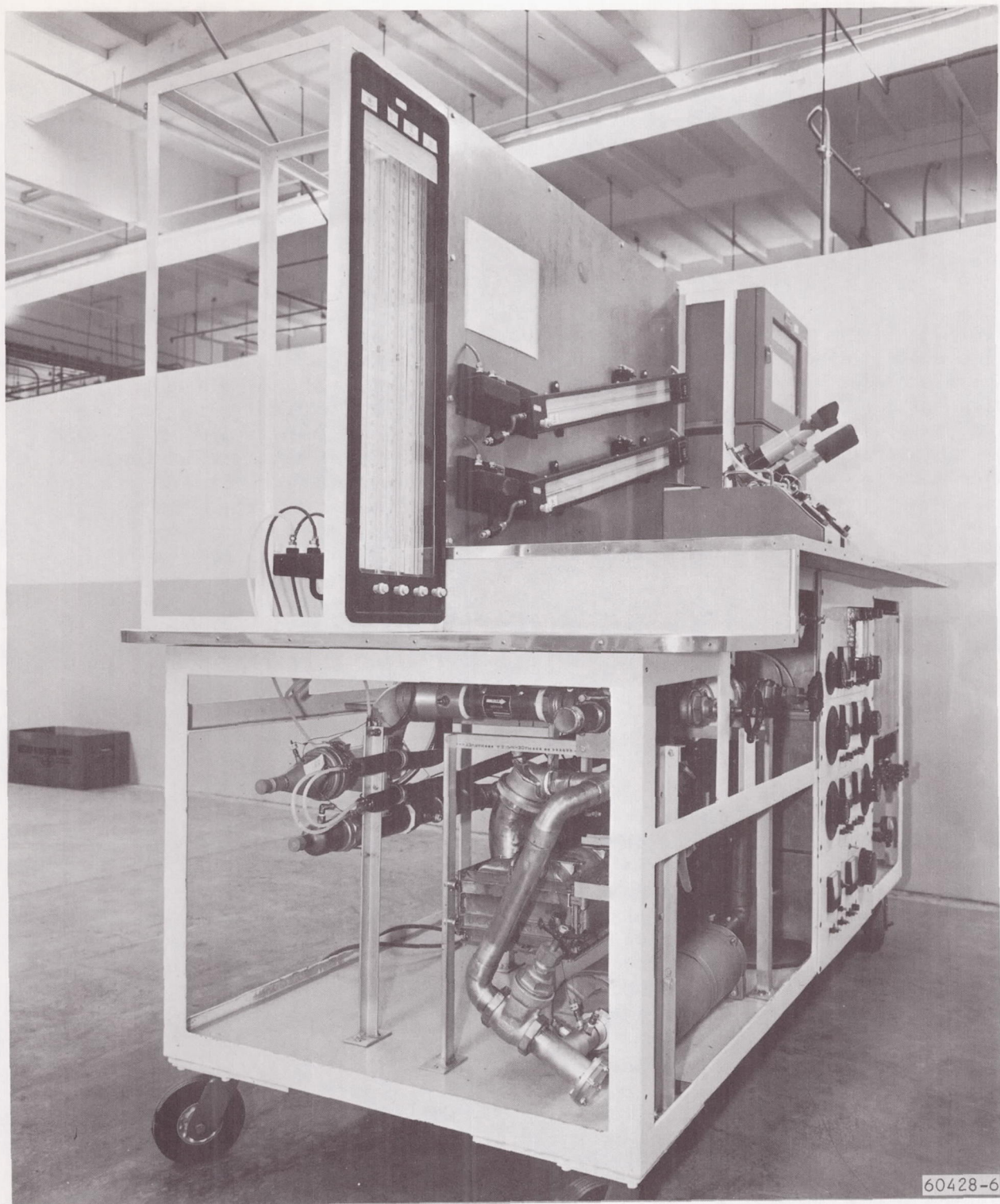


Figure 3-58. Mobile ECS, Left End View

tubes to their respective dew point cells. The gas enters the cell and passes over a glass/chromium mirror that is mounted on a copper base. The copper base extends into a carbon-dioxide-cooled methanol-alcohol bath heat sink that is used to lower the surface temperature of the mirror to the point where dew forms on the mirror. A nichrome-wire heating element is wound around the mirror base and is used to heat the mirror surface to any desired level above dew point temperature. When the electric current to the mirror heater is reduced, the mirror surface cools to the point where dew, caused by the water vapor in the gas, forms on the mirror.

An incandescent light inside the cell is normally reflected away from the mirror when it is dry and thus cannot be perceived. When dew forms, the light is immediately dispersed and reflected from the mirror and through a four-power microscope mounted on the dew point cell. The observer, or dew point instrument operator, can instantaneously perceive the reflected light. At this point, he presses a button on the instrument to index the temperature as analyzed from the mirror thermocouple measurement. This temperature trace is sensed by a thermocouple which is imbedded just beneath the surface of the mirror. In this manner, the mirror surface temperature, thus the dew point temperature, can be measured to $\pm 1^{\circ}\text{F}$. Technicians trained to use these instruments can confidently operate with a reproducibility of $\pm 0.5^{\circ}\text{F}$ of the actual dew point.

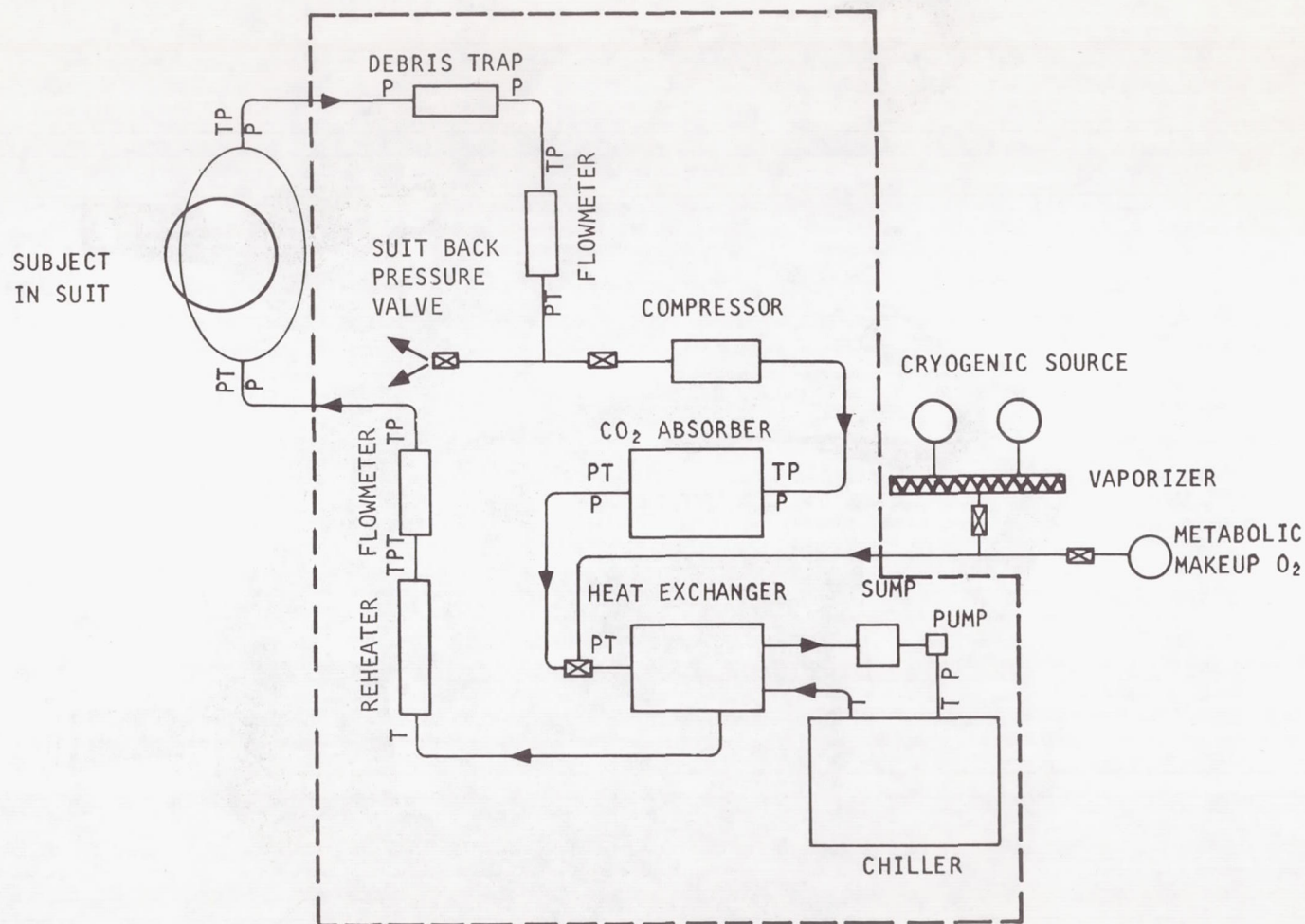
These instruments, along with the pressure manometers and temperature recorders are mounted on the tabletop of the ECS cart to minimize time constants and sample line lengths, i.e., sample transport time. Figure 3-59 is a schematic of the mobile ECS.

Mounting Shell

The mounting shells shown in Figure 3-60 were adapted for all methods of simulator suspension for simplicity and uniformity between suspensions. The shell encloses the torso of the pressure suit, distributes the suspension loads over large areas, and provides a stable and uniform structure for suspension and attachment of equipment. The hip and shoulder areas were cut so that the rigid shell does not interfere with leg or arm movements. The fiber-glass shell was lined with a plastic foam to eliminate irregularities in matching the suit configuration. The front piece shown on the right is cut out for the ventilation and instrumentation umbilicals and for the pressure suit helmet adjusting strap. The backpack is secured to this shell to ensure uniformity of position from test to test.

Basic Backpack and Respirometer

The backpack shown in Figure 3-61 is the basic backpack which was used for all tests on the inclined-plane simulator. The total Earth weight of the pack, including the weight of the shell and other equipment, is adjustable by placing lead weights as shown in the pack. These weights can be placed so that the pick-up suspension point of the pack is at the c.g. of the pack for any weight.



A-23289

Figure 3-59. Mobile ECS Schematic

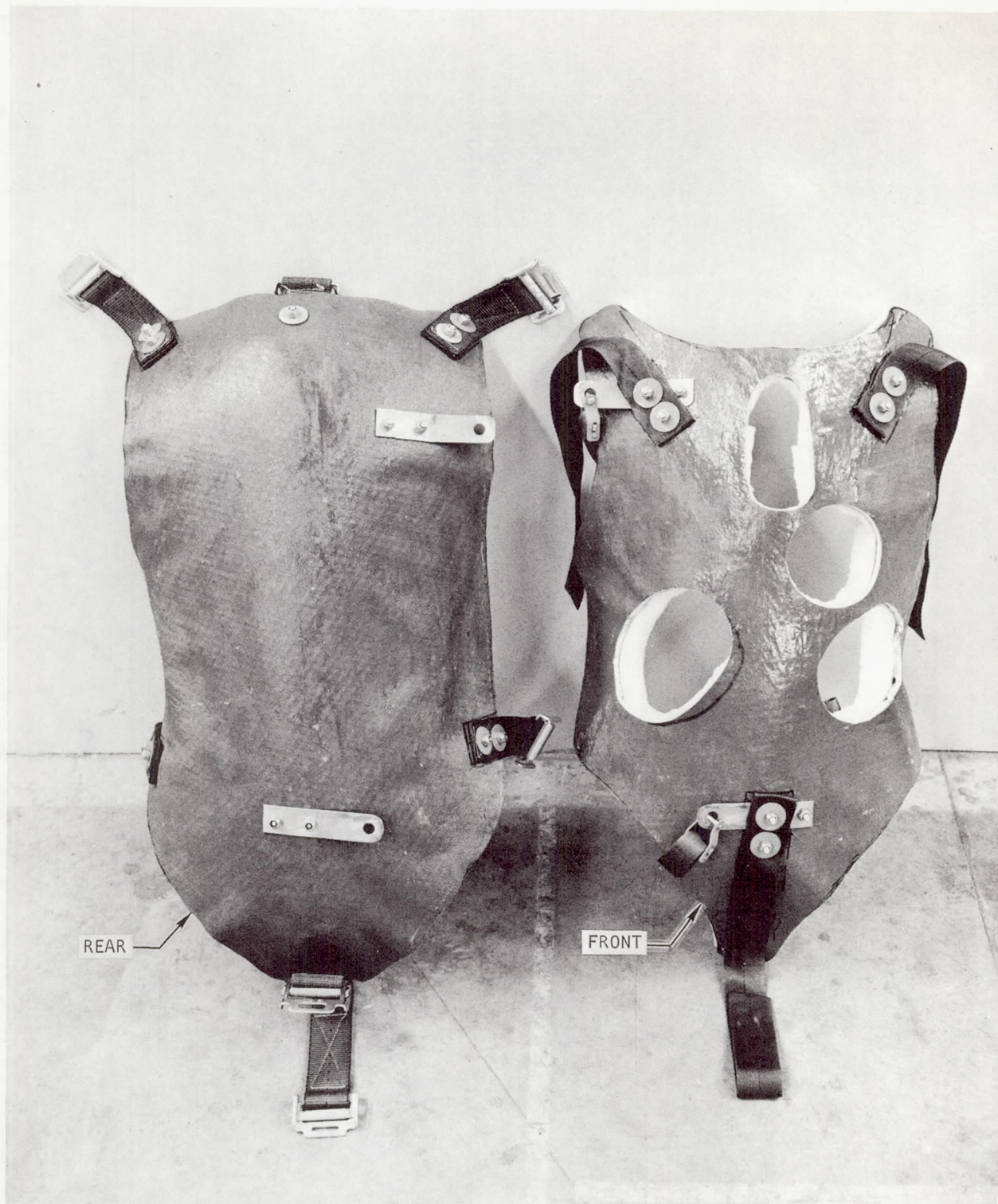


Figure 3-60. Mounting Shell

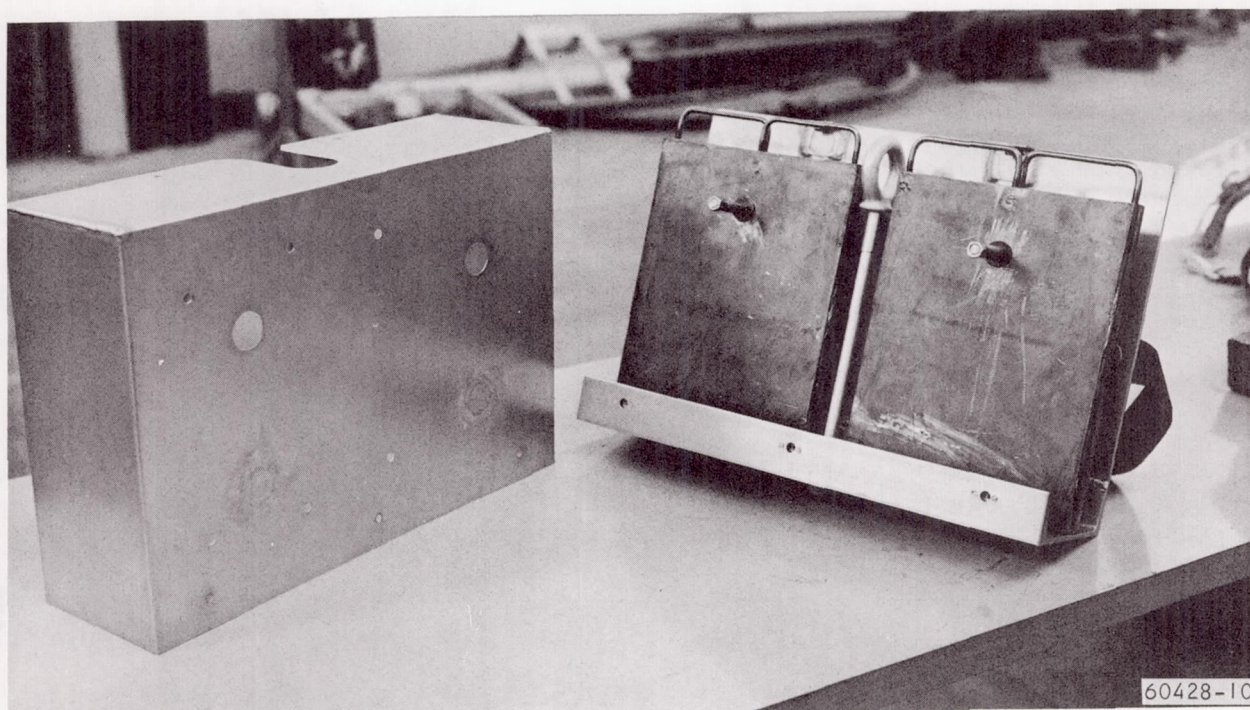


Figure 3-61. Basic Backpack with Weights Inserted and Cover Removed

The pack cover was provided for appearance and the mounting of other test gear as illustrated in Figure 3-62. This figure shows the respirometer used for respiration volume and for sampling of respired gases. Figure 3-63 shows a Max-Planck Institute respirometer enclosed in a special housing so that it is at the same pressure as the subject within the suit. This particular backpack was not usable with the vertical suspension "C" brace described earlier under "Lunar Gravity Simulators". However, the "C" brace, shell, and respirometer weighed slightly less than 70 lb and were weighted with ballast to bring the pack weight up to the 75 lb required for the tests. Individual item weights are shown in Table 3-13.

Liquid Air Backpack

Two liquid air backpacks used to ventilate and cool protective suits were modified to provide the ventilation, cooling, and pressurization of the suited subject for the basic training at Langley Research Center (LRC) and in initial subject orientation and training at AiResearch. The modification included increasing the flow rate by modification of the venturi orifice, sealing the system for pressurization adding a suit inlet hose adapter, a pressure gage, and a relief valve calibrated to relieve at 3.5 psig. This pack is shown in Figure 3-64 on a subject being trained on a small inclined-plane simulator. In this configuration, walkie talkie transceivers were adapted for intercom communication.

TABLE 3-13
INDIVIDUAL ITEM WEIGHTS

Item	Weight, lb
"C" frame with Franz-Mueller Respirometer mounted	60.38
Franz-Mueller hoses	3.03
Five clamps for hose connections	0.29
Fiber-glass front shell	4.83
Nosepiece, mouthpiece, and clamp	0.12
Helmet	5.05
Bifurcated mouthpiece with inspired hose	1.84
Total weight	75.54
Total backpack weight	70.37
Allowable balance weight	4.63

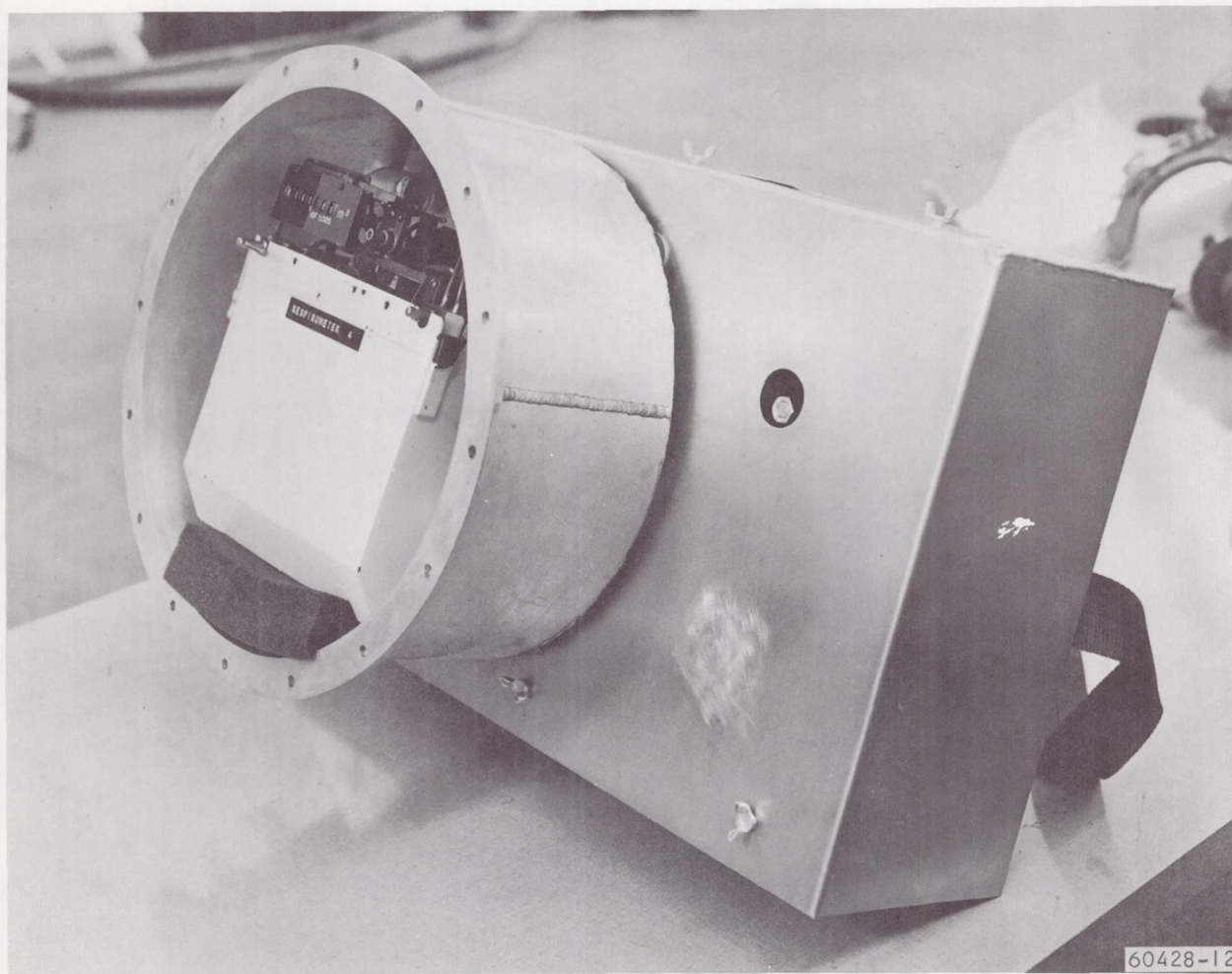
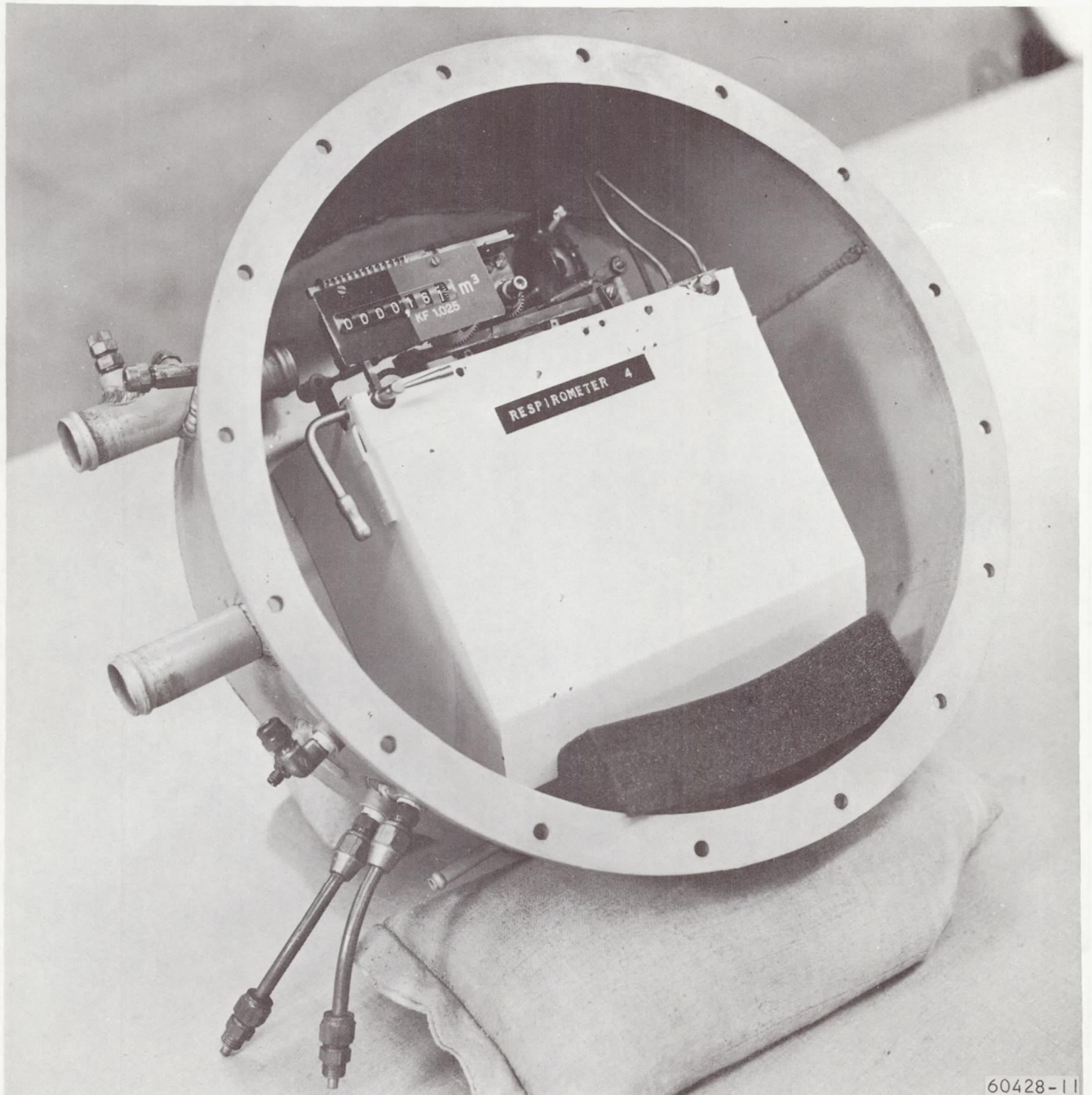


Figure 3-62. Weight Pack and Mounting of Respirometer



60428-11

Figure 3-63. Respirometer Assembly

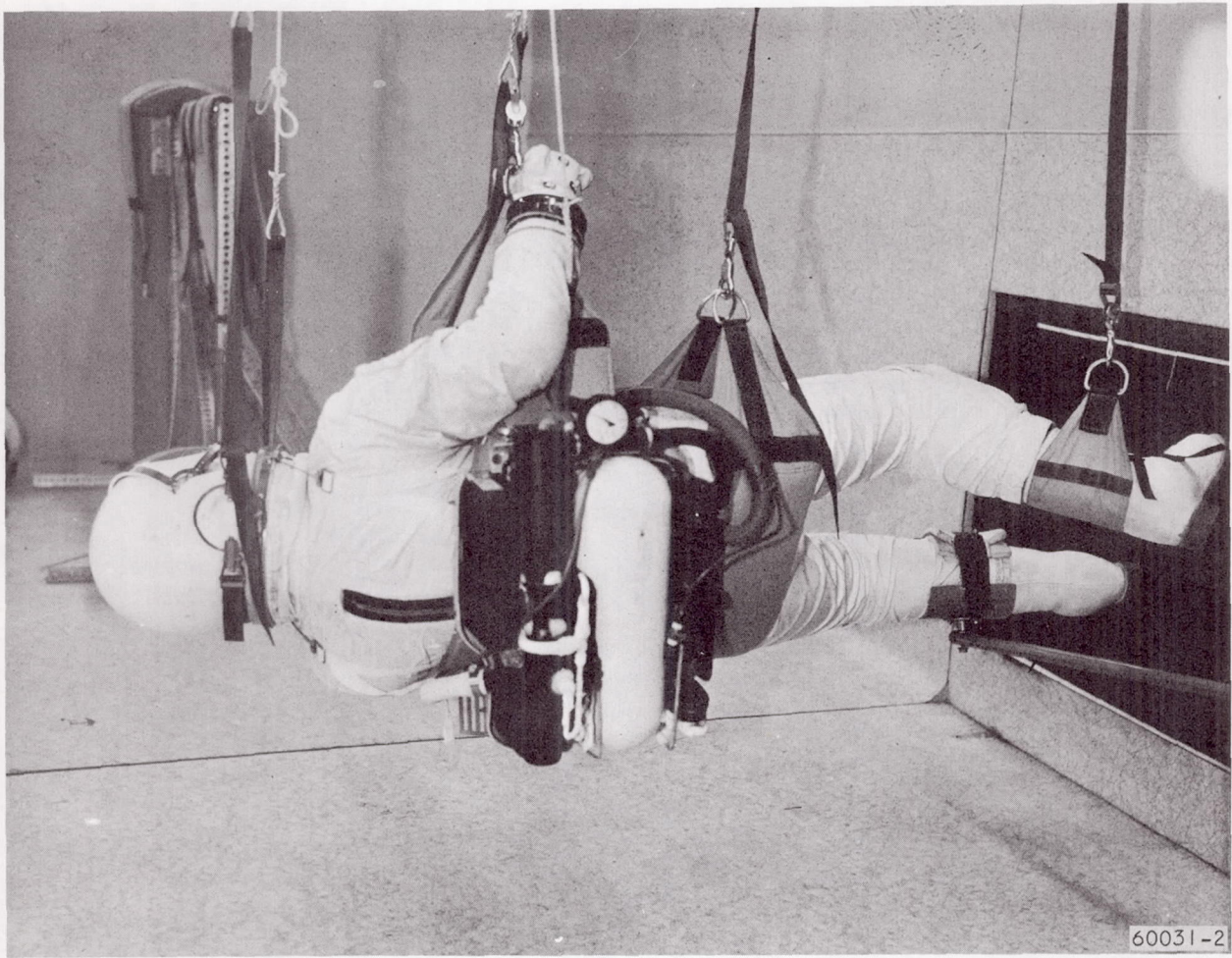


Figure 3-64 . Liquid Air Backpack on Subject in Training

Weighing Equipment

The scales used for weighing a subject are made by the Buffalo Company and are referred to as "Buffalo" scales. The weight of a subject can be determined to within ± 2 gm of his total body weight. These scales were cleaned, reassembled, and calibrated before testing started.

The ring load cells used for checking the simulated gravity in each system are constructed of a high-quality machined ring with attaching lugs on either end. A full bending bridge strain-gage arrangement is placed on the ring. This assembly is calibrated to read the tensile load applied in pounds.

Treadmill Speedometer

The treadmill speed was determined by a small generator assembly attached to the drive pulley of each treadmill system. Meters at the treadmill control and in the control room provided continual monitoring of belt speed. This system was calibrated by measuring actual belt length, timing the revolutions at various speeds with a stopwatch, and then adjusting the meter. The speed was checked again during each test and was held to ± 1 percent.

Ambient Pressure and Temperature Measurement

Ambient pressure was recorded for each test using a high quality aneroid barometer. The ambient temperature was measured using a thermocouple located in the test area and was recorded on the Brown recorder.

Air Supply

The air supply for the TOSS simulator was supplied by an AiResearch GPS-90 air turbine compressor.

GENERAL PROCEDURES

Preparation of Subjects

Test subjects were required to report for work one hour prior to a schedule test to permit time for medical checkup, weigh-in, application of instrumentation, and donning of a pressure suit. Each test subject was required to complete a questionnaire (Figure 3-65) prior to instrumentation and donning of the pressure suit. In addition, the subject was interviewed to determine if he had any symptoms that would indicate an ailment that might affect his ability to perform the tests or affect the data. If any doubt existed, the subject was examined by a physician and a decision was made on permitting the subject to participate in tests scheduled for that day.

SUBJECT QUESTIONNAIRE

DATE: _____

1. Name: _____ Nude wt: _____ Height: _____
2. How did you sleep last night? Soundly: _____
Light: _____
Fitfully: _____
If fitfully how many times did you
awaken? _____ times.
3. How many hours did you sleep? _____ hours.
4. Although directed not to imbibe alcohol, did you indulge?
What kind? _____ How many? _____
5. What were the basic components of last night's meal?

6. Did you have breakfast? _____
7. If so, what did you eat? _____

8. Did you have lunch? _____
9. What did you eat? _____
10. How do you feel generally? _____ Excellent _____ Good
_____ Fair _____ Poor
11. Do you have any significant symptoms to report?
(e.g., cold, aches, pains, etc.)
12. Do you think you will have any difficulty in completing today's test?

Figure 3-65. Subject Questionnaire

Basic instrumentation worn by the subject consisted of electrodes for continuous electrocardiogram recording and a thermister probe for recording rectal temperature. The electrocardiogram was taken using a three-electrode system consisting of a bipolar modified V_4 lead and a ground.

After the subject was cleared for test participation, the skin area at appropriate ECG electrode locations was shaved, then thoroughly cleaned with a 70-percent solution of isopropyl alcohol. The electrodes were attached using a double-adhesive colostomy tape and then covered with adhesive tape to prevent moisture penetration and to ensure adherence to the skin. The electrocardiogram tracings were then checked to determine signal adequacy.

Space suit donning was accomplished by the test subject with assistance from a suit technician. The subject then proceeded to the test area for hook-up with the applicable simulator.

Inclined-Plane Simulator Procedure

Upon arrival at the test site, the subject's bioinstrumentation was checked out by connecting the bioinstrumentation connector plug to the mating suit part. After completion of this check, the plug was disconnected to permit attachment of the molded fiber-glass shell to the subject. The shell was attached and positioned by utilizing straps equipped with quick-adjust fittings.

The ventilating gas hoses were attached to provide suit ventilation and the bioinstrumentation plug was again connected. The helmet was donned and all hose connections to the bifurcated mouthpiece and respirometer were completed. As a precaution, all connections were rechecked prior to pressurizing the suit to 3.5 psig.

The subject was then positioned on his left side with the feet on the inclined-plane treadmill and all support lines attached. The backpack for that specific test was mounted on the subject's back and locked in place. Alignment to the 9-1/2 deg treadmill was achieved by utilizing a special alignment bar to determine if the subject was vertical with respect to the treadmill surface. Adjustments were made as necessary.

The subject was then required to jump several times and to walk a short distance to determine if the trolley was functioning properly, if the left leg stabilizer bar had proper clearance, and if the backpack was positioned correctly and anchored firmly. Leakage at all hose connections, the bifurcated mouthpiece, and the respirometer were checked and instrumentation signals were observed prior to starting the actual test. Figure 3-66 is a procedure check sheet applicable to the inclined-plane tests.

Upon completion of the test, the subject was assisted from the simulator and permitted to remove the space suit, and the bioinstrumentation sensors were removed. The subject was then asked to comment on the test with respect to task difficulty, comfort, and other factors that may have affected performance.

SUBJECT _____ DATE _____

Item	Procedure	X	Comments
1	Check out bioinstrumentation		
2	Attach fiber-glass shell and position		
3	Attach vent hose and instrumentation plug		
4	Provide vent flow to subject		
5	Attach subject nose clip		
6	Don helmet and lock in place		
7	Connect hose to bifurcated mouthpiece and respirometer		
8	Pressurize suit		
9	Connect suspension lines to torso section		
10	Position subject on left side with feet on treadmill		
11	Attach safety line and helmet suspension line		
12	Attach leg suspension lines and step rate switch		
13	Position and attach backpack		
14	Exercise test subject and check recording and instrumentation		
15	Begin tests		

Figure 3-66. Inclined Treadmill Hookup Procedure and Check-out

TOSS Simulator Procedure

Prior to subject arrival, the turbine air compressor was activated and system airflow established. The "C" frame was neutrally balanced, and the air pads were pressurized and checked for correct operation. When the test subject arrived, a bioinstrumentation check identical to that performed on the inclined-plane simulator was made.

The test subject was then attached to the gimbal utilizing the fiberglass shell. Suit hoses and instrumentation plugs were connected and suit flow established. The subject's nose clip was applied and taped in place.

The helmet was donned and locked in place. The bifurcated mouthpiece and respirometer connections were made and checked. The suit was then pressurized to 3.5 psig.

After pressurization of the suit, turbine pressure was increased until a lifting force equal to the weight of the "C" frame assembly and subject was reached. The subject was then lifted from his feet and completely balanced in the pitch-and-roll axes by using lead weights as necessary. The pack system weight was brought to 75 lb, the subject's suit and system weight were determined, and the load cell was calibrated to zero.

At this point, turbine pressure was reduced and the subject was lowered to the treadmill to perform tasks such as jumping, walking, and standing to check out simulator performance. While these tasks were being performed, load-cell readings were taken to determine the correct turbine pressure setting to simulate the desired 1/6-g condition.

The basic procedure and checklist applicable to this simulator is shown in Figure 3-67.

Test Procedure

After check-out and calibration of all apparatus and instrumentation, the subject was placed in the simulator, the simulator check-out procedures were performed, and the tests were ready to commence. The first test point for every test condition was the measurement of resting metabolic rate. This was measured at time zero and +2 min. Upon recording +2 min of the data, the treadmill was started and the subject performed the scheduled task for a period of 14 min. Thus, at +16 min the treadmill was turned off. Recording of all physiological parameters continued until +22 min. The subject rested until all physiological parameters were normal for resting (e.g., heart rate, temperature). The second test could then commence. There was an absolute minimum period of 8 min (6 min at the end of one test, plus 2 min at the start of the next test) between periods of exercise on the treadmill. The average resting duration, however, was approximately 20 min.

SUBJECT _____ DATE _____

Item	Procedure	X	Comments
1	Activate TOSS turbine		
2	Balance "C" frame and check air pad		
3	Check out bioinstrumentation		
4	Attach subject to "C" frame using fiber-glass shell		
5	Connect bioinstrumentation plug and suit hoses		
6	Provide suit vent flow		
7	Attach subject's nose clip		
8	Install helmet and lock in place		
9	Connect bifurcated mouthpiece and respirometer hose		
10	Recheck all fittings and connections and communications		
11	Pressurize suit		
12	Lift subject off treadmill with turbine and balance subject in upright position		
13	Reset load cell		
14	Balance subject for pitch and roll		
15	Lower subject to treadmill surface		
16	Decrease turbine pressure until correct load cell reading is obtained		
17	Check load-cell function by having subject jump upward and land in vertical position		
18	Check system for leaks		
19	Begin tests		

Figure 3-67. TOSS Hookup Procedure and Check-out

The sequence of test events, especially velocities, was random among subjects to reduce the probability of other effects in the data.

Calibration of Gas Analyzers

All gas analyzer equipment was calibrated at least four times a day. Operating pressure for calibration was that of the gas analyzer during testing, i.e., suit pressure.

SECTION 4

SUBJECTS AND TRAINING

SUBJECT SELECTION

Six healthy male subjects were selected from the AiResearch test subject panel. Selection criteria were based upon suit fit, psychological and physiological reaction to stress-inducing situations, an ability to pass an FAA Class I flight physical, and physical fitness testing which included the Harvard Step Test and the Balke Test. The subjects chosen all had extensive experience in suit testing, in conjunction with a modified Hewes and Spady inclined-plane simulator and a 6-deg-of-freedom vertical suspension simulator.

The anthropomorphic data for the six subjects that participated in this program are given in Table 4-1. The obvious uniformity among the subjects is a result of the size requirements to fit the pressure suits available for this program. These subjects compare very closely to the body characteristics of the astronaut population, for this same reason. The only deviation from the characteristics of the astronauts is that the subjects in this program were younger.

TESTS FOR SELECTION

Basal Metabolic Rates

Basal and resting metabolic rates were determined to evaluate the possibility of any aberrations in the general condition of the body. Metabolic rates were determined by closed spirometry using a Goddard Pulmonet for all subjects. Each subject reported to the laboratory at the beginning of the work day and was instructed to lie down in a predesignated quiet area for a period of two hours. The subjects had been instructed not to eat any food after 9:00 P.M. the previous evening and were required to have at least seven hours of sleep. Upon completion of the two-hour rest, heart rate and oxygen consumption were measured in both the supine and sitting positions. The data are presented in Table 4-2.

Modified Harvard Step Test

Upon completion of the basal metabolic rate measurements, each subject performed a modified Harvard step test. The subject was required to step up to a raised surface, 45.7 cm from the floor, at a rate of 48 times per minute. The test was begun with the right foot on the raised surface and the left foot on the floor. At the first beat of a metronome, used as a guide for the subject's pace, the left foot was lifted to the raised surface; at the second beat, the foot was returned to the floor. This procedure continued until the

TABLE 4-1

ANTHROPOMORPHIC CHARACTERISTICS
OF TEST SUBJECTS

Subject	Age, years	Height,		Weight,		Body surface area, M ²	Lean body mass, kg
		in.	cm	lb	kg		
A (Billman)	24	68	172.7	149.3	67.73	1.81	56.46
B (Chidsey)	29	70	177.8	133.3	60.45	1.75	58.65
C (Gafvert)	24	68-3/4	174.6	147.3	66.82	1.82	52.01
D (Kern)	22	70-1/2	179.1	164.9	74.77	1.93	59.37
E (Paige)	31	70-1/2	179.1	148.3	67.27	1.85	57.18
F (Wallenius)	24	70	177.8	152.3	69.09	1.86	50.59

TABLE 4-2
 OXYGEN CONSUMPTION $\dot{V}O_2$ AND HARVARD STEP TEST RESULTS
 FOR TEST SUBJECTS

Subject	$\dot{V}O_2$ STPD, ml/min		V_{O_2}/BSA , ml/min/m ²		Step test duration		Pre-exercise heart rate	Post-exercise heart rate
	Supine	Seated	Supine	Seated	min	sec		
A (Billman)	197	231	125	146	3	0	64	116
B (Chidsey)	210	203	118	114	3	0	68	132
C (Gafvert)	223	246	119	132	3	0	48	136
D (Kern)	221	226	115	118	3	0	68	132
E (Paige)	232	260	126	141	3	0	64	124
F (Wallenius)	223	231	121	126	2	45	60	112

fifth time the left foot was lifted to the elevated surface; then the right foot was placed on the floor with the left foot kept on the raised surface. The right foot was then raised and lowered with every two beats of the metronome until the fifth time it was raised to the platform, at which time the procedure again reversed. This procedure was continued with the platform foot being changed with every tenth beat of the metronome for a period of three minutes, or until the subject stated he could not continue, whichever occurred first. Upon conclusion of the stepping exercises, the subject was seated in a chair and rested for one minute. After one minute, his heart rate was measured and recorded. The data for the heart rates are also presented in Table 4-2.

Modified Balke Test

Height, total body weight, and lean body mass of each subject were determined, and a modified Balke Test was accomplished. The data sheet used in determining the lean body mass of each subject is shown in Figure 4-1. The skinfold data used to derive the lean body mass of each subject is presented in Table 4-3. The results of these determinations and tests are presented in Table 4-4. The modified Balke test began with the subject walking at 3.5 mph on a 10-percent grade. The subject walked for two minutes and then breathed on a mouthpiece to a Tissot spirometer. He continued to walk for one more minute while gas samples were taken and data recorded. The grade was then increased to 12 percent, and after rest the subject resumed the same activities. This procedure was continued until the subject reached his maximum oxygen consumption rate. The oxygen consumption rates for each percent grade are compared by subject in Figure 4-2. The heart rates for each percent grade are compared by subject in Figure 4-3.

The results from the Harvard step test and the Balke Test indicated that all subjects were in above-average physical condition.

Preliminary Metabolic Rate Tests (1 G) Without Pressure Suit

Using a Goddard Pneumograph (spirometer) on a closed circuit, with the subject breathing 100-percent oxygen, a resting (seated) and a standing (1-g) metabolic rate was determined for each subject. The subjects were lightly clothed (shirt sleeves). Upon reporting for the test, the subject was seated for a 20-min period. After 20 min, he began breathing from the spirometer using a rubber mouthpiece and a nose clip. The subject breathed pure oxygen for 10 min. During the last 5 min, the volume of oxygen consumed was measured and the resting metabolic rate was computed from this.

Following the seated tests, the subject stopped breathing from the spirometer circuit, stood up, and remained standing for a total of 15 min. After the first 5 min, he again began breathing pure oxygen for another 10 min. During the last 5 min, the volume of oxygen consumed was measured and the standing metabolic rate was computed. Values obtained during these tests fall well within the expected normal range of values.

UNIVERSITY OF CALIFORNIA, LOS ANGELES
Department of Physical Education

Name: _____ Age: _____ Date: _____

Height: _____ ft. _____ cm.

Weight: _____ lbs. _____ kg. (M)

Vital Capacity: _____ mls. Residual Volume: _____ mls.

Skinfolds: Cheek: _____ mm Chin: _____ mm Chest: _____ mm Arm: _____ mm

Back: _____ mm Side: _____ mm Illiac Crest: _____ mm

Abdomen: _____ mm Knee: _____ mm Calf: _____ mm

Volumeter Readings:

Water Temp. (31°C): _____

(a) First Reading _____

(b) Intermediate Reading (navel) _____

(c) Total Submersion _____

Δ
a-c _____

Total Body Volume _____ Underwater Weight _____
(1cm = 12.5 lbs.)

VC + RV _____

Body Volume (V) _____

Specific Gravity _____

% Body Fat = $100 \left(\frac{4.201}{\text{Sp Gr}} - 3.813 \right)$

Fat = $4.861 (V) - 4.397 (M)$
= $(4.861) () - (4.397) ()$

= _____

LBM = $M - F$

= _____

Figure 4-1. Raw Data Sheet for Measurements Used in Calculating Lean Body Weight

TABLE 4-3
SUMMARY OF SKINFOLD DATA ON TEST SUBJECTS

Subject	Age, years	Height, in.	Weight, lb	Surface area, m ²	Skinfold data, mm										
					1 Cheek	2 Chin	3 Chest	4 Arm	5 Back	6 Side	7 Iliac crest	8 Abdomen	9 Knee	10 Calf	11 Total
A (Billman)	23	68	149	1.8	13	10	5.5	20	12	8	27	17	16.5	12	141.0
B (Chidsey)	28	70	133	1.75	12	7.5	5	8	7	4.5	18	11.5	7	7	87.5
C (Gafvert)	24	70.5	147	1.83	11	5.5	9	12	15	10	31.5	19.5	16	11	140.5
D (Kern)	22	70.5	164.5	1.92	13	9.5	12	15	15.5	13	42	31	13	11	175
E (Paige)	30	70.5	148	1.84	9.5	9.5	4.5	10.5	10	10	23	24.5	9.5	9	120
F (Wallenius)	23	70	152	1.86	13	5	9	14	13	8	27	22.5	10	7	128.5

References:

Skinfold - Ten Sites - Allen, T.H., et al.

"Prediction of Total Adiposity from Skinfold and the Curvilinear Relationship between External and Internal Adiposity," Metabolism, 5:346, 1956.

Computation of Residual Lung Volumes - Brozek, J.

"Age Differences in Residual Lung Volume and Vital Capacity of Normal Individuals," Journal of Gerontology, 15:155, 1960.

(Average values for young men, 24.4 percent of total lung capacity)

TABLE 4-4

SUMMARY DATA SHEET ON TEST SUBJECTS
FOR MODIFIED BALKE TEST

Subject	Age, years	Height, in.	Weight		Maximum heart rate, beats/min	Max \dot{V}_{O_2}		Max.R.Q.	Maximum ventilation	
			TBW, kg	LBM, kg		liters/min	ml/min/kg		liters/min, BTPS	Respiratory rate/min
A (Billman)	23	68	67.73	56.46	187	2.8	41.34	1.11	76.91	37
B (Chidsey)	28	70	60.45	58.65	185	2.21	36.56	1.17	93.04	48
C (Gafvert)	24	70.5	66.82	52.01	185	3.14	46.99	1.10	79.72	30
D (Kern)	22	70.5	74.77	59.37	198	3.16	42.26	1.18	97.7	33
E (Paige)	30	70.5	67.27	57.18	190	2.88	42.81	1.32	104.51	43
F (Wallenius)	23	70	69.09	50.59	178	3.08	44.58	1.19	106.91	40

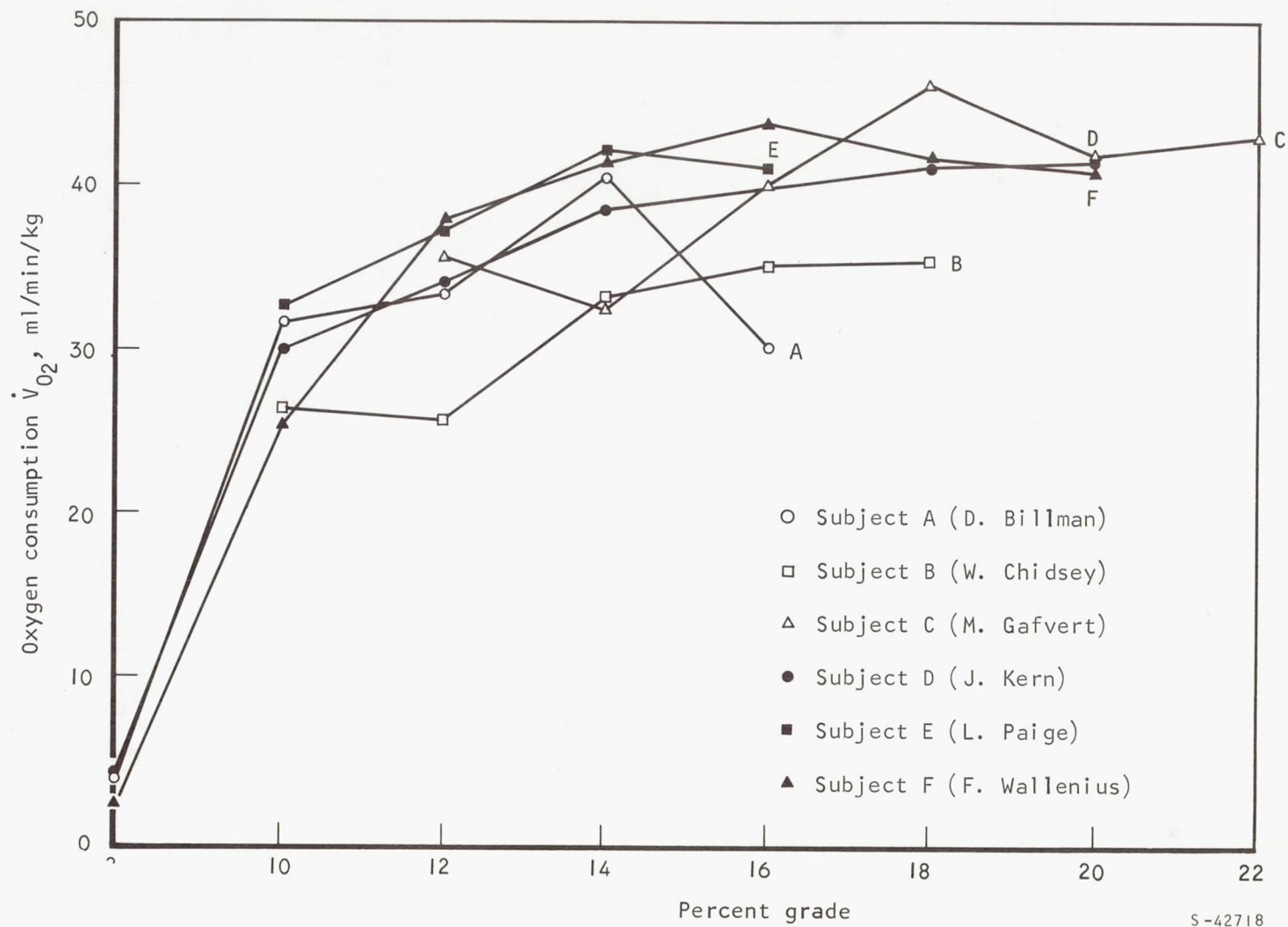


Figure 4-2. Oxygen Consumption Rate as a Function of Percent Grade

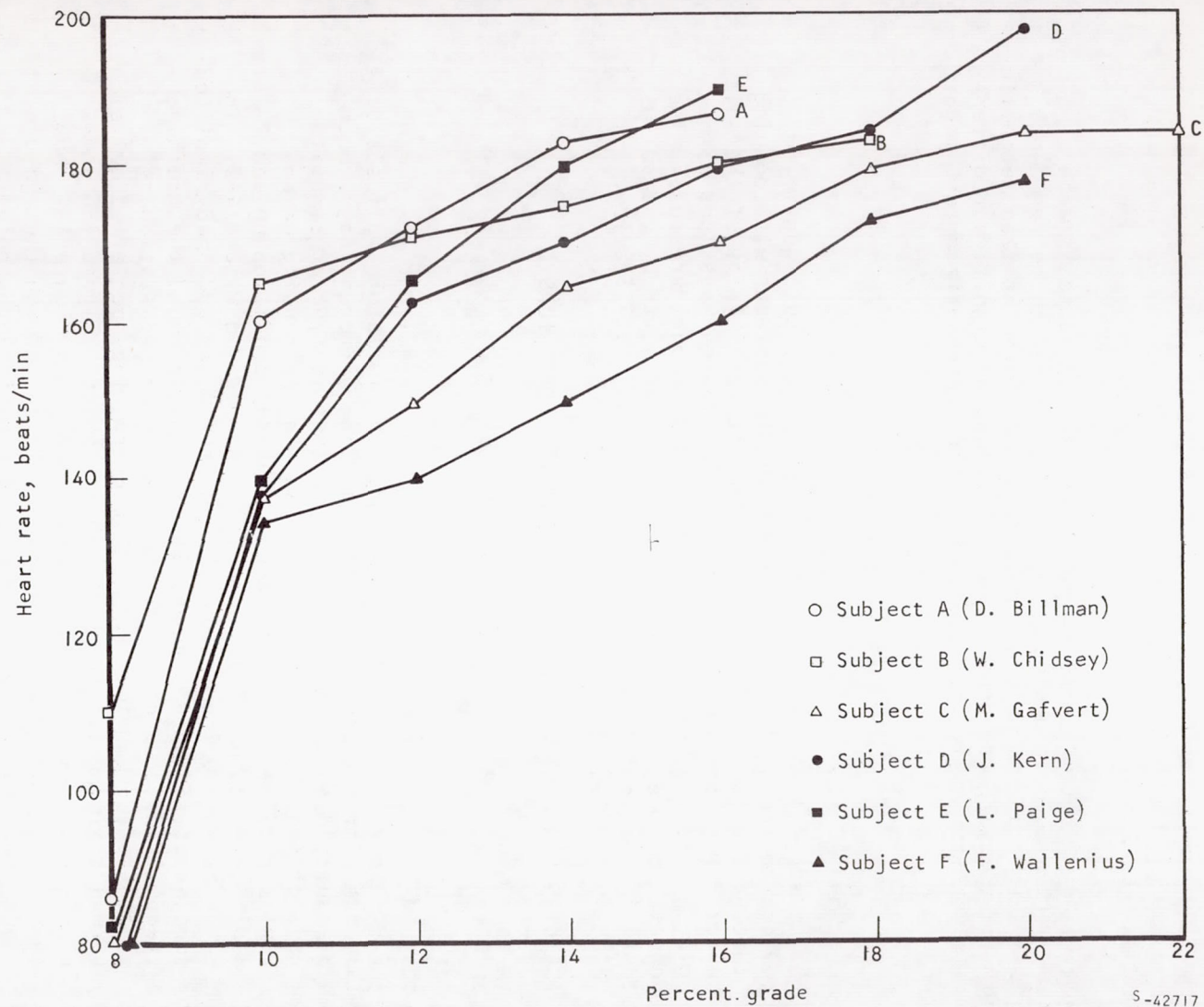


Figure 4-3. Heart Rate as a Function of Percent Grade

Preliminary Metabolic Rate Tests (1G) With Pressure Suit

Before testing began, the suited subject stood for 15 min in the vicinity of the inclined treadmill. His suit was ventilated but not pressurized. Using the same techniques as used for the treadmill tests (1/6 g), the subject's oxygen consumption rate was determined for the last 5 min of the standing test. During this time, the subject bore the weight of the 75-lb backpack used in the 1/6-g simulation tests. Tests were also performed by the same technique with the suit pressurized to 3.5 psig.

The metabolic rates (Figure 4-4) measured for the suited tests were higher than the shirt-sleeve values because the subjects had to perform work in supporting the weight of the suit and backpack. Although the mean metabolic rate increased when the suit was pressurized, there was no significant difference when compared statistically to the data from the unpressurized test mode.

SUIT TRAINING

Even though the subjects selected for this program were suit-qualified, training was provided on the Gemini suit to acquaint the subjects with donning and doffing of that particular suit and to minimize the possibility of the suit acting as a stressor during testing. Each subject had several sessions with the suit, including pressurization to 3.5 psig, the operational pressure. The training was adequate for the subjects to don and doff the suits by themselves and reduced potential emotional tensions involved with suit utilization.

TRAINING FOR LOCOMOTION IN LUNAR GRAVITY SIMULATORS

Inclined-Plane Simulator

All subjects had previously participated in studies requiring the use of a modified Hewes and Spady inclined-plane lunar gravity simulator. All subjects were given a minimum of three training sessions on three different days, both in mufti and in pressurized suits, to reorient them to this type of simulator. Normally, three days of training is adequate for walking or running on an inclined-plane simulator. The configuration for physical conditioning and training in the modified Hewes and Spady simulator is shown in Figure 4-5. The two subjects who also performed locomotion tasks on the Hewes and Spady inclined-plane simulator located at the NASA Langley Research Center found the training on the inclined treadmill quite adequate for performing on the stationary inclined board located at the Langley Research Center. They performed quite well after only 4 to 8 training trials on the 191-ft board. Figure 4-6 shows a subject in shirt sleeves walking in the LRC simulator, and Figure 4-7 shows a subject in a Gemini suit pressurized to 3.5 psi walking through the measurement grid on the same simulator. The only subjective differences noted between the inclined plane walkway and the treadmill were the push-off necessary to reach a given traversing velocity, the minor problems associated with maintaining a constant velocity and gait going through the measurement grid, and the problems of decelerating and stopping.

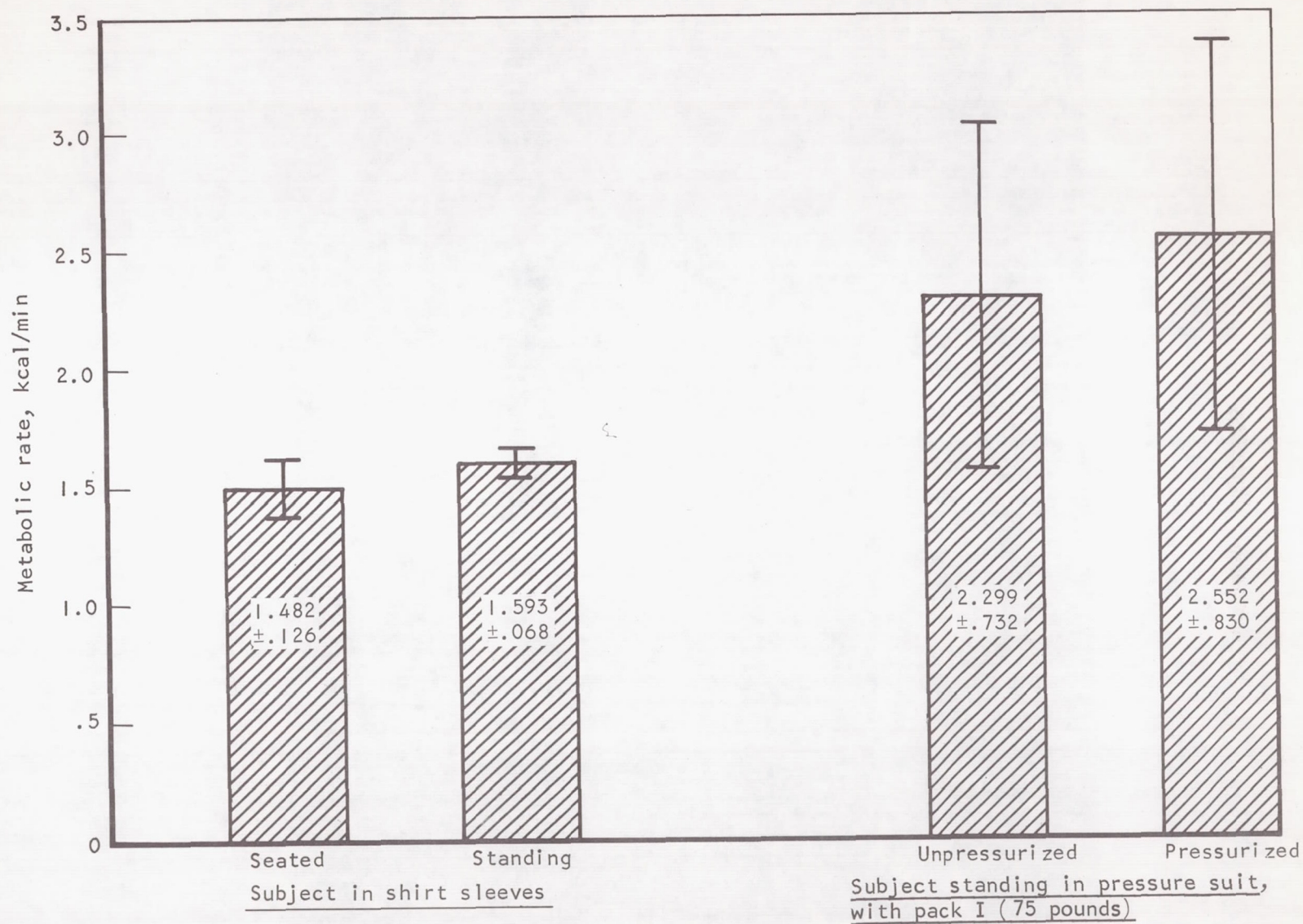


Figure 4-4. Baseline Metabolic Data (IG)

S-42686

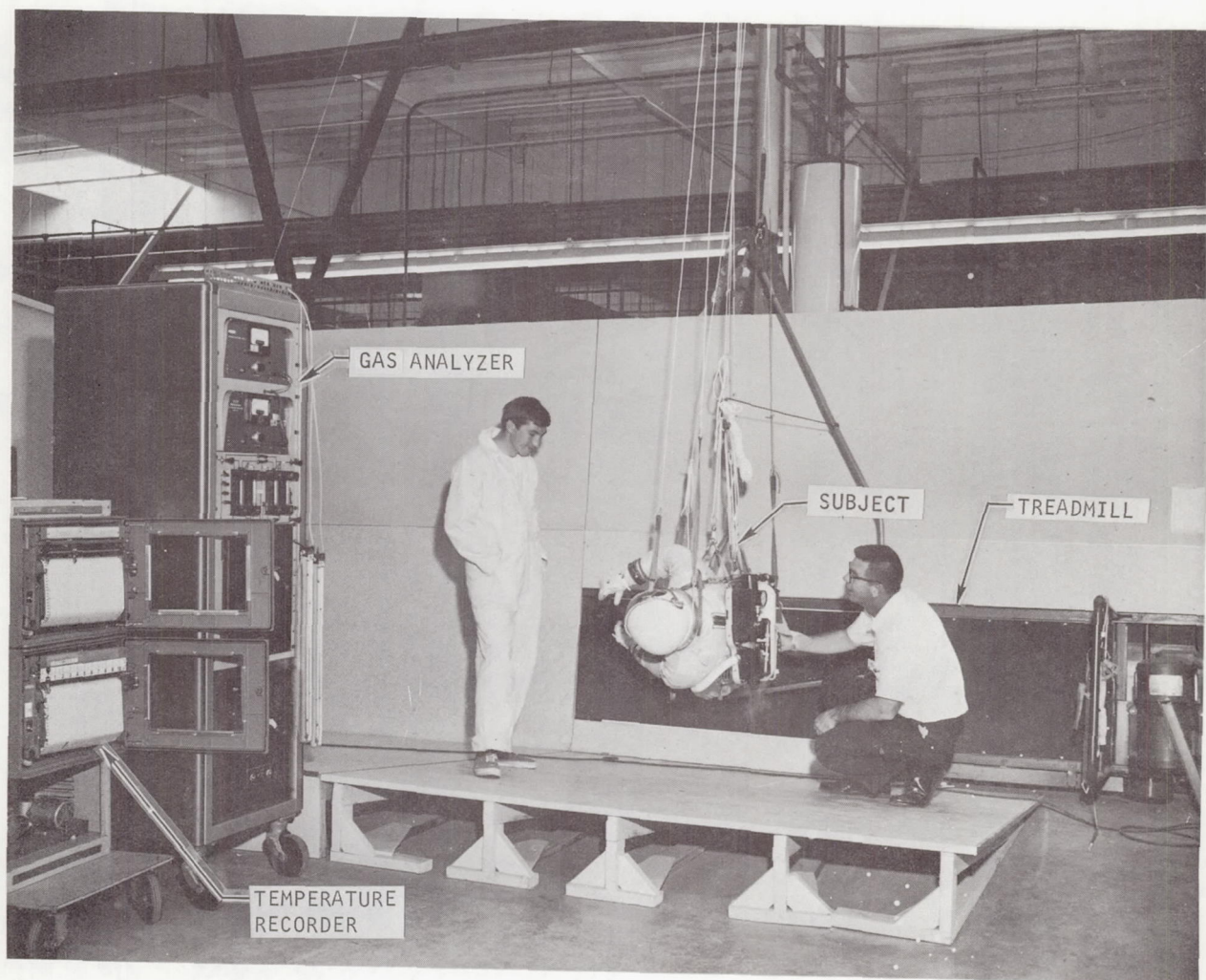


Figure 4-5. Physical Conditioning Training Configuration

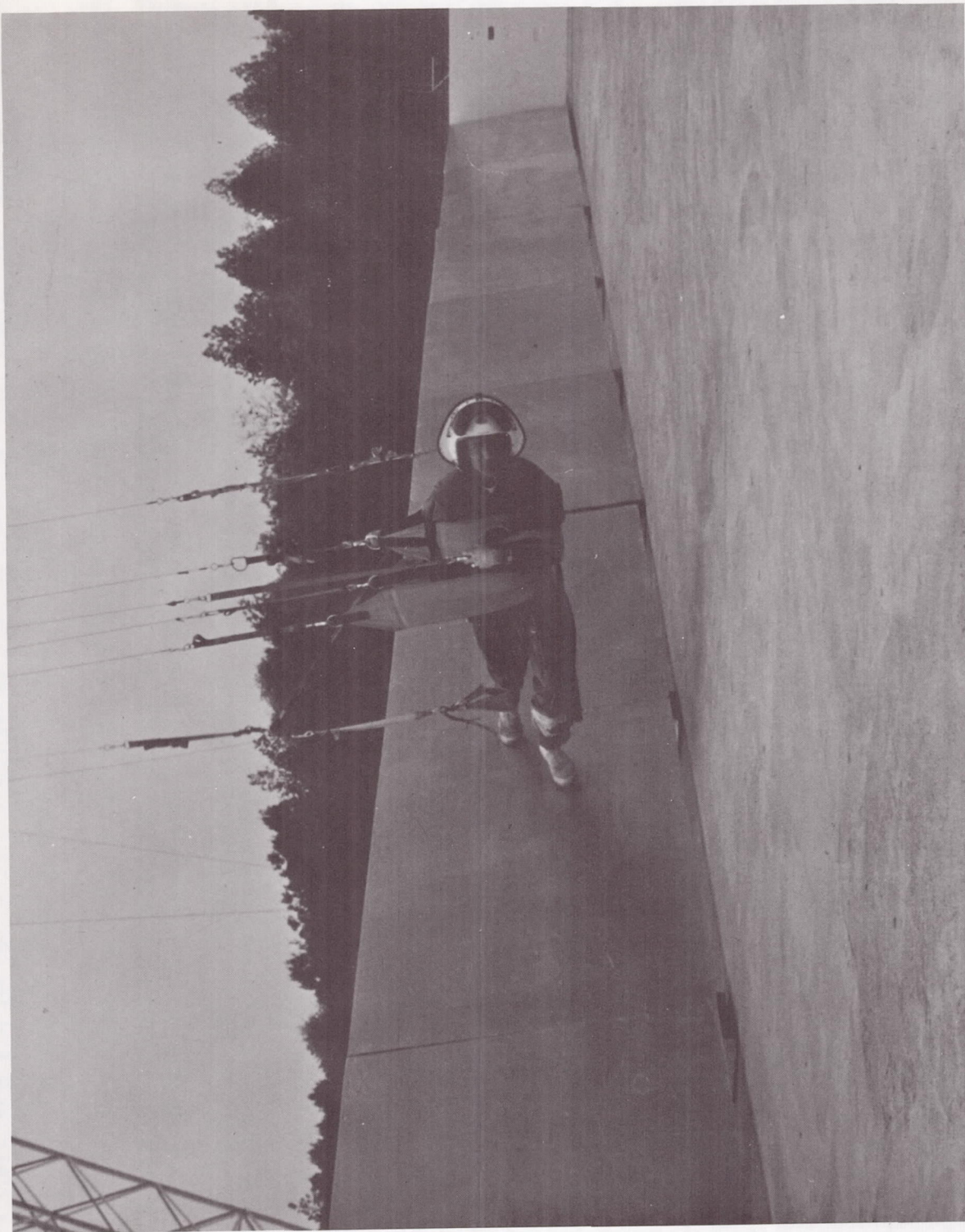


Figure 4-6. Test Subject Walking in LRC Inclined-Plane Simulator Without Pressure Suit

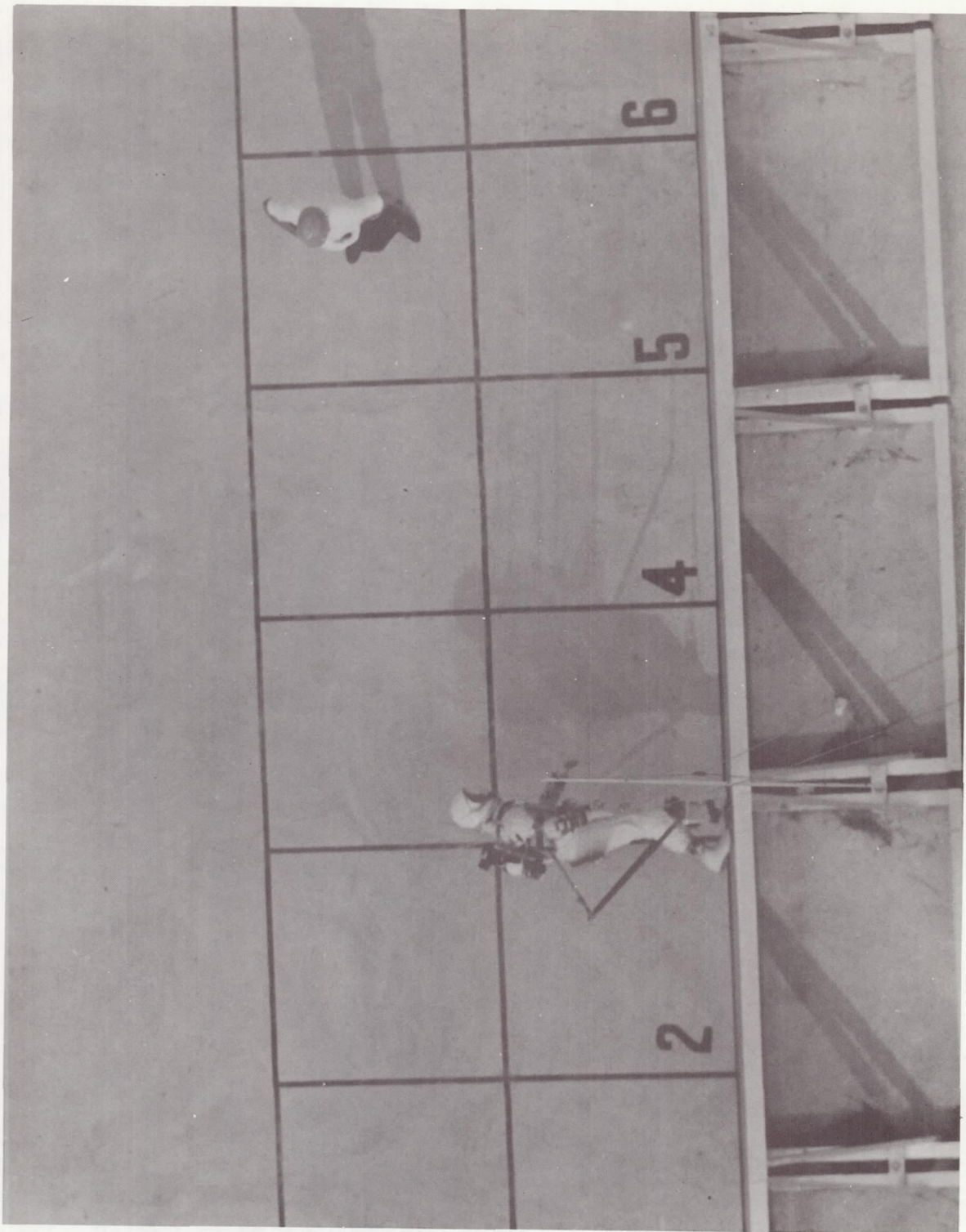


Figure 4-7. Test Subject in LRC Inclined-Plane Simulator with Pressurized Suit

Gait characteristics were recorded for two test subjects while using the LRC inclined-plane simulator. Complete film coverage of the various modes were provided by NASA Langley Research Center. Analysis of the specific gait characteristics for each of the subjects is presented in Section 5 of this report.

The various test modes, step rates, and times recorded are summarized in Tables 4-5 and 4-6. Table 4-5 defines the test modes by code letter and indicates the desired speed/time combination across a 13-meter grid as applicable to monitoring step rate and length of stride. Table 4-6 presents the mean data obtained for each subject during these tests.

Following completion of the tests for the modes shown in Table 4-6, each subject attempted an extended lope as a locomotion gait. The data obtained for five tests with each subject are shown in Table 4-7. Each subject indicated that initially the lope introduces balance problems and that extensive training would be required to master this locomotion technique. Table 4-7 also includes four data points for tests with the lope in the suited condition by test subject D (J. Kern).

This level of training, used just for familiarization with this type of simulation, is necessary to overcome the problems of postural positioning and missing degrees-of-freedom, and to learn to maneuver in a gravity field in which there is decreased traction provided at the feet. The postural problems relate to the individual supported essentially on his side at a 9-deg, 36-min angle to the ground. In this configuration, the subject must correct his visual and vestibular orientation so that he feels he is walking normally. This effect is rapidly compensated for and causes no problem. The inclined-plane simulator does not allow for lateral translation in the yaw degree-of-freedom and is quite restrictive in the roll degree-of-freedom. The subjects subjectively reported that they felt supported by the suspension so that directional stability was no problem. Decreased traction was quickly adjusted for with training.

Overall locomotion by walking or running in this type of simulator is quite easy to learn if repetitive learning trials are provided over time. Learning to perform a loping or leaping gait, however, is difficult for many individuals, probably because it is not a gait normally used in a 1-g environment. The requirement to perform a loping gait adds approximately two days to the training time.

Six-Degrees-of-Freedom Vertical Suspension Simulator

The subjects made the transition from the inclined-plane simulator to the vertical suspension simulator with approximately three days of training for each man. This added time was needed to adjust to problems of directional stability in the decreased traction field. The directional instability occurs mainly in the yaw degree-of-freedom. The subjects had to learn to impart approximately the same amount of force with each foot to keep from rotating either to the left or to the right. This effect was even more pronounced with the loping gait. All subjects were adequately trained within the three-day

TABLE 4-5

REQUIRED SPEEDS AND TIMES FOR LOCOMOTION THROUGH
THE LRC 13-METER CALIBRATION GRID

Mode	km/hr	cm/sec	Time, sec	ft/sec	mph
D	2	55.56	23.44	1.825	1.242
E	4	111.12	11.72	3.65	2.485
F	6	166.60	7.80	5.47	3.73
G	8	222.00	5.86	7.29	4.97
H	10	277.80	4.60	9.13	6.21
I	12	332.50	3.89	10.93	7.46
J	14	388.20	3.35	12.76	8.71
K	16	440.45	2.96	14.58	9.95
L	20	555.00	2.33	18.23	12.43

TABLE 4-6

MEAN TIME AND NUMBER OF STEPS FOR LOCOMOTION
THROUGH THE LRC 13-METER CALIBRATION GRID

Subject B (Chidsey)					Subject D (Kern)				
Mode	Shirt sleeves		Suited		Mode	Shirt sleeves		Suited	
	Steps	Time, sec	Steps	Time, sec		Steps	Time, sec	Steps	Time, sec
D	19.0	24.86	19.0	22.15	D	19.3	22.95	21.0	23.88
E	14.5	11.95	15.2	12.86	E	14.6	13.96	18.3	12.00
F	9.7	7.15	10.5	7.50	F	13.3	8.36	12.6	8.16
G	8.2	5.65	8.7	5.57	G	7.0	5.63	15.0	5.95
H	7.7	4.62	8.0	4.55	H	7.0	4.56	12.0	5.43
I	7.5	4.01	7.0	3.56	I	6.3	3.78	11.6	4.58
J	6.2	3.53	9.6	3.40	J	6.6	3.26	14.0	4.45
K	9.0	3.13		3.80	K	8.0	2.96		
L*					L	9.0	2.60		

*Mode L could not be attained by subject B.

TABLE 4-7

DATA FOR EXTENDED LOPE GAIT FOR TRAVERSING
THE LRC 13-METER CALIBRATION GRID

Subject B (Chidsey)		Subject D (Kern)	
Steps	Time, sec	Steps	Time, sec
3	4.4	8	3.4
3	3.7	3	4.4
2	5.4	4	3.7
3	4.6	5	3.8
3	4.4	4	3.3
		6*	6.4
		6*	4.6
		4*	5.0
		5*	4.9

*Subject in pressure suit; all other data are for shirt-sleeve condition.

period. It must be noted that each time a new series of tests was started (e.g., slope traversing, different loading, and surface changes), the subjects were given a brief period of training to ensure they could perform the modes requested and that the data would not be biased by a training effect. This procedure was used for each simulator.

As yet, subjects have not been trained directly onto the vertical suspension simulator without prior training on the inclined plane. Based on composite training times for both simulators, it would take six to eight days of respective trials to gain a reasonable level of performance in mufti. The use of pressure suits and unusual operating modes such as traversing with loads, up and down slopes, or with the soft surfaces would add to the training requirements.

Page Intentionally Left Blank

SECTION 5

RESULTS AND DISCUSSIONS

This section presents the test results on the effects of the independent variables (listed in Table 2-1, Section 2) on the dependent variables. The section is divided into two major subsections, physiological results and kinematic results, followed by a discussion of range computation. The first subsection presents physiological data such as metabolic rate, total energy expenditure, average energy expenditure, heart rate, respiratory rate, oxygen consumption, and carbon dioxide production. The second major subsection presents kinematic data such as stride length, stepping rate, and body positions (back angle, hip angle, knee angle).

PHYSIOLOGICAL RESULTS

The principal physiological dependent variable determined during this experimental program was metabolic rate. Metabolic rate was measured by indirect calorimetry using techniques for continuous on-line measurement, as described in Section 3.

With the indirect calorimetry method, the energy cost of a given activity was measured by calculation from the amounts of oxygen consumed and carbon dioxide produced. Inspired and expired gas samples were analyzed for oxygen and carbon dioxide content. From these data, the oxygen consumption, carbon dioxide production, and respiratory exchange ratio were calculated. Experimental pressure and temperature were also recorded to reduce oxygen consumption and carbon dioxide production to the conventional standard temperature and pressure dry conditions (STPD). The basic equations for the calculations are as follows:

$$\dot{V}_{O_2} = (\dot{V}_I F_{IO_2} - \dot{V}_E F_{EO_2}) \times \frac{P_T - P_{H_2O}}{760} \times \frac{273}{273 + T}$$

$$\dot{V}_{CO_2} = (\dot{V}_E F_{ECO_2} - \dot{V}_I F_{ICO_2}) \times \frac{P_T - P_{H_2O}}{760} \times \frac{273}{273 + T}$$

$$R = \frac{\dot{V}_{CO_2}}{\dot{V}_{O_2}}$$

where \dot{V}_{O_2} = oxygen consumption (STPD), liters/min

\dot{V}_{CO_2} = carbon dioxide production (STPD), liters/min

R = respiratory exchange ratio

F_{IO_2} = fraction of inspired oxygen

F_{EO_2} = fraction of expired oxygen

F_{ICO_2} = fraction of inspired carbon dioxide

F_{ECO_2} = fraction of expired carbon dioxide

\dot{V}_I = inspired volume per minute, liters/min

\dot{V}_E = expired volume per minute, liters/min

P_T = observed barometric pressure, mm Hg

P_{H_2O} = water vapor pressure at temperature (T), mm Hg

T = observed temperature, °C

C = kcal/liter \dot{V}_{O_2} at the measured R

Energy corresponding to oxygen consumption is calculated by the caloric equivalents for oxygen as related to the respiratory exchange ratio. The caloric equivalent of a liter of oxygen varies from 4.686 Kcal to 5.04 Kcal within the normal range of R.

Metabolic Rate Data

It is generally accepted that when the body is exercised the aerobic metabolic requirements should change as a step-function. However, the body reacts as a resistor-capacitor linked input so that the aerobic metabolic rate actually rises as an exponential to a steady-state level which is maintained until exercise is stopped (that is, a steady-state level is maintained unless there are additional inputs to the system). When the exercise is stopped there is an exponential decay to the pre-exercise resting value. The difference between the initial logarithmic rise and the assumed step function requirement

is the so-called "oxygen deficit" while the logarithmic decay is called "oxygen debt." Figure 5-1 is a curve of metabolic rate as a function of time and demonstrates these concepts.

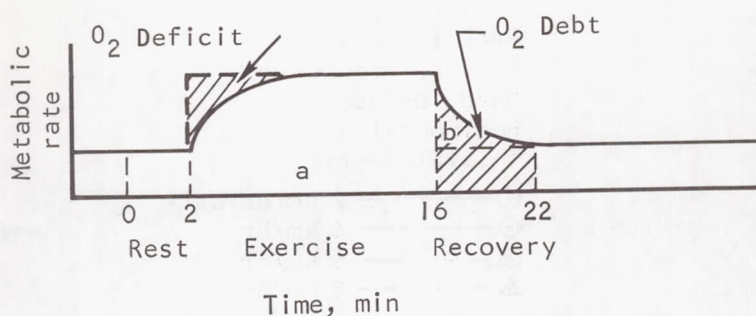


Figure 5-1. Typical Total Energy Cost Curve

The results presented are the average data for the six subjects studied. The standard deviations within tests are due mainly to variations between subjects. For example, the steady-state metabolic rates for each subject ascending the 7.5 deg grade on the TOSS hard surface at 2 km/hr and 8 km/hr are as follows:

(a) 2 km/hr - 3.80, 4.11, 4.14, 5.09, 5.21, and 5.76 kcal/min

(b) 8 km/hr - 9.85, 12.70, 14.53, 16.90, 17.70, and 19.60 kcal/min

The standard deviation is ± 0.78 for the 2 km/hr velocity and ± 3.57 for the 8 km/hr velocity. Comparison of these values demonstrates that the variations between subjects tended to increase as the metabolic cost of the work increased.

The curves for changes in metabolic rate with time have been faired to conform to the theories of physiology and are representative of the data (for example, see Figure 5-1). When several of the manually faired curves were checked against a computer-fitted curve, there were no appreciable differences; the manually faired curves were determined acceptable for graphing purposes.

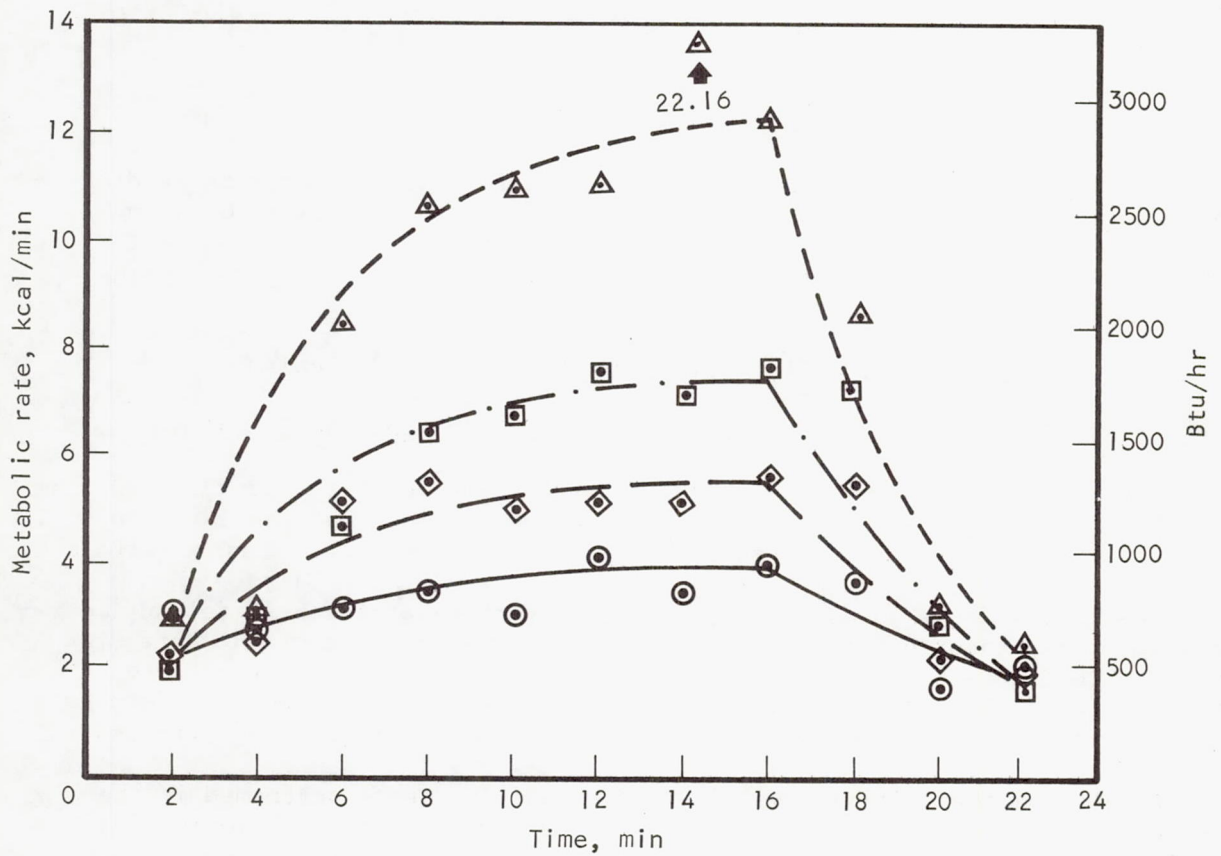
Results of the initial pressure-suited, walking tests performed in the inclined plane are presented in Figure 5-2; test results for the loping and running modes are shown in Figures 5-3 and 5-4. The first and second repeats of the 2-km/hr walk, the 6-km/hr lope, and the 8-km/hr run with all six subjects are presented in Figures A-4 and A-5 of Appendix A. There were no significant differences between the repeat data and the initial observations.

Statistical analysis of the repeated complete series by the two special subjects (see Figures A-6 through A-8, Appendix A) also found no significant differences between the initial tests and the repeat tests. The consistency of the results through repeated testing greatly enhances the reliability of all the metabolic data.

Conditions:

Inclined plane
Pack I (75 lb)
Suited, pressurized
Hard surface
Horizontal
Initial Tests

○ — 2 km/hr walk
◇ — 4 km/hr
□ — 6 km/hr
△ — 8 km/hr



S-42646

Figure 5-2. Time Course Changes in Metabolic Rates for Walking on the Inclined-Plane Simulator

Conditions:

Inclined plane
 Pack I (75 lb)
 Suited, pressurized
 Hard surface
 Horizontal initial tests

○ ————— 6 km/hr lope
 ◇ ————— 8 km/hr lope
 □ ————— 9.7 km/hr lope
 △ ————— 11.3 km/hr lope

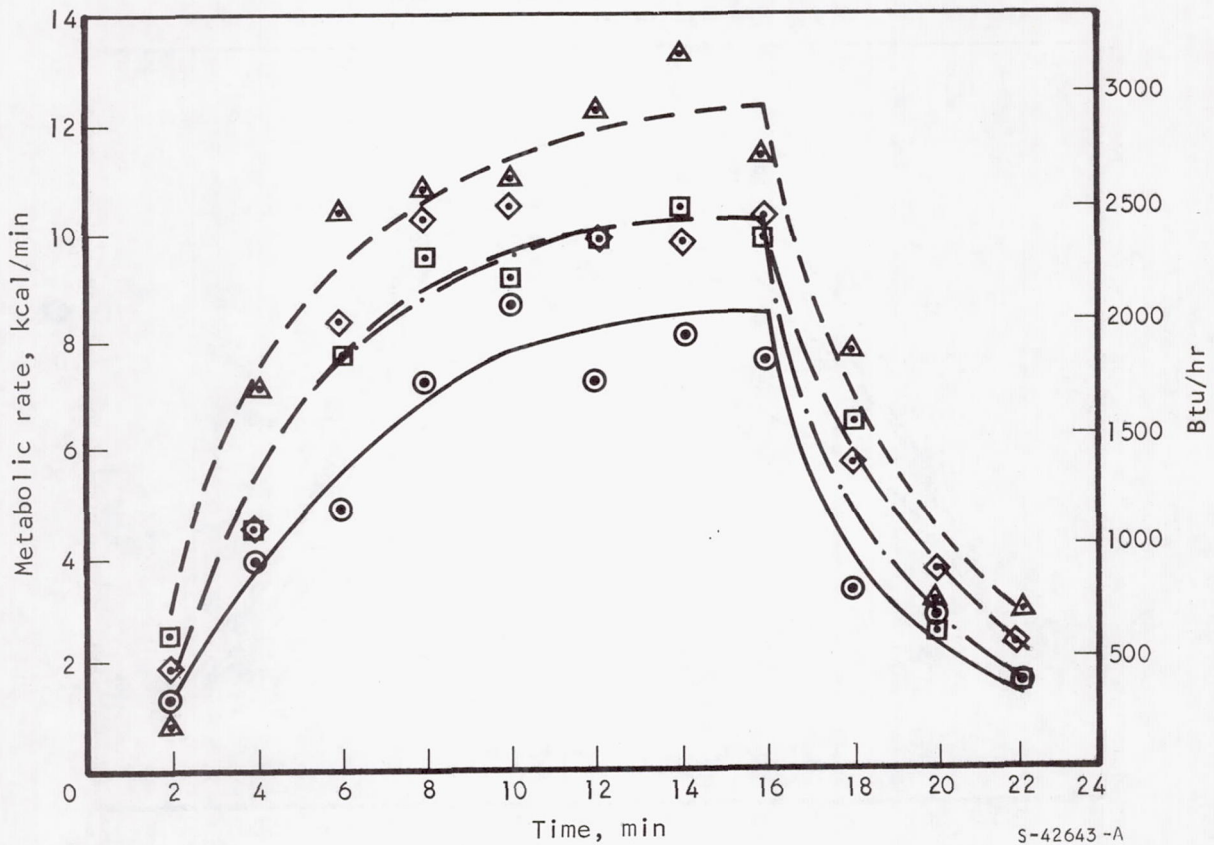


Figure 5-3. Time Course Changes in Metabolic Rates for Loping on the Inclined-Plane Simulator

Conditions:

Inclined plane
Pack I (75 lb)
Suited, pressurized
Hard surface
Horizontal
Initial Tests

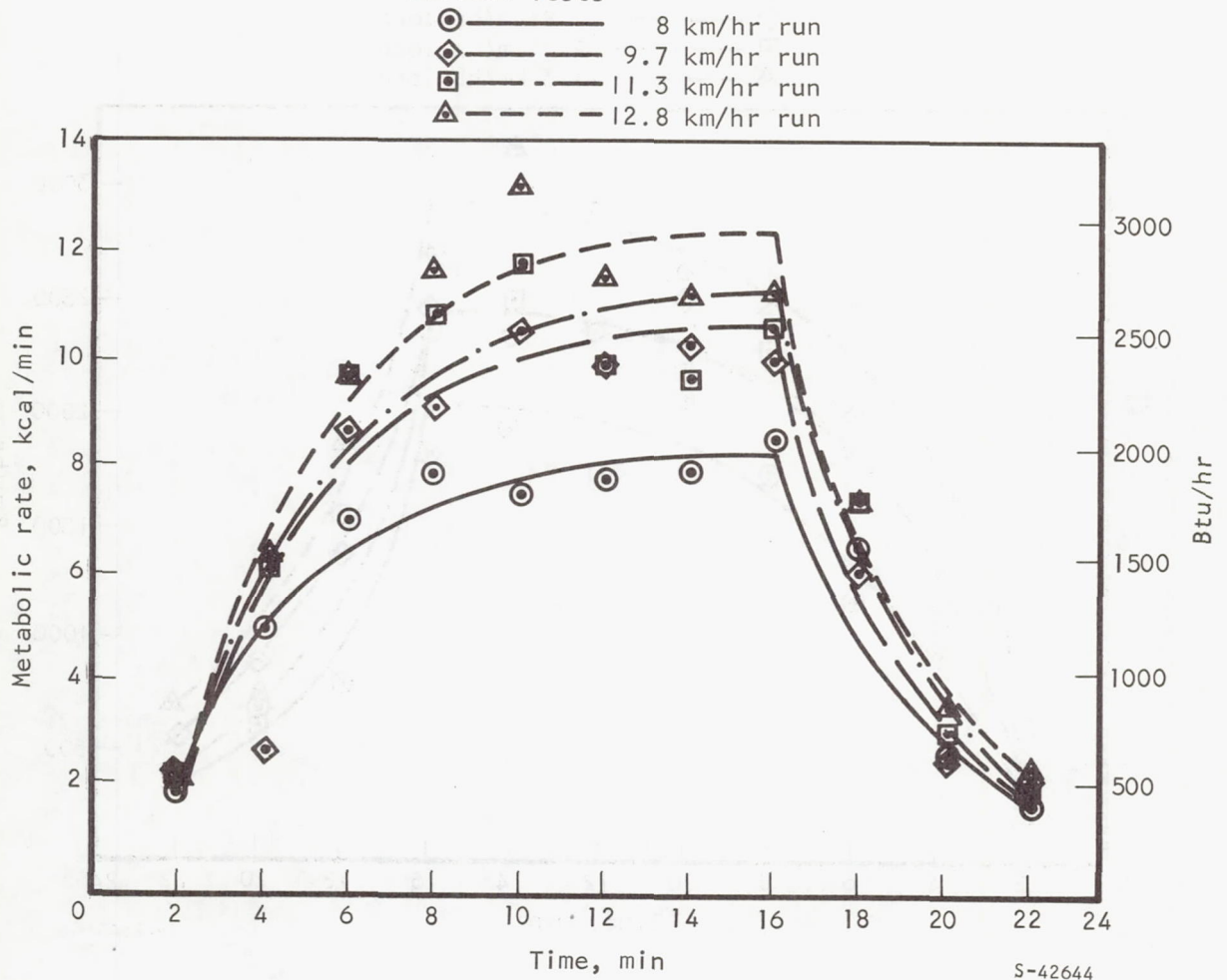


Figure 5-4. Time Course Changes in Metabolic Rates for Running on the Inclined-Plane Simulator

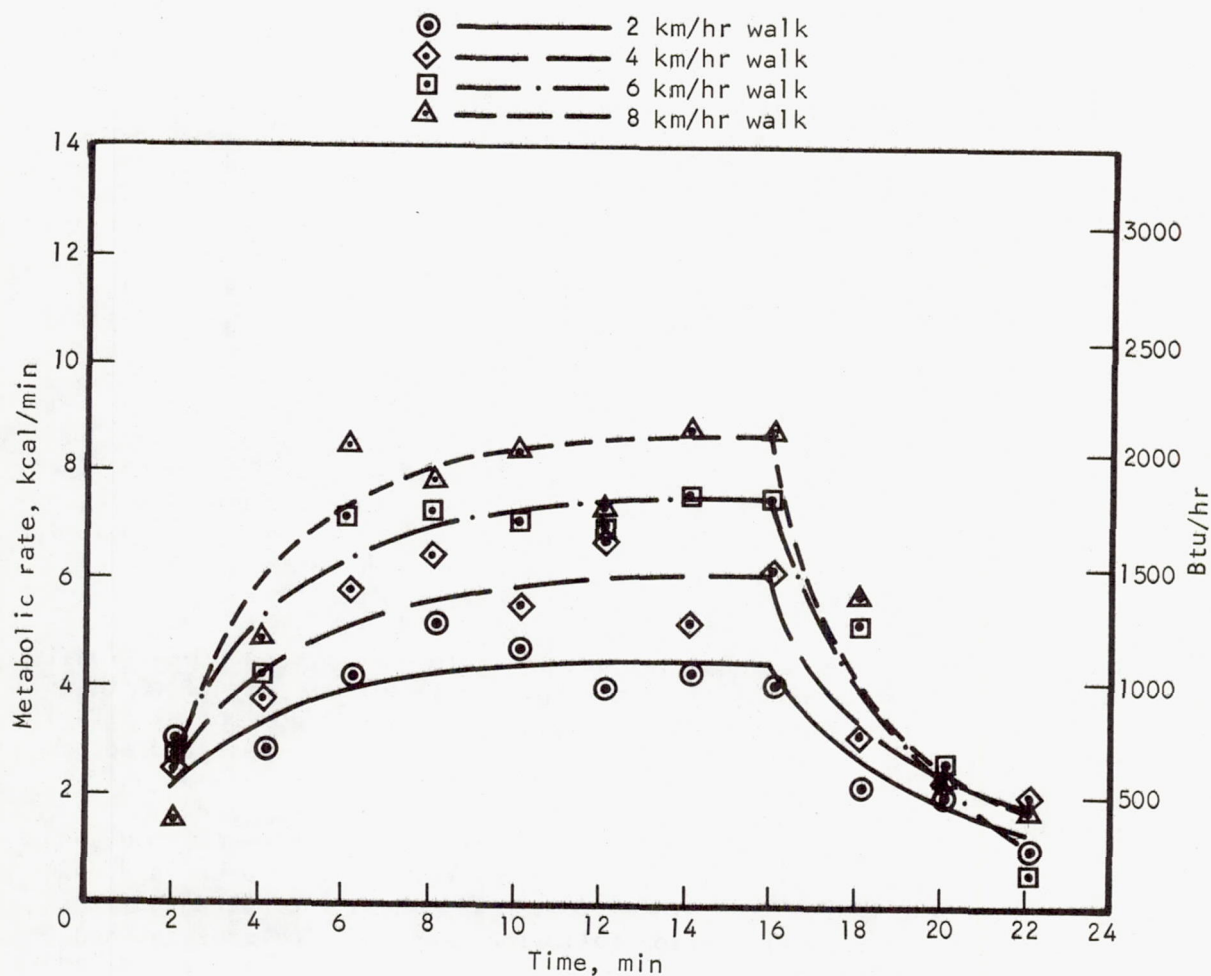
Figures 5-5, 5-6, and 5-7 present the time course changes in metabolic rate for the walking, loping, and running modes for tests performed with the TOSS simulator. Because of the redundancy in the shapes of the curves, and since the data are more meaningful in other forms, the curves presented here are shown to reflect the general form of the curves. The remainder of the energy expenditure profile curves for all modes with the various simulators are presented in Appendix A.

Metabolic rates obtained using the inclined plane. - The total energy in kcal required for locomoting over a 14-min period in each mode of the experimental design is summarized in Table 5-1. The values are presented as the mean \pm 1 standard deviation for the six subjects accomplishing each test, except for the first two rows of data which have been pooled. These data were combined because statistical analysis revealed no differences among the repeat tests. The data for the fatigue tests were not suitable for this type of analysis and were therefore not included in Table 5-1. The data for each mode are discussed in subsequent paragraphs. The total energy values in Table 5-1 represent the total area under the curve of metabolic rate vs time, as averaged for the six subjects. Areas were determined using Simpson's rule of integration which states that the area under a curve can be estimated by adding up the area of polygons fitted under the curve. Thus, the total area (energy) for the typical energy cost curve in Figure 5-1 is the sum of the area under the portion of the curve from the start of exercise (2 min) to the end of exercise (16 min) noted as "a," plus the logarithmic decay portion of the curves during recovery noted as the crosshatched area from the 15th min to the 22nd min.

Table 5-2 presents typical observations for total energy and proportional energy required for locomotion at 1/6 g carrying a 75-lb pack load (12.5 lb at 1/6 g) on the inclined plane simulator with the treadmill horizontal. The data represent the 3 locomotive gaits used, over the 12 velocities studied. Column I contains the total energy required during the work phase and the recovery period (total area under the curve from the 2nd to the 22nd min (Figure 5-7)). It is an average of the six subjects studied. Column II gives the average energy used by the subjects during the work period (area "a," under the curve from the 2nd to the 16th min). Column III shows the average of the total energy during the recovery period following exercise (the crosshatched area under the curve from the 16th to the 22nd min). Area "b," the so-called oxygen debt, represents the energy required to repay the oxygen deficit acquired during the work phase. Column IV gives the ratio of post exercise metabolism to the total energy requirement (Column III/Column I). Column V shows the average total energy cost of the work performed (Column VI x 14 min). Column VI gives the average energy cost per minute for the exercise task, (area "a" plus "b") divided by 14 min. Finally Column VII shows the actual average steady-state metabolic rate measured during the last portion of the exercise period.

Conditions:

T0SS
 Pack 1 (75 lb)
 Suited, pressurized
 Hard surface
 Horizontal



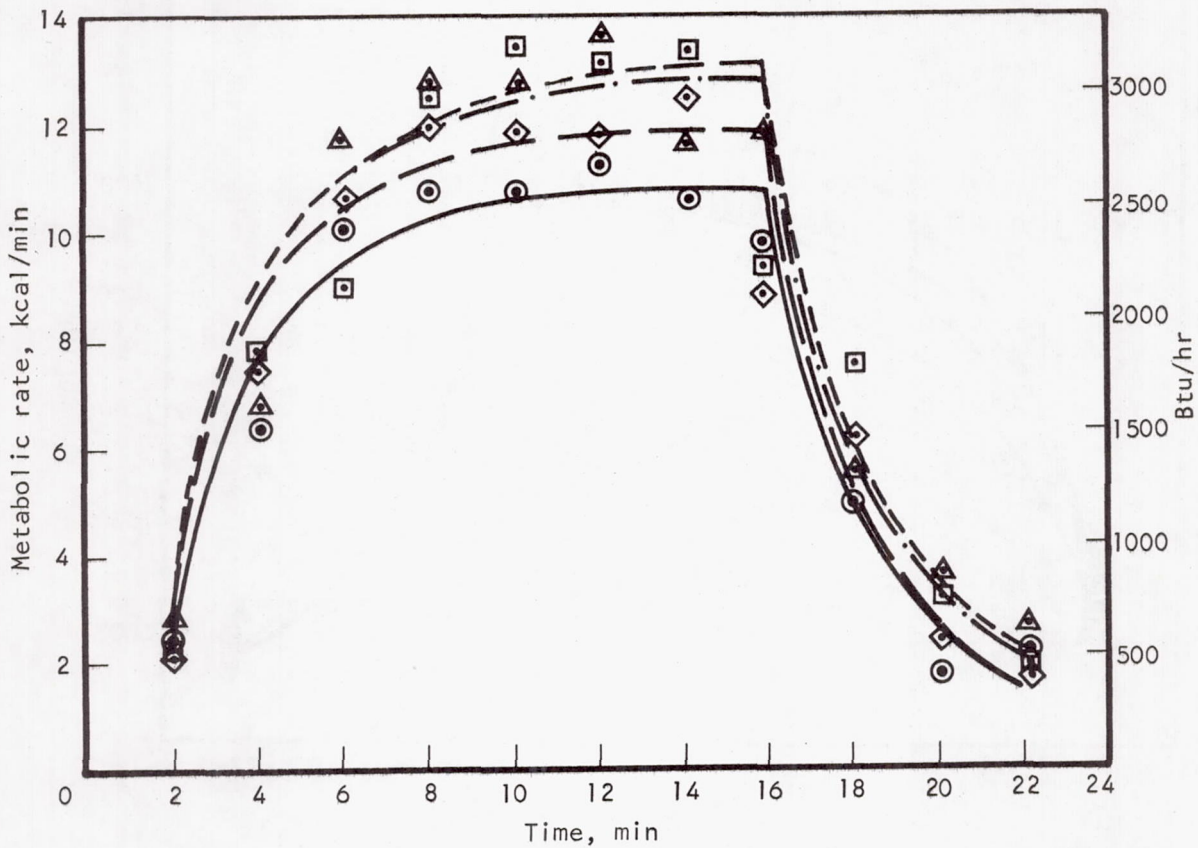
S-42647

Figure 5-5. Time Course Changes in Metabolic Rates for Walking with the T0SS (Turbine-Operated Suspension System) Simulator

Conditions:

TOSS
Pack I (75 lb)
Suited, pressurized
Hard surface
Horizontal

○ ————— 6 km/hr lope
 ◇ ————— 8 km/hr lope
 □ ————— 9.3 km/hr lope
 △ ————— 11.3 km/hr lope



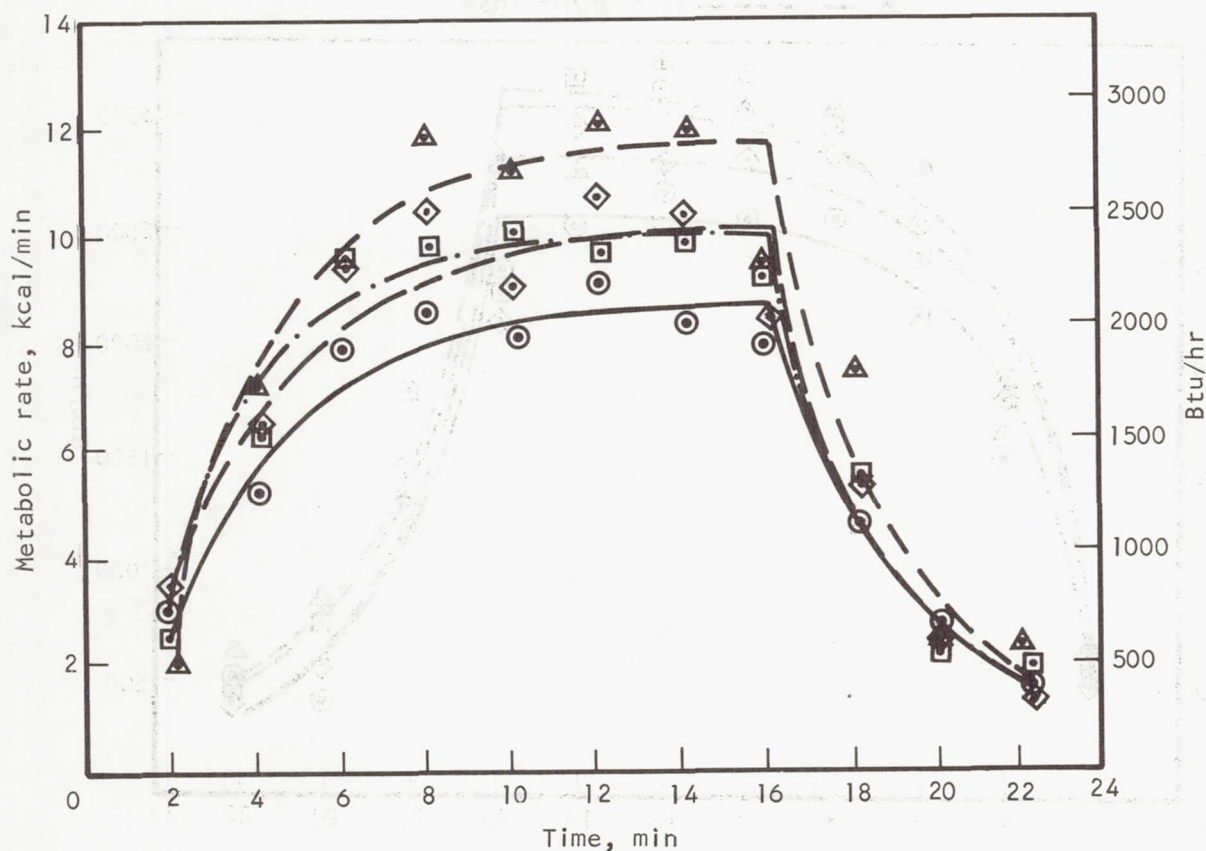
S-42645

Figure 5-6. Time Course Changes in Metabolic Rates for Loping with the TOSS Simulator

Conditions:

TOSS
Pack I (75 lb)
Suited, pressurized
Hard surface
Horizontal

○ — 8 km/hr run
 ◇ — 9.7 km/hr
 □ — 11.3 km/hr
 △ — 12.8 km/hr



S-42648

Figure 5-7. Time Course Changes in Metabolic Rates for Running with the TOSS Simulator

TABLE 5-1

TOTAL ENERGY COST (KCAL) FOR 14-MIN
LOCOMOTION IN EACH EXERCISE MODE

Experimental conditions							Results (mean and ± 1 standard deviation)							
Simulator and suit mode	Slope, deg	Surface condition	Pack	Number of velocities	Number of subjects	Total tests	Gait or ascend/descend	Velocity, km/hr						
								2	4	6	8	9.7	11.3	12.8
Inclined plane, pressurized (press.) suit	0 (horiz)	Hard	I, 75 lb	4 each; walk, lope and run	6, with 2 repeating once	96	Walk	62.90 \pm 16.09	83.49 \pm 26.40	99.64 \pm 37.53	168.69 \pm 52.32			
							Lope			126.09 \pm 30.89	153.26 \pm 48.66	148.89 \pm 20.28	179.45 \pm 37.59	
							Run				128.50 \pm 24.01	144.15 \pm 18.39	166.15 \pm 22.20	
Inclined plane, pressurized suit	0	Hard	I	1 each; walk, lope, and run	6, with all repeating twice	36	Walk							
							Lope							
							Run							
Inclined plane, subject in mufti (without press. suit)	0	Hard	I	4 each; walk, lope, and run	2	24	Walk	25.77 \pm 14.55	28.08 \pm 12.98	52.15 \pm 1.45	84.78 \pm 7.37			
							Lope			104.67 \pm 0.96	104.29 \pm 1.01	114.90 \pm 10.17	111.56 \pm 0.84	
							Run				62.00 \pm 8.61	63.96 \pm 12.51	86.96 \pm 16.00	94.12 \pm 20.84
Incl plane, mufti	0	Hard	I	Fatigue test	6	24								
Inclined plane, pressurized suit	0	Hard	I	Fatigue test	2	8								
Inclined plane, pressurized suit	0	Hard	II, 240 lb	4 each; walk, lope, and run	6	72	Walk	89.77 \pm 47.93	95.06 \pm 17.06	115.14 \pm 29.39	160.47 \pm 34.60			
							Lope			166.01 \pm 22.94	153.22 \pm 31.55	173.43 \pm 53.65	170.57 \pm 30.34	
							Run				137.27 \pm 21.42	145.09 \pm 29.56	144.59 \pm 23.73	
Inclined plane, pressurized suit	0	Hard	III, 400 lb	4 each; walk, lope, and run	2	24	Walk	61.04 \pm 1.24	94.99 \pm 2.10	121.57 \pm 22.13	117.04 \pm 2.54			
							Lope				181.62 \pm 30.03	138.63 \pm 12.95	207.78 \pm 39.99	237.42
							Run				152.94 \pm 51.11	113.73 \pm 4.86	163.73 \pm 15.19	154.72 \pm 22.88
TOSS (6-deg-of-freedom), pressurized suit	0	Hard	I	4 each; walk, lope, and run	6	72	Walk	76.71 \pm 10.61	99.35 \pm 12.17	119.50 \pm 33.87	130.68 \pm 22.01			
							Lope			159.22 \pm 33.92	173.29 \pm 26.79	184.55 \pm 10.22	189.07 \pm 20.96	
							Run				133.81 \pm 13.94	155.26 \pm 30.68	152.65 \pm 15.13	172.57 \pm 28.50
TOSS, press. suit	0	Smooth lunar	I	4 velocities	6	24		74.07 \pm 6.21	99.32 \pm 14.98	137.75 \pm 26.13	193.25 \pm 13.98			
TOSS, press. suit	0	Coarse lunar	I	4 velocities	6	24		64.85 \pm 4.18	110.33 \pm 12.51	153.65 \pm 15.90	169.69 \pm 11.40			
TOSS, pressurized suit	7.5	Hard	I	4 velocities	6	48	Ascend	75.00 \pm 12.36	118.90 \pm 7.13	161.0 \pm 23.2	197.5 \pm 52.2			
							Descend	54.15 \pm 7.17	71.52 \pm 10.69	83.87 \pm 13.26	101.75 \pm 17.93			
TOSS, pressurized suit	7.5	Smooth lunar	I	4 velocities	6	48	Ascend	90.00 \pm 18.89	139.42 \pm 23.59					
							Descend	74.08 \pm 6.21	99.32 \pm 14.98	137.75 \pm 26.14	193.25 \pm 13.98			
TOSS, pressurized suit	15	Hard	I	4 velocities	6	48	Ascend	94.18 \pm 12.03	177.49 \pm 26.21					
							Descend	51.96 \pm 9.04	62.55 \pm 6.32	67.52 \pm 5.57	82.85 \pm 14.20			
TOSS, pressurized suit	15	Smooth lunar	I	4 velocities	6	48	Ascend	117.84 \pm 9.14	182.21 \pm 16.93					
							Descend	53.61 \pm 5.78	65.74 \pm 6.59	78.26 \pm 12.69	87.52 \pm 14.07			
TOSS, pressurized suit	30	Hard	I	4 velocities	6	48	Ascend	162.27 \pm 36.24 ^a (at 1 km/hr)						
							Descend	58.76 \pm 11.76	66.32 \pm 9.13	74.34 \pm 6.06	86.66 \pm 8.23			
Inclined plane, pressurized suit	7.5	Hard	I	4 velocities	6	48	Ascend	57.36 \pm 11.59	85.87 \pm 27.57	120.15 \pm 49.85	138.80 \pm 43.40			
							Descend	54.37 \pm 9.75	67.83 \pm 14.66	77.17 \pm 14.31	85.27 \pm 13.57			
Inclined plane, pressurized suit	7.5	Hard	II	4 velocities	6	48	Ascend	74.97 \pm 16.40	111.46 \pm 24.74	148.46 \pm 28.70	181.92 \pm 37.72			
							Descend	58.94 \pm 8.47	74.55 \pm 14.01	88.20 \pm 11.18	102.51 \pm 13.68			
Inclined plane, pressurized suit	15	Hard	I	4 velocities	6	48	Ascend	74.20 \pm 9.38	116.45 \pm 15.08	151.18 \pm 10.52				
							Descend	51.96 \pm 9.04	62.55 \pm 6.32	67.52 \pm 5.56	82.85 \pm 14.20			
Inclined plane, pressurized suit	30	Hard	I	4 velocities	6	48	Ascend	122.0 \pm 33.2	171.7 \pm 38.5	216.6				
							Descend	59.82 \pm 6.90	72.27 \pm 15.16	87.20 \pm 13.16	104.08 \pm 16.99			

^aRate of 162.27 \pm 36.24 kcal/min was taken at 1-km/hr velocity

^aRate of 162.27 \pm 36.24 kcal/min was taken at 1-km/hr velocity

TABLE 5-2

TOTAL ENERGY AND PROPORTIONAL ENERGY REQUIREMENTS
LOCOMOTION ON HORIZONTAL INCLINED-PLANE SIMULATOR
WITH PACK I AND PRESSURIZED SUIT

Gait	Velocity, km/hr	Average total energy, kcal (Col I)	Average energy for work, kcal (Col II)	Average energy post-work, kcal (Col III)	Ratio of Col III/Col I (Col IV)	Total Energy During Work, kcal (Col V)	Average energy cost, kcal/min (Col VI)	Steady-state energy cost, kcal/min (Col VII)
Walk	2	62.90	47.78	15.12	0.240	645.5	3.25	3.67
	4	83.49	62.75	20.74	0.248	71.7	5.12	4.63
	6	99.65	74.18	25.47	0.256	90.0	6.43	6.42
	8	168.69	134.36	34.33	0.203	150.3	10.93	13.32
Lope	6	126.09	98.86	27.23	0.216	113.0	8.07	7.63
	8	153.26	122.06	31.20	0.204	142.5	10.18	9.96
	9.7	148.88	119.45	29.43	0.198	133.7	9.55	10.08
	11.3	179.45	143.64	35.81	0.200	173.6	12.40	12.31
Run	8	128.51	100.50	28.00	0.218	116.6	8.33	7.57
	9.7	120.58	95.30	25.28	0.210	108.2	7.73	9.56
	11.3	166.15	132.97	33.17	0.200	153.0	10.93	9.99
	12.8	181.12	145.66	35.46	0.196	167.6	11.97	11.37

A statistical analysis of the data in Table 5-2 showed an increase in energy for walking as velocity was increased ($p < 0.01$), no effect of velocity within the loping gait, and an increase with velocity for running ($p < 0.05$). Comparisons were also made between gaits used to achieve the same velocities. The energy costs of walking or loping were the same at 6 km/hr and matched the energy cost for the running gait at 8 km/hr. Differences between loping and running at 9.7 and 11.3 were insignificant.

Table 5-3 shows the comparative data for the same modes performed in shirt sleeves by the two special subjects. The tests were performed with a 75-lb (1-g) pack load (Pack I). These data are much lower than the suited data, thus yielding an index of the energy cost imposed by the suit. For walking and running gaits, use of the pressurized suit approximately doubled the energy cost for a given velocity. The increase with the suit for the loping gait, however, was approximately 50 percent. The loping modes had a higher energy cost than the other locomotive gaits ($p < 0.05$). This is in contrast to the thesis proposed previously by others which states that, based on kinematic data, the lope should have the lowest energy requirement (Reference 5-1).

The total energy requirements for increased weight carrying are presented in Table 5-4 for the 240-lb (1-g) Pack II and in Table 5-5 for the 400-lb (1-g) Pack III. In the 1/6-g environment, the subjects worked against the inertia of the 240-lb mass or the 400-lb mass while actually carrying 40 or 66-2/3 lb. The energy required for walking was significantly higher with increasing velocity for the walking gait with Pack II ($p < 0.05$). There was no velocity effect within the loping or running gait with Pack II. Loping with Pack II had a higher energy cost than walking at 6 km/hr ($p < 0.05$) but showed no difference at 8 km/hr. The energy cost of loping at 8, 9.7, and 11.3 km/hr was higher than running with the 240-lb Pack II ($p < 0.05$). The data for Pack III were inconclusive because of the number of tests performed. However, it would appear that had more tests been run, there would have been a significant statistical increase in loping as compared to walking at 6 km/hr, no difference between the 3 gaits at 8 km/hr, and a significant difference between loping and running at 9.7 km/hr, with the lope having the higher energy cost.

Statistical comparisons between the tests performed with the three different pack loads revealed no differences within the gaits for Packs I, II, and III. There was also no pack effect between gaits performed at the same velocity. Several conclusions can be drawn on the absence of significant differences between tests performed with the various packs. First, since the energy cost is not increased as the total work is increased, the subjects must be working with greater efficiency. That is, the energy cost per kg of weight carried is less, and the subjects are much more efficient. This increased efficiency may be due to the increased traction gained from the added weight as the load is increased (Reference 5-2). Although these conclusions are obvious, they may not in fact, be substantiated when comparative tests are performed in a 6-deg-of-freedom simulator where directional stability is a problem. The interaction of traction and stability are not completely understood, but it is assumed that increased traction should provide postural stability. Also, there must be a limit to the beneficial effects of increased weight either because of the inertial effects of handling a large mass or because the metabolic rate is increased to 1-g equivalents by increasing the weight of the subject back to that g field.

TABLE 5-3

TOTAL ENERGY AND PROPORTIONAL ENERGY REQUIREMENTS
 LOCOMOTION ON HORIZONTAL INCLINED-PLANE SIMULATOR
 WITH PACK I, SUBJECT IN MUFTI

Gait	Velocity, km/hr	Average total energy, kcal (Col I)	Average energy for work, kcal (Col II)	Average energy post-work, kcal (Col III)	Ratio of Col III/Col I (Col IV)	Total energy during work, kcal (Col V)	Average energy cost, kcal/min (Col VI)	Steady-state energy cost, kcal/min (Col VII)
Walk	2	25.77	19.44	6.33	0.246	21.3	1.52	1.46
	4	28.08	21.42	6.65	0.237	22.7	1.62	1.28
	6	52.15	40.30	11.85	0.227	44.4	3.17	3.05
	8	84.78	67.07	17.71	0.209	69.0	4.93	4.53
Lope	6	104.67	84.21	20.46	0.195	91.4	6.53	6.24
	8	104.29	82.17	22.12	0.212	92.0	6.57	6.21
	9.7	114.89	92.87	22.02	0.192	101.8	7.27	7.37
	11.3	111.56	88.89	22.66	0.203	98.6	7.04	6.89
Run	8	62.00	49.36	12.64	0.204	47.0	3.36	2.92
	9.7	63.95	47.49	16.46	0.257	54.5	3.89	3.31
	11.3	86.96	69.30	17.66	0.203	74.1	5.29	4.95
	12.8	94.12	75.92	18.20	0.193	81.6	5.83	5.63

TABLE 5-4

TOTAL ENERGY AND PROPORTIONAL ENERGY REQUIREMENTS
LOCOMOTION ON HORIZONTAL INCLINED-PLANE SIMULATOR
WITH PACK II

Gait	Velocity, km/hr	Average total energy, kcal (Col I)	Average energy for work, kcal (Col II)	Average energy post-work, kcal (Col III)	Ratio of Col III/Col I (Col IV)	Total energy during work, kcal (Col V)	Average energy cost, kcal/min (Col VI)	Steady-state energy cost, kcal/min (Col VII)
Walk	2	89.78	67.07	22.70	0.253	73.2	5.23	5.12
	4	95.06	72.15	22.91	0.241	85.0	6.07	5.52
	6	115.14	93.11	22.03	0.191	95.2	6.80	6.87
	8	160.47	130.66	29.81	0.186	145.3	10.38	10.08
Lope	6	166.00	131.27	34.73	0.209	151.5	10.82	10.43
	8	153.22	123.28	29.94	0.195	139.3	9.95	9.10
	9.7	173.43	142.02	31.41	0.181	153.3	10.95	10.51
	11.3	170.57	139.27	31.29	0.183	158.5	11.32	10.66
Run	8	137.26	110.17	27.09	0.197	123.1	8.79	8.49
	9.7	145.09	116.85	28.24	0.195	134.8	9.63	8.05
	11.3	144.59	116.97	27.62	0.191	132.6	9.47	8.73
	12.8	154.72	124.26	30.45	0.197	141.0	10.07	9.43

TABLE 5-5

TOTAL ENERGY AND PROPORTIONAL ENERGY REQUIREMENTS
LOCOMOTION ON HORIZONTAL INCLINED-PLANE SIMULATOR
WITH PACK III

Gait	Velocity km/hr	Average total energy, kcal (Col I)	Average energy for work, kcal (Col II)	Average energy post-work, kcal (Col III)	Ratio of Col III/Col I (Col IV)	Total Energy During Work, kcal (Col V)	Average energy cost, kcal/min (Col VI)	Steady-state energy cost, kcal/min (Col VII)
Walk	2	61.03	46.88	14.15	0.232	51.0	3.64	3.39
	4	94.99	74.28	20.70	0.218	77.7	5.55	5.33
	6	121.57	100.85	20.71	0.170	104.9	7.49	7.16
	8	117.03	94.47	22.56	0.193	103.5	7.39	7.68
Lope	6	181.62	150.78	30.83	0.170	156.0	11.14	10.3
	8	138.63	111.70	26.92	0.194	124.3	8.88	9.48
	9.7	207.77	153.52	54.25	0.261	196.3	14.02	12.53
	11.3	237.42	198.31	39.11	0.165	221.9	15.85	16.20
Run	8	152.93	126.99	25.94	0.170	136.4	9.74	9.57
	9.7	113.72	90.58	23.14	0.204	100.0	7.14	7.29
	11.3	163.72	122.92	40.80	0.249	150.6	10.76	10.77
	12.8	204.96	140.84	64.12	0.313	171.9	12.28	12.60

Table 5-6 presents the data for traversing slopes with either Pack I or Pack II.

Metabolic rates were significantly higher for ascending and descending slopes as a function of increased velocity ($p < 0.01$). The energy cost of ascending slopes was higher than walking level ($p < 0.01$), which in turn had a higher energy requirement than for descending slopes. Carrying a 240-lb pack further increased the energy cost for ascending or descending slopes. There was also a statistically significant interaction between velocity and slope, indicating that there is a curvilinear relationship between these parameters and their resultant effect on the dependent variable of total energy cost for locomotion.

No data are available for the 8-km/hr velocity for ascending a 30-deg slope because of the inability of any subject to perform this mode. At the 6-km/hr velocity with a 30-deg slope, only one subject completed the 14-min exercise period. The other subjects completed between 3 and 5-1/2 min of exercise before the tests were stopped because their heart rates had exceeded the established limits for safety.

Total energy and proportional energy required for locomotion at 1/6 g on the TOSS simulator. - The data obtained for locomotion in each of the 3 gaits across 4 velocities with the 75-lb load at 1/6 g on TOSS with a hard horizontal surface are presented in Table 5-7. The total energy required for walking was significantly increased with velocity ($p < 0.01$), but the change by velocity for the loping and running gaits was not significant. Where comparisons were made between gaits used to perform the same velocity, the lope had a higher energy cost than walking at both 6 and 8 km/hr ($p < 0.01$). Loping also had higher energy requirements than running at 8, 9.7, or 11.3 km/hr ($p < 0.01$). These differences between gaits at the same velocity are in direct contrast to results for locomotion on the inclined plane where no differences were found for similar comparisons.

The energy costs of ascending and descending slopes on a hard surface with Pack I are shown in Table 5-8. For ascending the 7.5-deg and 15-deg slopes, metabolic rates increased significantly with each 2-km/hr increment in velocity ($p < 0.01$). During descent of the 7.5-deg slope, energy costs increased as the velocity was changed from 2 to 4 km/hr ($p < 0.05$); no difference was noted between the 4- and 6-km/hr modes; and another significant increase occurred between the 6- and 8-km/hr ($p < 0.05$). During descent of the 15-deg slope, metabolic rates increased with velocity ($p < 0.05$). Similar differences were found for descending the 30-deg slope.

TABLE 5-6

TOTAL ENERGY AND PROPORTIONAL ENERGY REQUIREMENTS,
TRAVERSING SLOPES ON INCLINED-PLANE SIMULATOR

Pack	Slope incline, deg	Velocity, km/hr	Average total energy, kcal (Col I)	Average energy for work, kcal (Col II)	Average energy post-work, kcal (Col III)	Ratio of Col III/I (Col IV)	Total energy during work kcal (Col V)	Average energy cost, kcal/min (Col VI)	Steady-state energy cost, kcal/min (Col VII)
I (75 lb)	7.5 (ascending)	2	57.36	45.00	12.36	0.215	46.5	3.32	3.06
		4	85.87	68.97	16.90	0.197	76.2	5.44	5.42
		6	120.15	94.37	25.78	0.215	111.7	7.98	7.12
		8	138.81	109.46	29.34	0.211	124.6	8.90	8.84
	7.5 (descending)	2	54.36	41.54	12.82	0.236	41.6	2.97	2.52
		4	67.83	53.25	14.58	0.215	55.2	3.94	3.74
		6	77.17	61.12	16.05	0.208	64.1	4.58	4.42
		8	85.28	68.14	17.13	0.201	71.8	5.13	4.58
II (240 lb)	7.5 (ascending)	2	74.97	58.20	16.77	0.224	60.3	4.31	4.18
		4	111.47	89.36	22.10	0.198	98.6	7.04	7.04
		6	148.46	117.07	31.38	0.211	134.7	9.62	9.94
		8	181.92	142.90	39.02	0.214	170.8	12.20	12.09
	7.5 (descending)	2	58.95	45.78	13.17	0.223	42.6	3.04	2.89
		4	74.56	57.66	16.90	0.227	60.2	4.30	4.11
		6	88.20	68.58	19.62	0.222	71.8	5.13	4.93
		8	102.51	81.48	21.03	0.205	90.0	6.42	6.19
I	15 (ascending)	2	74.12	58.53	15.59	0.210	65.0	4.64	4.27
		4	116.45	91.59	24.85	0.213	104.3	7.45	7.11
		6	151.18	120.66	30.51	0.202	140.3	10.02	9.68
		8	176.43	143.24	33.19	0.188	166.6	11.90	X
	15 (descending)	2	53.49	41.00	12.49	0.233	40.6	2.90	2.57
		4	65.69	50.85	14.84	0.226	52.2	3.73	3.29
		6	78.28	61.90	16.39	0.209	65.7	4.69	4.18
		8	87.62	70.58	17.04	0.194	71.8	5.13	5.07
II	30 (ascending)	2	122.00	101.11	20.89	0.171	110.6	7.90	7.90
		4	171.72	139.82	31.90	0.186	156.0	11.14	11.14
		6	216.63	180.92	35.71	0.165	193.1	13.79	13.79
		8	X	X	X	X	X	X	X
	30 (descending)	2	59.83	45.18	14.65	0.245	44.9	3.21	2.88
		4	72.28	57.63	14.64	0.203	59.2	4.23	4.10
		6	87.20	68.80	18.40	0.211	72.2	5.16	4.73
		8	104.08	82.33	21.75	0.209	89.7	6.41	6.11

TABLE 5-7

TOTAL ENERGY AND PROPORTIONAL ENERGY REQUIREMENTS
LOCOMOTION ON HORIZONTAL TOSS SIMULATOR
WITH PACK I

Gait	Velocity km/hr	Average total energy, kcal (Col I)	Average energy for work, kcal (Col II)	Average energy post-work, kcal (Col III)	Ratio of Col III/Col I (Col IV)	Total energy during work, kcal (Col V)	Average energy cost, kcal/min (Col VI)	Steady-state energy cost, kcal/min (Col VII)
Walk	2	76.71	62.89	13.82	0.180	58.8	4.20	4.12
	4	99.35	80.35	19.01	0.191	84.1	6.01	5.99
	6	119.50	96.02	23.47	0.196	102.1	7.29	7.29
	8	130.69	104.16	26.52	0.203	121.7	8.69	8.21
Lope	6	159.22	134.29	24.93	0.157	146.2	10.44	10.44
	8	173.28	146.13	27.15	0.157	161.1	11.51	10.94
	9.7	184.55	152.33	32.22	0.175	171.9	12.28	11.81
	11.3	189.06	156.85	32.22	0.170	173.7	12.41	12.37
Run	8	133.81	109.61	24.21	0.181	117.6	8.40	8.42
	9.7	155.26	130.42	24.84	0.160	134.4	9.60	9.71
	11.3	152.65	126.36	26.29	0.172	137.6	9.83	9.53
	12.8	172.57	141.32	31.25	0.181	160.3	11.45	11.01

TABLE 5-8

TOTAL ENERGY AND PROPORTIONAL ENERGY REQUIREMENTS, TRAVERSING SLOPES
ON TOSS SIMULATOR WITH PACK I, HARD SURFACE

Slope incline, deg	Velocity, km/hr	Average total energy, kcal (Col I)	Average energy for work, kcal (Col II)	Average energy post-work, kcal (Col III)	Ratio of Col III/I (Col IV)	Total-energy during work kcal (Col V)	Average energy cost kcal/min (Col VI)	Steady-state energy cost, kcal/min (Col VII)
7.5 (ascending)	2	75.0 \pm 13.5	59.2 \pm 10.5	15.8 \pm 3.4	0.210	65.1	4.65	4.44
	4	118.9 \pm 7.8	95.8 \pm 7.8	23.1 \pm 1.1	0.194	109.8	7.84	7.56
	6	161.0 \pm 25.4	129.7 \pm 23.4	31.3 \pm 5.7	0.194	150.5	10.75	10.88
	8	197.5 \pm 57.2	157.6 \pm 53.8	40.0 \pm 8.3	0.202	185.5	13.25	14.19
7.5 (descending)	2	54.2 \pm 7.9	42.8 \pm 7.2	11.3 \pm 1.0	0.209	44.5	3.18	3.15
	4	71.5 \pm 11.7	57.7 \pm 9.6	13.8 \pm 2.5	0.193	60.9	4.35	4.45
	6	83.9 \pm 14.5	66.9 \pm 10.9	17.0 \pm 3.8	0.203	72.7	5.19	5.02
	8	101.7 \pm 19.6	83.4 \pm 16.9	18.4 \pm 3.9	0.180	85.3	6.09	6.50
15 (ascending)	2	94.2 \pm 13.2	75.6 \pm 10.3	18.6 \pm 3.3	0.197	86.0	6.14	5.60
	4	177.5 \pm 28.7	143.0 \pm 27.1	34.5 \pm 5.8	0.194	168.0	12.0	8.90
	6	209.2 \pm 39.1	165.9 \pm 39.6	43.3 \pm 11.5	0.207	199.0	14.2	12.64
	8							
15 (descending)	2	52.0 \pm 9.9	40.8 \pm 8.9	11.2 \pm 1.5	0.215	35.6	2.54	2.54
	4	62.6 \pm 6.9	50.1 \pm 6.3	12.5 \pm 1.6	0.199	50.8	3.63	3.71
	6	67.5 \pm 6.1	55.3 \pm 4.9	12.3 \pm 1.8	0.181	59.9	4.28	4.12
	8	82.9 \pm 16.6	66.9 \pm 13.6	16.0 \pm 2.3	0.193	72.7	5.19	5.22
30 (ascending)	1	162.3 \pm 36.2	132.3 \pm 27.2	29.9 \pm 9.6	0.184	151.3	10.81	10.81
30 (descending)	2	58.8 \pm 12.9	45.1 \pm 12.5	13.6 \pm 5.8	0.232	48.2	3.44	3.00
	4	66.3 \pm 10.0	51.5 \pm 10.6	14.8 \pm 4.6	0.223	54.7	3.91	3.92
	6	74.3 \pm 6.6	58.9 \pm 5.7	15.5 \pm 2.2	0.208	63.4	4.53	4.38
	8	86.7 \pm 9.0	69.3 \pm 7.2	17.3 \pm 2.2	0.200	71.5	5.11	4.93

Evaluation of the effects of traversing slopes shows that more energy was required for ascending the 7.5 deg slope than for horizontal locomotion at each velocity ($p < 0.01$) except at 2 km/hr. Increasing the slope to 15-deg further increased the energy cost at each velocity ($p < 0.01$) except at 2 km/hr. None of the subjects could accomplish the 8-km/hr mode on the 15-deg slope or any of the velocities on the 30-deg slope. As a result, the subjects were asked to attempt to accomplish 1-km/hr ascents at 30-deg. Four subjects managed to perform this task for at least 10 min. In each of the cases where the subjects could not perform the required mode, the causes were the loss of traction and the inability of the subjects to keep up with the treadmill even though they had not reached the limits for test termination based on physiological measures. The loss of traction and its effect in decreased cravity has been described by Wortz (Reference 5-2). It can be concluded from these data that climbing such extreme slopes will have an extremely high energy cost and should be avoided. These tests dictated constant-velocity locomotion, however, and do not indicate that slopes up to 30-deg could not be navigated under any circumstances.

Statistical comparisons of the data for ascending and descending slopes showed that metabolic rates were higher for the ascending modes than for the descending modes at both 7.5 and 15 deg ($p < 0.01$).

The total energy requirements for locomotion of the simulated smooth and coarse lunar soil under the various test conditions are presented in Table 5-9. Locomotion on the smooth lunar soil with a 0-deg slope resulted in an increased cost with increased velocity at each interval ($p < 0.05$). With the simulated coarse lunar soil, the same significance was obtained except that, although the total energy for walking at 8 km/hr was greater than at 6 km/hr, it did not significantly increase.

For ascending and descending slopes with the simulated smooth lunar soil, the total energy requirements increased with velocity. The difference between velocities was significant for ascending and descending 7.5-deg slopes ($p < 0.05$) and 15-deg slopes ($p < 0.05$), with the exception that there was no significant difference between 4- and 6-km/hr velocities for descending the 15-deg slope.

Energy costs were higher for ascending the 15-deg slope than the 7.5-deg slope ($p < 0.01$). On the other hand, the energy requirement for descending a 15-deg slope was much lower than for a 7.5-deg slope. Energy cost was significantly higher ascending for both the 7.5- and 15-deg slopes than for descending ($p < 0.01$).

TABLE 5-9

TOTAL ENERGY AND PROPORTIONAL ENERGY REQUIREMENTS, TRAVERSING SLOPES
ON TOSS SIMULATOR WITH PACK I, SIMULATED LUNAR SURFACE

Simulated lunar surface	Slope incline, deg	Velocity, km/hr	Average total energy, kcal (Col I)	Average energy for work, kcal (Col II)	Average energy post-work, kcal (Col III)	Ratio of Col III/I (Col IV)	Total energy during work (Col V)	Average energy cost, kcal/min (Col VI)	Steady-state energy cost, kcal/min (Col VII)
Smooth soil	0 (horizontal)	2	74.08	59.10	14.97	0.202	61.0	4.36	4.35
		4	99.32	81.03	18.29	0.184	87.2	6.23	6.24
		6	137.75	114.82	22.93	0.166	126.6	9.04	8.73
		8	193.25	160.58	32.67	0.169	17.9	12.80	12.28
Coarse soil	0	2	64.85	51.56	13.28	0.205	57.3	4.09	3.90
		4	110.33	89.67	20.66	0.187	100.0	7.14	6.91
		6	153.64	125.03	28.61	0.186	139.4	9.96	10.27
		8	169.69	138.09	31.60	0.186	155.5	11.11	11.09
Smooth soil	7.5 (ascending)	2	90.00	74.01	15.99	0.178	76.3	5.45	4.35
		4	139.42	117.75	21.67	0.155	128.8	9.20	6.24
		6	185.05	152.19	32.86	0.178	172.1	12.29	12.64
		8	210.33	178.55	31.78	0.151	197.8	14.13	
	7.5 (descending)	2	55.58	44.77	10.78	0.194	44.7	3.19	3.21
		4	80.09	63.93	16.16	0.202	69.0	4.93	4.95
		6	99.97	80.43	19.53	0.195	88.6	6.33	6.12
		8	119.12	96.23	22.89	0.192	106.4	7.60	7.42
	1.5 (ascending)	2	117.84	95.95	21.89	0.186	107.2	7.66	7.16
		4	182.21	145.83	36.38	0.200	169.0	12.07	13.18
	1.5 (descending)	2	53.61	41.29	12.32	0.230	46.9	3.35	2.99
		4	65.74	51.65	14.09	0.214	57.7	4.12	3.81
		6	78.26	62.71	15.55	0.199	69.0	4.93	5.04
		8	87.53	69.73	17.80	0.203	77.0	5.50	5.80

Effects of surfaces on total energy requirements with the TOSS simulator.-

Energy costs for ascending slopes on the simulated smooth lunar soil were higher than for the same modes performed on the hard surface. The increased energy with the lunar soil condition was also seen for descending a 7.5-deg slope ($p < 0.01$). For descending a 15-deg slope, the smooth lunar soil tests required higher, more significant energy levels ($p < 0.07$). The energy cost of locomotion on the simulated smooth lunar soil results from the reduction in traction. It is interesting to note that the subjects reported less difficulty with directional stability on the soil surface. This was attributed to the small differences in push-off with either foot being transmitted to or damped by the soil so that torquing did not occur at the same level as on the hard surface, and the subjects had better control of their balance. In addition, the subjects dragged their toes in the soil to correct directional stability rather than having to compensate by pushing harder with the opposite foot to correct for twisting.

The tests performed on the simulated coarse lunar soil did not produce significantly different total energy data when compared to the values from tests with simulated smooth lunar soil. There was a significant interaction between velocity and surface, however, showing a curvilinear relationship between these variables.

The simulated coarse lunar soil requires slightly lower energies than the smooth surface at 2 km/hr, higher energies at 4 and 6 km/hr, and about the same value at 8 km/hr. These data would indicate that the presence of rock in the soil increased traction at 2 km/hr and then affected directional stability at the higher velocities. Both the coarse and smooth lunar soils resulted in higher total energy requirements than needed for locomotion on the hard surface ($p < 0.01$).

Comparison of simulators based on total energy requirements for locomotion. - It has been of continuing interest to evaluate the degrees-of-freedom found in a simulator and the energy cost of performance in that simulator. The inclined plane is a 3-deg-of-freedom simulator, while the TOSS is a 6-deg-of-freedom simulator. Earlier studies, using a counterbalanced 6-deg-of-freedom simulator (References 5-3 and 5-4), indicated that the energy cost of locomotion was lower when compared to data obtained on an inclined-plane simulator. As noted in Table 5-1, the mean total energy value for each velocity is higher with TOSS than for the inclined plane, except for the 8-km/hr walk and the 12.8-km/hr run. However, statistical treatment of these data revealed that the differences in the means only approached significance ($p < 0.07$). It is believed that simulator differences were masked by the use of pressure suits that were highly restrictive to locomotive mobility. If similar tests were performed in the more mobile suits, significant simulator differences might be observed.

It was also interesting to note that locomotive tasks which resulted in lower total energy requirements, such as for descending slopes, minimized the differences between simulators. In contrast, ascending slopes which increased energy requirements magnified the differences between the simulators. The TOSS simulator produced higher metabolic data than the inclined-plane simulator. These differences were significant at the 0.01 level of confidence for ascending both the 7.5- and 15-deg slopes. There was also a significant interaction between simulators and slope direction ($p < 0.01$).

Additional considerations of proportional energies. - Several other facts can be derived from the tables of total and proportional energy (e.g., Table 5-2) shown in this section. The fourth column of each table shows that the ratio of the oxygen repayment period energy to the total energy for performing the exercise is relatively constant even though the metabolic cost is increased three to four times. This phenomenon is not understood at this time. Another factor of importance in these tables lies in the comparison of the fifth and sixth columns. The fifth column is derived by dividing the total energy required to perform each task by 14 (the number of minutes the subjects exercised). This provides a measure of the average energy per unit time (kcal/min) used to perform each mode and is comparable to the steady-state metabolic rates shown in the sixth column. Comparison of the values shown in these columns indicates that the total energy for performing a test can be evaluated simply by measuring the steady-state value and multiplying by the total time the exercise is performed. It must be noted that this consideration would only hold for a task repeated long enough for the individual to reach a true steady-state condition.

Steady-State Metabolic Rates

The data presented in this subsection correspond to the values noted in the time course curves when the curves had become asymptotic, usually by the sixth minute of exercise. This leveling of the curves indicates that the body has achieved new set-points for its physiological systems in response to the requirements imposed by the exercise and is operating at a new steady-state level. Table 5-10 presents the mean ± 1 standard deviation of the steady-state metabolic rate data in kcal/min for the subjects in all the exercise modes studied. The data missing in the cells for the 6-deg-of-freedom TOSS with a pressurized suit for the ascending modes at 15- and 30-deg on the hard surface and 7.5- and 15-deg on the simulated smooth lunar soil, and at 15- and 30-deg in the inclined plane with a hard surface represent the inability of the subjects to complete the modes; the reasons will be discussed later.

Suited tests on the horizontal inclined-plane simulator with a hard surface. - Three series of tests were accomplished to analyze the differences between repeated tests at the same conditions. Statistical analyses of these data showed no significant differences. Therefore, the data were pooled before other comparisons were made. The first row of Table 5-10 shows the pooled data for the duplicate tests across the six subjects. Comparison of these values to those shown in the second row for the two special test subjects

TABLE 5-10

STEADY-STATE METABOLIC RATES (KCAL/MIN)
FOR ALL SIMULATOR EXERCISE MODES

Experimental conditions							Results (mean and ± 1 standard deviation)							
Simulator and suit mode	Slope, deg	Surface condition	Pack	Number of velocities	Number of subjects	Total tests	Gait or ascend/descend	Velocity, km/hr						
								2	4	6	8	9.7	11.3	12.8
Inclined plane, pressurized (press.) suit	0 (horiz)	Hard	I, 75 lb	4 each; walk, lope and run	6, with 2 repeating once	96	Walk	3.67 \pm 0.75	4.63 \pm 1.92	6.42 \pm 3.16	13.32 \pm 5.39			
							Lope			7.63 \pm 1.73	9.96 \pm 4.24	10.08 \pm 2.53	12.31 \pm 2.96	
							Run				7.57 \pm 1.19	9.56 \pm 1.35	9.99 \pm 1.75	11.37 \pm 3.09
Inclined plane, pressurized suit	0	Hard	I	1 each; walk, lope, and run	6, with all repeating twice	36	Walk	3.65 \pm 1.47						
							Lope			7.43 \pm 2.28				
							Run				7.59 \pm 2.76			
Inclined plane, subject in mufti (without press. suit)	0	Hard	I	4 each; walk, lope, and run	2	24	Walk	1.46 \pm 0.84	1.28 \pm 1.01	2.99 \pm 0.41	4.65 \pm 0.83			
							Lope			5.92 \pm 0.45	6.47 \pm 0.28	6.97 \pm 0.26	6.89 \pm 0.78	
							Run				2.97 \pm 0.46	9.39 \pm 1.19	4.95 \pm 0.85	5.63 \pm 2.04
Incl plane, mufti	0	Hard	I	Fatigue test	6	24	Run				3.10 \pm 0.96*	3.15 \pm 0.86*	3.43 \pm 0.67*	4.55 \pm 1.01*
Inclined plane, pressurized suit	0	Hard	I	Fatigue test	2	8	1-hr duration				5.27 \pm 1.11*	8.56 \pm 0.95*	10.00 \pm 1.09*	6.28 \pm 0.30*
											4.91 \pm 0.88**	8.30 \pm 0.98**	6.69 \pm 3.24**	8.64 \pm 0.78**
Inclined plane, pressurized suit	0	Hard	II, 240 lb	4 each; walk, lope, and run	6	72	Walk	5.12 \pm 2.34	5.52 \pm 1.03	6.87 \pm 2.16	10.09 \pm 3.07			
							Lope				10.44 \pm 2.55	10.94 \pm 2.28	11.81 \pm 1.28	12.37 \pm 1.99
							Run					8.49 \pm 1.40	8.05 \pm 2.23	8.73 \pm 1.32
														9.43 \pm 1.18
Inclined plane, pressurized suit	0	Hard	III, 400 lb	4 each; walk, lope, and run	2	24	Walk	3.39 \pm 0.01	5.33 \pm 0.07	7.16 \pm 1.45	7.68 \pm 0.46			
							Lope				10.3 \pm 0.39	9.48 \pm 0.32	12.53 \pm 1.97	16.20
							Run					9.57 \pm 3.91	7.29 \pm 0.02	10.77 \pm 0.62
														12.59
TOSS (6-deg-of-freedom), pressurized suit	0	Hard	I	4 each; walk, lope, and run	6	72	Walk	4.12 \pm 1.25	5.99 \pm 1.08	7.28 \pm 2.19	8.20 \pm 1.32			
							Lope				10.44 \pm 2.55	10.94 \pm 2.28	12.17 \pm 0.97	
							Run					8.42 \pm 0.83	9.71 \pm 2.43	9.53 \pm 1.41
														11.01 \pm 2.19
TOSS, press. suit	0	Smooth lunar	I	4 velocities	6	24		4.35 \pm 0.56	6.24 \pm 0.73	8.73 \pm 1.78	12.28 \pm 1.21			
TOSS, press. suit	0	Coarse lunar	I	4 velocities	6	24		3.90 \pm 0.31	6.91 \pm 0.62	10.27 \pm 0.82	11.09 \pm 1.09			
TOSS, pressurized suit	7.5	Hard	I	4 velocities	6	48	Ascend	4.44 \pm 0.78	7.51 \pm 0.68	10.88 \pm 1.49	14.19 \pm 3.07			
							Descend	3.15 \pm 0.57	4.45 \pm 0.96	5.02 \pm 0.78	6.50 \pm 1.02			
TOSS, pressurized suit	7.5	Smooth lunar	I	4 velocities	6	48	Ascend	5.60 \pm 1.37	8.90 \pm 1.41	12.64 \pm 1.30				
							Descend	3.21 \pm 0.25	4.95 \pm 0.44	6.12 \pm 0.86	7.42 \pm 1.32			
TOSS, pressurized suit	15	Hard	I	4 velocities	6	48	Ascend	6.00 \pm 0.46	12.22 \pm 1.79					
							Descend	2.54 \pm 0.55	3.71 \pm 0.76	4.12 \pm 0.47	5.22 \pm 1.08			
TOSS, pressurized suit	15	Smooth lunar	I	4 velocities	6	48	Ascend	7.16 \pm 0.66	13.18 \pm 0.94					
							Descend	2.99 \pm 0.33	3.81 \pm 0.43	5.04 \pm 0.98	5.80 \pm 0.90			
TOSS, pressurized suit	30	Hard	I	4 velocities	6	48	Ascend	10.81*** (at 1 km/hr)						
							Descend	3.00 \pm 0.61	3.92 \pm 0.77	4.38 \pm 0.38	4.93 \pm 0.70			
Inclined plane, pressurized suit	7.5	Hard	I	4 velocities	6	48	Ascend	3.06 \pm 0.92	5.42 \pm 1.74	7.12 \pm 3.49	8.84 \pm 3.01			
							Descend	2.52 \pm 0.54	3.74 \pm 1.10	4.42 \pm 0.91	4.58 \pm 0.98			
Inclined plane, pressurized suit	7.5	Hard	II	4 velocities	6	48	Ascend	4.18 \pm 0.54	7.04 \pm 1.47	9.94 \pm 1.92	12.09 \pm 2.85			
							Descend	2.89 \pm 0.45	4.11 \pm 0.97	4.93 \pm 0.66	6.19 \pm 1.41			
Inclined plane, pressurized suit	15	Hard	I	4 velocities	6	48	Ascend	4.27 \pm 0.71	7.11 \pm 1.13	9.68 \pm 0.64				
							Descend	2.57 \pm 0.28	3.29 \pm 0.87	4.18 \pm 0.89	5.07 \pm 0.98			
Inclined plane, pressurized suit	30	Hard	I	4 velocities	6	48	Ascend	7.90	11.14	13.79				
							Descend	2.88 \pm 0.44	4.10 \pm 1.08	4.73 \pm 0.79	6.11 \pm 1.08			

***Rate of 10.81 kcal/min was taken at 1-km/hr velocity

*45 to 60 min interval, mean ± 1 std duration

**Mean ± 1 std, deviation of last 10 min of test

*45 to 60 min interval, mean ± 1 std duration
**Mean ± 1 std deviation of last 10 min of test

***Rate of 10.81 kcal/min was taken at 1-km/hr velocity

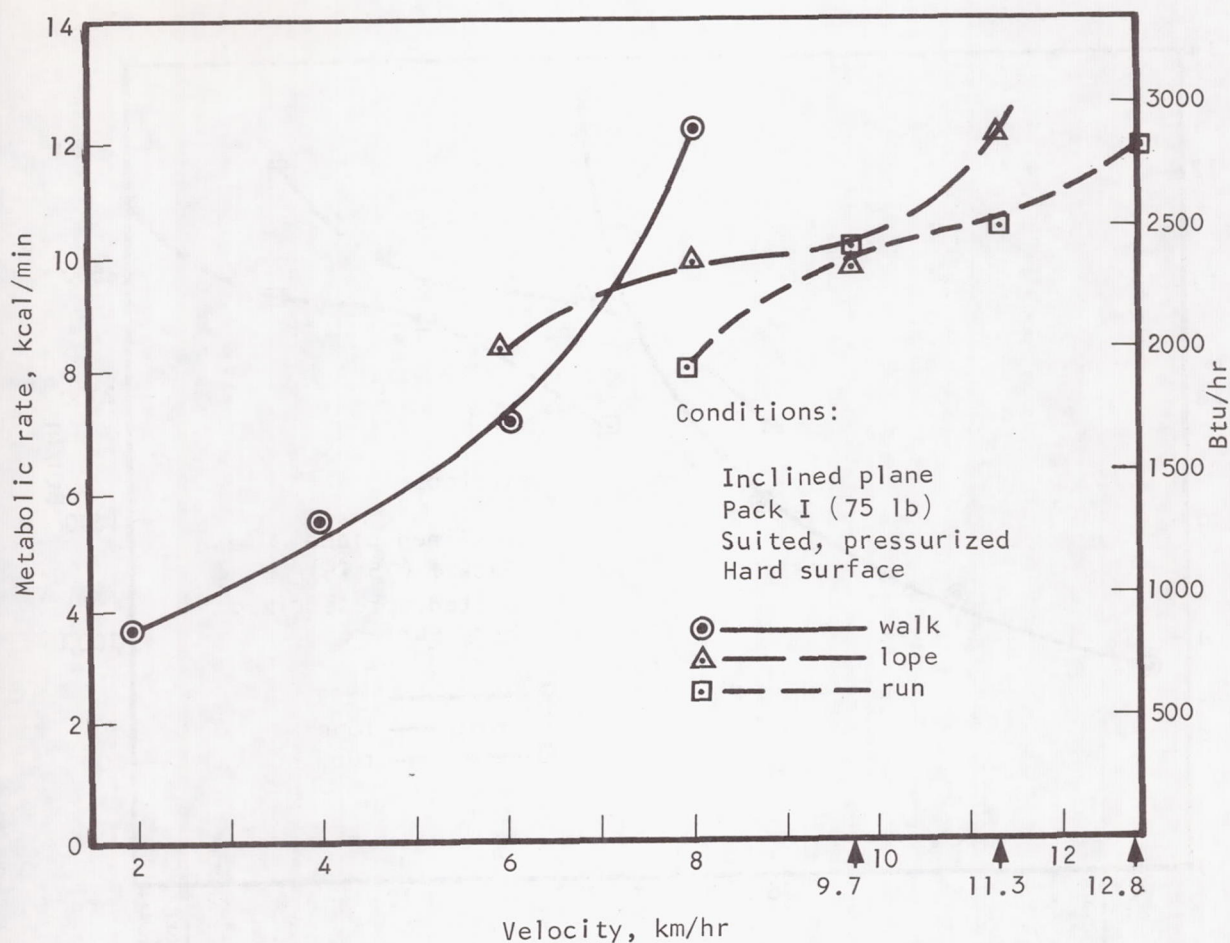
indicates the repeatability of the data. Pooling all the values minimized the effect of the variance of the data and increased the effectiveness of the statistical comparisons.

The steady-state metabolic rates for the initial tests with the 75-lb pack are shown graphically in Figure 5-8. Comparison of the curves for the pooled data shown in Figure 5-9 shows that the data are from the same population of values. The general forms of the curves obtained are as expected. If the subjects had been able to choose their gait to perform any given velocity, however, the curve for walking would probably have led directly into the curve for running to produce a straight line. The curve for the loping data lies above this imaginary line.

The metabolic costs of walking were increased significantly by velocity ($p < 0.01$) with the energy cost for the 8-km/hr walk being disproportionately high. In trying to walk at this velocity the subjects were forced to use an unusually long stride (refer to subsection on kinematics) while striving to maintain the double support required for walking. Hogberg (Reference 5-5) reported in 1952 that for running, the most economical stride length lies in the region of a freely chosen one, while an increase of stride length over this optimum yields a larger increase in energy cost than a corresponding shortening of the stride. Although Hogberg's studies were performed at 1-g, the same phenomenon has been demonstrated by Sanborn in a 1/6-g environment (Appendix C, Figure C-3) (Reference 5-6). This effect, coupled with the physical characteristics of the suit which impose an undue stress in performing the walking tasks, accounts for the exceptionally high energy cost of the 8-km/hr walk. The metabolic costs for loping at 1/6 g increased with velocity, but the increases were not significant. The running modes resulted in an increase in energy cost with velocity ($p < 0.05$).

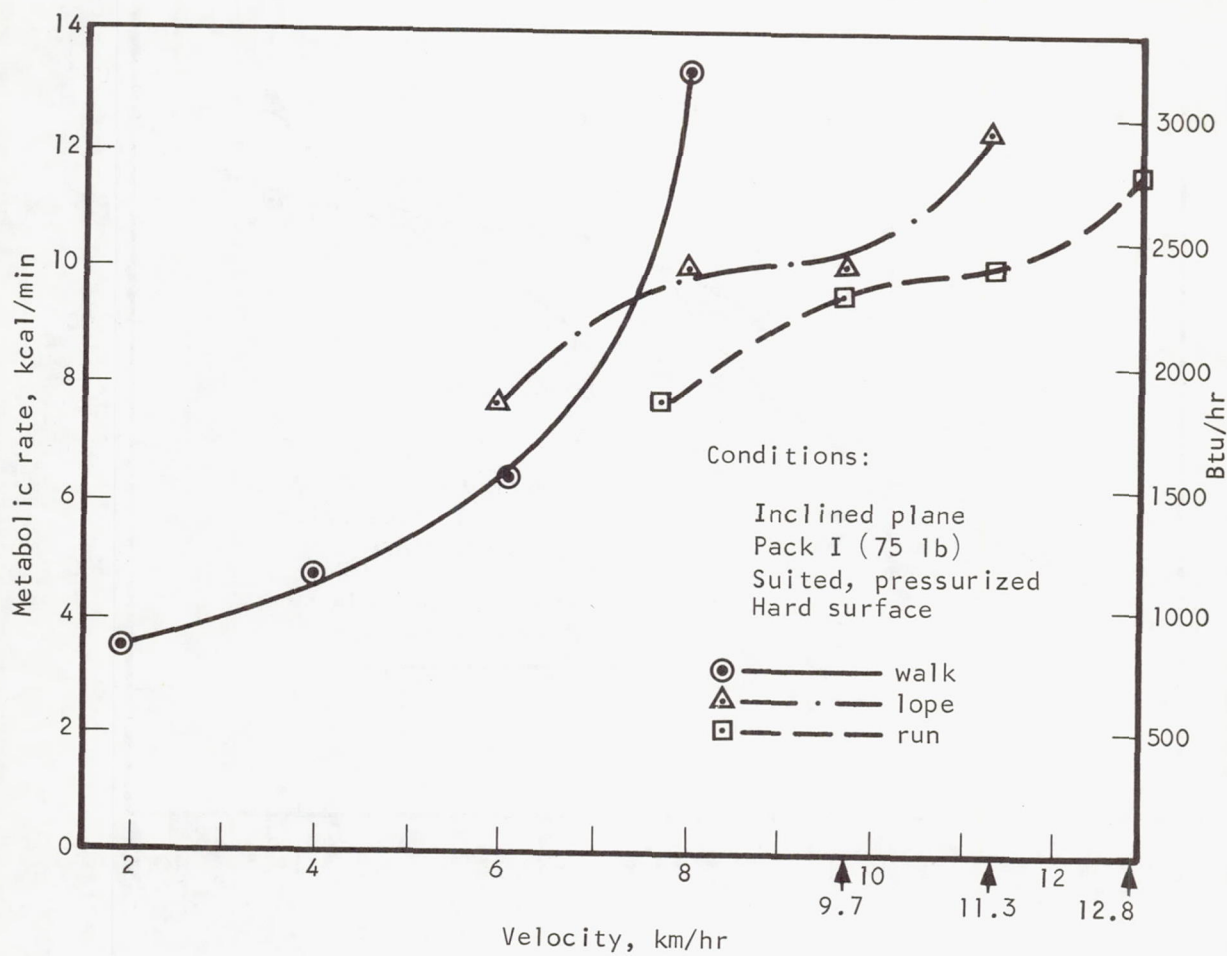
Statistical comparisons were also made between gaits where there was overlap of velocity. Thus, comparisons could be made between the walk and lope gaits at 6-km/hr, and between the lope and run gaits at 9.7 and 11.3 km/hr. With Pack I, there were no differences between the metabolic costs of walking or loping at 6 km/hr; walking, loping, or running at 8 km/hr; and loping or running at 9.7 and 11.3 km/hr. This would indicate that based on metabolic rate alone, there would be little choice between the lope and run gaits for these velocities with a 75-lb (1-g) pack.

Data shown in Figure 5-10 for subjects in shirt sleeves are significantly lower ($p < 0.01$) for each velocity than the data in Figure 5-8 for subjects in pressurized suits. The lope gait required significantly higher energy levels than either of the other gaits regardless of velocity ($p < 0.05$). The higher energy cost for loping is undoubtedly due to the requirement for performing more antigravity work than is the case in walking or running. Benedict and Marchauser (Reference 5-7) report that the energy requirements are higher for running than for walking at the same speed at 1 g due to the greater elevation of the body with the increased cost required to perform antigravity work. Supporting evidence has been presented by Fern (Reference 5-8) and Cavagna (Reference 5-9). Extrapolation of their conclusions to the 1/6-g environment supports the data obtained during this program and offers a



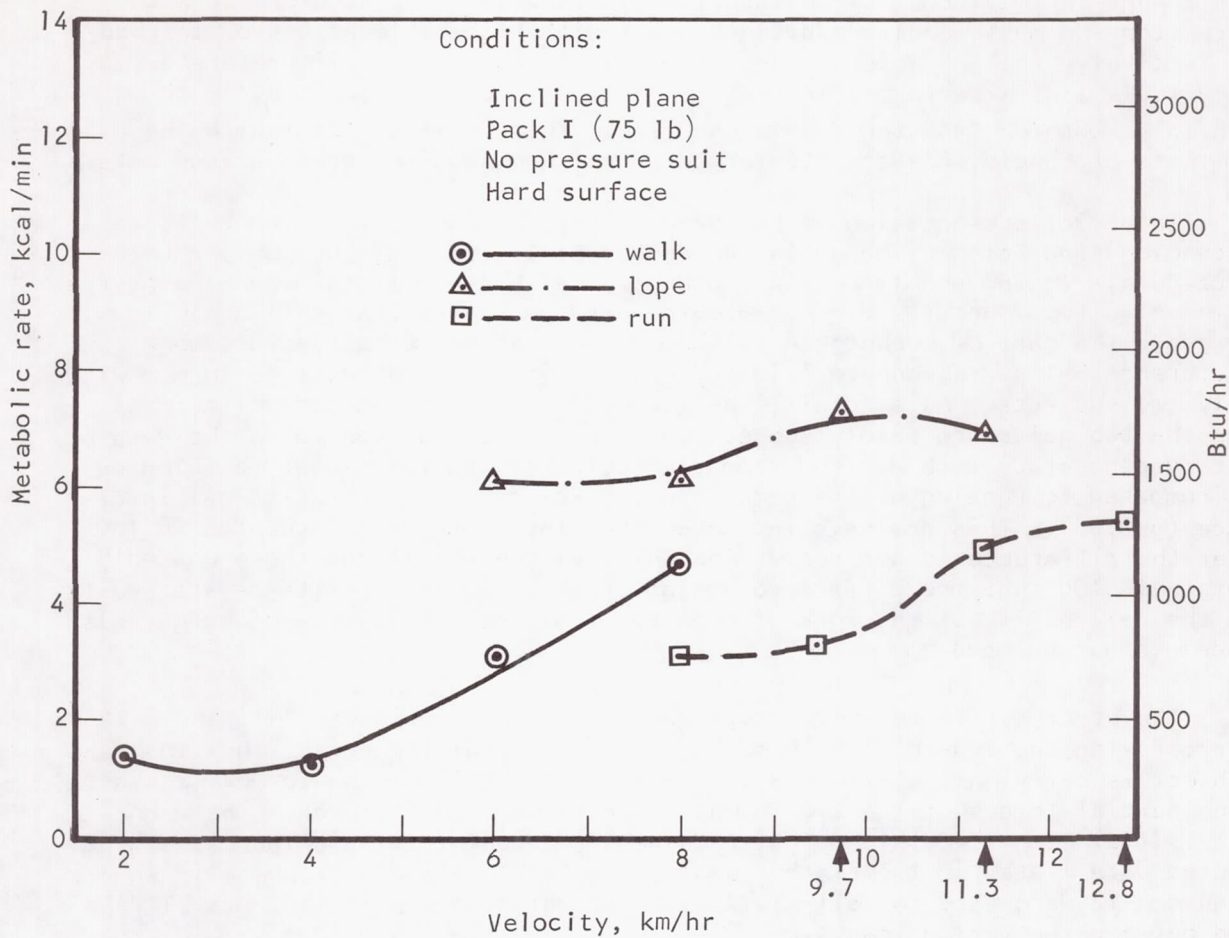
S-42660

Figure 5-8. Steady-State Metabolic Rates for Initial Trials on the Horizontal Inclined-Plane Simulator, Subject Carrying Pack I



S-42662

Figure 5-9. Steady-State Metabolic Rates for All Trials (Pooled Data) on the Horizontal Inclined-Plane Simulator with Pack I



S-42661

Figure 5-10. Steady-State Metabolic Rates for Locomotion on the Inclined-Plane Simulator, Pack I, Without Pressure Suit

probable explanation for the higher energy cost for loping. The energy cost for raising the body would be lower at 1/6-g, but proportional changes should be similar to the 1-g condition. Raising the body may be only a portion of the change in total cost of loping since the body must be decelerated with each step and must require additional cost with higher elevations of the body. Subjectively, the subjects all reported that if they had their preference, they would always perform a locomotive gait that could be performed with minimal excursion from the walking surface. This is in contrast with the comments of Langley Research Center personnel who have performed as subjects.

In a 1967 presentation to the Seventh International Symposium on Space Technology and Science, Margaria (Reference 5-10) reported that on a theoretical basis loping should not have a higher metabolic cost than running at the same velocity. Margaria did not provide data to substantiate his analysis. However, the data of Kuehnegger tends to give credence to Margaria's work (Reference 5-11). Kuehnegger's data, however is based on tests performed with only two subjects. As a result, the comparison between the metabolic costs for the two gaits are purely subjective comparisons. In contrast, the data of the current study were derived from six subjects, and the higher cost loping as compared to running at the same velocity was derived by statistical inference ($p < 0.05$). This analysis indicates that there are only 5 chances in 100 that the difference is not real. For shirt sleeve conditions there was only 1 chance in 100 that the difference was not real. Similar confidence statements on the reliability of the work of Kuehnegger or the sufficiency of Margaria's model cannot be made.

The steady-state metabolic rate data are shown in Figures 5-11 and 5-12 for carrying the 240-lb (1-g) Pack II, with the resulting effect that the subject is carrying a 40-lb load at 1/6-g, but is still having to work against the inertial forces of the 240-lb mass. There were no differences between the initial Pack II data and that obtained in repeat testing. Therefore, the pooled data listed in the sixth row of Table 5-10 and shown graphically in Figure 5-12 were used for all statistical comparisons within the Pack II data and between the various packs.

Statistical inferences indicate a significant increase in metabolic rate with velocity for walking with Pack II ($p < 0.01$). There were no differences with velocity for either the loping or running gaits. At 6 km/hr the energy cost for loping was higher than for walking ($p < 0.01$). There were no differences between the walking and running at 8 km/hr. The lope and run at 8, 9.7, and 11.3 km/hr were different ($p < 0.05$), with the lope having the higher energy cost.

Locomotion with Pack III required the subjects to transport a 400-lb (1-g) load which resulted in the subject carrying 66-2/3 lb in the 1/6-g environment while still affected by the inertial mass of 400 lb. Since only two subjects were used in these tests, and the variance between only two subjects tends to mask differences between mean values, the statistical analyses were not particularly meaningful. Since the number of degrees-of-freedom with only two subjects is one, the statistical tests are very insensitive to differences.

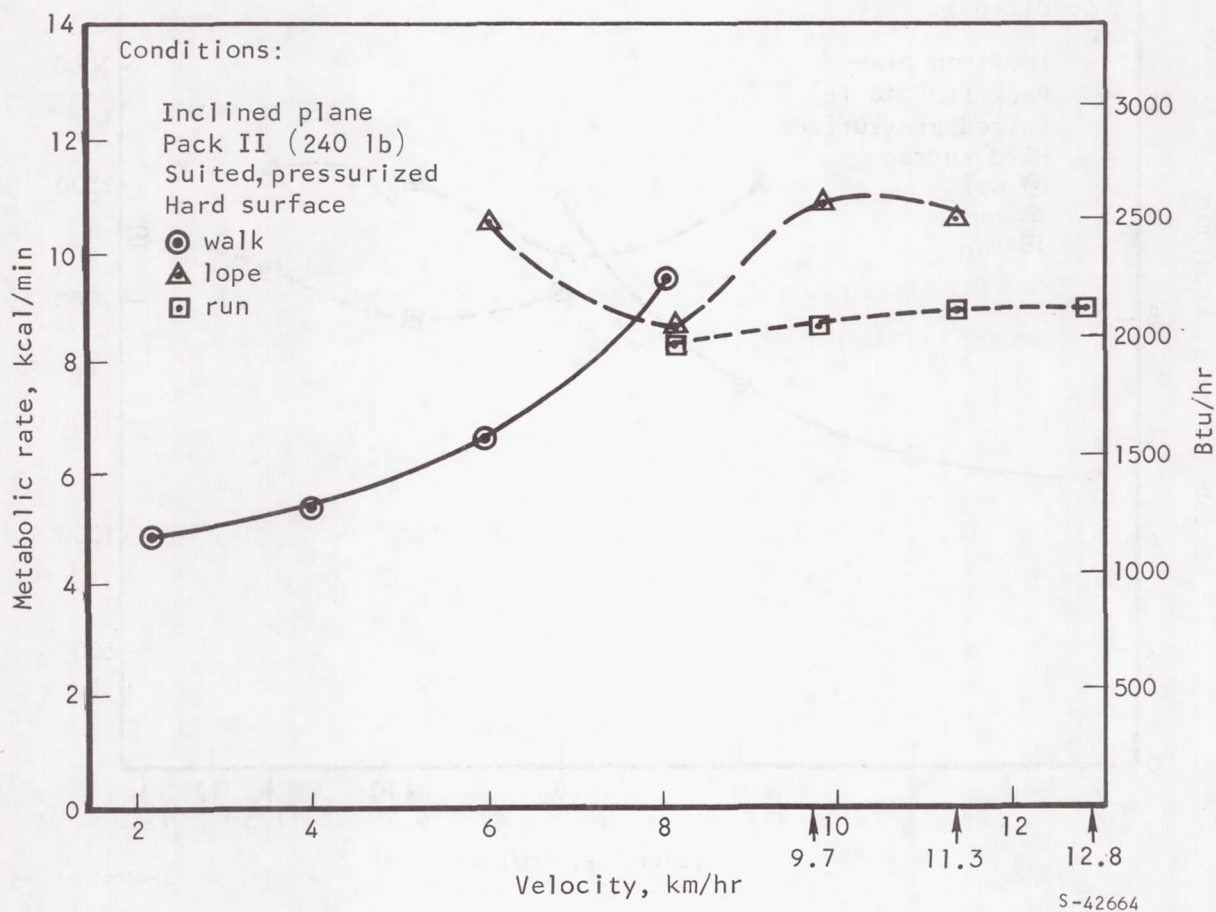


Figure 5-11. Steady-State Metabolic Rates for Initial Trials on the Inclined-Plane Simulator, Pack II

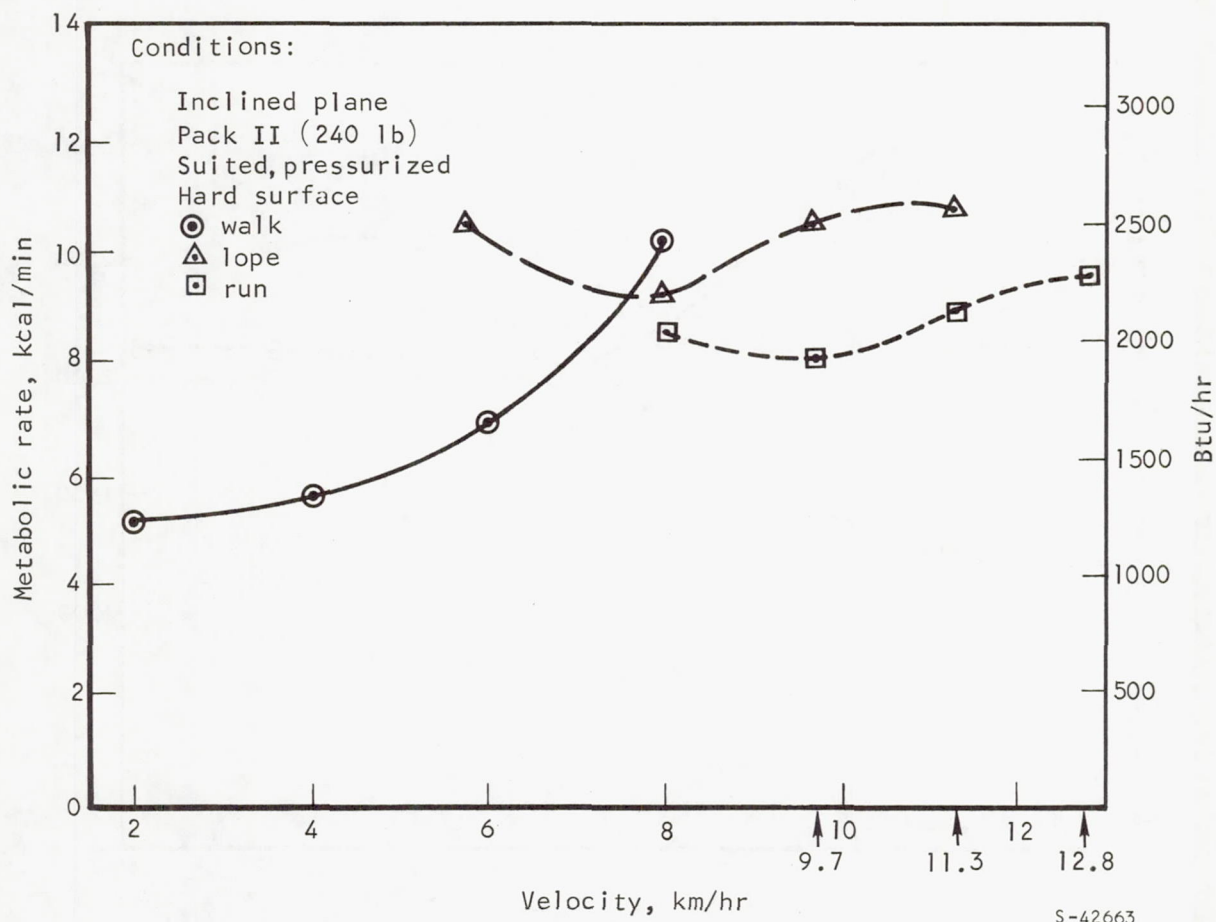


Figure 5-12. Steady-State Metabolic Rates for All Trials (Pooled Data) on the Inclined-Plane Simulator, Pack II

A comparison of Figure 5-13, which shows the results of testing with Pack III, with Figure 5-12 indicates that except for the two highest lope and the two highest run velocities, the data between Packs II and III were quite similar. At the higher velocities, the energy cost was very high. All the costs for the 2-km/hr and 8-km/hr walks were lower. The points of inflection in the 8-km/hr lope and the 9.7-km/hr run curves would infer that these velocities were better for locomotion than the other lope or run velocities.

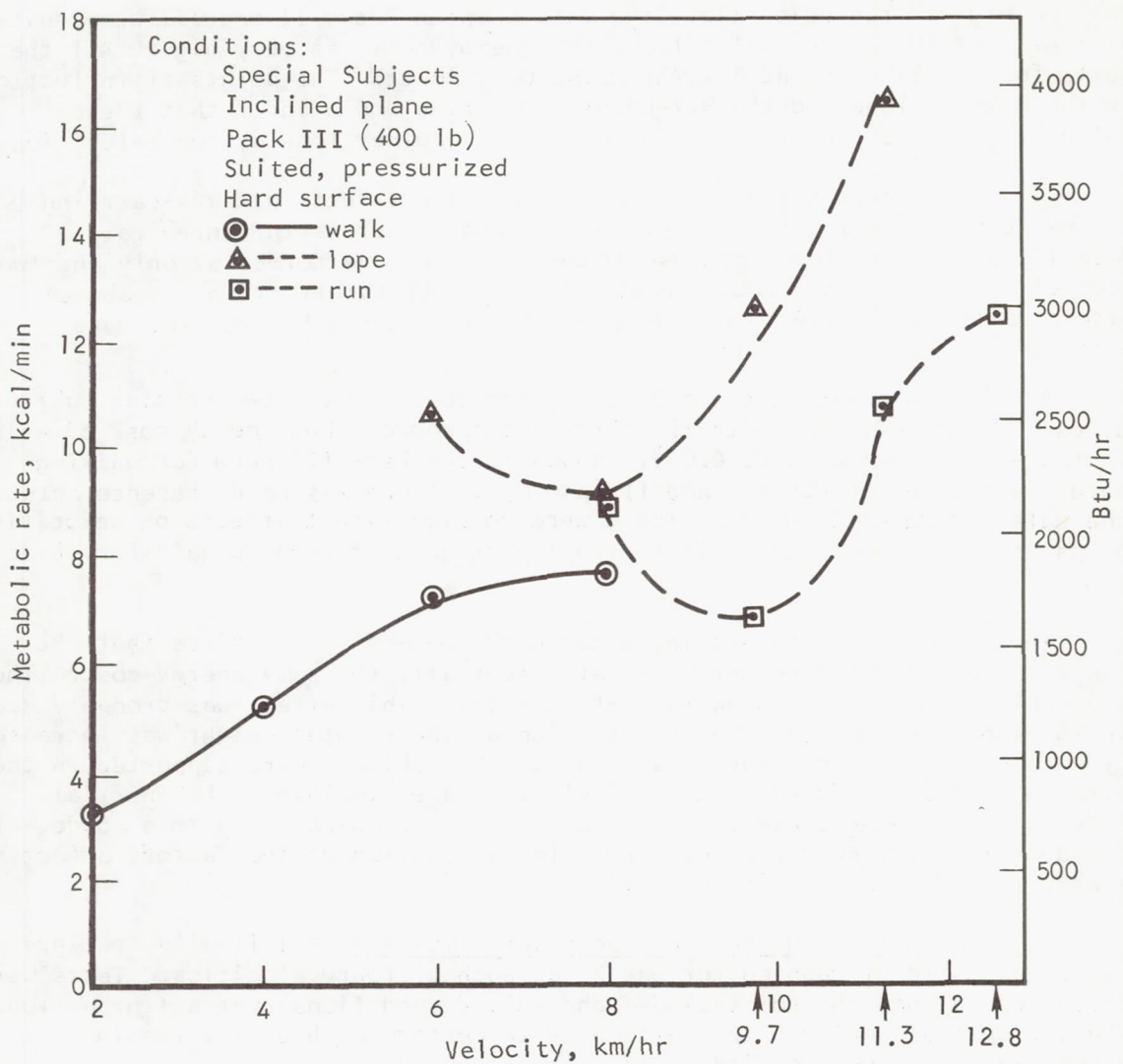
A multiple analysis of variance to test the effects of pack-carrying was performed on all the data for Packs I and II across the three gaits. Pack III was not included because those tests were performed by only the two special subjects. This analysis showed the velocity effects noted above within gaits and failed to demonstrate any differences between the data obtained for Packs I and II.

A multiple analysis of variance of the data for the two special subjects, across the three gaits, with the three packs, showed that energy cost of walking increased with velocity ($p < 0.01$). However, the Pack III data for walking were lower than for Packs I and II ($p < 0.05$). There was no difference between the data for Packs I and II. There were no significant effects of velocities or packs on metabolic cost within the loping gait or running gait for these two subjects.

The lack of significant increases with load-carrying infers that the subjects were performing more work at essentially the same energy cost. Thus, the subjects were performing more efficiently. This effect was probably due to the subjects obtaining better traction as their total weight was increased by adding weight with a pack load. Since the subjects were supported in the missing degrees-of-freedom in the inclined-plane simulator, the inertial effects of carrying these loads are not clear. Load-carrying in a 6-deg-of-freedom simulator should be performed for evaluation of the factors affecting energy expenditure with load-carrying.

Fatigue testing on the inclined-plane simulator. - Initially, fatigue tests consisted of running for one hr at each of four velocities. Tests were performed in both the shirt-sleeve and suited conditions over a 1-hr period. The two special subjects then attempted to perform each of the running velocities for a 4-hr period while suited.

The data for the 1-hr testing is shown in Figure 5-14. The energy costs of the shirt-sleeve activity were lower than for the suited tests. The metabolic costs of exercise for the suited condition were approximately 200 percent greater than for the shirt-sleeve condition. It is obvious from these curves that the subjects could perform the required exercise level with no adverse effect for one hr. Each subject's subjective response for the suited modes was one of extreme fatigue for all velocities. The mean values for these curves are not different from the steady-state data reported in Table 5-10 for the same velocities.



S-42641

Figure 5-13. Steady-State Metabolic Rates for Locomotion on the Inclined-Plane Simulator, Pack III

Conditions:
 Special Subjects
 Inclined plane
 Pack I
 Hard surface

Shirt sleeves	Suited, pressurized	Run km/hr
○ —————	● —————	8
◇ —————	◆ —————	9.7
□ —	■ —	11.3
△ —	▲ —	12.8

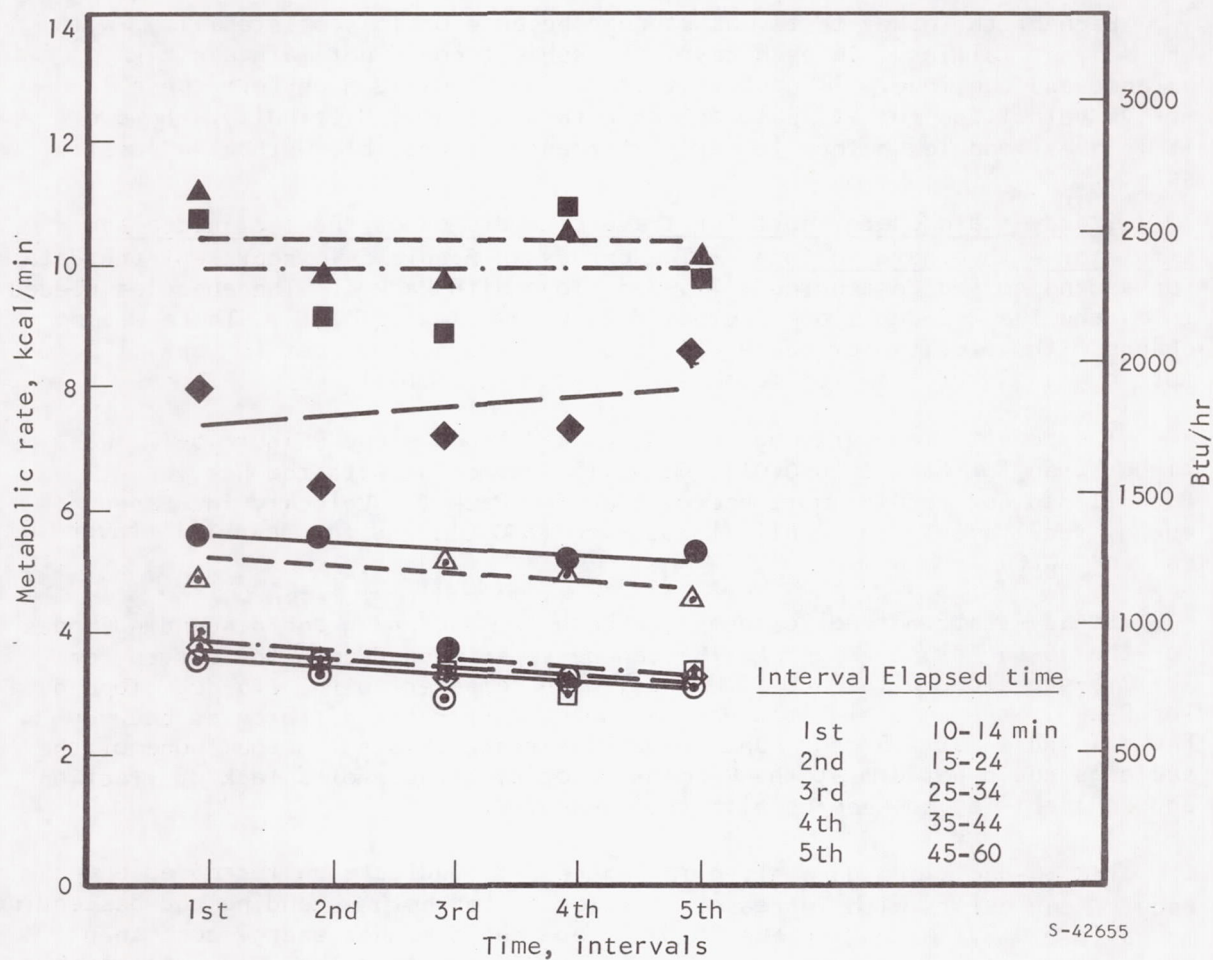


Figure 5-14. Fatigue Testing on the Inclined-Plane Simulator (One-Hour Tests)

The extended fatigue test data are shown in Figure 5-15. The values for the first interval (10-14 min of exercise) compare favorably with the steady-state data from Table 5-10. The downward slope of each faired curve is not understood. A number of factors could account for this phenomenon, such as warming of the legs with increased blood supply (nutrient supply) which could result in greater efficiency or an increase in anaerobic metabolism indicating a greater oxygen debt. Only one subject was able to perform for a full 4-hr period, and this was for the 9.7-km/hr run. The increase in metabolic rate after the fourth interval is indicative of fatigue occurring. Although the subject completed the 4-hr task, he was completely fatigued and did not fully recover until the fourth day after the test.

Each of the other tests was stopped because of loss of stability, with the subject falling. In each case, the subject could not maintain his balance and continue. It appears that an individual can perform these locomotive velocities for at least one hr without serious difficulty. However, it is questionable whether longer performance is possible without a loss in safety.

Steady-state energy cost for traversing slopes on the inclined-plane simulator with a hard surface. - The curves in Figure 5-16 represent the data for ascending and descending a 7.5-deg slope with Pack I. The energies needed to ascend the 7.5-deg slope increased with velocity ($p < 0.01$). There was no change with velocity for descending the same grade. The cost for uphill locomotion was higher than for downhill locomotion ($p < 0.01$).

The penalty for carrying Pack II up a 7.5-deg slope (Figure 5-17) was higher than for Pack I ($p < 0.01$). Downhill locomotion with the heavier Pack II did not require more energy than for Pack I. Velocity increased energy requirements for uphill locomotion ($p < 0.01$) and for downhill traversal ($p < 0.05$).

Steady-state metabolic costs for both the ascending and descending modes for the 15-deg slope (Figure 5-18) can be superimposed upon the curves for the 7.5-deg slope with Pack II. Thus, when compared to the 7.5-deg slope data for Pack I, the same significance was noted as for the differences between Packs I and II at 7.5 deg. One major difference exists, in that none of the subjects could perform at the 8-km/hr velocity because of a lack of traction and an inability to keep up with the treadmill.

The 30-deg slope data given in Figure 5-19 indicate an increased energy requirement exists with increases in velocity for both ascending and descending modes ($p < 0.01$). Ascending the 30-deg slope had a higher energy cost than traversing a level surface or descending a 30-deg slope ($p < 0.01$). Although all subjects were able to accomplish the 2-km/hr velocity when ascending the 30-deg slope, only two of the subjects were able to accomplish the 4-km/hr velocity, and only one of these completed the 6-km/hr mode. No differences were noted for negotiating the downhill slopes for within the 7.5-, 15-, or 30-deg slopes.

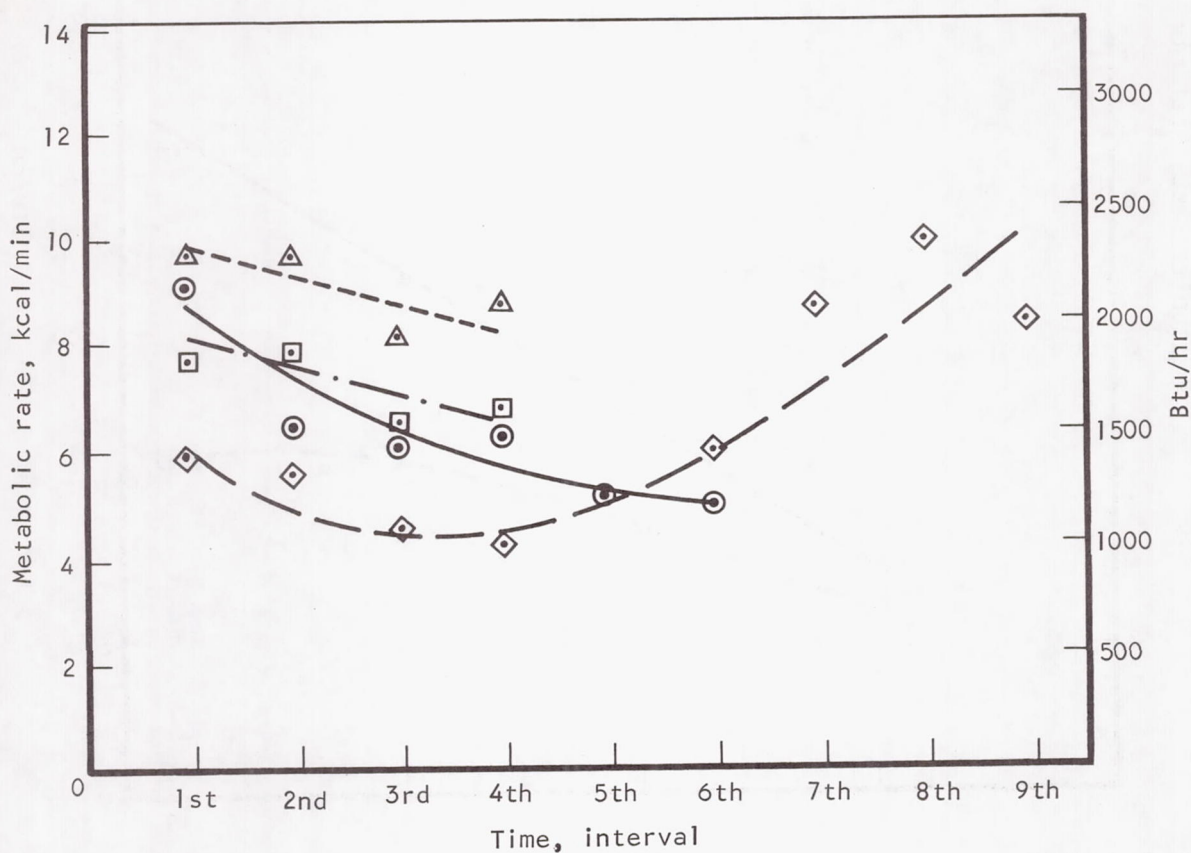
Interval	Elapsed time, min
----------	-------------------

1st	10-14
2nd	15-44
3rd	45-74
4th	75-104
5th	105-134
6th	135-164
7th	165-194
8th	195-224
9th	225-254

Conditions:

Special Subjects
Inclined plane
Pack I (75 lb)
Suited, pressurized
Hard surface

○	Run 8 km/hr
◇	Run 9.7 km/hr
□	Run 11.3 km/hr
△	Run 12.8 km/hr



S-42651-A

Figure 5-15. Extended Fatigue Testing on the Inclined-Plane Simulator

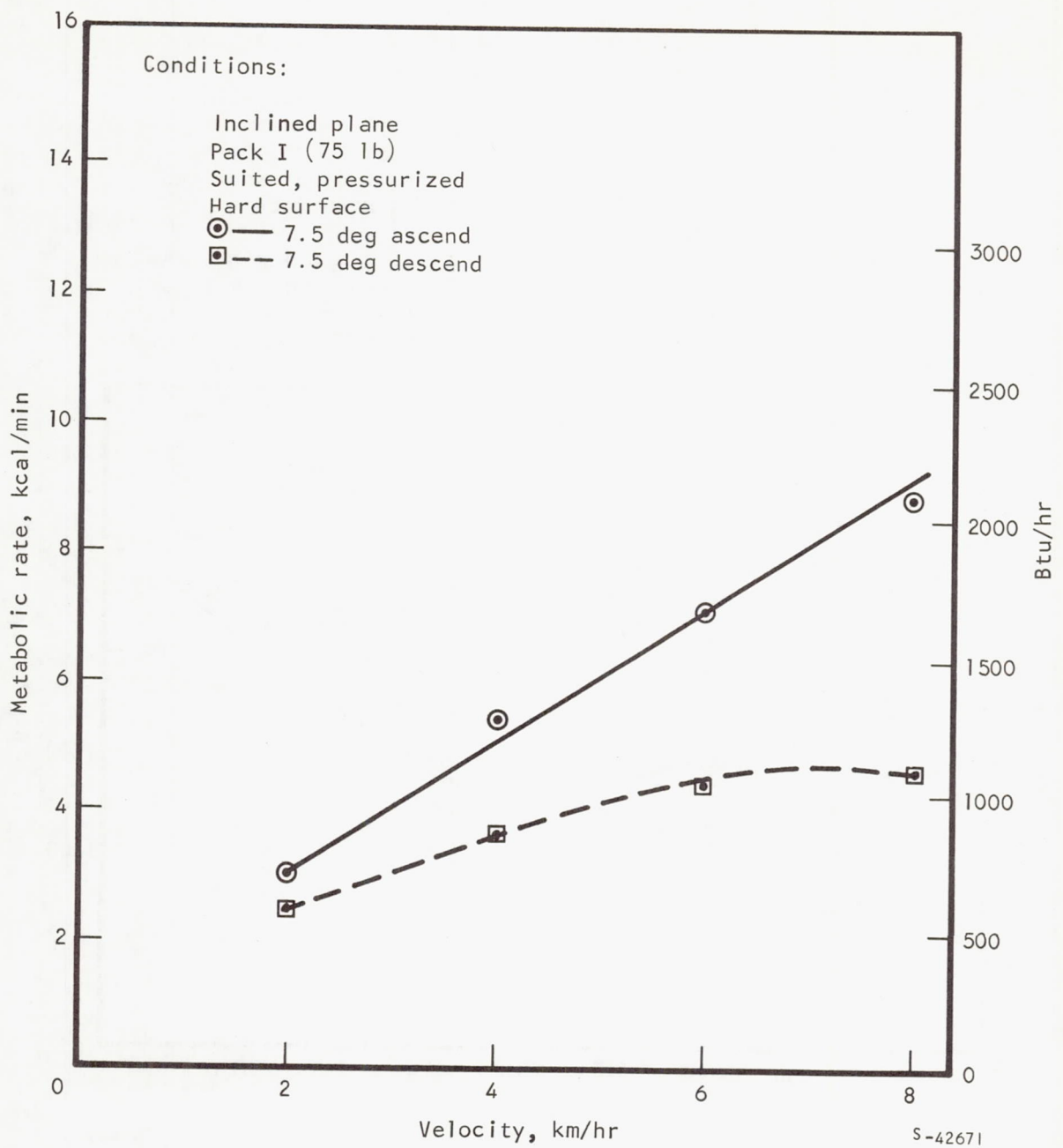


Figure 5-16. Steady-State Energy Cost for Traversing a 7.5-deg Slope on the Inclined-Plane Simulator with Pack I

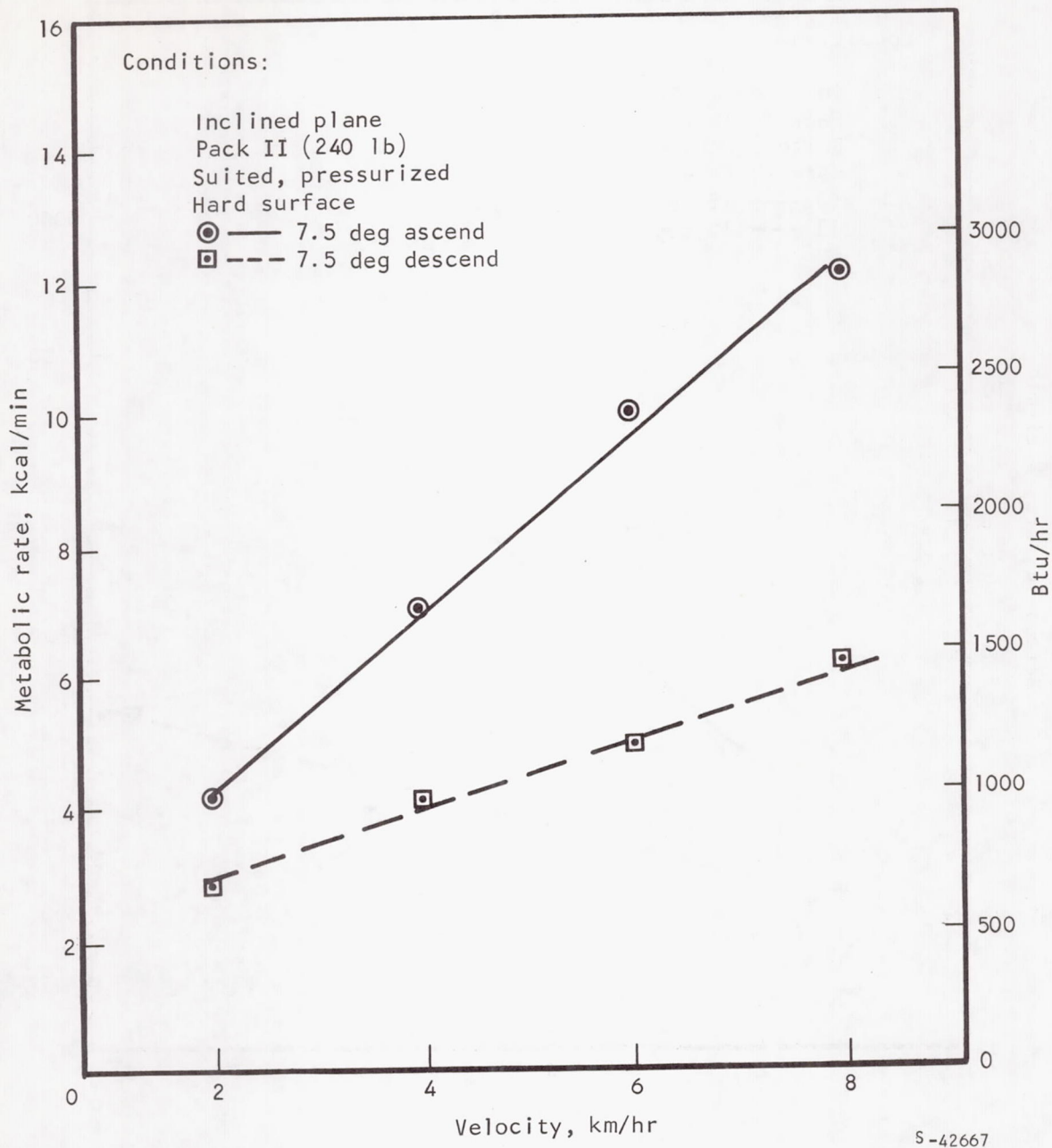


Figure 5-17. Steady-State Energy Cost for Traversing a 7.5-deg Slope, Inclined Plane, Pack II

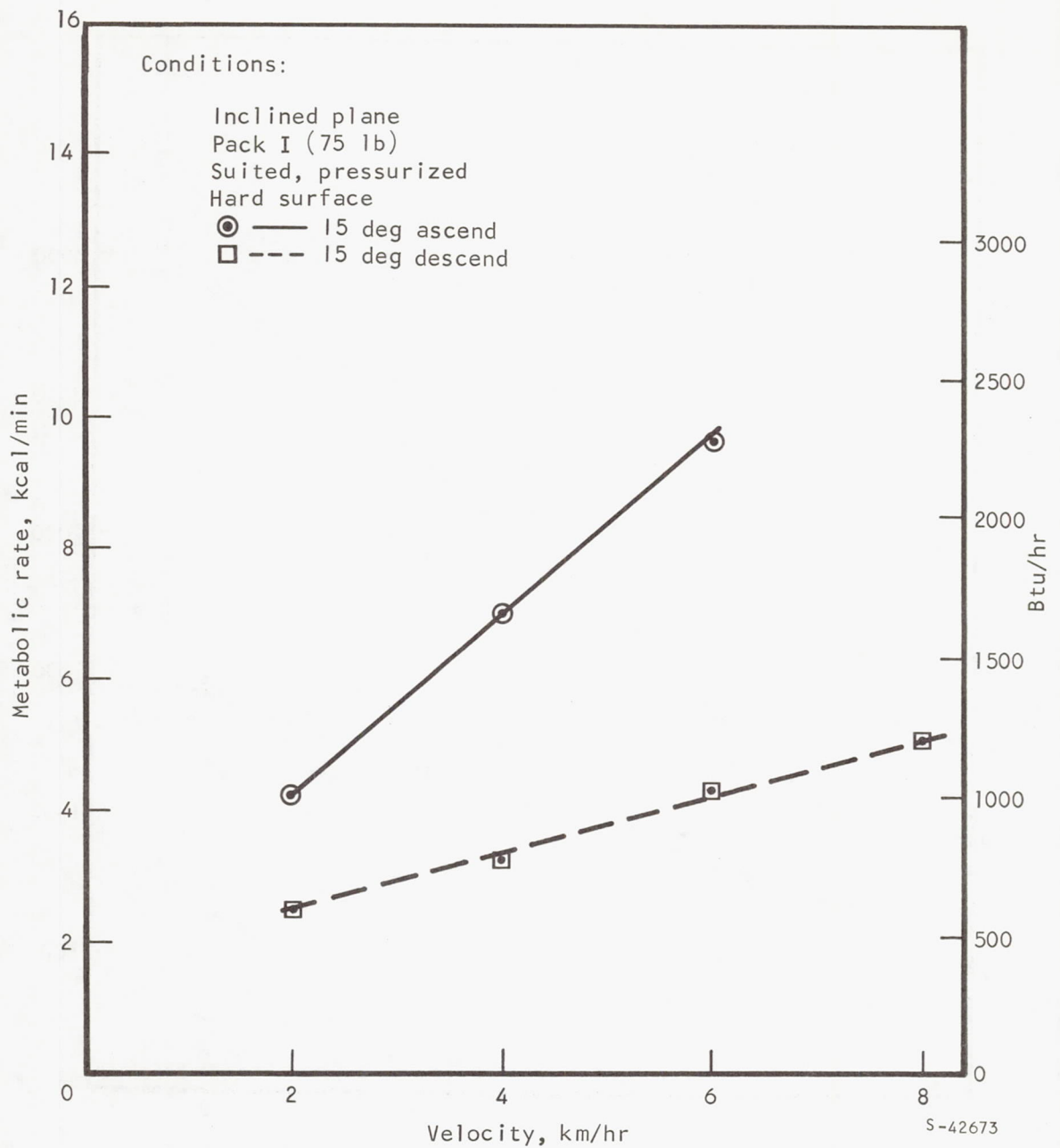


Figure 5-18. Steady-State Energy Cost for Traversing a 15-deg Slope, Inclined Plane, Pack I

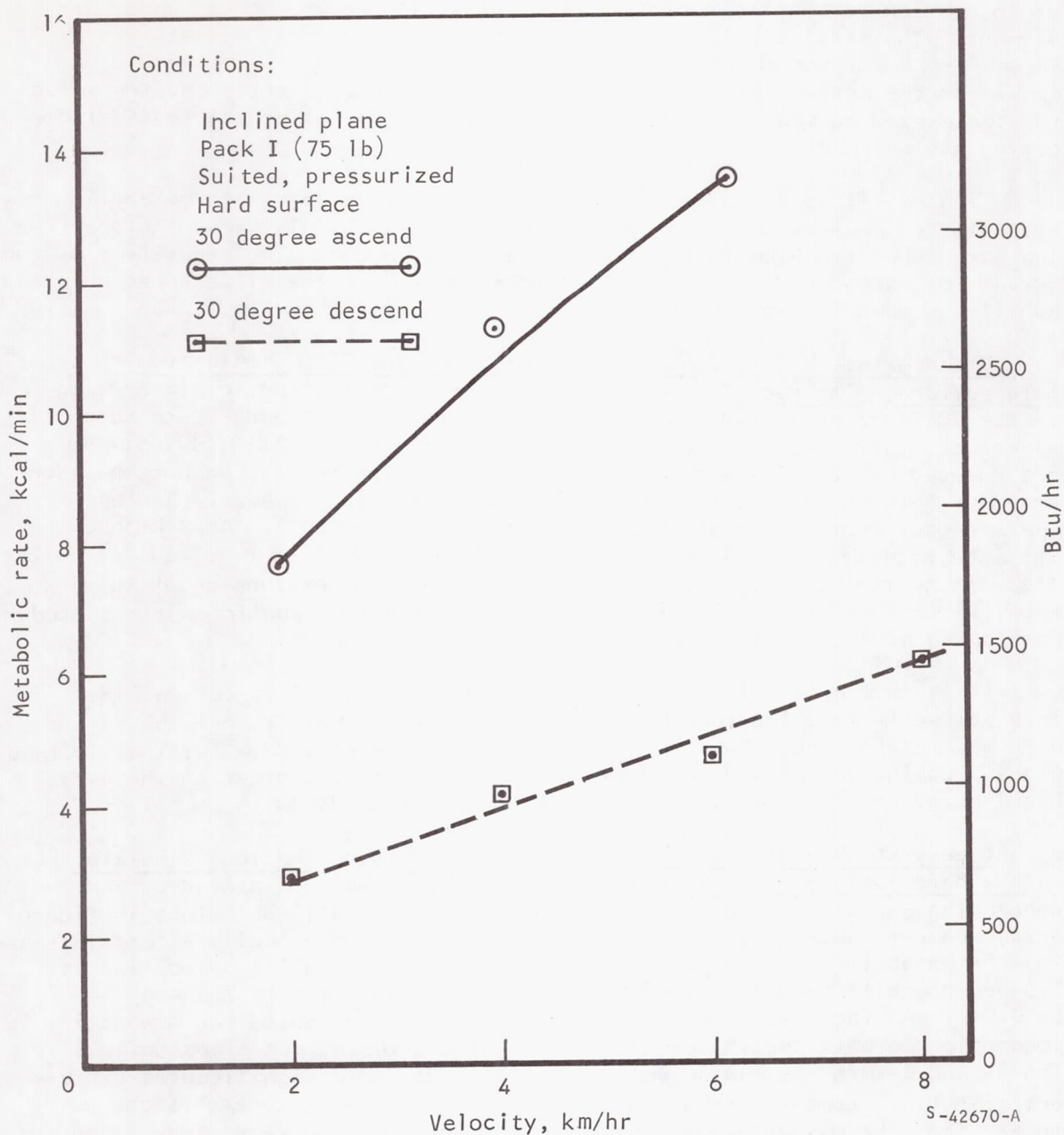


Figure 5-19. Steady-State Energy Cost for Ascending a 30-deg Slope on the Inclined-Plane Simulator

Figure 5-20 presents a summary plot of the steady-state metabolic cost of locomotion on the inclined-plane simulator with Pack I at 2, 4, 6, and 8 km/hr. The statistical relationships for the differences between these curves are described above. All the descending values lie below the curve for the horizontal test, indicating a lower energy cost; and the values for the ascending modes lie above the values for the horizontal tests, indicating a higher cost.

Figure 5-21 is a replica of the data from Figure 5-19 with metabolic rate plotted against the slope within each velocity. This presentation of the data shows graphically the differences noted above. The separation of the curves for ascending and descending slopes points out the differences between uphill and downhill locomotion.

Steady-state energy cost for locomotion on the TOSS simulator with a hard surface, with Pack I. - The data for the metabolic cost of locomotion in the TOSS are presented graphically in Figure 5-22. Steady-state metabolic rates were increased by velocity within the walking gait ($p < 0.01$), but were not changed by velocity within the lope or running modes. When comparisons are made between gaits performed at the same velocity, however, the lope had a higher energy cost than the walk at 6 km/hr ($p < 0.05$). At 8 km/hr, the lope resulted in a higher energy expenditure than that required for either the walk or run gaits ($p < 0.05$). The costs of walking or running at this velocity were not statistically different. A higher metabolic cost resulted for lope at 9.7 and 11.3 km/hr than for running ($p < 0.01$).

It is interesting to note that the curve in Figure 5-22 for walking leads directly into the running curve, and the total points could be fitted with a straight line. This was also noted in the Pack I data for the inclined plane. Loping values are completely above this curve, indicating the very high energy cost for performing the loping gait with TOSS.

Steady-state energy cost for traversing slopes on the TOSS simulator with a hard surface, with Pack I. - The metabolic costs of ascending and descending a 7.5-deg slope are shown in Figure 5-23, a 15-deg slope in Figure 5-24, and descending a 30-deg slope in Figure 5-25. A velocity effect increasing the metabolic cost of locomotion was noted between all 4 velocities at 7.5-deg downhill ($p < 0.05$) and for all 4 uphill velocities at 7.5 deg ($p < 0.01$). An increased cost across all velocities was noted for downhill locomotion on both the 15-deg slope ($p < 0.05$) and the 30-deg slope ($p < 0.05$). The 2- and 4-km/hr ascending velocities at 15-deg were significantly different ($p < 0.01$). Comparisons between requirements to navigate each slope showed that the oxygen needs for climbing a 15-deg slope were higher than for the 7.5-deg slope ($p < 0.01$). Traversing downhill slopes indicated that the 7.5-deg slope required more energy than either the 15-deg or 30 deg slope ($p < 0.01$), and there was no difference between the 15-deg and 30-deg data. Climbing uphill had a high cost than going downhill at all velocities with both slopes ($p < 0.01$).

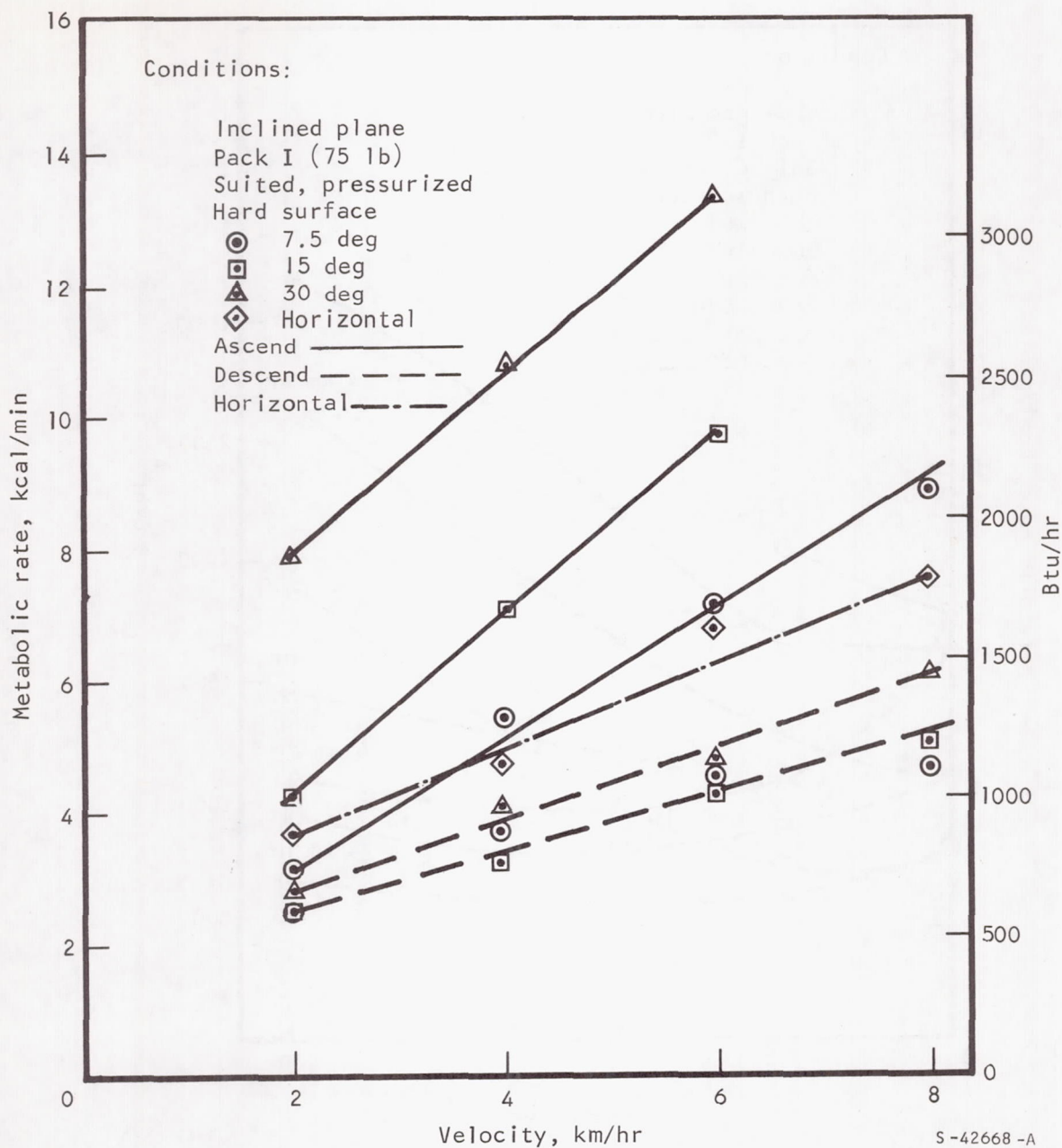
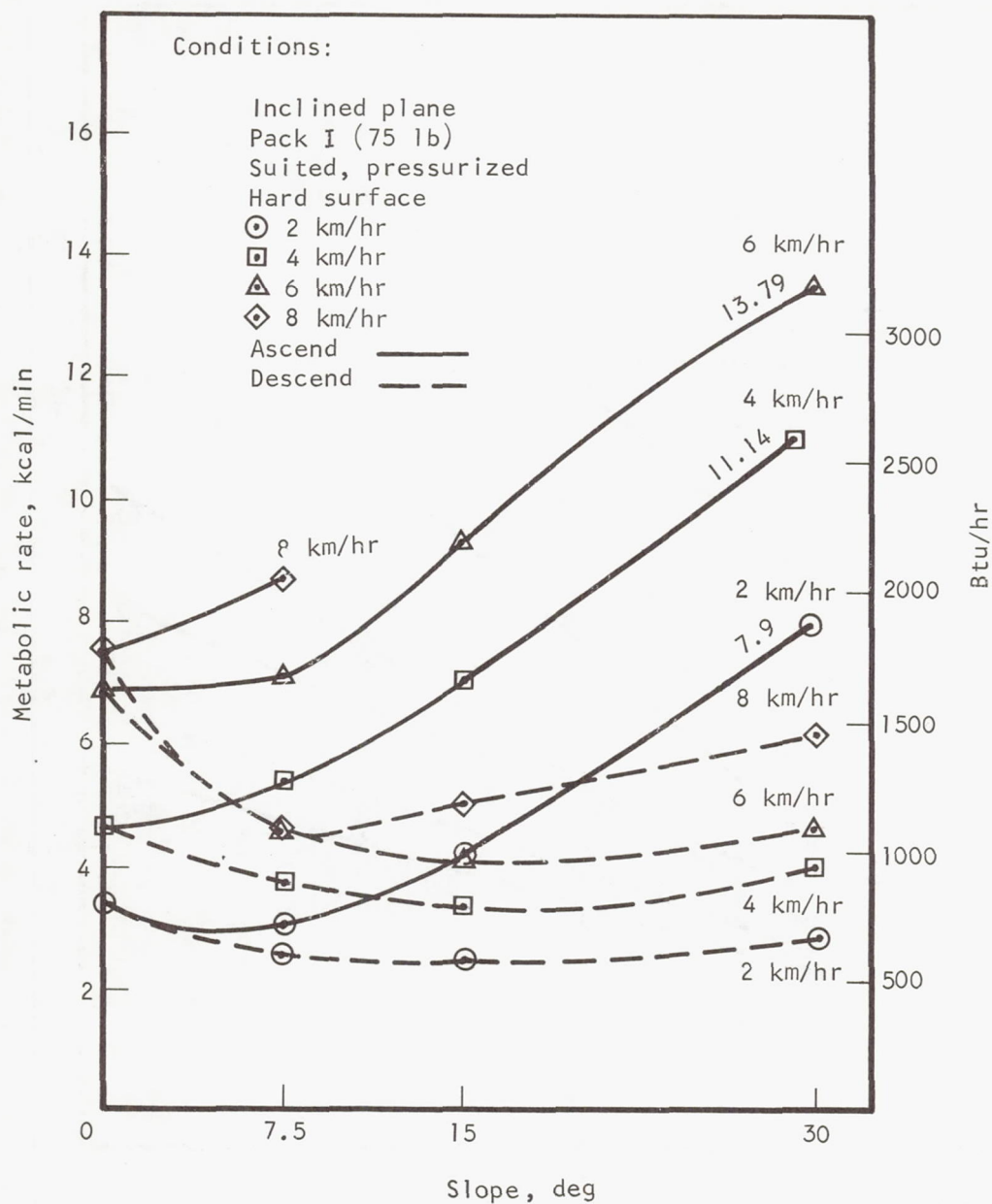
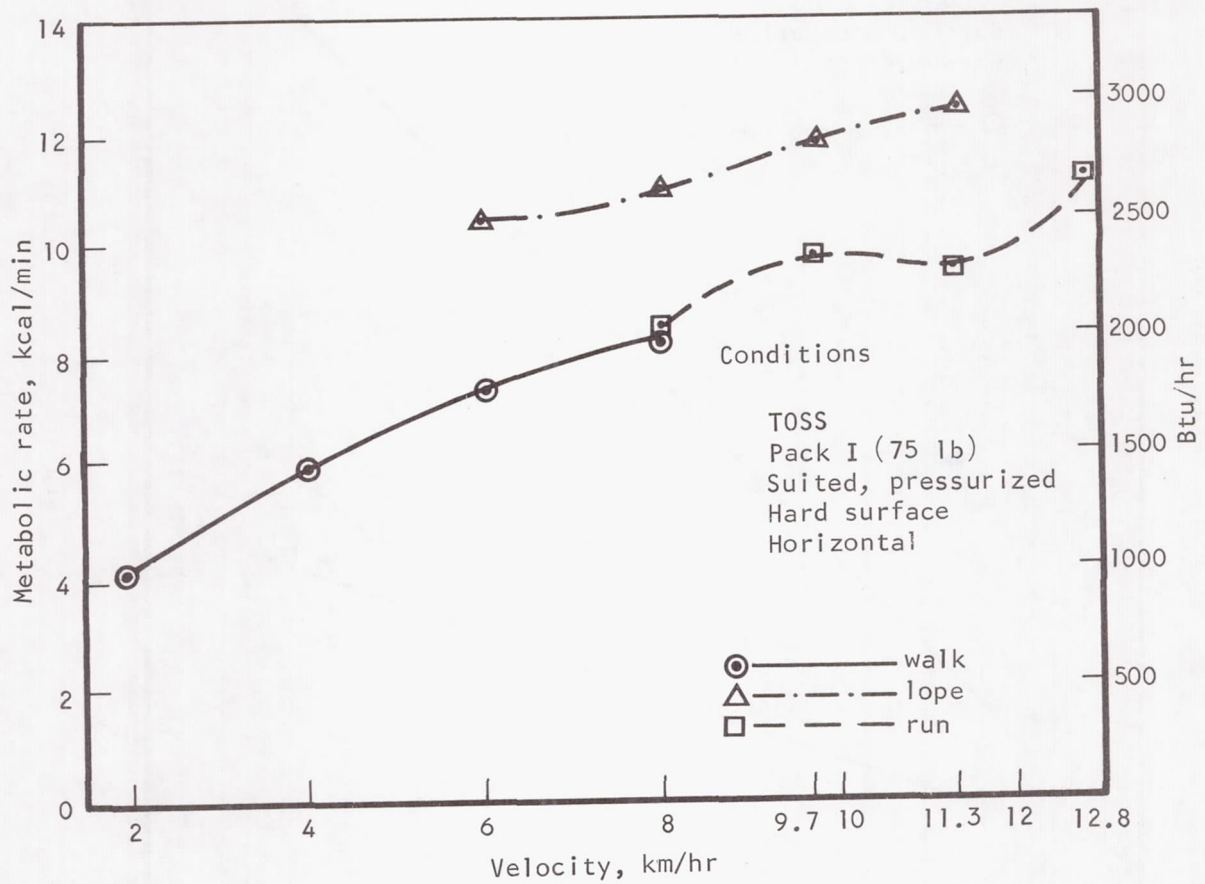


Figure 5-20. Summary Plot of Steady-State Data from All Tests for Traversing Slopes on the Inclined-Plane Simulator



S-42653-A

Figure 5-21. Summary Curves of Steady-State Energy Cost for Locomotion on Slopes with the Inclined-Plane Simulator



S-42666

Figure 5-22. Effect of Gait and Velocity on Steady-State Energy Cost of Locomotion with the TOSS Simulator

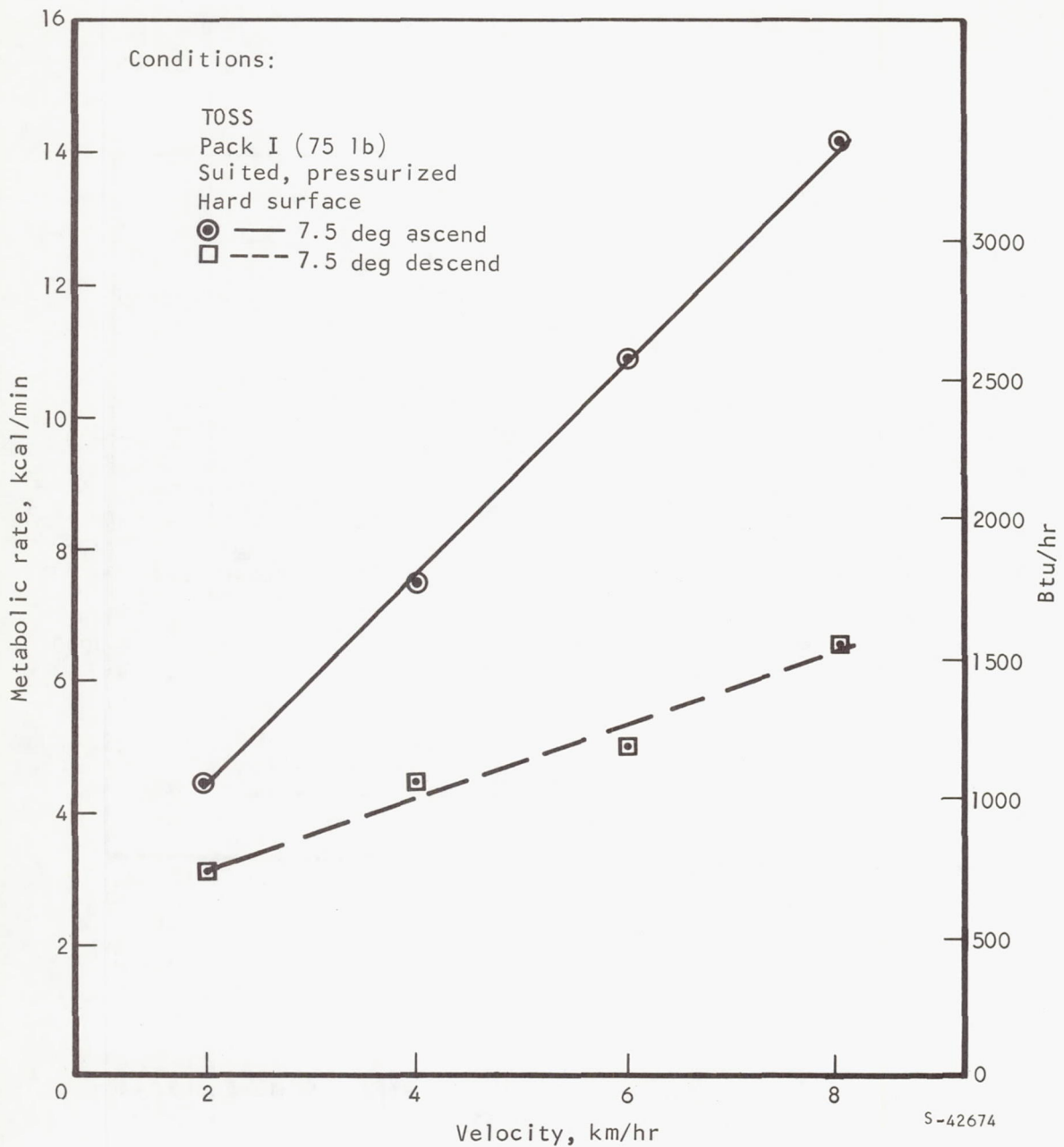


Figure 5-23. Energy Cost for Traversing a 7.5-deg Slope, Hard Surface, T0SS Simulator

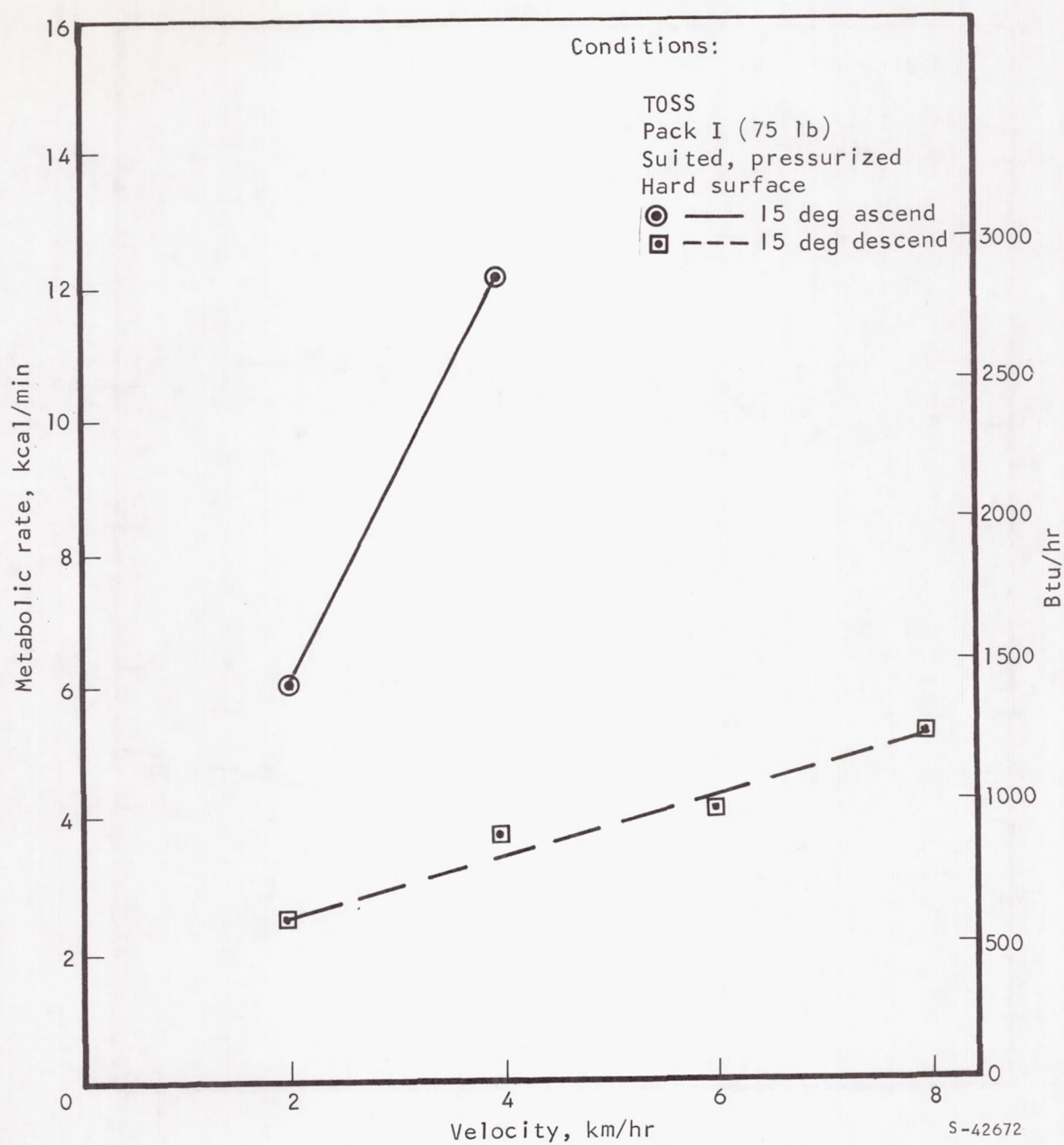


Figure 5-24. Energy Cost for Traversing a 15-deg Slope, Hard Surface, T0SS Simulator

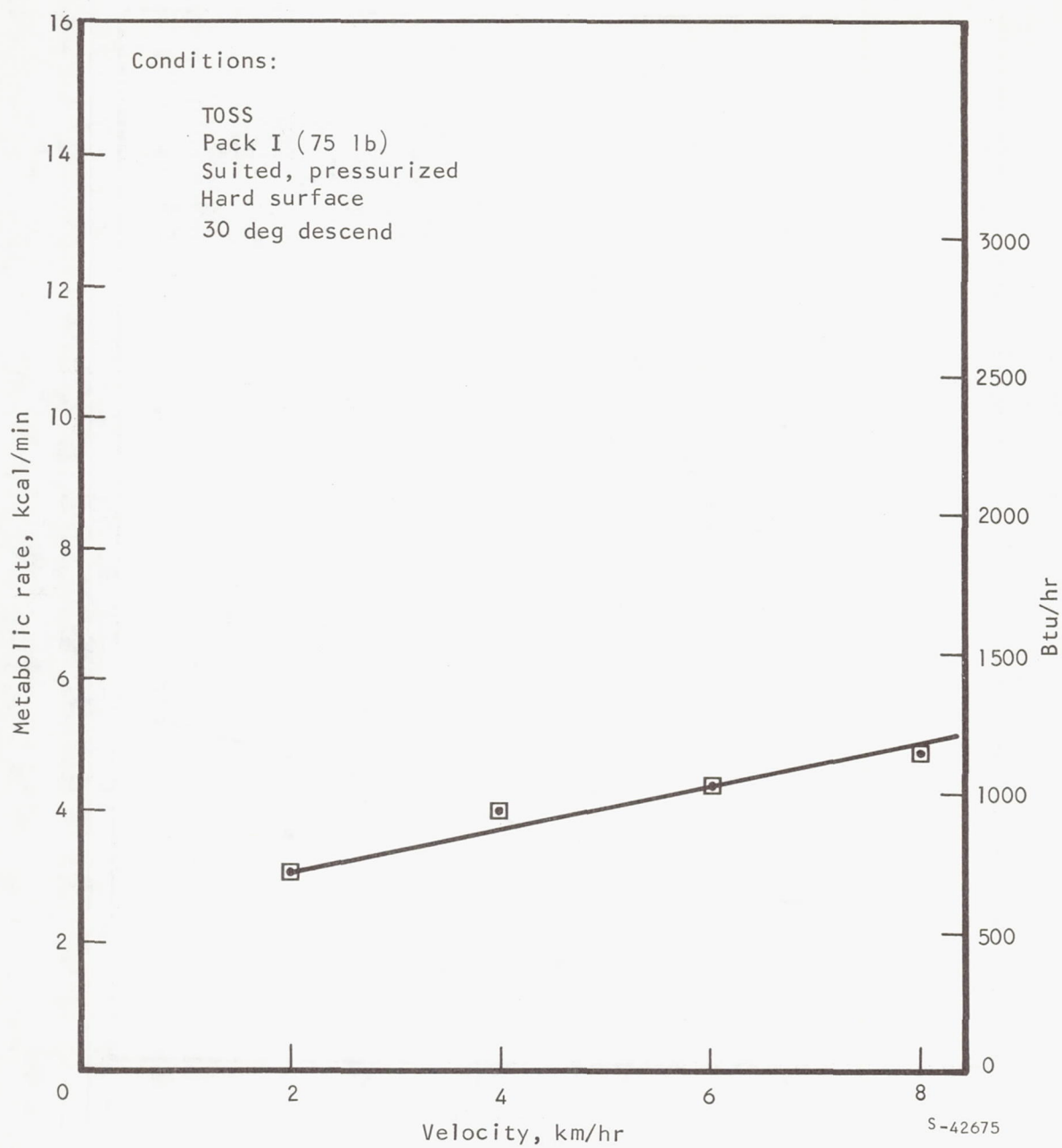


Figure 5-25. Energy Cost for Descending a 30-deg Slope, Hard Surface, TOSS Simulator

Figure 5-26 summarizes the slope data for tests performed on TOSS and is comparable to the presentation made in Figure 5-20 for the inclined-plane tests. The effects described for Figure 5-20 fit equally well to these data, with only the magnitude of the data being different. The downhill data is lower than the horizontal values, which in turn are lower than for the ascending modes. This separation is much more pronounced than for the inclined plane. These curves are replotted in Figure 5-27 and are similar to those shown for the inclined plane in Figure 5-21.

The differences between the data from the subjects in each of the simulators is demonstrated by the locomotive modes they could not complete. On the inclined plane, the subjects were able to accomplish all of the descending modes and ascending the 7.5- and 15-deg slopes. When attempting to ascend the 30-deg slope on the inclined plane, the subjects were able to complete the 2- and 4-km/hr velocities with little difficulty. At the 6-km/hr velocity, however, only one subject completed the standard 14-min exercise period. The other subjects completed between 2 and 5-1/2 min of exercise before the tests were stopped because their heart rates had exceeded the established safe limits. At 8-km/hr, none of the subjects were able to perform on the 30-deg slope. The major reason for this was the inability to maintain traction and position (inability to keep up) on the treadmill. On the other hand, with the TOSS simulators, the subjects were able to perform all of the descending-slope tests and the 7.5-deg ascending tests. At a 15-deg ascending slope, the subjects were able to perform only the 2- and 4-km/hr velocities. In the 6- and 8-km/hr tests, they each exceeded a heart rate of 180 beats/min prior to reaching a steady-state condition. Only one of the six subjects could perform the 2-km/hr velocity while ascending the 30-deg slope, and he was able to maintain the exercise for only 5 min before his heart rate reached test cutoff limits.

Steady-state energy cost for locomotion on simulated smooth lunar soil with the TOSS simulator. - Data obtained from tests performed with the simulated smooth lunar soil are depicted in Figure 5-28 for walking on the horizontal, Figure 5-29 for ascending and descending 7.5 deg slopes, and Figure 5-30 for traversing a 15-deg slope. Metabolic costs increased with velocity for the horizontal tests ($p < 0.01$). For 7.5- and 15-deg ascent, the cost was increased by velocity ($p < 0.05$), while for descending modes, velocity increased the cost at 7.5 and 15 deg ($p < 0.05$). Energy costs for descending modes were lower than for either locomotion on a horizontal surface ($p < 0.01$) or the ascending modes ($p < 0.01$). The uphill values at 7.5 deg were not statistically different from the data on the horizontal smooth lunar surface, but the 15-deg values were different from the data obtained for tests both on the 7.5-deg slope and in the horizontal plane ($p < 0.01$).

Results of testing with simulated coarse lunar soil on the TOSS simulator. - Steady-state metabolic rate requirements for locomotion on the simulated coarse lunar soil on TOSS with the treadmill horizontal are shown in Figure 5-31. Statistical comparisons show that metabolic costs increased as velocity increased.

Comparison between effects of various surfaces on metabolic rates. - The multiple analysis of variance used to compare the values obtained from testing with the three surfaces showed that the simulated smooth lunar surface effected

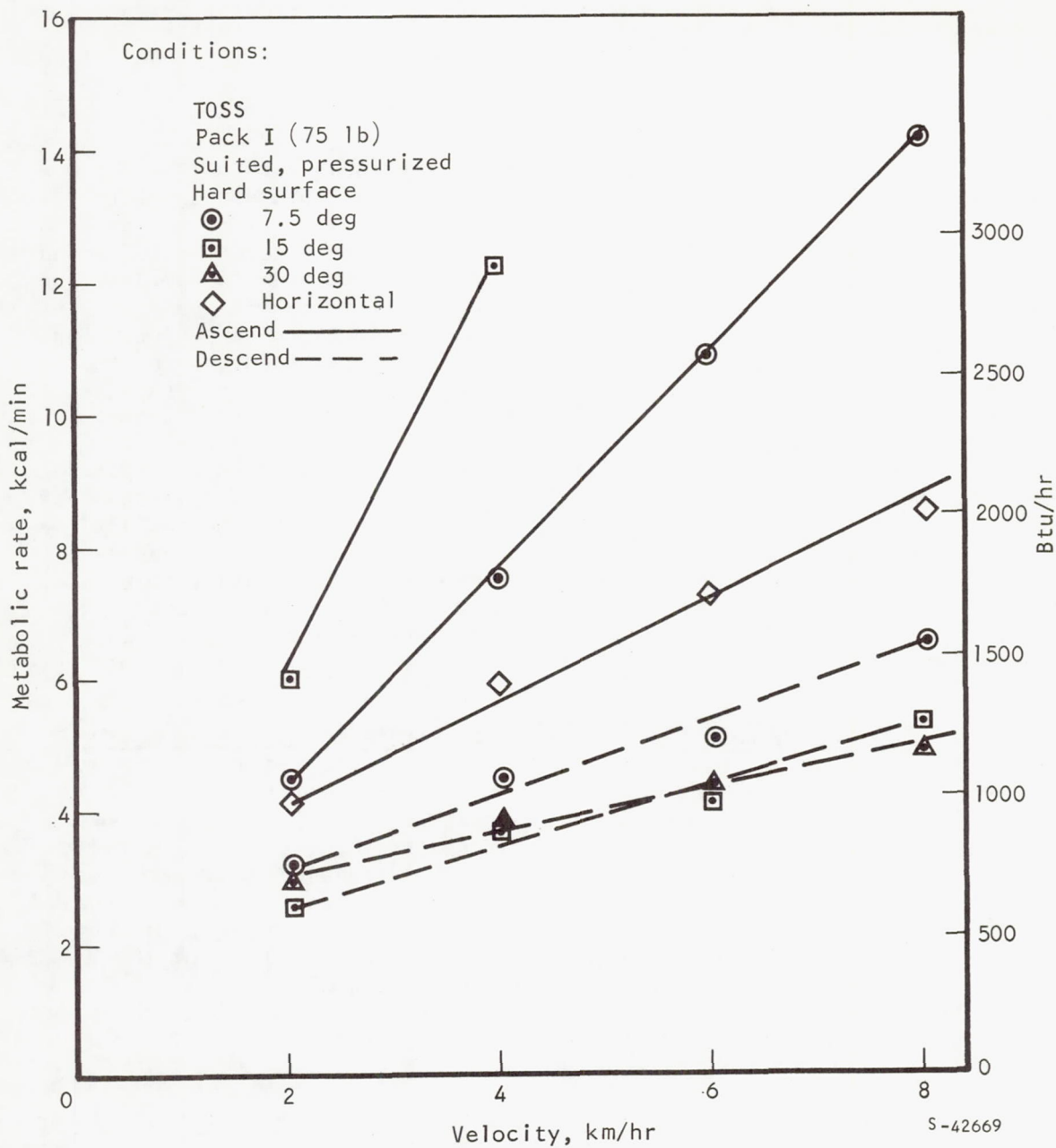


Figure 5-26. Summary Plot of Metabolic Rates for Traversing Hard-Surface Slopes, TOSS Simulator

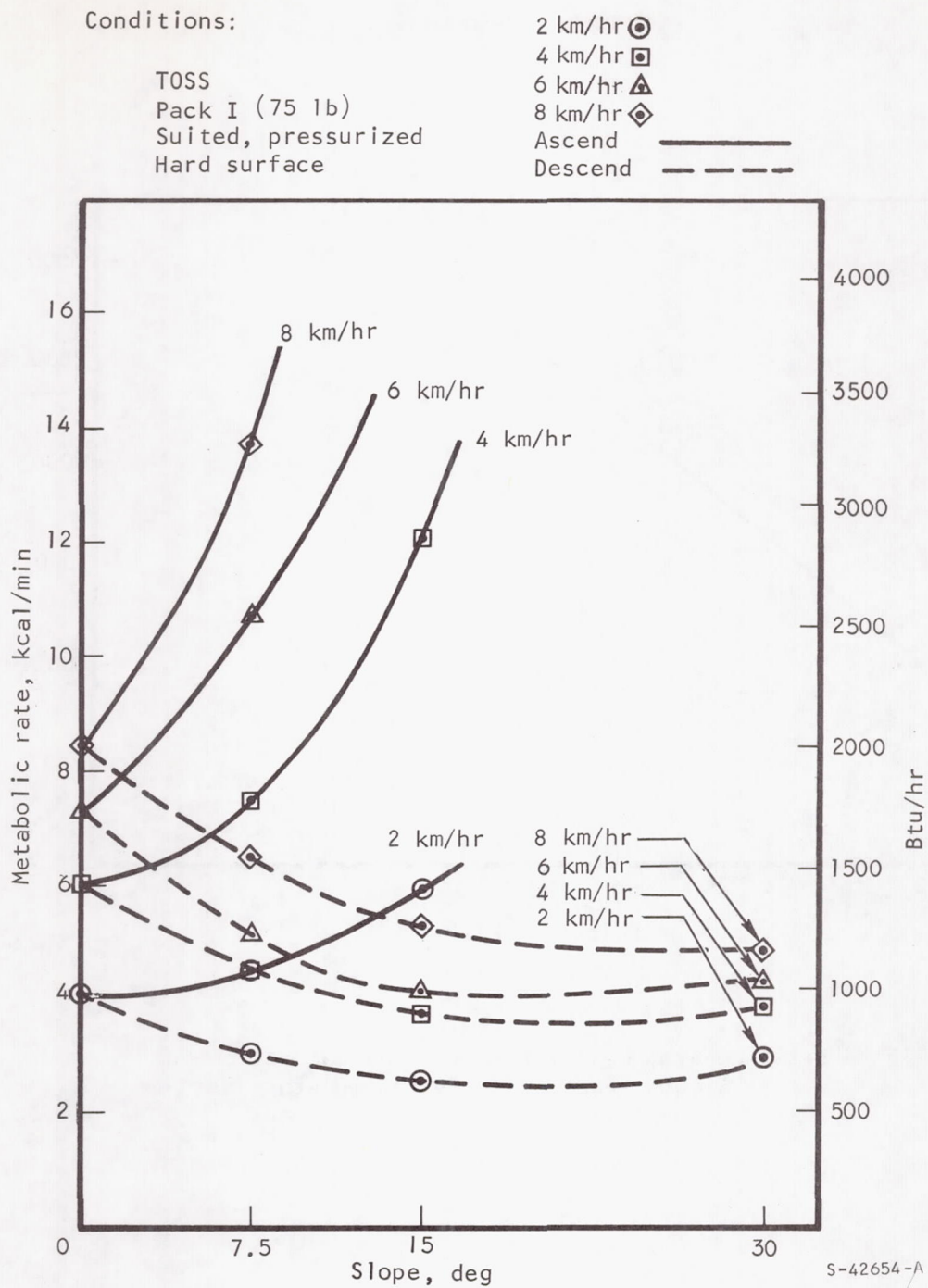


Figure 5-27. Summary Curves of Energy Cost for Locomotion on Hard-Surface Slopes, TOSS Simulator

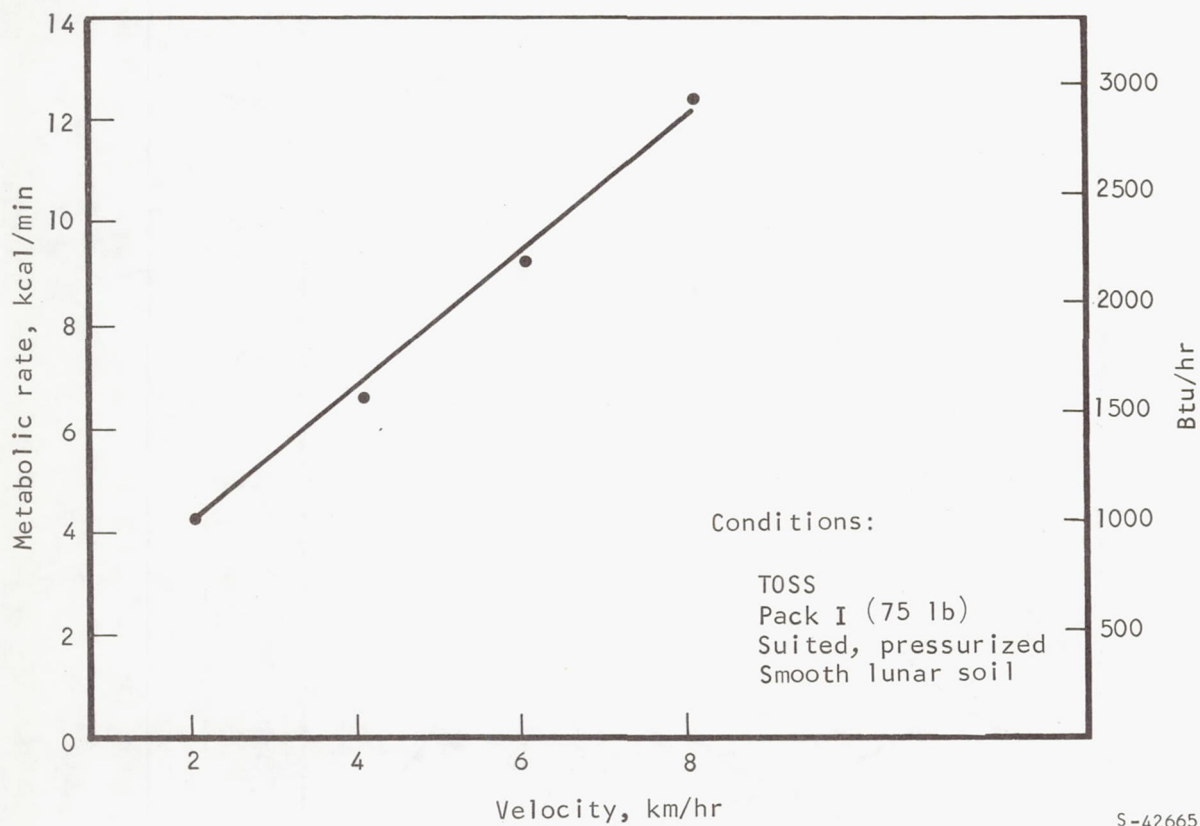
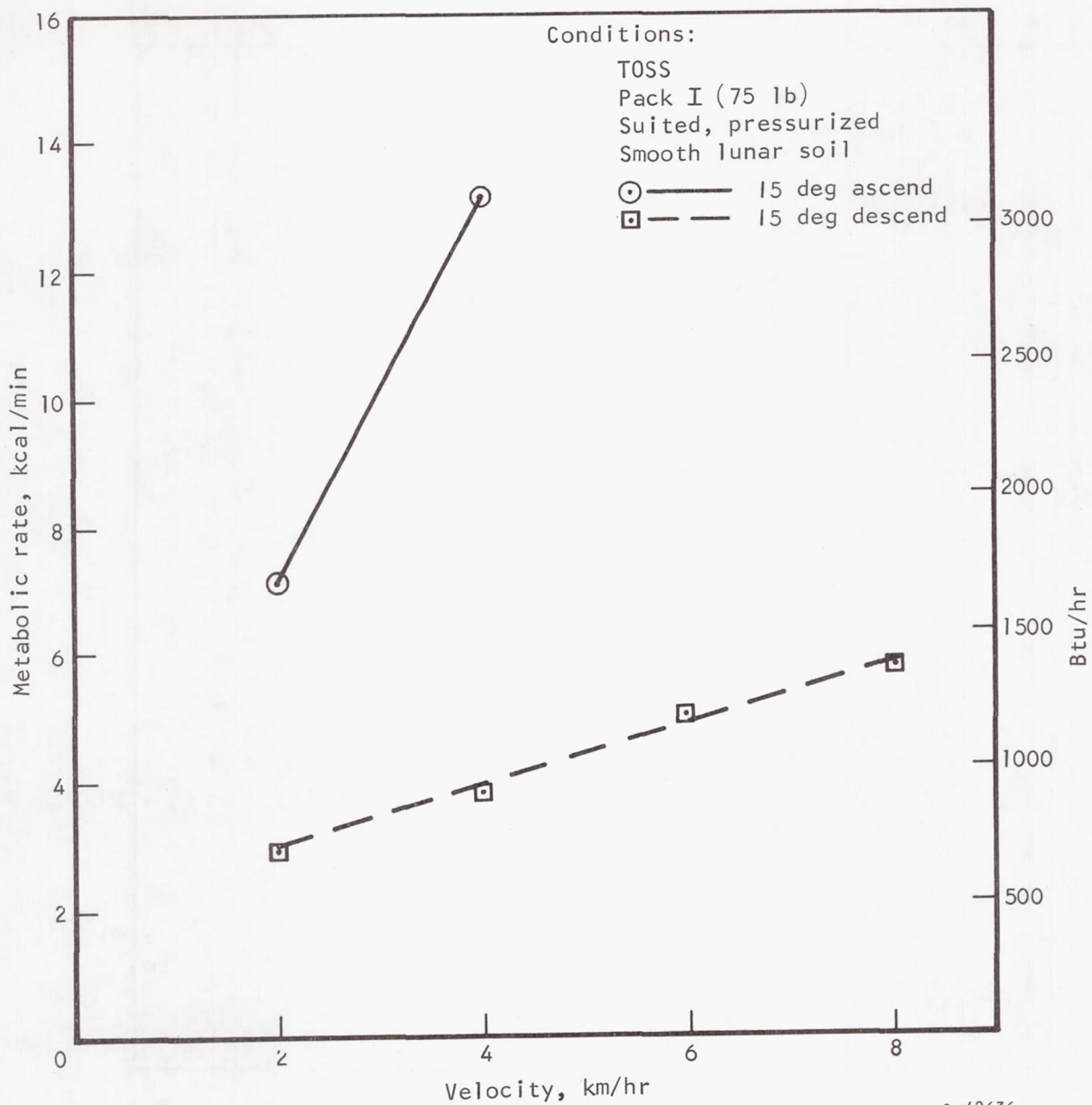


Figure 5-28. Energy Cost for Horizontal Locomotion on Smooth Lunar Soil, TOSS Simulator



S-42636

Figure 5-29. Energy Cost for Traversing a 7.5-deg Slope, Smooth Lunar Soil, T0SS Simulator

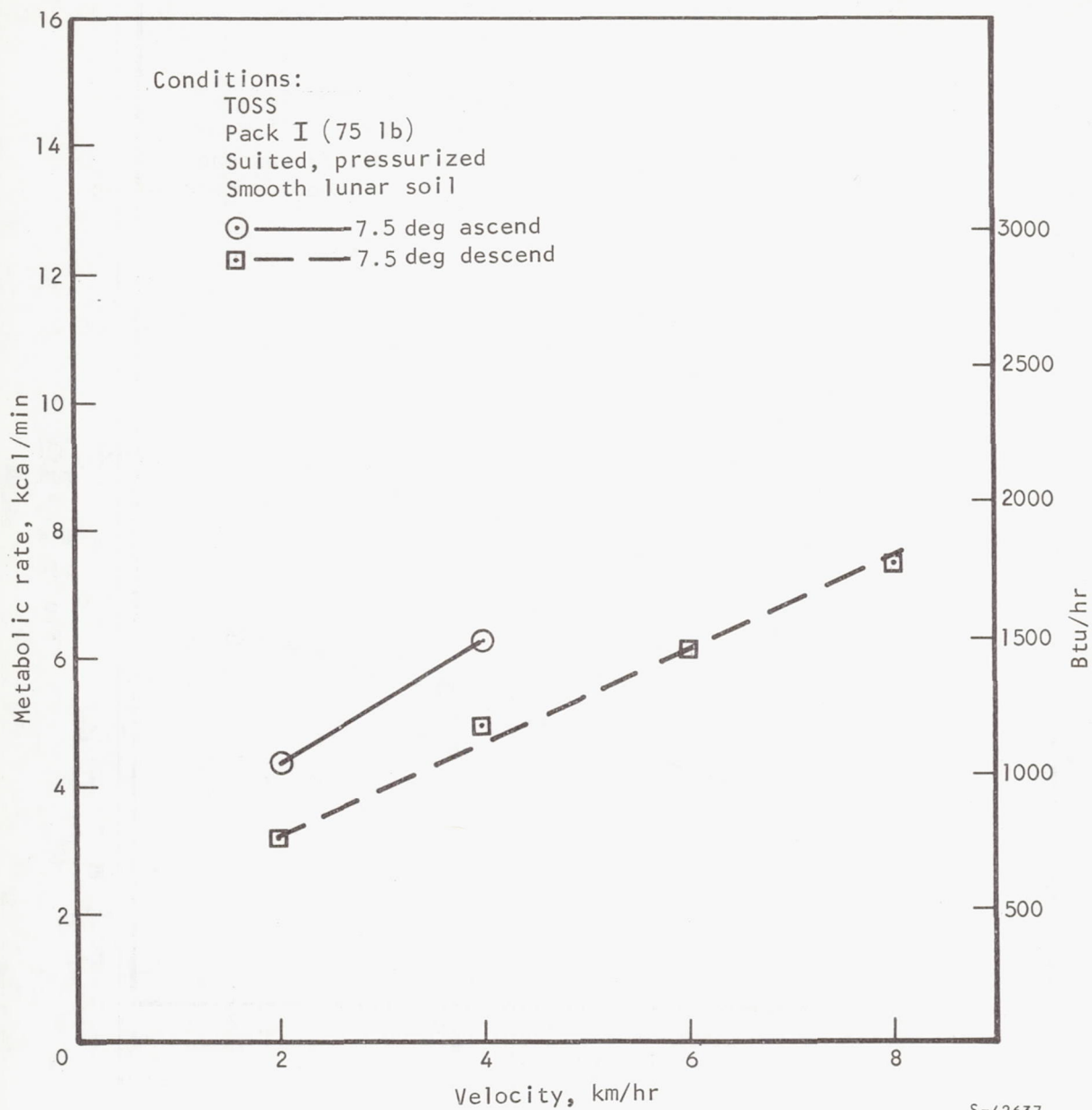


Figure 5-30. Energy Cost for Traversing a 15-deg Slope, Smooth Lunar Soil, TOSS Simulator

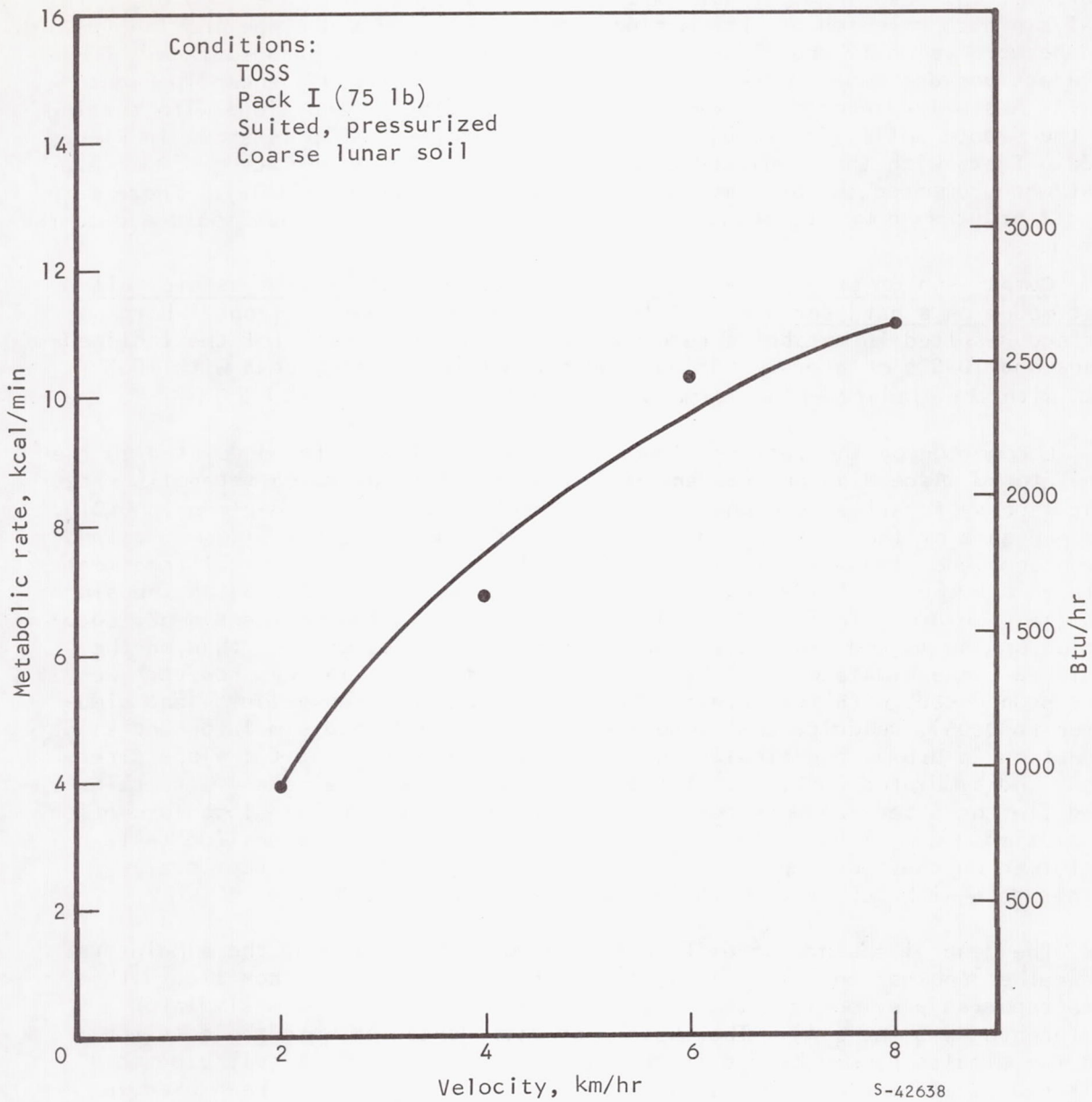


Figure 5-31. Energy Cost for Horizontal Locomotion on Coarse Lunar Soil, TOSS Simulator

a greater increase in metabolic rates than did the hard surface ($p < 0.01$). This analysis also revealed an interaction between velocity and slope incline ($p < 0.01$) and between velocity and slope direction ($p < 0.01$) for the hard surface. These interactions are descriptive of the curvilinear relationship shown in Figure 5-27. A similar interaction was found between velocity and slope with testing on the smooth soil. The resulting curvilinear relationship is shown in Figure 5-32. Tests with the simulated coarse lunar soil showed an increase in energy cost when compared to the same tasks on the hard surface ($p < 0.01$). There were no differences, however, between the values for testing on the smooth and coarse surfaces.

Comparison of steady-state metabolic rates between simulators over all test modes on a hard surface. - Walking or sprinting on a horizontal hard surface resulted in metabolic rates which were not different for the inclined-plane and TOSS simulators. Loping produced a higher energy cost with TOSS than with the inclined-plane simulator ($p < 0.05$).

Locomotion on the various slopes pointed out other effects related to the simulators. Ascending and descending a 7.5-deg slope produced metabolic rates that were systematically higher for TOSS than for the inclined-plane ($p < 0.01$). The presence of the roll and yaw degrees-of-freedom with TOSS allowed motion in these planes and may affect the cost of locomotion. Statistical treatment pointed out the significance of the interaction between direction on the slope and the simulator, indicated by the data plots in Figures 5-27 and 5-32. Locomotion on the 15-deg slope again produced higher values on TOSS than on the inclined-plane simulator ($p < 0.01$). The interactions at 15 deg, however, were very pronounced, with the interactions being found between velocity and simulator ($p < 0.05$), velocity and slope direction ($p < 0.01$), and simulator and slope direction ($p < 0.01$), and finally an interaction between velocity, slope direction, and simulator ($p < 0.05$). The effects noted above are mainly a function of differences between data for the two simulators for uphill slope locomotion. Locomotion downhill on slopes up to 30 deg showed no differences for tests performed on the two simulators. Uphill slopes resulted in exceptionally higher data with TOSS than with the inclined plane ($p < 0.01$).

The general absence of differences between the data from the simulators was rather unexpected. This lack of difference is in direct conflict with data reported previously with a counterweight 6-deg-of-freedom simulator (References 5-3 and 5-4). The absence of differences between the data for the two simulators may be due in part to the highly immobile suit used in this study. If one of the relatively mobile Apollo suits had been used in this study, it is probable that many more differences would have been noted, including information on the effects of the presence or lack of the various degrees-of-freedom.

Conditions:

T0SS
 Pack I (75 lb)
 Suited, pressurized
 Smooth lunar soil
 ○ — ascend
 □ — descend

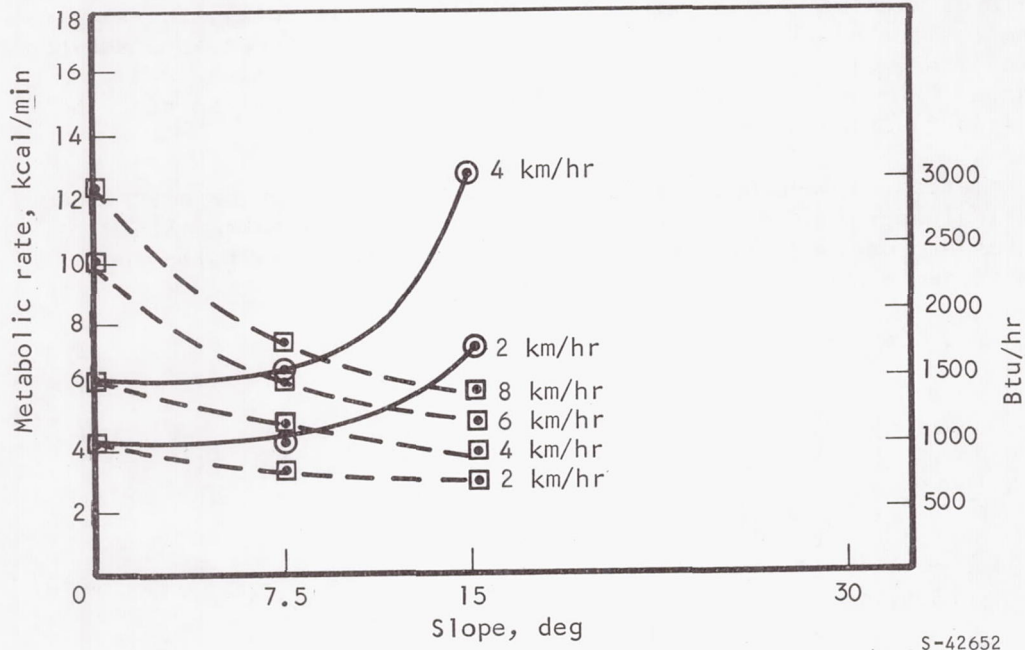


Figure 5-32. Summary Curves of Energy Cost for Locomotion on Slopes, Smooth Lunar Soil, T0SS Simulator

Heart Rate Data

Table 5-11 presents the heart rates in beats/min obtained for all the exercise modes performed. Data not shown in the second row are pooled with the data in the first row since there were no significant differences between repeat tests. In the fourth and fifth rows, no data are presented because of the nature of the tests performed. Where other data points are missing, the subjects were unable to accomplish the exercise mode.

Although a statistical treatment of the heart rate data was made, the individual differences are not described here. Since heart rates are positively correlated with metabolic rates ($R = 0.80$ for these data), the statistical differences for heart rates in general mirror the differences described for metabolic rates, although the variance for heart rate is much larger. Inferences noted for the metabolic rates can be used in general to describe heart rates as a function of the various exercise modes.

The correlation between heart rate and metabolic rate can be described by a mathematical approach to this basic physiological principle. Since metabolic rates are derived from oxygen consumption rates, the following equation for oxygen consumption describes the relationship:

$$\dot{V}_{O_2} = \dot{Q} (Ca_{O_2} - \bar{C}\bar{V}_{O_2}) \quad (5-1)$$

$$\dot{V}_{O_2} = \text{H.R.} \times \text{S.V.} (Ca_{O_2} - \bar{C}\bar{V}_{O_2}) \quad (5-2)$$

$$\text{H.R.} = \frac{\dot{V}_{O_2}}{\text{S.V.} (Ca_{O_2} - \bar{C}\bar{V}_{O_2})} \quad (5-3)$$

where

\dot{V}_{O_2} = oxygen consumption in liters/min at standard temperature and pressure dry (STPD)

\dot{Q} = cardiac output in liters/min

Ca_{O_2} = oxygen content of the arterial blood

$\bar{C}\bar{V}_{O_2}$ = oxygen content of the mixed venous blood

H.R. = heart rate in beats/min

S.V. = stroke volume in liters/beat

$\dot{Q} = \text{H.R.} \times \text{S.V.}$

TABLE 5-11

HEART RATES (BEATS/MIN) FOR ALL SIMULATOR EXERCISE MODES

Experimental conditions							Results (mean and ± 1 standard deviation)							
Simulator and suit mode	Slope, deg	Surface condition	Pack	Number of velocities	Number of subjects	Total tests	Gait or ascend/ descend	Velocity, km/hr						
								2	4	6	8	9.7	11.3	12.8
Inclined plane, pressurized (press.) suit	0 (horiz)	Hard	I, 75 lb	4 each; walk, lope and run	6, with 2 repeating once	96*	Walk	77.3 \pm 15.0	85.0 \pm 10.0	106.4 \pm 15.8	132.7 \pm 17.6			
							Lope			120.9 \pm 17.8	121.3 \pm 19.7	128.8 \pm 14.8	131.8 \pm 23.2	
							Run				103.9 \pm 12.6	114.3 \pm 19.1	114.3 \pm 23.6	126.0 \pm 18.4
Inclined plane, pressurized suit	0	Hard	I	1 each; walk, lope, and run	6, with all repeating twice	36*	Walk							
							Lope							
							Run							
Inclined plane, subject in mufti (without press. suit)	0	Hard	I	4 each; walk, lope, and run	2	24	Walk	74 \pm 6	82 \pm 4.2	86 \pm 3.7	109.5 \pm 2.8			
							Lope			111 \pm 10.2	123 \pm 1.6	126 \pm 14.2	129 \pm 4.1	
							Run				85.5 \pm 2.6	91.5 \pm 8.7	93 \pm 1.1	107.5 \pm 6.2
Incl plane, mufti	0	Hard	I	Fatigue test	6	24								
Inclined plane, pressurized suit	0	Hard	I	Fatigue test	2	8								
Inclined plane, pressurized suit	0	Hard	II, 240 lb	4 each; walk, lope, and run	6	72	Walk	83.6 \pm 9.6	89.6 \pm 10.5	108.3 \pm 14.9	139.2 \pm 13.9			
							Lope			132.3 \pm 4.6	142.0 \pm 8.5	149.7 \pm 10.7	153.8 \pm 20.4	
							Run				126.0 \pm 13.4	127.0 \pm 15.3	136.6 \pm 15.8	142.0 \pm 10.2
Inclined plane, pressurized suit	0	Hard	III, 400 lb	4 each; walk, lope, and run	2	24	Walk	86.0 \pm 12.0	105.0 \pm 21.0	109.0 \pm 13.0	139.0 \pm 1			
							Lope			141.0 \pm 9.0	148.5 \pm 16.5	152.5 \pm 2.5	162.0	
							Run				124.0 \pm 28.0	140.0 \pm 20.0	151.5 \pm 10.5	156
TOSS (6-deg-of-freedom), pressurized suit	0	Hard	I	4 each; walk, lope, and run	6	72	Walk	105.7 \pm 10.5	108.0 \pm 10.4	128.6 \pm 13.3	137.0 \pm 8.3			
							Lope			154.2 \pm 11.7	164.2 \pm 9.5	177.2 \pm 4.8	176.7 \pm 7.1	
							Run				140.7 \pm 18.5	145.3 \pm 17.5	158.7 \pm 12.2	168.2 \pm 13.4
TOSS, press. suit	0	Smooth lunar	I	4 velocities	6	24		96.33 \pm 6.65	110.5 \pm 12.51	140.2 \pm 18.07	169.0 \pm 6.60			
TOSS, press. suit	0	Coarse lunar	I	4 velocities	6	24		99.5 \pm 11.81	114.5 \pm 10.54	147.5 \pm 14.07	158.33 \pm 8.25			
TOSS, pressurized suit	7.5	Hard	I	4 velocities	6	48	Ascend	110.8 \pm 6.7	123.8 \pm 13.9	160.0 \pm 7.0	172.8 \pm 5.5			
							Descend	89.2 \pm 10.8	95.8 \pm 10.1	101.8 \pm 12.5	114.2 \pm 11.2			
TOSS, pressurized suit	7.5	Smooth lunar	I	4 velocities	6	48	Ascend	106.83 \pm 7.7	151.16 \pm 16.9	167.6 \pm 3.87				
							Descend	81.5 \pm 10.8	93.33 \pm 10.67	105.25 \pm 10.18	129.25 \pm 23.85			
TOSS, pressurized suit	15	Hard	I	4 velocities	6	48	Ascend	119.3 \pm 10.6	157.5 \pm 9.5	173.5 \pm 4.2				
							Descend	79.8 \pm 15.3	82.2 \pm 16.3	89.3 \pm 15.6	100.3 \pm 21.7			
TOSS, pressurized suit	15	Smooth lunar	I	4 velocities	6	48	Ascend	127 \pm 11.47	172 \pm 5.09					
							Descend	82.6 \pm 12.33	89.8 \pm 11.14	102.6 \pm 15.52	108.8 \pm 16.60			
TOSS, pressurized suit	30	Hard	I	4 velocities	6	48	Ascend							
							Descend	83.3 \pm 8.7	92.3 \pm 9.1	99.8 \pm 11.5	107.7 \pm 10.0			
Inclined plane, pressurized suit	7.5	Hard	I	4 velocities	6	48	Ascend	88.8 \pm 15.7	106.8 \pm 19.4	118.3 \pm 26.4	125.0 \pm 27.0			
							Descend	78.8 \pm 11.0	84.5 \pm 12.8	92.2 \pm 12.9	92.7 \pm 15.0			
Inclined plane, pressurized suit	7.5	Hard	II	4 velocities	6	48	Ascend	96.5 \pm 11.14	117.8 \pm 17.2	138.0 \pm 13.9	155.3 \pm 11.2			
							Descend	74.3 \pm 13.4	83.3 \pm 14.0	95.7 \pm 11.3	103.0 \pm 16.1			
Inclined plane, pressurized suit	15	Hard	I	4 velocities	6	48	Ascend	99.0 \pm 10.8	123.7 \pm 11.8	145.8 \pm 11.2				
							Descend	75.5 \pm 10.0	85.8 \pm 13.0	90.2 \pm 13.3	99.8 \pm 12.6			
Inclined plane, pressurized suit	30	Hard	I	4 velocities	6	48	Ascend							
							Descend	80.0 \pm 6.0	88.5 \pm 10.7	102.7 \pm 14.0	114.0 \pm 17.6			
*Pooled data														

Stroke volume normally varies only over narrow limits due to limited distensibility of the myocardium. Therefore, heart rate is the major determinant of cardiac output. Since the body tends to keep the extraction of oxygen from the blood at a fairly constant level (approximately 5 volume %), provided that cardiac output is adequate, the heart rate can be considered one of the most important factors in determining oxygen consumption. If stroke volume and arteriovenous arterial difference are, in fact, relative constants, Equation (5-3) can be written as

$$\text{H.R.} = k \dot{V}_{O_2} \quad (5-4)$$

The above discussion represents an oversimplification of the physiological facts. They do, however, represent the general case. The information as stated should not be extended to defend the thesis that heart rate can be used to predict heart rate. Increases in oxygen requirements by the body are only one of many physiological inputs that can change heart rates. The presence of any other stress factor which affects heart rate, in combination with the requirement for added oxygen, will cause perturbations in the relationship stated in Equation (5-4), resulting in high heart rates. Considerations of heart rate and metabolic rate interrelationships as measured for this effort are presented later.

Figures 5-33 through 5-38 are graphic presentations of typical heart rate data. The general forms of the curves approximate those obtained for the metabolic rates shown earlier. There were no unusual findings from the statistical analysis that would warrant a complete discussion of statistical differences for heart rates. The major use of these data was the real-time observation of the heart rate during each test to ensure safety of the subjects.

Respiratory Rates

Respiratory rates have rarely been usable as a meaningful physiological measure during exercise testing. The level of respiratory rate response to emotional stimuli usually results in the high rates descriptive of the hyper-ventilation syndrome. Statistical analysis of the data obtained from these tests indicates that little can be derived from the data.

Table 5-12 presents the respiratory data obtained; it is apparent that full treatment of the data was not justified and would have been wasteful. The general conclusion is that respiratory rate increased with the increased oxygen requirement generated as a function of exercise. Respiratory rate is important as one of the two determinants of ventilatory volume. Expired minute ventilation (\dot{V}_E) is

$$\dot{V}_E = \text{respiratory rate} \times \text{tidal volume}$$

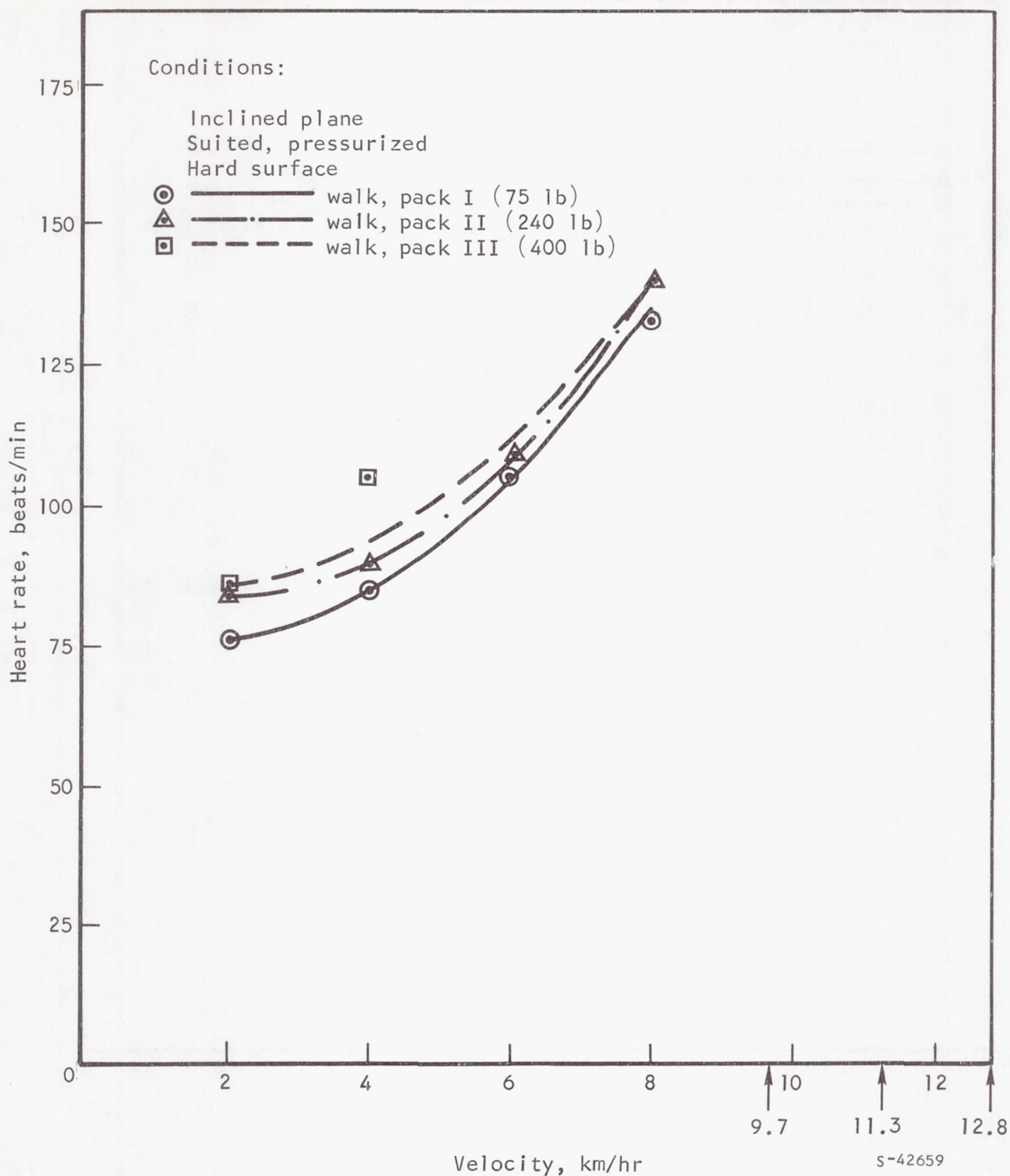


Figure 5-33. Heart Rates for Walking on the Horizontal Inclined-Plane Simulator

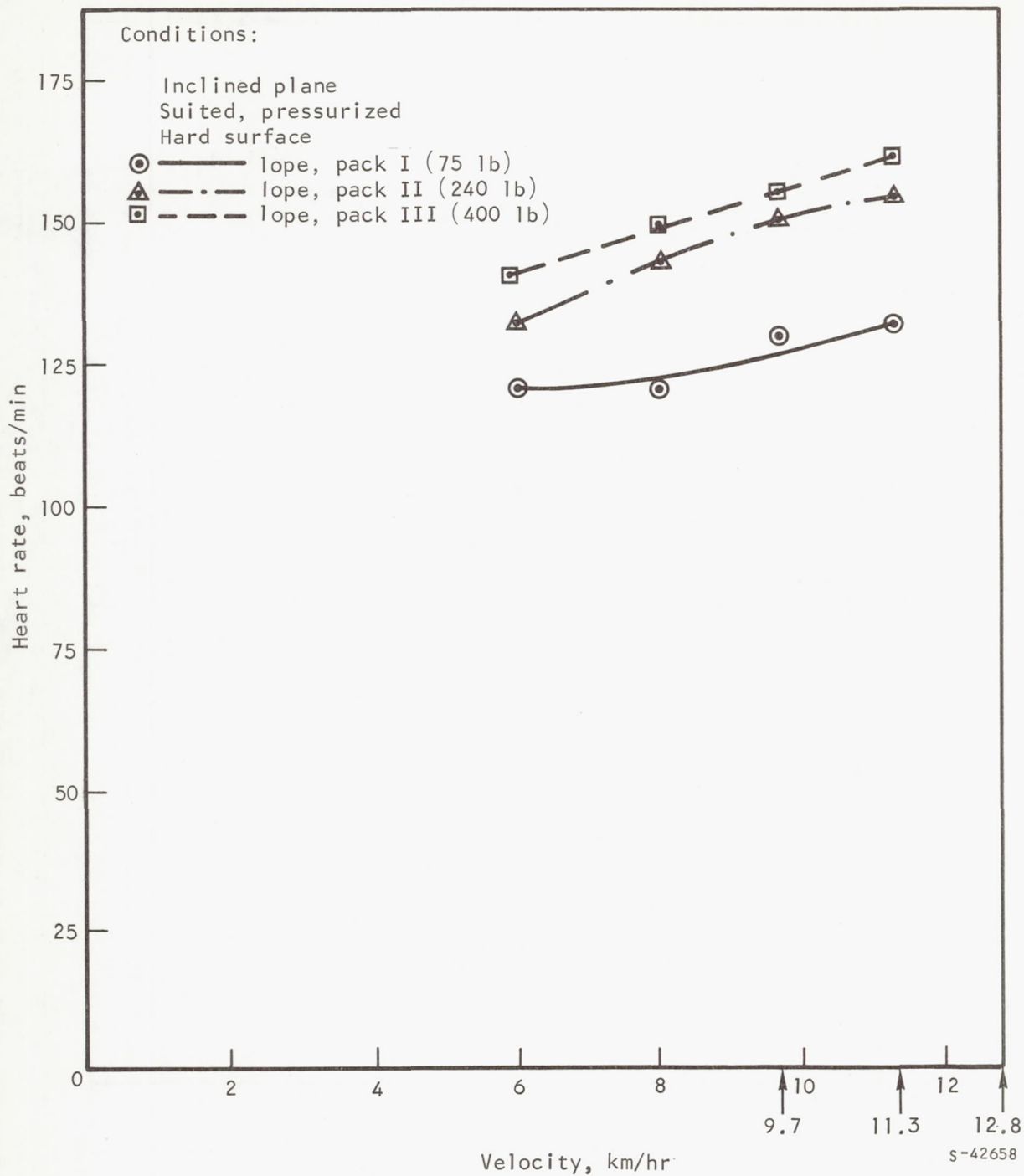


Figure 5-34. Heart Rates for Loping on the Horizontal Inclined-Plane Simulator

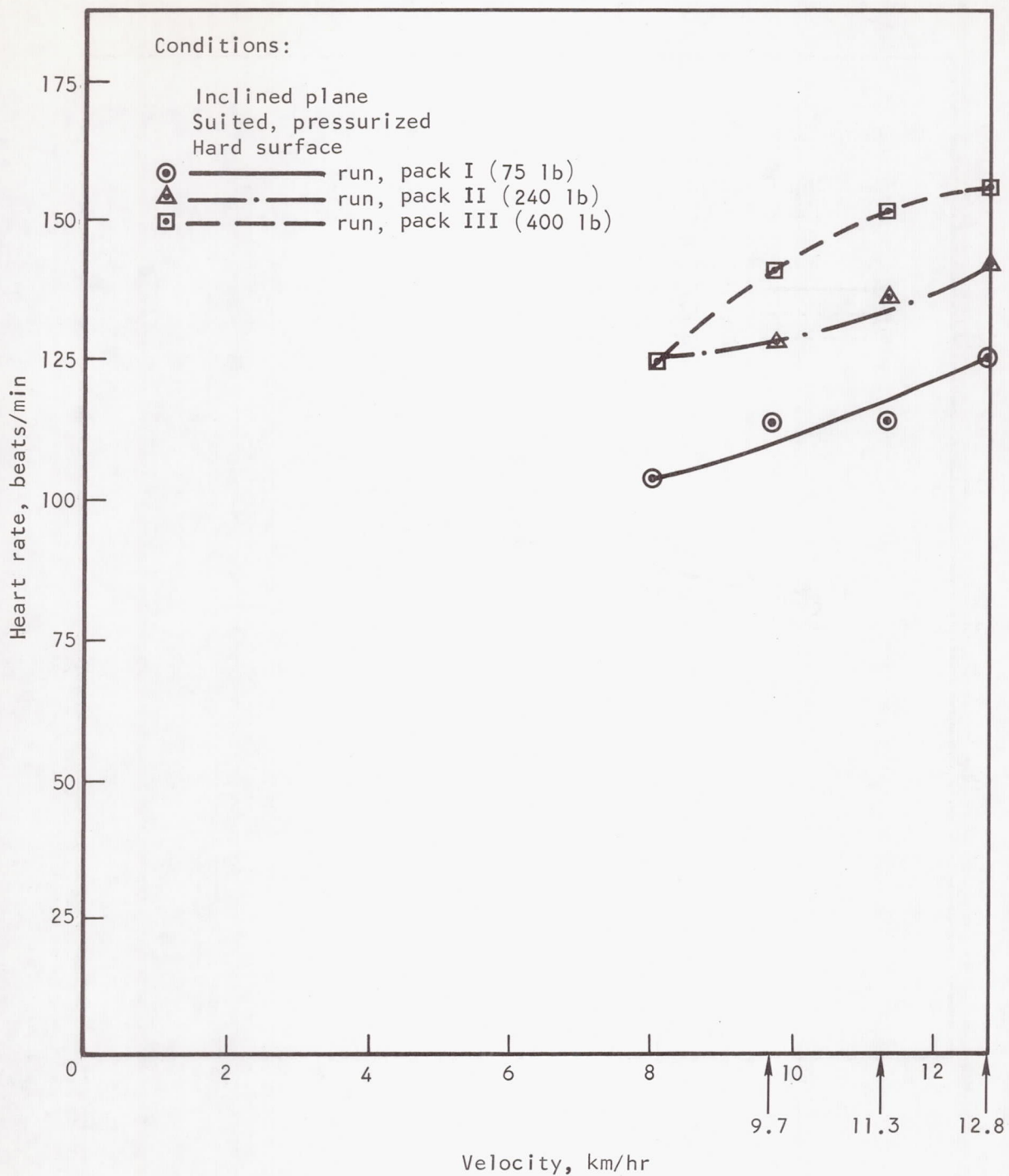


Figure 5-35. Heart Rates for Running on the Horizontal Inclined-Plane Simulator

S-42656

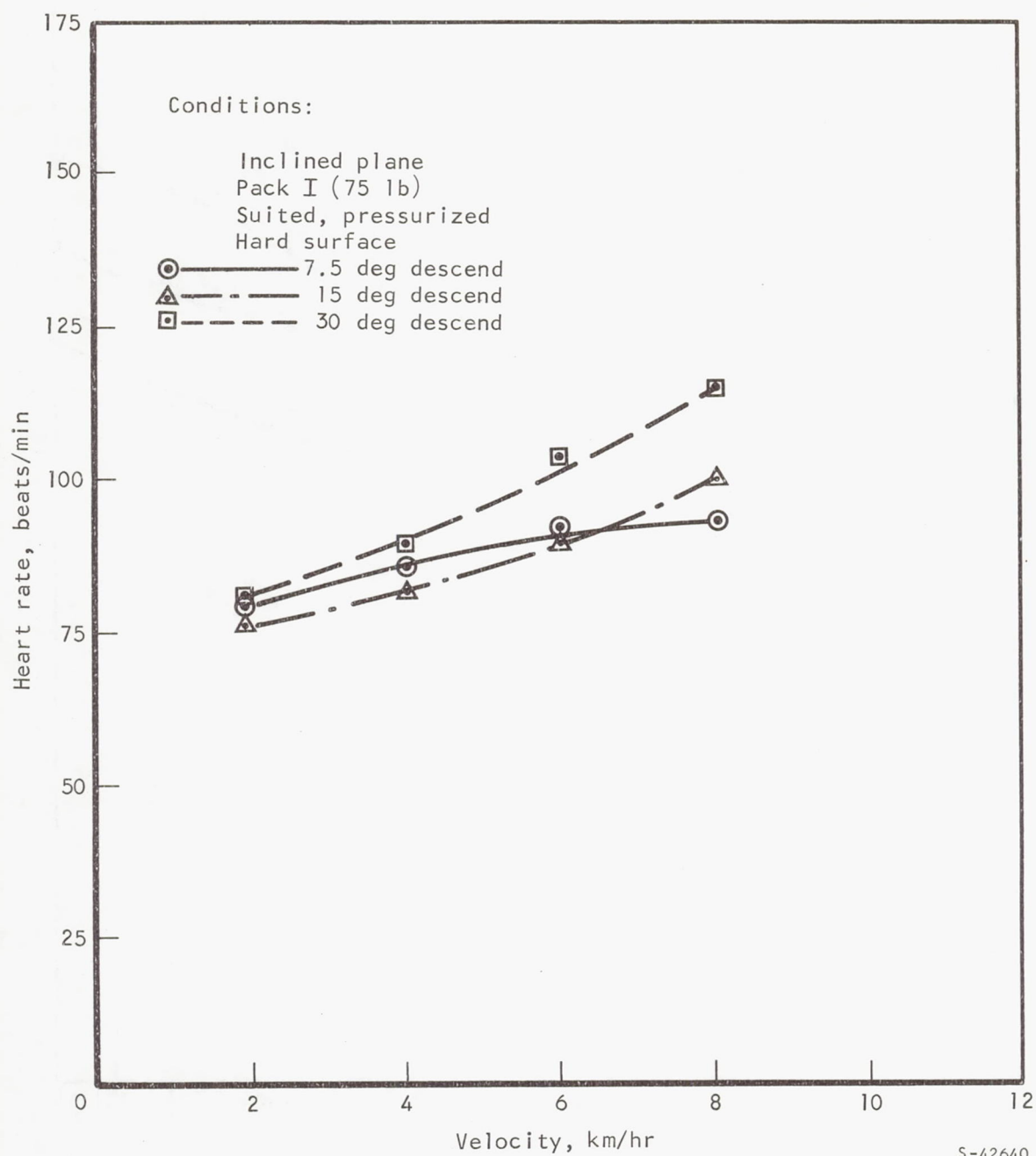
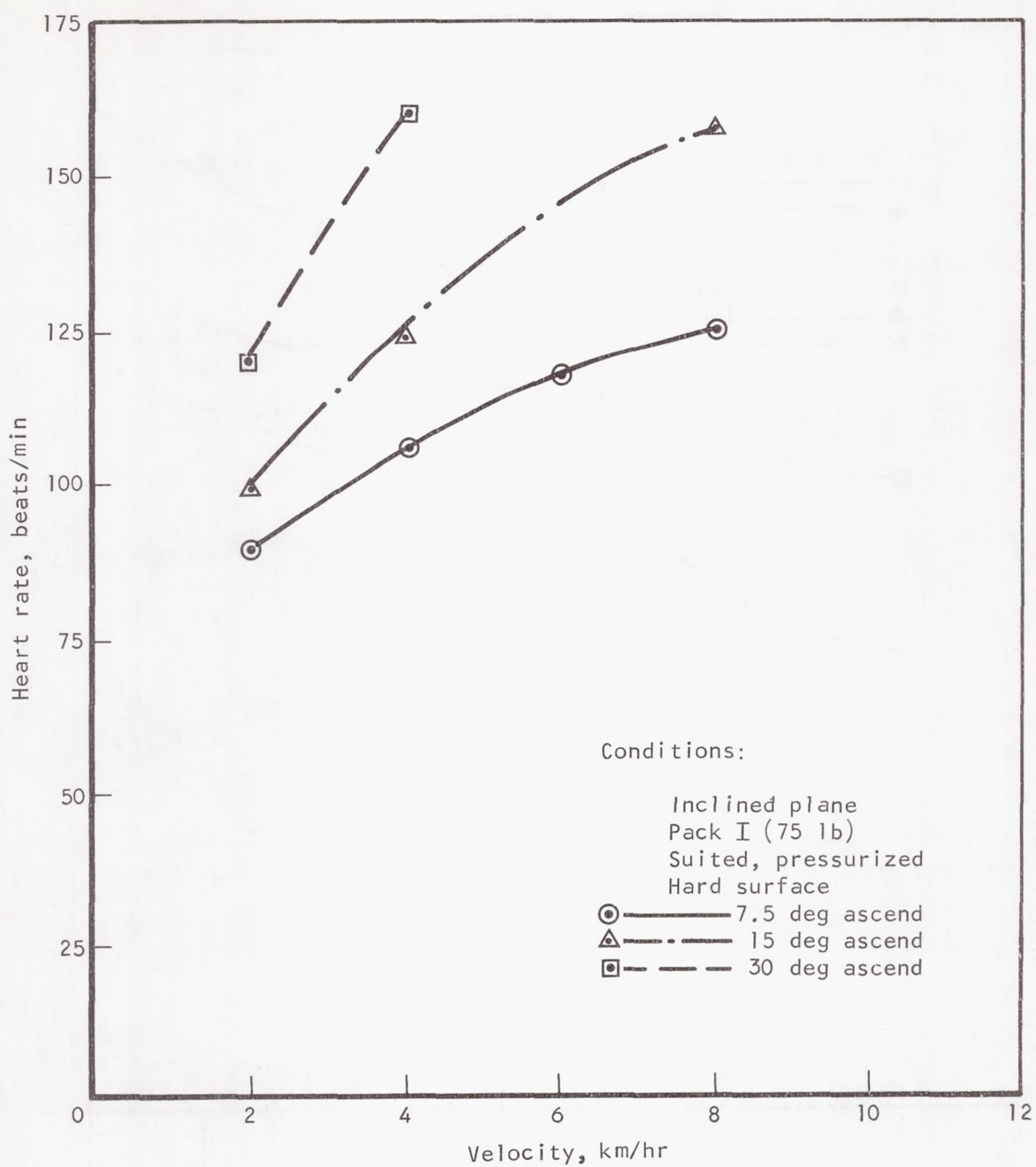


Figure 5-36. Heart Rates for Descending Slopes on the Inclined-Plane Simulator



S-42639

Figure 5-37. Heart Rates for Ascending Slopes on the Inclined-Plane Simulator

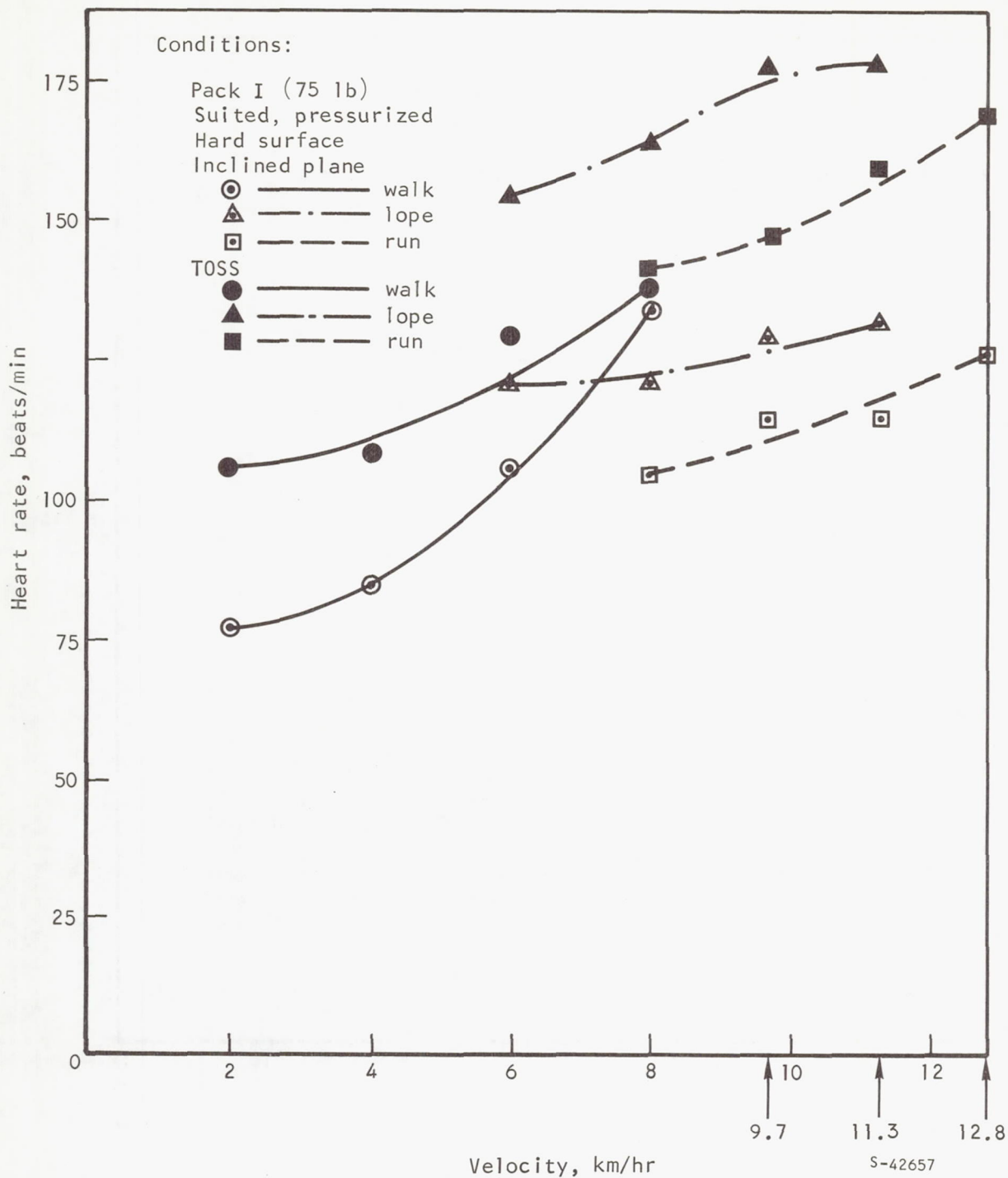


Figure 5-38. Comparison of Heart Rates for Horizontal Locomotion with the Inclined-Plane Simulator and the T0SS Simulator

TABLE 5-12

RESPIRATORY RATES (BREATHS/MIN) FOR
ALL SIMULATOR EXERCISE MODES

Experimental conditions							Results (mean and ± 1 standard deviation)							
Simulator and suit mode	Slope, deg	Surface condition	Pack	Number of velocities	Number of subjects	Total tests	Gait or ascend/descend	Velocity, km/hr						
								2	4	6	8	9.7	11.3	12.8
Inclined plane, pressurized (press.) suit	0 (horiz)	Hard	I, 75 lb	4 each; walk, lope and run	6, with 2 repeating once	96*	Walk	19.1 \pm 4.2	19.7 \pm 3.3	24.9 \pm 3.5	29.5 \pm 3.6			
							Lope			22.9 \pm 3.6	26.6 \pm 5.6	28.3 \pm 7.4	28.7 \pm 5.3	
							Run				22.5 \pm 5.2	23.5 \pm 5.7	24.0 \pm 6.6	25.0 \pm 4.9
Inclined plane, pressurized suit	0	Hard	I	1 each; walk, lope, and run	6, with all repeating twice	36*	Walk							
							Lope							
							Run							
Inclined plane, subject in mufti (without press. suit)	0	Hard	I	4 each; walk, lope, and run	2	24	Walk							
							Lope							
							Run							
Incl plane, mufti	0	Hard	I	Fatigue test	6	24								
Inclined plane, pressurized suit	0	Hard	I	Fatigue test	2	8								
Inclined plane, pressurized suit	0	Hard	II, 240 lb	4 each; walk, lope, and run	6	72	Walk	17.7 \pm 2.7	18.5 \pm 3.7	24.5 \pm 9.1	23.0 \pm 6.2			
							Lope			25.3 \pm 3.8	24.7 \pm 2.8	28.5 \pm 2.3	29.2 \pm 2.7	
							Run				21.3 \pm 7.9	21.0 \pm 5.0	21.8 \pm 7.4	28.3 \pm 13.8
Inclined plane, pressurized suit	0	Hard	III, 400 lb	4 each; walk, lope, and run	2	24	Walk	13 \pm 1	21 \pm 1	24 \pm 2	25 \pm 1			
							Lope			25 \pm 1	26	27 \pm 1	34	
							Run				24 \pm 2	21 \pm 9	25 \pm 11	18
TOSS (6-deg-of-freedom), pressurized suit	0	Hard	I	4 each; walk, lope, and run	6	72	Walk	18.2 \pm 4.6	19.2 \pm 3.0	20.1 \pm 4.7	24.0 \pm 4.8			
							Lope			23.5 \pm 4.3	27.5 \pm 5.5	30.3 \pm 6.6	32.2 \pm 6.8	
							Run				22.3 \pm 6.4	22.2 \pm 6.4	25.0 \pm 8.4	31.3 \pm 13.1
TOSS, press. suit	0	Smooth lunar	I	4 velocities	6	24		18.33 \pm 2.92	20.83 \pm 2.73	20.60 \pm 2.33	25.4 \pm 5.64			
TOSS, press. suit	0	Coarse lunar	I	4 velocities	6	24		19.16 \pm 4.09	19.66 \pm 5.08	25.66 \pm 7.78	23.5 \pm 5.70			
TOSS, pressurized suit	7.5	Hard	I	4 velocities	6	48	Ascend	21.3 \pm 1.9	20.5 \pm 3.8	28.3 \pm 6.4	32.7 \pm 6.8			
							Descend	19.2 \pm 3.8	18.3 \pm 2.4	21.0 \pm 3.3	22.2 \pm 5.0			
TOSS, pressurized suit	7.5	Smooth lunar	I	4 velocities	6	48	Ascend	21.3 \pm 3.4	24.33 \pm 3.14	26.8 \pm 8.4				
							Descend	19.16 \pm 4.01	19.66 \pm 3.35	19.83 \pm 6.15	23 \pm 3.68			
TOSS, pressurized suit	15	Hard	I	4 velocities	6	48	Ascend	22.7 \pm 3.2	25.3 \pm 5.6	32.3 \pm 7.6				
							Descend	18.2 \pm 1.5	18.7 \pm 1.9	21.3 \pm 2.7	21.2 \pm 2.9			
TOSS, pressurized suit	15	Smooth lunar	I	4 velocities	6	48	Ascend	21.5 \pm 3.68	30.4 \pm 9.41					
							Descend	17.16 \pm 4.09	18.16 \pm 3.93	21.66 \pm 4.42	22.16 \pm 5.52			
TOSS, pressurized suit	30	Hard	I	4 velocities	6	48	Ascend							
							Descend	19.7 \pm 3.1	20.8 \pm 3.5	22.5 \pm 2.3	23.3 \pm 3.4			
Inclined plane, pressurized suit	7.5	Hard	I	4 velocities	6	48	Ascend	17.0 \pm 3.0	20.2 \pm 4.9	21.3 \pm 7.5	22.7 \pm 4.4			
							Descend	16.7 \pm 2.5	17.5 \pm 2.9	18.5 \pm 2.2	19.5 \pm 3.9			
Inclined plane, pressurized suit	7.5	Hard	II	4 velocities	6	48	Ascend	17.8 \pm 2.7	21.7 \pm 4.4	23.2 \pm 6.3	26.2 \pm 8.0			
							Descend	15.7 \pm 2.1	17.0 \pm 1.4	19.7 \pm 3.1	19.6 \pm 4.8			
Inclined plane, pressurized suit	15	Hard	I	4 velocities	6	48	Ascend	19.0 \pm 2.8	20.8 \pm 3.6	24.7 \pm 2.8	28.0 \pm 4.7			
							Descend	16.7 \pm 3.3	19.2 \pm 2.0	20.0 \pm 2.0	20.2 \pm 2.3			
Inclined plane, pressurized suit	30	Hard	I	4 velocities	6	48	Ascend							
							Descend	17.8 \pm 1.9	20.0 \pm 2.3	21.7 \pm 3.3	22.0 \pm 4.2			
*Pooled data														

Oxygen Consumption, Carbon Dioxide Production, and Minute Expired Ventilation

The data for these three variables are discussed together because of their interrelationships. Oxygen consumption data (Table 5-13) and carbon dioxide production data (Table 5-14) were based on the expired minute volumes (Table 5-15) and the appropriate inspired and expired gas fractions. The following equations show these interrelationships. Correction factors for converting values from ambient temperature, pressure, and humidity to the appropriate conditions for the particular variable being evaluated (e.g., standard temperature and pressure saturated for \dot{V}_{O_2} are omitted for simplification).

Oxygen consumptions are calculated based on the following equation:

$$\dot{V}_{O_2} = \dot{V}_I F_{I_{O_2}} - \dot{V}_E F_{E_{O_2}} \quad (5-5)$$

where

\dot{V}_{O_2} = oxygen consumption (liters/min)

\dot{V}_I = inspired minute volume (liters/min)

\dot{V}_E = expired minute volume (liters/min)

$F_{I_{O_2}}$ = oxygen fraction in inspired air

$F_{E_{O_2}}$ = oxygen fraction in expired air

Since only \dot{V}_E was measured, however, \dot{V}_I was calculated by

$$\dot{V}_I F_{I_{N_2}} = \dot{V}_E F_{E_{N_2}} \quad (5-6)$$

which is based on the fact that nitrogen is neither taken up nor given off by the body at constant pressure. Equation (5-6) can be rewritten as

$$\dot{V}_I = \dot{V}_E \left(\frac{F_{E_{N_2}}}{F_{I_{N_2}}} \right) \quad (5-7)$$

TABLE 5-13

STEADY-STATE OXYGEN CONSUMPTION \dot{V}_{O_2} (LITERS/MIN, STPD)
FOR ALL SIMULATOR EXERCISE MODES

Experimental conditions							Results (mean and ± 1 standard deviation)							
Simulator and suit mode	Slope, deg	Surface condition	Pack	Number of velocities	Number of subjects	Total tests	Gait or ascend/descend	Velocity, km/hr						
								2	4	6	8	9.7	11.3	12.8
Inclined plane, pressurized (press.) suit	0 (horiz)	Hard	I, 75 lb	4 each; walk, lope and run	6, with 2 repeating once	96	Walk	0.661 \pm 0.176	0.957 \pm 0.448	1.30 \pm 0.55	3.03 \pm 0.29			
							Lope		1.63 \pm 0.47	2.03 \pm 0.11	2.11 \pm 0.63	2.75 \pm 0.89		
							Run			1.64 \pm 0.31	2.02 \pm 0.28	1.96 \pm 0.41	2.32 \pm 0.85	
Inclined plane, pressurized suit	0	Hard	I	1 each; walk, lope, and run	6, with all repeating twice	36	Walk							
							Lope							
							Run							
Inclined plane, subject in mufti (without press. suit)	0	Hard	I	4 each; walk, lope, and run	2	24	Walk	0.324 \pm 0.014	0.452 \pm 0.293	0.477 \pm 0.020	0.931 \pm 0.016			
							Lope			1.31 \pm 0.10	1.41 \pm 0.15	1.36 \pm 0.16	1.29 \pm 0.19	
							Run				0.858 \pm 0.144	0.704 \pm 0.259	1.05 \pm 0.24	0.817 \pm 0.36
Incl plane, mufti	0	Hard	I	Fatigue test	6	24								
Inclined plane, pressurized suit	0	Hard	I	Fatigue test	2	8								
Inclined plane, pressurized suit	0	Hard	II, 240 lb	4 each; walk, lope, and run	6	72	Walk	0.982 \pm 0.573	1.071 \pm 0.308	1.35 \pm 0.308	2.19 \pm 0.67			
							Lope			2.23 \pm 0.48	2.00 \pm 0.45	2.19 \pm 0.88	2.09 \pm 0.41	
							Run			1.60 \pm 0.49	1.71 \pm 0.45	1.80 \pm 0.40	1.96 \pm 0.35	
Inclined plane, pressurized suit	0	Hard	III, 400 lb	4 each; walk, lope, and run	2	24	Walk	0.595 \pm 0.031	1.07 \pm 0.124	1.31 \pm 0.43	1.61 \pm 0.23			
							Lope			2.00 \pm 0.10	2.00 \pm 0.14	2.70 \pm 0.33	3.01 \pm 0.00	
							Run			1.94 \pm 0.62	1.43 \pm 0.18	1.85 \pm 0.13	3.29 \pm 0.00	
TOSS (6-deg-of-freedom), pressurized suit	0	Hard	I	4 each; walk, lope, and run	6	72	Walk	0.897 \pm 0.327	1.09 \pm 0.33	1.58 \pm 0.32	1.81 \pm 0.36			
							Lope			2.16 \pm 0.73	2.58 \pm 0.50	2.73 \pm 0.36	2.36 \pm 0.59	
							Run				1.73 \pm 0.30	2.13 \pm 0.55	2.02 \pm 0.38	2.41 \pm 0.61
TOSS, press. suit	0	Smooth lunar	I	4 velocities	6	24		0.85 \pm 0.21	1.27 \pm 0.26	1.70 \pm 0.36	2.60 \pm 0.55			
TOSS, press. suit	0	Coarse lunar	I	4 velocities	6	24		0.68 \pm 0.14	1.49 \pm 0.28	2.31 \pm 0.34	2.25 \pm 0.38			
TOSS, pressurized suit	7.5	Hard	I	4 velocities	6	48	Ascend	0.97 \pm 0.24	1.45 \pm 0.34	2.08 \pm 0.27	2.92 \pm 0.75			
							Descend	0.70 \pm 0.16	0.68 \pm 0.27	1.02 \pm 0.21	1.44 \pm 0.38			
TOSS, pressurized suit	7.5	Smooth lunar	I	4 velocities	6	48	Ascend	0.99 \pm 0.16	1.79 \pm 0.41					
							Descend	0.62 \pm 0.12	0.99 \pm 0.13	1.20 \pm 0.28	1.47 \pm 0.33			
TOSS, pressurized suit	15	Hard	I	4 velocities	6	48	Ascend	1.13 \pm 0.15	2.48 \pm 0.40					
							Descend	0.53 \pm 0.22	0.75 \pm 0.37	0.91 \pm 0.13	1.06 \pm 0.12			
TOSS, pressurized suit	15	Smooth lunar	I	4 velocities	6	48	Ascend	1.46 \pm 0.18	2.46 \pm 0.34					
							Descend	0.58 \pm 0.10	0.79 \pm 0.18	1.02 \pm 0.16	1.20 \pm 0.26			
TOSS, pressurized suit	30	Hard	I	4 velocities	6	48	Ascend							
							Descend	0.59 \pm 0.23	0.75 \pm 0.33	0.87 \pm 0.17	1.03 \pm 0.21			
Inclined plane, pressurized suit	7.5	Hard	I	4 velocities	6	48	Ascend	0.66 \pm 0.18	1.04 \pm 0.40	1.52 \pm 0.75	2.07 \pm 0.61			
							Descend	0.52 \pm 0.09	0.78 \pm 0.28	0.74 \pm 0.21	0.96 \pm 0.20			
Inclined plane, pressurized suit	7.5	Hard	II	4 velocities	6	48	Ascend	0.88 \pm 0.21	1.44 \pm 0.31	1.98 \pm 0.52	2.55 \pm 0.68			
							Descend	0.65 \pm 0.21	0.89 \pm 0.20	0.97 \pm 0.20	1.38 \pm 0.42			
Inclined plane, pressurized suit	15	Hard	I	4 velocities	6	48	Ascend	0.96 \pm 0.21	1.60 \pm 0.30	1.92 \pm 0.22				
							Descend	0.58 \pm 0.31	0.59 \pm 0.20	0.87 \pm 0.34	1.21 \pm 0.20			
Inclined plane, pressurized suit	30	Hard	I	4 velocities	6	48	Ascend							
							Descend	0.65 \pm 0.16	0.75 \pm 0.15	1.04 \pm 0.21	1.39 \pm 0.17			

TABLE 5-14

CARBON DIOXIDE PRODUCTION \dot{V}_{CO_2} (LITERS/MIN, STPD)
FOR ALL SIMULATOR EXERCISE MODES

Experimental conditions							Results (mean and ± 1 standard deviation)							
Simulator and suit mode	Slope, deg	Surface condition	Pack	Number of velocities	Number of subjects	Total tests	Gait or ascend/descend	Velocity, km/hr						
								2	4	6	8	9.7	11.3	12.8
Inclined plane, pressurized (press.) suit	0 (horiz)	Hard	I, 75 lb	4 each; walk, lope and run	6, with 2 repeating once	96	Walk	0.452 \pm 0.128	0.689 \pm 0.198	1.05 \pm 0.290	1.96 \pm 0.927			
							Lope			1.44 \pm 0.543	1.76 \pm 0.70	1.84 \pm 0.39	1.87 \pm 0.42	
							Run				1.18 \pm 0.35	1.43 \pm 0.15	1.28 \pm 0.22	1.52 \pm 0.47
Inclined plane, pressurized suit	0	Hard	I	1 each; walk, lope, and run	6, with all repeating twice	36	Walk							
							Lope							
							Run							
Inclined plane, subject in mufti (without press. suit)	0	Hard	I	4 each; walk, lope, and run	2	24	Walk	0.229 \pm 0.038	0.453 \pm 0.166	0.417 \pm 0.024	0.704 \pm 0.166			
							Lope			0.865 \pm 0.067	1.04 \pm 0.18	1.22 \pm 0.42	0.927 \pm 0.080	
							Run				0.601 \pm 0.177	0.532 \pm 0.077	0.921 \pm 0.074	0.683 \pm 0.059
Incl plane, mufti	0	Hard	I	Fatigue test	6	24								
Inclined plane, pressurized suit	0	Hard	I	Fatigue test	2	8								
Inclined plane, pressurized suit	0	Hard	II, 240 lb	4 each; walk, lope, and run	6	72	Walk	0.62 \pm 0.22	0.75 \pm 0.26	1.03 \pm 0.27	1.59 \pm 0.23			
							Lope			1.62 \pm 0.38	1.74 \pm 0.22	2.13 \pm 0.47	2.21 \pm 0.39	
							Run				1.37 \pm 0.31	1.57 \pm 0.31	1.67 \pm 0.16	1.87 \pm 0.22
Inclined plane, pressurized suit	0	Hard	III, 400 lb	4 each; walk, lope, and run	2	24	Walk	0.401 \pm 0.008	0.741 \pm 0.035	1.17 \pm 0.42	1.33 \pm 0.19			
							Lope			1.76 \pm 0.20	1.57 \pm 0.03	2.14 \pm 0.18	2.16 \pm 0.00	
							Run				1.50 \pm 0.41	1.41 \pm 0.22	1.53 \pm 0.30	2.68 \pm 0.00
TOSS (6-deg-of-freedom), pressurized suit	0	Hard	I	4 each; walk, lope, and run	6	72	Walk	0.639 \pm 0.140	0.745 \pm 0.216	1.22 \pm 0.25	1.38 \pm 0.18			
							Lope			1.72 \pm 0.64	1.95 \pm 0.37	2.24 \pm 0.46	2.10 \pm 0.54	
							Run				1.30 \pm 0.32	1.64 \pm 0.43	1.77 \pm 0.60	2.20 \pm 0.59
TOSS, press. suit	0	Smooth lunar	I	4 velocities	6	24		0.70 \pm 0.17	1.05 \pm 0.21	1.38 \pm 0.27	2.21 \pm 0.42			
TOSS, press. suit	0	Coarse lunar	I	4 velocities	6	24		0.56 \pm 0.12	1.18 \pm 0.22	1.87 \pm 0.22	1.84 \pm 0.29			
TOSS, pressurized suit	7.5	Hard	I	4 velocities	6	48	Ascend	0.85 \pm 0.12	1.29 \pm 0.22	1.93 \pm 0.40	2.58 \pm 0.57			
							Descend	0.58 \pm 0.13	0.55 \pm 0.22	0.85 \pm 0.17	1.19 \pm 0.31			
TOSS, pressurized suit	7.5	Smooth lunar	I	4 velocities	6	48	Ascend	0.87 \pm 0.13	1.57 \pm 0.38					
							Descend	0.52 \pm 0.10	0.81 \pm 0.11	1.10 \pm 0.13	1.23 \pm 0.26			
TOSS, pressurized suit	15	Hard	I	4 velocities	6	48	Ascend	0.93 \pm 0.12	2.05 \pm 0.33					
							Descend	0.44 \pm 0.18	0.62 \pm 0.31	0.75 \pm 0.11	0.88 \pm 0.10			
TOSS, pressurized suit	15	Smooth lunar	I	4 velocities	6	48	Ascend	1.25 \pm 0.16	2.29 \pm 0.33					
							Descend	0.48 \pm 0.08	0.65 \pm 0.15	0.85 \pm 0.14	0.99 \pm 0.21			
TOSS, pressurized suit	30	Hard	I	4 velocities	6	48	Ascend							
							Descend	0.49 \pm 0.19	0.62 \pm 0.27	0.71 \pm 0.14	0.85 \pm 0.18			
Inclined plane, pressurized suit	7.5	Hard	I	4 velocities	6	48	Ascend	0.57 \pm 0.17	0.88 \pm 0.32	1.30 \pm 0.58	1.59 \pm 0.42			
							Descend	0.38 \pm 0.04	0.60 \pm 0.20	0.65 \pm 0.22	0.82 \pm 0.19			
Inclined plane, pressurized suit	7.5	Hard	II	4 velocities	6	48	Ascend	0.73 \pm 0.18	1.19 \pm 0.26	1.64 \pm 0.44	2.11 \pm 0.56			
							Descend	0.46 \pm 0.15	0.67 \pm 0.17	0.75 \pm 0.16	1.02 \pm 0.30			
Inclined plane, pressurized suit	15	Hard	I	4 velocities	6	48	Ascend	0.78 \pm 0.17	1.31 \pm 0.26	1.72 \pm 0.20				
							Descend	0.40 \pm 0.08	0.45 \pm 0.13	0.63 \pm 0.15	0.88 \pm 0.11			
Inclined plane, pressurized suit	30	Hard	I	4 velocities	6	48	Ascend							
							Descend	0.45 \pm 0.11	0.57 \pm 0.11	0.85 \pm 0.18	0.98 \pm 0.12			

TABLE 5-15

MINUTE EXPIRED VOLUME \dot{V}_E (LITERS/MIN, BTPS)
FOR ALL SIMULATOR EXERCISE MODES

Experimental conditions							Results (mean and ± 1 standard deviation)							
Simulator and suit mode	Slope, deg	Surface condition	Pack	Number of velocities	Number of subjects	Total tests	Gait or ascend/descend	Velocity, km/hr						
								2	4	6	8	9.7	11.3	12.8
Inclined plane, pressurized (press.) suit	0 (horiz)	Hard	I, 75 lb	4 each; walk, lope and run	6, with 2 repeating once	96*	Walk	16.71 \pm 3.16	24.35 \pm 5.39	38.37 \pm 10.43	64.06 \pm 21.23			
							Lope			44.35 \pm 13.32	55.75 \pm 23.12	60.82 \pm 12.60	59.81 \pm 10.66	
							Run				37.64 \pm 8.33	45.56 \pm 2.57	41.74 \pm 5.65	48.34 \pm 13.86
Inclined plane, pressurized suit	0	Hard	I	1 each; walk, lope, and run	6, with all repeating twice	36*	Walk							
							Lope							
							Run							
Inclined plane, subject in mufti (without press. suit)	0	Hard	I	4 each; walk, lope, and run	2	24	Walk	7.39 \pm 0.29	13.26 \pm 3.5	11.49 \pm 0.28	20.44 \pm 0.95			
							Lope			26.98 \pm 3.35	27.75 \pm 0.04	31.84 \pm 7.70	26.78 \pm 5.98	
							Run				17.76 \pm 2.59	15.01 \pm 3.64	25.63 \pm 4.78	20.47 \pm 2.28
Incl plane, mufti	0	Hard	I	Fatigue test	6	24								
Inclined plane, pressurized suit	0	Hard	I	Fatigue test	2	8								
Inclined plane, pressurized suit	0	Hard	II, 240 lb	4 each; walk, lope, and run	6	72	Walk	21.89 \pm 6.94	27.09 \pm 8.61	35.24 \pm 8.35	52.95 \pm 7.15			
							Lope			52.56 \pm 12.43	54.32 \pm 5.52	61.82 \pm 13.41	69.42 \pm 8.96	
							Run			43.99 \pm 9.66	49.46 \pm 7.61	49.97 \pm 3.69	57.52 \pm 14.93	
Inclined plane, pressurized suit	0	Hard	III, 400 lb	4 each; walk, lope, and run	2	24	Walk	13.67 \pm 0.89	26.40 \pm 0.51	41.87 \pm 12.25	45.67 \pm 6.40			
							Lope			57.80 \pm 6.76	54.68 \pm 1.63	70.47 \pm 10.38	77.69 \pm 0.00	
							Run				54.38 \pm 13.85	42.99 \pm 3.82	51.46 \pm 0.48	81.11
TOS (6-deg-of-freedom), pressurized suit	0	Hard	I	4 each; walk, lope, and run	6	72	Walk	23.14 \pm 4.83	23.66 \pm 6.21	38.62 \pm 7.67	44.18 \pm 5.90			
							Lope			52.21 \pm 15.27	60.62 \pm 10.08	70.65 \pm 14.00	66.46 \pm 11.73	
							Run				41.26 \pm 11.38	49.75 \pm 12.10	54.55 \pm 16.19	81.11 \pm 0.00
TOS, press. suit	0	Smooth lunar	I	4 velocities	6	24		23.36 \pm 5.30	33.22 \pm 5.47	42.48 \pm 9.40	70.77 \pm 20.02			
TOS, press. suit	0	Coarse lunar	I	4 velocities	6	24		19.60 \pm 5.57	36.21 \pm 5.96	55.29 \pm 10.01	52.88 \pm 11.33			
TOS, pressurized suit	7.5	Hard	I	4 velocities	6	48	Ascend	27.76 \pm 4.66	36.23 \pm 6.76	56.53 \pm 10.74	77.92 \pm 19.97			
							Descend	20.96 \pm 4.66	18.35 \pm 7.30	27.06 \pm 4.69	37.53 \pm 8.95			
TOS, pressurized suit	7.5	Smooth lunar	I	4 velocities	6	48	Ascend	29.03 \pm 3.82	48.12 \pm 12.33					
							Descend	18.87 \pm 3.57	27.33 \pm 4.12	36.45 \pm 5.82	37.92 \pm 6.16			
TOS, pressurized suit	15	Hard	I	4 velocities	6	48	Ascend	28.04 \pm 4.05	56.71 \pm 10.77					
							Descend	16.38 \pm 5.04	21.76 \pm 10.99	25.56 \pm 2.15	29.26 \pm 3.99			
TOS, pressurized suit	15	Smooth lunar	I	4 velocities	6	48	Ascend	39.89 \pm 3.30	68.17 \pm 13.96					
							Descend	17.50 \pm 3.08	23.17 \pm 5.65	29.06 \pm 4.50	32.81 \pm 6.18			
TOS, pressurized suit	30	Hard	I	4 velocities	6	48	Ascend							
							Descend	17.65 \pm 6.12	22.33 \pm 9.55	25.74 \pm 5.21	28.90 \pm 6.45			
Inclined plane, pressurized suit	7.5	Hard	I	4 velocities	6	48	Ascend	19.90 \pm 5.53	29.83 \pm 13.33	43.39 \pm 23.50	48.89 \pm 13.60			
							Descend	14.06 \pm 1.51	20.69 \pm 6.37	21.31 \pm 6.40	27.14 \pm 6.54			
Inclined plane, pressurized suit	7.5	Hard	II	4 velocities	6	48	Ascend	24.21 \pm 5.40	38.64 \pm 10.08	50.16 \pm 15.32	62.79 \pm 15.11			
							Descend	16.32 \pm 4.44	22.82 \pm 5.31	25.34 \pm 6.79	33.64 \pm 10.34			
Inclined plane, pressurized suit	15	Hard	I	4 velocities	6	48	Ascend	25.84 \pm 6.46	40.39 \pm 10.28	52.41 \pm 6.34				
							Descend	14.72 \pm 3.17	15.74 \pm 4.90	21.74 \pm 5.04	29.90 \pm 4.80			
Inclined plane, pressurized suit	30	Hard	I	4 velocities	6	48	Ascend							
							Descend	15.74 \pm 4.07	20.29 \pm 5.08	28.71 \pm 6.41	32.10 \pm 3.96			
*Pooled data														

where $F_{E_{N_2}}$ = nitrogen fraction in the expired air

$F_{I_{N_2}}$ = nitrogen fraction in the inspired air

Substituting in Equation (5-5),

$$\dot{V}_{O_2} = \left(\frac{\dot{V}_E F_{E_{N_2}}}{F_{I_{N_2}}} \right) F_{I_{O_2}} - \dot{V}_E F_{E_{O_2}} \quad (5-8)$$

or

$$\dot{V}_{O_2} = \dot{V}_E \left(\frac{F_{E_{N_2}} F_{I_{O_2}}}{F_{I_{N_2}}} - F_{E_{O_2}} \right) \quad (5-9)$$

Carbon dioxide production is calculated in a similar manner as follows:

$$\dot{V}_{CO_2} = \dot{V}_E F_{E_{CO_2}} - \dot{V}_I F_{I_{CO_2}} \quad (5-10)$$

where \dot{V}_{CO_2} = carbon dioxide production (liters/min)

$F_{E_{CO_2}}$ = carbon dioxide fraction in the expired gas

$F_{I_{CO_2}}$ = carbon dioxide fraction in the inspired gas

If the substitution of Equation (5-7) is made in Equation (5-10) and the components are rearranged, the following equation is obtained:

$$\dot{V}_{CO_2} = \dot{V}_E \left(F_{E_{CO_2}} - \frac{F_{E_{N_2}} F_{I_{CO_2}}}{F_{I_{N_2}}} \right) \quad (5-11)$$

In addition, metabolic rates as described earlier were also derived from these data by

$$\text{Metabolic rate} = C \dot{V}_{O_2} \quad (5-12)$$

where the function is derived from the caloric equivalent of a liter of oxygen as determined by the ratio of carbon dioxide production to oxygen consumption, usually noted as the respiratory ratio. The respiratory ratio, R , can be written

$$R = \frac{\dot{V}_{CO_2}}{\dot{V}_{O_2}} \quad (5-13)$$

or substituting from Equations (5-9) and (5-10) and rearranging, we obtain

$$R = \frac{F_{E_{CO_2}} F_{I_{N_2}} - F_{I_{CO_2}} F_{E_{N_2}}}{F_{I_{O_2}} F_{E_{N_2}} - F_{E_{O_2}} F_{I_{N_2}}} \quad (5-14)$$

Values of R normally vary between 0.8 and 1.0 and are determined by small differences in the fractions of gases in the respired air. While these minor changes occur from the resting state to extreme exercise, expired minute volumes vary from 8 liters/min at rest to as high as 80 liters/min for running with a 400-lb (1 g) load at 12.8 km/hr. It is readily evident that the expired minute volume is the major determinant of gas exchange, while the gas fractions remain essentially constant.

The interrelationships between these variables are therefore very apparent, and it is fairly obvious that they are self-correlating. Presentation of the statistical evaluation of these data would shed little additional information not provided by the evaluation presented for the steady-state metabolic rates.

Special Considerations of the Physiological Data

Metabolic rates. - Although it was initially thought that the energy cost of locomotion would be increased on the lunar surface (Reference 5-12), the use of artificial-gravity simulators has shown that the energy requirements for locomotion at decreased gravity will be less (References 5-4, and 5-13 through 5-17). Current test results support this latter thesis.

Figure 5-39 presents most of the data available, including those obtained by this effort on the energy cost of locomotion during simulated 1/6 g in mufti. The summary data for the 1-g data are prepared after Passmore and Durin (Reference 5-18). The curves shown are trend lines drawn by visual averaging. It is readily apparent that the lower curve drawn for the 1/6-g data is a reasonable fit for all the data from the three different test series. It is significant that the data for these tests were obtained by different techniques.

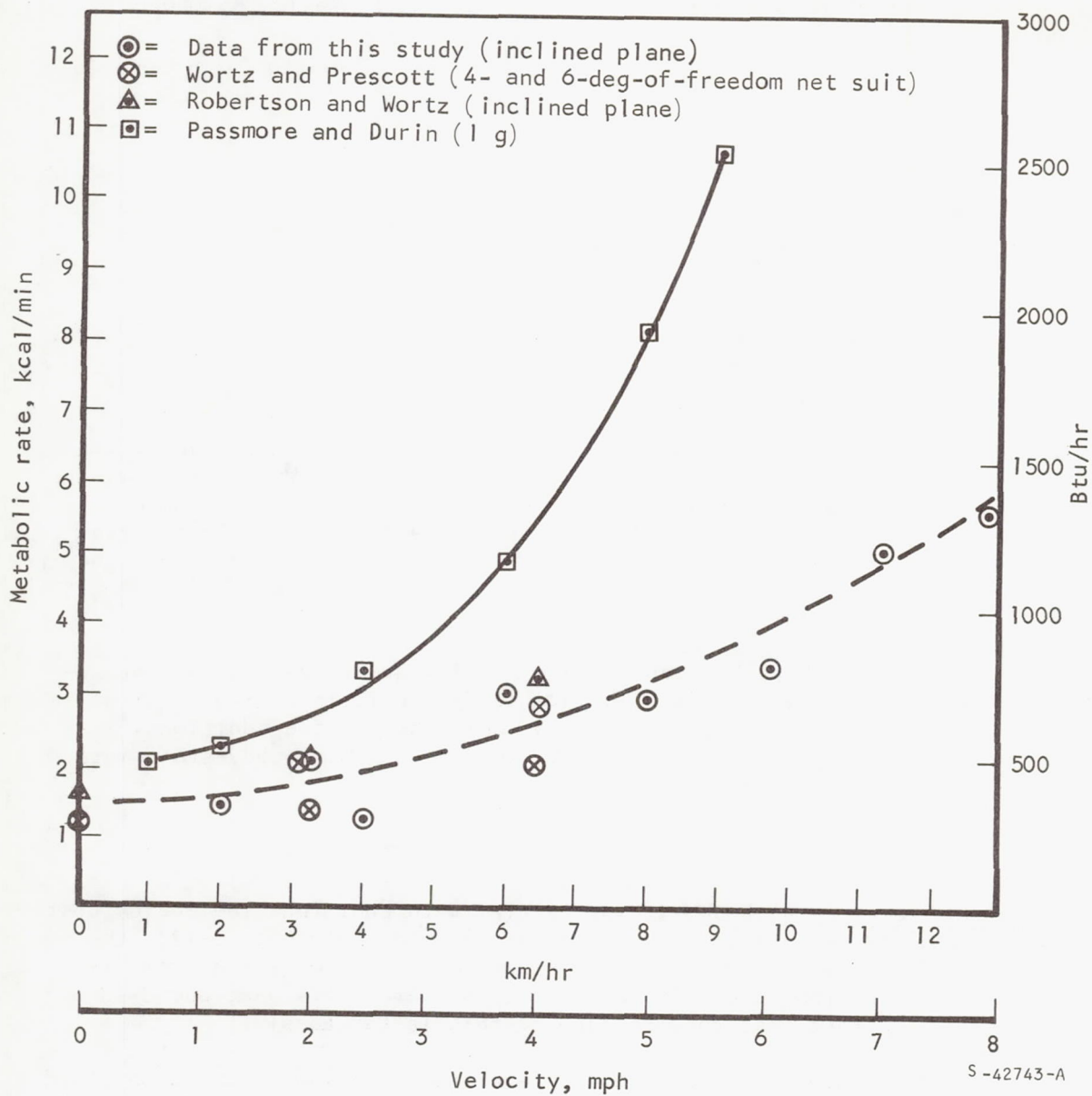


Figure 5-39. Energy Cost for Walking and Running at 1 G and 1/6 G, Horizontal, Without Pressure Suit

The data shown in Figure 5-39 dramatically point out the decrease in metabolic rate with decreased gravity. When considering locomotion in the reduced-gravity environment, several parameters such as gait and traction are relevant. A simplified view of the problem is to consider locomotion as analogous to walking while carrying weights. As gravity is reduced, the weight carried is reduced concomitantly, and the energy required for comparative locomotive tasks is similarly reduced. Wortz (Reference 5-2) described a series of experiments that confirmed the above by adding weights to the subjects to return them to their 1-g equivalent weight with metabolic rates that were similar to 1-g tests. These results substantiate the concept that weight reduction is a primary mechanism in producing metabolic costs for locomotion that are lower at reduced gravity than at 1 g.

The factors of traction are also important. This is amply demonstrated by a significant decrease in the efficiency of locomotion even though the total energy expenditure is dramatically reduced with reduced gravity. This relationship was cogently illustrated by the data of Robertson and Wortz (Reference 5-3), which shows that energy cost per kg of body weight at lunar gravity is significantly higher than for comparative tasks at 1 g, indicating a substantial reduction in efficiency.

Figure 5-40 summarizes the data available for the metabolic cost of locomotion in various pressure suits at 1 g (References 5-3, 5-12, 5-19, and 5-20). These data are shown to indicate the mobility characteristics of the various suits and for comparisons with the 1/6-g data shown in Figure 5-41. Three of the suits characterized in Figure 5-40 were developed as early-generation Apollo suits. These suits are the Litton RX-2A, the International Latex Corporation pre-prototype suit ILC, and the A5L. The G-2C manufactured by David Clark, the ILC, and the A5L suits all represent approximately the same weight penalty to the subject. In contrast to this, the RX-2A weighed 83 lb, a penalty of approximately 50 lb over the other suits.

The curves shown for these data are faired curves. The values are so diverse between suits, however, that certain conclusions can be drawn. First and most important, the development of mobile joints has led to the evolution of suits which allow locomotion at greatly reduced metabolic cost. The A5L, the latest ILC suit, is by far the most mobile design based on this criterion. The G-2C suit is the least mobile of the soft-suit concepts. The RX-2A is a hard suit, weighing 83 lb. The extremely high metabolic cost of locomotion with the RX-2A suit was a function of carrying this excessive weight, rather than being related to the mobility of the suit.

Comparing the shirt-sleeve data of Passmore and Durin (Figure 5-39) with the suited data of Figure 5-40 at the 1- and 2-mph velocity intervals shows that the 3 relatively rigid suits increased the metabolic cost 250 percent. The more mobile A5L suit increased the cost of locomotion by only 150 percent. It should also be noted that the data for suited subjects reached 8.4 kcal/min (2000 Btu/hr) at a velocity of only 2 mph, while in mufti this level was not reached until 5 mph.

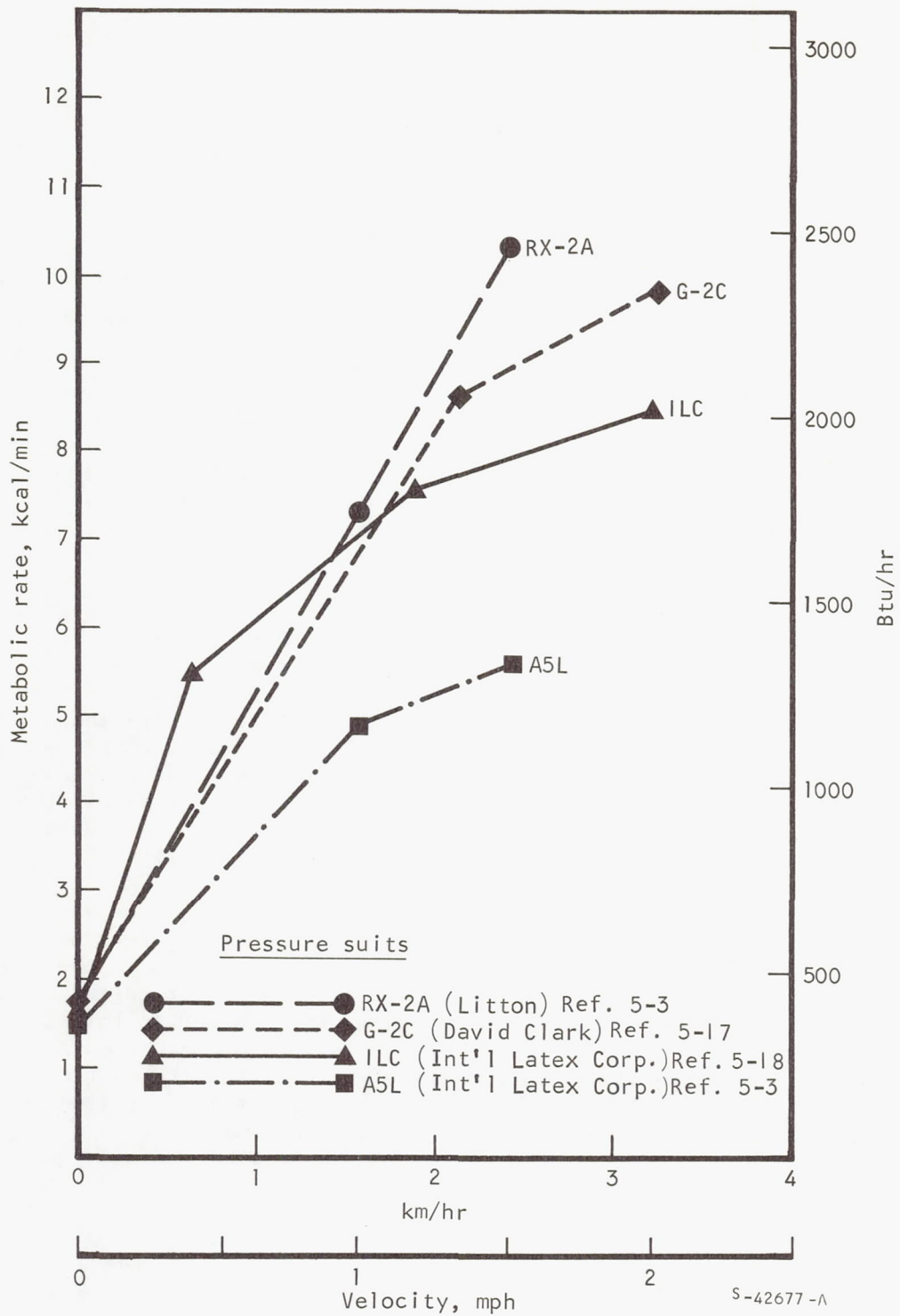


Figure 5-40. Energy Cost for Walking at 1 G, Horizontal, Various Pressurized Suits (No Pack)

- ——— AiResearch data, RX-2A suit, 6 subjects, inclined plane
- ——— AiResearch data, RX-2A suit, 6 subjects, gimbal (6 deg of freedom)
- △ — ····· AiResearch data, A5L suit, 6 subjects, inclined plane
- ▲ — ····· AiResearch data, A5L suit, 6 subjects, gimbal (6 deg of freedom)
- ——— AiResearch data, G-2C suit, 6 subjects, inclined plane
- ——— AiResearch data, G-2C suit, 6 subjects, TOSS (6 deg of freedom)

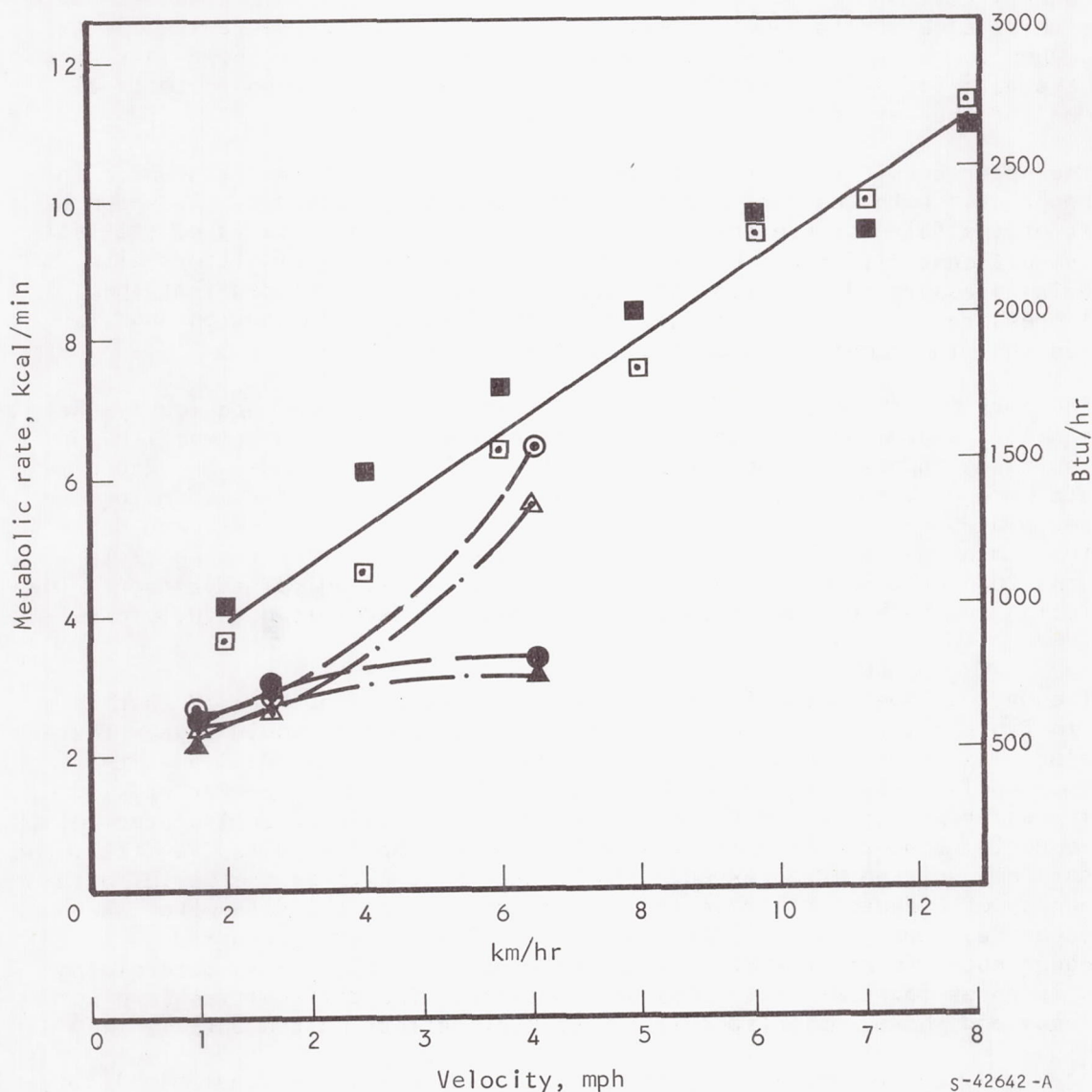


Figure 5-41. Energy Cost for Walking and Running at 1/6 G, Horizontal, Pressurized Suits, on a Level Hard Surface

Figure 5-41 reviews the metabolic cost of locomotion in pressurized suits in a simulated lunar-gravity environment (Reference 5-3) including the data from this effort. When compared to the 1-g data from Figure 5-40, the decreased total energy cost of locomotion for suited subjects is obvious. The evaluation of the shirt-sleeve data shown in Figure 5-39 explains this decreased energy cost. When compared to the shirt-sleeve data for 1/6-g tests shown in Figure 5-39, the data for suit tests show similar increments in metabolic costs as reported for the 1-g data as a function of the suit worn.

The upper curve in Figure 5-41 presents the data contained elsewhere in this report for both the inclined-plane and the TOSS simulators. As shown by the fit of the faired curve and the analysis of variance there is no statistically significant difference between the data from the two simulators with the Gemini pressure suit. From these data, it must be concluded that the Gemini pressure suit imposed the greatest restriction to locomotion and incurred the higher metabolic cost of the suits shown here.

The data for the A5L and RX-2A suits have been described previously (Reference 5-3). In comparing data for the Gemini suit, the greater mobility of these suits is apparent. The differences between the inclined-plane and gimbal data were originally attributed to the missing degrees-of-freedom in the inclined plane, requiring energy (References 5-3 and 5-13). The lower data with the gimbal, shown in Figure 5-41, may have resulted from the subjects using the counterbalance of that simulator to their mechanical advantage. The conflicting evidence on the effects of degrees-of-freedom is not fully understood.

The data of Kuehnegger for locomotion in a pressurized Mark IV suit is shown in Table 5-16. By comparison with the other data it would appear that for velocities up to 4 km/hr minimum, the Mark IV suit is as mobile as the prototype Apollo suits. Since the Mark IV suit was not designed for walking in the pressurized state and did not have specially designed articulated joints, it is doubtful that the Mark IV is as mobile as the Apollo suits. In fact, the data for this suit would be expected to be nearly as high as the Gemini data. The paucity of Kuehnegger's data leaves many questions; the data were taken with essentially only one subject, and no repetitions were performed. Kuehnegger noted in his report that he experienced difficulty in determining metabolic rates for tests with pressurized suits. The difficulties were not described, and there was no speculation on their effect on the data.

In addition to testing on a horizontal, inclined-plane lunar simulator, Kuehnegger performed a small number of studies with locomotion on slopes. The table below summarizes his metabolic data for ascending slopes and the comparable data from the current study. Values are shown in kcal/min.

TABLE 5-16

DATA FROM NASA CR 66119

Test Series 1000 Subjects				Test Series 3120 Subjects			Test Series 3200 Subjects			Test Series 500 Subjects		
Velocity mph	A Btu/hr	B Btu/hr	C Btu/hr	Velocity mph	A Btu/hr	C Btu/hr	Velocity mph	A Btu/hr	C Btu/hr	Velocity mph	A Btu/hr	C Btu/hr
0	270	271.77	319	0	497	343	0	518	619	0	236	339
0.5	396	343.45	355	4	1426	1651	4	943	-	0.5	318	344
1.0	463	373.82	402	5	1575	1243	5	1352	1698	1	366	386
2.0	655	482.78	534	6	1258	2227	6	1411	1990	2	441	467
3.0	858	722.29	750				7	2230	836	3	674	656
4.0	996	858.04	902							4	845	750
5.0	1115	965.00	992							5	1044	883
6.0	1652	1457.00	1197							6	1331	1298
7.0	1287	1626.00	1386									
8.0	1441	-	-									
1/6 g, shirtsleeves Walking and running Pack I (12.02 kg)				1/6 g, pressurized Jumping horizontally Pack II (34.374 kg)			1/6 g, pressurized Loping horizontally Pack II (34.374 kg)			1/6 g, shirtsleeve Walking and running without pack		

Velocity, km/hr	Ascending slope, deg				
	7.5	10	15	20	30
2	3.06 kcal/min	3.5	4.27	7.8	7.9
4	5.42 kcal/min	5.8	7.11		11.14

The 10- and 20-deg slope data are from Kuehnegger's data, while the 7.5- , 15- , and 30-deg values are from the current study. Since tests were not performed on the same slope grades, it is difficult to make comparisons. cursory examination, however, reveals no notable differences.

Comparative metabolic rate data for descending slopes are listed in the following table in kcal/min:

Velocity km/hr	Descending slope, deg		
	7.5	10	15
2	2.52 kcal/min	3.2	2.57
4	3.74	4.0	3.29

The values for descending slopes are slightly higher for Kuehnegger's data (10-deg slope) than for this study. However, the values are too close to discriminate any real differences.

Comparisons can also be made for loping values between these two studies. The values obtained for the metabolic cost of loping (in kcal/min) are as follows:

Velocity, km/hr	Kuehnegger's data	Current study
8	6.41 kcal/min	9.96 kcal/min
10	7.16	10.08*
11.3	8.33	12.31

*This value was actually obtained at 9.7 km/hr.

Results in this study are much higher than those reported by Kuehnegger.

In general, definitive conclusions between the studies cannot be drawn. The magnitude of the data of this study, however, combined with the statistical evaluations and error analyses performed, lends credence to the validity of the data for this effort. Similar conclusions cannot be drawn based on the documentation of Kuehnegger's work due to the lack of data.

Heart rate vs metabolic rate. - Figures 5-42 through 5-45 show typical relationships between heart rates and metabolic rates. As expected, the two variables are positively correlated as explained in a previous section. The dispersion of data, however, is quite different between test series. Figure 5-46 is given for evaluation of the effect of data dispersion on the predictions of metabolic rate from heart rates over a large population of values.

In Figure 5-46(A), 500 data points are plotted relating heart rate and metabolic rate. The mean ± 1 standard deviation over the 500 heart rates is 117.6 ± 30.7 beats/min, while for the metabolic rates the value was 7.01 ± 3.56 kcal/min. The central solid line is the regression line with respect to y and is expressed by the equation $y = 69.24 + 6.91x$. The broken line on either side of this regression line is the value of two standard deviations from the mean regression line. The regression line with respect to x is shown by the broken center line and is expressed by the equation $x = -2.11 + 0.08y$; the solid lines are ± 2 standard deviations from this line.

A correlation of 0.80 was found for the relationship between heart rate and metabolic rate. This relatively high correlation in the presence of the obvious dispersion of data points is a result of the extensive range of both heart rate and metabolic rate.

A complete analysis of these curves yields a standard error in determining the heart rate from a given metabolic rate of 18.42 beats/min. The standard error of metabolic rate, given a heart rate, equals 2.14 kcal/min. These standard errors represent the utility of these data in predicting the value of either variable, having the value of the other. Individual subject variability is illustrated in Table 5-17 and Figure 5-46(B). The technique of predicting metabolic rate from heart rate leaves much to be desired from the standpoint of accuracy and requires the determination of the level of acceptability prior to its use. Andrews (Reference 5-21) reviewed this technique and reported: "The acceptability of the increased experimental error which is introduced by the substitution of the regression method for respiratory calorimetry will depend upon the nature and objective of each particular investigation. The simplicity and convenience of the regression method must be weighed against the loss of precision which it entails."

There are currently two schools of thought on the utility of using heart rate to accurately predict metabolic rate (References 22, 23, and 24). It is generally accepted that under closely controlled laboratory conditions, a subject can be calibrated for heart rate and metabolic rate, and his metabolic rate determined by only a heart rate measurement. It is also well understood that this relationship only holds when no outside stress factors such as heat or carbon dioxide are present (Reference 5-25). For conditions where pressure suit wear is mandatory or desirable (e.g., for testing), external stresses are

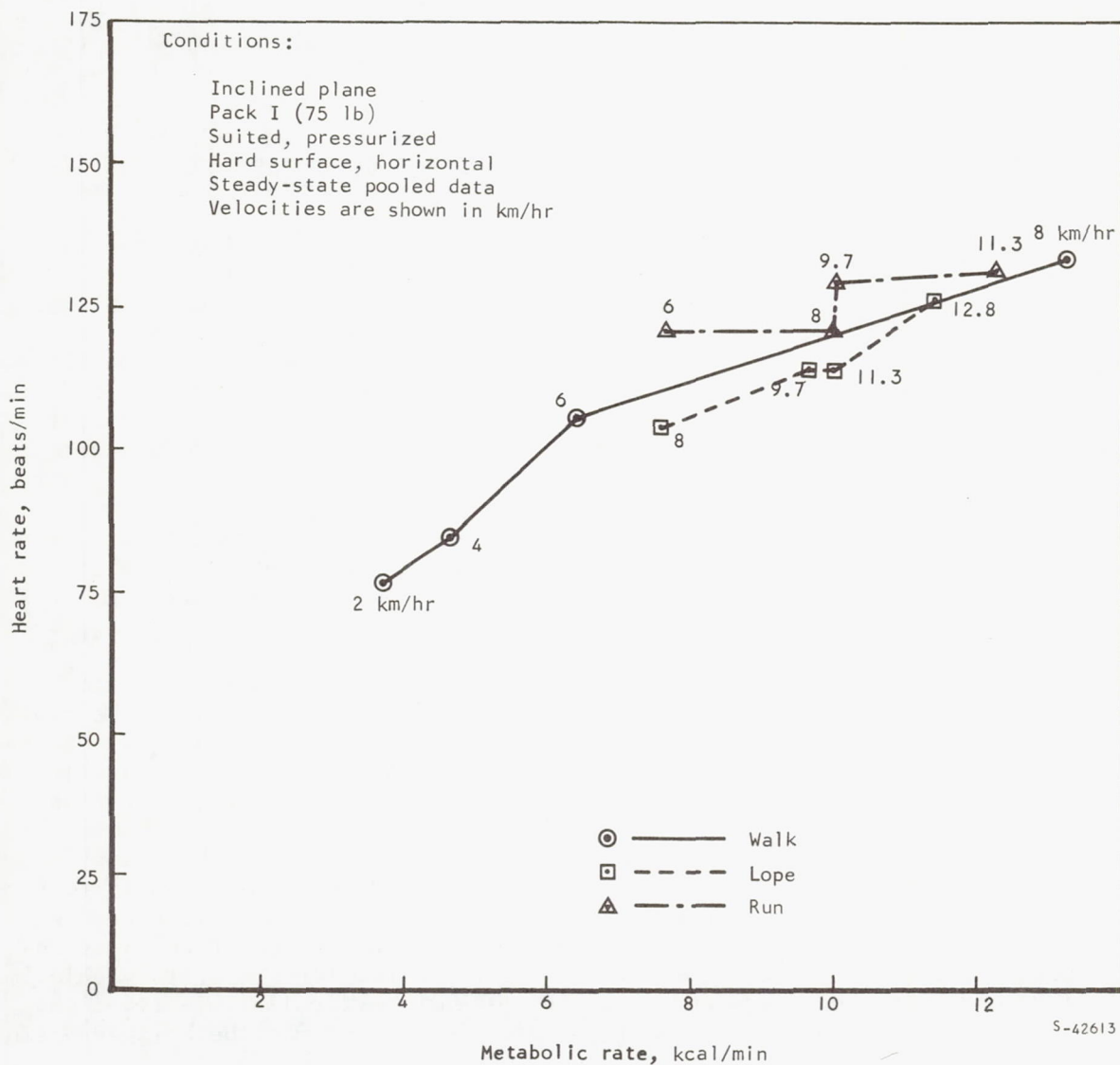


Figure 5-42. Heart Rate vs Metabolic Rate on the Inclined Plane Simulator with Pack I

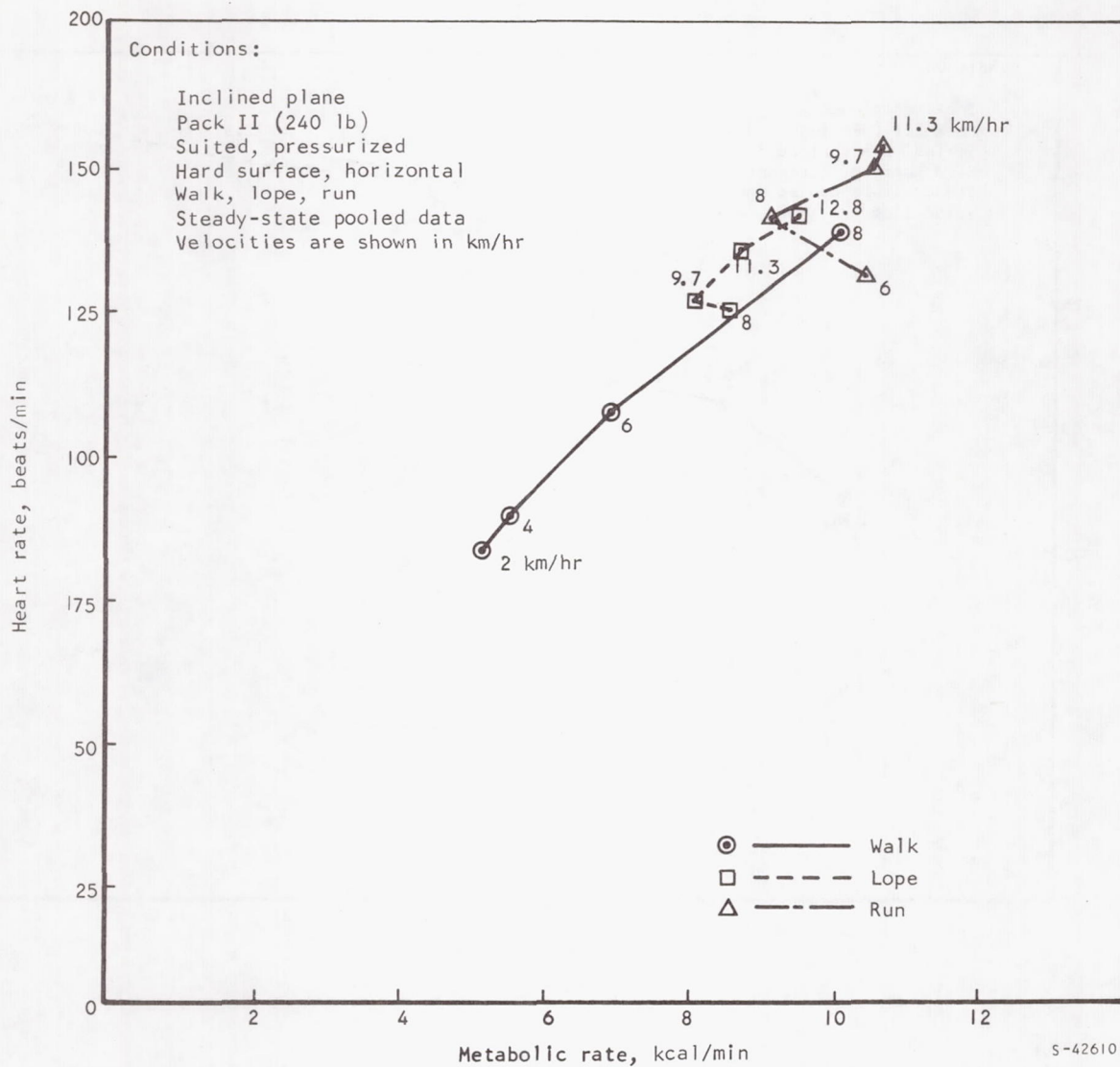


Figure 5-43. Heart Rate vs Metabolic Rate, Inclined Plane, Pack II

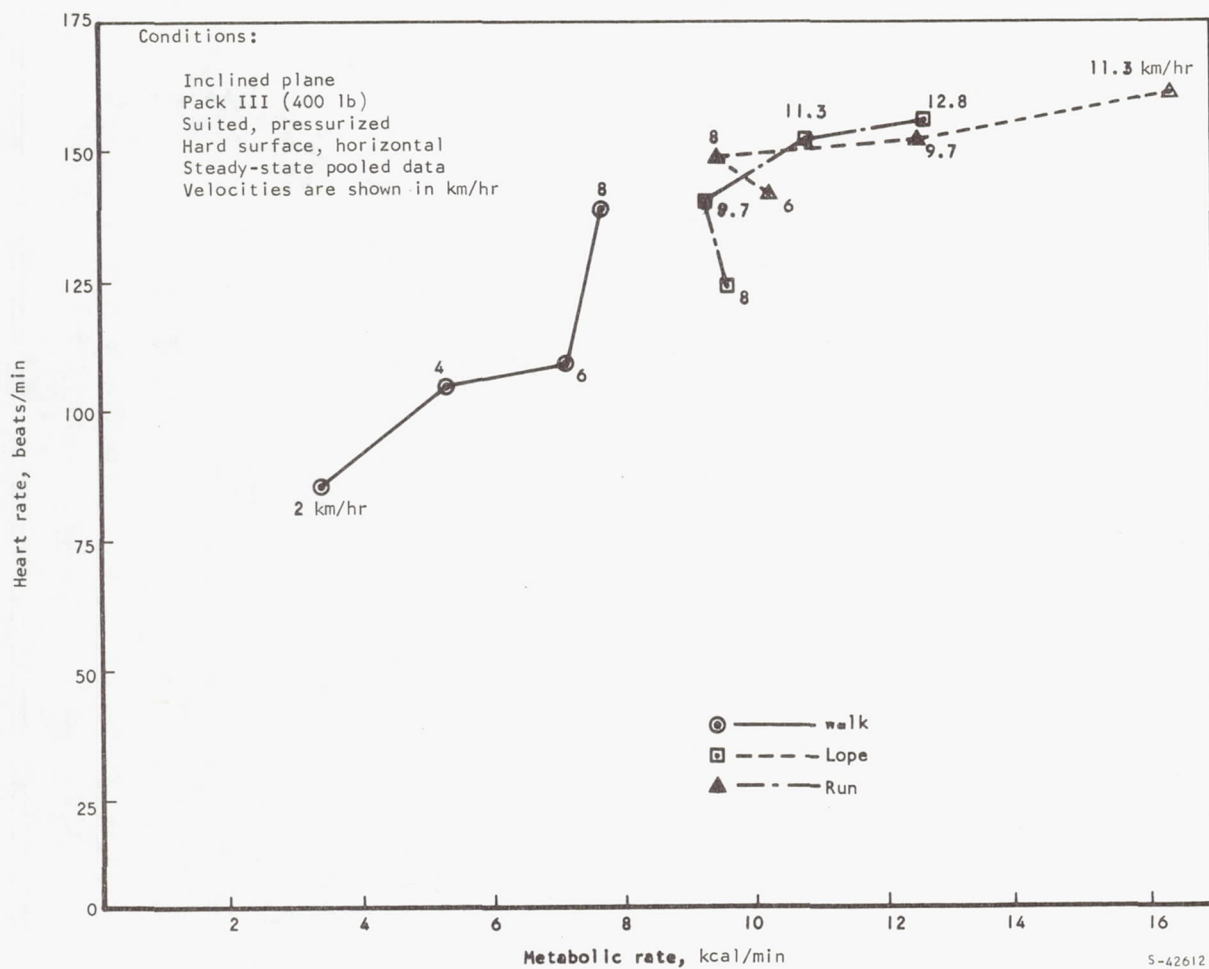


Figure 5-44. Heart Rate vs Metabolic Rate, Inclined Plane, Pack III

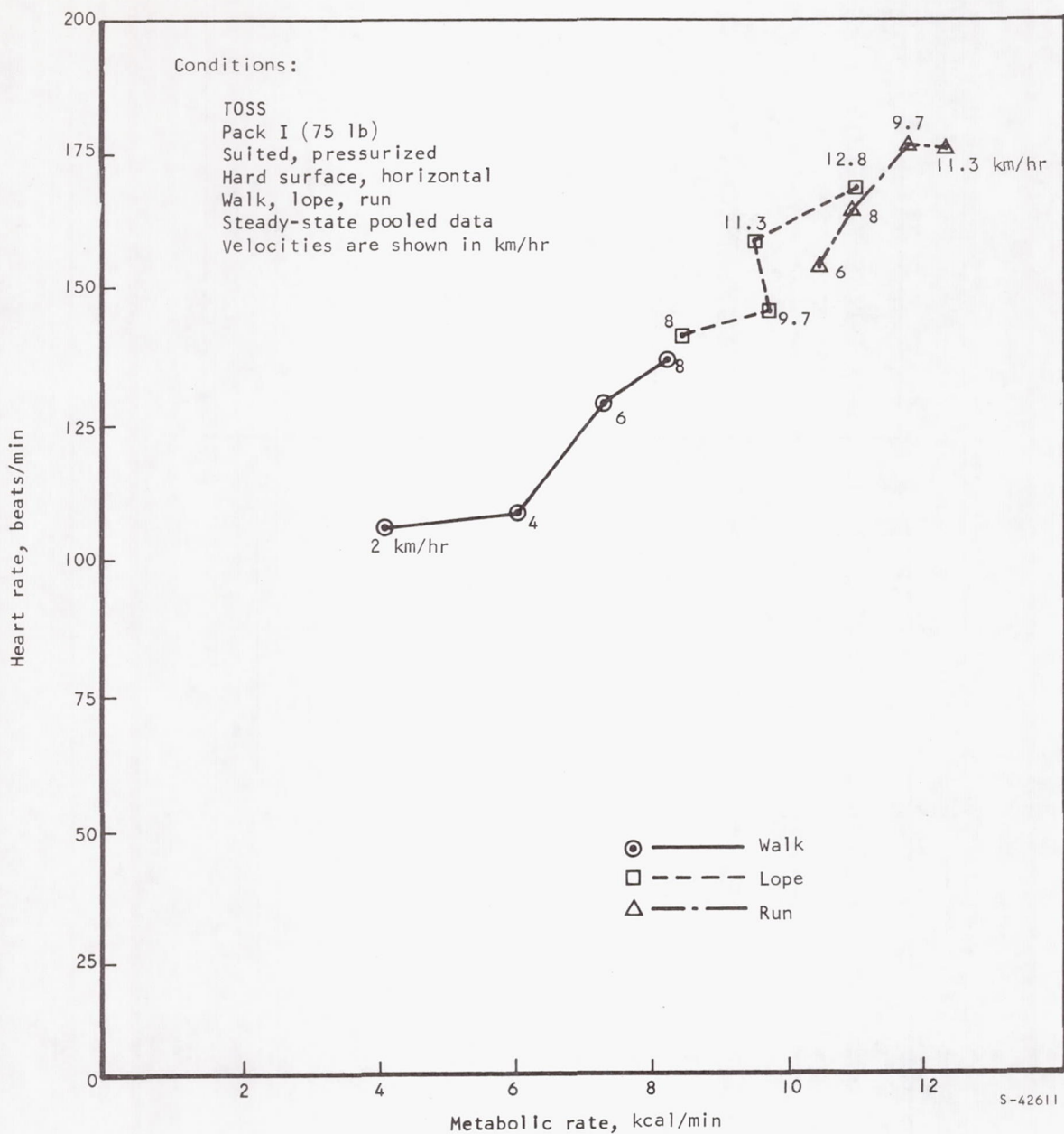


Figure 5-45. Heart Rate vs Metabolic Rate on the T0SS Simulator with Pack I

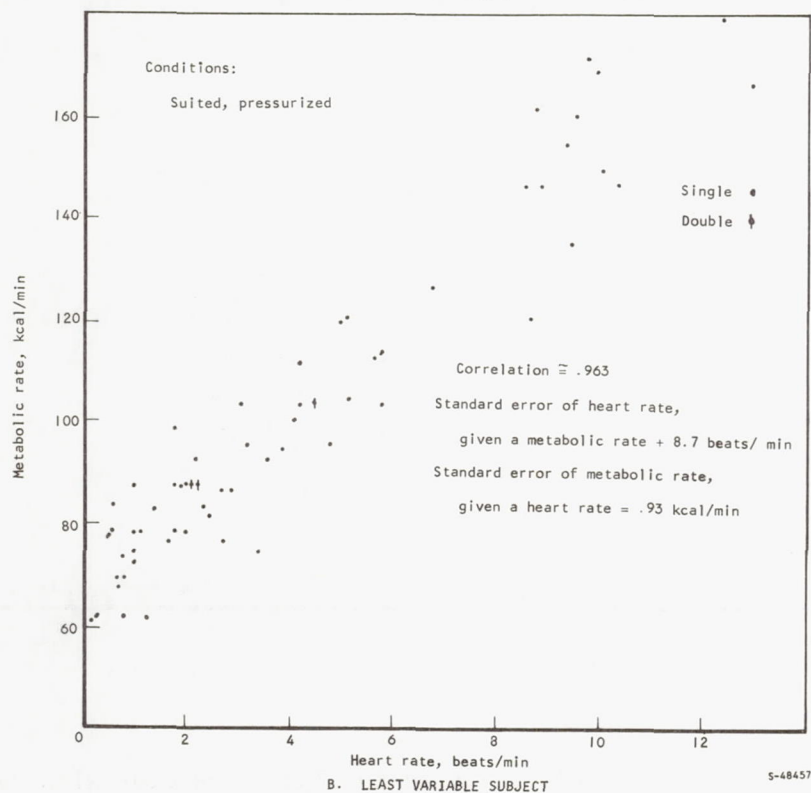
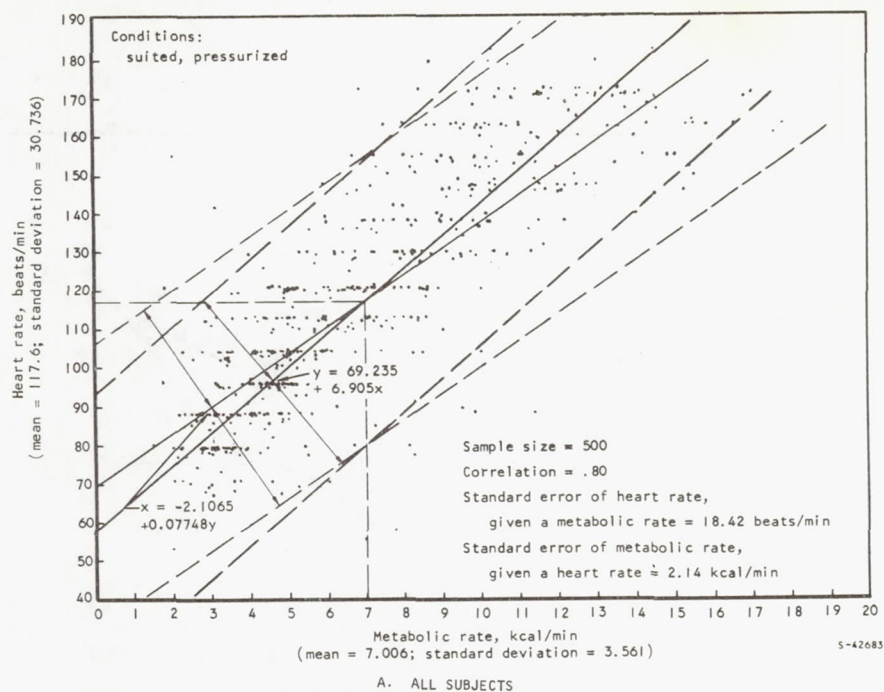


Figure 5-46. Plot of Data Points Relating Heart Rate and Metabolic Rate

TABLE 5-17

SUBJECT VARIABILITY IN PREDICTABILITY OF HEART RATE FROM
METABOLIC RATE AND METABOLIC RATE FROM HEART RATE

Standard error of estimate for	Subject	
	DB	MG
Heart Rate	22.78	8.67
Metabolic Rate Kcal/min	2.31	0.94

always present, particularly in terms of carbon dioxide rebreathing and emotional stresses; the heart-rate technique of determining metabolic rate is therefore highly inaccurate. Errors of 30 to 50 percent are to be expected. Such errors may be acceptable under conditions where metabolic rates cannot be measured, but such errors can never be accepted if the use of the technique is based on either convenience or lack of technical capability to measure metabolic rates directly.

Heart rate vs expired minute volume. - Figure 5-47 shows a plot of 500 simultaneous data points of heart rate and expired minute ventilation. The regression line of y on x is $y = 73.74 + 1.21x$, and for x on y is $x = -24.51 + 0.52y$. The two variables are correlated by a rate of $R = 0.79$. This relatively high level of correlation can be explained through the equations developed earlier in the test.

The mean heart rate for this plot is 119.1 ± 30.7 beats/min, and the mean ventilatory rate is 37.3 ± 20.1 liters/min. Prediction of heart rate from a measured minute volume would give a value ± 18.7 beats/min; Ventilatory rate as evaluated from heart rate would be within ± 12.2 liters/min.

The similarity between Figures 5-46 and 5-47 is obvious and in fact they are almost identical. If heart rate were plotted against oxygen consumption or carbon dioxide production, plots superimposable upon Figures 5-46 and 5-47 would be obtained. These conclusions are based on equations presented in this report.

Interactions of Gait Characteristics and Metabolic Rates

The relationship of locomotive index η vs metabolic rates for Packs I, II, and III is shown in Figures 5-48 through 5-50. Since locomotive index η is an artificial parameter derived from kinematic data to delineate between gaits, comparison to metabolic rate is not meaningful. The vertical separation representing gait differences, however, indicates the great differences between gaits. The differences in metabolic rates with η tend to mimic differences in stride length, an indirect determinant of η . These differences can be discussed accurately only for stride length.

The curves for stride length vs metabolic rate are presented in Figures 5-51, 5-52, and 5-53. Since Hogberg (Reference 5) demonstrated the dependence of metabolic rate on stride length, it was anticipated that these curves would provide some insight on efficiency of locomotion by revealing those stride lengths at which the metabolic rates would be lowest. If such could be determined, the best gait for each velocity to perform a given locomotive task could be defined. The idea must also be tempered by the high probability (refer to Appendix C) that there is an optimum stride length for any stepping rate for any given velocity. Thus, the probability of ascertaining the most efficient stride length from these data is very low.

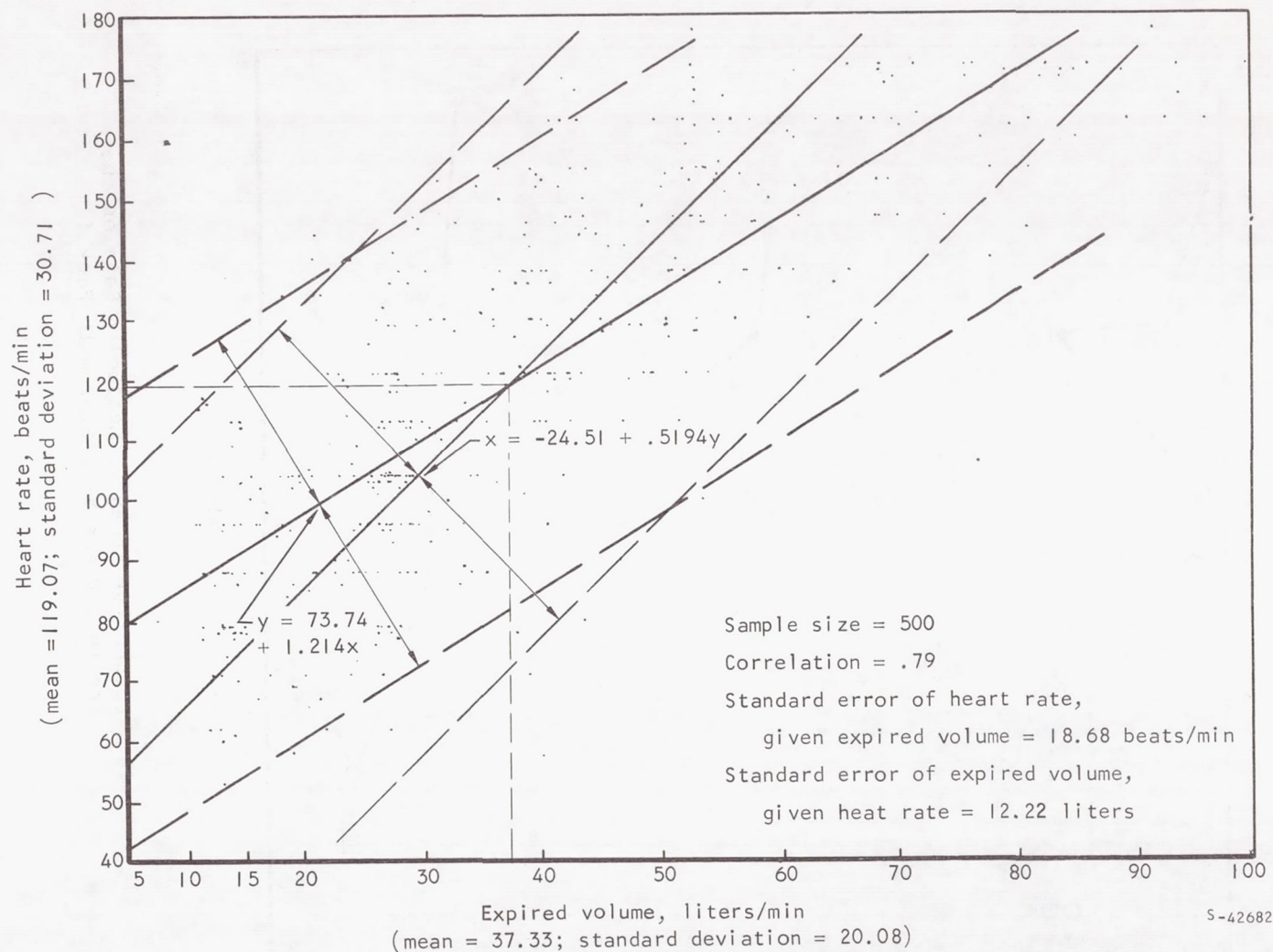
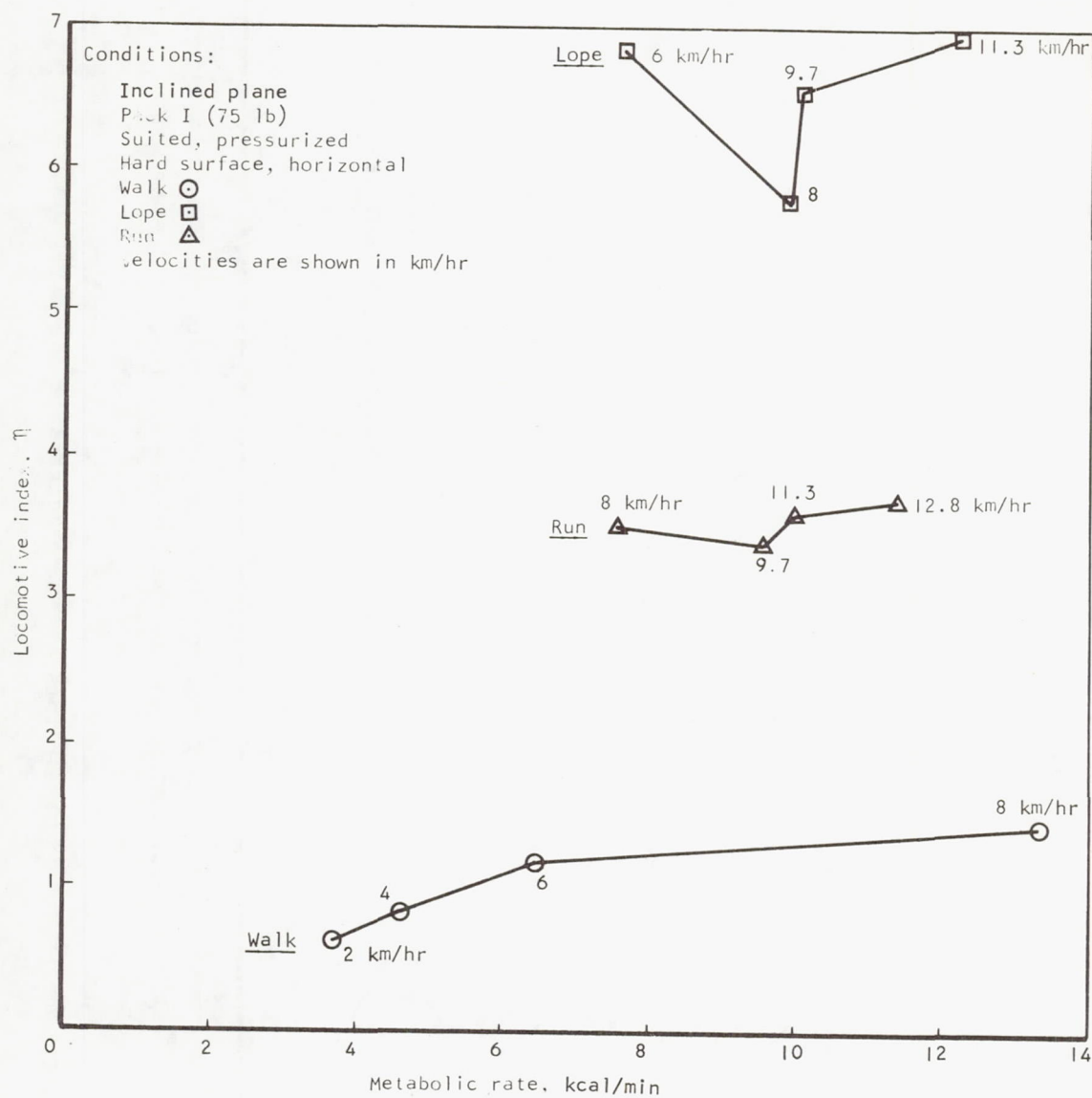


Figure 5-47. Plot of Data Points Relating Heart Rate and Expired Volume



S-42438

Figure 5-48. Locomotive Index vs Metabolic Rate on the Inclined-Plane Simulator with Pack I

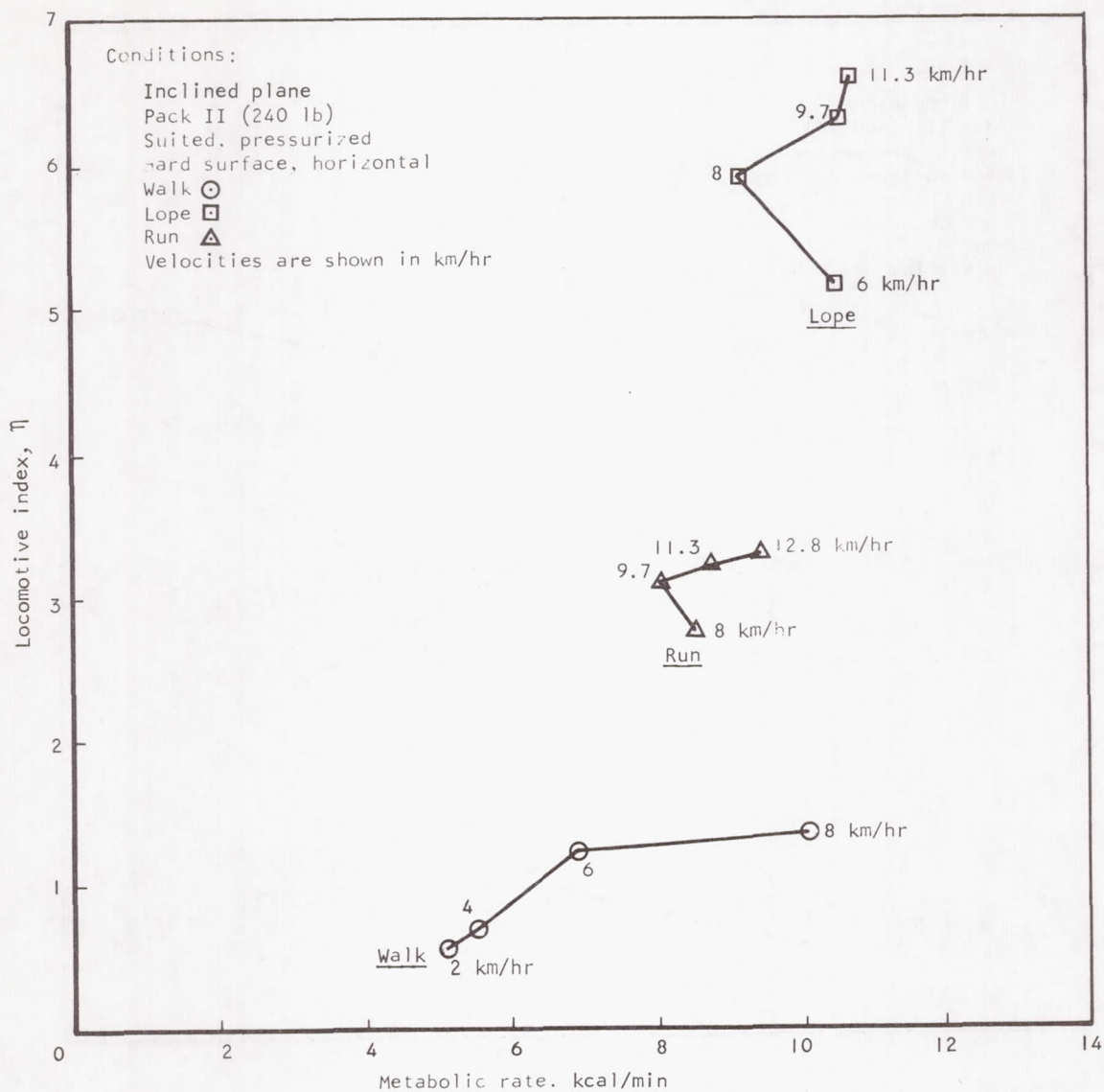


Figure 5-49. Locomotive Index vs Metabolic Rate, Inclined Plane, Pack II

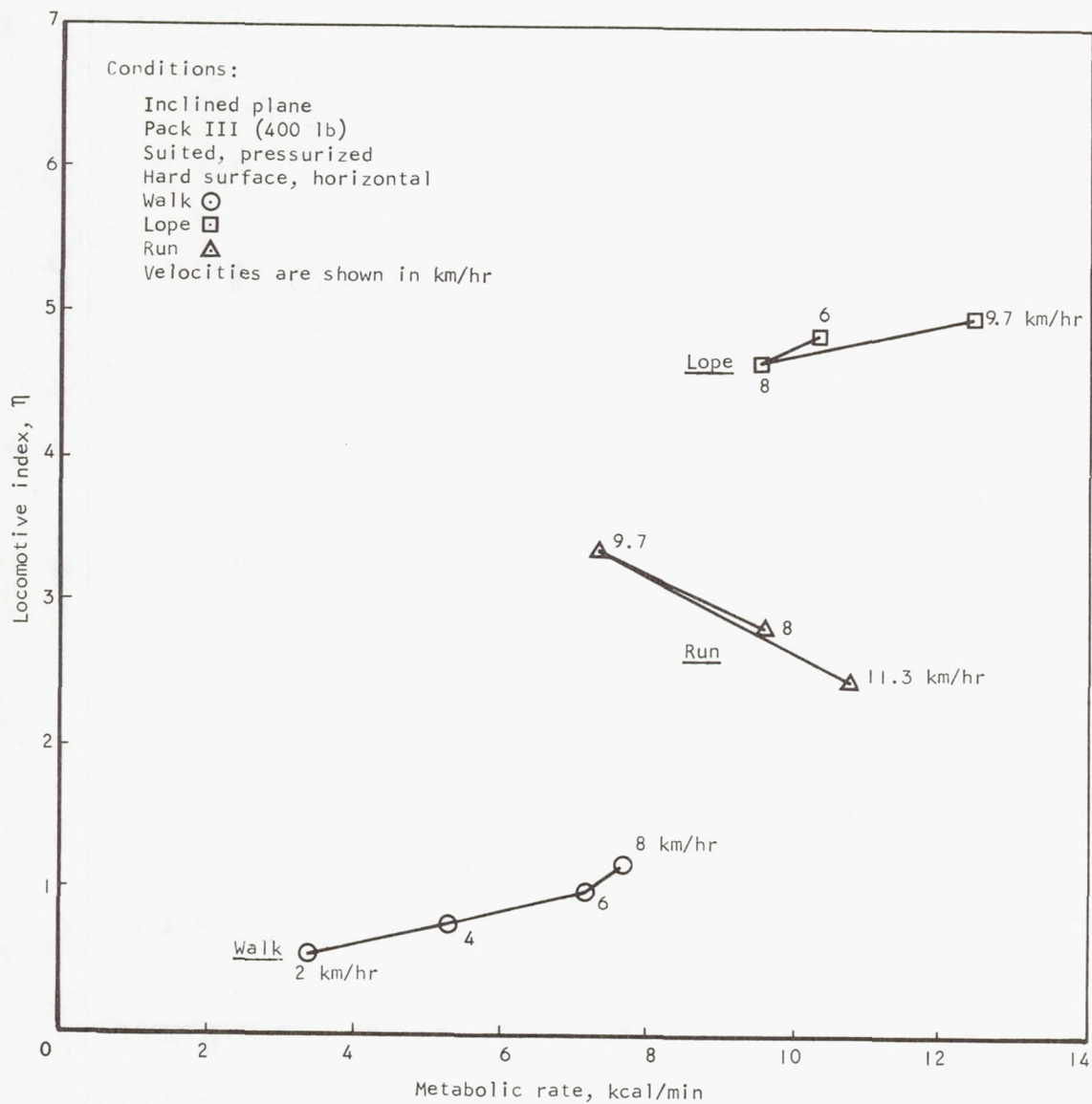
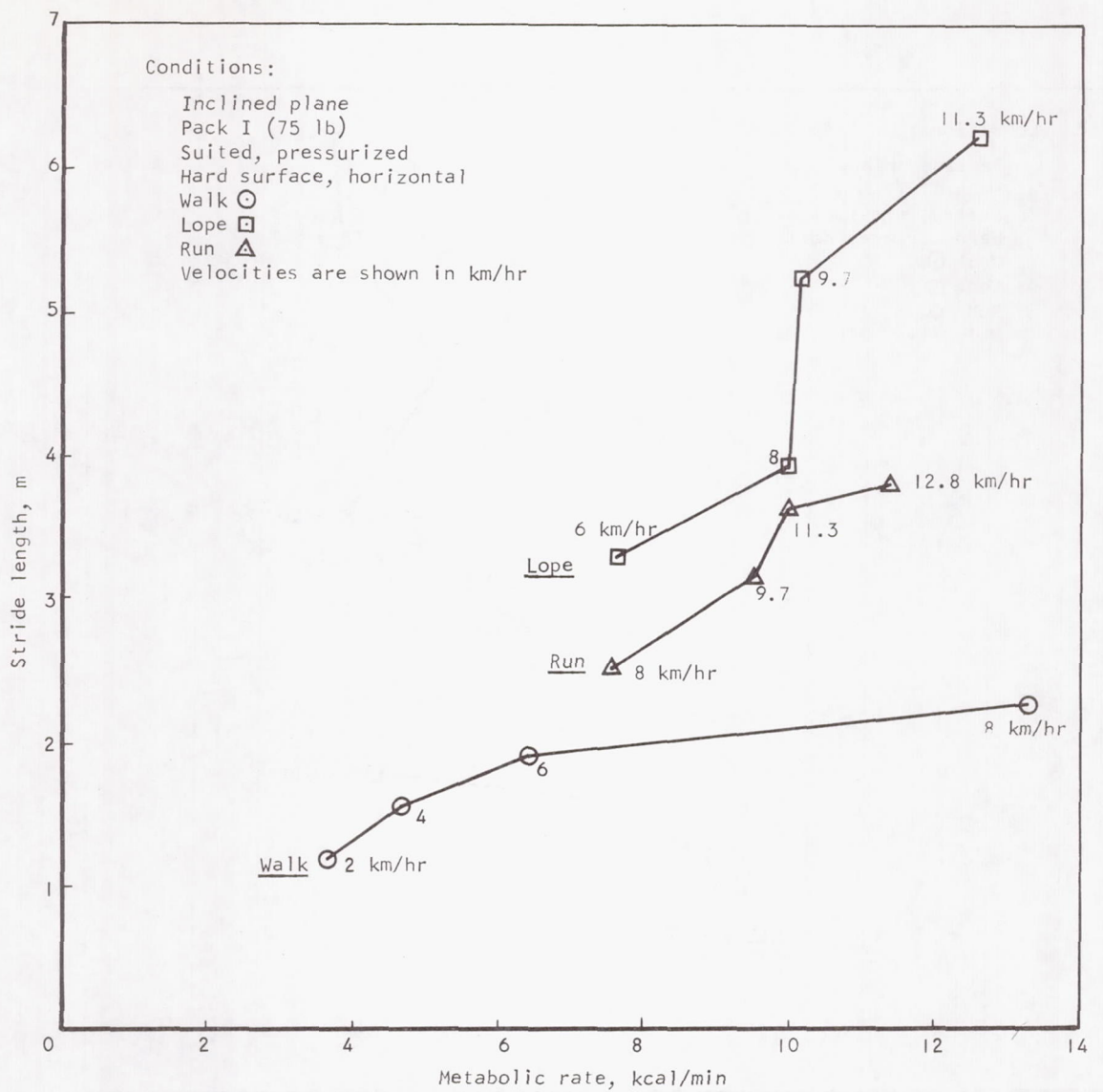


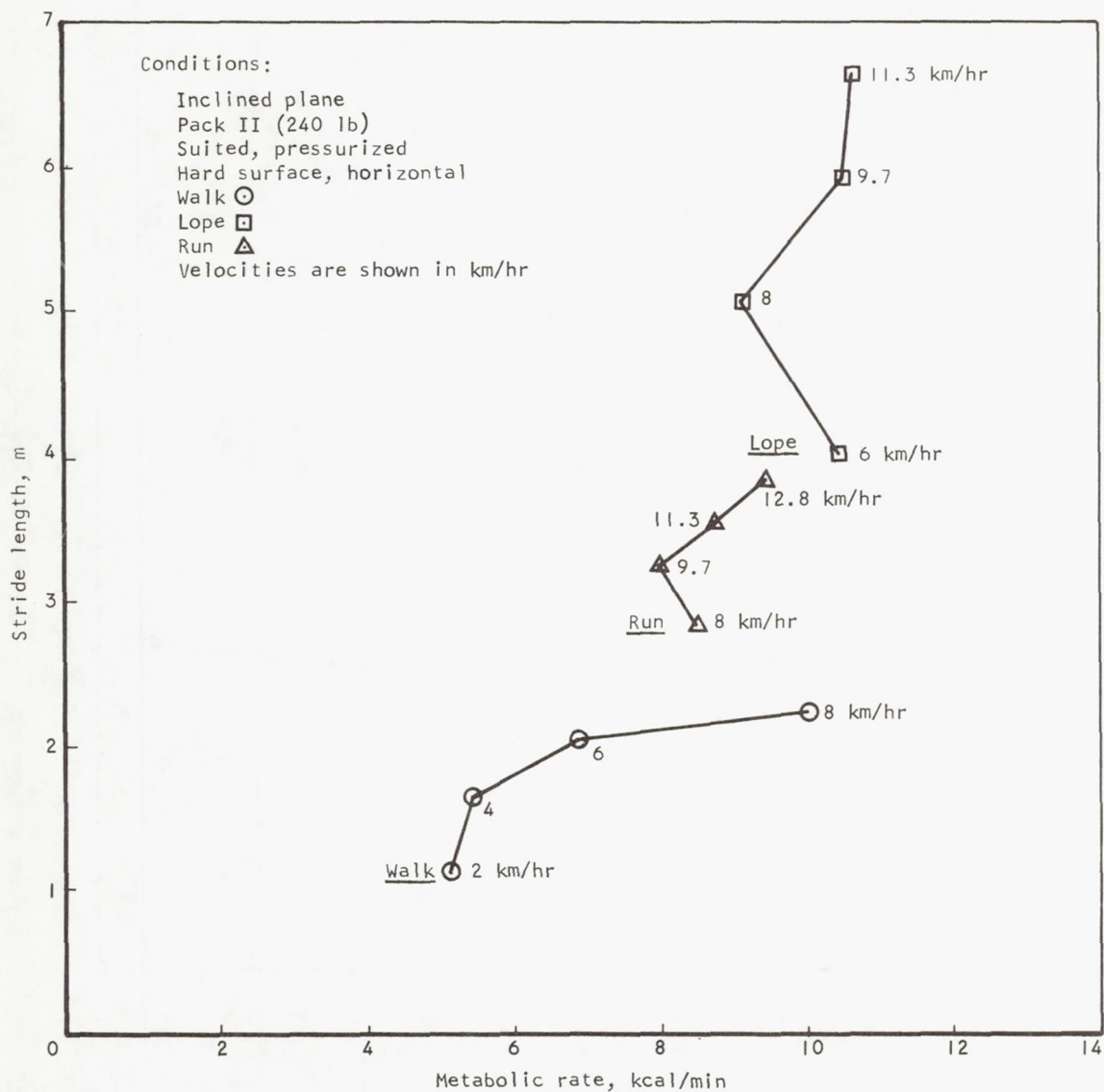
Figure 5-50. Locomotive Index vs Metabolic Rate, Inclined Plane, Pack III

S-42439



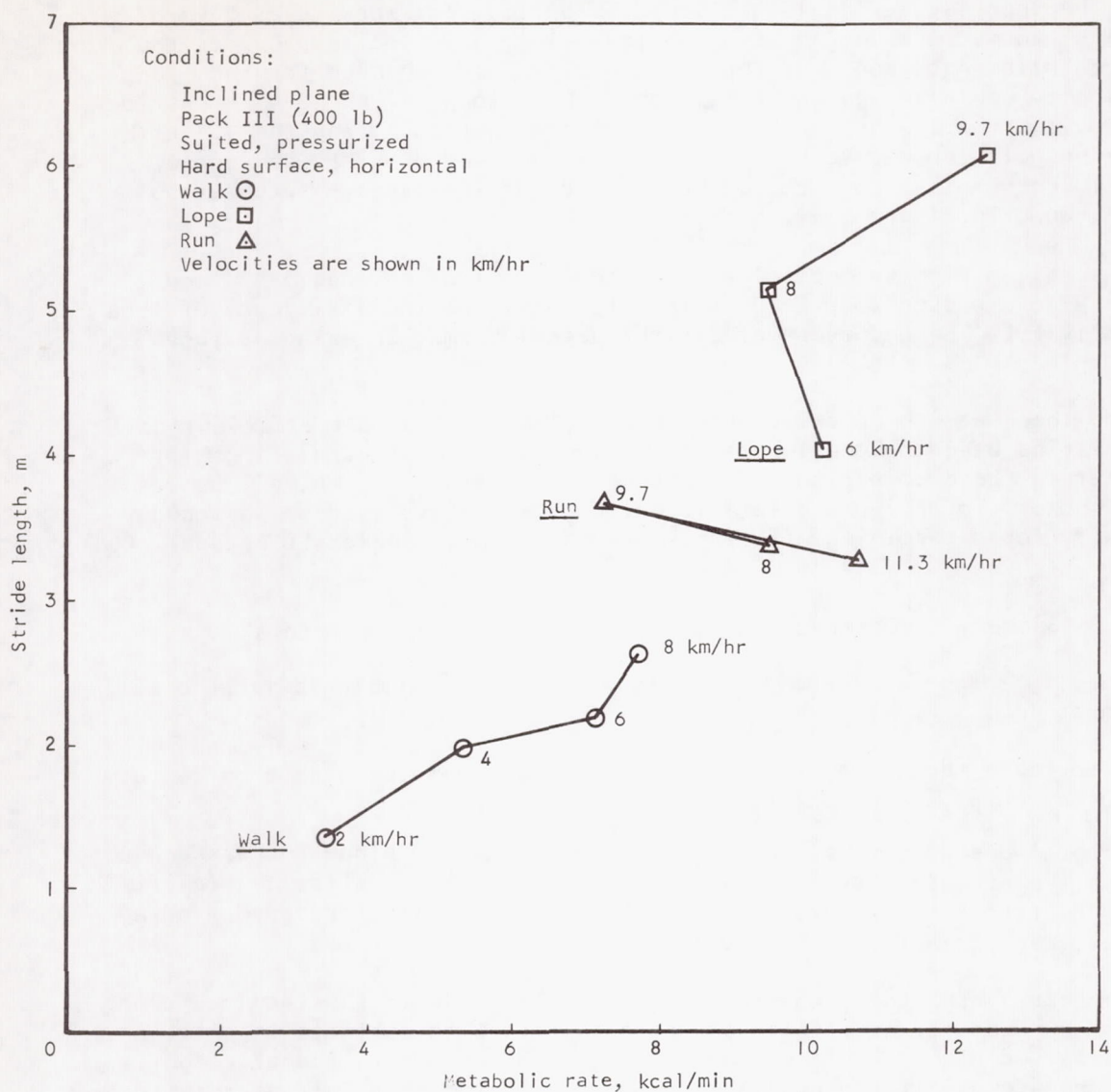
S-42443

Figure 5-51. Stride Length vs Metabolic Rate, Inclined Plane Simulator, Pack I



S-42445

Figure 5-52. Stride Length vs Metabolic Rate, Inclined Plane, Pack II



S-42444

Figure 5-53. Stride Length vs Metabolic Rate, Inclined Plane, Pack III

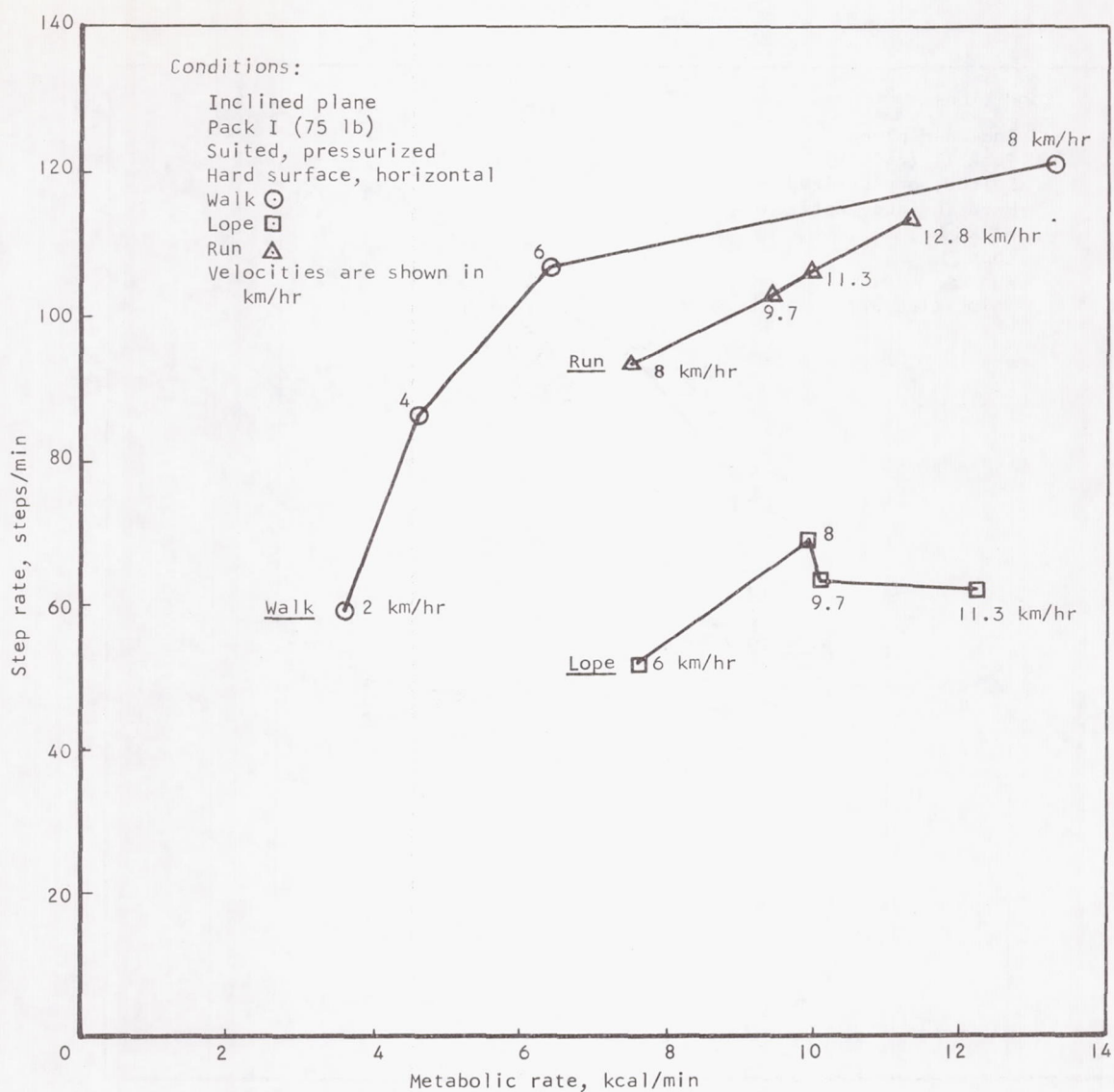
From an evaluation of these curves it would appear that, for Pack I, the shortest stride length used with each gait attempted would be the best. With Pack II, the shortest stride length would be optimum for working at 2 km/hr. For running, the stride length used for the 9.7-km/hr velocity provides the lowest metabolic cost, and with loping, the stride length used for the 9.7-km/hr velocity would be the most efficient. For Pack III, the 2-km/hr stride length provided the lowest metabolic rate within that gait, and the 9.7-km/hr lope and run gaits appear to be the most efficient based on stride length. These efficiency points conform to those noted for the steady-state metabolic rate data shown in Figures 5-9, 5-11, and 5-12.

The stepping rate vs metabolic rate shown in Figures 5-54, 5-55, and 5-56 were also expected to provide some information on the efficiency of locomotive activity. These curves reflect the same information as noted above for stride length vs metabolic rate.

Since there was no specific attempt to determine the most efficient gait characteristics based on the lowest metabolic cost, the interrelationships that appear in these comparisons are not valid; for this reason, all curves were not shown. To derive usable information, definitive studies designed specifically for determining efficiency are essential. (Refer to Appendix C.)

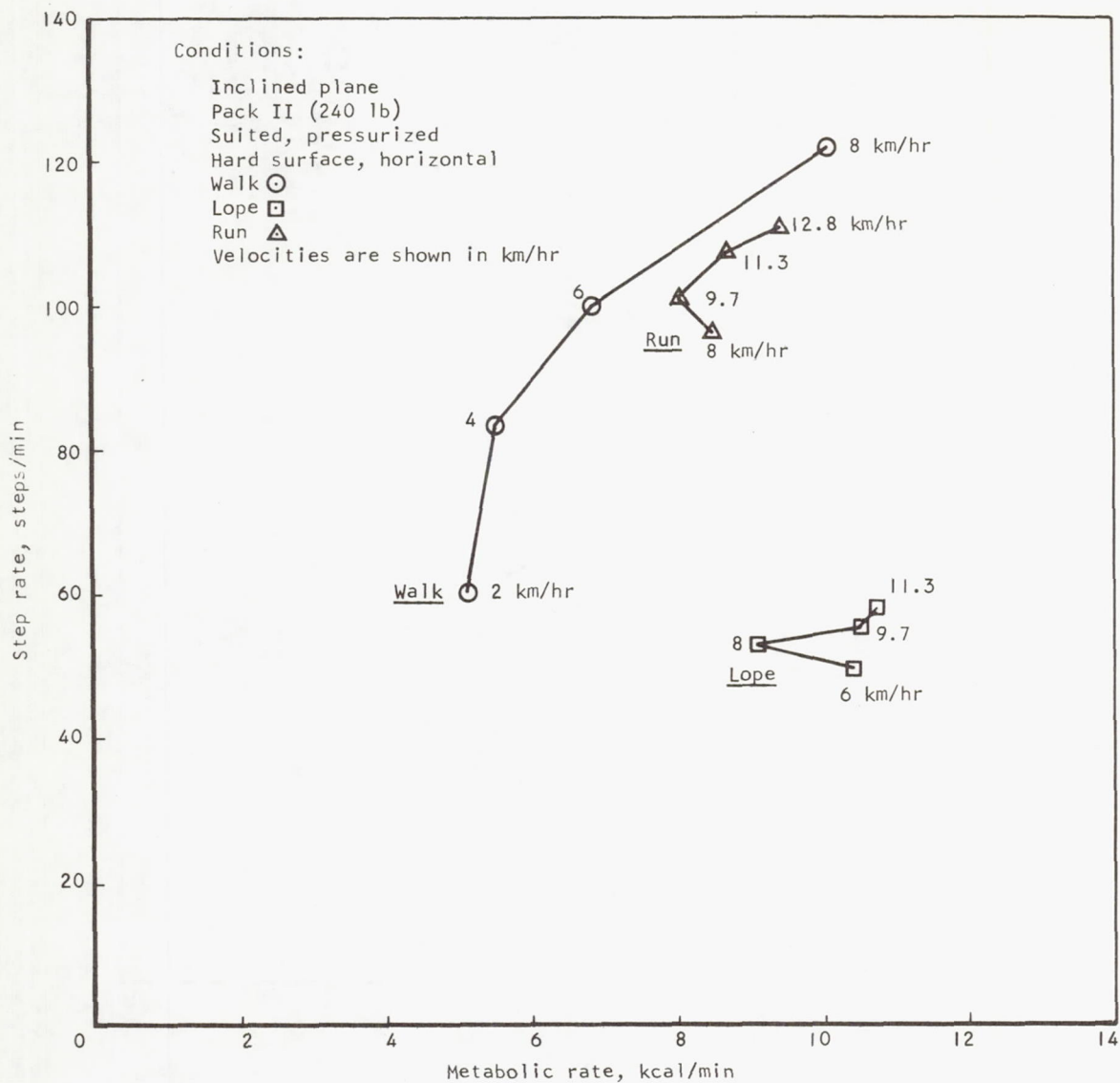
Summary of Observations on the Physiological Parameters

1. Metabolic rates for locomotive tasks are lower at simulated lunar gravity than at 1 g.
2. The forms of the curves for changes in metabolic rates with time conform to accepted physiological principles.
3. The total energy cost of locomotion on the inclined plane increased as velocity increased for all gaits. There were no statistically significant differences in energy expenditures between gaits for performing a given velocity where such data could be compared.
4. As expected, the total cost of locomotion in mufti in the inclined plane is lower than for tests with pressure suits. With subjects in shirt sleeves, loping had a higher energy cost than the other locomotive gaits. The absence of differences for loping in a suit must result as an effect of the suit constraints masking this effect.
5. Total metabolic costs for load-carrying on the inclined plane increased as a function of velocity. However, there were no differences within gaits for the three loads carried. Thus, more work was being performed with the same energy, indicating an increase in efficiency as a result of increased weight. This increased efficiency may result from the increased traction gained by the added weight as the load is increased.
6. Total energy costs were higher for ascending slopes than for horizontal locomotion. Energy costs for ascending slopes and for horizontal locomotion were higher than for descending. An increased load further increases the cost of locomotion on slopes.



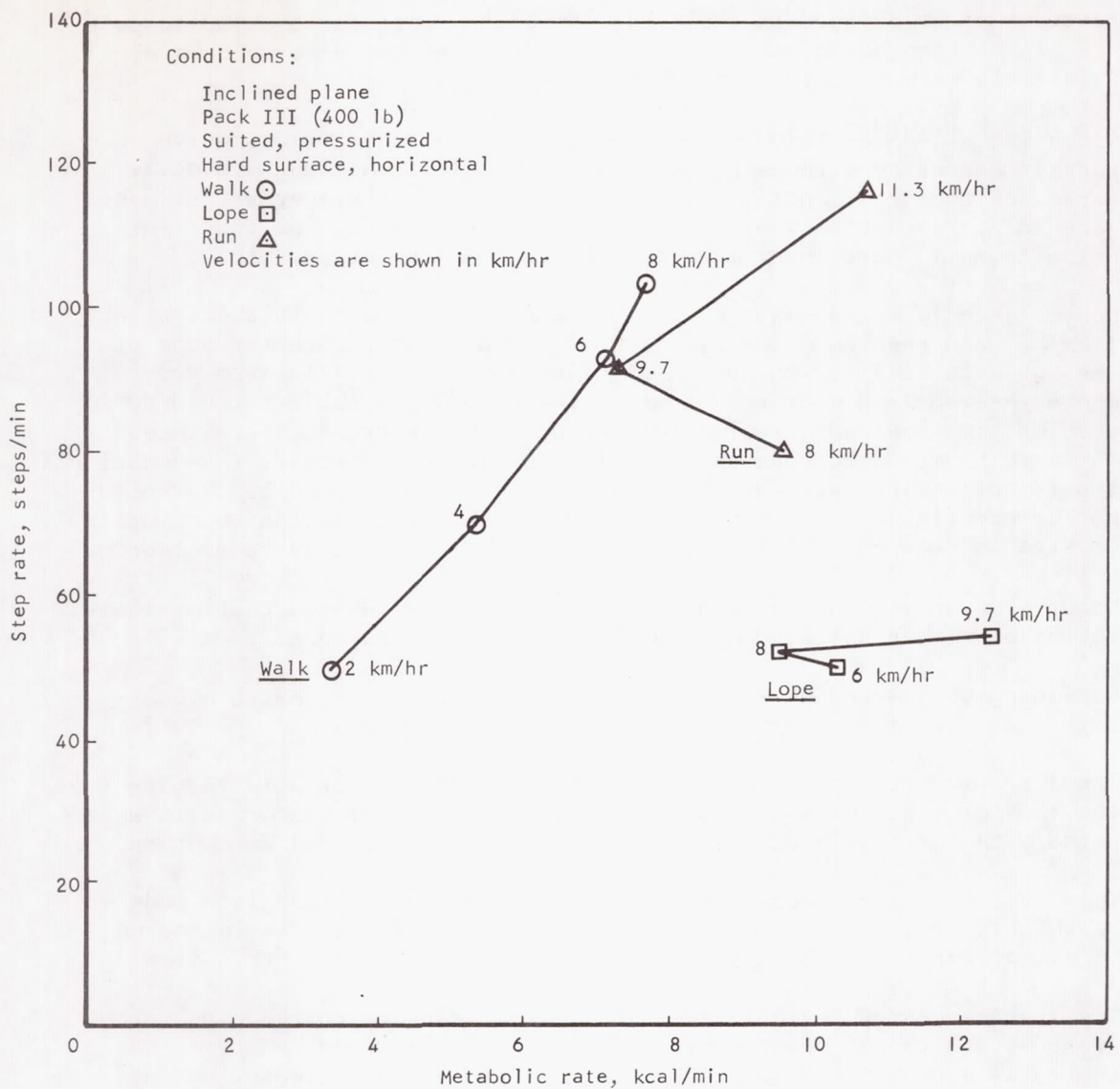
S-42442

Figure 5-54. Step Rate vs Metabolic Rate on Inclined Plane Simulator with Pack I



S-42441

Figure 5-55. Step Rate vs Metabolic Rate, Inclined Plane, Pack II



S-42440

Figure 5-56. Step Rate vs Metabolic Rate, Inclined Plane, Pack III

7. Testing on the TOSS simulator showed an increase in total energy as a function of velocity. In addition, the energy cost for the loping gait was higher than for either walking or running at the same velocities. This is in direct contrast to the inclined-plane results.
8. Ascending slopes on TOSS increased total energy requirements, which were further increased with each increase in velocity. Although velocity increased the total energy for descending slopes, the energy cost was lowered by descending slopes within a given velocity. The costs for going downhill were lower than for horizontal locomotion.
9. Subjects could not negotiate the 30-deg uphill slope on TOSS except at 1 km/hr, and then only 4 subjects could accomplish the test. None of the subjects could climb the 15-deg slope at 8 km/hr. In each case where the required mode could not be performed, the subject could not develop the required traction to keep up with the treadmill. Since these tests mandated constant-velocity locomotion, however, these data should not be interpreted as indicating that slopes up to 30 deg could not be negotiated. The conclusion that can be drawn is that locomotion on steep slopes has extremely high energy cost and should be avoided.
10. Locomotion on a simulated lunar soil increases the energy cost of locomotion over that observed with a normal treadmill surface.
11. Ascending or descending slopes on the smooth lunar soil had a higher cost than the same modes performed on the hard surface.
12. The increased cost of locomotion on the simulated lunar soil results from the loss of traction due to shearing of the soil. Similar results were noted with the simulated coarse lunar soil for horizontal locomotion.
13. The ratios of oxygen repayment to total oxygen cost for a given mode were reasonably constant even though the total metabolic cost is increased three to four times. This phenomenon is not understood at this time.
14. The average energy per unit time in kcal/min closely corresponds to the steady-state values measured for each task. This would indicate that the total energy for a task can be simply evaluated by measuring the steady-state value and multiplying by the total time the exercise is performed. It must be noted that this consideration would hold only for a task repeated long enough for a steady-state condition to be reached.
15. Steady-state metabolic costs are significantly increased by velocity. Comparisons of requirements between gaits to perform the same velocity in the inclined plane indicate that based on metabolic rate alone, there would be little choice between gaits with a 75-lb (1 g) pack.
16. Loping in mufti revealed a much higher steady-state cost than other gaits at the same velocity. This is undoubtedly due to the added cost to perform antigravity work.

17. There were no statistically significant differences between carrying the 75-lb or 240-lb pack on the inclined-plane simulator. Lower rates were noted with the 400-lb pack. These findings support the thesis of better efficiency of work due to increased traction as a function of increased weight.
18. All subjects could perform at velocities ranging from 8 to 12.8 km/hr on the hard surface with the inclined-plane simulator for periods of 1 hr either suited or in mufti (at 1/6 g).
19. Fatigue tests of 4-hr duration were attempted while suited and pressurized, and only one subject was able to complete a 4-hr test. This test was run at 9.7 km/hr on a horizontal hard surface. The extreme fatigue of the subject indicated that such modes should be avoided.
20. Steady-state metabolic costs were higher for ascending slopes than for horizontal locomotion. Costs were further decreased with downhill locomotion. Downhill locomotion decreased the metabolic cost below that required for horizontal locomotion.
21. The steady-state data with the TOSS simulator showed higher energy cost for loping than for other gaits at the same velocity.
22. Differences in data for walking and running on a horizontal hard surface were not statistically significant for the inclined-plane or the TOSS simulators. Loping produced a higher energy cost with TOSS than with the inclined-plane simulator.
23. Locomotion on the uphill slopes showed TOSS differing from the inclined plane. Downhill slopes did not produce any differences between simulators.
24. The general absence of differences between simulators in this study may have resulted from the use of the highly immobile pressure suit used in these tests. Tests must be performed in more mobile suits or in mufti to properly evaluate any differences between simulators.
25. Testing with pressurized suits at 1 g will tend to differentiate between the suits, based on mobility, as long as the total system weight is similar.
26. The mobile A5L suit was shown in other studies to increase the cost of locomotion by 150 percent over the shirt-sleeve condition. In this study, the more rigid Gemini suit increased the metabolic rate by 250 percent.
27. Heart rates are positively correlated with metabolic rates, $r = 0.80$. Using the regression technique of evaluating metabolic rates from heart rates, the accuracy that could be obtained from 500 observations was ± 2.14 kcal/min for any measured heart rate. The utility of this technique is limited, and estimation of metabolic rates from heart rates has basic inherent errors.

28. Heart rate and minute ventilatory volume are positively correlated with $r = 0.79$.
29. Respiratory rates were of little use in these studies other than to monitor the emotional state of the subject during rest periods for checking for hyperventilation.

KINEMATICS

Several comprehensive reviews of the pertinent literature on gait analysis have been made (References 5-26 through 5-37) which describe the characteristics of gait with locomotion. The kinematics of locomotion at lunar-gravity conditions have been studied primarily by Hewes, et al. (Reference 5-29) and Kuehnegger (Reference 5-11).

The fundamental considerations of Hewes, Spady, and Harris (Reference 5-29) are used in the following analysis to characterize locomotion/gait. The principal locomotion gaits employed by man are walking and running. The generally accepted distinction between them is that in walking, there is double support (i.e., both feet are on the ground sometime during any given stride), and in running, double support is absent and both feet are simultaneously off the ground sometime during any given stride. Locomotion without double support can be further divided into loping and sprinting. The lope, typical of the lower running speeds, is characterized by a long, leaping stride, normally achieved with a relatively low stepping rate. The sprint, which utilizes a short stride with a fast stepping rate, achieves higher running speeds. These authors (Reference 5-29) provide a convenient method, termed locomotive index and defined as the ratio of leg swing to leg stroke, to differentiate between walking and running. When the calculated locomotive index is less than 1, the subject is walking; when the index is greater than 1, the subject is running. No distinction had previously been made in the locomotive index between running and loping. Prior differentiations of these two gaits have been by subjective evaluation.

To evaluate and compare the kinematic effects of the independent variables in this program, measurements were made of the maximum back angle, maximum hip angle, maximum knee angle, step rate, treadmill speed, and leg stroke for all tests. The step rate (number of steps taken by subject during one minute) was counted and recorded by an observer using a stopwatch to measure the elapsed time between the first and last step counted. A recording tachometer was used to determine the treadmill speed and, in addition, an observer corroborated the tachometer readings by measuring the time required for the treadmill surface to travel through 10 revolutions and by referring to a chart listing the speed for the respective elapsed time, based on calculations from treadmill belt length, the number of belt revolutions, and the time elapsed during these revolutions.

The measurements of body angle and leg stroke (meters traversed during portion of stride when a reference foot is in contact with the treadmill) were obtained from projected images of motion pictures taken during the tests. This data film was taken at 24 frames per second. A special manikin protractor device was developed to obtain the angle determinations (Figure 5-57). The movie film was stopped at the frame in which the subject's feet had reached the maximum distance apart for a particular stride, the right foot being forward. The manikin, equivalent to a 50th percentile man on a 1/8 scale, was then superimposed upon the image contour, and the maximum hip angle and maximum back angles were recorded. Figure 5-58 defines the three angles. For a few of the test modes, the maximum value of angles occurred at different periods in the stride cycle. When this was the case, different image contours were analyzed. For instance, in the slower walking modes the subjects sometimes had both feet on the treadmill for a prolonged period of time. This, coupled with the stiffness of the suit, created a forward pitch, i.e., back angle, that was greater at a different point in the stride cycle. The maximum knee angle was usually observed at that point in the stride cycle when the right leg had just begun its forward motion. This condition was found to exist in all work carried out in the Gemini suit, but varied for tests performed by subjects wearing overalls.

Leg stroke was determined by counting the number of picture frames during which the right foot was in contact with the treadmill and substituting this value into the equation:

$$D = D_1 V_1 / V_2$$

where D = foot contact in picture frames

D_1 = leg contact in picture frames

V_1 = treadmill speed, meters/sec

V_2 = camera speed, frames/sec

Stride (distance traversed during one stride cycle completed when body members regain initial relative positions) was computed from step rate and treadmill speed by the equation:

$$S = 2V_3 / N$$

where S = stride length, meters

N = step rate, steps/min

V_3 = treadmill speed in meters/min

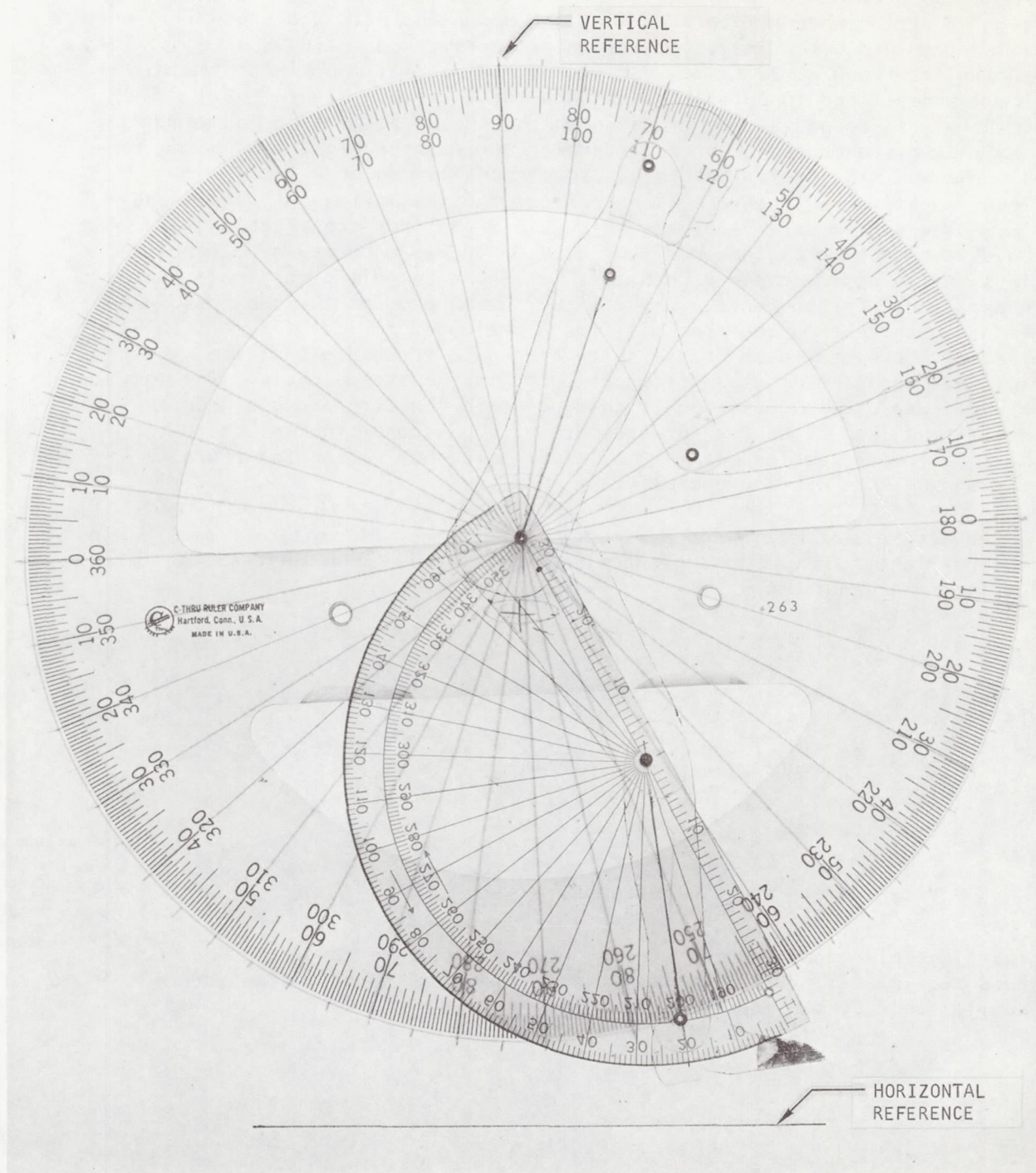


Figure 5-57. Manikin Protractor

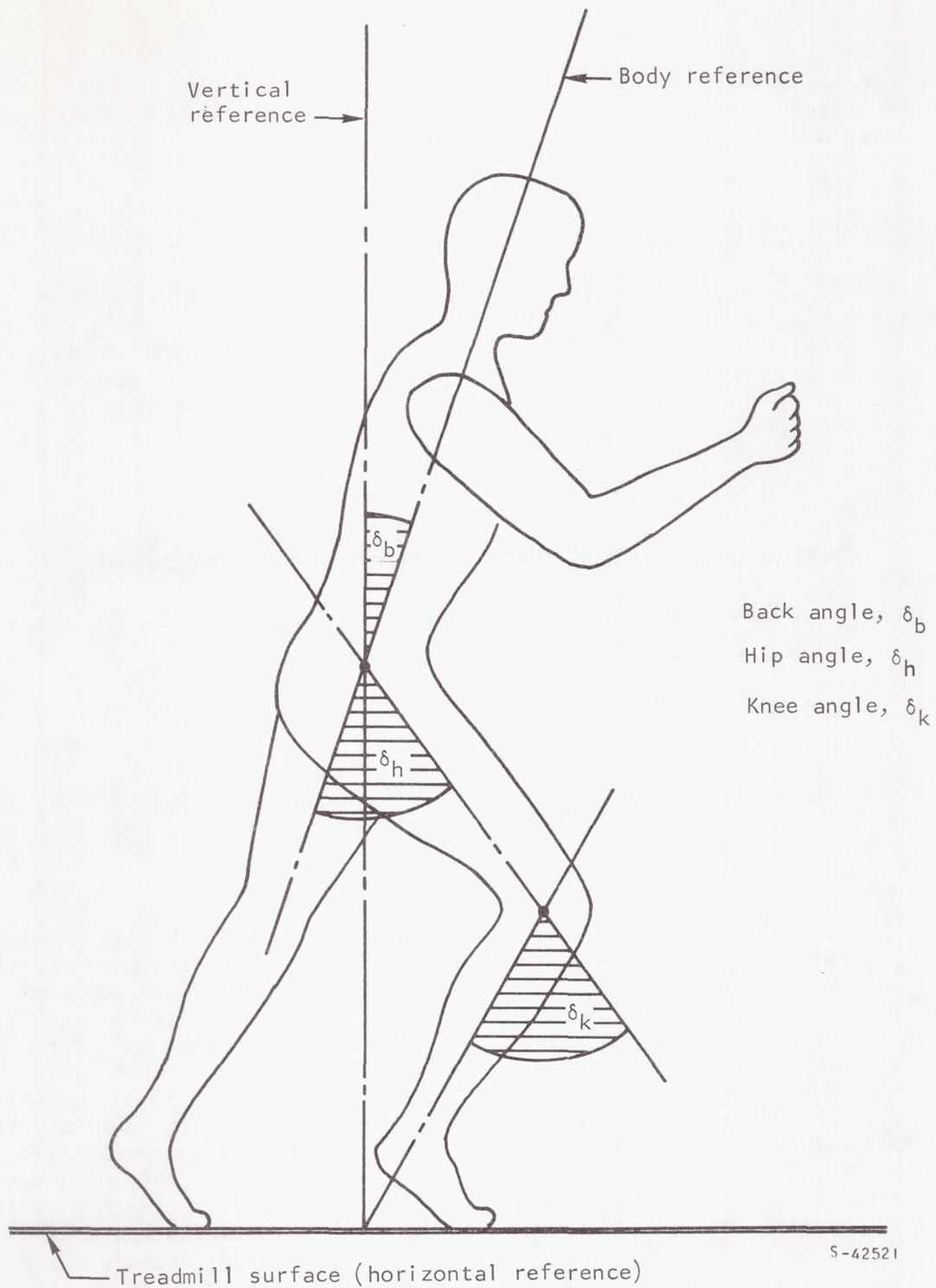


Figure 5-58. Definition of Body Angles

The ratio of leg swing (meters traversed during portion of stride when the reference foot is free of the treadmill) to leg stroke was determined by the equation:

$$\eta = (S-D)/D$$

where η = ratio of leg swing to leg stroke (locomotive index)

As a test of the measurement procedure, the body angle measurements (excluding maximum knee angle) for the walking, loping, and running velocities of the subjects carrying the 240-lb pack on the inclined-plane simulator were correlated with a second set of measurements taken from these same tests one week following the first determinations. The correlation coefficients are presented in Table 5-18.

TABLE 5-18
TYPICAL BODY ANGLE MEASUREMENT-REMEASUREMENT CORRELATIONS

Gait	Max. Hip Angle	Max. Back Angle
Walk	0.73	0.80
Lope	0.83	0.88
Run	0.79	0.79
Total	0.82	0.88

The maximum back angle measurement appears to have the highest reliability, followed by the maximum hip angle. Contingencies that create the less-than-perfect correlations include gait inconsistencies and measurement errors. The subjects were instructed to find their gait in the first few minutes of the test mode and maintain it throughout the remainder of the test period. Some subjects, however, were inconsistent in the more physiologically demanding modes. A number of problems were encountered in the measurement process. The first of these arises when the body angles of the subject within the suit differ from the actual pressure suit angles. When the suit is pressurized, it is larger than the man: the thighs are greater in diameter, the torso is greater in diameter, and the overall length is greater. Differences also exist between simulators because of the stretching and consequent lengthening of the pressure suit as the suit and man are lifted by the TOSS simulator. This stretching was sufficient to require some subjects to wear a pressure suit that was too short in the normal standing condition but which stretched to the proper length in the TOSS simulator.

The loosely fitting suit cover layers created size discrepancy between the manikin and the projected image, and this in turn was detrimental to accurate angle measurement. The cover layer is quite bulky in the knee area of some suits. A typical measurement of the maximum knee angle of one test without estimations for cover layer bulkiness resulted in a 53-deg angle reading. When allowances were estimated for the cover layer on the same projected image, the estimate became 58 deg.

Other conditions that confounded the measurement problem included camera projection angle and suit fit. When the subject was exercising directly in line with the camera lens opening, more accurate measurements could be made than when the subject was in the periphery of the projection field. This problem was of little significance for the inclined-plane tests because the camera was mounted on the tower quite a distance from the subject. Due to area limitations, the camera was much closer to the subject for the TOSS tests. In addition, the measurement of the body angles using the side profile was made more difficult on the TOSS simulator due to the additional degrees-of-freedom provided the subject and the resultant roll and yaw motions during exercise. The projection angle also created some problems in determination of the locomotive index. In all of the TOSS and 30-deg descending inclined-plane tests, some difficulty was encountered in determining exactly when the subject's foot actually touched and when it actually left the treadmill surface.

Although it was the intent to have each subject wear a particular pressure suit from the beginning of the program until its conclusion, there was some interchanging of suits primarily because of suit failure. In addition, each suit went through numerous alterations throughout the program. Arms were lengthened and shortened, and shoulders were raised and lowered. These changes in suit fit may have affected the reliability of the measurements.

Discussion of Kinematic Data

The kinematic results of this program are summarized in the following pages. The data are presented in tabular and graphical forms, together with a discussion of each parameter. Means and standard deviations were determined for each test condition by machine computation. The graphs are plots of means for the dependent variables against treadmill speed, pack weight, or slope. The level tests completed on the hard surface for the inclined-plane and TOSS simulators included four velocities for which the subject was instructed to walk, four for running, and four for loping. The velocities range from 2 to 12.8 km/hr. The curves presented for these tests are separated by gait. The gaits were differentiated by the subject in the test situation through kinesthetic and proprioceptive feedback, in conjunction with confirmation from the test conductor. Sensations perceived by the subject during a gait confirmed as a walk by the test conductor were different than those for a run or a lope. Criteria used by the test subject for differentiating these gaits are as follows:

Walk. - The walk is characterized by a heel-toe action during which both feet are on the treadmill at the same time during some part of the stride cycle.

Run. - The run is differentiated from the walk by both of the subject's feet being off the surface at some point in the stride cycle.

Lope. - The lope was primarily differentiated from the run by an attempt to achieve maximum practical stride lengths which increased the vertical displacement of the subject over that of the walk or run.

Judgments rather than measurements were used by the test conductor in specifying whether a subject was walking, running, or loping. A principal problem in evaluating gait is the large range of individual differences between subjects. For example, gaits were not as consistent for loping with the 240-lb pack as with the 75-lb pack. In addition, stride length decreased for loping with the heavier pack. Also, when tests were run on the TOSS system, judgments as to an allowable walk were changed because the additional degrees-of-freedom that was allowed the subject resulted in a different walking gait.

Upon conclusion of the horizontal tests on the inclined-plane and TOSS simulators, a change in the experimental design was incorporated to eliminate forced gaits during locomotion. For the remainder of the tests, the subjects were allowed to choose that gait which was of least difficulty for them to maintain throughout each particular test mode. For these tests, treadmill velocities ranged from 2 to 8 km/hr at intervals of 2 km/hr. Since gait was no longer controlled, complete comparisons of the kinematic dependent variables could not be meaningfully accomplished by variance. Consequently, the use of tests of significance were limited.

Locomotive Index, Step Rate, and Stride Length

The means and standard deviations for locomotive index, step rate, and stride length measured in this program are tabulated in Tables 5-19, 5-20, and 5-21. These three variables are presented together in subsequent figures because the effects that change one parameter must result in changes in the others.

Locomotive index, step rate, and stride length with the horizontal inclined-plane simulator. - Figure 5-59 shows the data for a pressure-suited subject carrying a 75-lb load on the horizontal inclined-plane treadmill. It can be seen in this figure that stride length, step rate, and locomotive index all increase as velocity increases. It is also apparent that step rate and locomotive index distinctly differ between gaits, while the velocity effects on stride length for running is a continuation of that for walking. Locomotive index significantly increases with velocity for walking ($p < 0.01$). The effect of velocity on locomotive index for the running or loping mode, however, is not statistically significant. Locomotive index is also significantly different for each of the gaits ($p < 0.01$).

Step rate is significantly affected by velocity in the walking ($p < 0.01$) and loping modes ($p < 0.05$). Step rate was not significantly altered by velocity changes between 8 and 12.8 km/hr during the running gait. On the other hand, step rate is significantly different for each of the three gaits.

TABLE 5-19

LOCOMOTION INDEX (η) FOR ALL SIMULATOR EXERCISE MODES

Experimental conditions							Results (mean and \pm standard deviation)							
Simulator and suit mode	Slope, deg	Surface condition	Pack	Number of velocities	Number of subjects	Total tests	Gait or ascend/descend	Velocity, km/hr						
								2	4	6	8	9.7	11.3	12.8
Inclined plane, pressurized (press.) suit	0 (horiz)	Hard	I, 75 lb	4 each; walk, lope and run	6, with 2 repeating once	96	Walk	0.625 \pm 0.098	0.831 \pm 0.131	1.167 \pm 0.343	1.451 \pm 0.283			
							Lope			6.827 \pm 0.750	5.747 \pm 1.053	6.543 \pm 1.125	6.898 \pm 1.287	
							Run				3.489 \pm 0.587	3.388 \pm 0.712	3.617 \pm 0.667	3.676 \pm 0.770
Inclined plane, pressurized suit	0	Hard	I	1 each; walk, lope, and run	6, with all repeating twice	36	Walk	0.617 \pm 0.148						
							Lope			7.152 \pm 0.768				
							Run				3.400 \pm 0.654			
Inclined plane, subject in mufti (without press. suit)	0	Hard	I	4 each; walk, lope, and run	2	24	Walk	0.866 \pm 0.311	0.860 \pm 0.010	1.142 \pm 0.167	0.976 \pm 0.037			
							Lope			5.764 \pm 0.112	6.676 \pm 0.112	7.922 \pm 0.290	9.050 \pm 0.036	
							Run				2.324 \pm 0.478	3.061 \pm 0.069	2.648 \pm 0.018	2.968 \pm 0.058
Incl plane, mufti	0	Hard	I	Fatigue test	6	24								
Inclined plane, pressurized suit	0	Hard	I	Fatigue test	2	8								
Inclined plane, pressurized suit	0	Hard	II, 240 lb	4 each; walk, lope, and run	6	72	Walk	0.559 \pm 0.060	0.692 \pm 0.155	1.239 \pm 0.250	1.351 \pm 0.441			
							Lope			5.167 \pm 0.33	5.918 \pm 0.490	6.305 \pm 0.521	6.627 \pm 0.722	
							Run				2.745 \pm 0.581	3.114 \pm 0.413	3.128 \pm 0.534	3.312 \pm 0.204
Inclined plane, pressurized suit	0	Hard	III, 400 lb	4 each; walk, lope, and run	2	24	Walk	0.538 \pm 0.060	0.763 \pm 0.080	1.008 \pm 0.076	1.247 \pm 0.009			
							Lope			4.863 \pm 0.933	4.673 \pm 0.146	4.983 \pm 0.280		
							Run				2.840 \pm 0.536	3.376 \pm 0.888	2.509 \pm 0.00	2.548 \pm 0.00
TOSS (6-deg-of-freedom), pressurized suit	0	Hard	I	4 each; walk, lope, and run	6	72	Walk	1.06 \pm 0.00	No film	1.09 \pm 0.00	1.54 \pm 0.09			
							Lope			5.56 \pm 0.41	5.62 \pm 0.34	6.38 \pm 0.96	7.67 \pm 0.22	
							Run				1.86 \pm 0.26	1.98 \pm 0.37	2.11 \pm 0.27	2.61 \pm 0.3
TOSS, press. suit	0	Smooth lunar	I	4	6	24		0.77 \pm 0.15	0.97 \pm 0.13	1.14 \pm 0.07	1.32 \pm 0.22			
TOSS, press. suit	0	Coarse lunar	I	4	6	24		0.88 \pm 0.11	1.54 \pm 0.54	2.53 \pm 0.92	1.61 \pm 0.55			
TOSS, pressurized suit	7.5	Hard	I	4	6	48	Ascend	0.99 \pm 0.6	1.10 \pm 0.16	2.34 \pm 0.84	2.44 \pm 1.13			
							Descend	0.87 \pm 0.43	1.61 \pm 0.48	2.25 \pm 0.59	3.11 \pm 1.01			
TOSS, pressurized suit	7.5	Smooth lunar	I	4	6	48	Ascend	0.69 \pm 0.11	1.02 \pm 0.13	1.52 \pm 0.4	2.45 \pm 0.46			
							Descend	0.81 \pm 0.1	1.76 \pm 0.48	2.15 \pm 0.55	2.81 \pm 1.17			
TOSS, pressurized suit	15	Hard	I	4	6	48	Ascend	0.91 \pm 0.32	1.17 \pm 0.08	1.72 \pm 0.33	1.58 \pm 0.09			
							Descend	1.42 \pm 0.69	2.71 \pm 0.98	3.97 \pm 1.44	4.82 \pm 1.89			
TOSS, pressurized suit	15	Smooth lunar	I	4	6	48	Ascend							
							Descend	0.93 \pm 0.24	1.98 \pm 0.32	2.88 \pm 0.75	3.85 \pm 0.71			
TOSS, pressurized suit	30	Hard	I	4	6	48	Ascend	2.89 \pm 0.78* N=1						
							Descend	1.18 \pm 0.13	3.17 \pm 0.70	5.2 \pm 2.5	4.29 \pm 1.02			
Inclined plane, pressurized suit	7.5	Hard	I	4	6	48	Ascend	0.56 \pm 0.07	1.16 \pm 0.7	3.16 \pm 0.86	3.64 \pm 0.82			
							Descend	0.59 \pm 0.12	1.32 \pm 0.94	3.35 \pm 0.86	3.67 \pm 0.77			
Inclined plane, pressurized suit	7.5	Hard	II	4	6	48	Ascend	0.64 \pm 0.1	1.35 \pm 0.57	2.42 \pm 0.43	2.7 \pm 0.34			
							Descend	0.59 \pm 0.09	0.85 \pm 0.06	2.91 \pm 0.56	3.01 \pm 0.78			
Inclined plane, pressurized suit	15	Hard	I	4	6	48	Ascend	0.74 \pm 0.15	1.54 \pm 0.85	2.82 \pm 0.69	3.04 \pm 0.47			
							Descend	0.67 \pm 0.17	0.96 \pm 0.17	2.99 \pm 1.02	4.13 \pm 0.97			
Inclined plane, pressurized suit	30	Hard	I	4	6	48	Ascend	25 \pm 0.35	3.08 \pm 0.42	3.36 \pm 0.34				
							Descend	0.69 \pm 0.12	1.57 \pm 0.83	4.56 \pm 1.02	5.12 \pm 1.01			

*At 1 km/hr, locomotive index η was 1.84 \pm 0.48, N = 2

TABLE 5-20

STEP RATE (STEPS/MIN) FOR ALL SIMULATOR EXERCISE MODES

Experimental conditions							Results (mean and ± 1 standard deviation)							
Simulator and suit mode	Slope, deg	Surface condition	Pack	Number of velocities	Number of subjects	Total tests	Gait or ascend/descend	Velocity, km/hr						
								2	4	6	8	9.7	11.3	12.8
Inclined plane, pressurized (press.) suit	0 (horiz)	Hard	I, 75 lb	4 each; walk, lope and run	6, with 2 repeating once	96	Walk	59.2 \pm 13.4	86.2 \pm 10.1	107.0 \pm 16.0	120.7 \pm 17.6			
							Lope			51.8 \pm 3.3	68.7 \pm 7.1	63.0 \pm 7.3	62.2 \pm 9.4	
							Run				93.2 \pm 9.8	102.8 \pm 9.6	105.7 \pm 13.4	114.3 \pm 12.5
Inclined plane, pressurized suit	0	Hard	I	1 each; walk, lope, and run	6, with all repeating twice	36	Walk	57.4 \pm 14.2						
							Lope			47.0 \pm 6.34				
							Run				93.3 \pm 12.4			
Inclined plane, subject in mufti (without press. suit)	0	Hard	I	4 each; walk, lope, and run	2	24	Walk	48.0 \pm 8.0	69.0 \pm 5.0	90.0 \pm 7.0	108.0 \pm 6.0			
							Lope			37.0 \pm 1.0	40.5 \pm 0.5	38.0 \pm 1.0	39.5 \pm 1.5	
							Run				92.5 \pm 8.5	88.5 \pm 1.5	98.5 \pm 0.5	103.5 \pm 1.5
Incl plane, mufti	0	Hard	I	Fatigue test	6	24								
Inclined plane, pressurized suit	0	Hard	I	Fatigue test	2	8								
Inclined plane, pressurized suit	0	Hard	II, 240 lb	4 each; walk, lope, and run	6	72	Walk	59.8 \pm 6.9	82.8 \pm 14.5	100.2 \pm 10.2	122.0 \pm 15.0			
							Lope			50.2 \pm 3.2	53.3 \pm 3.2	55.2 \pm 2.5	57.0 \pm 2.9	
							Run				95.8 \pm 11.0	100.8 \pm 10.3	107.7 \pm 8.4	111.3 \pm 5.3
Inclined plane, pressurized suit	0	Hard	III, 400 lb	4 each; walk, lope, and run	2	24	Walk	49.5 \pm 4.5	69.5 \pm 8.5	92.5 \pm 0.5	102.5 \pm 4.5			
							Lope			50.0 \pm 3.0	52.0 \pm 0.00	53.5 \pm 2.5		
							Run				80.0 \pm 7.0	90.5 \pm 12.5	117.0 \pm 0.00	135.0 \pm 0.00
TOSS (6-deg-of-freedom), pressurized suit	0	Hard	I	4 each; walk, lope, and run	6	72	Walk	80.17 \pm 8.03	113.33 \pm 13.91	137.17 \pm 13.23	152.83 \pm 13.47			
							Lope			49.67 \pm 9.91	61.33 \pm 10.2	61.17 \pm 10.02	59.0 \pm 10.24	
							Run				136.67 \pm 16.08	145.17 \pm 24.18	158.8 \pm 14.11	168.67 \pm 29.11
TOSS, press. suit	0	Smooth lunar	I	4 velocities	6	24		87.83 \pm 17.53	114.67 \pm 17.33	138.33 \pm 7.82	152.4 \pm 8.73			
TOSS, press. suit	0	Coarse lunar	I	4 velocities	6	24		69.17 \pm 10.07	83.83 \pm 13.32	86.33 \pm 27.40	137.67 \pm 24.67			
TOSS, pressurized suit	7.5	Hard	I	4 velocities	6	48	Ascend	87.17 \pm 14.78	118.33 \pm 12.36	114.33 \pm 27.39	139.67 \pm 34.18			
							Descend	82.33 \pm 18.99	104.0 \pm 19.39	114.83 \pm 19.45	114.0 \pm 25.15			
TOSS, pressurized suit	7.5	Smooth lunar	I	4 velocities	6	48	Ascend	96.0 \pm 10.47	134.17 \pm 5.65	142.4 \pm 8.14	153.5 \pm 10.83			
							Descend	78.83 \pm 20.61	85.0 \pm 14.59	93.67 \pm 13.63	90.8 \pm 23.08			
TOSS, pressurized suit	15	Hard	I	4 velocities	6	48	Ascend	89.0 \pm 17.61	124.67 \pm 16.19	147.8 \pm 19.57	175.0 \pm 15.8			
							Descend	62.83 \pm 17.36	73.5 \pm 18.91	79.0 \pm 23.19	81.33 \pm 32.42			
TOSS, pressurized suit	15	Smooth lunar	I	4 velocities	6	48	Ascend	90.0 \pm 36.26	140.2 \pm 8.47					
							Descend	62.33 \pm 8.7	67.33 \pm 7.77	64.17 \pm 12.71	62.67 \pm 14.21			
TOSS, pressurized suit	30	Hard	I	4 velocities	6	48	Ascend	42.5 \pm 6.42* N = 1						
							Descend	54.0 \pm 8.57	67.5 \pm 16.43	69.67 \pm 25.96	76.67 \pm 30.55			
Inclined plane, pressurized suit	7.5	Hard	I	4 velocities	6	48	Ascend	62.8 \pm 13.96	86.6 \pm 15.49	92.0 \pm 18.41	97.83 \pm 17.89			
							Descend	66.33 \pm 17.9	87.0 \pm 10.12	92.33 \pm 16.88	97.5 \pm 15.44			
Inclined plane, pressurized suit	7.5	Hard	II	4 velocities	6	48	Ascend	67.33 \pm 14.03	89.17 \pm 13.7	93.67 \pm 12.83	102.33 \pm 11.11			
							Descend	67.33 \pm 12.51	80.0 \pm 13.2	92.0 \pm 17.15	100.83 \pm 15.01			
Inclined plane, pressurized suit	15	Hard	I	4 velocities	6	48	Ascend	76.83 \pm 17.94	97.67 \pm 17.74	103.5 \pm 16.8	108.0 \pm 9.58			
							Descend	66.5 \pm 17.57	76.83 \pm 12.9	95.17 \pm 18.15	97.67 \pm 17.44			
Inclined plane, pressurized suit	30	Hard	I	4 velocities	6	48	Ascend	71.0 \pm 18.13	85.67 \pm 20.21	91.67 \pm 17.73				
							Descend	56.83 \pm 13.22	78.0 \pm 15.61	81.0 \pm 17.1	86.83 \pm 19.39			

*At 1 km/hr, step rate was 67.2 \pm 4.6 steps/min, N = 4

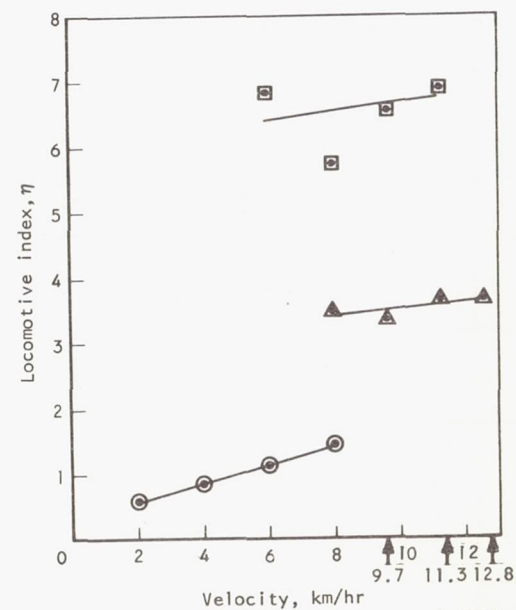
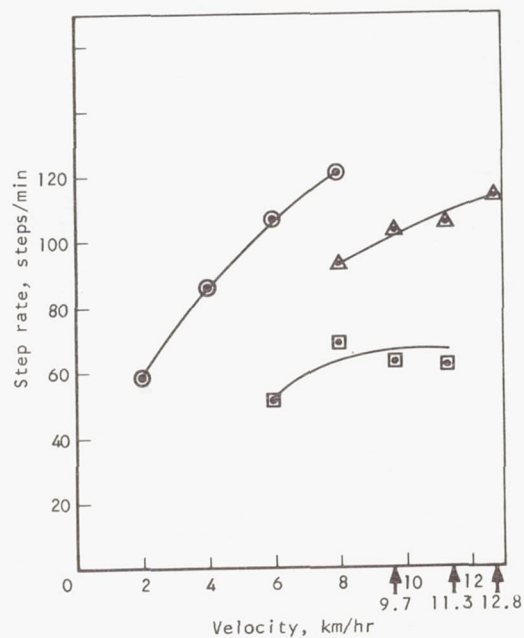
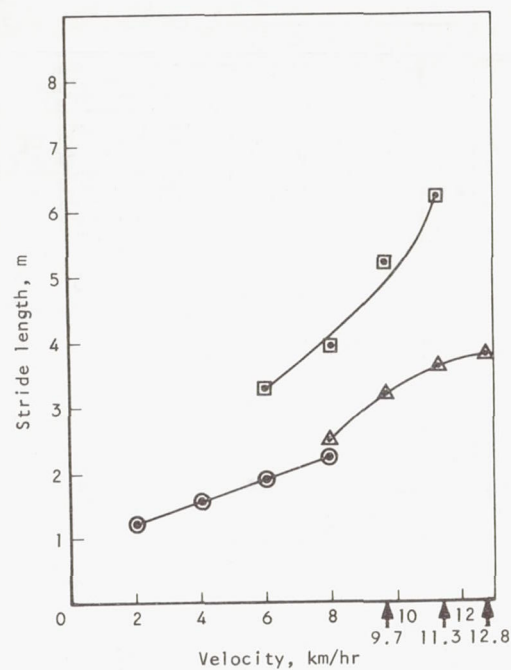
*At 1 km/hr, step rate was 67.2 \pm 41.6 steps/min, N = 4

TABLE 5-21

STRIDE LENGTH (M) FOR ALL SIMULATOR EXERCISE MODES

Simulator and suit mode	Experimental conditions						Results (mean and ± 1 standard deviation)							
	Slope, deg	Surface condition	Pack	Number of velocities	Number of subjects	Total tests	Gait or ascend/descend	Velocity, km/hr						
								2	4	6	8	9.7	11.3	12.8
Inclined plane, pressurized (press.) suit	0 (horiz)	Hard	I, 75 lb	4 each; walk, lope and run	6, with 2 repeating once	96	Walk	1.207 \pm 0.276	1.567 \pm 0.187	1.917 \pm 0.326	2.267 \pm 0.376			
							Lope		3.285 \pm 0.305		3.925 \pm 0.414	5.212 \pm 0.679	6.212 \pm 1.01	
							Run				2.533 \pm 0.296	3.175 \pm 0.328	3.630 \pm 0.525	3.783 \pm 0.500
Inclined plane, pressurized suit	0	Hard	I	1 each; walk, lope, and run	6, with all repeating twice	36	Walk	1.23 \pm 0.30						
							Lope		2.89 \pm 0.36					
							Run				2.19 \pm 0.34			
Inclined plane, subject in mufti (without press. suit)	0	Hard	I	4 each; walk, lope, and run	2	24	Walk	1.43 \pm 0.24	1.94 \pm 0.14	2.24 \pm 0.17	2.48 \pm 0.14			
							Lope		5.41 \pm 0.15	6.59 \pm 0.08	8.52 \pm 0.22	9.55 \pm 0.36		
							Run			2.91 \pm 0.27	3.66 \pm 0.06	3.82 \pm 0.02	4.12 \pm 0.06	
Incl plane, mufti	0	Hard	I	Fatigue test	6	24								
Inclined plane, pressurized suit	0	Hard	I	Fatigue test	2	8								
Inclined plane, pressurized suit	0	Hard	II, 240 lb	4 each; walk, lope, and run	6	72	Walk	1.132 \pm 0.138	1.660 \pm 0.302	2.018 \pm 0.208	2.215 \pm 0.258			
							Lope		4.005 \pm 0.251		5.018 \pm 0.284	5.875 \pm 0.267	6.630 \pm 0.334	
							Run				2.825 \pm 0.387	3.242 \pm 0.325	3.520 \pm 0.256	3.842 \pm 0.181
Inclined plane, pressurized suit	0	Hard	III, 400 lb	4 each; walk, lope, and run	2	24	Walk	1.355 \pm 0.125	1.950 \pm 0.240	2.160 \pm 0.010	2.605 \pm 0.115			
							Lope		4.015 \pm 0.245	5.130 \pm 0.00	6.055 \pm 0.285			
							Run			3.360 \pm 0.290	3.645 \pm 0.505	3.220 \pm 0.00	3.160 \pm 0.00	
TOSS (6-deg-of-freedom), pressurized suit	0	Hard	I	4 each; walk, lope, and run	6	72	Walk	0.84 \pm 0.08	1.19 \pm 0.14	1.47 \pm 0.13	1.76 \pm 0.15			
							Lope		4.15 \pm 0.7	4.45 \pm 0.66	5.41 \pm 0.79	6.54 \pm 0.95		
							Run			1.98 \pm 0.23	2.28 \pm 0.33	2.39 \pm 0.2	2.6 \pm 0.4	
TOSS, press. suit	0	Smooth lunar	I	4	6	24		0.79 \pm 0.16	1.19 \pm 0.18	1.45 \pm 0.07	1.75 \pm 0.08			
TOSS, press. suit	0	Coarse lunar	I	4	6	24		0.98 \pm 0.11	1.64 \pm 0.34	2.58 \pm 0.89	2.03 \pm 0.52			
TOSS, pressurized suit	7.5	Hard	I	4	6	48	Ascend	0.79 \pm 0.15	1.14 \pm 0.11	1.85 \pm 0.43	2.1 \pm 0.8			
							Descend	0.86 \pm 0.21	1.34 \pm 0.29	1.8 \pm 0.37	2.46 \pm 0.57			
TOSS, pressurized suit	7.5	Smooth lunar	I	4	6	48	Ascend	0.7 \pm 0.07	1.0 \pm 0.03	1.48 \pm 0.17	1.17 \pm 0.5, N=2			
							Descend	0.89 \pm 0.21	1.63 \pm 0.38	2.19 \pm 0.39	3.18 \pm 0.98			
TOSS, pressurized suit	15	Hard	I	4	6	48	Ascend	0.78 \pm 0.17	1.09 \pm 0.14	1.38 \pm 0.21	1.53 \pm 0.13			
							Descend	1.14 \pm 0.32	1.94 \pm 0.51	2.81 \pm 1.01	3.87 \pm 1.51			
TOSS, pressurized suit	15	Smooth lunar	I	4	6	48	Ascend	1.23 \pm 1.32	0.95 \pm 0.05					
							Descend	1.08 \pm 0.12	2.0 \pm 0.21	3.23 \pm 0.6	4.45 \pm 0.9			
TOSS, pressurized suit	30	Hard	I	4	6	48	Ascend	1.57 \pm 0.06*						
							Descend	1.26 \pm 0.16	2.1 \pm 0.53	3.31 \pm 1.19	4.05 \pm 1.51			
Inclined plane, pressurized suit	7.5	Hard	I	4	6	48	Ascend	1.12 \pm 0.27	1.59 \pm 0.28	2.27 \pm 0.47	2.84 \pm 0.66			
							Descend	1.08 \pm 0.28	1.56 \pm 0.2	2.25 \pm 0.45	2.81 \pm 0.49			
Inclined plane, pressurized suit	7.5	Hard	II	4	6	48	Ascend	1.04 \pm 0.23	1.53 \pm 0.24	2.18 \pm 0.35	2.63 \pm 0.28			
							Descend	1.03 \pm 0.21	1.71 \pm 0.26	2.25 \pm 0.42	2.70 \pm 0.44			
Inclined plane, pressurized suit	15	Hard	I	4	6	48	Ascend	0.93 \pm 0.3	1.42 \pm 0.33	2.0 \pm 0.41	2.49 \pm 0.2			
							Descend	1.08 \pm 0.32	1.78 \pm 0.29	2.20 \pm 0.53	2.83 \pm 0.61			
Inclined plane, pressurized suit	30	Hard	I	4	6	48	Ascend	1.01 \pm 0.27	1.66 \pm 0.45	2.27 \pm 0.48				
							Descend	1.23 \pm 0.25	1.77 \pm 0.31	2.58 \pm 0.54	5.12 \pm 1.01			

*At 1 km/hr, stride length was 0.62 \pm 0.21, N = 4



Conditions:

- Inclined plane
- Pack I (75 lb)
- Suited, pressurized
- Hard surface, horizontal

Legend:

- walk
- lope
- ▲ run

Figure 5-59. Locomotive Parameters vs Velocity on Inclined-Plane Simulator, Horizontal Hard Surface, Pack I

Figure 5-60 illustrates the effects on these parameters when a 240-lb pack is carried. Locomotive index significantly increased with velocity for both the walking and loping modes ($p < 0.01$). There was no velocity effect on locomotive index during the running mode. The locomotive index between the three gaits with this pack, however, was significantly different ($p < 0.01$).

The trend of step rate data with the 240-lb pack is similar to that with the 75-lb pack. Locomotive index is significantly different between gaits ($p > 0.01$) and significantly increases by velocity for walking and loping ($p > 0.01$). The change observed for the running mode was not significant.

The data for stride length indicate that this dependent parameter is significantly altered by gait and by velocity within each gait ($p < 0.01$).

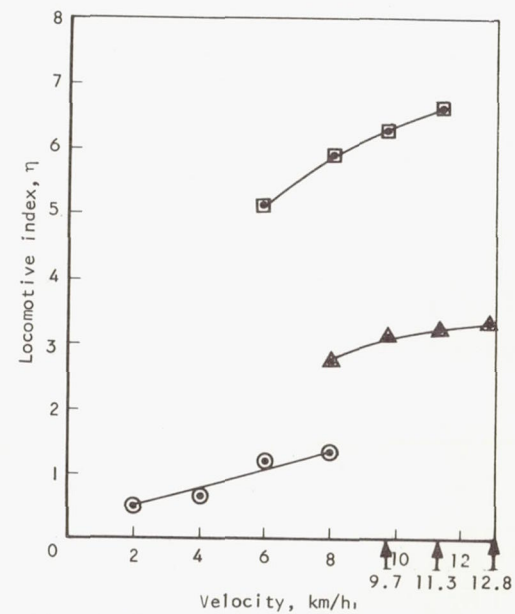
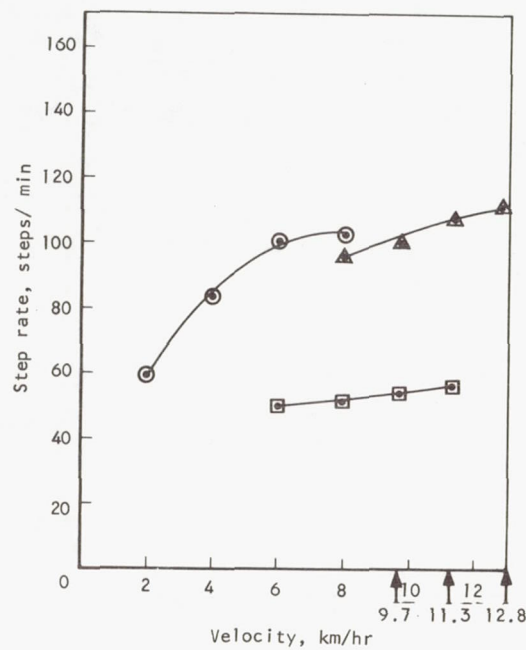
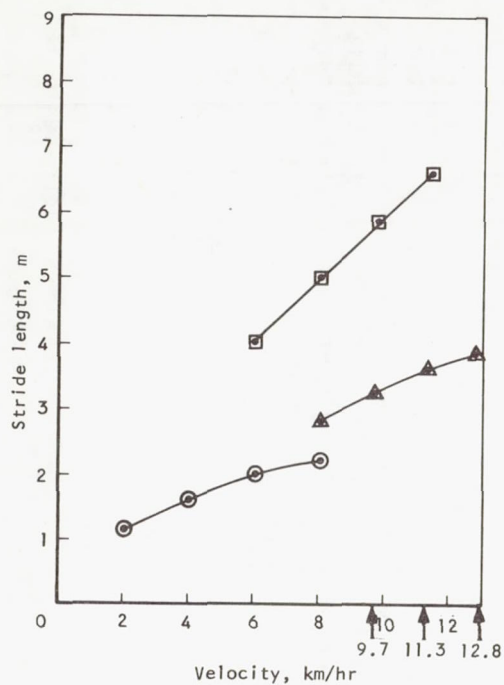
The data from tests with two subjects carrying 400-lb packs are presented in Figure 5-61. Because of the small number of subjects, statistical treatment of the data is not relevant. General observations from the 400-lb pack data are similar, however, to the 75- and 240-lb pack condition. These are generally increases in step rate, stride length, and locomotive index with increasing velocities, and there are marked distinctions between all three gaits for these dependent variables.

With respect to differences between packs, the only significant effect of pack weight within gait is a significantly lower locomotive index during running ($p < 0.01$) for the heavier pack. Also there was no statistically significant effect of pack weight on the parameter η as a function of gait, except at 6 km/hr where a significant interaction effect is observed between the walk and lope gaits with the 240- and 400-lb packs.

The only significant effect of pack weight on step rate was noted for the loping gait, in which the 240-lb pack produced a systematically ($p > 0.01$) lower step rate than was observed for the 75-lb pack. This effect is reflected in stride length where again the only effect of pack weight was to affect the loping stride length by an increase for the 240-lb pack over that obtained with the 75-lb pack. A significant interaction effect between pack and velocity was also observed for the loping gait, which indicates that the extent of the effect of pack weight on stride length is altered by velocity ($p < 0.01$).

Locomotive index, step rate, and stride length with the horizontal TOSS simulator. - The locomotive kinematic parameters for the TOSS simulator are plotted as a function of velocity in Figure 5-62. Velocity has a significant effect on each of the dependent parameters for each of the three gaits ($p < 0.01$). In addition, the differences exhibited between each of the gaits are statistically significant ($p < 0.01$). It should be noted, however, that the running stride length and locomotive index appear to be simple extensions of the walking data. This is probably due to the elimination of walking in the simulator at a velocity somewhere between 2 and 6 km/hr. These observations accurately reflect the energy expenditure data.

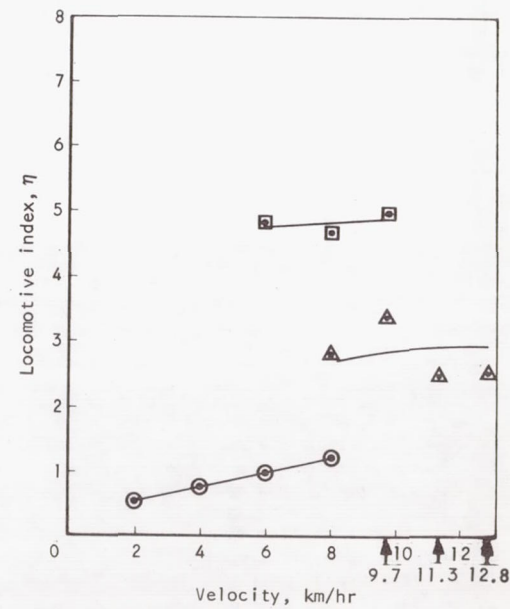
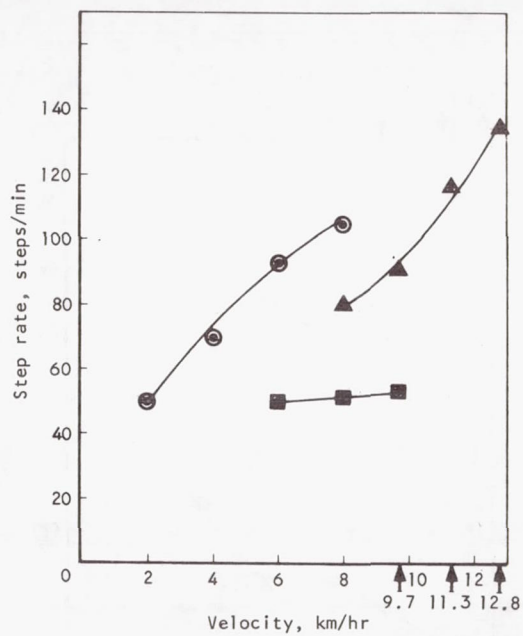
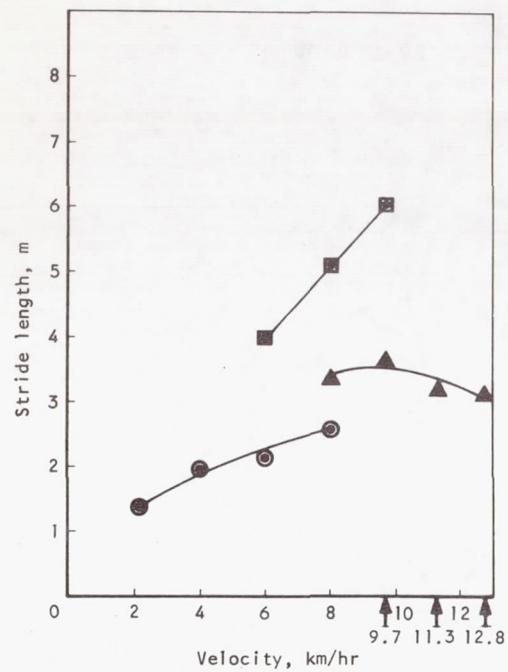
Lunar surface conditions. - The effects of lunar surface conditions on stride length, step rate, and locomotive index are shown as a function of velocity in Figure 5-63. In general, each of these parameters increases with



Conditions:

- Inclined plane
- Pack II (240 lb)
- Suited, pressurized
- Hard surface, horizontal
- walk
- lope
- ▲ run

Figure 5-60. Locomotive Parameters vs Velocity on Inclined-Plane Simulator, Horizontal Hard Surface, Pack II

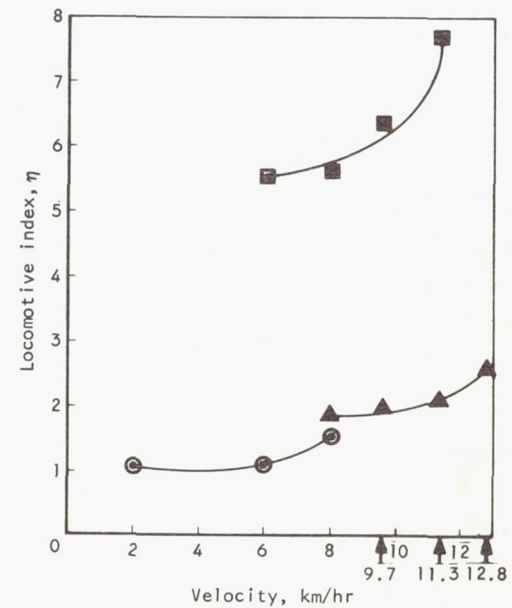
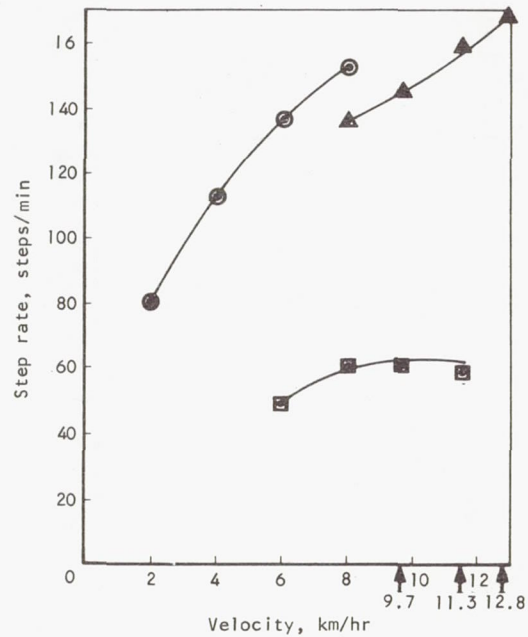
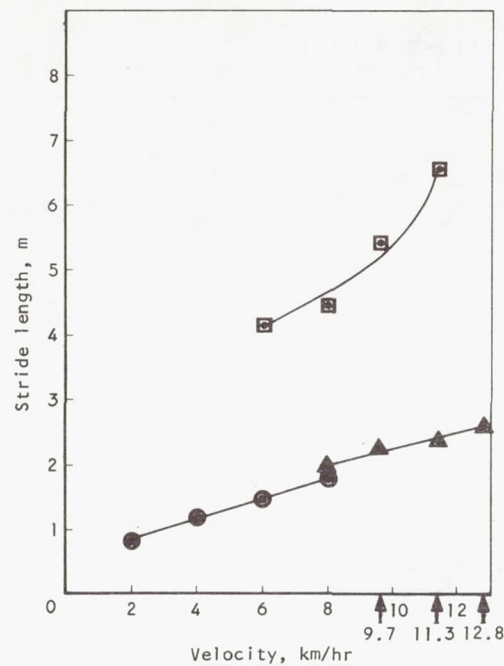


Conditions:

Inclined plane
 Pack III (400 lb)
 Suited, pressurized
 Hard surface, horizontal

○ walk
 □ lope
 ▲ run

Figure 5-61. Locomotive Parameters vs Velocity on Inclined-Plane Simulator, Horizontal Hard Surface, Pack III



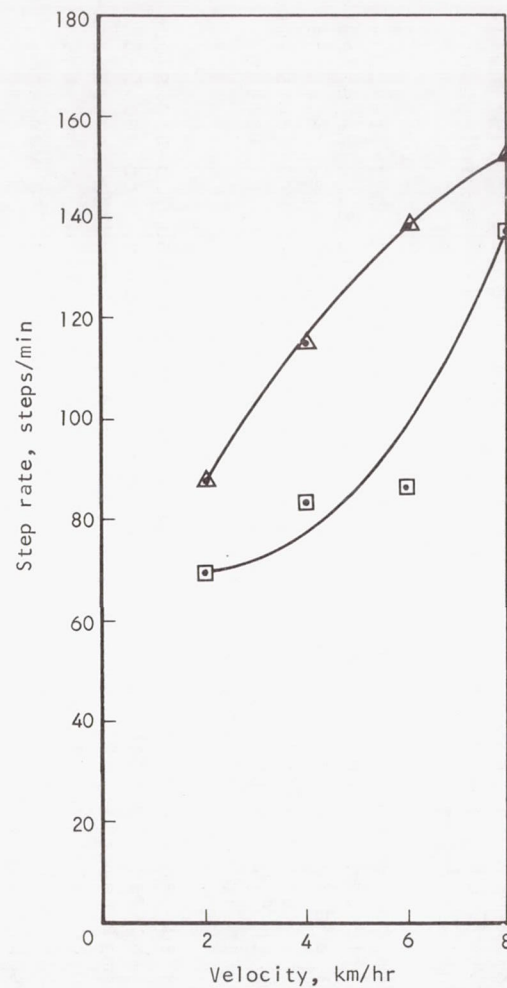
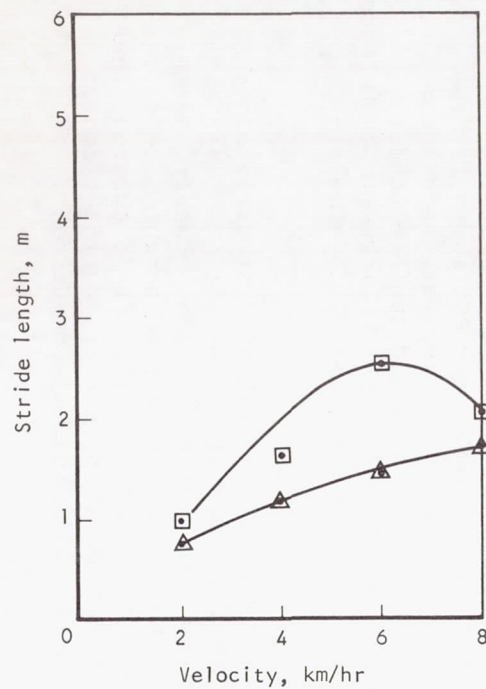
Conditions:

TOSS
Pack I (75 lb)
Suited, pressurized
Hard surface, horizontal

● walk
■ lope
▲ run

Figure 5-62. Locomotive Parameters vs Velocity on TOSS Simulator, Horizontal Hard Surface, Pack I

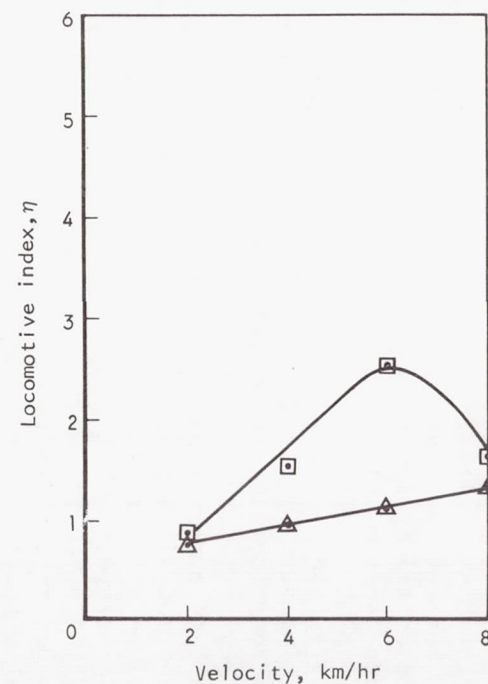
S-42749



Conditions:

T0SS
Pack I (75 lb)
Suited, pressurized
Horizontal

▲ Smooth lunar soil
□ Coarse lunar soil



5-42734

Figure 5-63. Locomotive Parameters vs Velocity on T0SS Simulator, Horizontal, Lunar Surface Conditions, Pack I

velocity for the simulated smooth lunar surface ($p > 0.01$). With the simulated coarse lunar surface, however, stride length and locomotive index have a curvilinear relationship with velocity. This interaction effect is statistically significant for both parameters ($p > 0.05$). In addition, the main effect of this surface on all three parameters is a significant increase in values as velocity increases $p > 0.01$.

Slope traverse. - The following subsection presents the evaluation of the locomotive kinematic data for slope traversing. The data are presented in comparative form for simulators and surface conditions, as appropriate.

Figure 5-64 presents data for stride length, step rate, and locomotive index for the two simulators and two of the surface conditions for descending a 7.5-deg slope at different velocities. Figure 5-65 presents data for ascending a 7.5-deg slope.

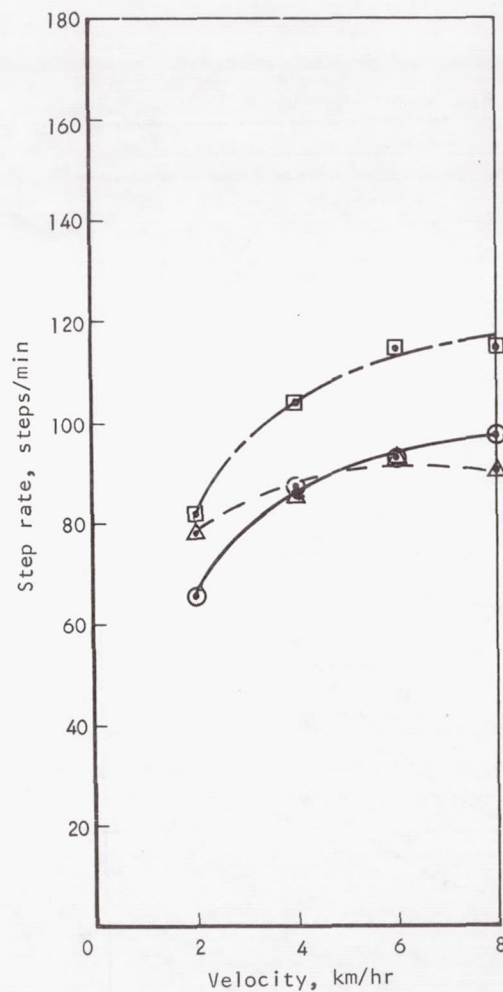
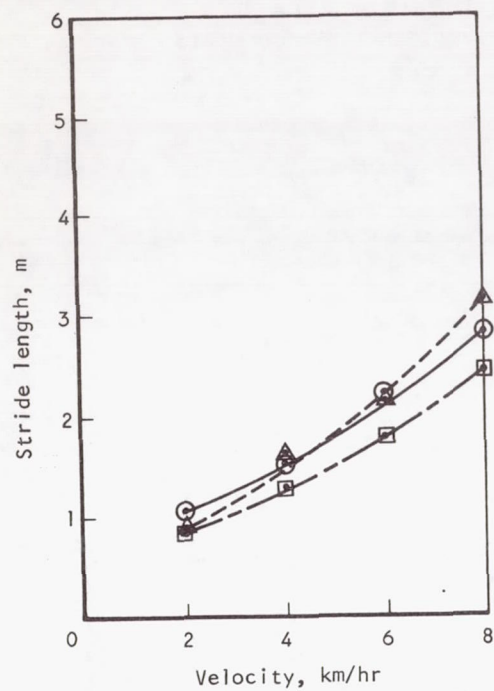
During descent, there is a significant effect of velocity on step rate, stride length, and locomotive index for all three simulator conditions ($p > 0.05$). There is no difference between simulator conditions for stride length or locomotive index. The differences in step rate by simulators are statistically significant ($p < 0.01$). The descending data are quite similar regardless of simulator surface or velocity.

The data for ascent of a 7.5-deg slope, Figure 5-65, demonstrate considerable difference between simulators and surface conditions. The effects of simulator and surface conditions, as well as velocity, on step rate and stride length are significant ($p > 0.01$). However, only velocity affects locomotive index ($p < 0.01$). Locomotive index was not significantly different between the simulator and surface conditions.

All six subjects carried the 240-lb pack up and down the 7.5-deg slope condition. The data for this activity, presented in Figures 5-66 and 5-67, show the normal velocity effect on the kinematic data. The data are remarkably similar between the ascent and descent conditions. In addition, the additional pack weight apparently has the effect of reducing the variance in the kinematic parameters.

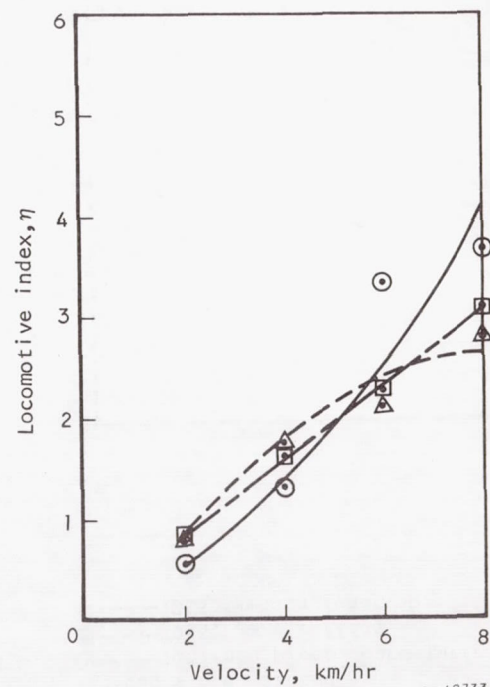
The data for descending and ascending a 15-deg slope are shown in Figures 5-68 and 5-69. The velocity effect on stride length, step rate, and locomotive index is statistically significant for each simulator and surface condition ($p > 0.01$). Because of large variance in the data, the only significant difference for the three conditions is between the inclined-plane and TOSS simulators ($p < 0.01$).

The ascending data, on the other hand, exhibit significant differences between simulators for all three locomotive parameters ($p < 0.01$), as well as a significant effect of velocity. A comparison cannot be made, however, between the lunar surface condition and the other conditions during ascent, due to the limited number of subjects that could complete this task. It is apparent that step rate increases very rapidly with increases in velocity during ascent, while stride length increases more rapidly with velocity on descent.



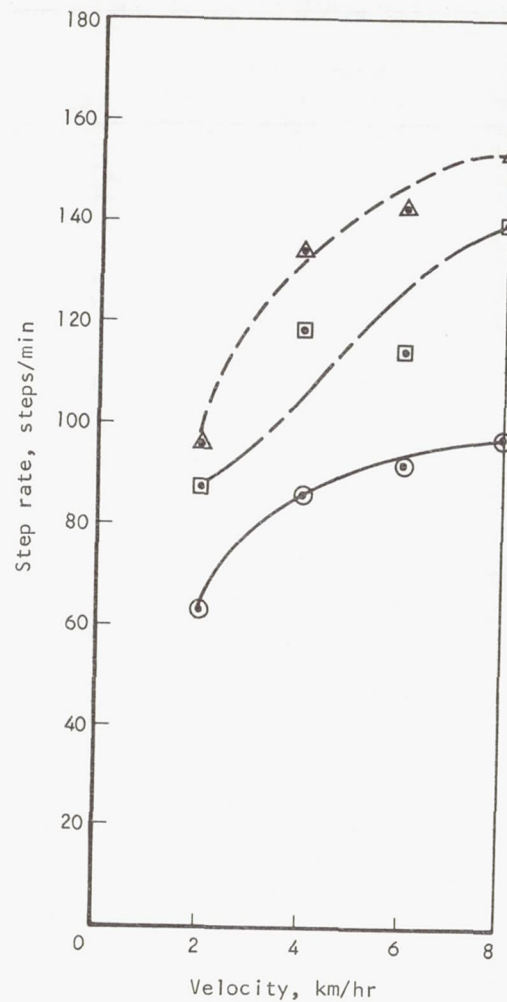
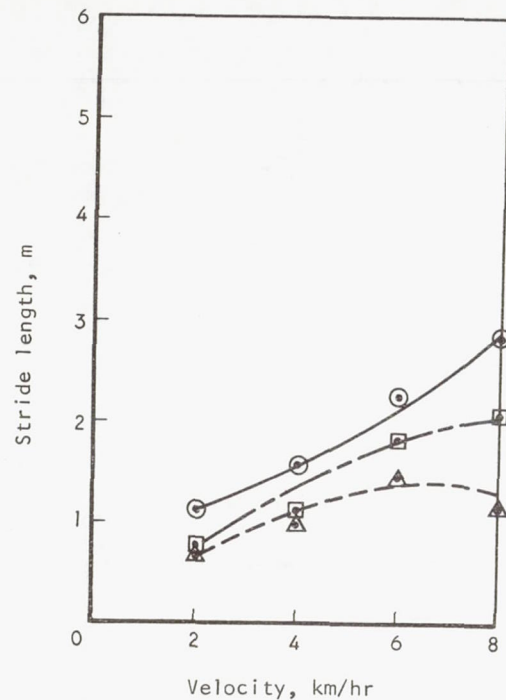
Conditions:

Pack I (75 lb)
 Suited, pressurized
 7.5-deg slope, descend
 ○— inclined plane, hard surface
 □— T0SS, hard surface
 △— T0SS, smooth lunar soil



S-42733

Figure 5-64. Comparison of Simulators and Surface Conditions Using Locomotive Kinematic Data for Descending a 7.5-deg Slope with Pack I



Conditions:

Pack I (75 lb)

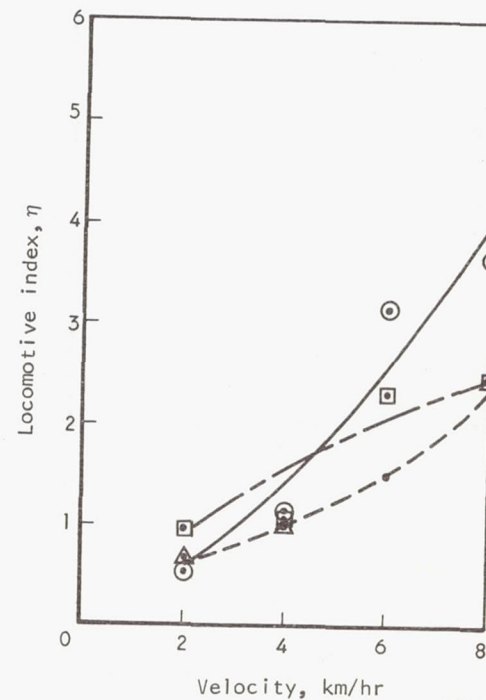
Suited, pressurized

7.5-deg slope, ascend

⊙—Inclined plane, hard surface

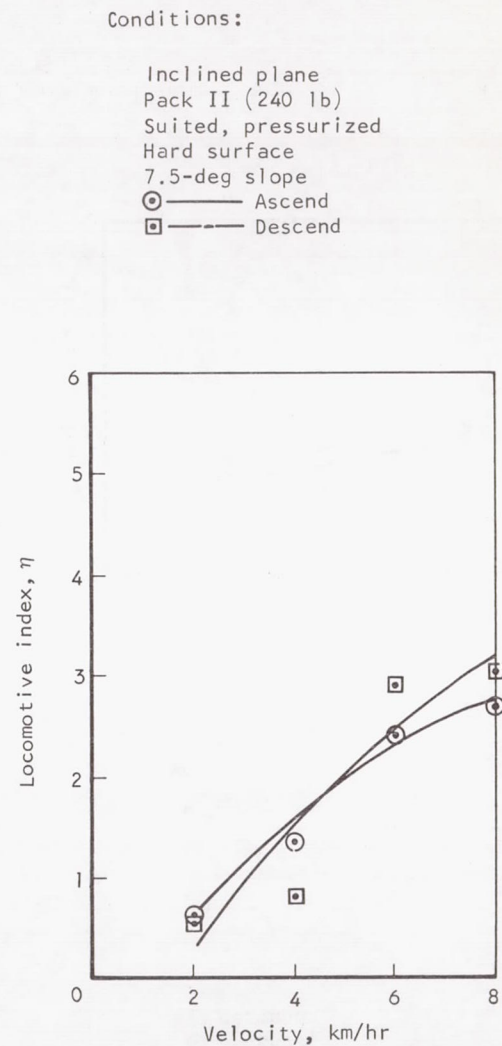
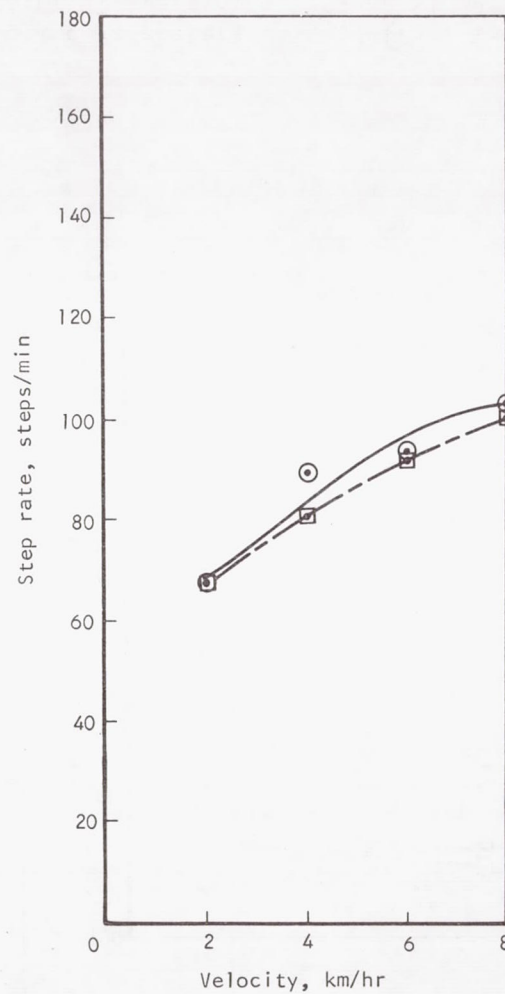
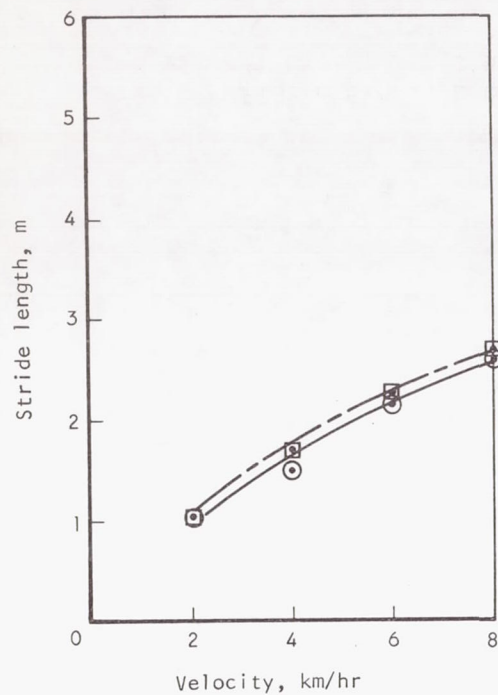
□—TOSS, hard surface

△—TOSS, smooth lunar soil



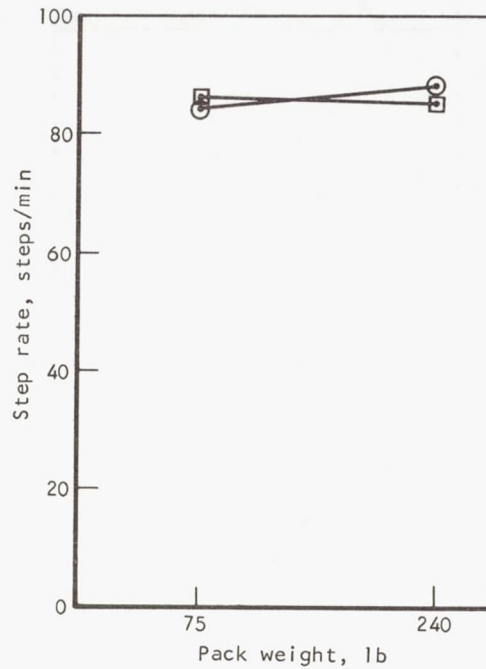
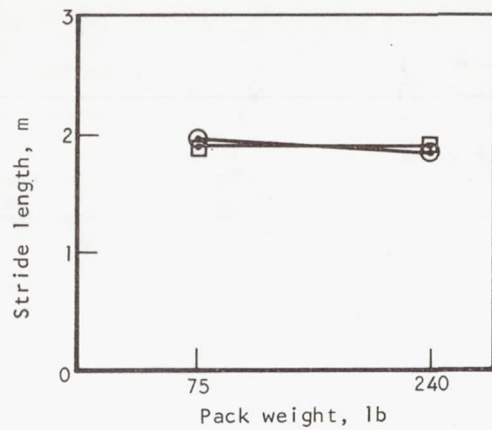
S-42731

Figure 5-65. Comparison of Simulators and Surface Conditions Using Locomotive Kinematic Data, Ascending a 7.5-deg Slope with Pack I



S-42732

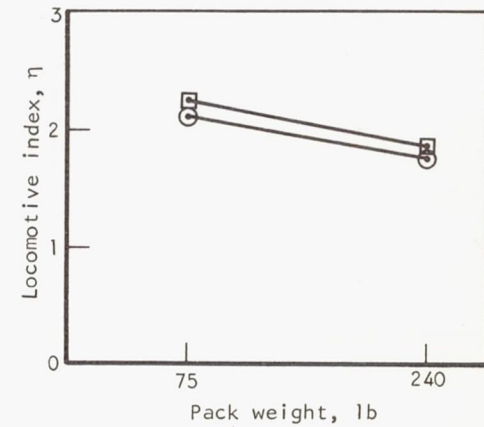
Figure 5-66. Locomotive Parameters vs Velocity on Inclined-Plane Simulator, Traversing a 7.5-deg Slope, Hard Surface, Pack II



Conditions:

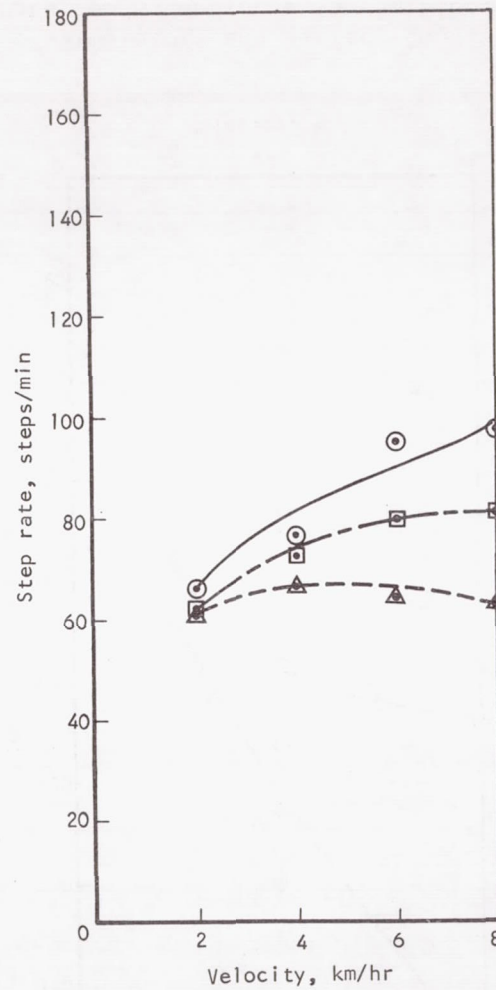
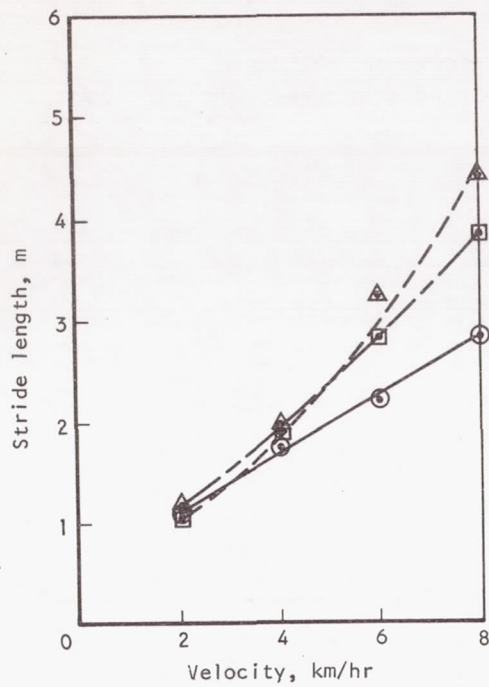
Inclined plane
Pack II (240 lb)
Suited, pressurized
7.5-deg slope, hard surface

○ ascend
□ descend



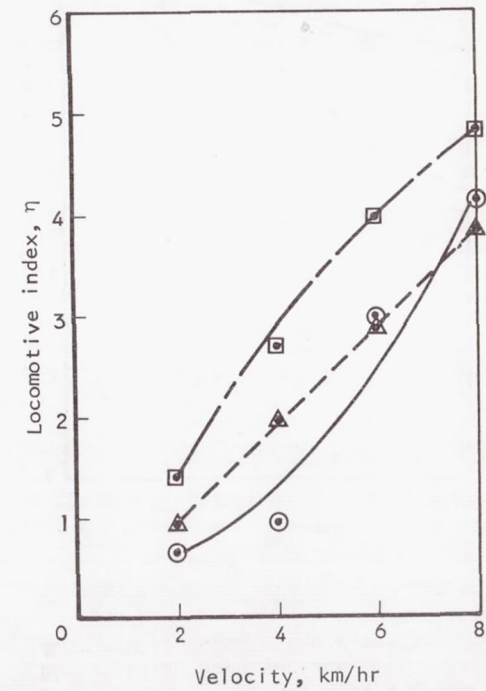
S-42745

Figure 5-67. Locomotive Parameters vs Load (Pack Weight) on Inclined-Plane Simulator, Traversing a 7.5-deg Slope, Hard Surface



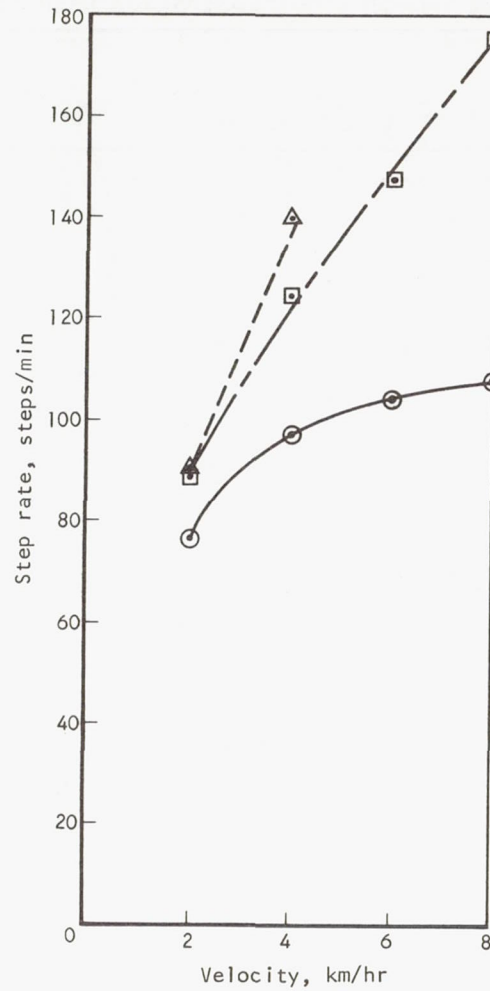
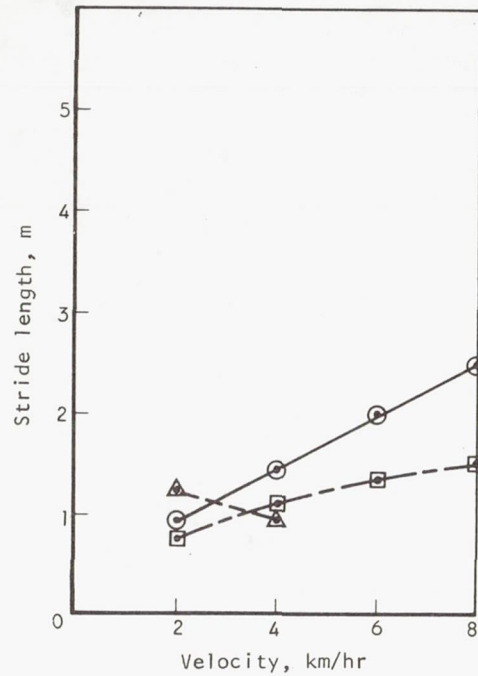
Conditions:

Pack I (75 lb)
 Suited, pressurized
 15-deg slope, descend
 (●) — Inclined plane, hard surface
 (□) — TQSS, hard surface
 (△) — TQSS, smooth lunar soil



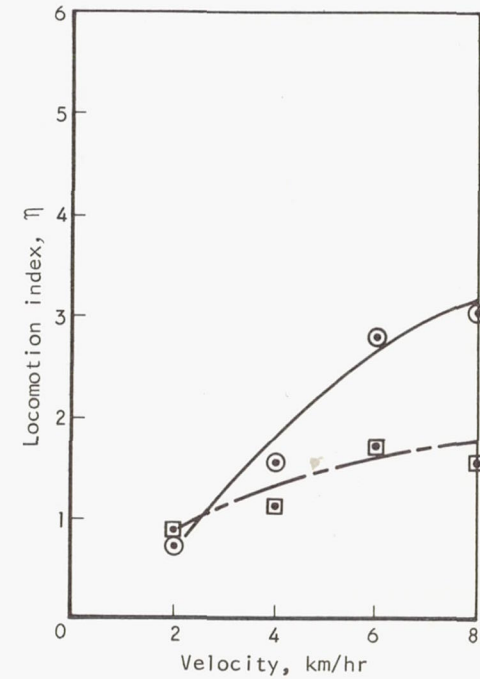
S-42729

Figure 5-68. Comparison of Simulators and Surface Conditions Using Locomotive Kinematic Data for Descending a 15-deg Slope with Pack I



Conditions:

Pack I (75 lb)
 Suited, pressurized
 15-deg slope, ascend
 ○— Inclined plane, hard surface
 □— TOSS, hard surface
 △— TOSS, smooth lunar soil



5-42736

Figure 5-69. Comparison of Simulators and Surface Conditions Using Locomotive Kinematic Data for Ascending a 15-deg Slope with Pack I

Descending and ascending a 30-deg slope produces the values of locomotive index, step rate, and stride length shown in Figures 5-70 and 5-71. There are no differences between simulators for descent; however, the velocity effect shown is significant for all parameters on each simulator ($p < 0.01$). The ascending data cannot be treated for simulator comparisons because of the paucity of data on the TOSS simulator. The velocity effect during ascent with the inclined-plane simulator is significant for all parameters ($p < 0.01$).

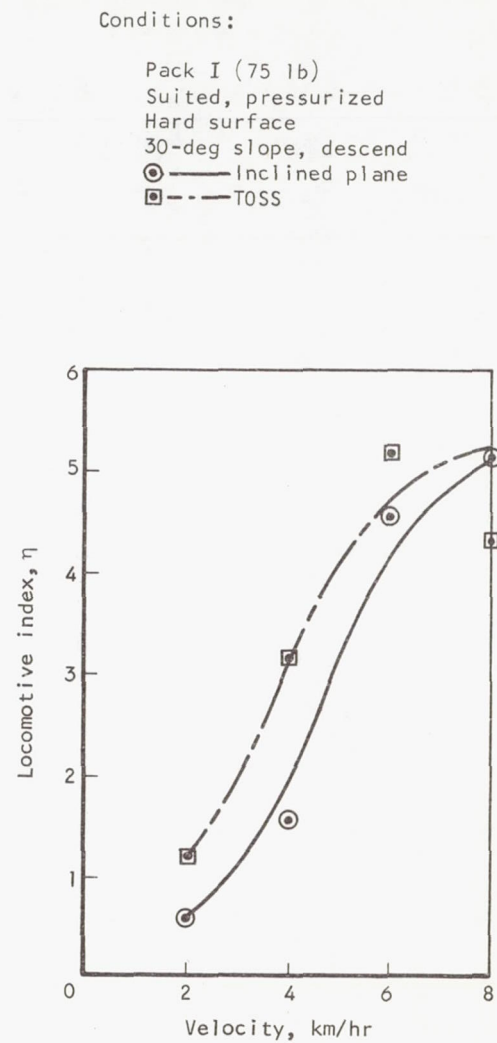
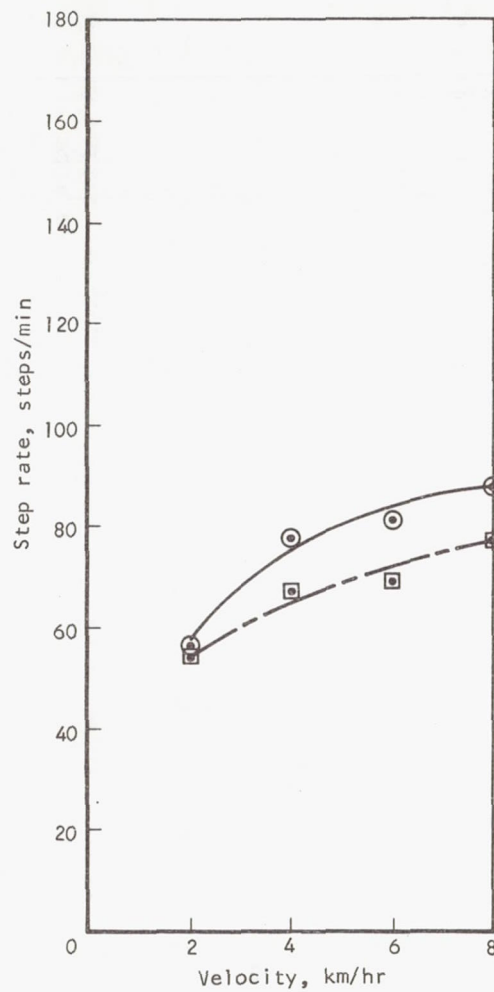
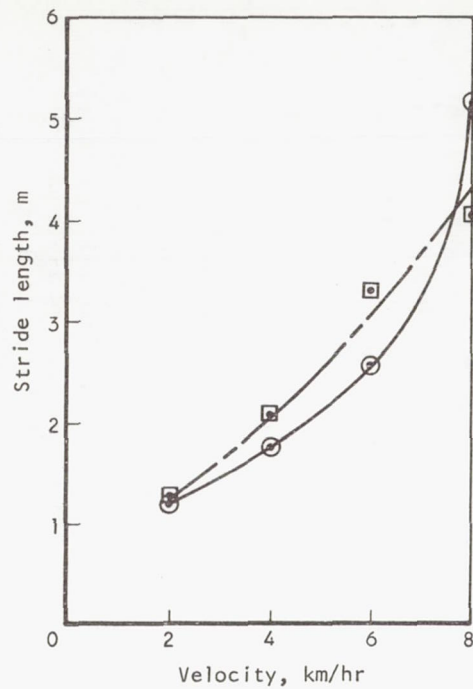
Simulator comparisons. - The primary simulator comparison to be made, in addition to the slope traverse data in the previous subsection, is concerned with the horizontal surface data. Figure 5-72 illustrates comparative data for the TOSS simulator for the three surface conditions, the inclined-plane simulator, and the inclined board at Langley Research Center. Figure 5-72 shows that the inclined-plane treadmill and the inclined-plane walkway produce similar kinematic data at comparable velocities. There is very little difference between simulators in the shape of the curves of velocity effect on stride length. The TOSS simulator produces lower stride lengths and higher step rates than is found with the inclined plane. Locomotive index, however, is very similar for all simulators at velocities under 6 km/hr. At 8 km/hr, locomotive index is widely dispersed between all simulators and conditions. The most novel effect is, of course, with the TOSS simulator and the coarse lunar surface where each parameter exhibits a curvilinear effect of velocity which is opposite to the effect for the same simulator with other surfaces or with the inclined-plane simulator.

Figures 5-73 and 5-74 extend the simulator comparisons that can be made for locomotion to differences between the inclined-plane treadmill and the inclined walkway at Langley Research Center. These figures display data taken on subjects both in pressurized suits and in shirt sleeves. The shirt-sleeve condition shows the best correspondence between simulators for the data taken. The suited data show good correspondence; however, differences were observed in step rate and locomotive index which may be partly due to differences in pack weight.

Comparison of shirt-sleeve and pressurized suit conditions for stride length, step rate, and locomotive index confirm the contention of Spady and Harris (1968) that pressurization of the suit does not appreciably affect step rate and extends this observation to stride length and locomotive index.

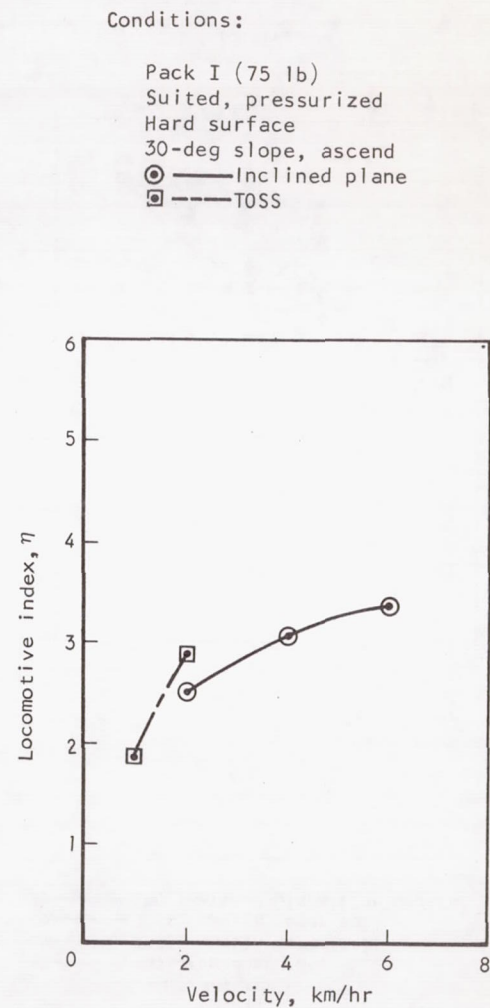
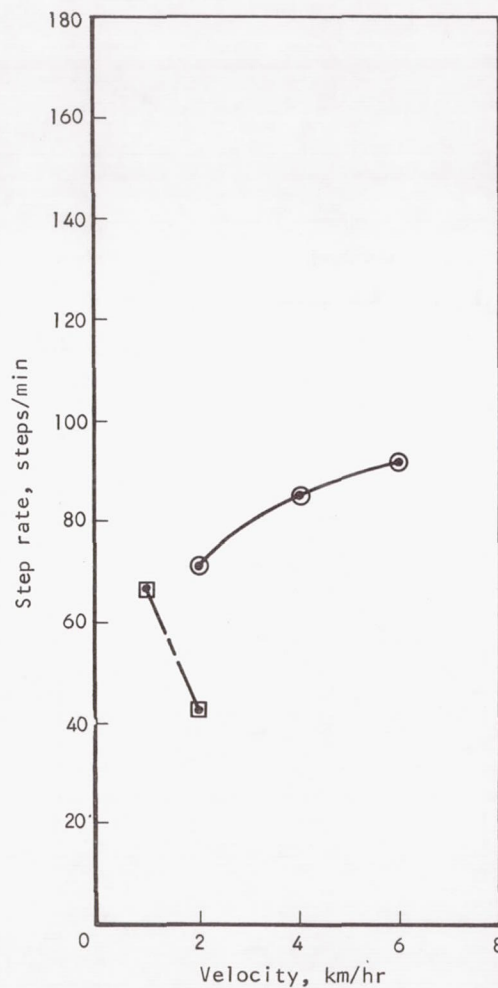
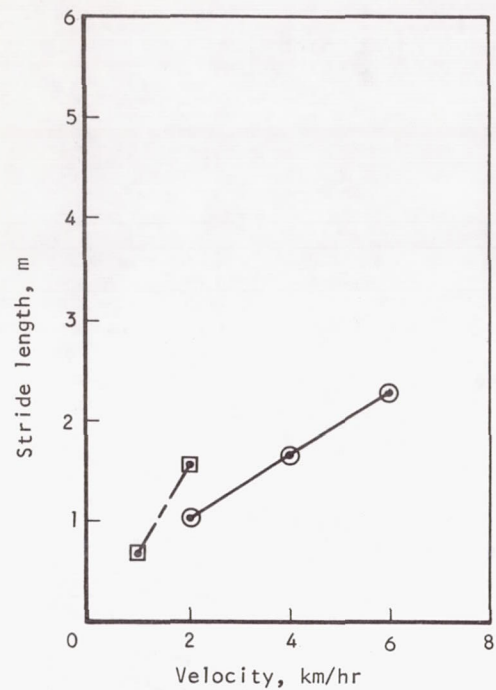
Summary of Observations on Stride Length, Step Rate, and Locomotive Index

1. In general, the values of stride length, step rate, and locomotive index η increase as velocity increases.
2. The walk, lope, and run gaits are definitely distinct in terms of locomotive index. Generally, the probability of distinguishing gait in terms of η is $p > 0.90$. Mean values of η for the horizontal inclined-plane simulator at velocities less than 8 km/hr range from 0.625 to 1.16 for walking, 3.49 to 3.68 for running, and 6.83 to 6.90 for loping. On



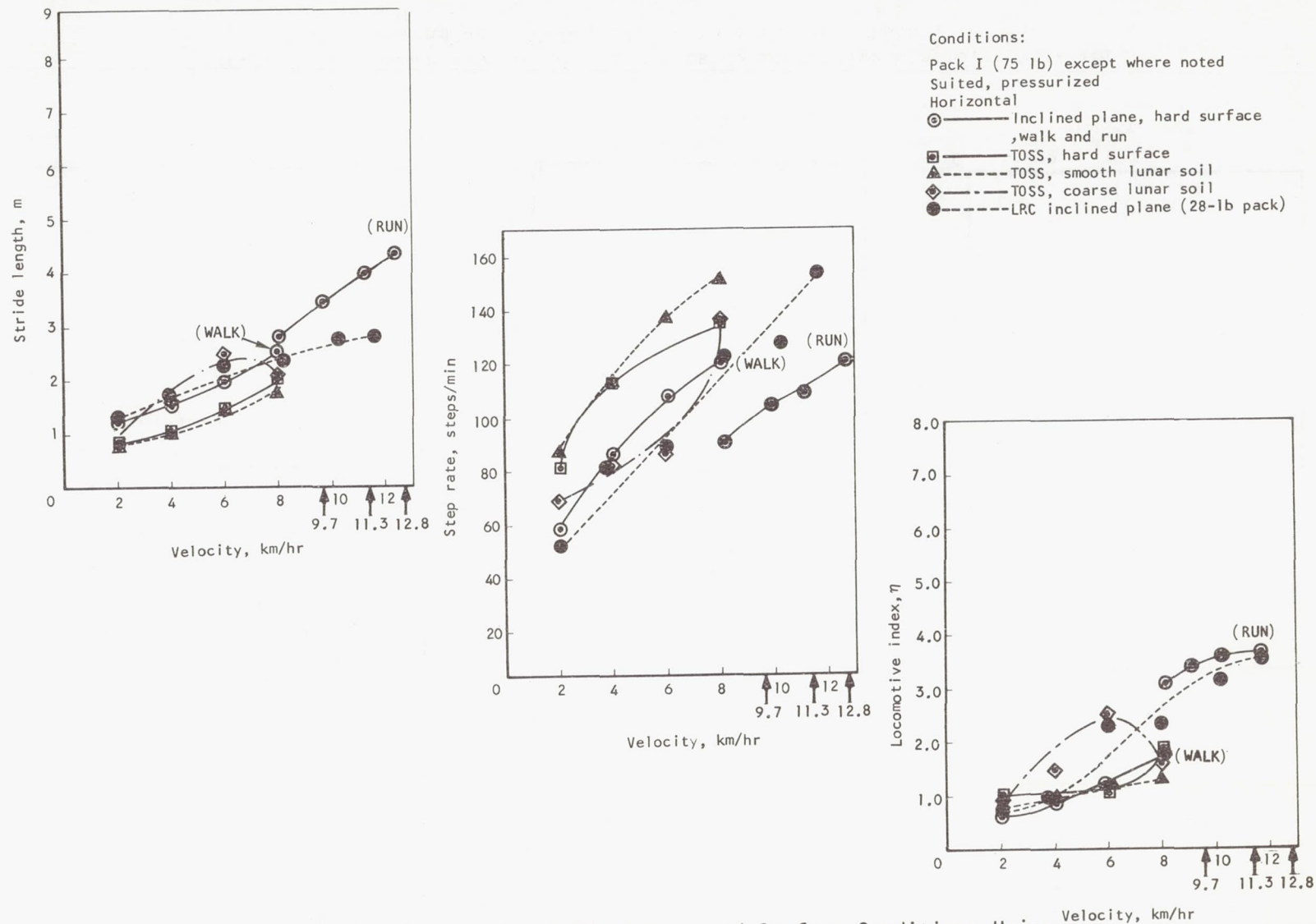
S-42137

Figure 5-70. Comparison of Simulators Using Locomotive Kinematic Data for Descending a 30-deg Slope, Hard Surface, Pack I



S-42730

Figure 5-71 Comparison of Simulators Using Locomotive Kinematic Data for Ascending a 30-Deg Slope, Hard Surface, Pack I



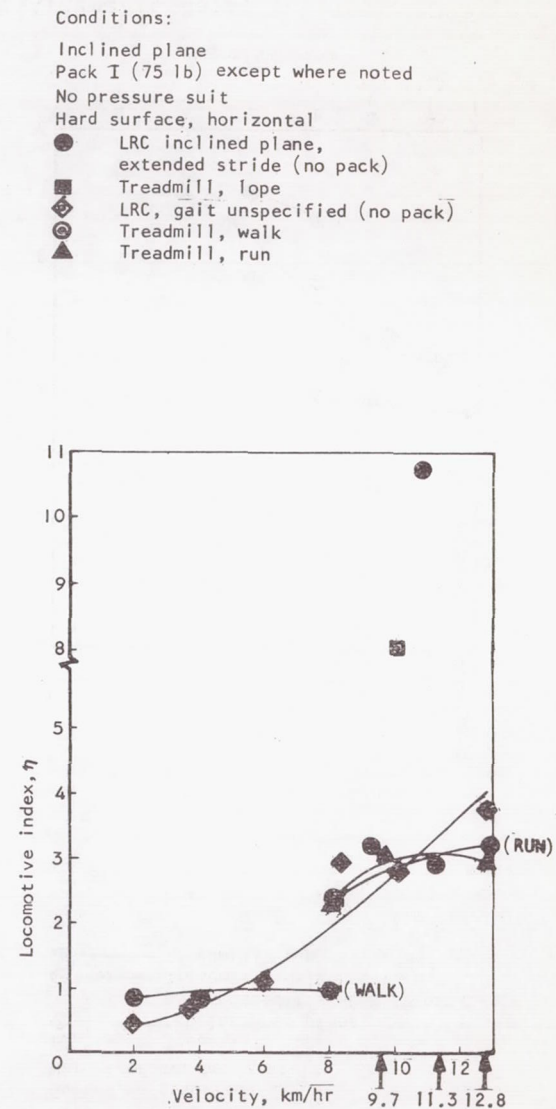
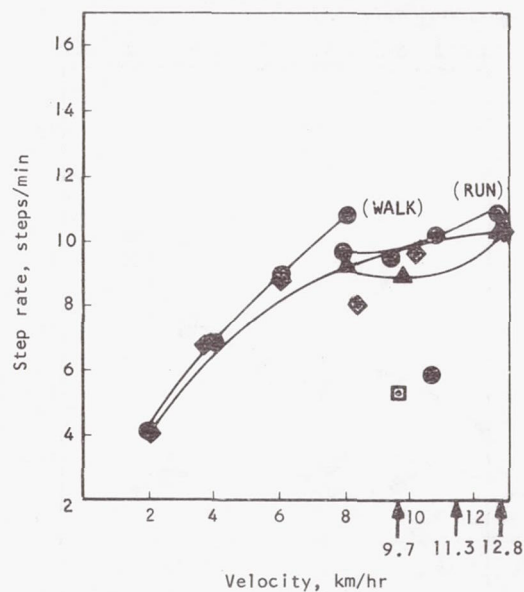
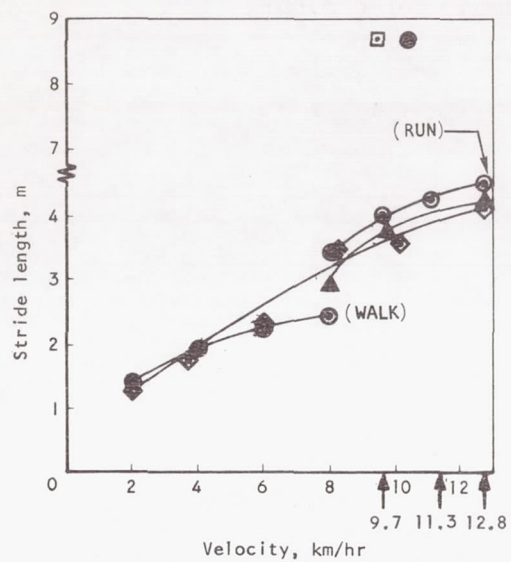
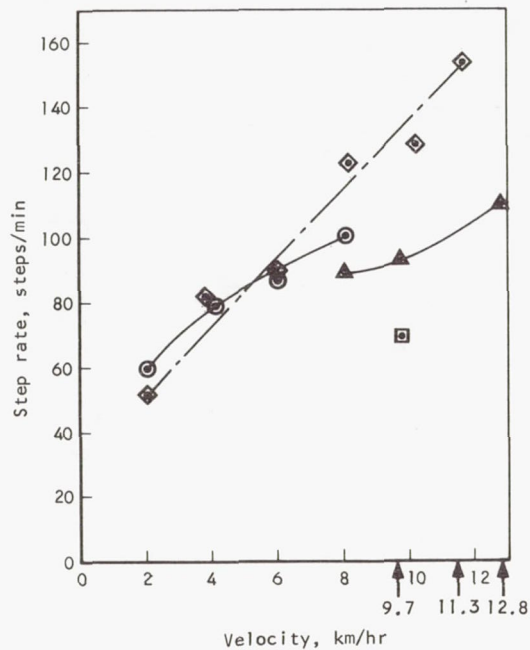
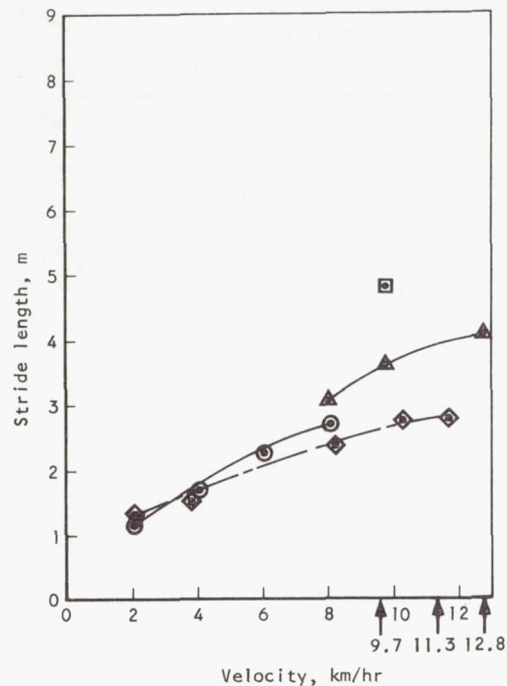


Figure 5-73. Comparison of Simulators Using Locomotive Kinematic Data, Horizontal Hard Surface, Without Pressure Suits



Conditions:

- Inclined plane
- Pack I (75 lb) except where noted
- Suited, pressurized
- Hard surface, horizontal
- Treadmill, lope
- ◇ LRC inclined plane, gait unspecified (28-lb pack)
- Treadmill, walk
- △ Treadmill, run

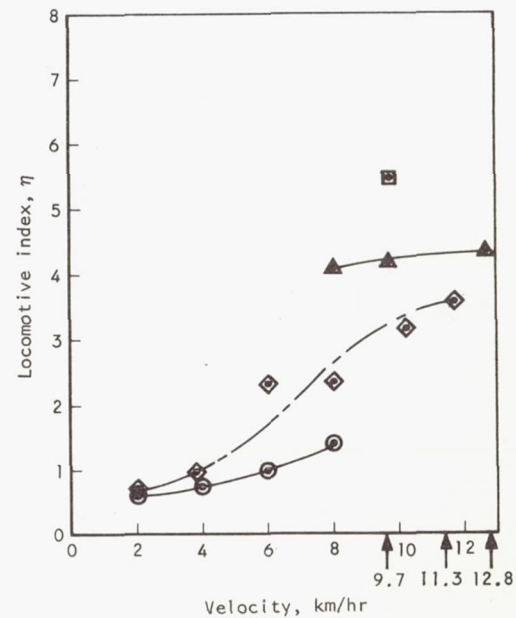


Figure 5-74. Comparison of Simulators Using Locomotive Kinematic Data, Horizontal Hard Surface, Pressurized Suits

the TOSS simulator these values ranged from 0.77 to 1.09 for walking, 1.14 to 2.53 for running, and 5.56 to 7.67 for loping. In this simulator, loping is distinct from either walking or running. Walking phases into running between 4 and 6 km/hr.

3. The subjects encountered difficulty in obtaining a consistent gait for the 6-km/hr lope and the 8-km/hr run, indicating that these velocities may have been somewhat low for the gaits. Walking in the TOSS simulator is not the same as in the inclined plane. The inclined-plane simulator provides freedom for the subject to pitch, to walk forward and backward, and to displace himself vertically. No freedom is allowed for moving from side to side or for roll and yaw motions. The suspension is such that the distance between the feed is relatively fixed. This makes it possible for the subject to maintain a desired leg position without exerting muscular forces. Subjects in the TOSS simulator did not have this advantage. On the faster lope velocities, it was necessary for the subject to extend the foot as far forward as possible when coming down onto the treadmill surface. To achieve this, it was also necessary to use the thigh muscles to hold the suit legs closer together. This action was tiring and sometimes painful. For one subject, heart rate was increased more than 20 beats/min for standing with legs held together, as compared to standing relaxed with the legs apart. The preferred gait for subjects in the TOSS simulator included a yaw motion while walking and running. The yaw action reduces the period during which both feet can be on the surface at the same time.
4. Heavy pack loads reduce the variance in kinematic parameters and may well aid stability during locomotion under lunar-gravity conditions.
5. Treadmill and walkway kinematic data are quite similar for the inclined-plane technique of simulation.
6. Kinematic data are also similar for the inclined-plane and TOSS simulation at velocities under 6 km/hr.
7. Stride lengths for walking and running in the TOSS simulator appear to increase almost linearly with velocity. The stride lengths for the loping gait show the same effect only much greater. Stride length is consistently less for walking and running in the TOSS system than for those gaits with the inclined-plane simulator. For loping, stride length is greater in the TOSS system than in the inclined-plane system.
8. In comparing the step rate curves with the locomotive index curves, a consistent relationship of decreasing step rate with increasing locomotive index within velocity and pack is shown. For example, the comparison of the locomotive indexes for the different gaits at the 8-km/hr velocity show the walking gait as the lowest, followed by the running gait, with the loping gait as the highest. The plotted step rates for the 8-km/hr velocity show the loping gait as the lowest stepping rate, followed by running, with the walking gait as the highest. This relationship is also brought out by comparison of the gait curves across all

the velocities. The two highest locomotive indexes for suited subjects loping with 75-lb packs occur at 6 and 11.8 km/hr, with the lowest occurring at 8 km/hr. The two lowest step rates for suited subjects loping with 75-lb packs occur at 6 and 11.3 km/hr, with the highest occurring at 8 km/hr.

9. Comparison of the walking data for the two simulators shows that step rates are higher and stride lengths are lower for the TOSS simulator.
10. Locomotive index, step rate, and stride length increased with velocity for the simulated smooth lunar soil condition. This was also the case for the coarse lunar soil condition, with the exception of the locomotive index and stride length at the 8-km/hr velocity. At this velocity, it was necessary to increase the step rate to improve stability after stepping on the rocks. The curves for the smooth lunar soil condition are almost linear. When compared to the data for the smooth lunar soil, the locomotive index and stride lengths were greater for the coarse soil condition at all velocities, and step rates were lower.
11. On the TOSS simulator, the step rate is greater for the hard surface than for the simulated smooth lunar soil and becomes increasingly greater as velocity increases. This effect may be due to the decreased traction on the smooth lunar soil, with increasing velocity as a function of the shearing of the soil. Sensory feedback as to when the foot has touched the surface arises sooner when stepping on a hard surface than when stepping on a yielding surface. The shear strength of the soil provides the subject poor traction with lowered feedback at the higher velocities; consequently, the time taken to end one step and start another increases, resulting in a decreased step rate. The depth of penetration into the soil increases the duration of application of both decelerating and accelerating forces by the foot. The penetration of the foot into the soil makes it difficult to determine from photographic data, exactly when the foot left the surface. This probably resulted in some errors in data reduction.
12. Values of locomotive index, step rate, and stride length are almost identical for the shirt-sleeve and pressurized suit conditions:

Body Position Data

The body position data taken during this experiment are the maximum changes in angle that occur with movement of the various body parts. The angles measured include back angle, δ_b (the deviation of the back from vertical), hip angle, δ_h (the angle between the thigh and the body reference line during extension),^h and knee angle, δ_k (the angle between the thigh and lower leg, as defined in Figure 5-58). The mean values and standard deviations for these parameters are recorded in Tables 5-22, 5-23, and 5-24.

Back angle, δ_b . - The effect of the independent variable on back angle, δ_b , is shown in Figures 5-75 through 5-80. Although there is an apparent increase in back angle with velocity, at no time is this increase statistically significant during any tests of horizontal locomotion with any simulator.

TABLE 5-22

MAXIMUM BACK ANGLE (δ_D) FOR ALL SIMULATOR EXERCISE MODES

Experimental conditions							Results (mean and ± 1 standard deviation)							
Simulator and suit mode	Slope, deg	Surface condition	Pack	Number of velocities	Number of subjects	Total tests	Gait or ascend/descend	Velocity, km/hr						
								2	4	6	8	9.7	11.3	12.8
Inclined plane, pressurized (press.) suit	0 (horiz)	Hard	I, 75 lb	4 each; walk, lope and run	6, with 2 repeating once	96	Walk	12.18 \pm 2.33	14.33 \pm 3.94	13.33 \pm 6.45	14.17 \pm 3.13			
							Lope			20.33 \pm 3.44	22.17 \pm 4.37	17.07 \pm 3.80	18.20 \pm 2.97	
							Run				19.58 \pm 6.73	18.67 \pm 5.71	18.50 \pm 6.02	16.67 \pm 3.68
Inclined plane, pressurized suit	0	Hard	I	1 each; walk, lope, and run	6, with all repeating twice	36	Walk	12.1 \pm 3.0						
							Lope			21.2 \pm 6.86				
							Run				20.9 \pm 6.13			
Inclined plane, subject in mufti (without press. suit)	0	Hard	I	4 each; walk, lope, and run	2	24	Walk	12.0 \pm 0.0	12.0 \pm 4.0	23.0 \pm 0.00	14.0 \pm 4.0			
							Lope			25.0 \pm 3.0	22.5 \pm 2.5	25.5 \pm 1.5	25.5 \pm 0.5	
							Run				17.5 \pm 3.5	15.5 \pm 5.5	24.0 \pm 4.0	20.5 \pm 4.5
Incl plane, mufti	0	Hard	I	Fatigue test	6	24								
Inclined plane, pressurized suit	0	Hard	I	Fatigue test	2	8								
Inclined plane, pressurized suit	0	Hard	II, 240 lb	4 each; walk, lope, and run	6	72	Walk	12.50 \pm 8.92	15.50 \pm 8.42	17.17 \pm 6.57	14.83 \pm 4.84			
							Lope			24.50 \pm 7.04	26.83 \pm 5.70	25.67 \pm 7.09	23.67 \pm 7.06	
							Run			22.67 \pm 5.82	28.67 \pm 4.96	23.50 \pm 6.08	22.20 \pm 5.37	
Inclined plane, pressurized suit	0	Hard	III, 400 lb	4 each; walk, lope, and run	2	24	Walk	15.0 \pm 0.00	18.0 \pm 5.00	16.5 \pm 4.5	19.0 \pm 2.0			
							Lope			29.0 \pm 5.0	28.5 \pm 4.5	22.0 \pm 0.00		
							Run			22.50 \pm 0.500	26.00 \pm 0.000	21.00 \pm 1.00	27.00 \pm 0.000	
TOSS (6-deg-of-freedom), pressurized suit	0	Hard	I	4 each; walk, lope, and run	6	72	Walk	12.0 \pm 0.00		15.0 \pm 0.0	16.5 \pm 1.5			
							Lope			17.5 \pm 2.06	18.0 \pm 3.74	17.8 \pm 5.0	18.4 \pm 1.62	
							Run				11.0	13.0 \pm 3.56	13.75 \pm 5.31	11.4 \pm 3.07
TOSS, press. suit	0	Smooth lunar	I	4	6	24		17.5 \pm 3.64	18.33 \pm 3.86	18.6 \pm 4.08	20.8 \pm 1.6			
TOSS, press. suit	0	Coarse lunar	I	4	6	24		18.5 \pm 3.73	20.5 \pm 2.22	21.67 \pm 6.26	21.17 \pm 3.48			
TOSS, pressurized suit	7.5	Hard	I	4	6	48	Ascend	29.5 \pm 5.44	31.83 \pm 1.77	32.83 \pm 3.48	32.17 \pm 2.54			
							Descend	8.67 \pm 3.59	8.5 \pm 5.25	9.5 \pm 4.23	11.67 \pm 4.68			
TOSS, pressurized suit	7.5	Smooth lunar	I	4	6	48	Ascend	30.17 \pm 2.34	34.83 \pm 4.71	31.5 \pm 4.09	31.5 \pm 3.5, N=2			
							Descend	11.0 \pm 2.58	9.67 \pm 3.99	9.67 \pm 4.38	9.67 \pm 3.99			
TOSS, pressurized suit	15	Hard	I	4	6	48	Ascend	40.0 \pm 4.2	41.33 \pm 2.92	42.0 \pm 3.16	33.0 \pm 7.0			
							Descend	-2.5 \pm 2.93	-1.33 \pm 4.78	-2.17 \pm 6.72	-4.17 \pm 6.36			
TOSS, pressurized suit	15	Smooth lunar	I	4	6	48	Ascend	36.33 \pm 3.99	38.0 \pm 2.74					
							Descend	3.67 \pm 2.36	4.83 \pm 2.61	7.67 \pm 4.75	5.5 \pm 3.1			
TOSS, pressurized suit	30	Hard	I	4	6	48	Ascend	40.5 \pm 5.5*						
							Descend	-20.2 \pm 2.93	-20.0 \pm 4.83	-23.17 \pm 2.79	-25.4 \pm 2.06			
Inclined plane, pressurized suit	7.5	Hard	I	4	6	48	Ascend	21.25 \pm 5.12	22.0 \pm 7.97	28.5 \pm 5.36	29.2 \pm 6.43			
							Descend	13.17 \pm 4.02	13.67 \pm 6.77	15.17 \pm 7.47	13.5 \pm 7.21			
Inclined plane, pressurized suit	7.5	Hard	II	4	6	48	Ascend	38.17 \pm 5.84	40.0 \pm 7.79	36.83 \pm 4.34	38.17 \pm 5.37			
							Descend	17.83 \pm 4.84	18.5 \pm 5.35	21.0 \pm 3.9	18.0 \pm 5.13			
Inclined plane, pressurized suit	15	Hard	I	4	6	48	Ascend	38.0 \pm 3.58	42.67 \pm 9.86	41.17 \pm 3.72	40.0 \pm 2.08			
							Descend	4.33 \pm 5.06	8.00 \pm 6.27	4.17 \pm 7.29	2.33 \pm 3.64			
Inclined plane, pressurized suit	30	Hard	I	4	6	48	Ascend	54.4 \pm 3.93	52.83 \pm 5.93	51.5 \pm 4.5				
							Descend	-12.8 \pm 4.58	-11.0 \pm 6.35	-12.33 \pm 6.88	-10.4 \pm 3.72			

*At 1 km/hr, maximum back angle (δ_0) was 49.6 \pm 3.77

*At 1 km/hr, maximum back angle (δ_D) was 49.6 \pm 3.77

TABLE 5-23

MAXIMUM HIP ANGLE (δ_h) FOR ALL SIMULATOR EXERCISE MODES

Experimental conditions							Results (mean and ± 1 standard deviation)							
Simulator and suit mode	Slope, deg	Surface condition	Pack	Number of velocities	Number of subjects	Total tests	Gait or ascend/descend	Velocity, km/hr						
								2	4	6	8	9.7	11.3	12.8
Inclined plane, pressurized (press.) suit	0 (horiz)	Hard	I, 75 lb	4 each; walk, lope and run	6, with 2 repeating once	96	Walk	37.88 \pm 5.25	40.5 \pm 5.22	44.0 \pm 4.32	44.17 \pm 3.76			
							Lope			40.83 \pm 2.73	44.83 \pm 5.55	42.20 \pm 1.95	44.07 \pm 1.74	
							Run				43.08 \pm 5.84	42.67 \pm 7.16	43.50 \pm 5.19	42.83 \pm 5.01
Inclined plane, pressurized suit	0	Hard	I	1 each; walk, lope, and run	6, with all repeating twice	36	Walk	37.05 \pm 5.03						
							Lope			40.75 \pm 7.27				
							Run				40.58 \pm 5.92			
Inclined plane, subject in mufti (without press. suit)	0	Hard	I	4 each; walk, lope, and run	2	24	Walk	31.0 \pm 0.0	35.0 \pm 4.0	46.0 \pm 0.0	40.0 \pm 4.0			
							Lope			49.0 \pm 7.0	42.5 \pm 1.5	50.0 \pm 0.0	50.0 \pm 1.0	
							Run				42.0 \pm 1.0	42.5 \pm 5.5	53.5 \pm 6.5	50.5 \pm 5.5
Incl plane, mufti	0	Hard	I	Fatigue test	6	24								
Inclined plane, pressurized suit	0	Hard	I	Fatigue test	2	8								
Inclined plane, pressurized suit	0	Hard	II, 240 lb	4 each; walk, lope, and run	6	72	Walk	36.83 \pm 7.65	39.83 \pm 6.54	41.33 \pm 4.53	39.17 \pm 3.72			
							Lope			41.67 \pm 7.34	45.00 \pm 4.47	48.00 \pm 9.38	48.00 \pm 8.19	
							Run				41.17 \pm 4.14	49.33 \pm 3.30	45.00 \pm 6.32	45.8 \pm 5.70
Inclined plane, pressurized suit	0	Hard	III, 400 lb	4 each; walk, lope, and run	2	24	Walk	34.5 \pm 2.5	39.0 \pm 6.0	40.0 \pm 3.0	49.5 \pm 2.5			
							Lope			47.0 \pm 4.0	51.5 \pm 9.5	48.0 \pm 0.00		
							Run				45.0 \pm 3.0	45.5 \pm 1.5	43.0 \pm 3.0	50.0 \pm 0.00
TOSS (6-deg-of-freedom), pressurized suit	0	Hard	I	4 each; walk, lope, and run	6	72	Walk	35.0 \pm 0.00		35.0 \pm 0.0	40.0 \pm 4.00			
							Lope			38.0 \pm 8.34	40.25 \pm 3.49	43.0 \pm 4.2	44.0 \pm 3.03	
							Run				33.67 \pm 0.47	39.67 \pm 6.13	39.5 \pm 5.17	36.6 \pm 5.89
TOSS, press. suit	0	Smooth lunar	I	4	6	24		37.5 \pm 2.18	38.33 \pm 5.56	40.0 \pm 3.52	43.4 \pm 1.50			
TOSS, press. suit	0	Coarse lunar	I	4	6	24		39.33 \pm 2.87	40.0 \pm 1.83	43.17 \pm 6.99	43.33 \pm 3.04			
TOSS, pressurized suit	7.5	Hard	I	4	6	48	Ascend	39.17 \pm 4.52	44.33 \pm 2.98	44.67 \pm 3.50	45.83 \pm 3.76			
							Descend	34.33 \pm 3.40	34.0 \pm 4.80	35.5 \pm 3.55	39.5 \pm 2.43			
TOSS, pressurized suit	7.5	Smooth lunar	I	4	6	48	Ascend	45.83 \pm 2.19	51.5 \pm 4.31	51.5 \pm 8.02	48.5 \pm 6.5, N=2			
							Descend	34.83 \pm 3.58	34.17 \pm 4.14	34.67 \pm 2.81	37.0 \pm 4.20			
TOSS, pressurized suit	15	Hard	I	4	6	48	Ascend	42.8 \pm 4.26	46.17 \pm 2.61	46.6 \pm 3.83	44.0 \pm 7.00			
							Descend	26.67 \pm 6.32	28.17 \pm 4.95	29.17 \pm 4.88	27.33 \pm 7.82			
TOSS, pressurized suit	15	Smooth lunar	I	4	6	48	Ascend	47.67 \pm 3.99	50.5 \pm 4.50					
							Descend	35.0 \pm 4.93	35.5 \pm 2.69	39.17 \pm 3.24	37.33 \pm 4.23			
TOSS, pressurized suit	30	Hard	I	4	6	48	Ascend	25.5 \pm 20.5						
							Descend	30.4 \pm 4.36	32.17 \pm 3.34	31.17 \pm 5.52	31.8 \pm 3.76			
Inclined plane, pressurized suit	7.5	Hard	I	4	6	48	Ascend	34.0 \pm 11.02	38.25 \pm 9.5	42.0 \pm 5.15	44.4 \pm 8.16			
							Descend	41.17 \pm 5.34	39.17 \pm 4.71	43.17 \pm 6.36	42.0 \pm 2.38			
Inclined plane, pressurized suit	7.5	Hard	II	4	6	48	Ascend	43.33 \pm 6.75	47.0 \pm 5.60	51.0 \pm 5.48	51.0 \pm 4.83			
							Descend	42.33 \pm 5.79	43.5 \pm 5.02	43.4 \pm 4.72	42.0 \pm 5.45			
Inclined plane, pressurized suit	15	Hard	I	4	6	48	Ascend	46.0 \pm 6.81	51.17 \pm 8.88	48.0 \pm 3.27	50.67 \pm 2.75			
							Descend	39.5 \pm 6.53	42.0 \pm 6.98	41.67 \pm 5.62	40.67 \pm 1.97			
Inclined plane, pressurized suit	30	Hard	I	4	6	48	Ascend	47.2 \pm 4.96	50.83 \pm 5.84	58.0 \pm 1.00				
							Descend	34.0 \pm 2.61	36.33 \pm 3.30	34.17 \pm 7.58	35.0 \pm 4.29			

*At 1 km/hr, maximum hip angle (δ_h) was 43.0 \pm 3.29

*At 1 km/hr, maximum hip angle (δ_h) was 43.0 \pm 3.29

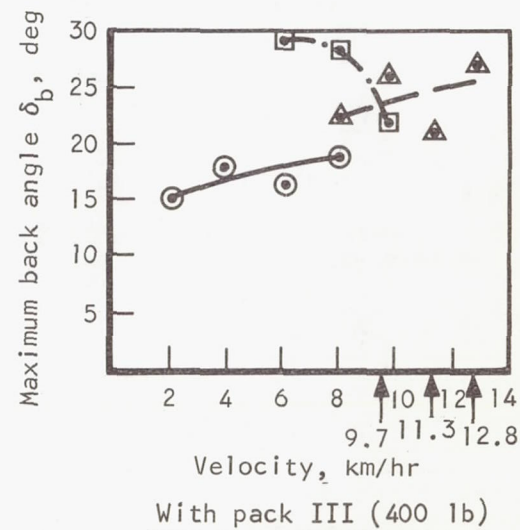
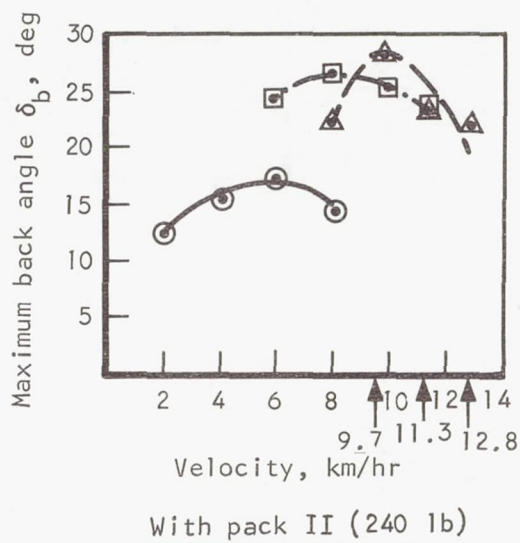
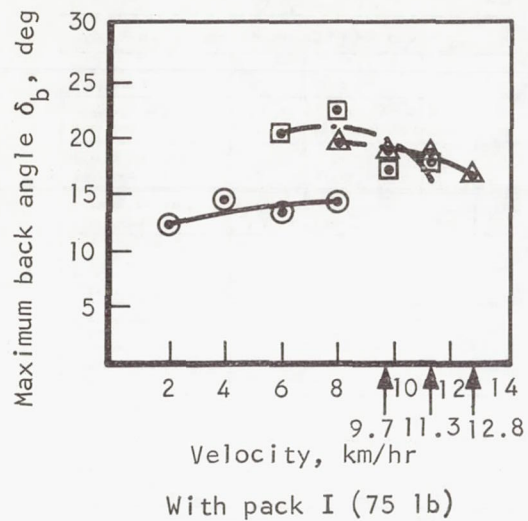
TABLE 5-24

MAXIMUM KNEE ANGLE (δ_k) FOR ALL SIMULATOR EXERCISE MODES

Experimental conditions							Results (mean and ± 1 standard deviation)							
Simulator and suit mode	Slope, deg	Surface condition	Pack	Number of velocities	Number of subjects	Total tests	Gait or ascend/descend	Velocity, km/hr						
								2	4	6	8	9.7	11.3	12.8
Inclined plane, pressurized (press.) suit	0 (horiz)	Hard	I, 75 lb	4 each; walk, lope and run	6, with 2 repeating once (Note 1)	96	Walk	54.33 \pm 13.42	61.33 \pm 6.47	62.33 \pm 8.96	61.83 \pm 8.27			
							Lope			64.83 \pm 4.15	66.17 \pm 3.58	70.8 \pm 5.81	68.8 \pm 6.58	
							Run				63.33 \pm 6.07	63.67 \pm 6.90	69.33 \pm 9.01	66.33 \pm 5.68
Inclined plane, pressurized suit	0	Hard	I	1 each; walk, lope, and run	6, with all repeating twice (Note 2)	36	Walk	55.8 \pm 14.02						
							Lope			72.5 \pm 4.35				
							Run				67.5 \pm 3.45			
Inclined plane, subject in mufti (without press. suit)	0	Hard	I	4 each; walk, lope, and run	2	24	Walk	53.0 \pm 0	61.0 \pm 1.0	60.0 \pm 0	61.0 \pm 4.0			
							Lope			84.5 \pm 15.5	82.0 \pm 2.0	79.5 \pm 0.5		
							Run				71.5 \pm 2.5	74.0 \pm 1.0	66.5 \pm 3.5	75.5 \pm 4.5
Incl plane, mufti	0	Hard	I	Fatigue test	6	24	Run				71.5 \pm 9.14	76.83 \pm 12.69	81.0 \pm 7.85	70.67 \pm 8.58
Inclined plane, pressurized suit	0	Hard	I	Fatigue test	2	8	Run				65.0 \pm 0.0	60.0 \pm 0.0	70.0 \pm 0.0	75.0 \pm 0.0
Inclined plane, pressurized suit	0	Hard	II, 240 lb	4 each; walk, lope, and run	6	72	Walk	44.83 \pm 9.63	49.5 \pm 7.65	55.0 \pm 5.83	60.17 \pm 3.8			
							Lope			70.33 \pm 8.03	65.0 \pm 5.97	69.83 \pm 6.36	68.33 \pm 2.87	
							Run				61.5 \pm 5.99	60.33 \pm 10.35	64.33 \pm 4.15	68.6 \pm 5.89
Inclined plane, pressurized suit	0	Hard	III, 400 lb	4 each; walk, lope, and run	2	24	Walk	39.0 \pm 1.0	47.0 \pm 1.0	46.5 \pm 0.5	48.5 \pm 1.5			
							Lope			61.0 \pm 3.0	63.0 \pm 3.0	65.0 \pm 0.0	0.00 \pm 0.0	
							Run				57.0 \pm 2.0	65.0 \pm 0.0	59.0 \pm 1.0	35.0 \pm 0.0
TOSS (6-deg-of-freedom), pressurized suit	0	Hard	I	4 each; walk, lope, and run	6	72	Walk	54.0 \pm 0.00		62.0 \pm 0.00	50.0 \pm 2.0			
							Lope			63.75 \pm 4.6	62.25 \pm 10.47	61.0 \pm 12.93	59.8 \pm 10.44	
							Run				60.67 \pm 7.76	55.0 \pm 15.51	61.5 \pm 5.85	64.2 \pm 8.89
TOSS, press. suit	0	Smooth lunar	I	4	6	24		46.75 \pm 2.77	48.0 \pm 2.83	59.8 \pm 7.81	65.4 \pm 3.44			
TOSS, press. suit	0	Coarse lunar	I	4	6	24		45.5 \pm 6.63	49.5 \pm 1.61	56.83 \pm 3.24	61.83 \pm 5.49			
TOSS, pressurized suit	7.5	Hard	I	4	6	48	Ascend	38.5 \pm 6.37	40.0 \pm 9.49	43.17 \pm 8.88	45.83 \pm 3.8			
							Descend	52.83 \pm 5.18	54.17 \pm 9.92	57.5 \pm 4.72	60.67 \pm 6.87			
TOSS, pressurized suit	7.5	Smooth lunar	I	4	6	48	Ascend	37.17 \pm 2.11	52.67 \pm 3.64	55.75 \pm 3.63	55.5 \pm 4.5			
							Descend	52.17 \pm 8.43	61.0 \pm 6.14	62.0 \pm 2.0	64.33 \pm 3.54			
TOSS, pressurized suit	15	Hard	I	4	6	48	Ascend	37.8 \pm 2.71	41.5 \pm 6.83	46.6 \pm 4.32	47.5 \pm 0.5			
							Descend	58.33 \pm 5.12	54.5 \pm 7.14	63.0 \pm 6.16	69.5 \pm 3.69			
TOSS, pressurized suit	15	Smooth lunar	I	4	6	48	Ascend	43.67 \pm 3.2	49.5 \pm 8.26					
							Descend	61.17 \pm 4.22	59.83 \pm 8.17	67.83 \pm 8.39	69.5 \pm 9.14			
TOSS, pressurized suit	30	Hard	I	4	6	48	Ascend	66.5 \pm 3.5*						
							Descend	84.4 \pm 5.95	66.5 \pm 5.53	76.33 \pm 6.37	87.0 \pm 4.0			
Inclined plane, pressurized suit	7.5	Hard	I	4	6	48	Ascend	44.75 \pm 4.55	52.25 \pm 8.95	61.0 \pm 2.92	59.0 \pm 4.98			
							Descend	65.5 \pm 5.85	66.67 \pm 8.2	65.33 \pm 6.7	68.5 \pm 11.5			
Inclined plane, pressurized suit	7.5	Hard	II	4	6	48	Ascend	39.0 \pm 8.77	42.0 \pm 6.06	50.0 \pm 10.71	55.33 \pm 10.78			
							Descend	57.5 \pm 5.56	54.67 \pm 16.74	59.8 \pm 7.33	64.83 \pm 10.71			
Inclined plane, pressurized suit	15	Hard	I	4	6	48	Ascend	37.6 \pm 5.24	49.0 \pm 7.42	58.0 \pm 6.3	64.67 \pm 8.58			
							Descend	77.0 \pm 5.16	76.67 \pm 6.16	71.5 \pm 8.42	79.5 \pm 8.4			
Inclined plane, pressurized suit	30	Hard	I	4	6	48	Ascend	46.0 \pm 4.52	54.33 \pm 11.86	49.5 \pm 1.5				
							Descend	92.0 \pm 3.95	79.5 \pm 8.98	78.17 \pm 13.5	84.2 \pm 11.58			

*At 1 km/hr, maximum knee angle (δ_k) was 47.6 \pm 4.08

*At 1 km/hr, maximum knee angle (δ_k) was 47.6 \pm 4.08



Conditions:

Inclined plane
 Suited, pressurized
 Hard surface, horizontal

○ ——— walk

□ ——— lope

△ ——— run

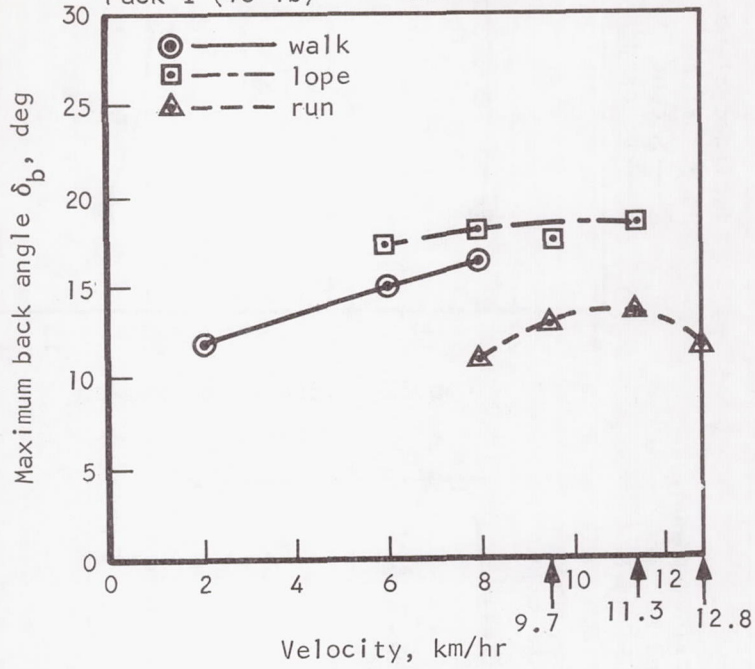
Figure 5-75. Effect of Gait on Maximum Back Angle, Horizontal Inclined-Plane Simulator

S-42726

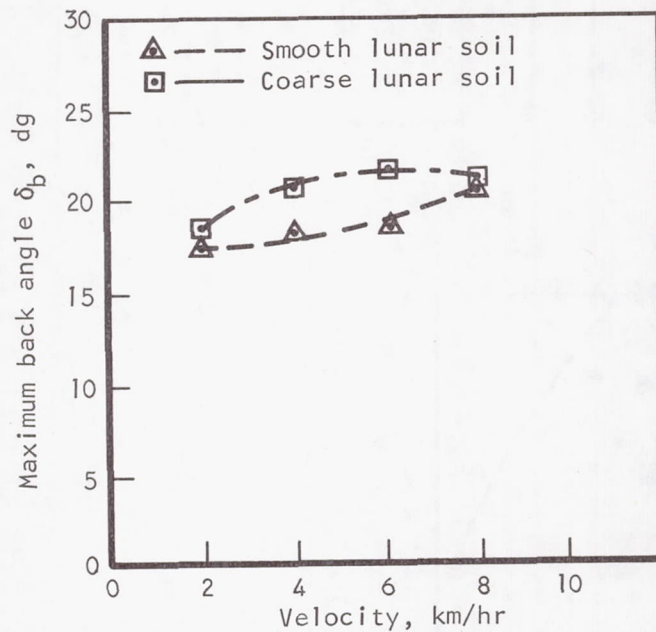
Conditions:

TOSS
Pack I (75 lb)

Suited, pressurized
Horizontal



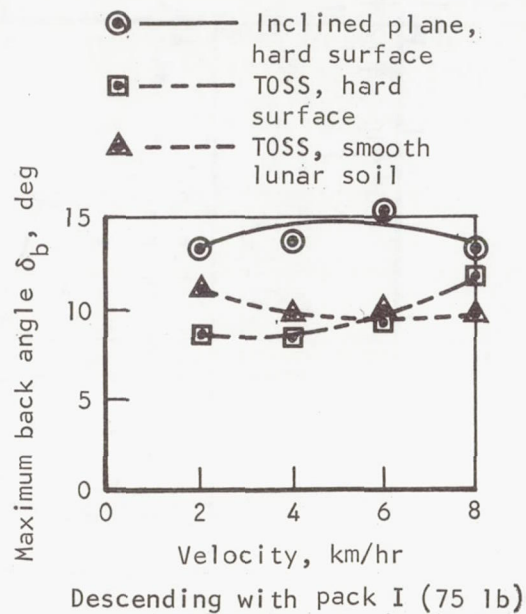
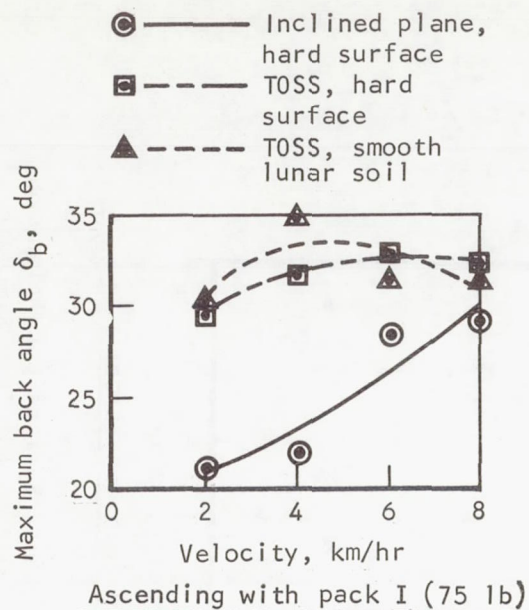
Hard surface



Lunar surface conditions

S-42727

Figure 5-76. Effect of Gait and Lunar Surface Conditions on Maximum Back Angle, Horizontal TOSS Simulator



Conditions:

Suited, pressurized
7.5-deg slope

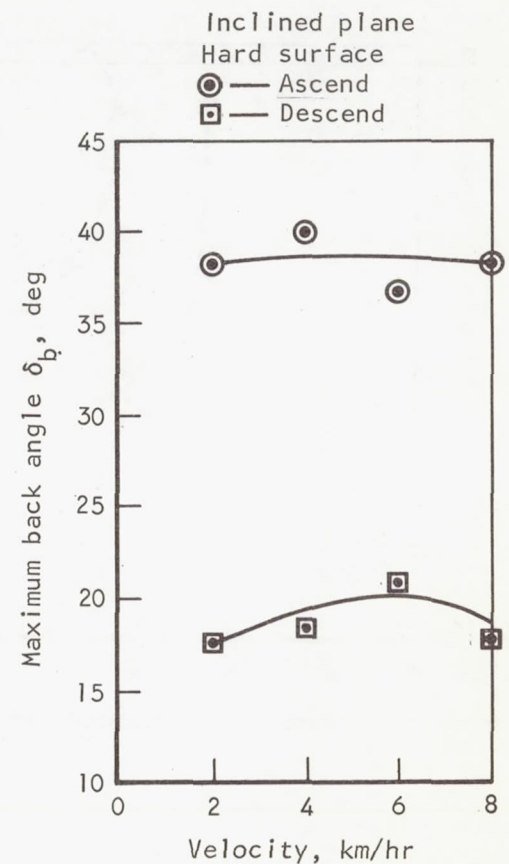


Figure 5-77. Maximum Back Angle vs Velocity, Comparison of Simulators and Surface Conditions, Traversing a 7.5-deg Slope

S-42766

Conditions:

Pack I (75 lb)
Suited, pressurized
15-deg slope

○ ——— Inclined plane, hard surface
□ — · — · — TOSS, hard surface
△ — — — — TOSS, smooth lunar soil

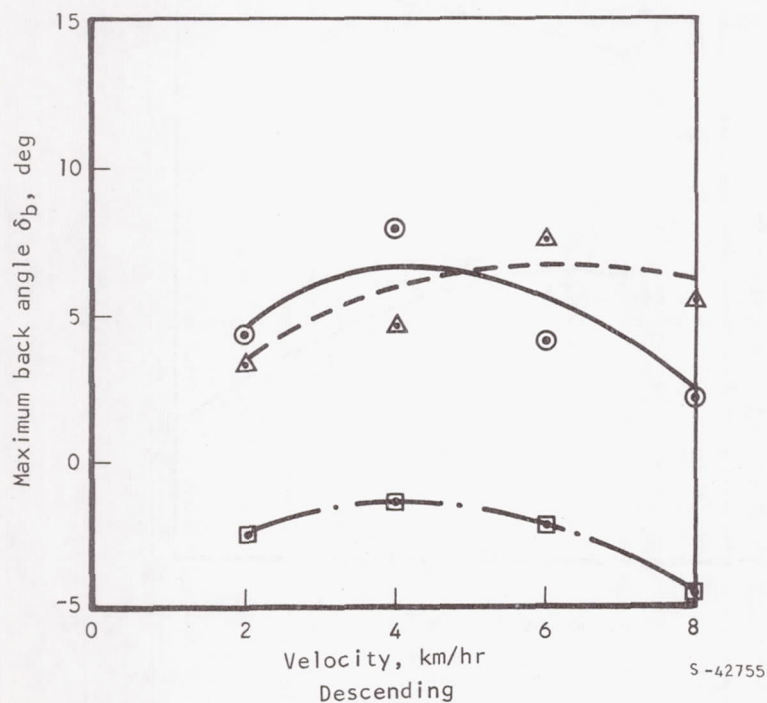
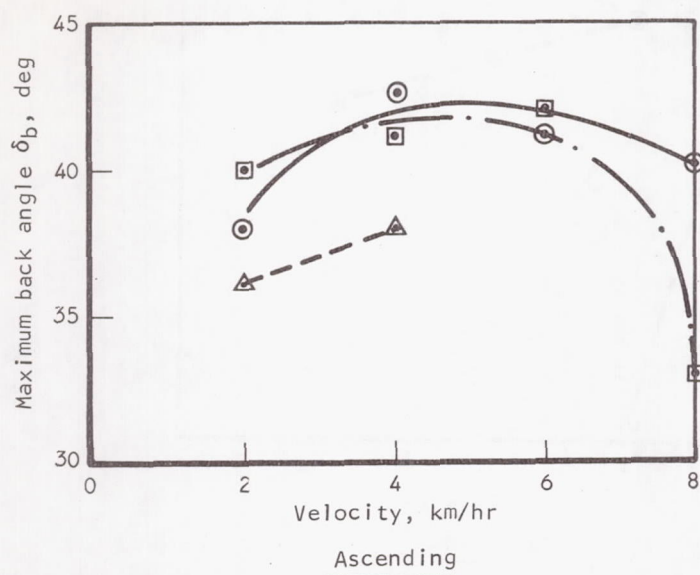


Figure 5-78. Maximum Back Angle vs Velocity. Comparison of Simulators and Surface Conditions, Traversing a 15-deg Slope

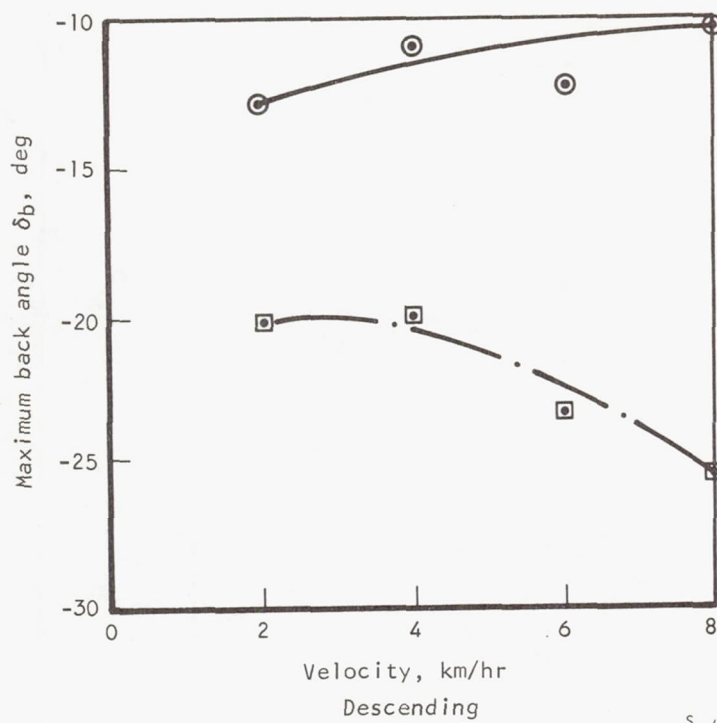
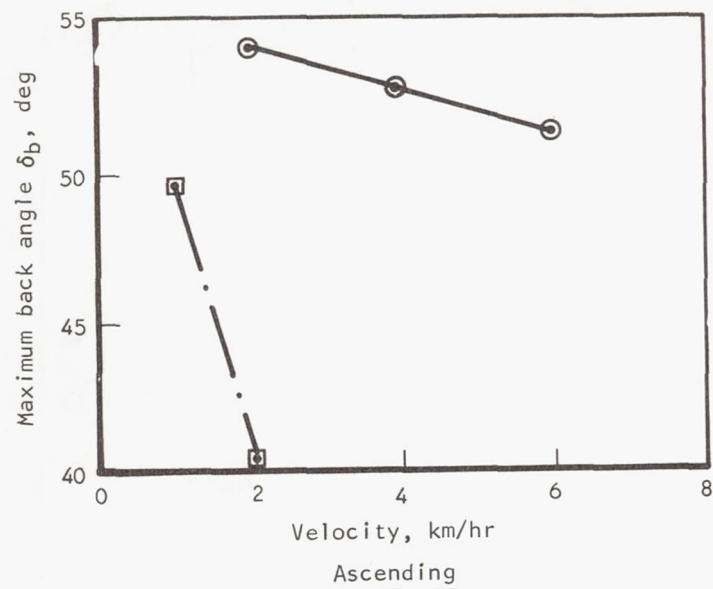
Conditions:

Pack I (75 lb)

Suited, pressurized

30-deg slope

○ ——— Inclined plane, hard surface
 □ - - - T0SS, hard surface



S-42768

Figure 5-79. Maximum Back Angle vs Velocity, Comparison of Simulators, Traversing a 30-deg Slope, Hard Surface

Conditions:

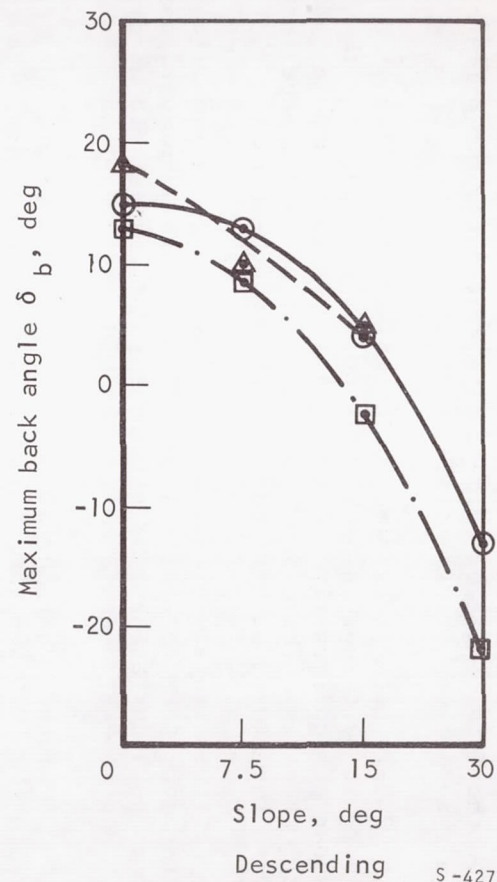
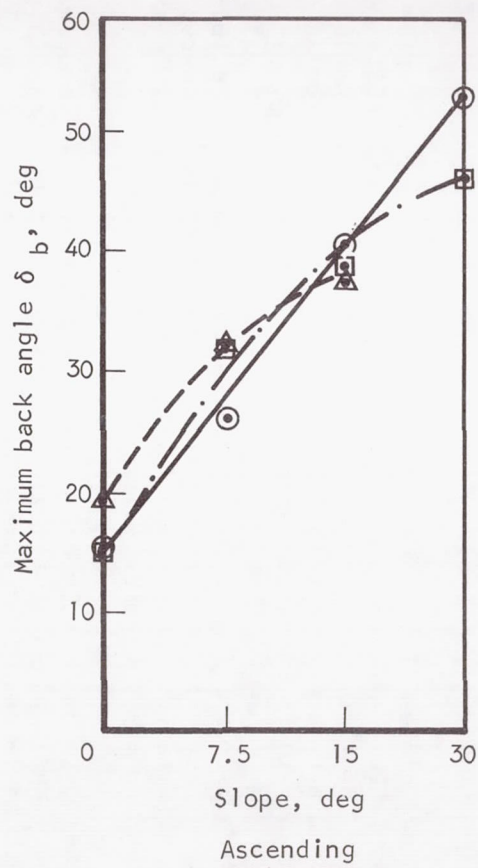
Pack I (75 lb)

Suited, pressurized

⊙— Inclin plane, hard surface

□— ··· TOSS, hard surface

△— - - TOSS, smooth lunar soil



S-42756

Figure 5-80. Maximum Back Angle vs Slope, Comparison of Simulators and Surface Conditions, Traversing with Pack I

There is a significant effect on back angle, however, caused by gait. Data on the inclined-plane simulator (Figure 5-75) show that increase in back angle between walk and run and between walk and lope is significant ($p < 0.01$). On the TOSS simulator (Figure 5-74), however, the difference between all gait conditions is significant ($p < 0.01$).

When the 240-lb pack is carried during walking on the inclined-plane simulator there is no change in back angle over that observed with the 75-lb pack. Back angle significantly increases with this pack, however, for both the run and lope gaits. There does not appear to be much change in this parameter when the 240-lb pack is replaced by the 400-lb pack.

Using the TOSS simulator (Figure 5-76), back angle is significantly higher for the lope than for the run ($p < 0.01$). The run, however, has a significantly lower back angle than the walk at 8 km/hr. There are no differences between walk and lope at 6 and 8 km/hr.

When the simulated lunar surface conditions are employed for horizontal locomotion with the TOSS simulator, back angle increases significantly over that formed with the hard surface ($p < 0.01$). There is no difference in back angle for the two lunar surface conditions (Figure 5-76).

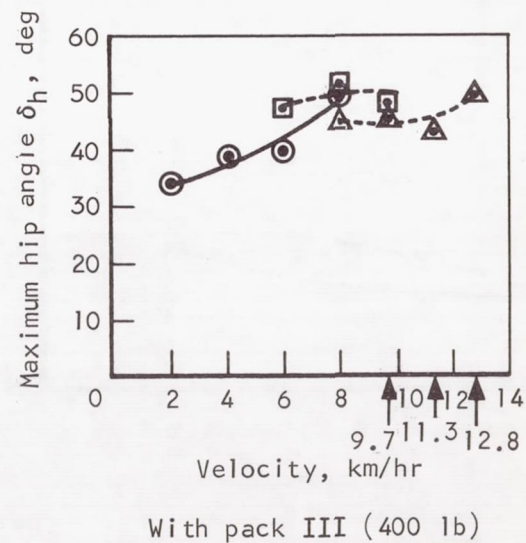
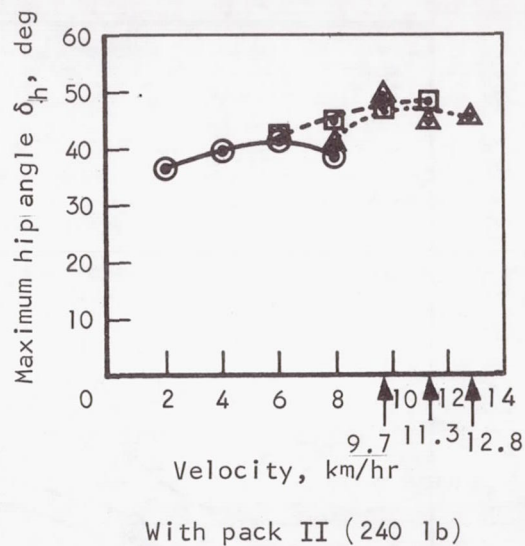
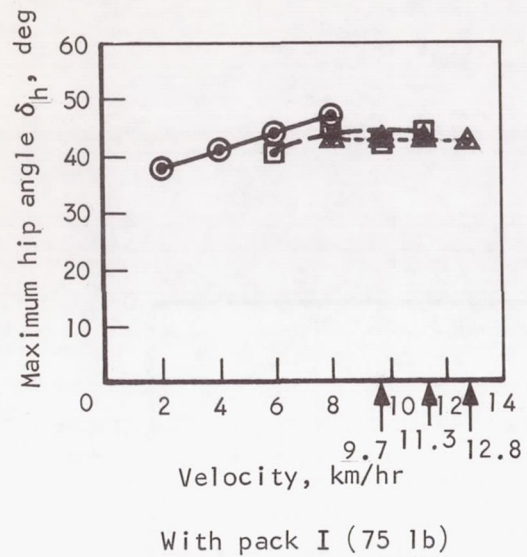
As shown in Figure 5-77, for ascending a 7.5-deg slope, a lower back angle is exhibited on the inclined-plane simulator than on the TOSS simulator ($p < 0.01$). Back angle is significantly higher on ascent than on descent for all conditions ($p < 0.01$).

For 15-deg slopes (Figure 5-78), there is no difference between simulators during ascent. During descent, however, back angle on the TOSS simulator is significantly lower for the hard surface condition than for the lunar soil or the inclined-plane simulator ($p < 0.01$). There was no difference in the data for the inclined-plane simulator and the lunar soil condition.

For 30-deg slopes (Figure 5-79), the ascending data on the TOSS simulator is insufficient for simulator comparisons. It was observed, however, that during descent, the subjects leaned farther back from vertical in the TOSS simulator than in the inclined-plane simulator.

Since velocity had little effect on back angle, a mean value was obtained from the individual values at all velocities; Figure 5-80 shows this mean value of back angle as a function of slope during ascent. It can be seen that there is a systematic increase of back angle with ascent and a systematic decrease with descent. Figure 5-80 illustrates a minimal difference between simulator conditions.

Hip angle, δ_h . - The mean values of the data obtained on hip angle, δ_h , during this program are shown in Figures 5-81 through 5-86. In general, hip angle was only occasionally influenced by velocity. Hip angle was altered only by velocity during the tests under the simulated lunar soil conditions.



Conditions:

Inclined plane
Suited, pressurized
Hard surface, horizontal

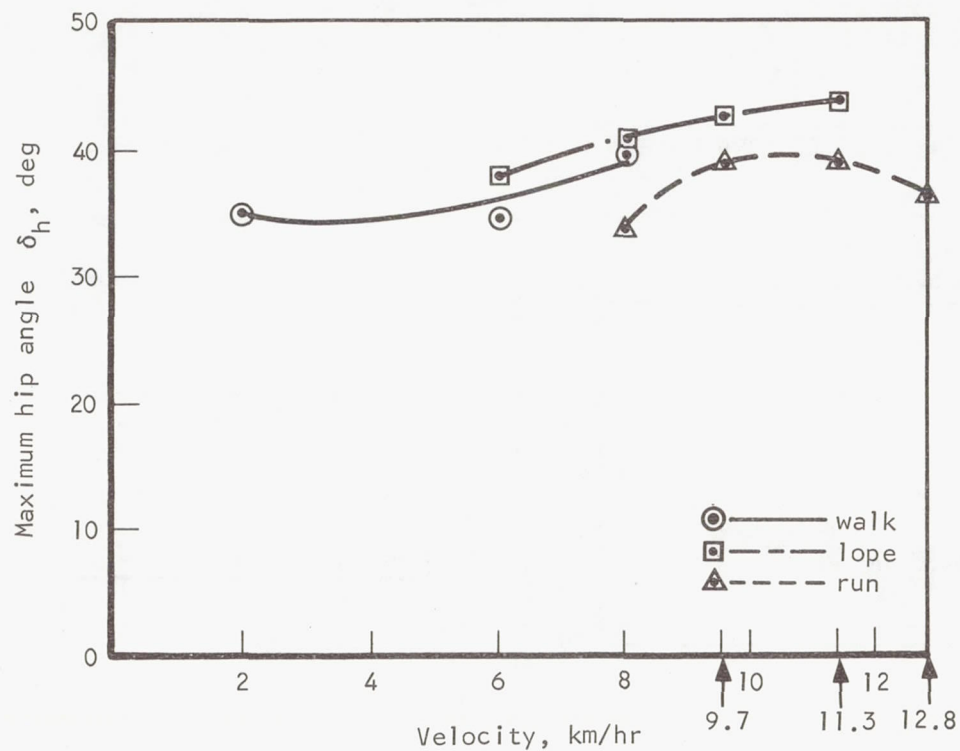
○— walk
□— lope
△— run

Figure 5-81. Maximum Hip Angle vs Velocity, Inclined-Plane Simulator, Horizontal Hard Surface

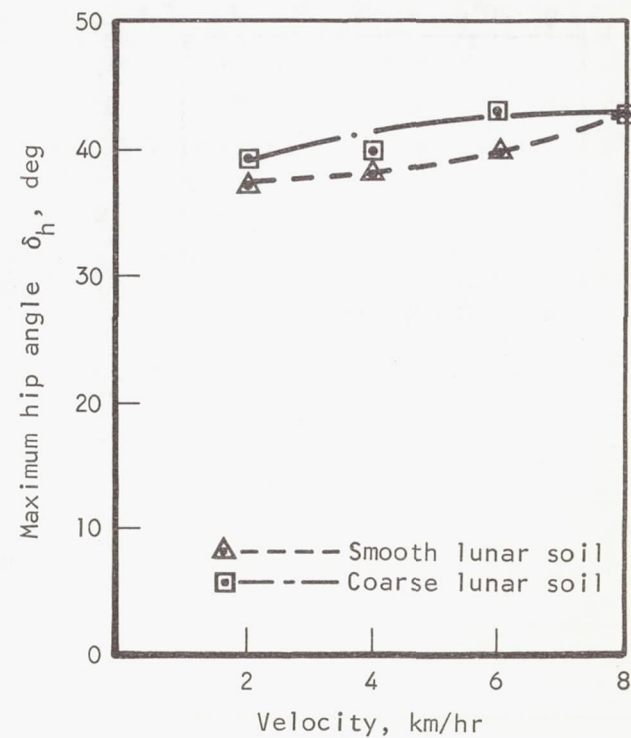
S-42735

Conditions:

TOSS
Pack I (75 lb)
Suited, pressurized
Horizontal



With hard surface



With lunar surface conditions

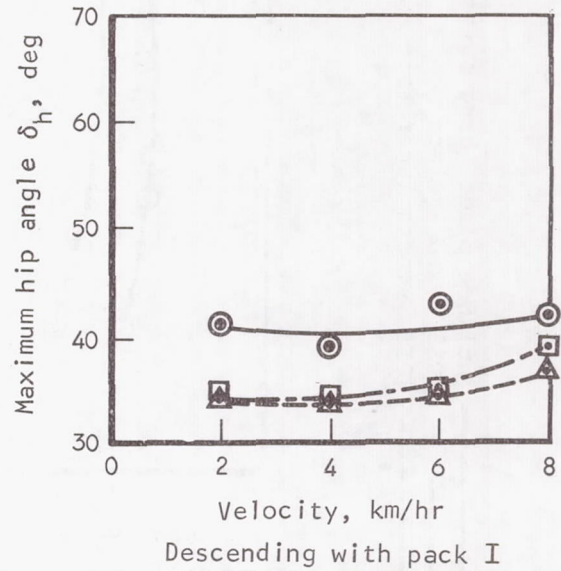
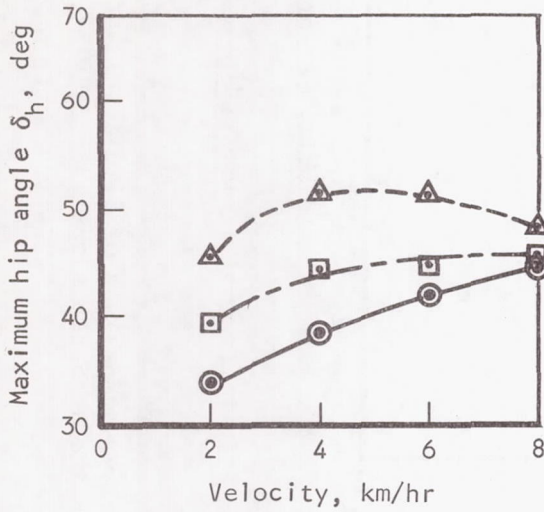
S-42764

Figure 5-82. Maximum Hip Angle vs Velocity, Horizontal TOSS Simulator

Conditions:

Pack I (75 lb)
Suited, pressurized
7.5-deg slope

○— Inclined plane, hard surface
□— TOSS, hard surface
△— TOSS, smooth lunar soil

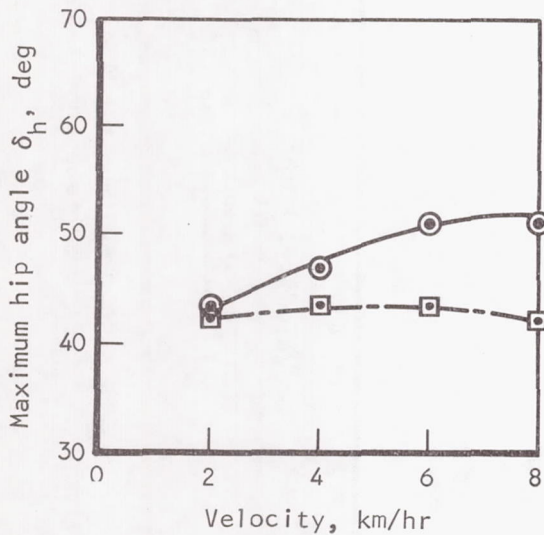


Traversing with pack II

Conditions:

Inclined plane
Pack II (240 lb)
Suited, pressurized
Hard surface

○— 7.5-deg slope, ascend
□— 7.5-deg slope, descend



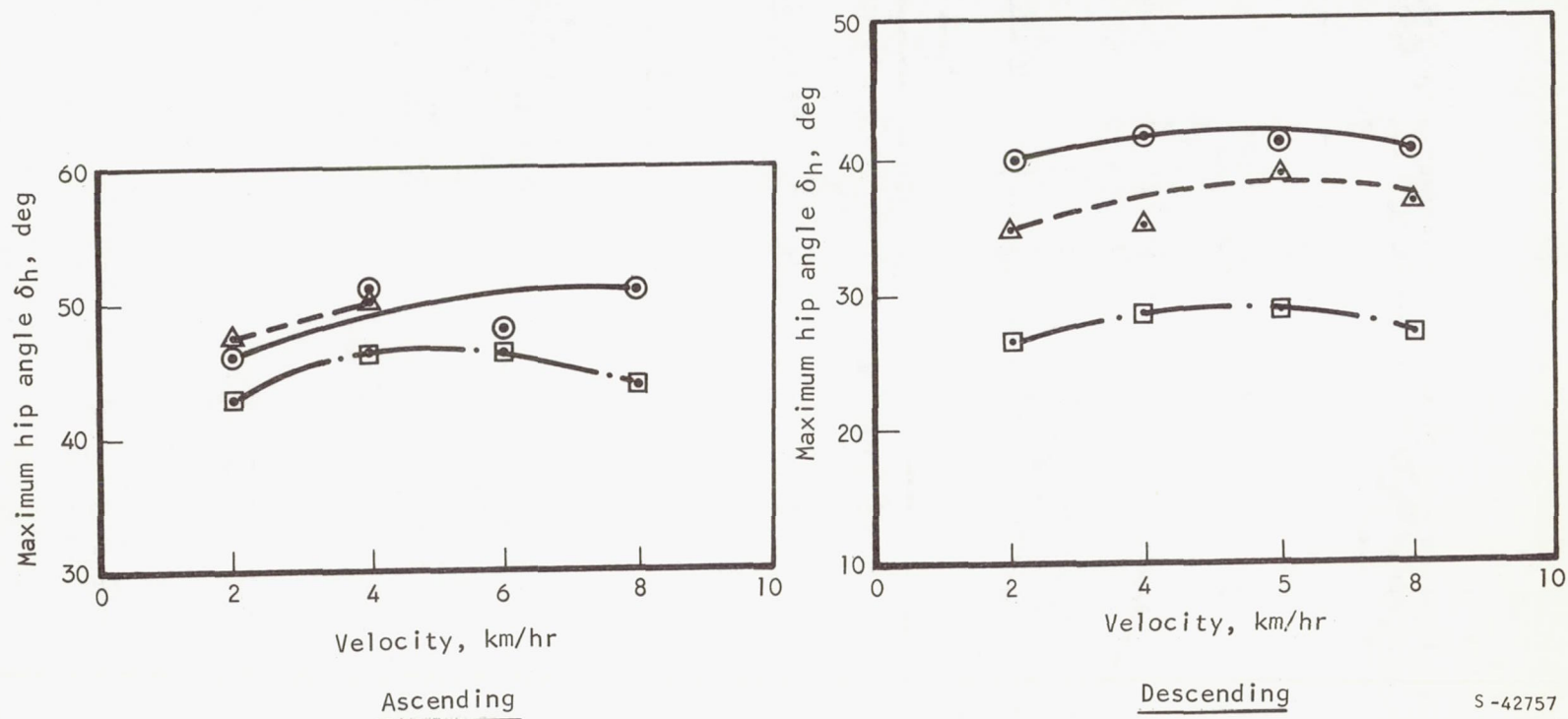
S-42765

Figure 5-83. Maximum Hip Angle vs Velocity, Comparison of Simulators and Surface Conditions, Traversing a 7.5-deg Slope

Conditions:

Pack I (75 lb)
 Suited, pressurized
 15-deg slope

○ ————— Inclined plane, hard surface
 □ — · · · · · TOSS, hard surface
 △ — - - - - TOSS, smooth lunar soil



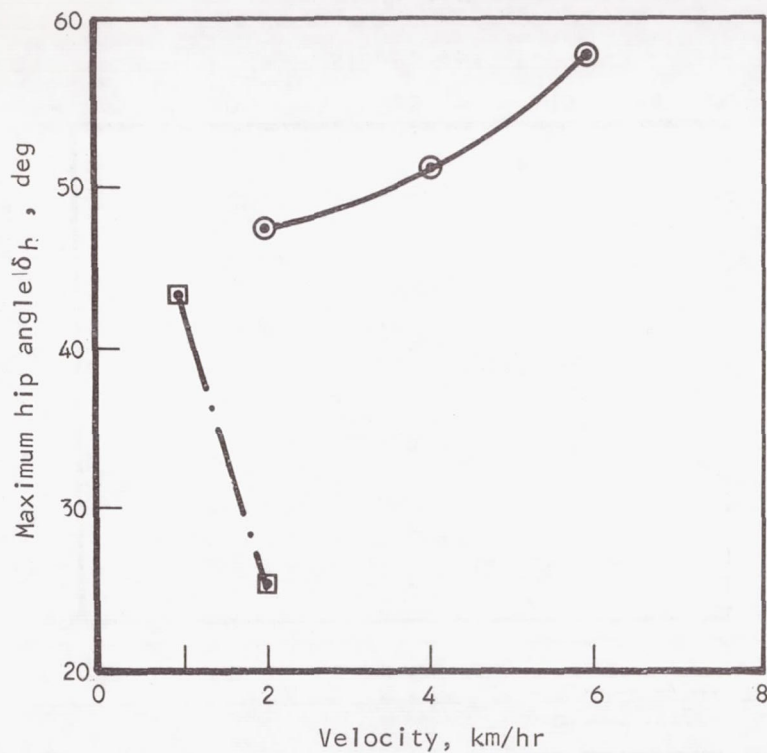
S-42757

Figure 5-84. Maximum Hip Angle vs Velocity, Comparison of Simulators and Surface Conditions, Traversing a 15-deg slope

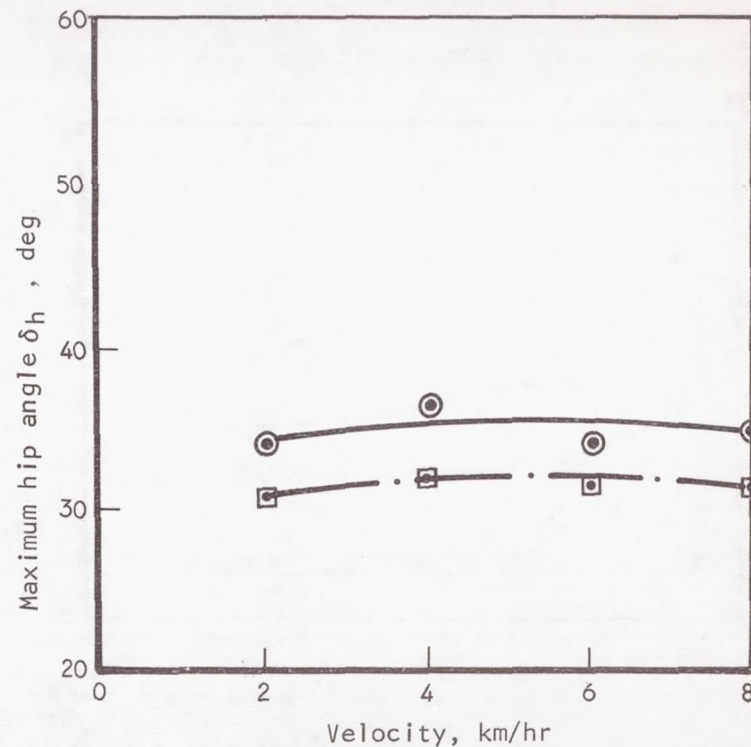
Conditions:

Pack I (75 lb)
 Suited, pressurized
 30-deg slope
 Hard surface

⊙ ——— Inclined plane
 □ — · — TOSS



Ascending



Descending

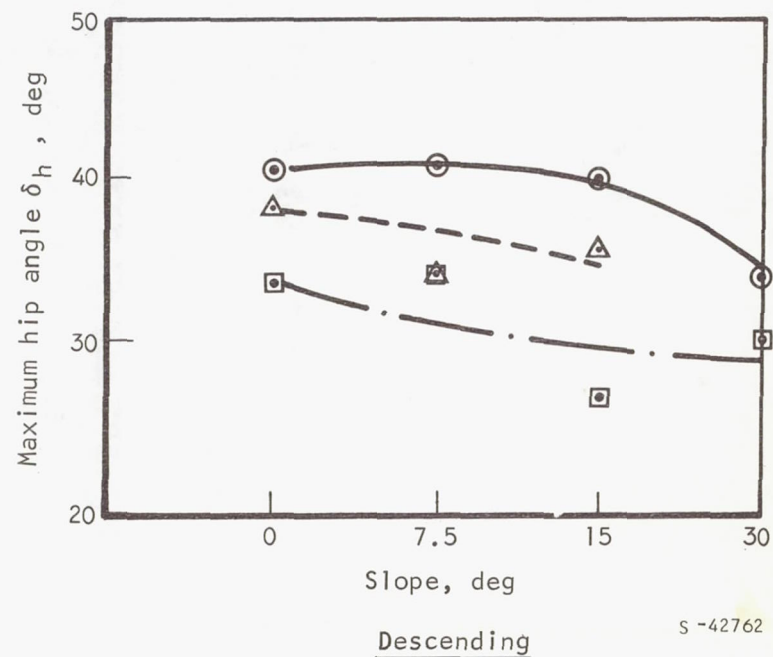
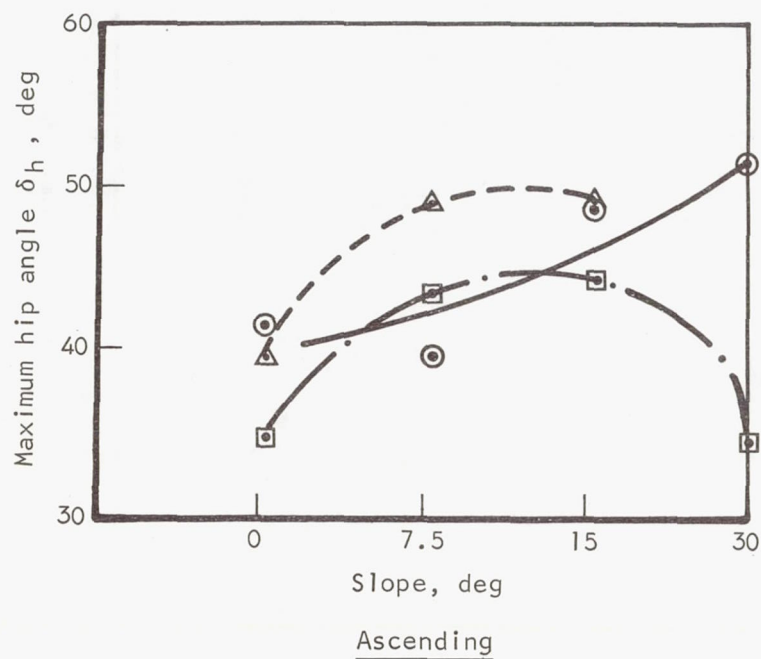
S-42763

Figure 5-85. Maximum Hip Angle vs Velocity, Comparison of Simulators, Traversing a 30-deg Slope, Hard Surface

Conditions:

Pack I (75 lb)
Suited, pressurized

- ⊙ ————— Inclined plane, hard surface
- — · — · — TOSS, hard surface
- △ — — — — TOSS, smooth lunar soil



S -42762

Figure 5-86. Maximum Hip Angle vs Slope, Comparison of Simulators and Surface Conditions, Traversing with Pack I

A significantly higher hip angle results with the 240-lb pack than with the 75-lb pack ($p < 0.05$), during lope and run modes on the inclined-plane simulator (Figure 5-81). This was the only statistically significant effect on hip angle observed with the inclined-plane simulator.

With the TOSS simulator and a hard surface (Figure 5-82), the loping gait produced a higher hip angle than did the running gait ($p < 0.01$). With the TOSS simulator and lunar soil conditions, hip angle significantly increased as velocity increased ($p < 0.01$). There were no differences, however, as a function of the two lunar soil conditions, and no significant differences between lunar surfaces and hard surfaces.

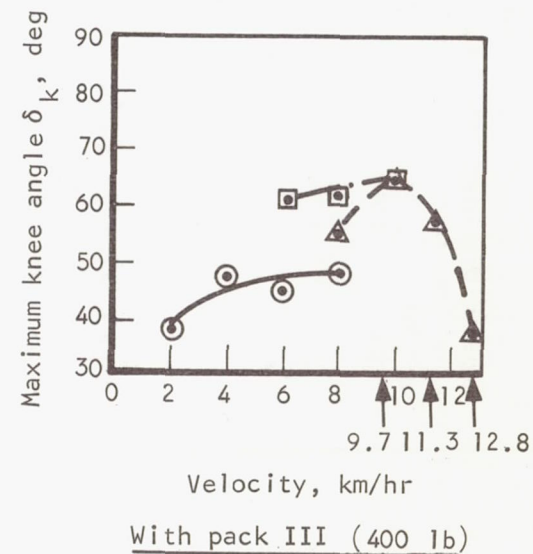
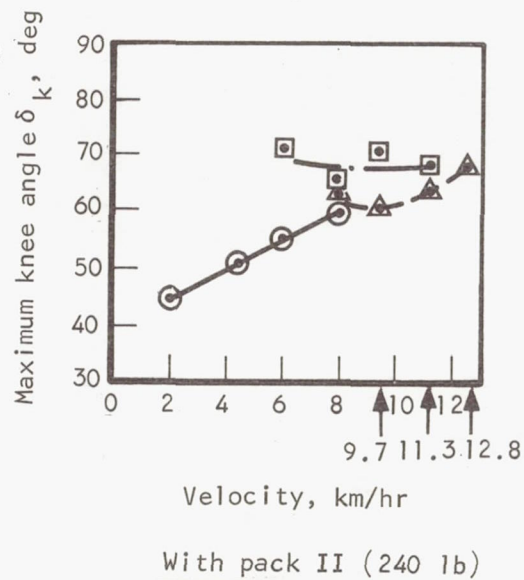
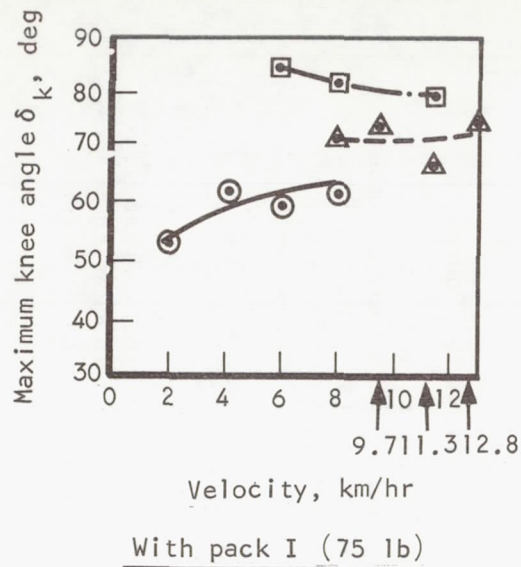
During locomotion tests on the 7.5-deg slope, hip angle for the inclined plane was significantly lower than for the TOSS simulator during ascent ($p < 0.01$) and significantly higher during descent ($p < 0.01$) (Figure 5-83). In addition, during ascent at 7.5 deg, hip angle was significantly increased by velocity ($p < 0.01$) for the inclined plane, TOSS/hard surface, and TOSS/smooth lunar surface conditions. At 7.5 deg on the inclined-plane simulator, a 240-lb pack load produces a higher hip angle during ascent than is observed for descending conditions (Figure 5-83).

During ascent at 15 deg, there is a significant effect of velocity ($p < 0.05$), with the higher velocities producing higher values for hip angle, but no demonstrable difference between simulators (Figure 5-84). On the other hand, there is no velocity effect during descent, but the difference between each simulator condition is significant ($p < 0.01$), with the highest values for hip angle occurring on the inclined-plane simulator, and the TOSS/hard surface and TOSS/lunar smooth surface producing lower values (Figure 5-84).

For a 30-deg slope (Figure 5-85), there are significant differences between simulators ($p < 0.01$), with the inclined-plane simulator producing higher values of hip angle during both ascent and descent. Since velocity had little effect on hip angle, the data were averaged across velocity and are shown in Figure 5-86 as a function of slope.

Knee angle, δ_k . - Mean values of knee angle, δ_k , are shown in Figures 5-87 through 5-92. Like hip angle, knee angle is unaffected by velocity during runs on the horizontal hard surface with either simulator (Figure 5-87). There is, however, a significant difference between each of the gaits on the inclined plane ($p < 0.01$), with higher values of knee angle for running than for walking, and with loping higher than running. This relationship holds for the 75-lb, 240-lb, and 400-lb pack conditions. There is also an effect from pack loads, with each heavier pack producing a significantly lower knee angle.

With the TOSS simulator horizontal (Figure 5-88), there is no gait or velocity effect with the hard surface. With the two simulated lunar surfaces, however, there is a significant velocity effect, with knee angle increasing with velocity ($p < 0.01$). There is no differential effect between the two lunar soil conditions.



Conditions:

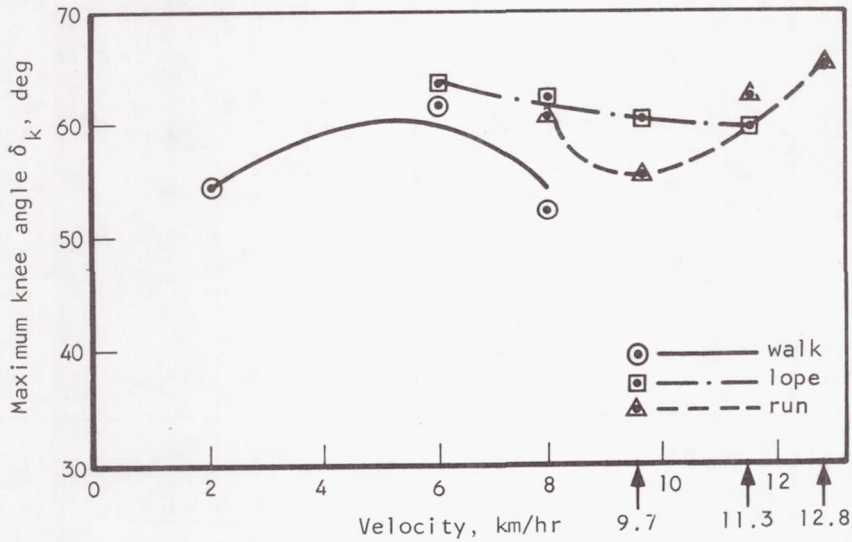
Inclined plane
Suited, pressurized
Hard surface, horizontal

○ — walk
□ — lope
△ — run

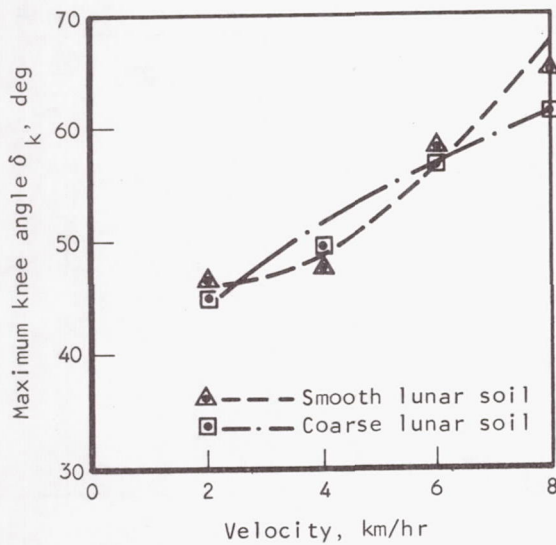
Figure 5-87. Maximum Knee Angle vs Velocity, Inclined-Plane Simulator, Horizontal Hard Surface

S-42758

Conditions:
 TOSS
 Pack I (75 lb)
 Suited, pressurized
 Horizontal



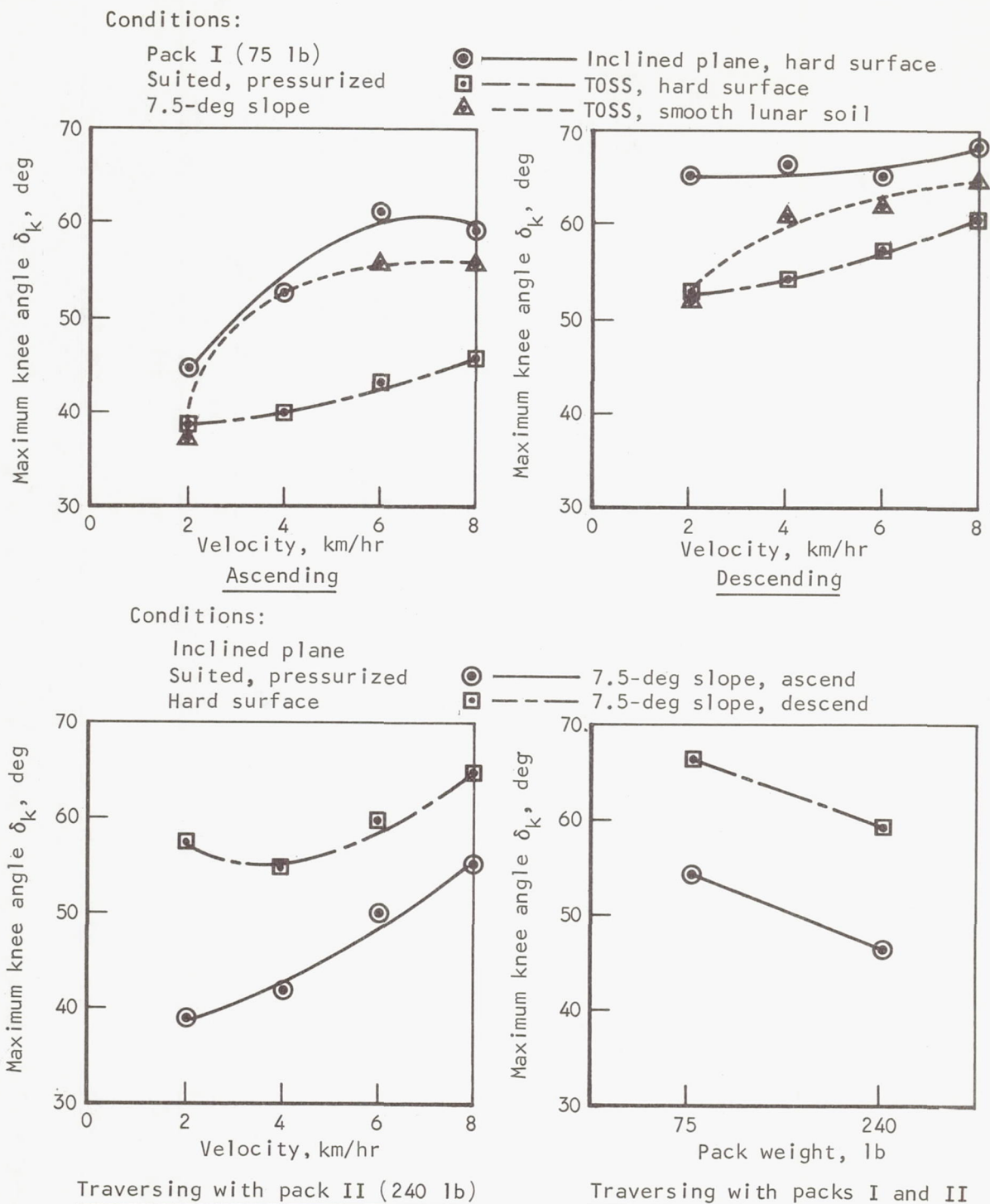
With hard surface conditions



With lunar surface conditions

S-42767

Figure 5-88. Maximum Knee Angle vs Velocity, Horizontal TOSS Simulator.



S-42753

Figure 5-89. Maximum Knee Angle vs Velocity and Load, Traversing a 7.5-deg Slope

Conditions:

Pack I (75 lb)
Suited, pressurized
15-deg slope

○—Inclined plane, hard surface
□—T0SS, hard surface
△—T0SS, smooth lunar soil

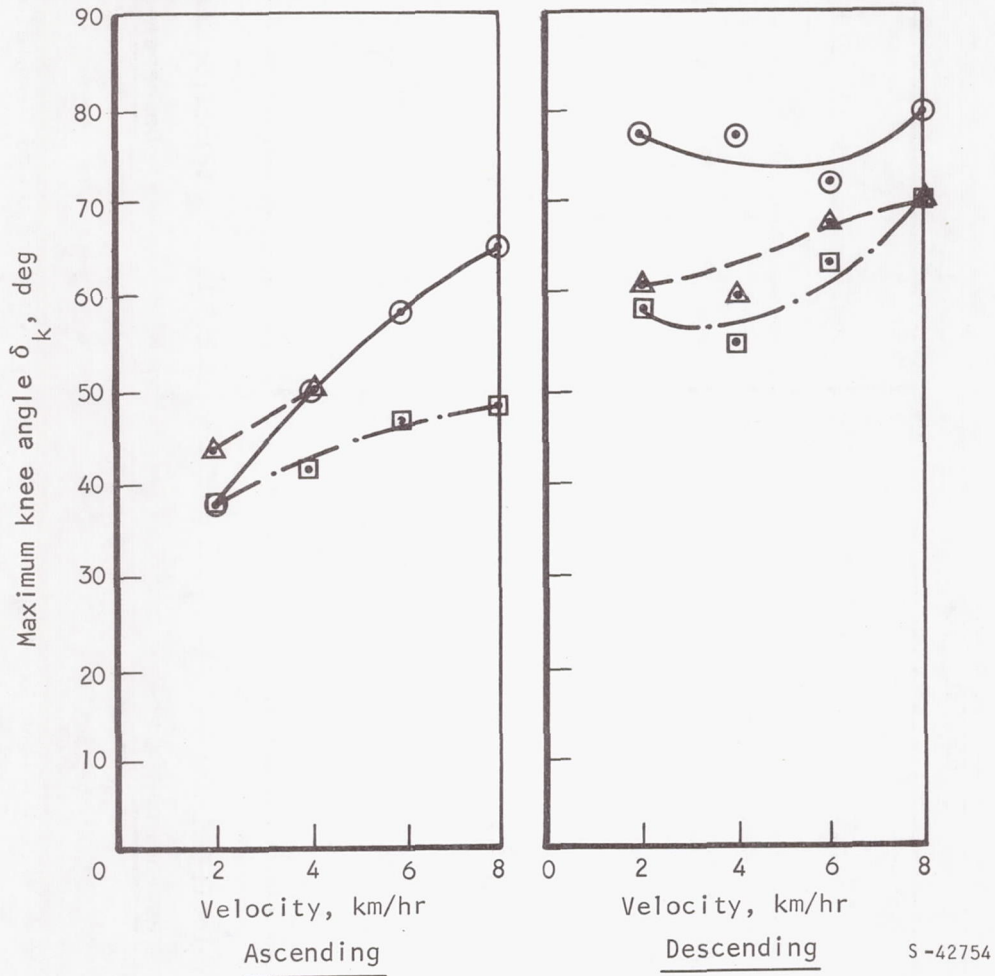
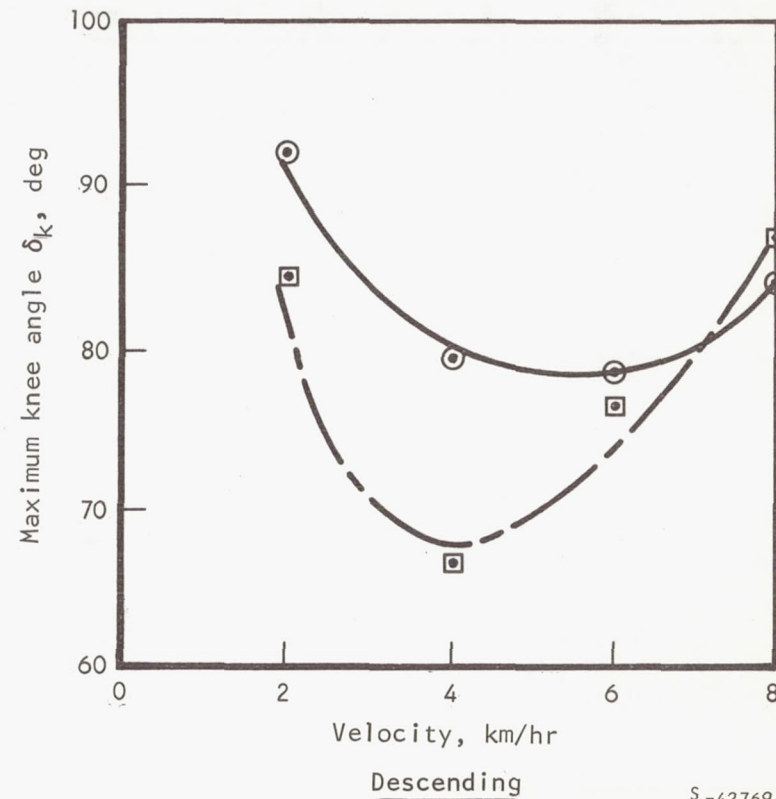
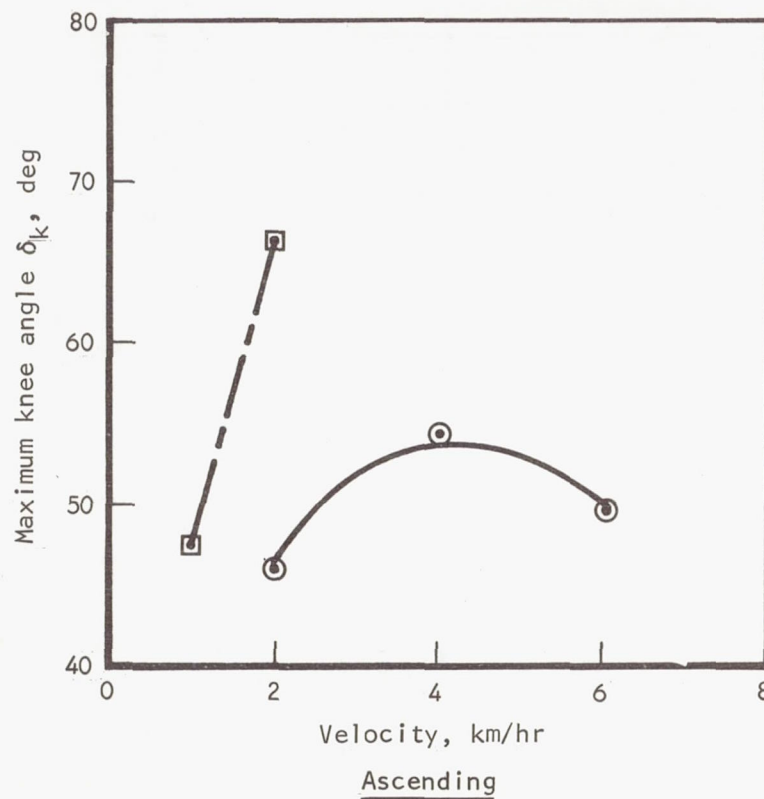


Figure 5-90. Maximum Knee Angle vs Velocity, Comparison of Simulators and Surface Conditions, Traversing a 15-deg Slope

Conditions:

Pack I (75 lb)
Suited, pressurized
30-deg slope
Hard surface

○ — Inclined plane
□ — TOSS



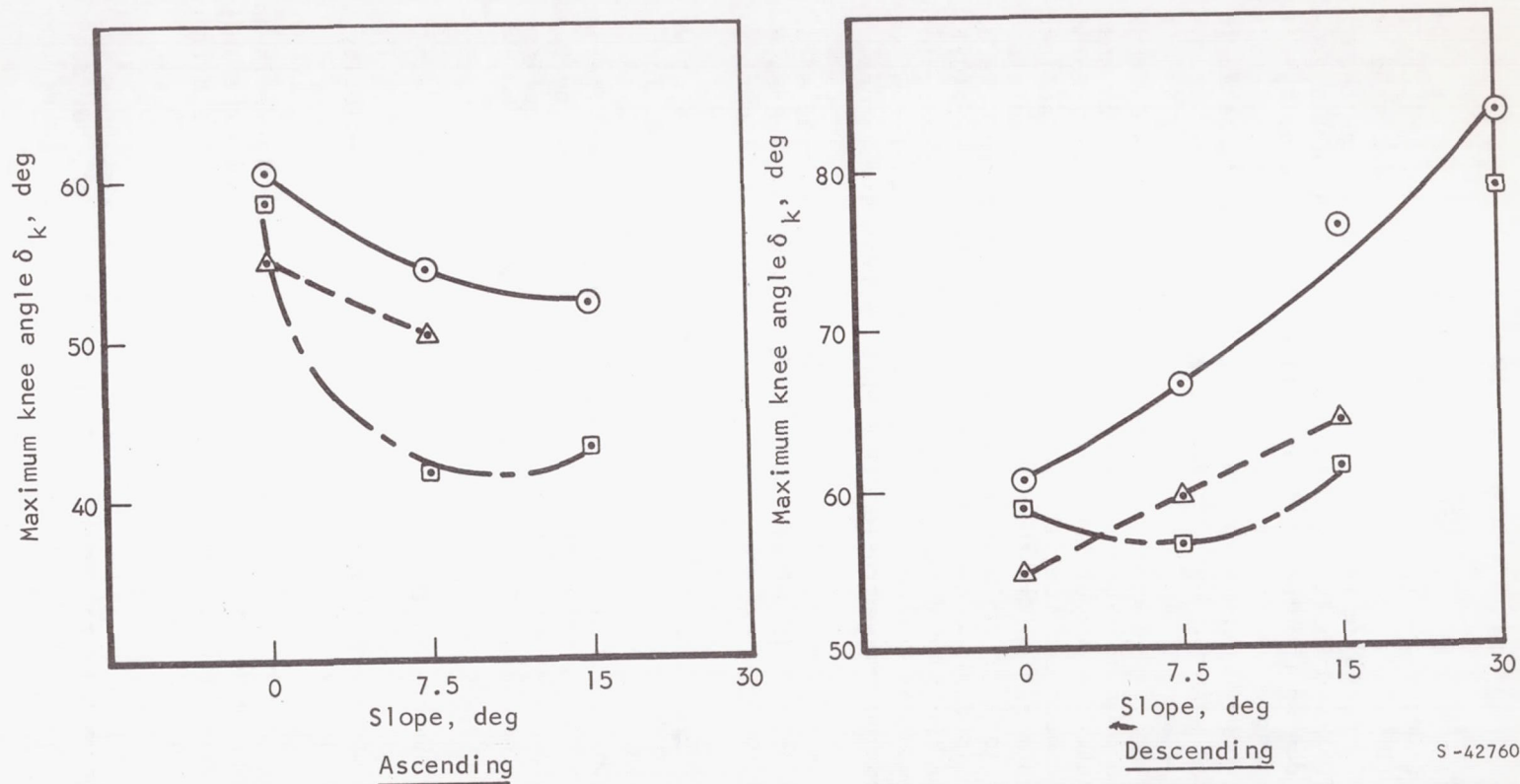
S-42769

Figure 5-91. Maximum Knee Angle vs Velocity, Comparison of Simulators, Traversing a 30-deg Slope, Hard Surface

Conditions:

Pack I (75 lb)
Suited, pressurized

- ——— Inclined plane, hard surface
 □ ——— TOSS, hard surface
 ▲ ——— TOSS, smooth lunar soil



S-42760

Figure 5-92. Maximum Knee Angle vs Slope, Comparison of Simulators and Surface Conditions, Traversing with Pack I

As shown in Figure 5-89, velocity and simulator effects are significant for ascending a 7.5-deg slope ($p < 0.01$), while only simulator effects are significant on descent ($p < 0.01$). In both ascent and descent cases, the inclined plane produces a higher value for knee angle at all velocities than the TOSS/hard surface and TOSS/smooth lunar surface conditions. When the 240-lb pack is carried at 7.5 deg on the inclined-plane simulator, a velocity effect is observed with knee angle increasing with velocity. Knee angle is also systematically greater on descent than ascent and is higher with the 75-lb pack than with the 240-lb pack during both ascent and descent.

In contrast, the 15-deg ascending slope tests (Figure 5-90) show that velocity and simulator conditions produce significant effects on knee angle ($p < 0.01$), with greater values of knee angle occurring at the higher velocities. During tests on the hard surface, the values obtained on the inclined-plane simulator increased more rapidly than they did on the TOSS simulator. No significant change in knee angle occurred with velocity during the descending tests, but the inclined plane had higher values than for either surface on the TOSS. The data for the 30-deg slope (Figure 5-91) are too sparse for ascent to allow comparison. For descent, however, there is a significant velocity effect ($p < 0.01$), but no demonstrable difference between simulators.

The mean values for knee angle across velocity are plotted as a function of slope in Figure 5-92. The effect of increasing slope to increase knee angle during descent and to decrease knee angle during ascent is significant ($p < 0.01$).

Shirt-sleeve conditions. - Body position data are compared between shirt-sleeve and pressurized suit conditions at comparable velocities in Figures 5-93, 5-94, and 5-95. It can be seen from this data that, as with locomotive index, stride length, and step rate, back angle shows little difference between the shirt-sleeve and the pressurized suit modes. This is not the case for hip angle and knee angle. Hip angle is larger and knee angle is smaller in the shirt-sleeve modes than when a pressurized suit is worn.

Summary of Observations on Body Angles

1. There is no significant change in back angle, δ_b , with velocity changes for horizontal locomotion.
2. The type of gait, however, does influence back angle. There is an increase in back angle between the walk and run gaits and between the walk and lope gaits on the inclined-plane simulator. Back angle is different for all gaits on the TOSS simulator.
3. When the 240-lb pack is substituted for the 75-lb pack, back angle does not change for walking on the inclined-plane simulator, but does increase with lope and run gaits. Back angle increases for all gaits when the 400-lb pack is substituted for the 75-lb pack.

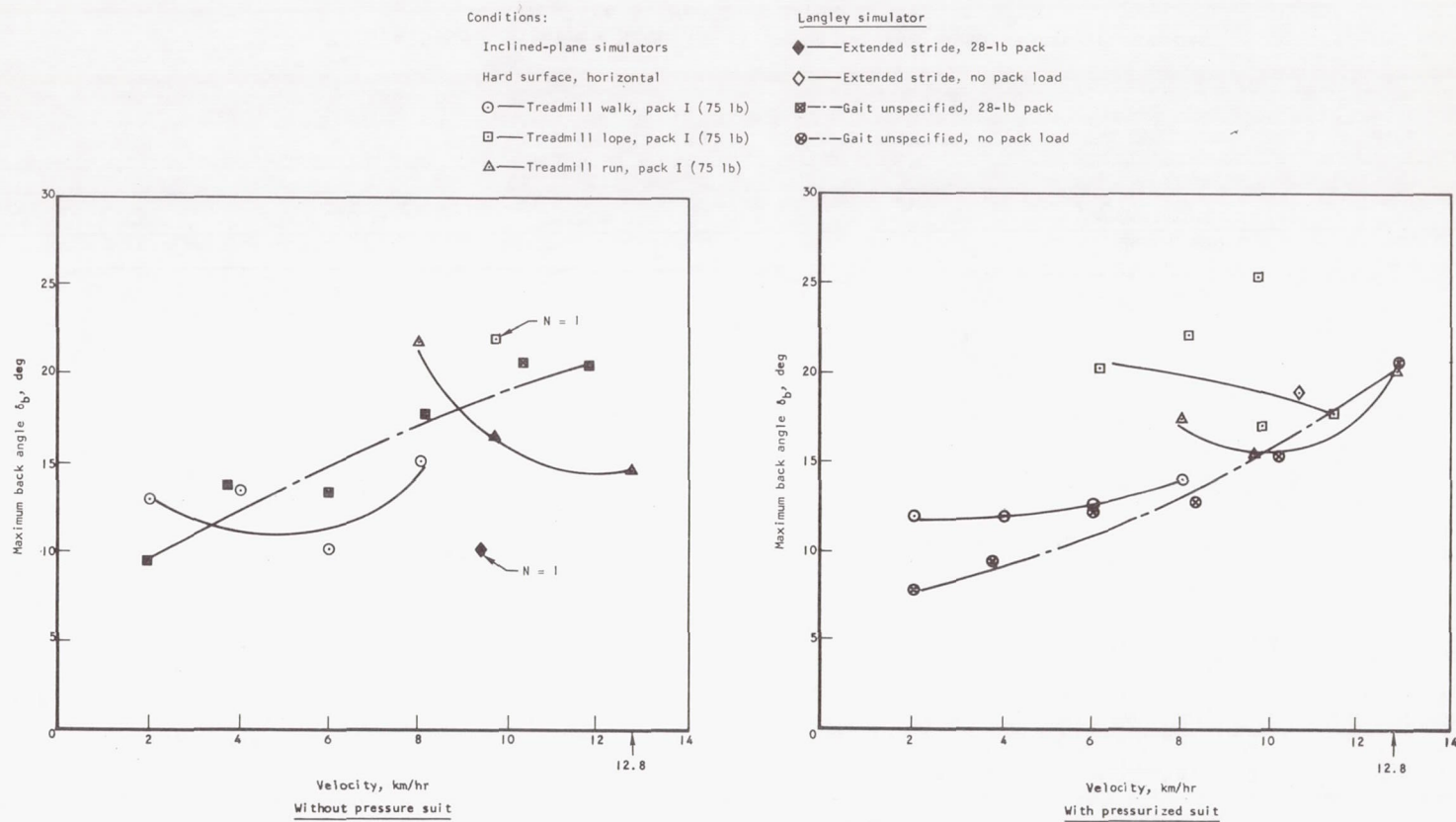


Figure 5-93 Maximum Back Angle vs Velocity, Comparison of Various Simulators, Horizontal Hard Surface

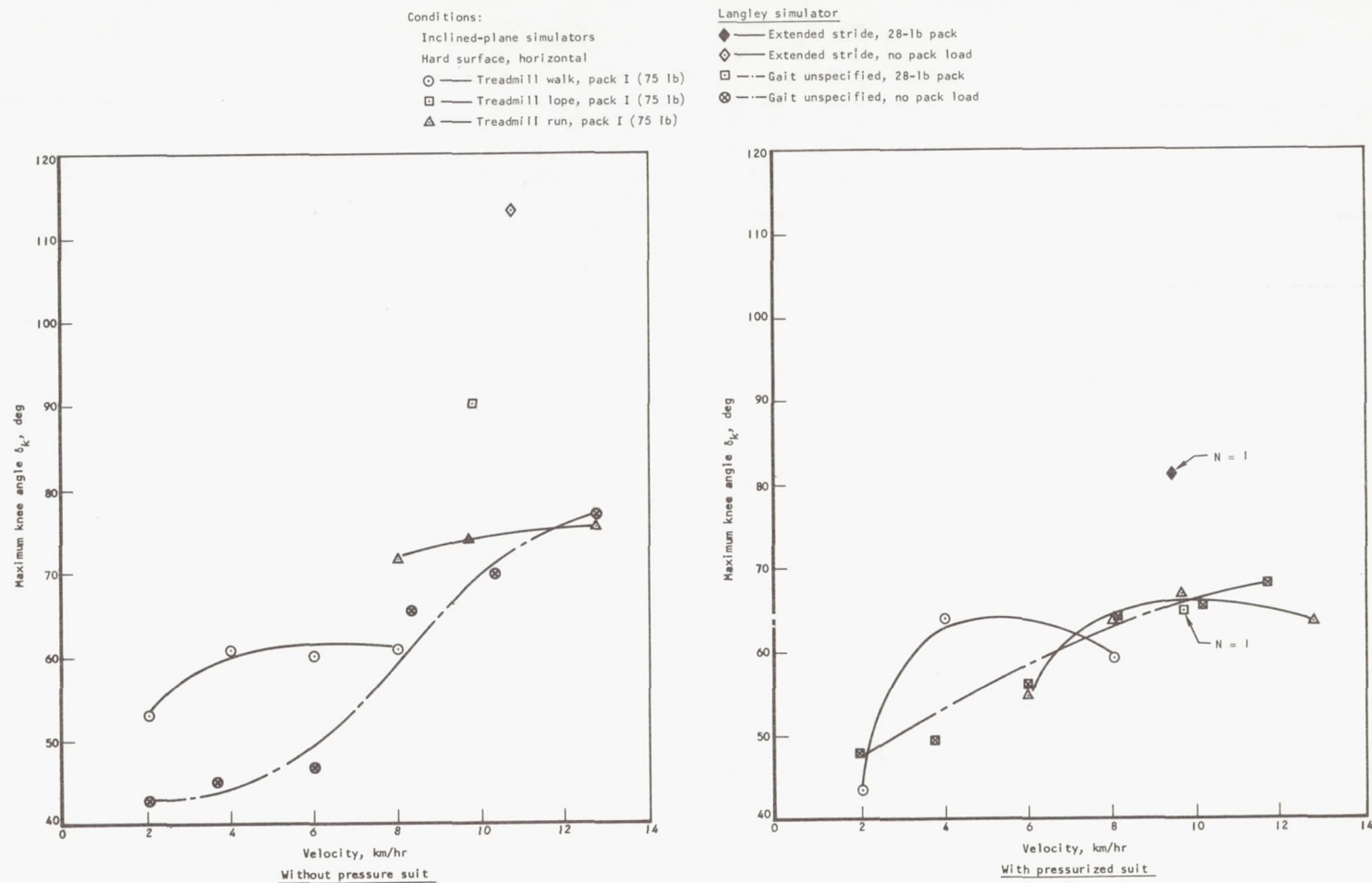


Figure 5-95. Maximum Knee Angle vs Velocity, Comparison of Various Simulators, Horizontal Hard Surface

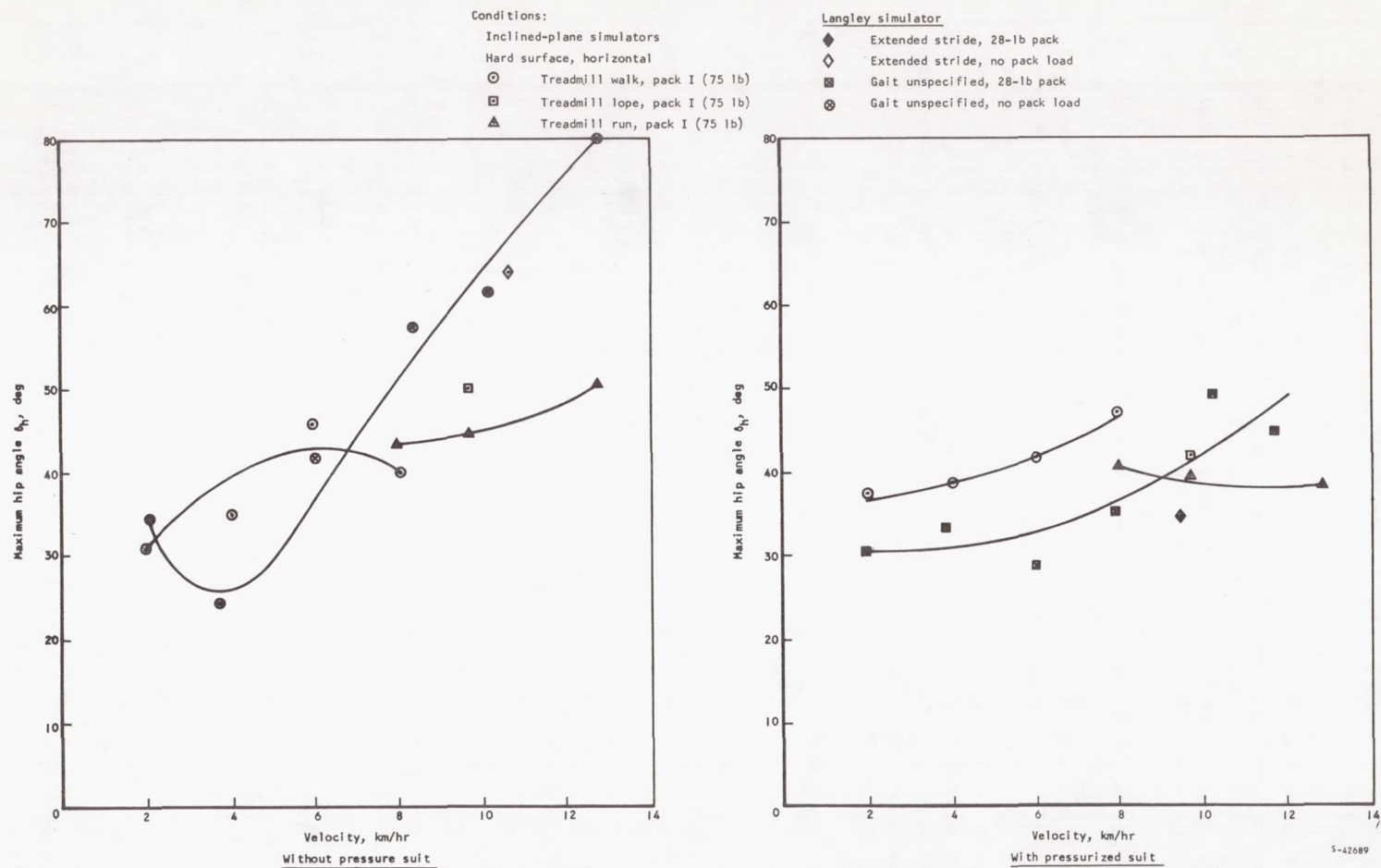


Figure 5-94. Maximum Hip Angle vs Velocity, Comparison of Various Simulators, Horizontal Hard Surface

4. Back angle increases for simulated lunar soil conditions as compared to the hard surface with the horizontal TOSS simulator. There is no difference in back angle between the two types of simulated lunar surfaces. Whether ascending or descending at 7.5-deg slope on the TOSS simulator, no differences occurred in back angle for either the hard surface or the simulated smooth lunar surface. For a 15-deg slope, a significantly lower back angle was observed on the hard surface than on the simulated smooth lunar surface. The data on 15-deg ascending are insufficient for comparisons between hard surface and simulated lunar soil conditions.
5. The only difference in back angle between the inclined-plane and TOSS simulators on a horizontal hard surface occurs during the run gait, where back angle is lower on the TOSS simulator. For 7.5-deg ascent, however, a lower back angle is exhibited on the inclined-plane simulator than on the TOSS simulator. For a 15-deg slope, there is no difference between simulators while ascending. There is insufficient data for 30-deg ascending on TOSS to allow comparisons. Back angle is significantly higher on the inclined-plane simulator than on the TOSS simulator for descending 7.5- , 15- , and 30-deg slopes, because the subjects leaned farther back from vertical in the TOSS simulator than in the inclined-plane simulator.
6. Back angle is higher for all conditions when ascending than when descending.
7. Hip angle, δ_h , is not greatly influenced by velocity during horizontal locomotion. Ascending slopes, however, increase hip angle as velocity increases, but descending slopes do not affect it.
8. Using the inclined-plane simulator, the only influence of gait on hip angle was seen with the heavier packs, especially in the run and lope modes where the hip angle was higher than with the 75-lb pack. With the TOSS simulator and a hard surface, the lope gait produced a higher hip angle than did the run gait.
9. With the TOSS simulator lunar soil conditions, an increase in hip angle was seen as velocity increased. There was no difference between the lunar surfaces and the hard surface or between the two types of lunar surfaces.
10. During ascent at 7.5 deg, the inclined-plane simulator produced a lower hip angle than did the TOSS simulator. There was no difference between the simulator during ascent at 15 and 30 deg. The effects were reversed during descent, and the inclined-plane data showed higher hip angle at all slopes than did the TOSS data.
11. Knee angle is unaffected by velocity during runs on the horizontal hard surface with either simulator. During ascent at 7.5 and 15 deg, however, knee angle increased with velocity, and the inclined-plane simulator showed greater values of knee angle during the descending slope tests than did the TOSS simulator, but neither system tended to show changes in knee angle with changes in velocity during descent.

12. On a horizontal hard surface with the TOSS simulator, there is no change in knee angle associated with gait. On the inclined-plane simulator, there is a significant increase in knee angle with the lope, run, and walk gaits.
13. Each heavier pack produced a lower knee angle.
14. With the two lunar surfaces, a velocity effect is noted on knee angle, but there is no difference between the two types of soil conditions.
15. The inclined-plane simulator produces higher knee angles at all velocities than does the TOSS simulator with a hard surface or smooth lunar soil.
16. Increased slope increases knee angle during descent and decreases knee angle during ascent.

Comparison of Kinematics Data with Previous Studies

Figures 5-96 through 5-101 compare data points from this program with those reported by Hewes and Spady in NASA TND-3363. Step rate, stride length, and locomotive index are essentially identical for the treadmill and the inclined walkway at velocities up through 6 km/hr. At 8 km/hr, there is a higher step rate and lower stride length on the treadmill than observed on the inclined walkway. These differences may be due to the difficulty of achieving a steady-state at higher velocities on the inclined walkway, or to mechanical differences in the simulators, or may result because in one case a gait was specified and in the other it was not.

With respect to back angle, hip angle, or knee angle, however, substantial differences exist between the set of data obtained under this program and that reported by Hewes and Spady. The differences between these sets of data are greater than differences between the treadmill and inclined-plane data where the same subjects are used. This suggests that these differences may be due to variations among subjects. It has been observed that subjects in this program appear to assume lower back angles, as compared with subjects at NASA-LRC.

Comparison of the data from this program with that obtained by Kuehnegger (under Contract NAS 1-4449) for walking on a horizontal surface reveals no difference in stride length or step rate (Figures 5-102 and 5-103). Although a substantial variation in back angle is shown in Figure 5-104, the differences between subjects C and A reported by Kuehnegger are greater than the differences between subject C and the average data for the six subjects used in this program. Comparison of data for traversing slopes shows that stride length is quite similar for both ascent and descent (Figures 5-105 and 5-106). Step rate (Figures 5-107 and 5-108) also demonstrates good correspondence between programs. Although the back angle data (Figures 5-109 and 5-110) show low correspondence for horizontal walking, the correspondence is quite good for ascent or descent on a 10-deg slope.

Conditions:

Inclined plane
No pressure suit
Hard surface, horizontal

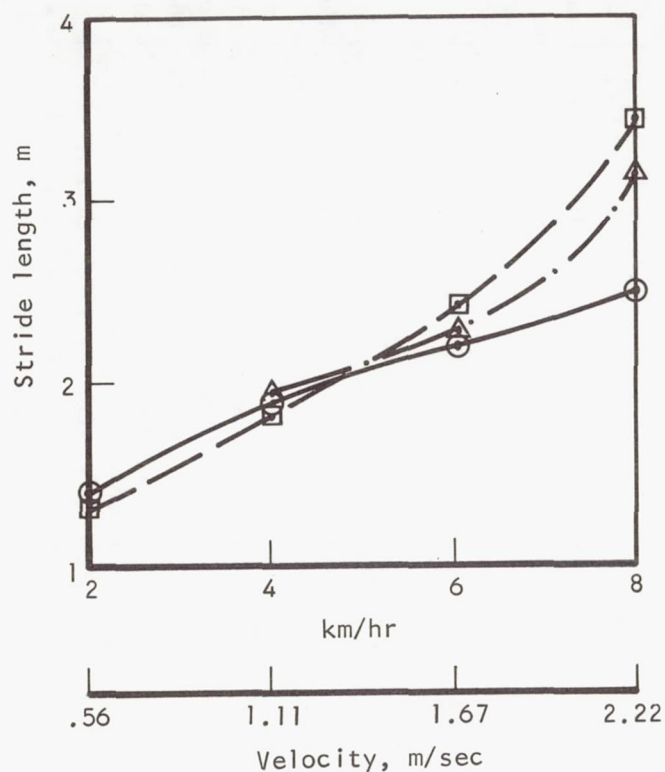
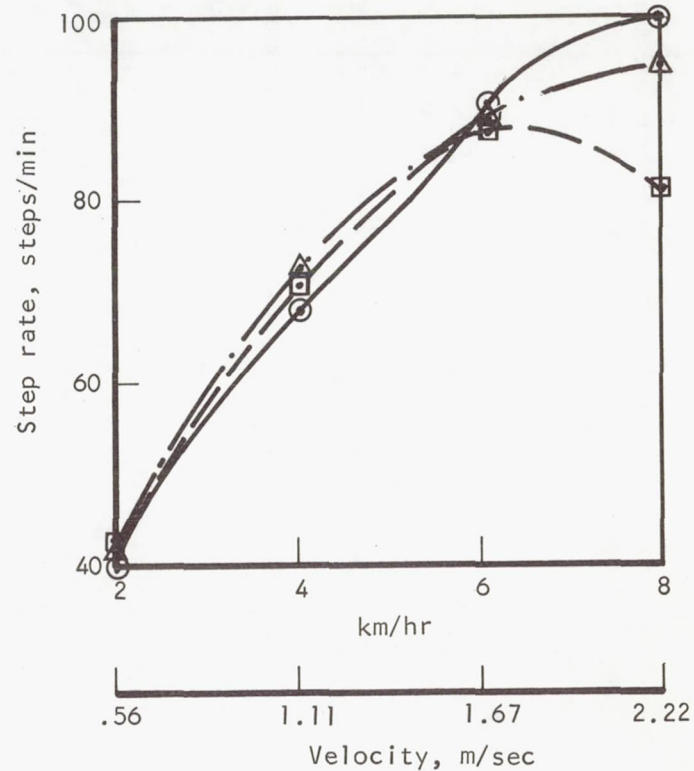


Figure 5-96. Comparison of Stride Length Between Programs, Without Pressure Suit

- — LRC inclined plane, gait unspecified, no pack load (Contract NAS 1-7053)
- — Treadmill, walk, pack I (75 lb) (Contract NAS 1-7053)
- △ — Langley, Hewes & Spady, TN D-3363



S-42761

Figure 5-97. Comparison of Step Rate Between Programs, Without Pressure Suit

Conditions:

Inclined plane
No pressure suit
Hard surface, horizontal

- ▣ LRC inclined plane, gait unspecified, no pack load (Contract NAS 1-7053)
- ⊙ Treadmill, walk, pack I (75 lb) (Contract NAS 1-7053)
- ▲ Langley, Hewes & Spady, TN D-3363

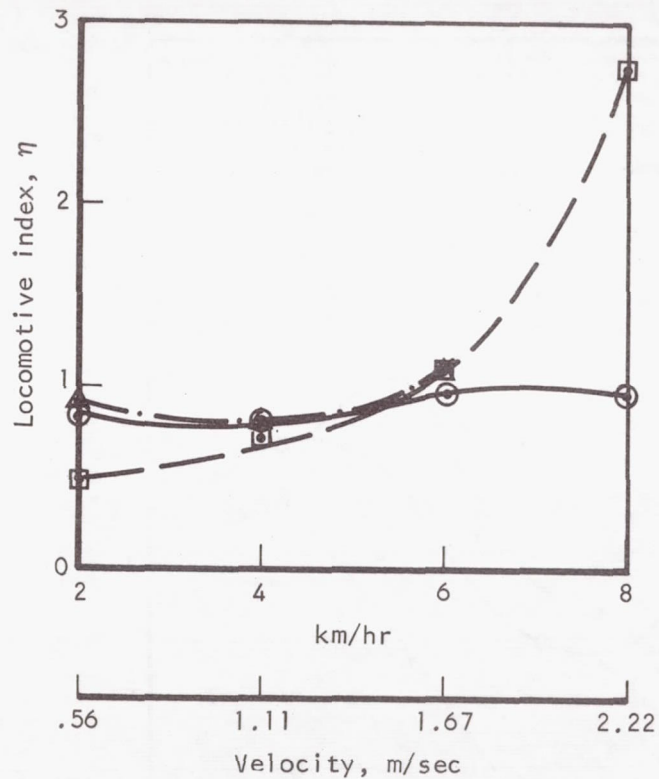


Figure 5-98. Comparison of Locomotive Index Between Programs, Without Pressure Suit

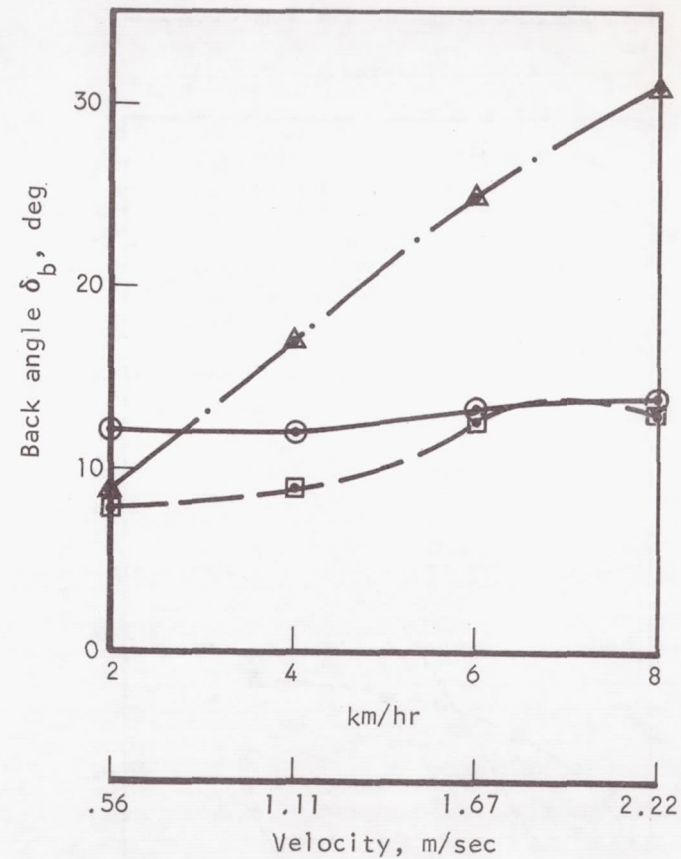


Figure 5-99. Comparison of Back Angle Between Programs, Without Pressure Suit

S-42759

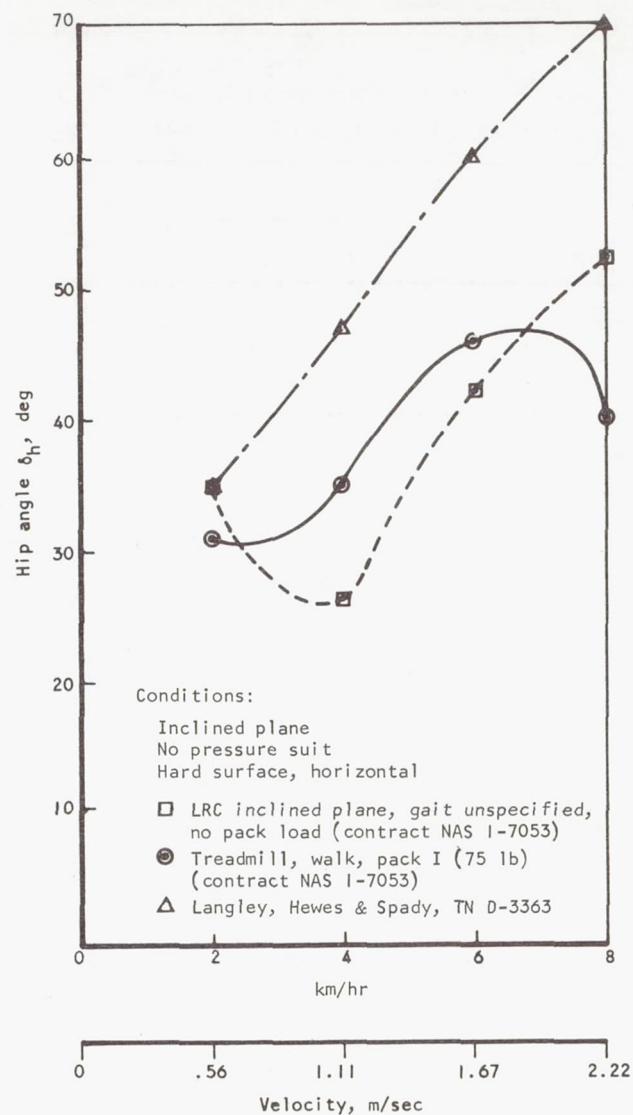


Figure 5-100. Comparison of Hip Angle Between Programs, Without Pressure Suit

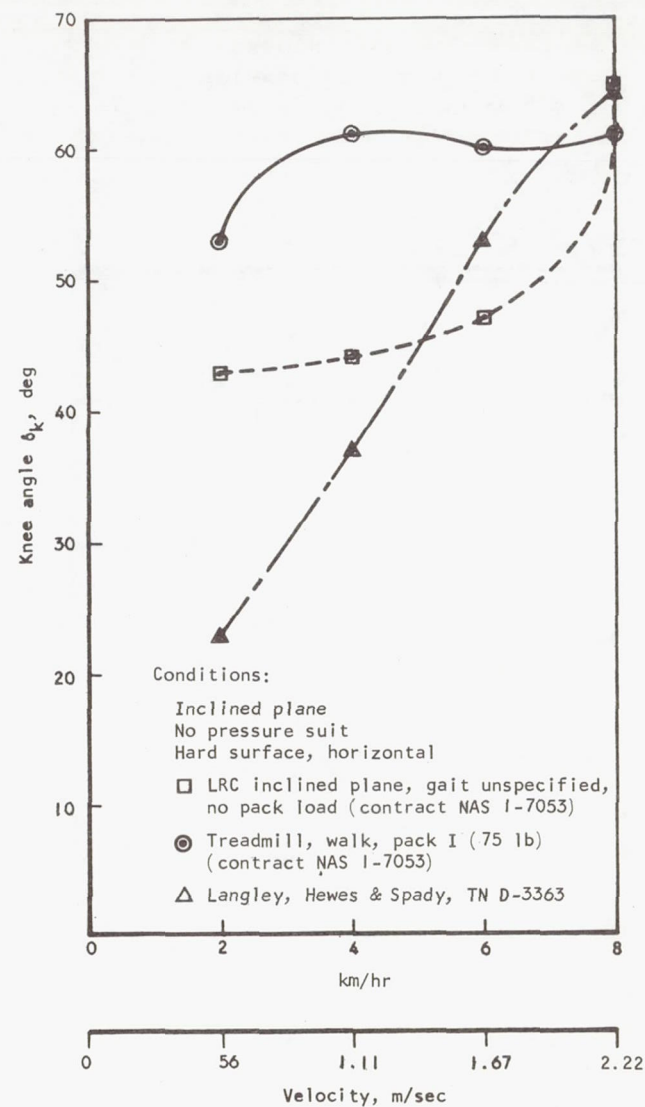
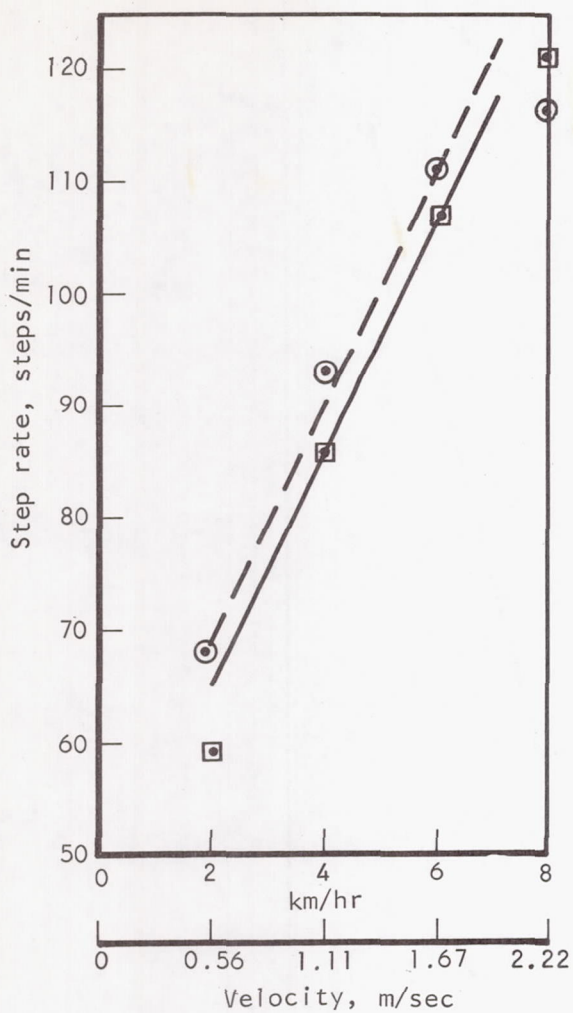


Figure 5-101. Comparison of Knee Angle Between Programs, Without Pressure Suit

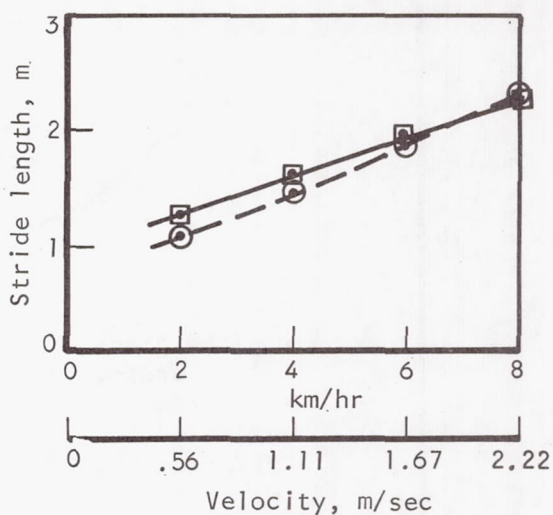


Conditions:

Inclined plane
Suited, pressurized
Hard surface, horizontal
Walking

□ — Garrett (NAS 1-7053),
pack I (75 lb)

○ — Northrop (NAS 1-4449)



S-42741

Figure 5-102. Comparison of Step Rate Between Programs, Pressurized Suit

Figure 5-103. Comparison of Stride Length Between Programs, Pressurized Suit

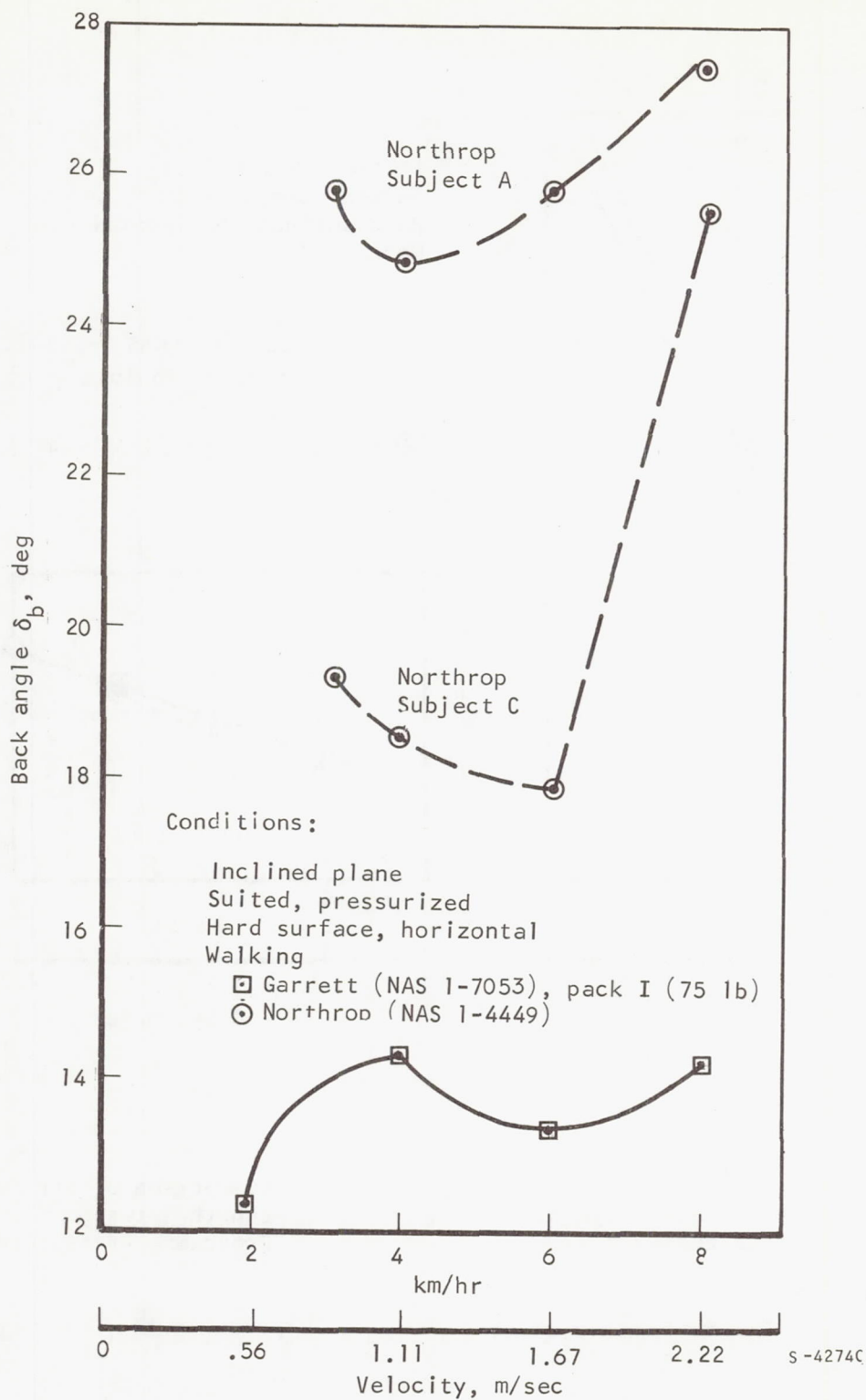


Figure 5-104. Comparison of Back Angle Between Programs, Pressurized Suit

Conditions:

Inclined plane
Suited, pressurized
Hard surface
Walking, velocities shown in km/hr

□ — Garrett (NAS 1-7053), pack I (75 lb)
○ — Northrop (NAS 1-4449)

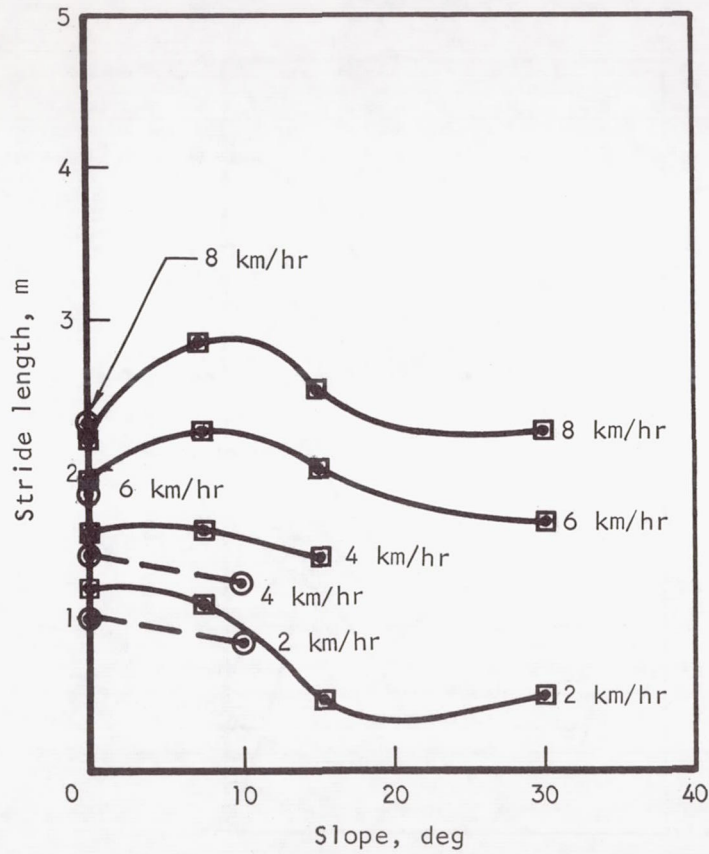


Figure 5-105. Comparison of Stride Lengths for Ascending Slopes, Pressurized Suit

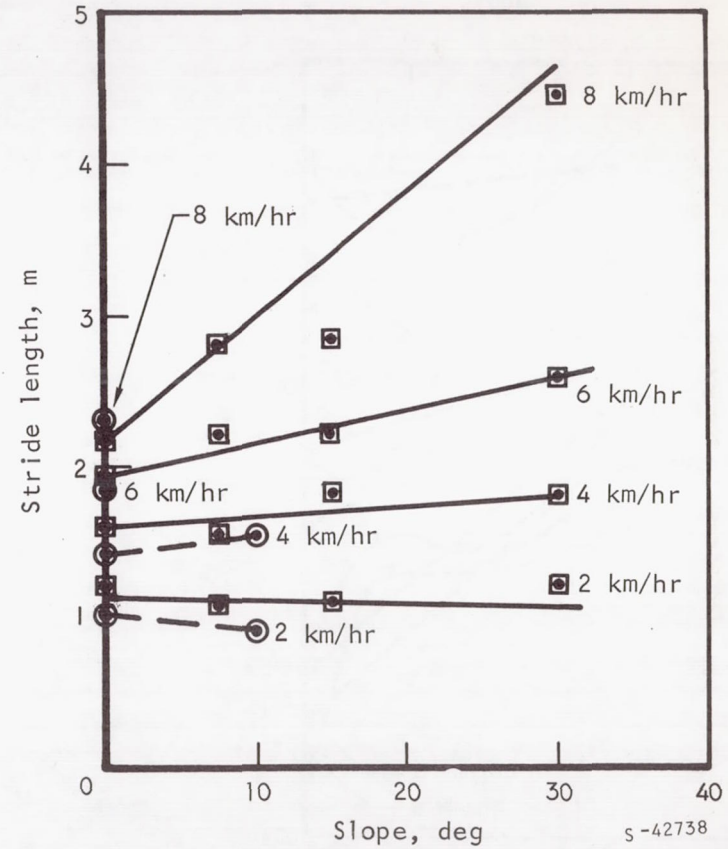


Figure 5-106. Comparison of Stride Lengths for Descending Slopes, Pressurized Suit

Conditions:

Inclined plane
 Suited, pressurized
 Hard surface
 Walking, velocities shown in km/hr

□ — Garrett (NAS 1-7053), pack I (75 lb)
 ○ — Northrop (NAS 1-4449)

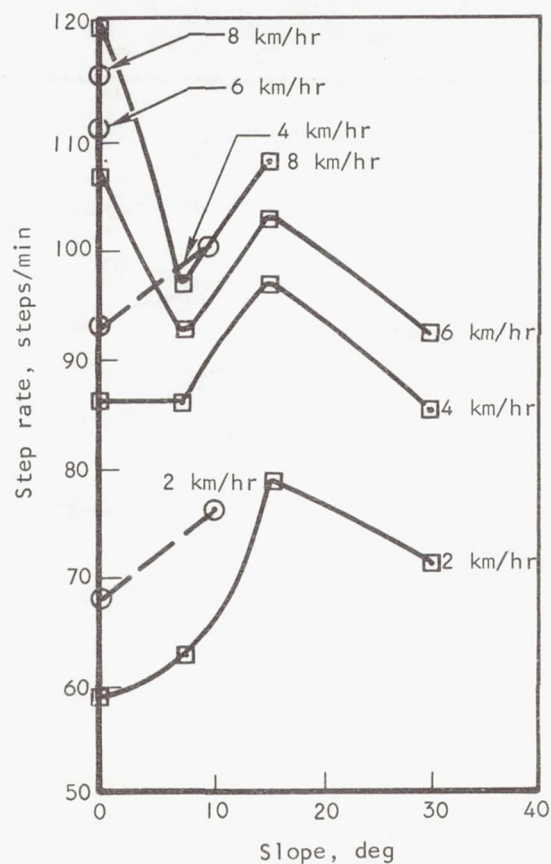


Figure 5-107. Comparison of Step Rates for Ascending Slopes, Pressurized Suits

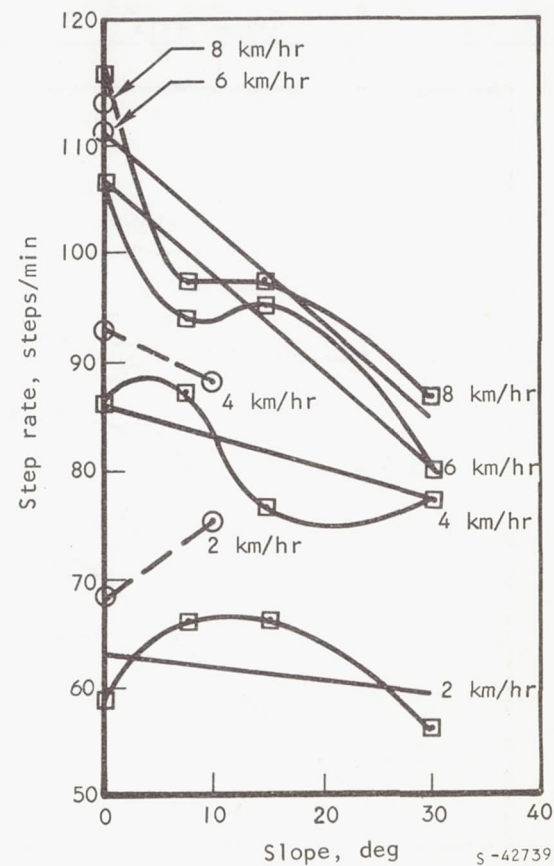


Figure 5-108. Comparison of Step Rates for Descending Slopes, Pressurized Suits

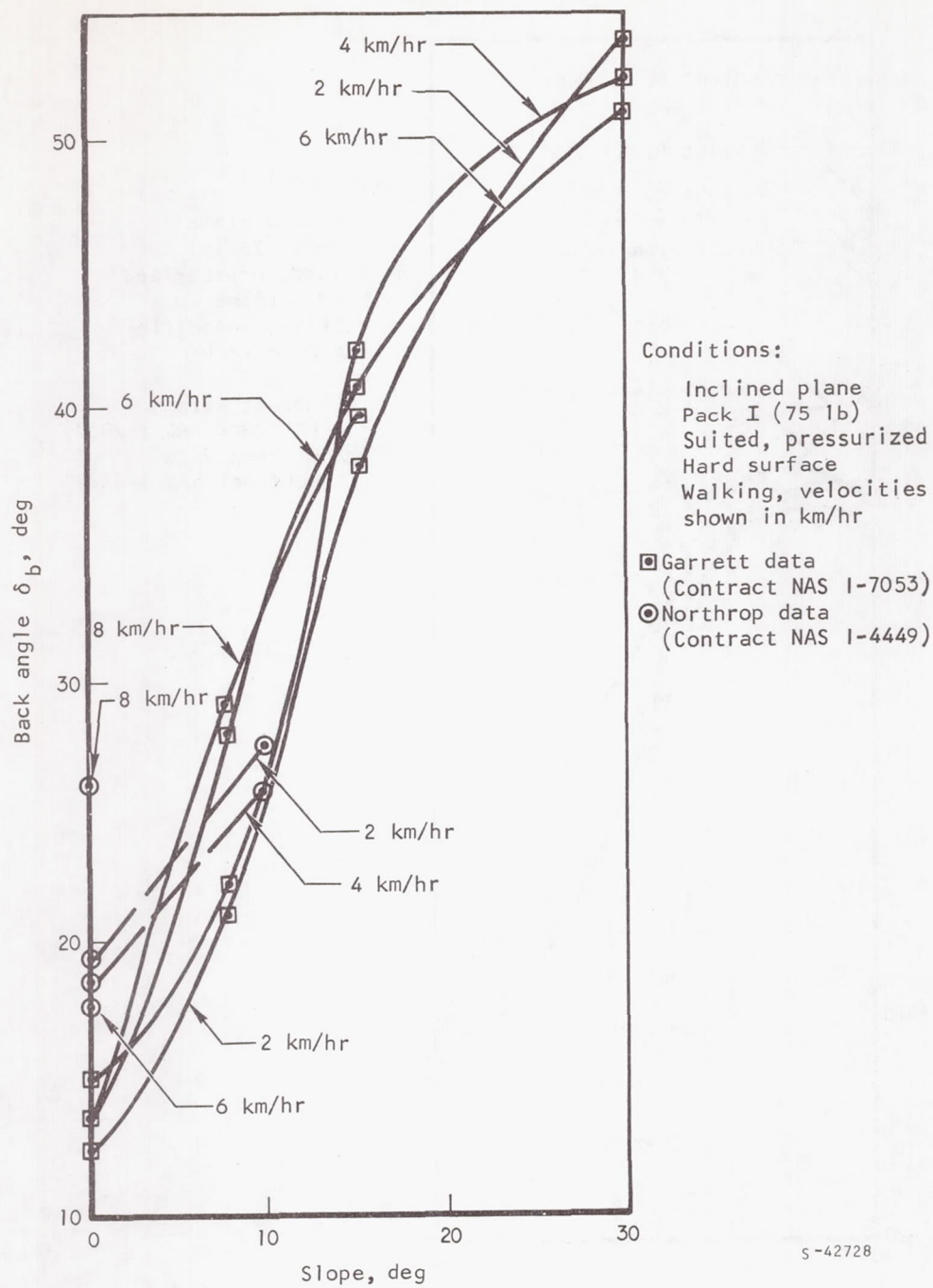
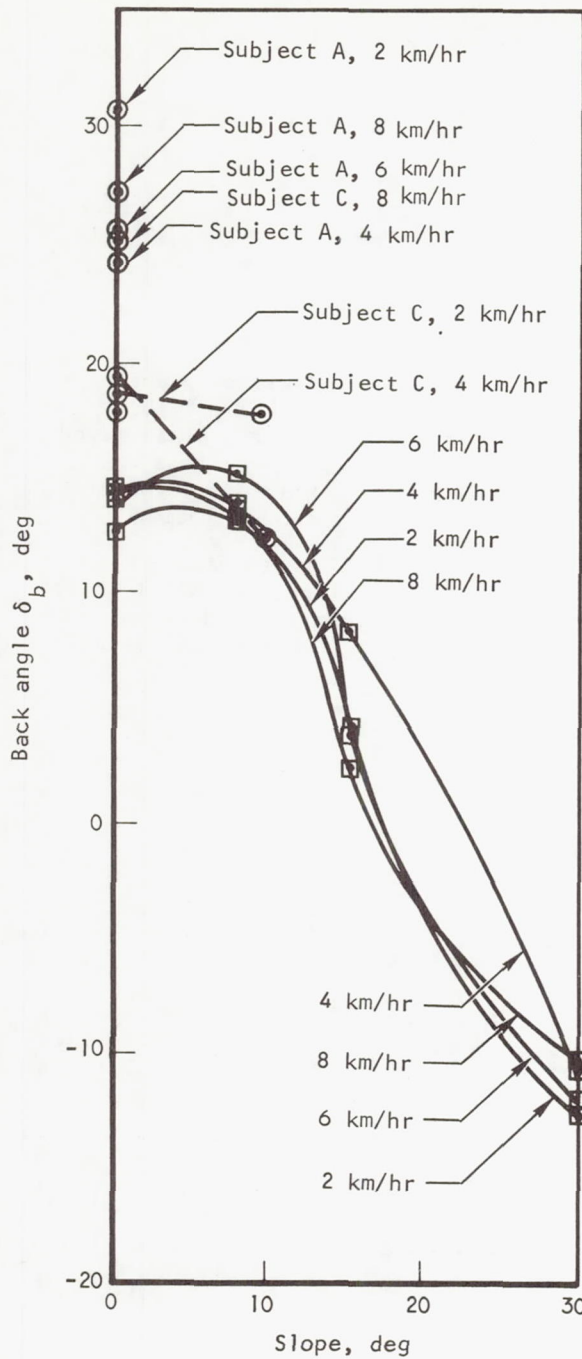


Figure 5-109. Comparison of Back Angle, Ascending Slopes. Pressurized Suits



Conditions:

Inclined plane
Pack I (75 lb)
Suited, pressurized
Hard surface
Walking, velocities
shown in km/hr

- ▣ Garrett data
(Contract NAS 1-7053)
- Northrop data
(Contract NAS 1-4449)

S-42744

Figure 5-110. Comparison of Back Angle, Descending Slopes, Pressurized Suits

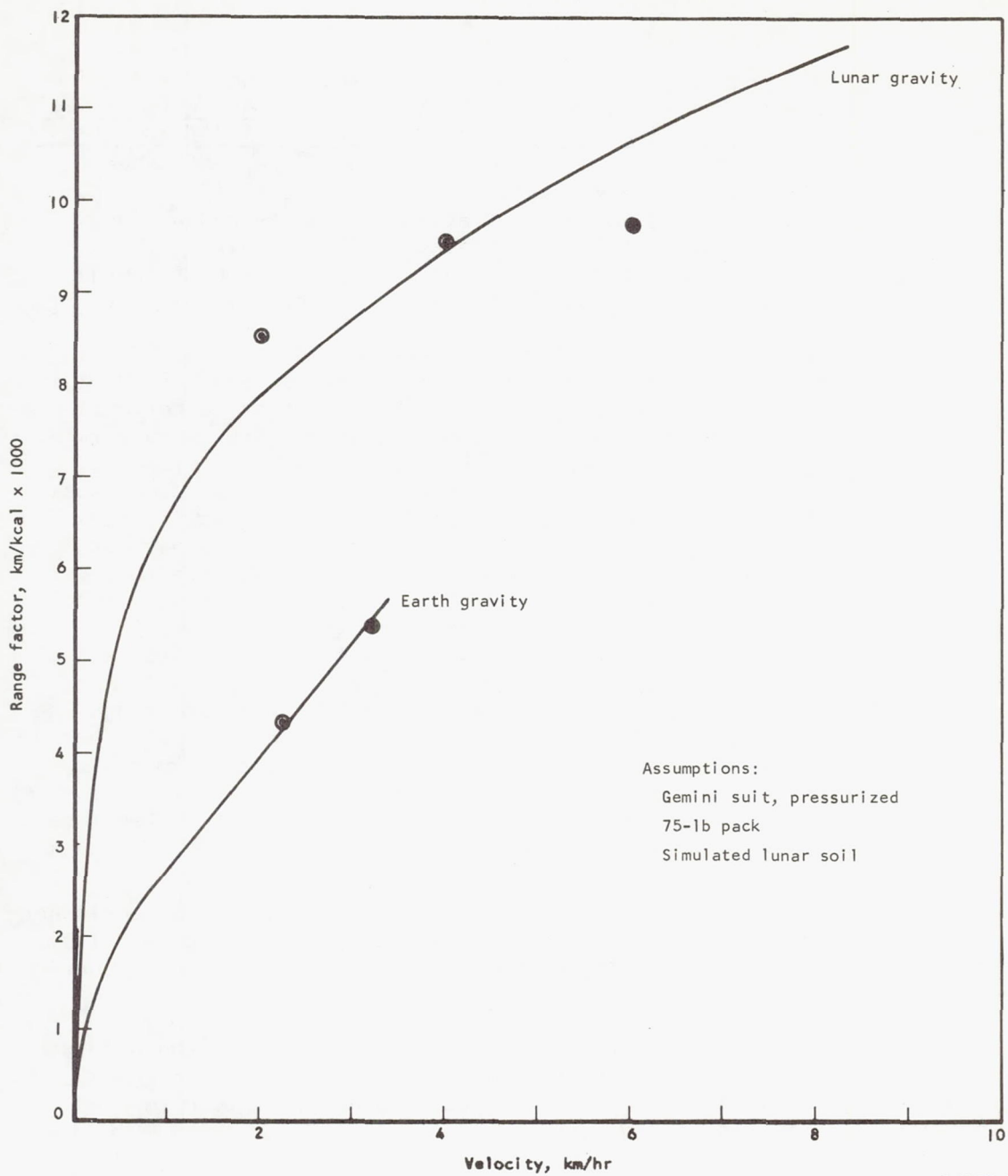
RANGE COMPUTATION

The prediction of range capabilities for men walking on the lunar surface has been thoroughly treated by D. E. Hewes in NASA TN D-3934, Analysis of Self-Locomotive Performance of Lunar Explorers Based on Experimental Reduced Gravity Studies, May 1967 (Reference 5-30). Hewes developed the concept of range factor as equal to $V/Q \times 1000$ where V = velocity and Q = metabolic rate. Computation of range factors for the Gemini suit at Earth gravity and at lunar gravity with a simulated lunar soil is illustrated in Figure 5-III. The substantial increase in distance achieved on the lunar surface per unit energy expenditure over that observed under Earth conditions is readily apparent.

If the results of the current program are extrapolated to hypothetical operational situations, some interesting observations can be made. To do this, however, it is necessary to look at the constraints for locomotion on the lunar surface imposed by a portable environmental control system. Approximate values for total metabolic capacity (total oxygen supply and total heat rejection capability) for two candidate systems are 1200 kcal (4750 Btu) and 2000 kcal (7900 Btu). In addition the current practical maximum rate of heat removal from a space suit is approximately 500 kcal/hr (1999 Btu/hr). The assumed values for these constraints can be applied to the experimental data to ascertain both the range limit of the self-locomoting astronaut and his duration "in the field" as a function of the velocity of his traverse. Figure 5-II2 illustrates the ranges that can be achieved with these two assumed ECS pack capacities as a function of velocity. It can be seen from Figure 5-II2 that range increases by velocity from 2 through 4 km/hr. Beyond 4 km/hr, range is slightly affected as a function of velocity up through 8 km/hr. At 8 km/hr, a range of 15 km could be achieved with the 1200-kcal pack, and 24 km could be achieved with the 2000-kcal pack. If, however, the heat dissipation from the suit was limited to 500 kcal and little or no heat storage by the astronaut was allowed, the range would become substantially limited.

The ranges achievable for the two assumed pack capacities are accomplished in durations that decrease with increasing velocity as shown in Figure 5-II3, which plots the maximum duration for walking on the lunar surface as a function of velocity.

In reviewing these comments, it should be borne in mind that these data assume the use of a Gemini suit, that the surface is horizontal (zero grade), and that the characteristics of the lunar surface are quite similar to the simulated lunar soil used in this program.



S-42688-A

Figure 5-III. Range Factors at Earth Gravity and at Lunar Gravity, with Simulated Lunar Soil and Gemini Suit

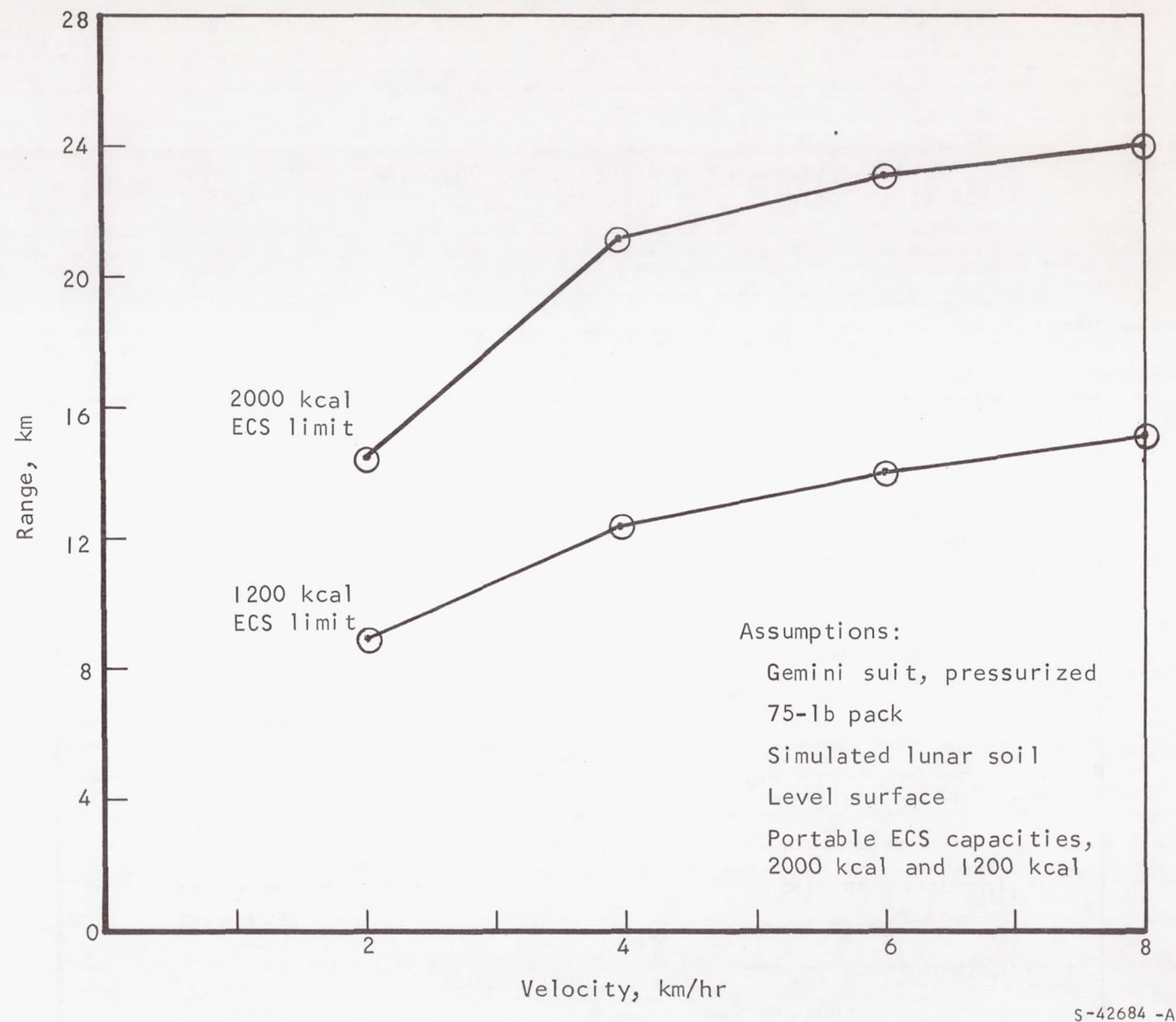


Figure 5-112. Range Limit as a Function of Velocity,
Assuming Two Portable ECS Capacities

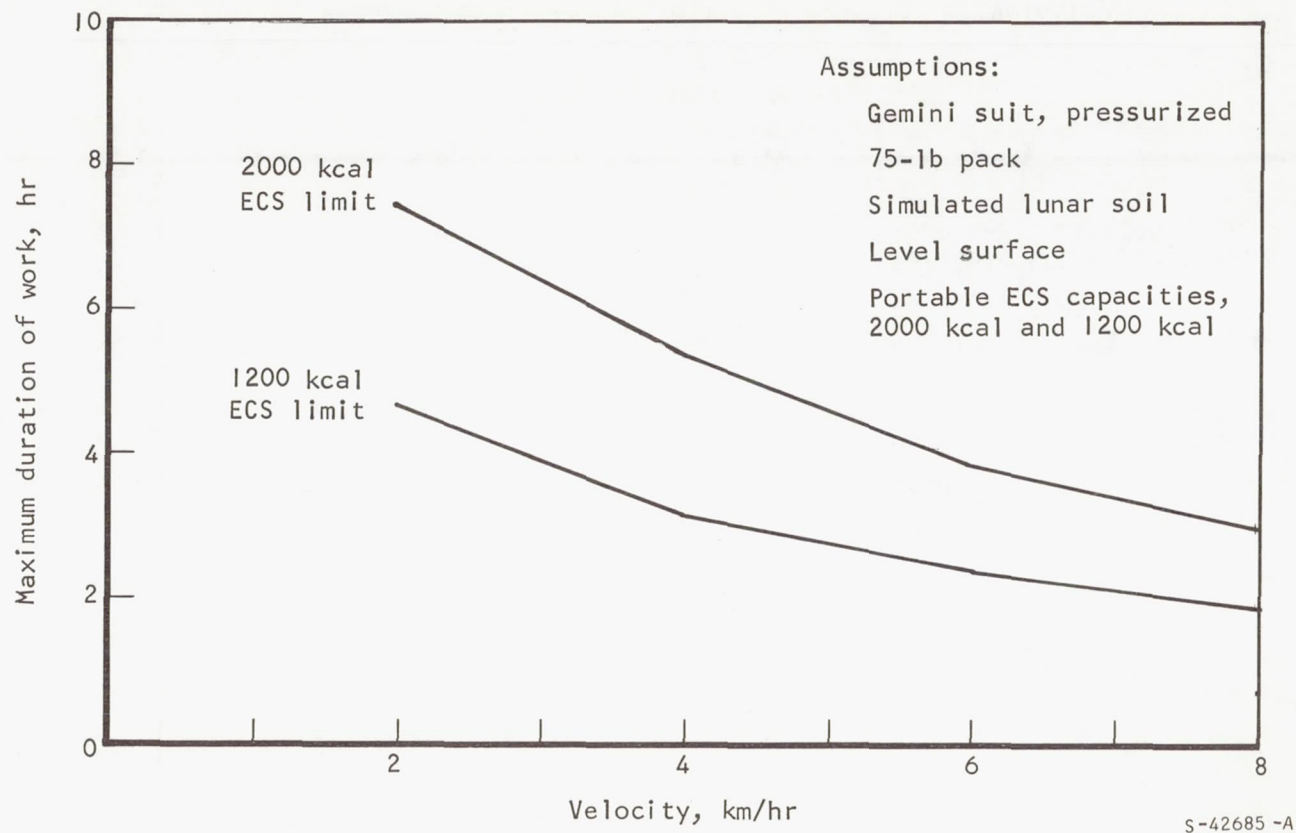


Figure 113 Duration of Lunar Walk as a Function of Velocity
(Assuming Two Portable ECS Capacities)

SECTION 6

CONCLUSIONS

1. Metabolic rates are lower during locomotion in simulated lunar gravity than at 1 g. The decrease is approximately 30.5 percent at 2 km/hr and 64.6 percent at 8 km/hr in mufti, and 51.1 percent at 2 km/hr and 37.9 percent at 8 km/hr in the Gemini space suit.
2. Energy cost for a loping gait is higher than for either walking or running. This observation is consistent for subjects either with or without space suits.
3. The metabolic rate for walking in a Gemini space suit on a level surface at any given gait and velocity with a 75-lb pack is unchanged by substitution of 240- or 400-lb pack weights.
4. For self-locomotion on level grades with a simulated lunar surface, energy expenditures range from 4.35 kcal/min at a 2/km-hr velocity to 12.28 kcal/min at 8 km/hr.
5. Metabolic costs for locomotion on a horizontal lunar surface increase sharply for ascending slopes: 36 percent greater for 7.5-deg slopes and 88 percent for 15-deg slopes. Metabolic costs for descending these grades, over horizontal locomotion, decrease by 29.1 percent (7.5 deg) and 41.3 percent (15 deg). On ascending or descending slopes, the metabolic cost for carrying a 240-lb pack increases over that for a 75-lb pack.
6. Locomotion on simulated lunar soil increases energy cost over that required on a hard surface (i.e., normal treadmill surface) for horizontal walking, as well as for ascending or descending slopes.
7. In the walking or running gaits, there are no differences in energy costs between the 3-deg-of-freedom simulator and the 6-deg-of-freedom simulator. For the lope gait, higher levels of energy expenditure occur with the 6-deg-of-freedom simulator.
8. The ratio of oxygen repayment to total oxygen cost is relatively constant, regardless of test conditions or level of energy expenditure.
9. The average energy expenditure rate is essentially identical to the instantaneous rate of energy expenditure at the end of any given test.
10. Heart rate and metabolic rate are correlated $R = 0.80$; however, the standard error about the regression line is ± 1.07 kcal/min (~ 514 Btu/hr). Consequently, the 95-percent confidence interval is ± 2.09 kcal/min ($\sim \pm 875$ Btu/hr or 1750 Btu/hr) for predicting energy expenditure from heart rate.
11. In general, the values of step rate, stride length, and locomotive index (η) increase as velocity increases.

12. When heavy packs are carried, the variance in kinematic parameters is reduced.

13. Treadmill and walkway kinematic data are quite similar for the inclined-plane technique of simulation.

14. Kinematic data is similar for both the 3-deg-of-freedom and the 6-deg-of-freedom simulations at velocities under 6 km/hr.

15. Values of locomotive index (η), step rate, and stride length are essentially identical for either shirt-sleeve or pressurized suit conditions.

16. There is no significant change in back angle (δ_b) with velocity changes for horizontal locomotion on either simulator.

17. The type of gait does influence back angle (δ_b). Back angle increases between walk and run and between walk and lope on the 3-deg-of-freedom simulator. Back angle differs for all gaits on the 6-deg-of-freedom simulator.

18. When the 240-lb pack is substituted for the 75-lb pack, back angle (δ_b) does not change while walking on the inclined-plane simulator but does increase for the lope and run gaits. Back angle increases for all gaits when the 400-lb pack is substituted for the 75-lb pack.

19. Back angle (δ_b) for horizontal locomotion is greater for lunar soil conditions than for hard surfaces and greater for ascending than for descending slopes under all conditions.

20. Hip angle (δ_h) is not greatly influenced by velocity on a horizontal surface. For ascending slopes, hip angle increases as velocity increases. Hip angle is not affected on descending slopes. Hip angle (δ_h) does not differ between the lunar surfaces and the hard surface or between the two types of lunar surfaces.

APPENDIX A METABOLIC RATE TIME COURSE CHANGES

Fig. No.	Simulator		Pressurized suit		Pack			Surface			Gait			Slope, deg ascend(A), descend(D)						
	Inclined plane	TOSS	With	With- out	I	II	III	Hard	Lunar		Walk	Lope	Run	0	7.5		15		30	
									Smooth	Coarse					A	D	A	D	A	D
A-1	X		X		X			X			X			X						
A-2	X		X		X			X				X		X						
A-3	X		X		X			X					X	X						
A-4	X		X		X			X			X	X	X	X						
A-5	X		X		X			X			X	X	X	X						
A-6	X		X		X			X			X			X						
A-7	X		X		X			X				X		X						
A-8	X		X		X			X					X	X						
A-9	X			X	X			X			X			X						
A-10	X			X	X			X				X		X						
A-11	X			X	X			X					X	X						
A-12	X		X			X		X			X			X						
A-13	X		X			X		X				X		X						
A-14	X		X			X		X					X	X						
A-15	X		X				X	X			X			X						
A-16	X		X				X	X				X		X						
A-17	X		X				X	X					X	X						
A-18	X		X		X			X							X					
A-19	X		X		X			X									X			
A-20	X		X		X			X											X	
A-21	X		X			X		X							X					
A-22	X		X		X			X								X				
A-23	X		X		X			X										X		
A-24	X		X		X			X												X
A-25	X		X			X		X								X				
A-26	X		X		X			X			X			X						
A-27		X	X		X			X				X		X						
A-28		X	X		X			X					X	X						
A-29		X	X		X			X							X					
A-30		X	X		X			X									X			
A-31		X	X		X			X											X	
A-32		X	X		X			X								X				
A-33		X	X		X			X										X		
A-34		X	X		X			X												X
A-35		X	X		X				X		X			X						
A-36		X	X		X					X	X			X						
A-37		X	X		X				X						X					
A-38		X	X		X				X							X				
A-39		X	X		X				X								X			
A-40		X	X		X				X									X		

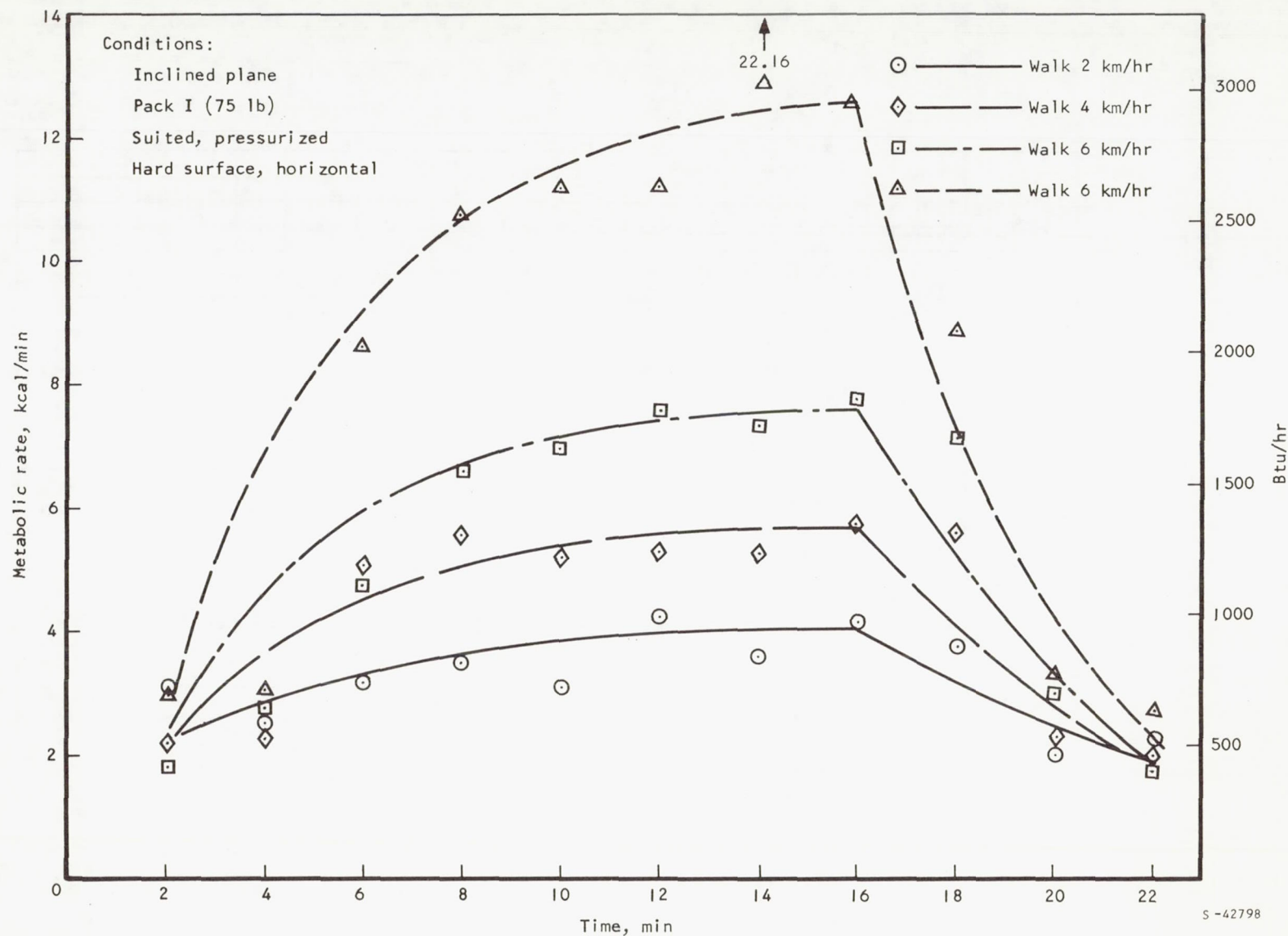


Figure A-1. Initial Tests, Inclined-Plane Simulator, Pack I, Walk

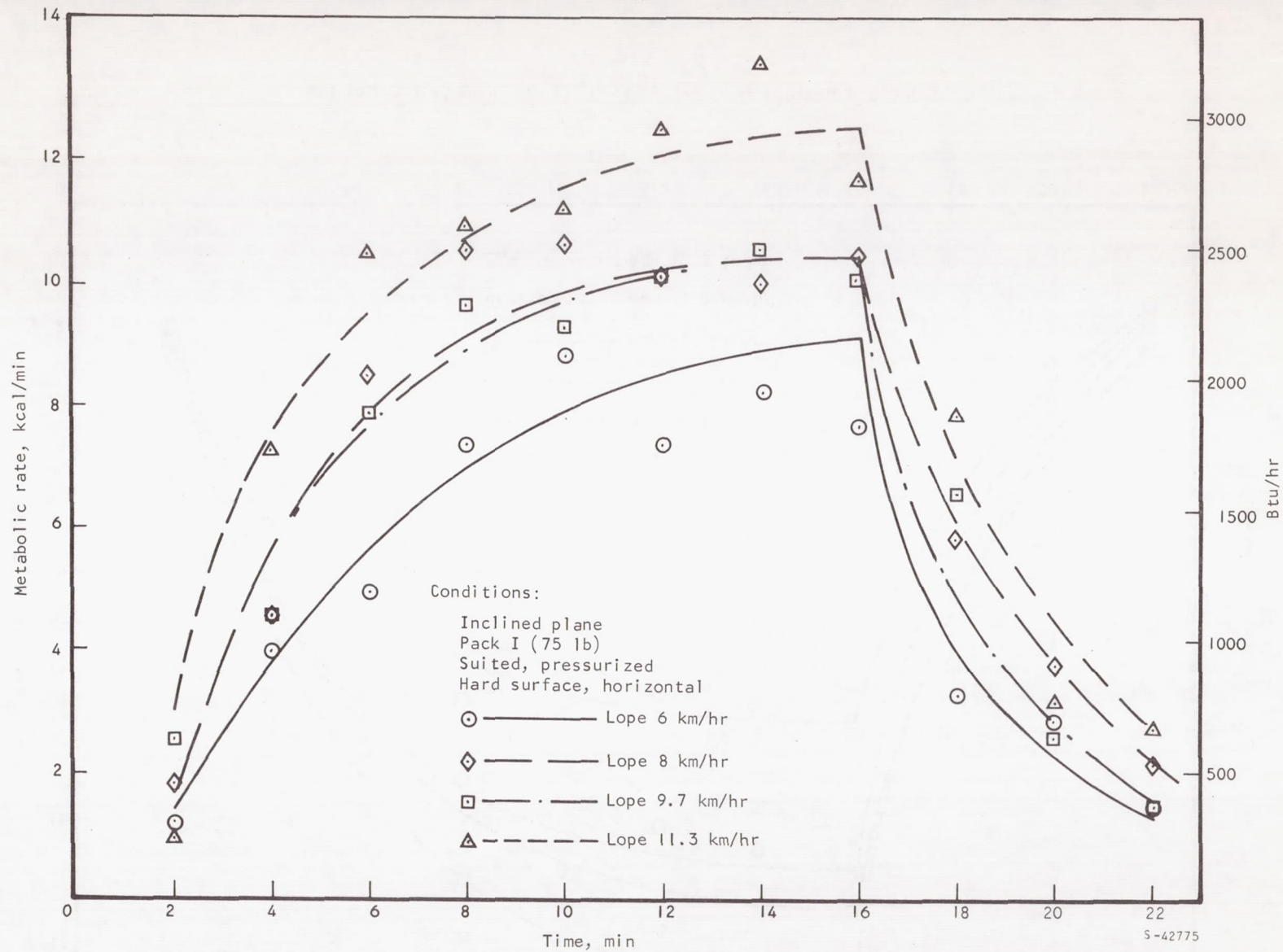


Figure A-2. Initial Tests, Inclined Plane, Pack I, Lope

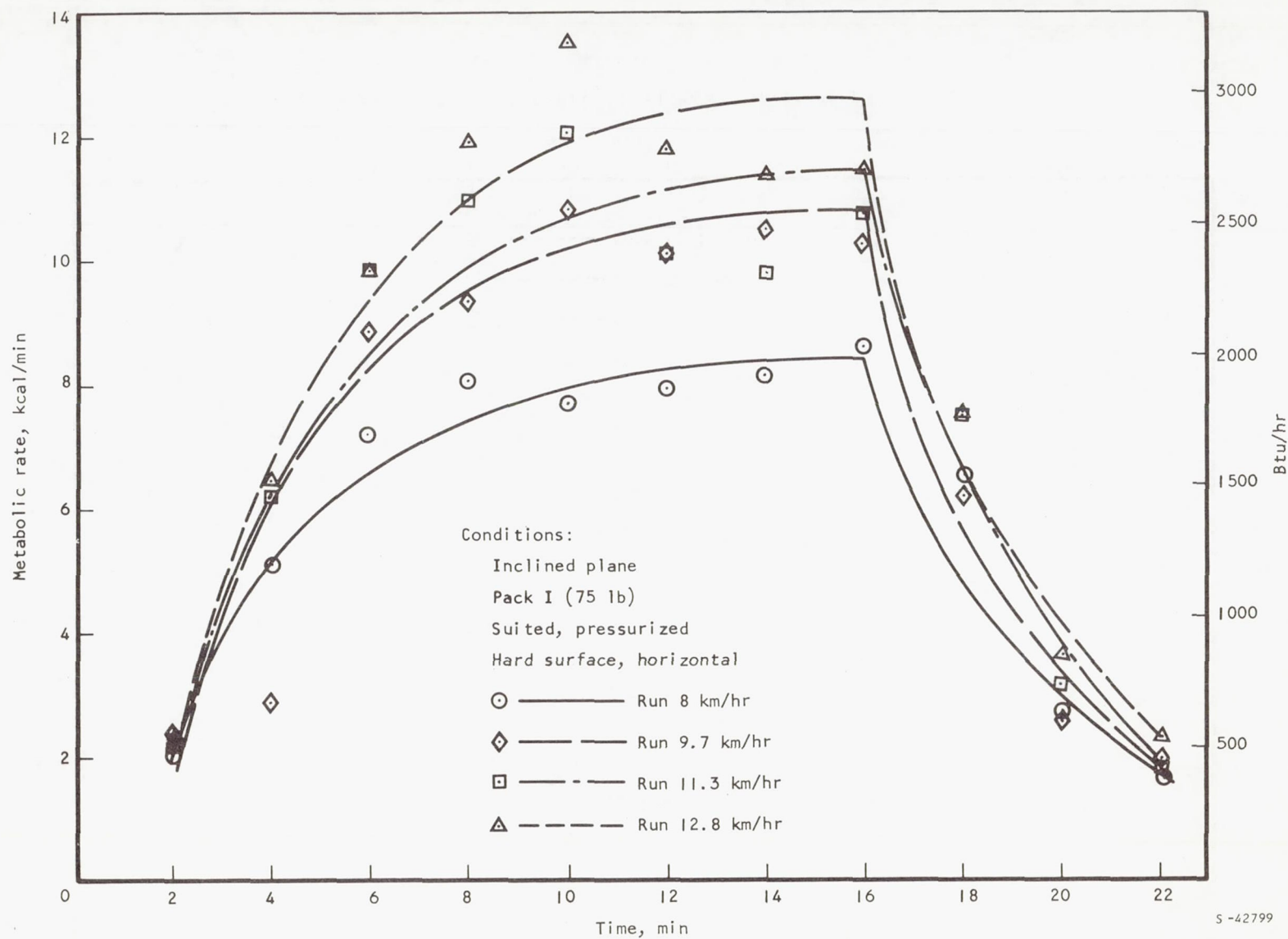


Figure A-3. Initial Tests, Inclined Plane, Pack I, Run

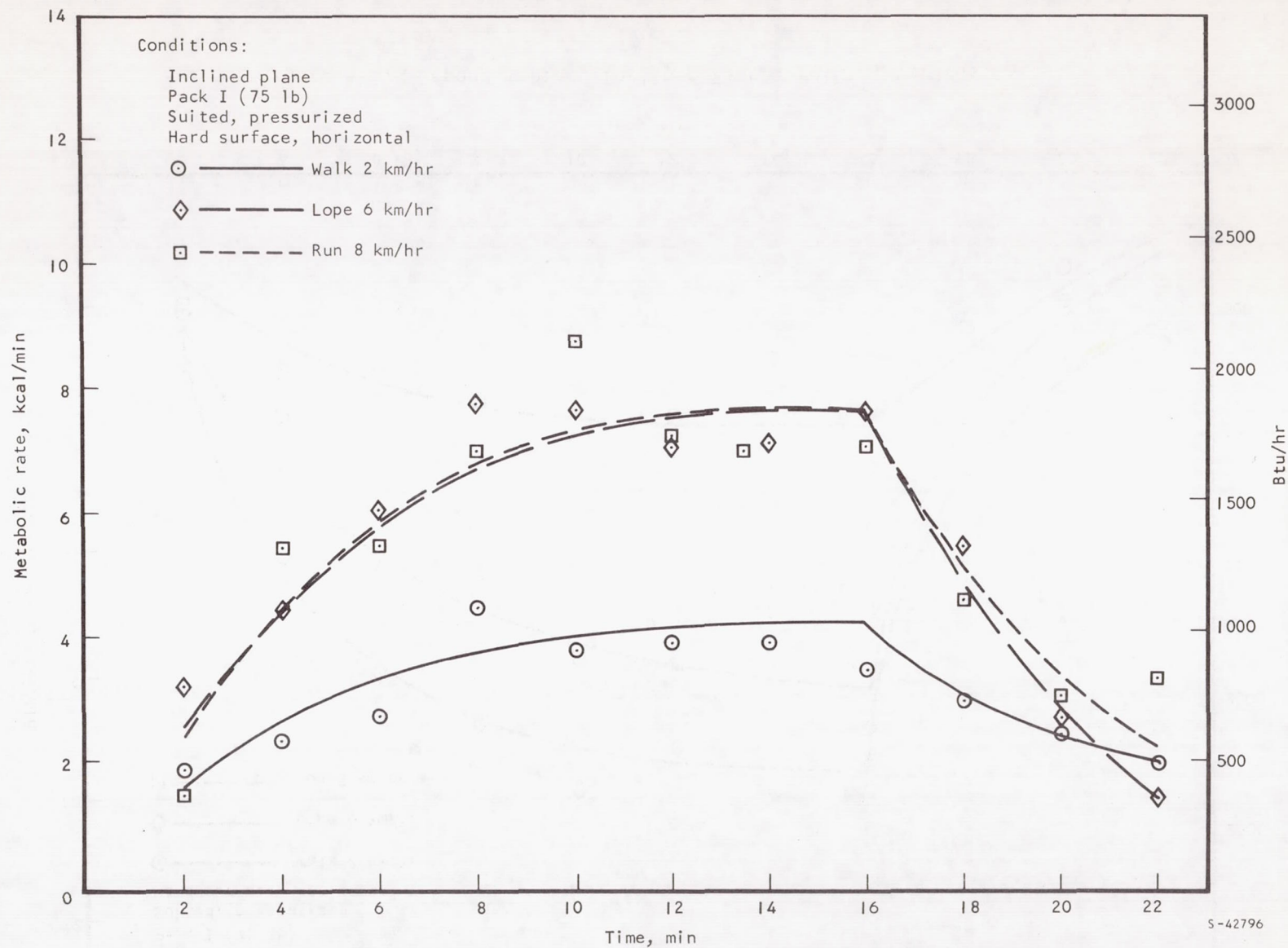


Figure A-4.. First Repeat, Inclined Plane, Pack I, Various Gaits

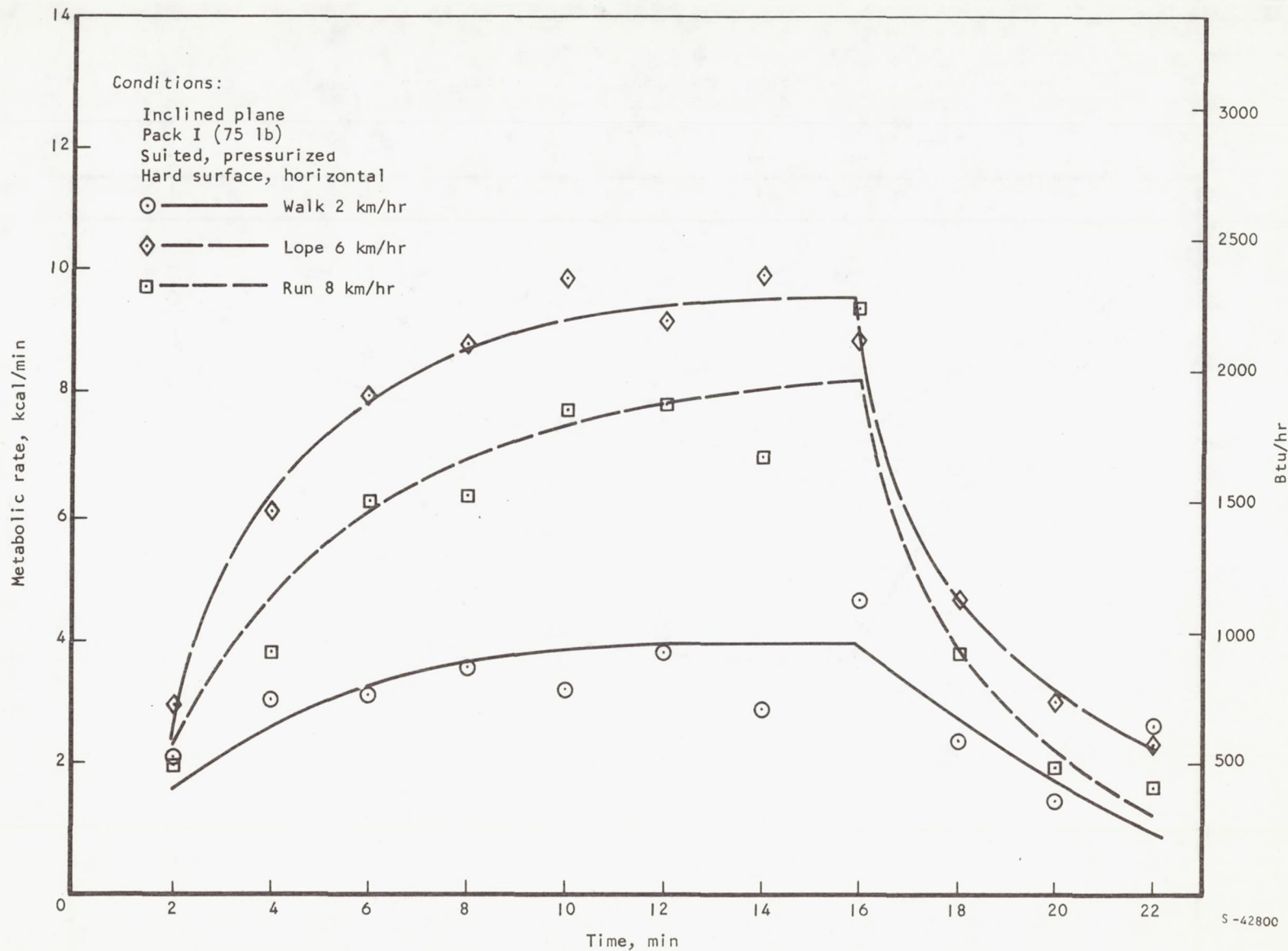


Figure A-5. Second Repeat, Inclined Plane, Pack I, Various Gaits

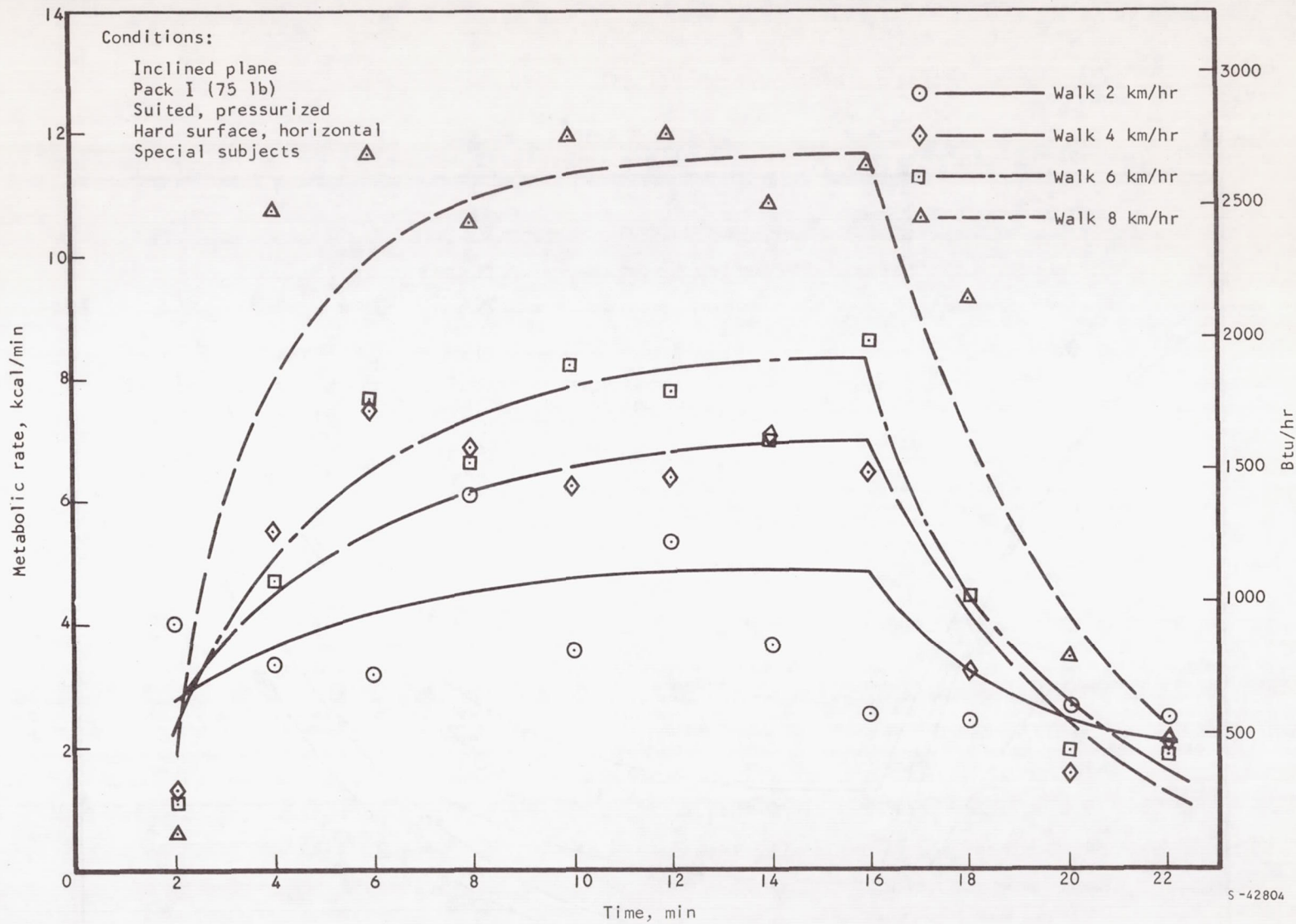


Figure A-6. Repeat, Inclined Plane, Pack I, Walk

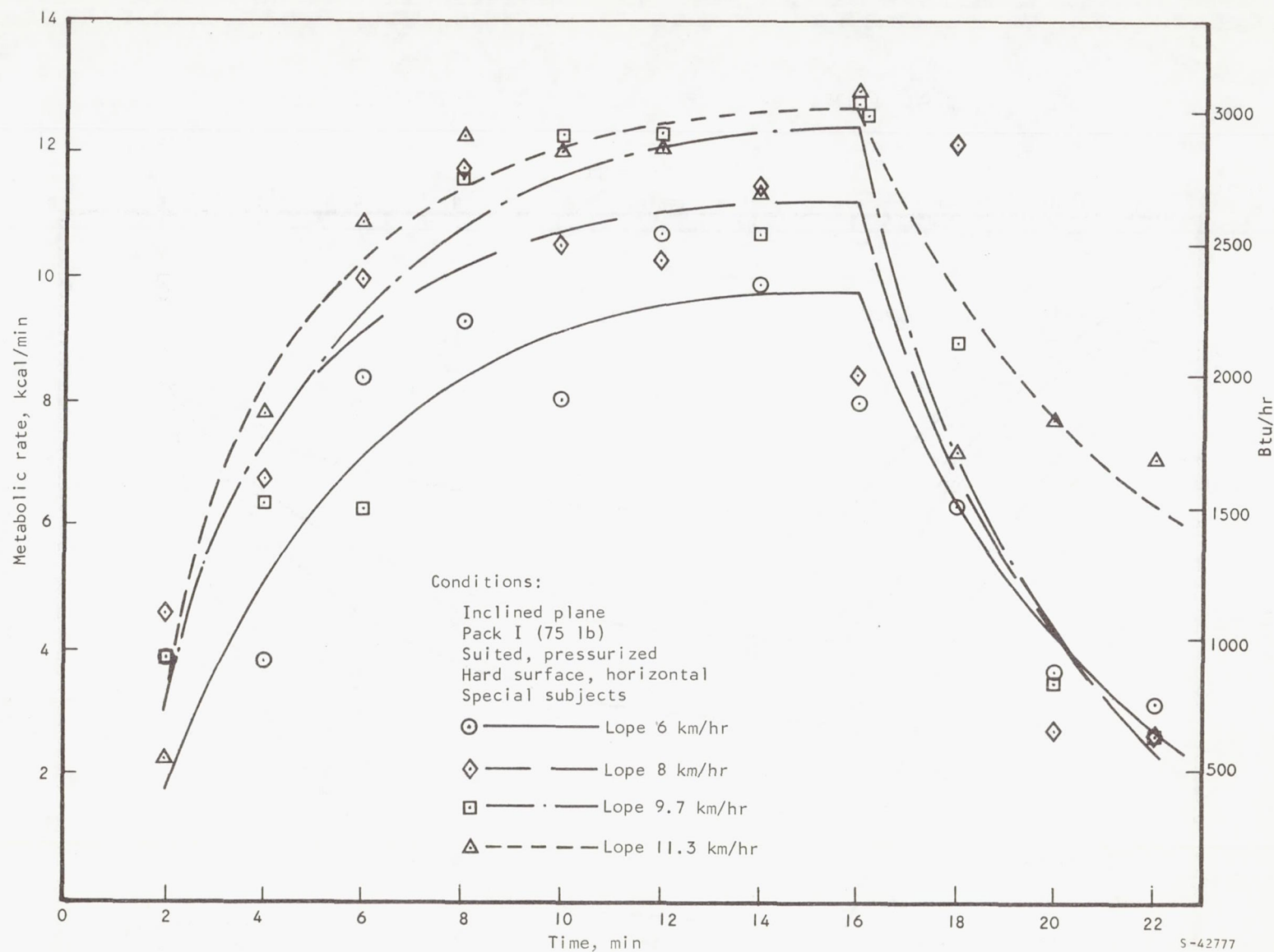


Figure A-7. Repeat, Inclined Plane, Pack I, Lope

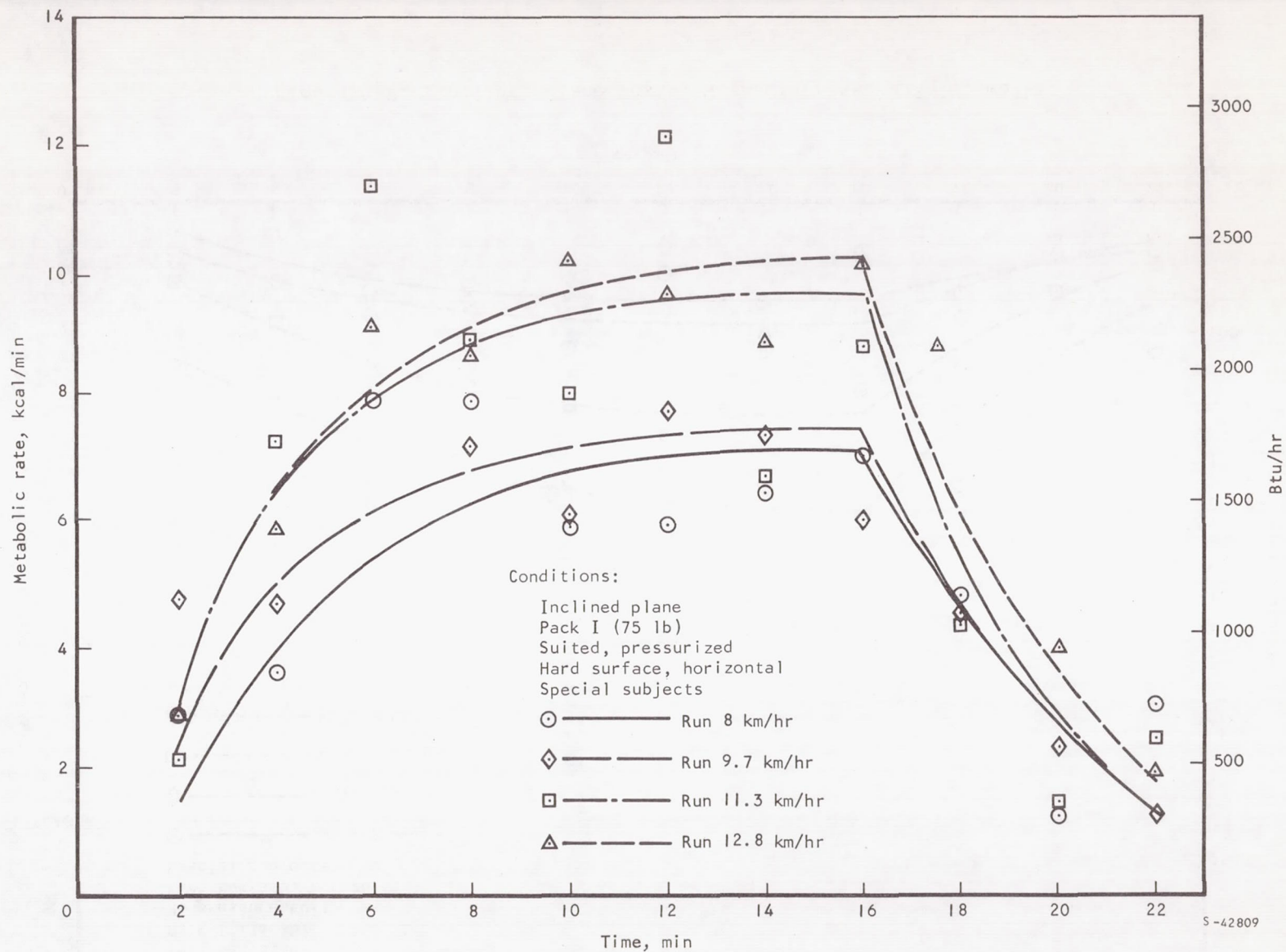
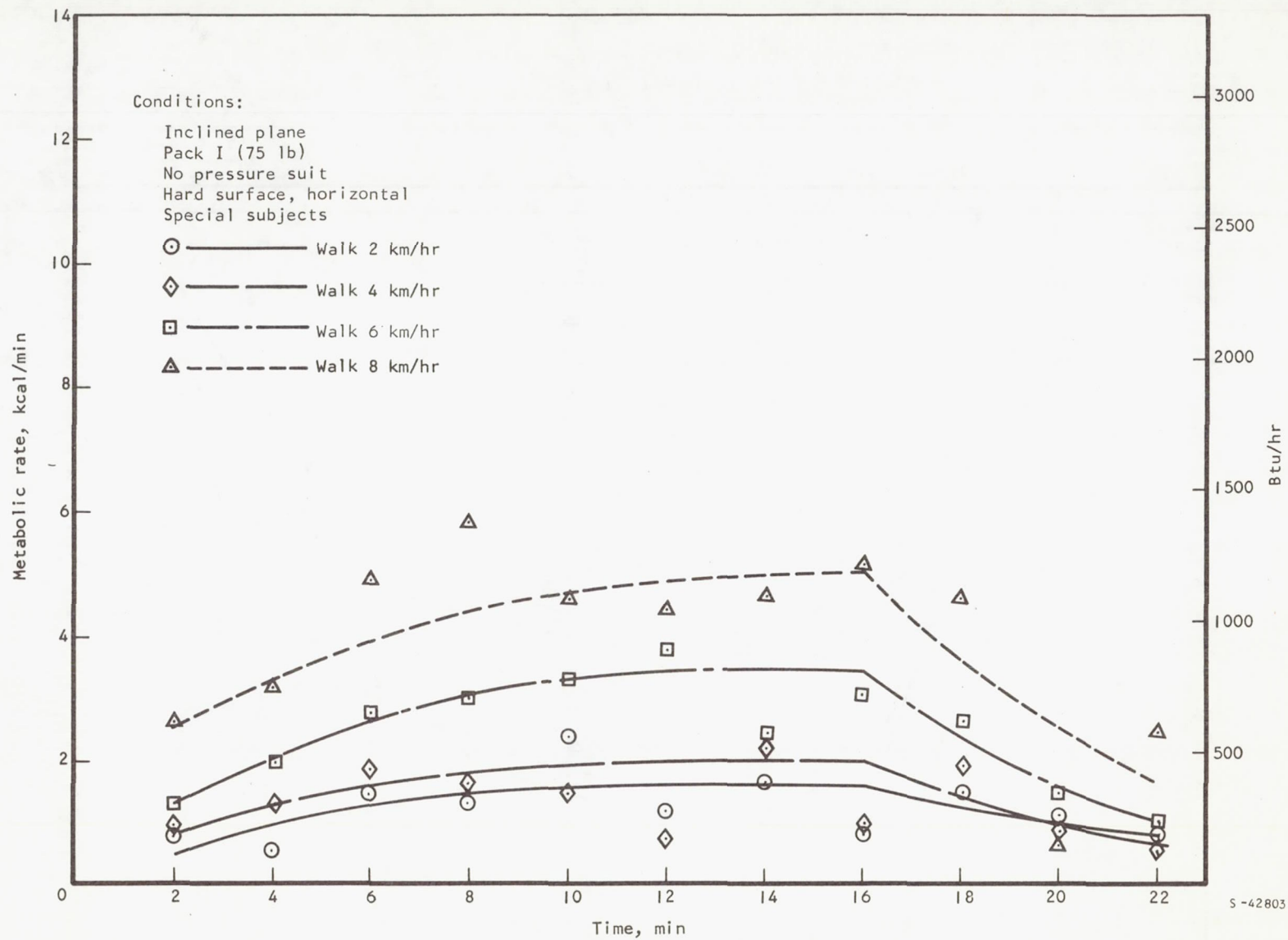


Figure A-8. Repeat, Inclined Plane, Pack I, Run



S-42803

Figure A-9. Inclined-Plane Tests, Without Pressure Suit, Walk

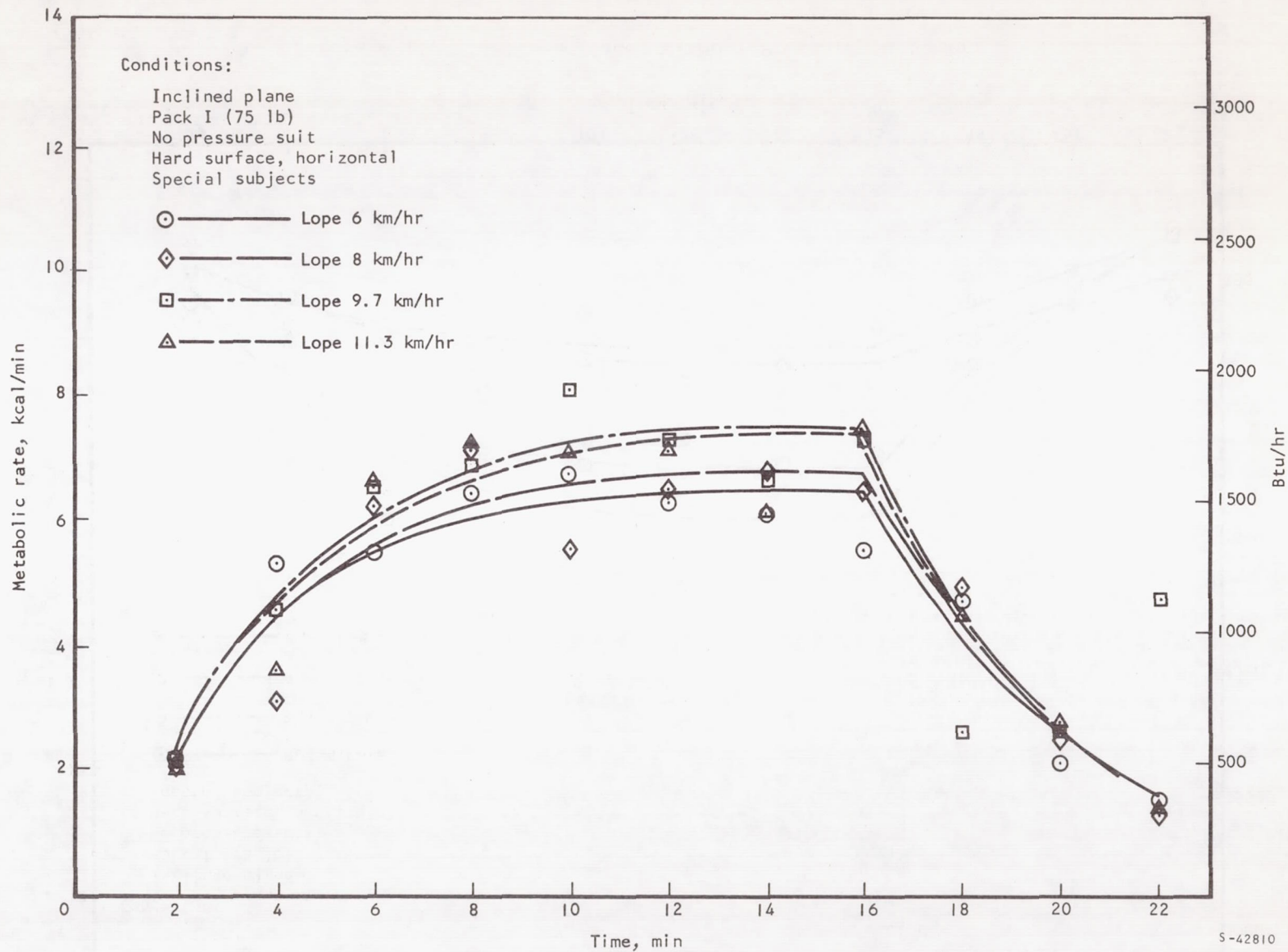


Figure A-10. Inclined Plane, Without Pressure Suit, Lope

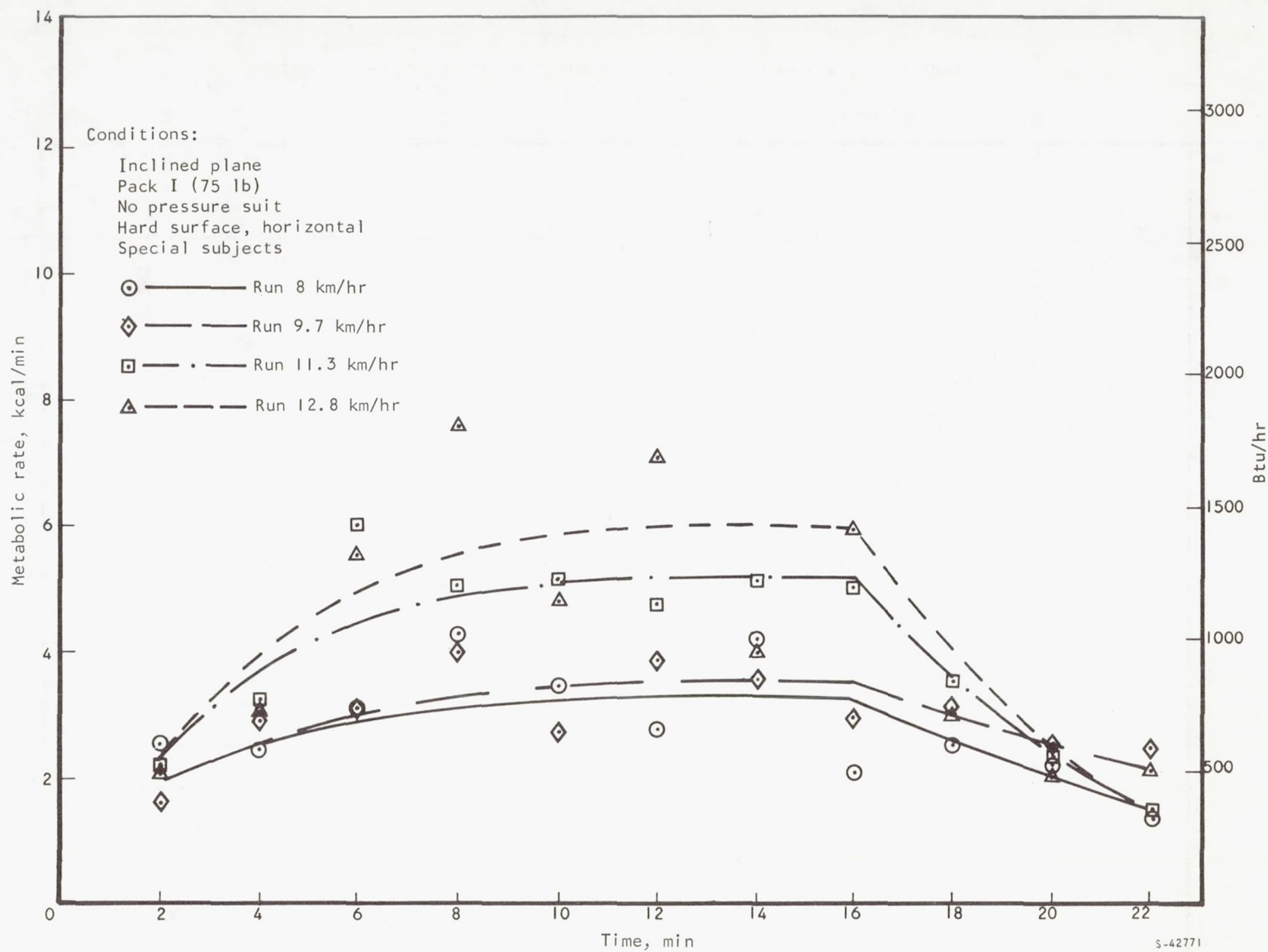


Figure A-II. Inclined Plane, Without Pressure Suit, Run

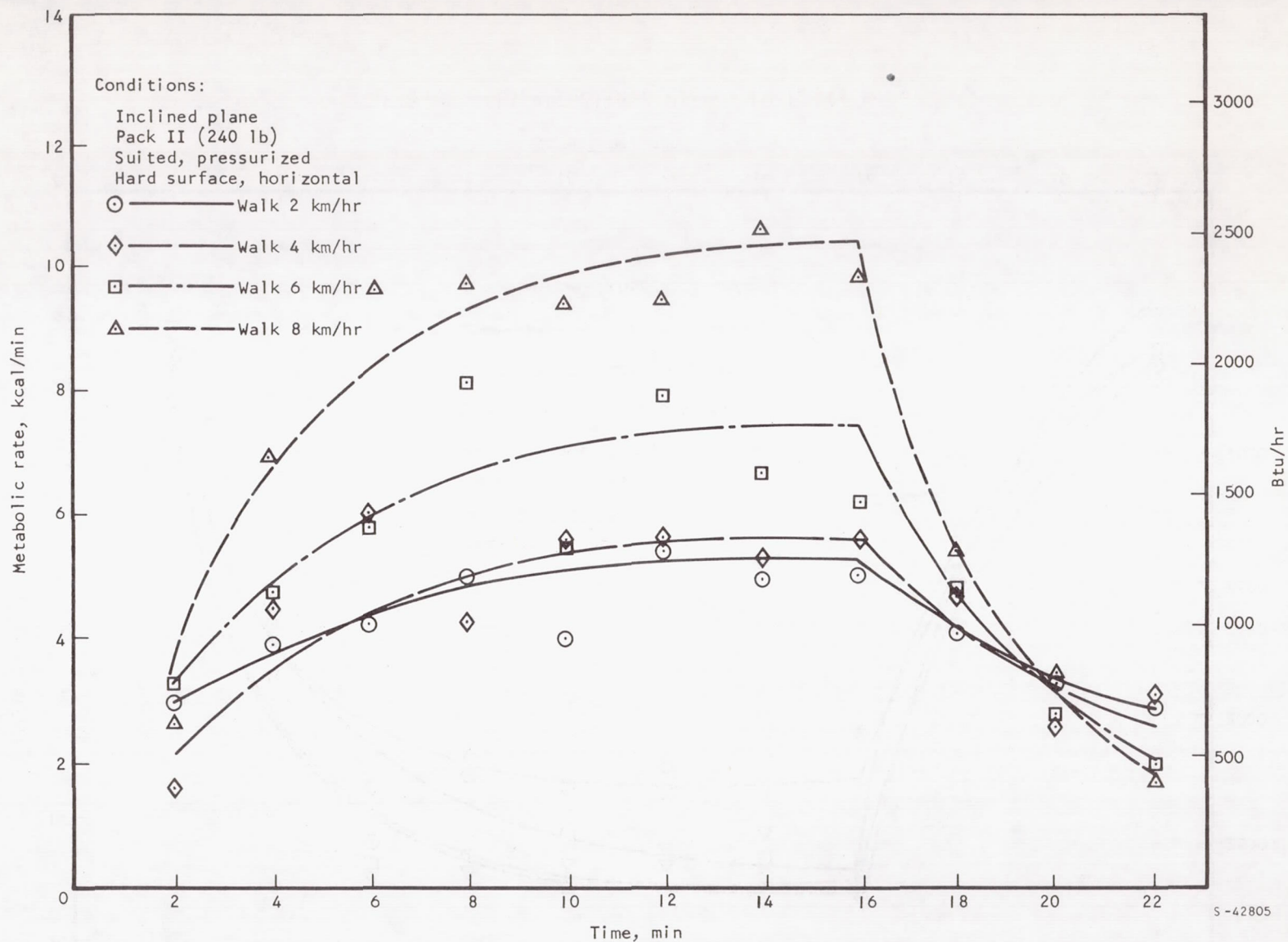


Figure A-12. Inclined Plane, Pack II, Walk

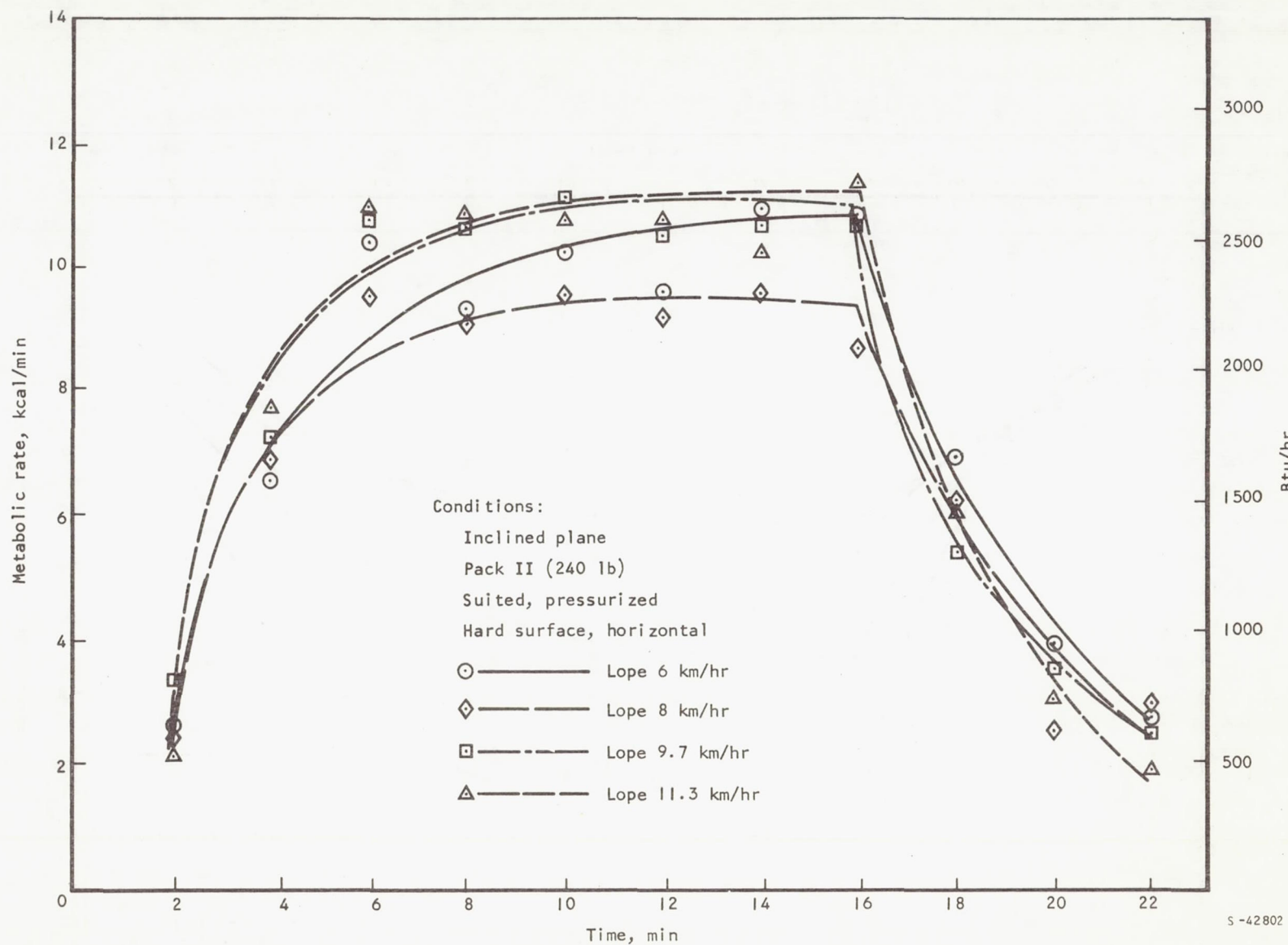
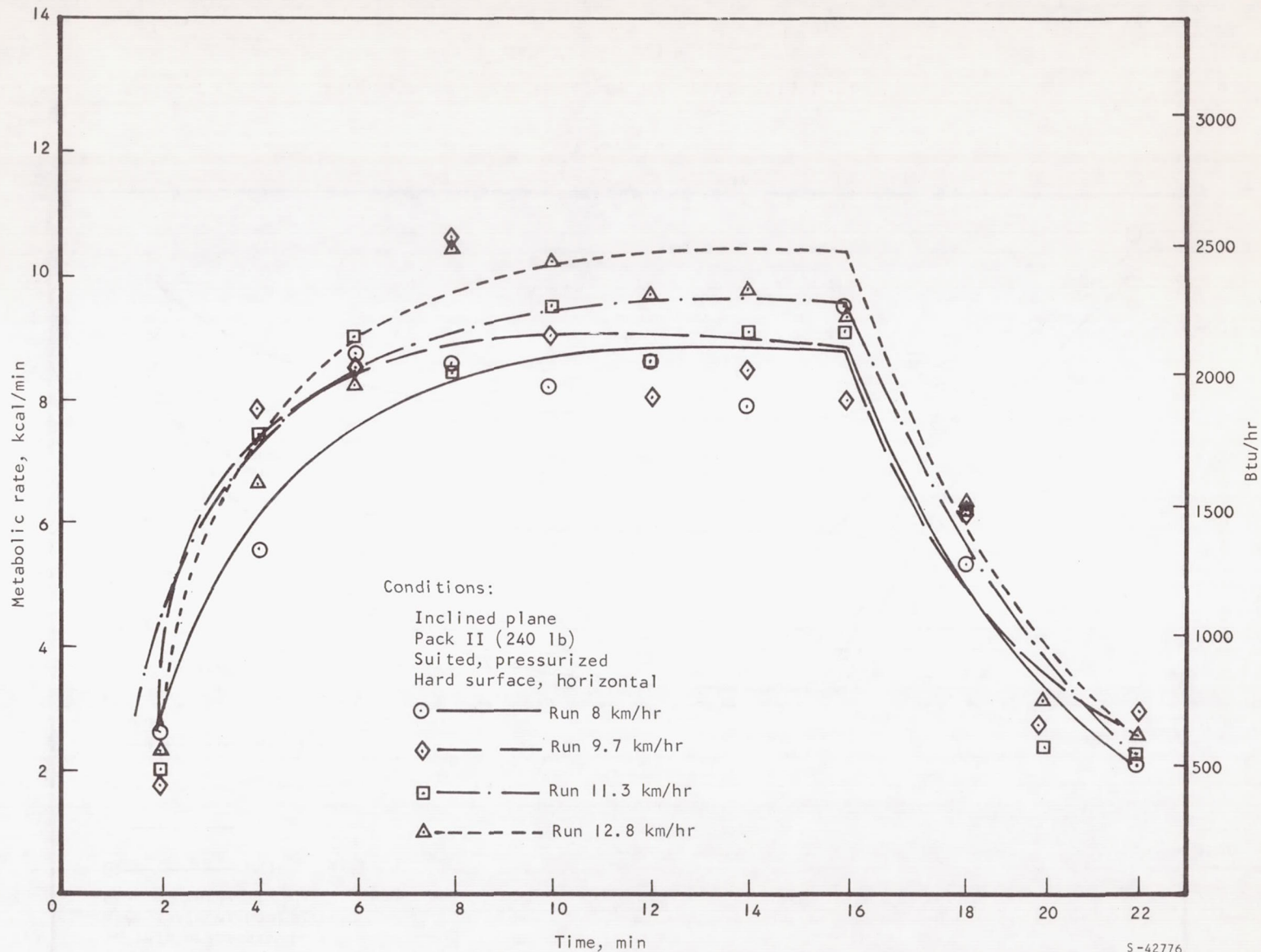


Figure A-13. Inclined Plane, Pack II, Lope



S-42776

Figure A-14. Inclined Plane Pack II, Run

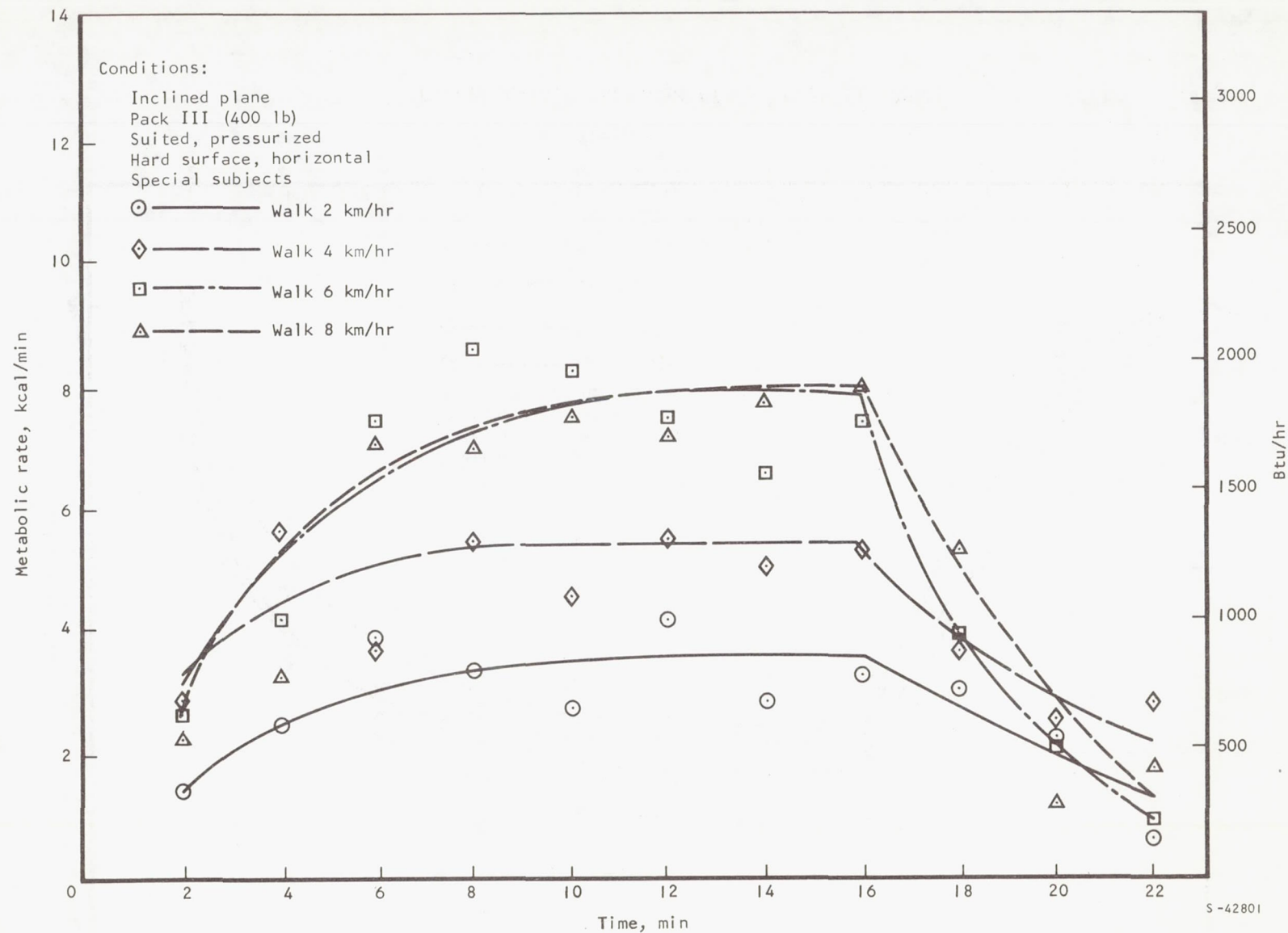


Figure A-15. Inclined Plane, Pack III, Walk

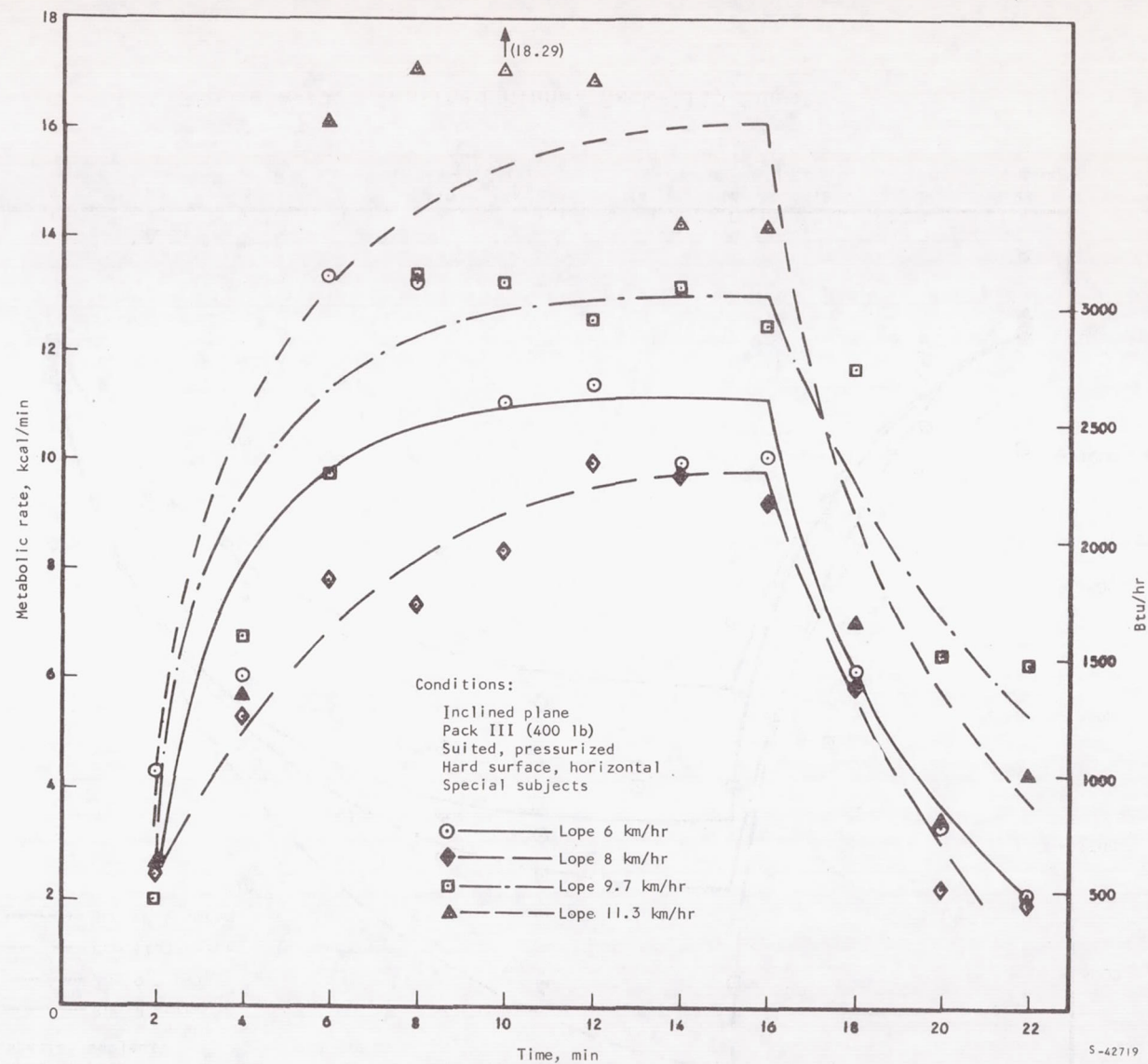


Figure A-16. Inclined Plane, Pack III, Lope

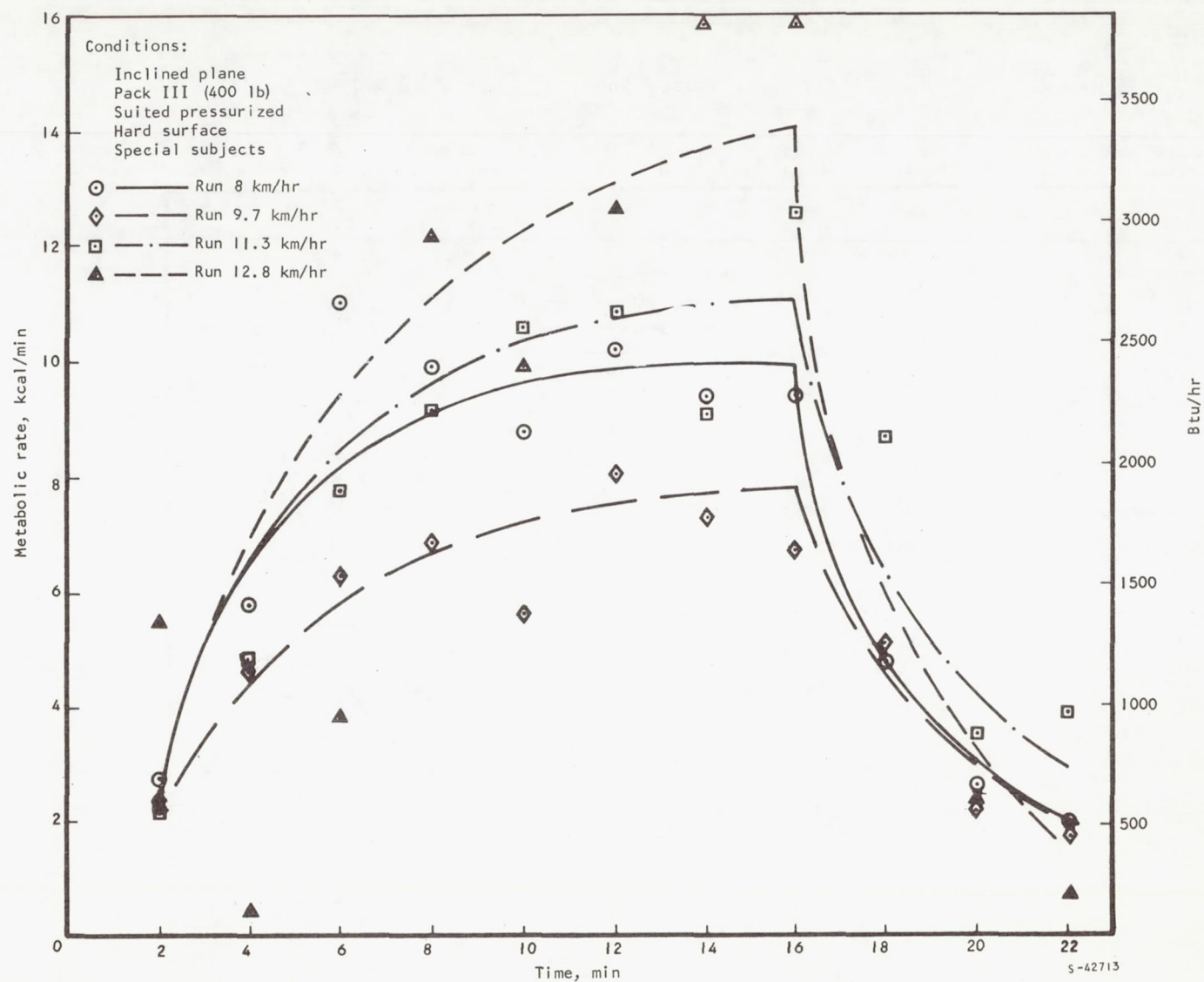


Figure A-17. Inclined Plane, Pack III, Run

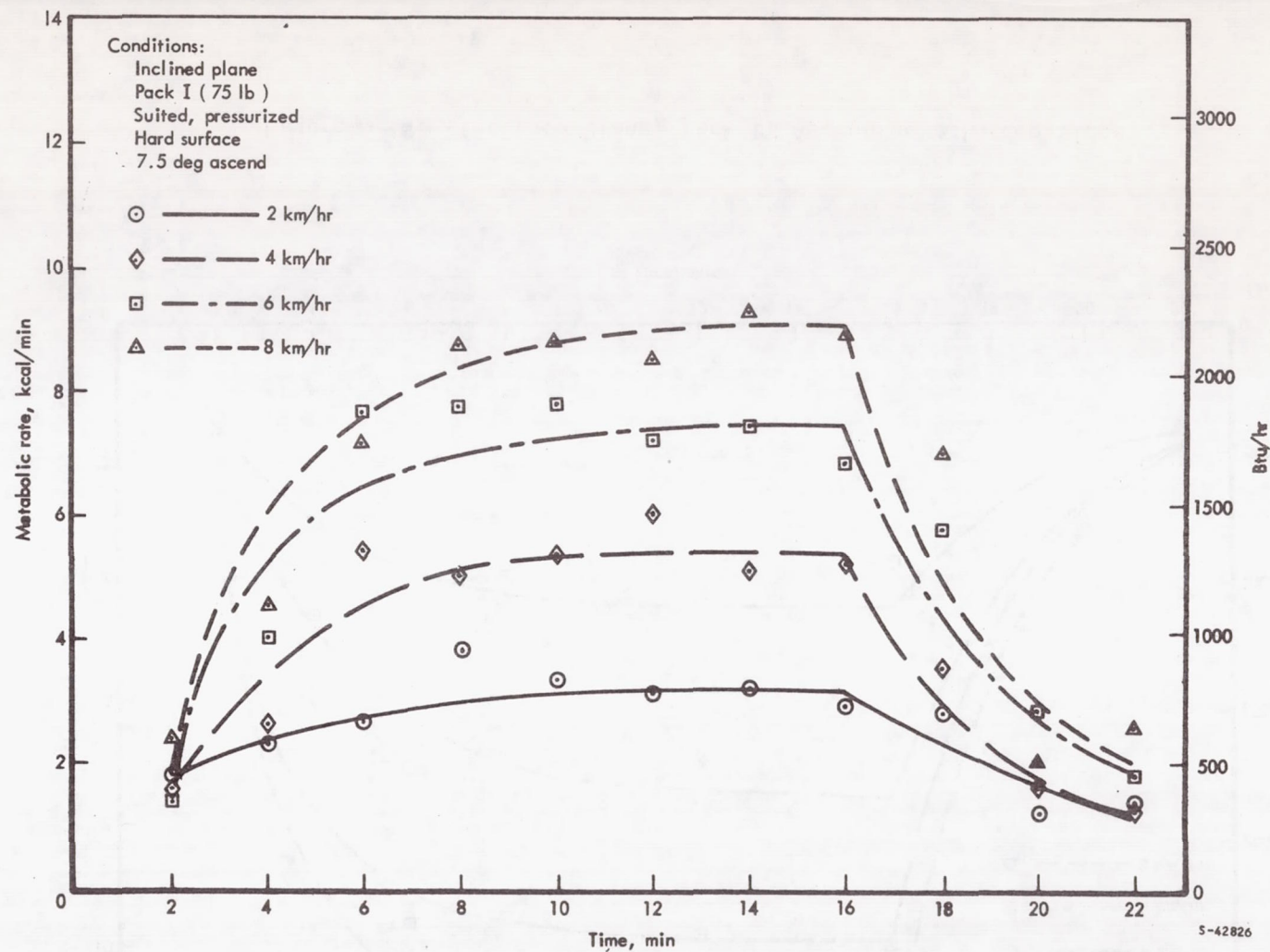


Figure A-18. Inclined Plane, Pack I, Ascending a 7.5-deg Slope

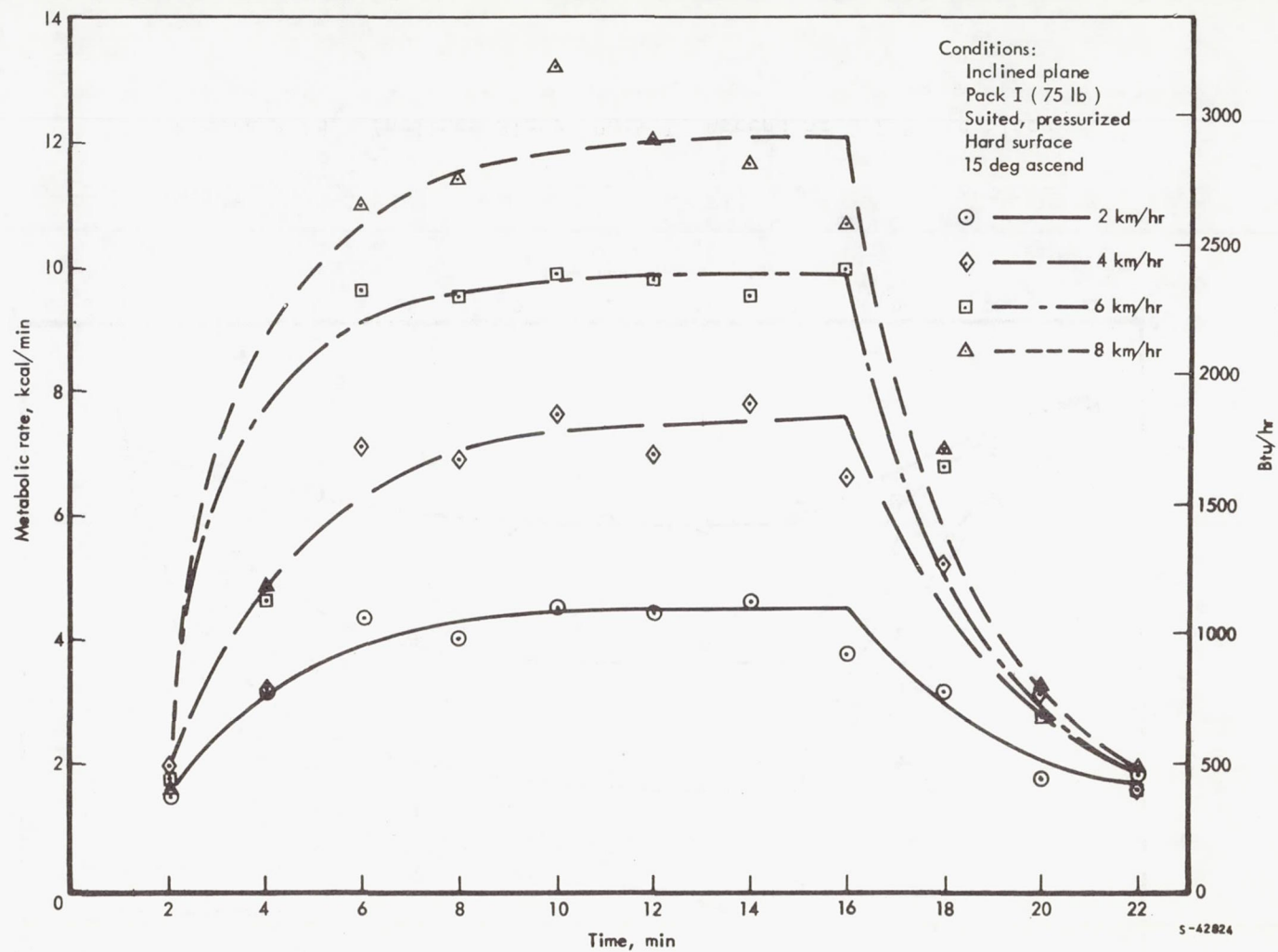


Figure A-19. Inclined Plane, Pack I, Ascending a 15-deg Slope

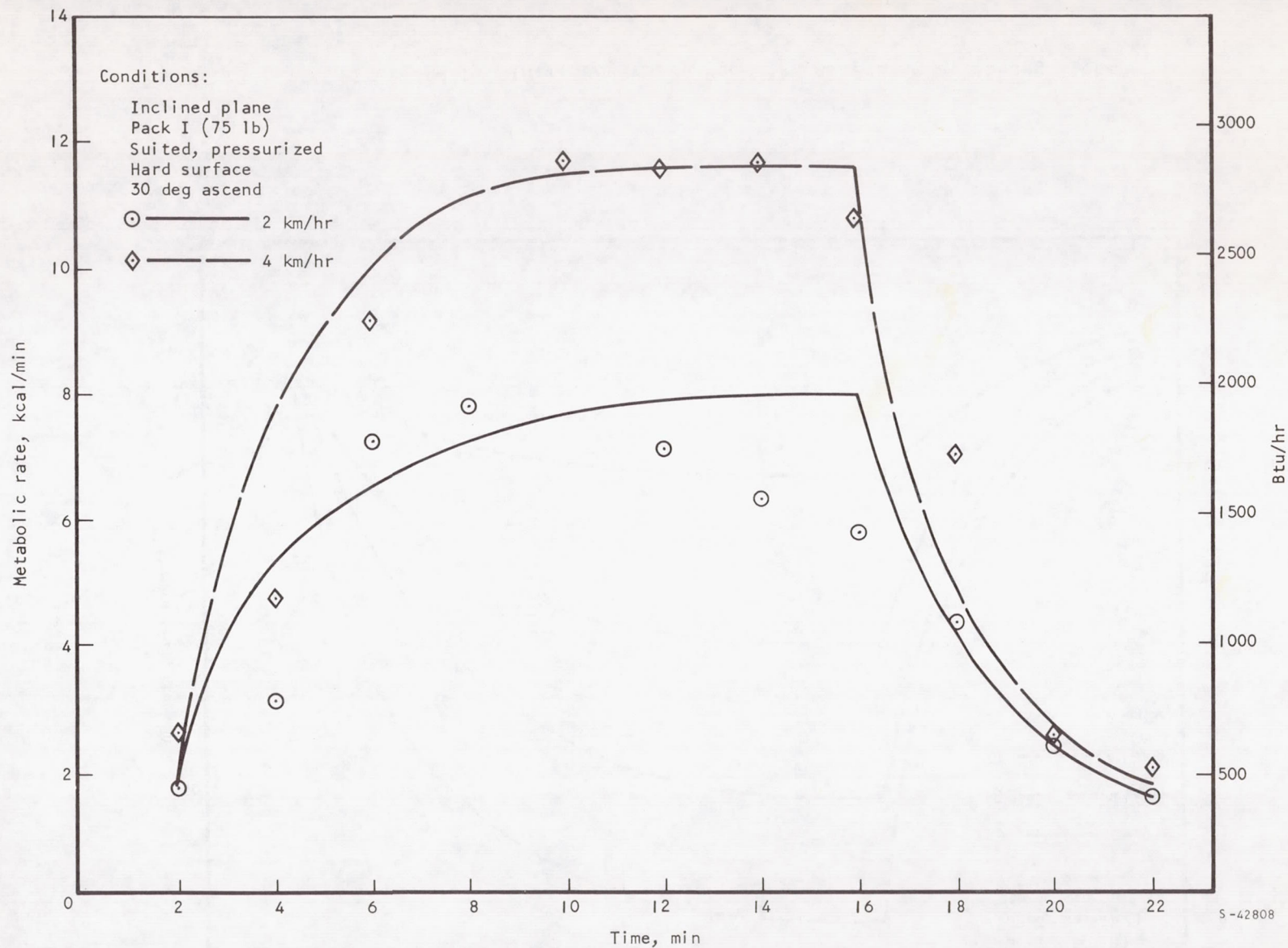


Figure A-20. Inclined Plane, Pack I, Ascending a 30-deg Slope

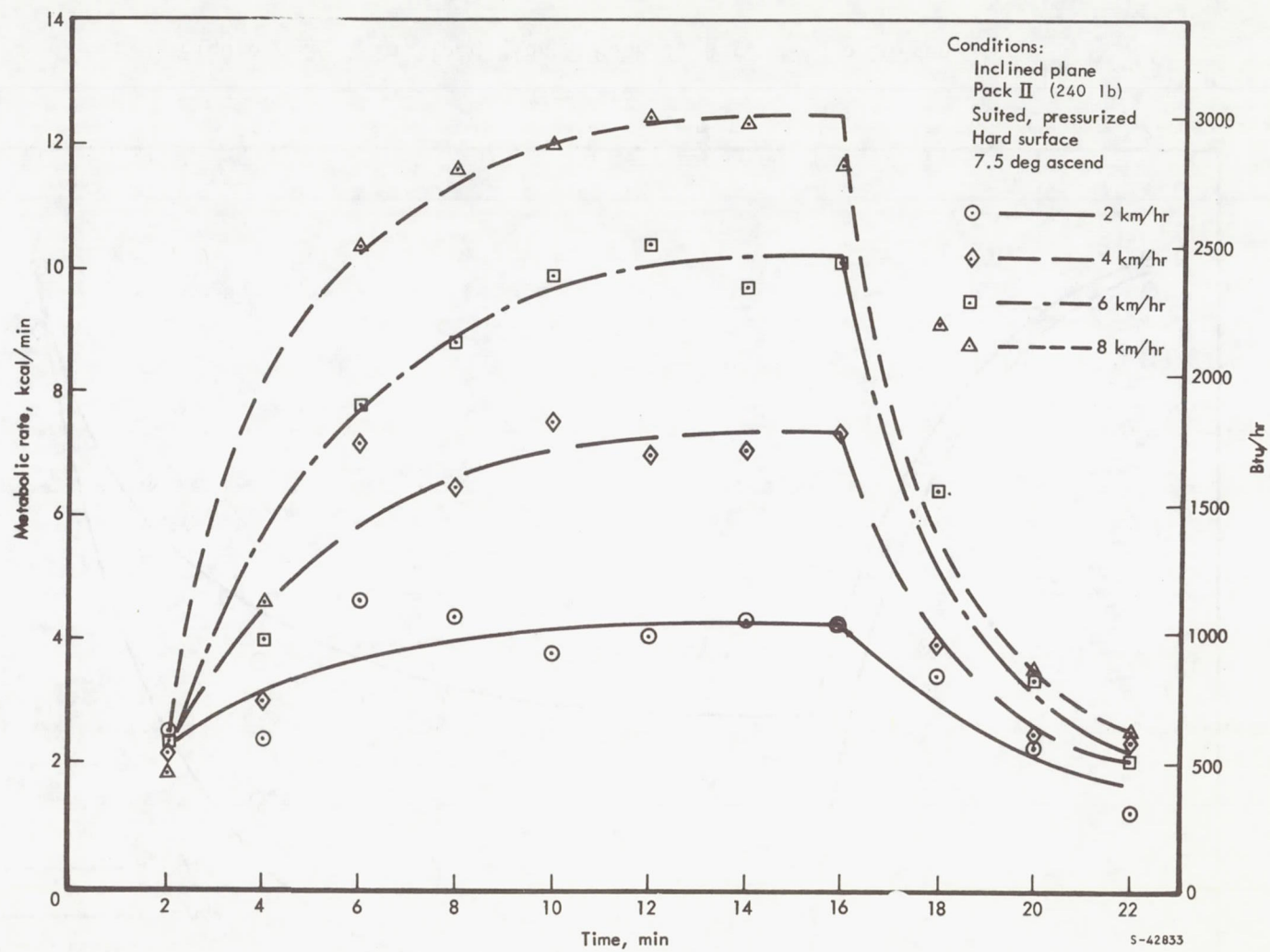


Figure A-21. Inclined Plane, Pack II, Ascending a 7.5-deg Slope

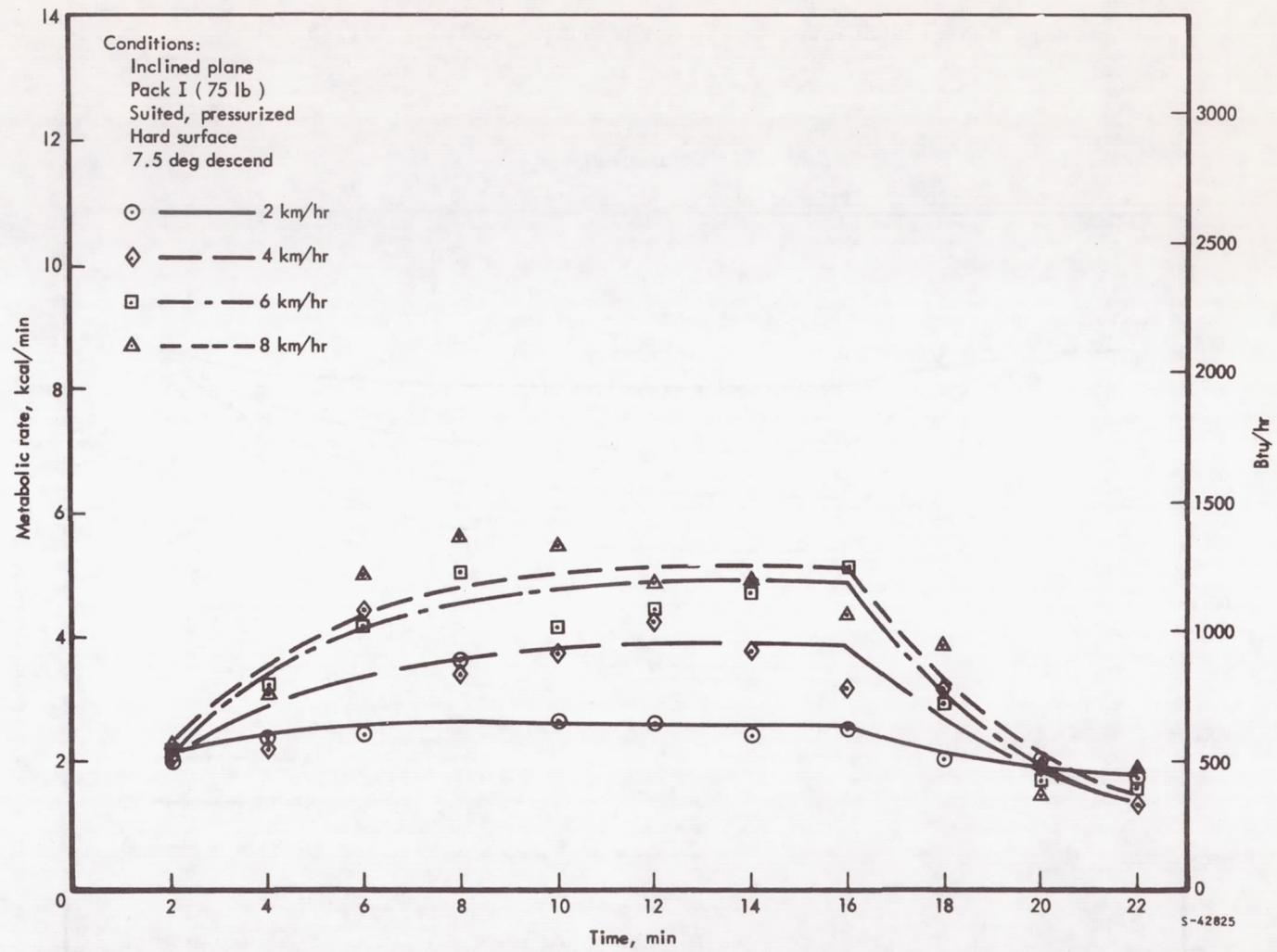


Figure A-22. Inclined Plane, Pack I, Descending a 7.5-deg Slope

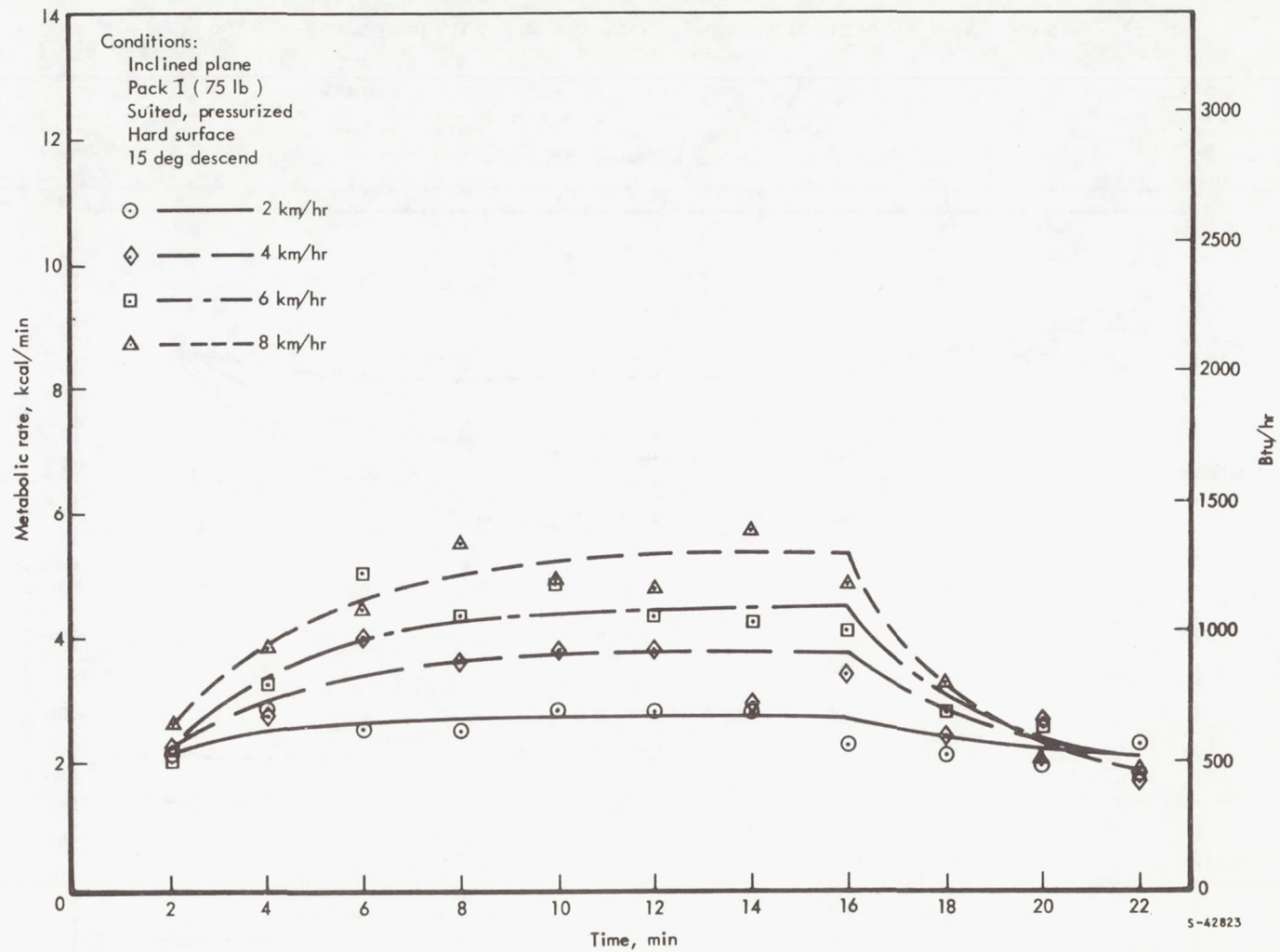


Figure A-23. Inclined Plane, Pack I, Descending a 15-deg Slope

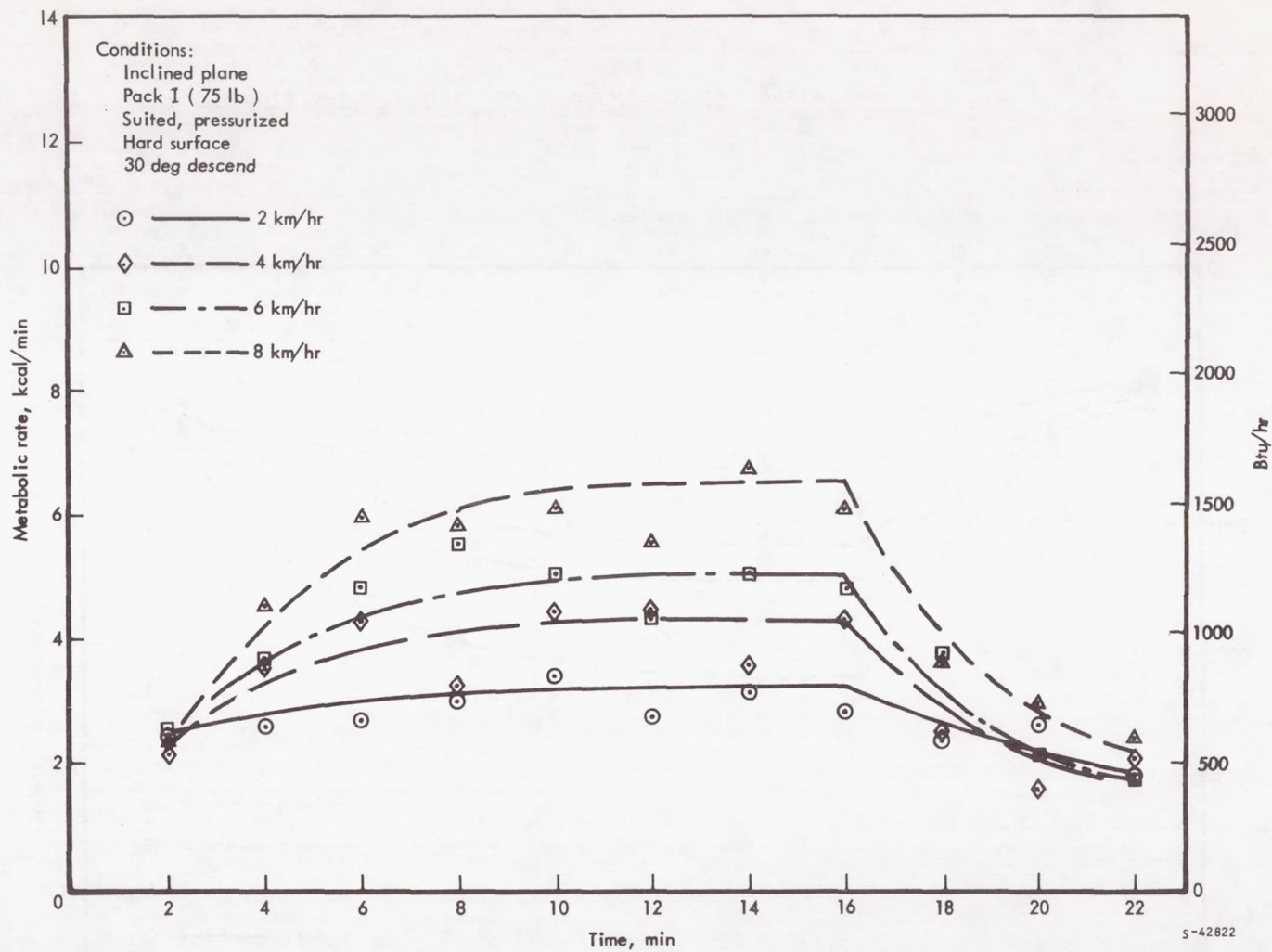


Figure A-24. Inclined Plane, Pack I, Descending a 30-deg Slope

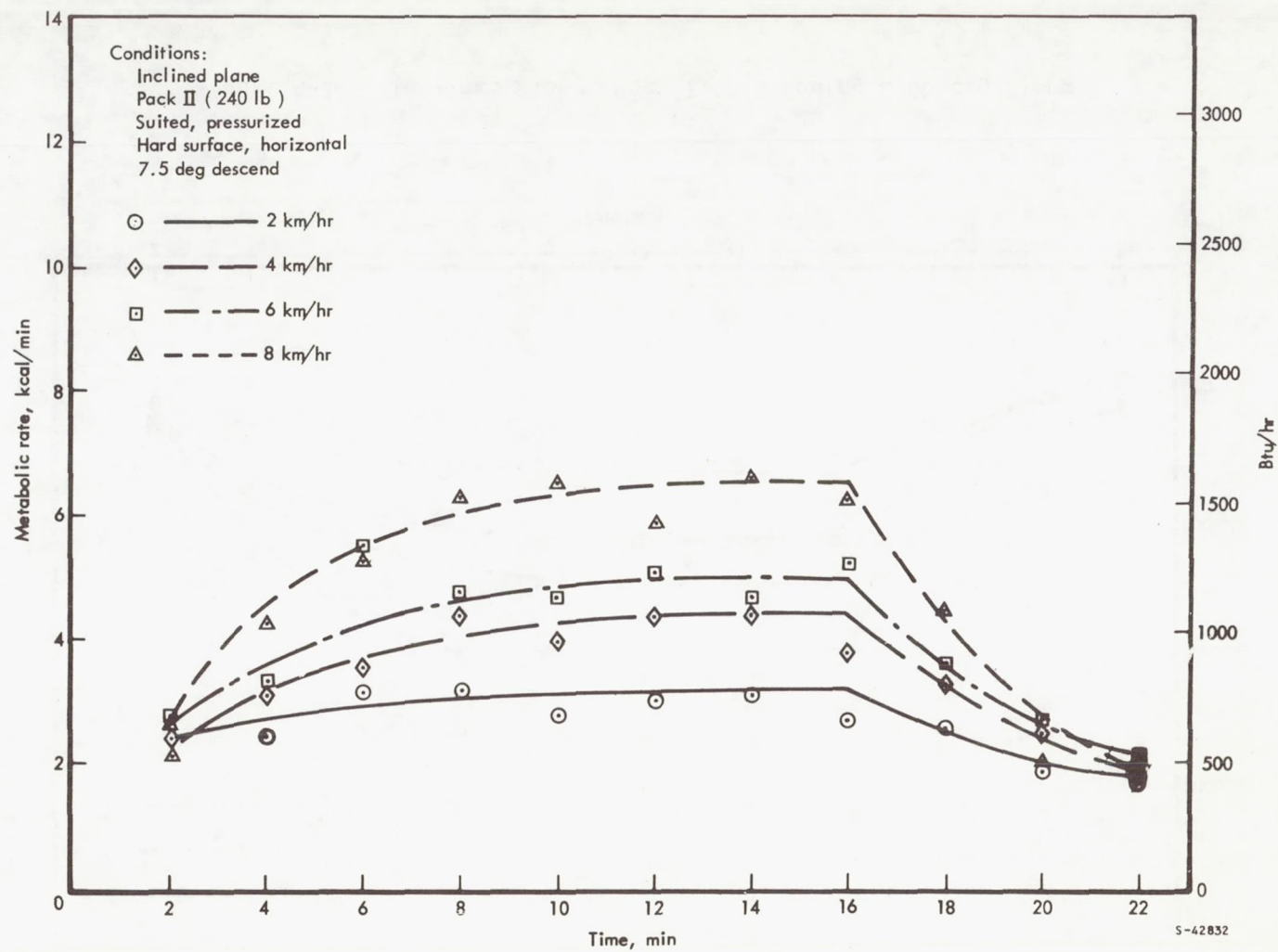


Figure A-25. Inclined Plane, Pack II, Descending a 7.5-deg Slope

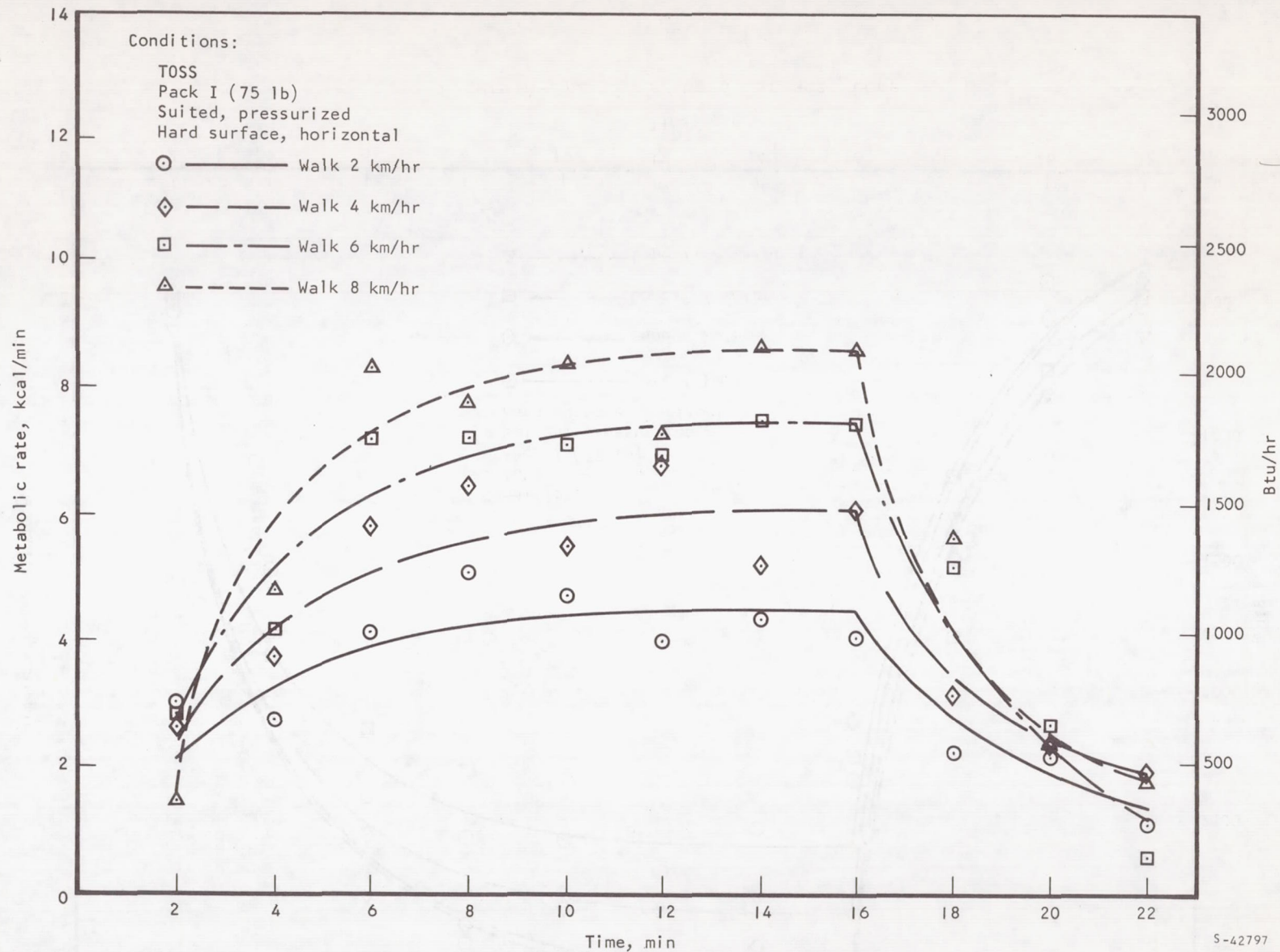


Figure A-26. TOSS Simulator, Hard Surface, Walk

S-42797

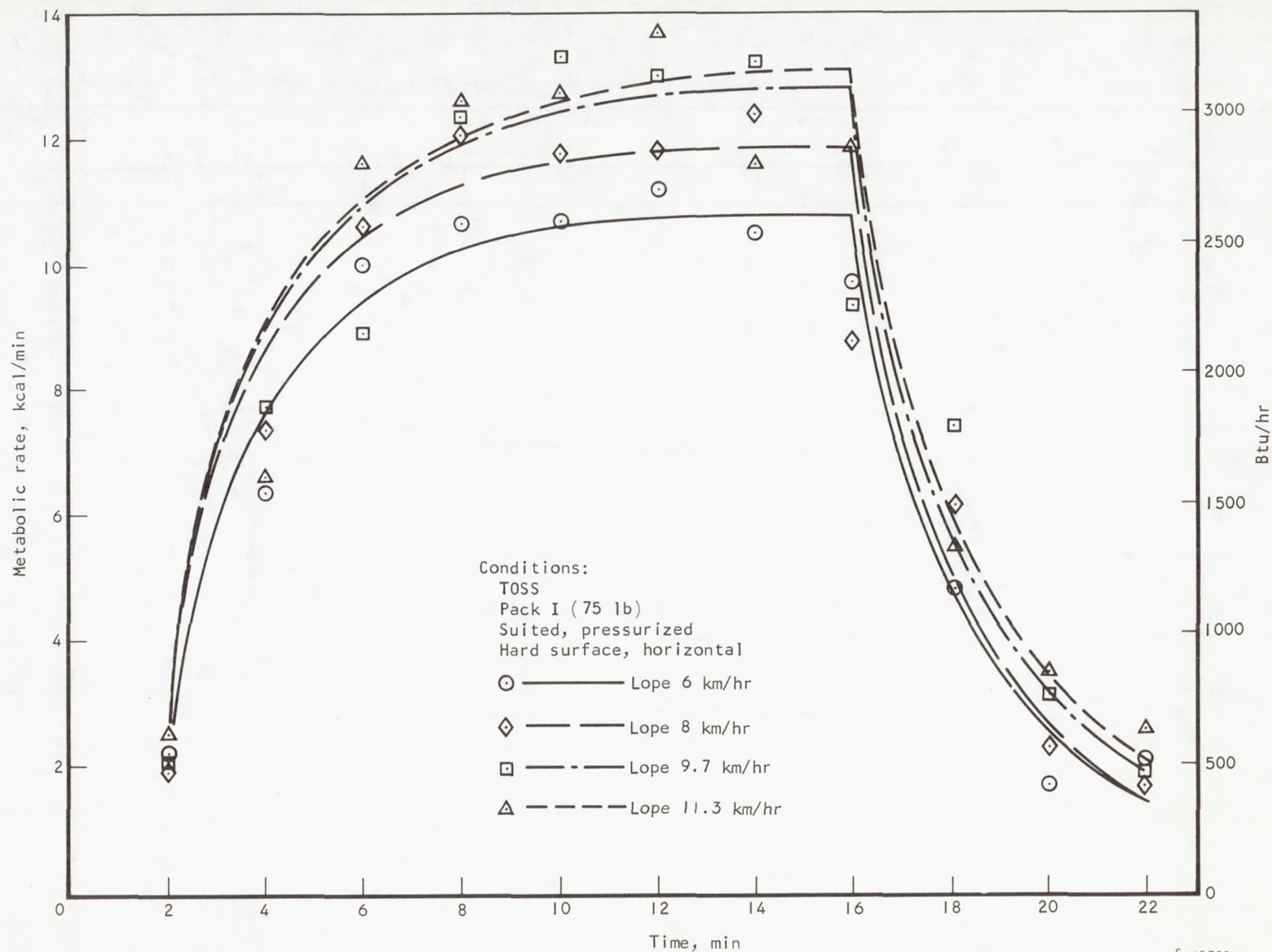


Figure A-27. T0SS, Hard Surface, Lope

S-42780

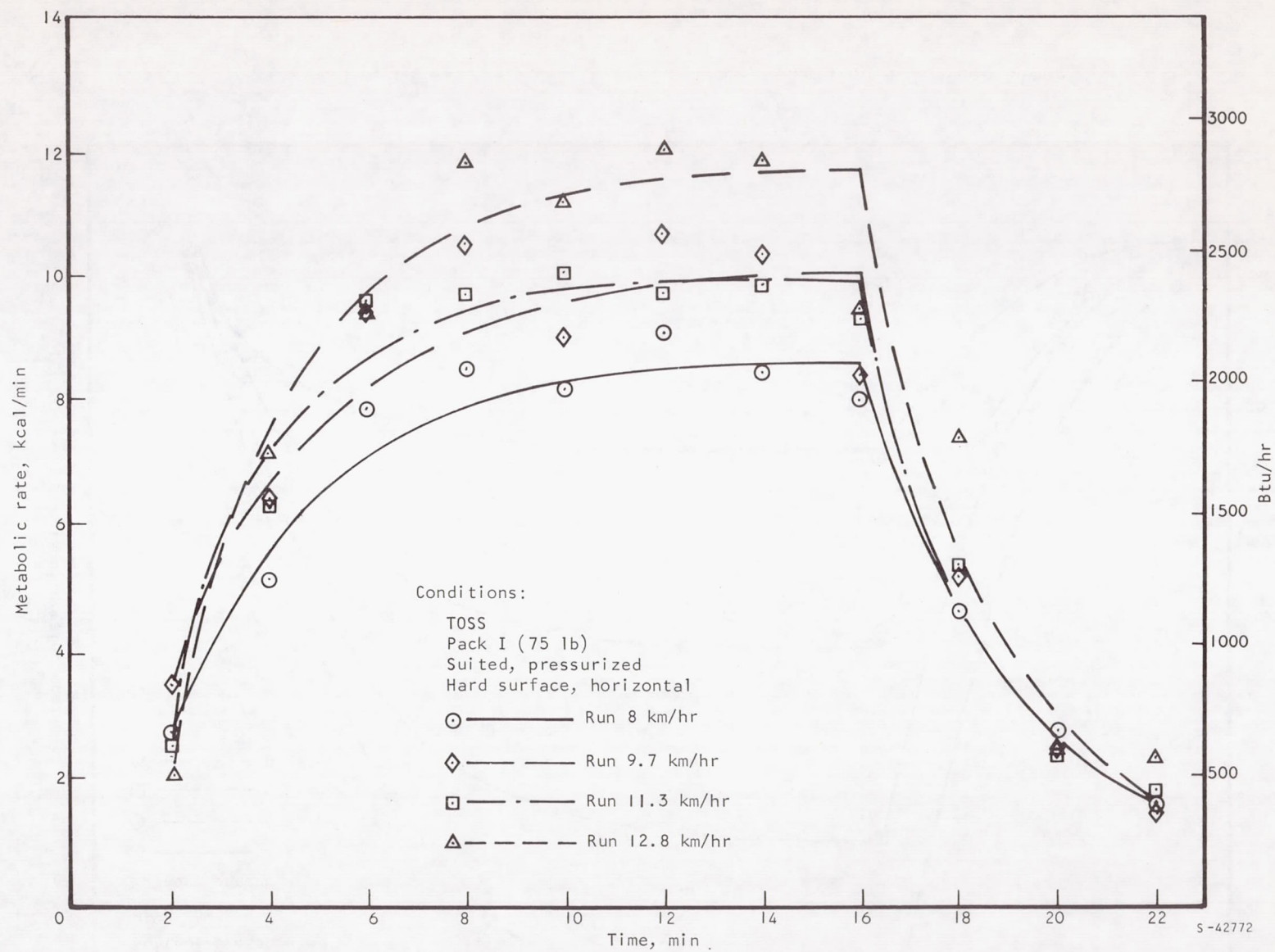


Figure A-28. TOSS, Hard Surface, Run

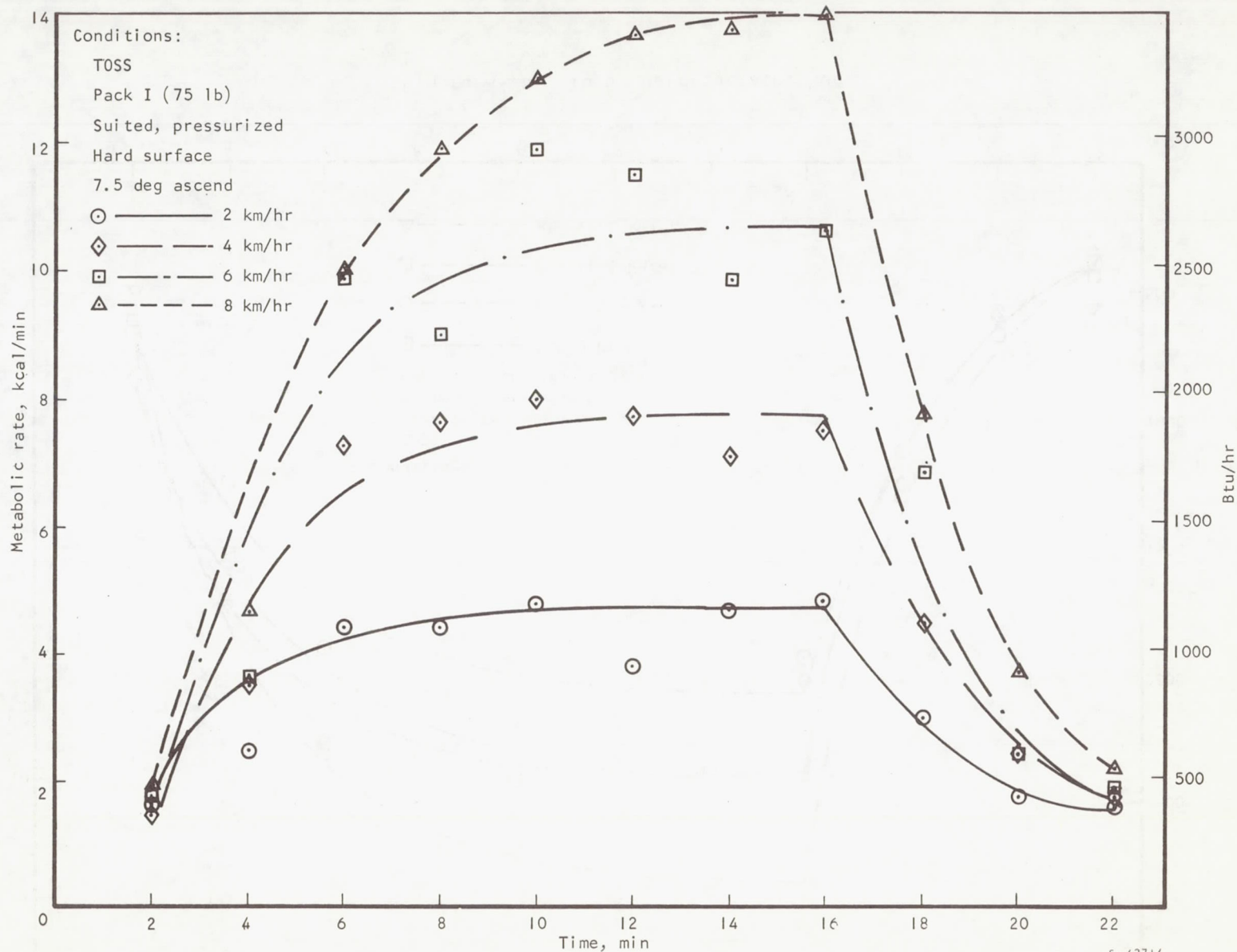


Figure A-29. TOSS, Hard Surface, Ascending a 7.5-deg Slope

S-42714

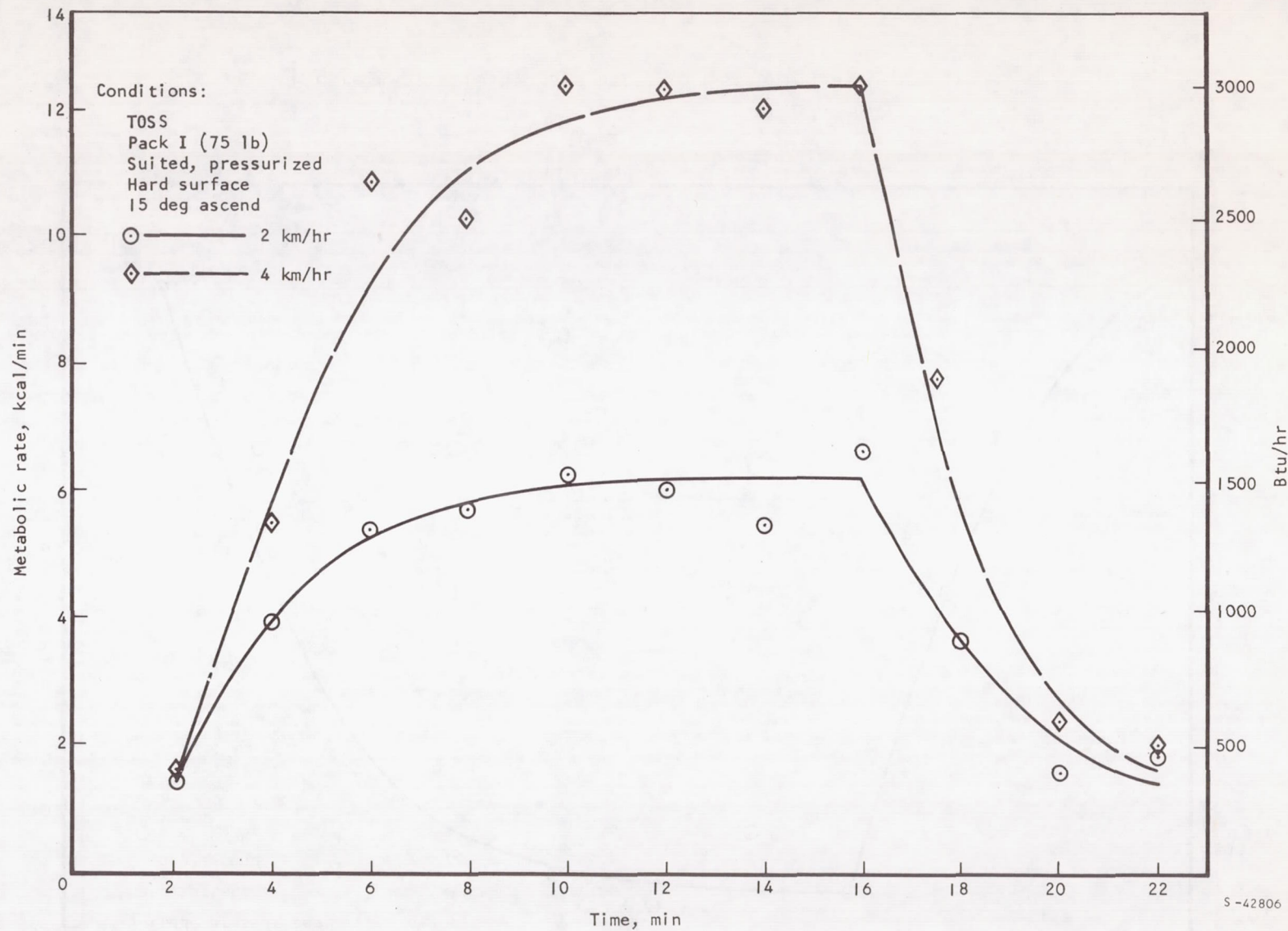


Figure A-30. T0SS, Hard Surface, Ascending a 15-deg Slope

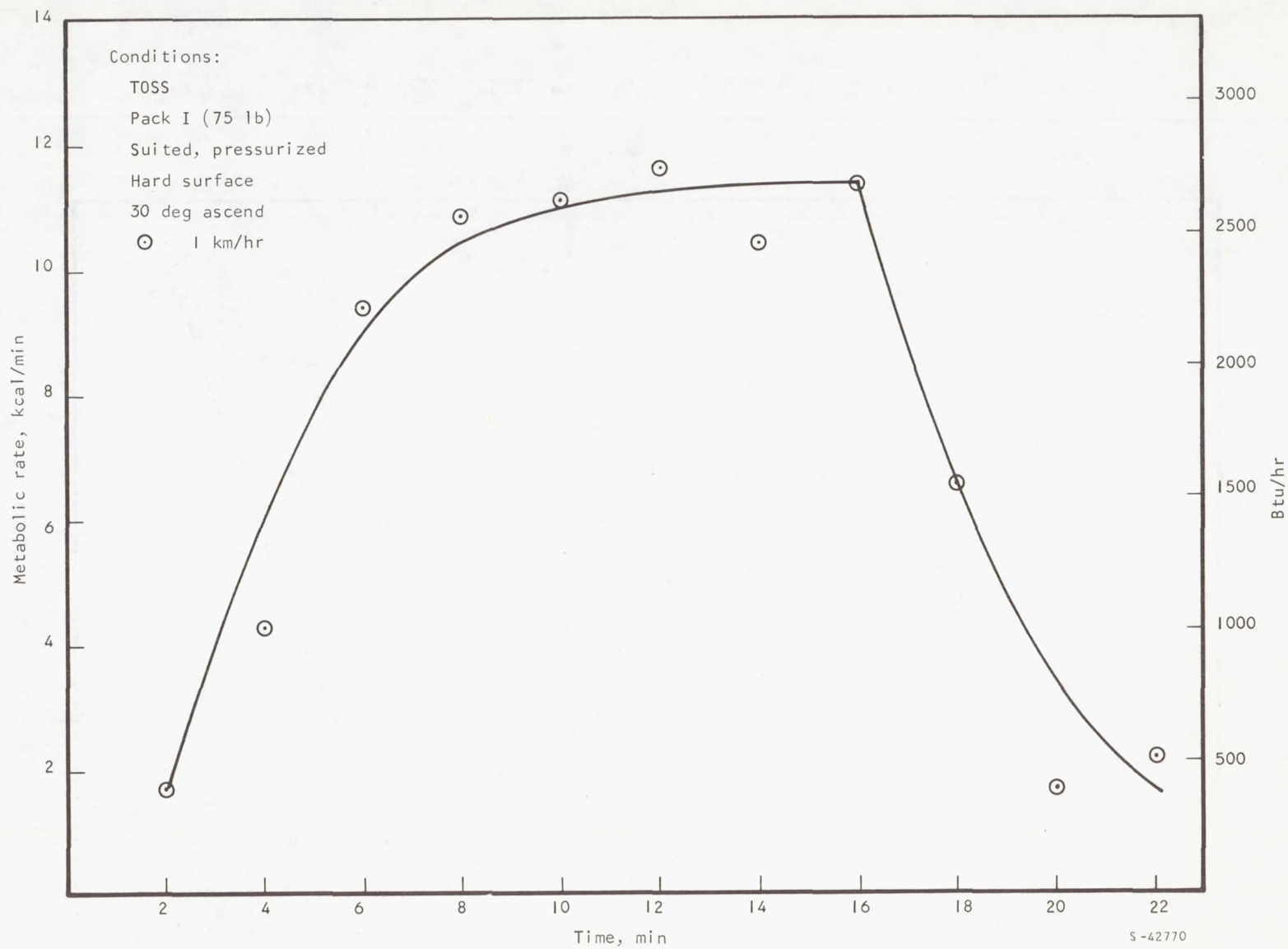


Figure A-31. TOSS, Hard Surface, Ascending a 30-deg Slope

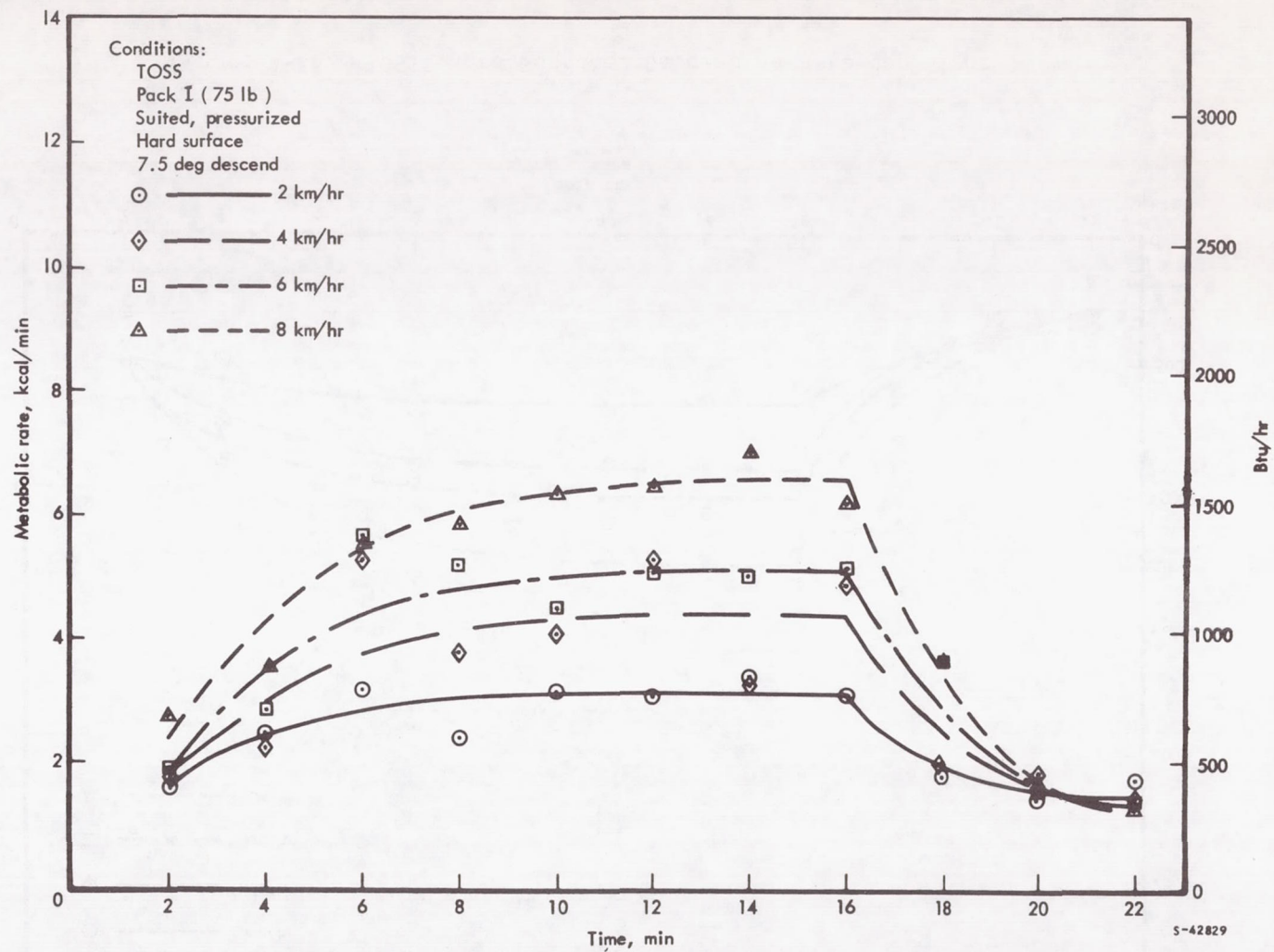


Figure A-32. TOSS, Hard Surface, Descending a 7.5-deg Slope

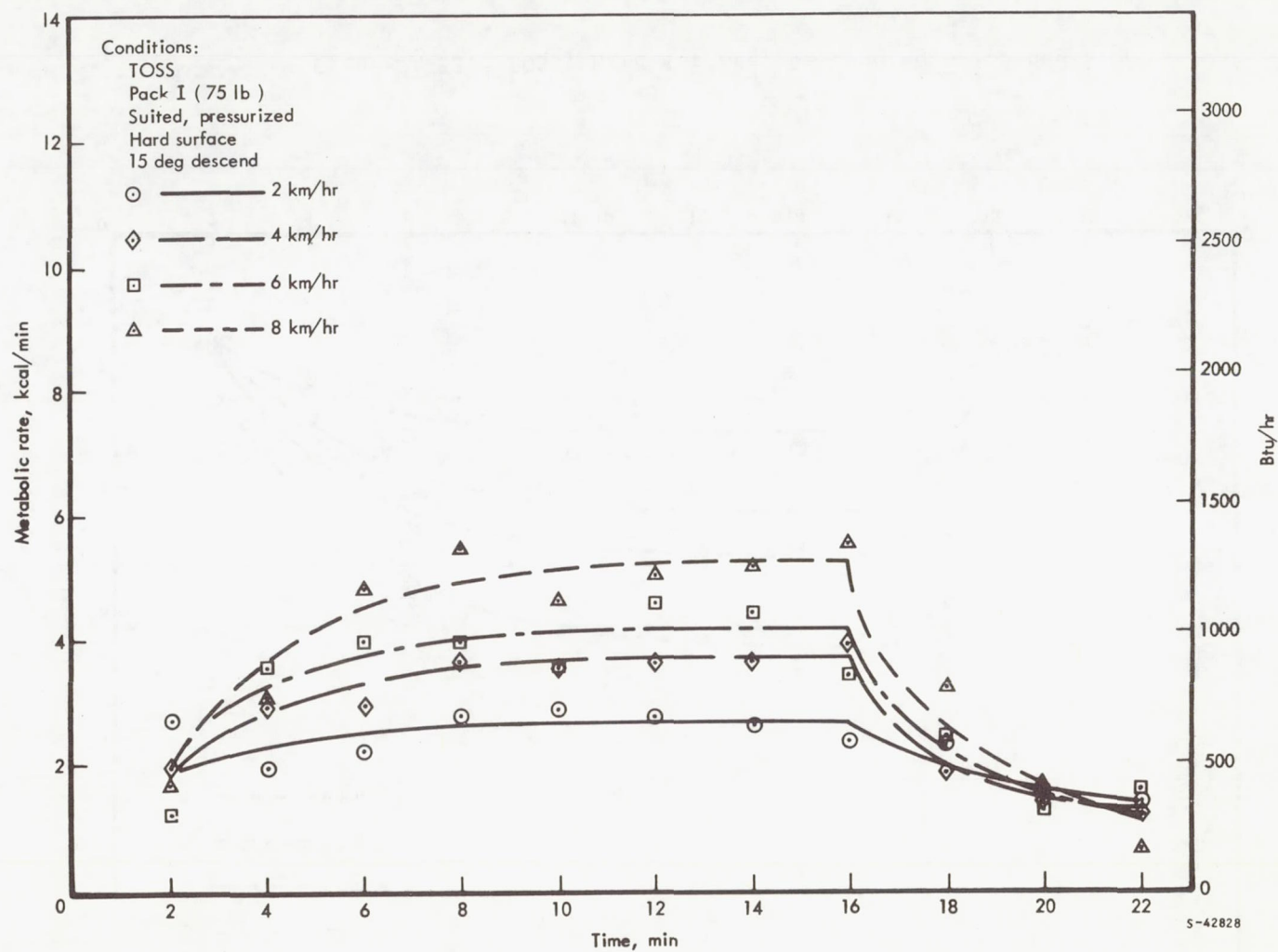


Figure A-33. TOSS, Hard Surface, Descending a 15-deg Slope

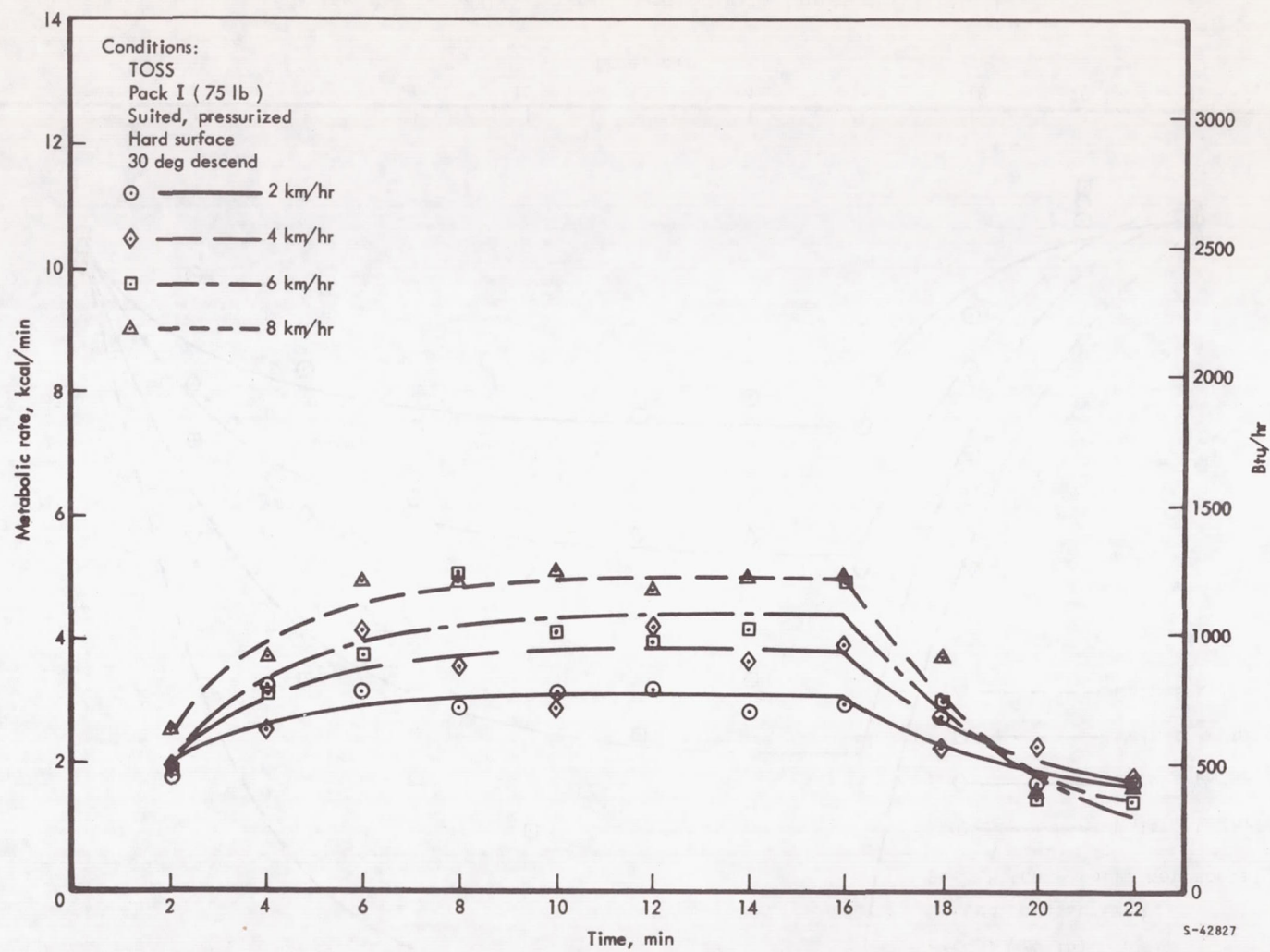


Figure A-34. TOSS, Hard Surface, Descending a 30-deg Slope

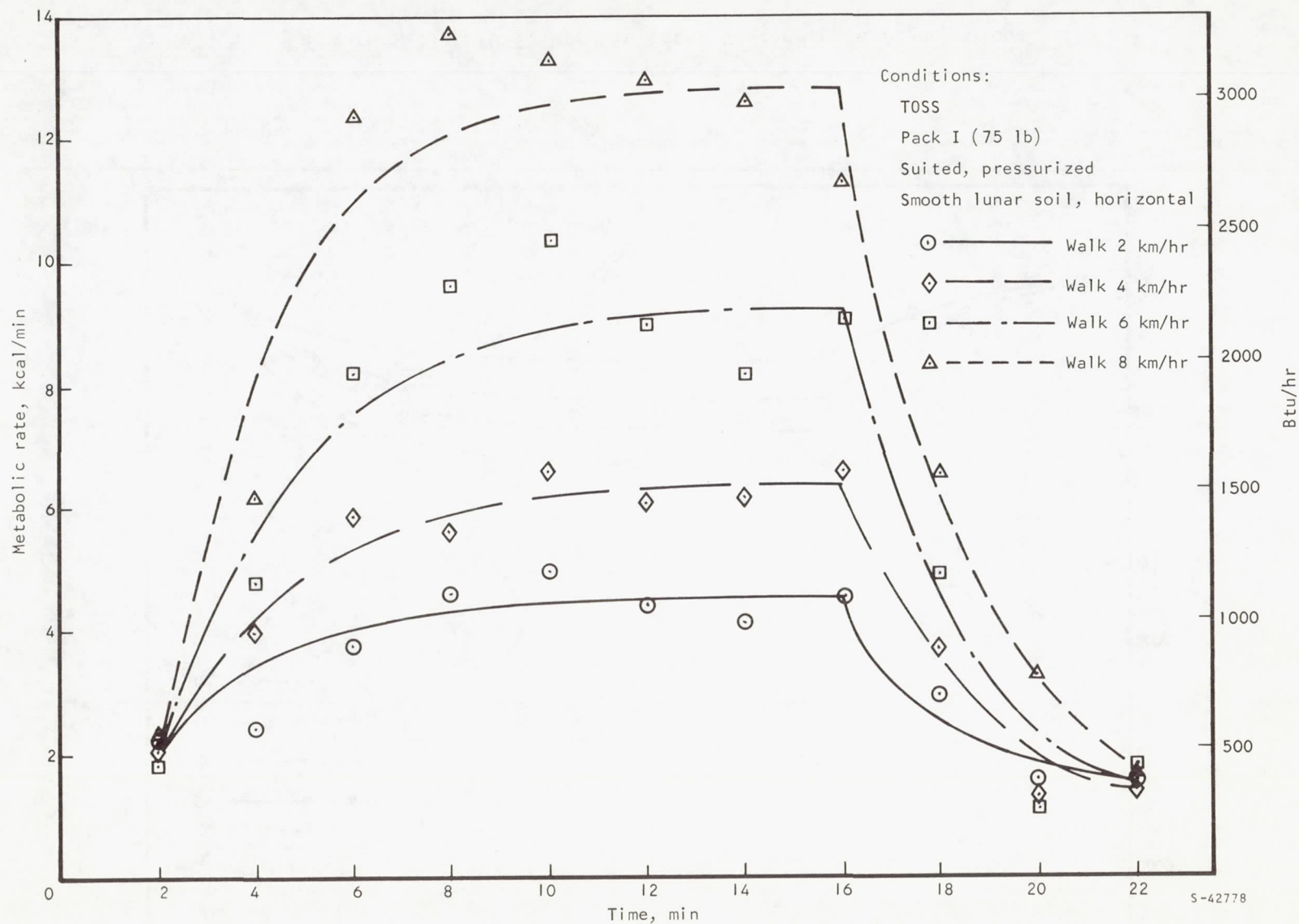


Figure A-35. T0SS, Simulated Smooth Lunar Soil, Walk

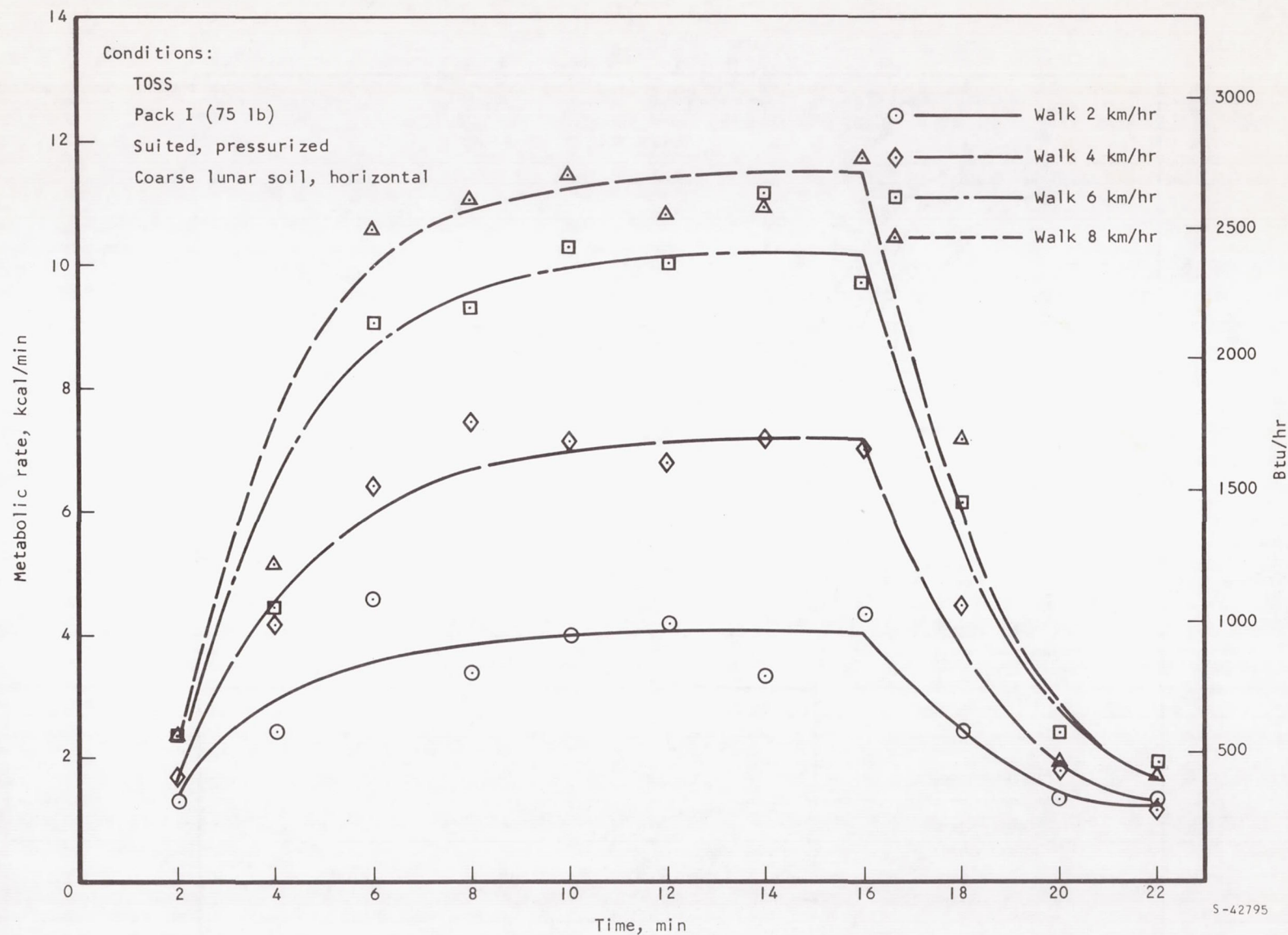


Figure A-36. TOSS, Coarse Lunar Soil, Walk

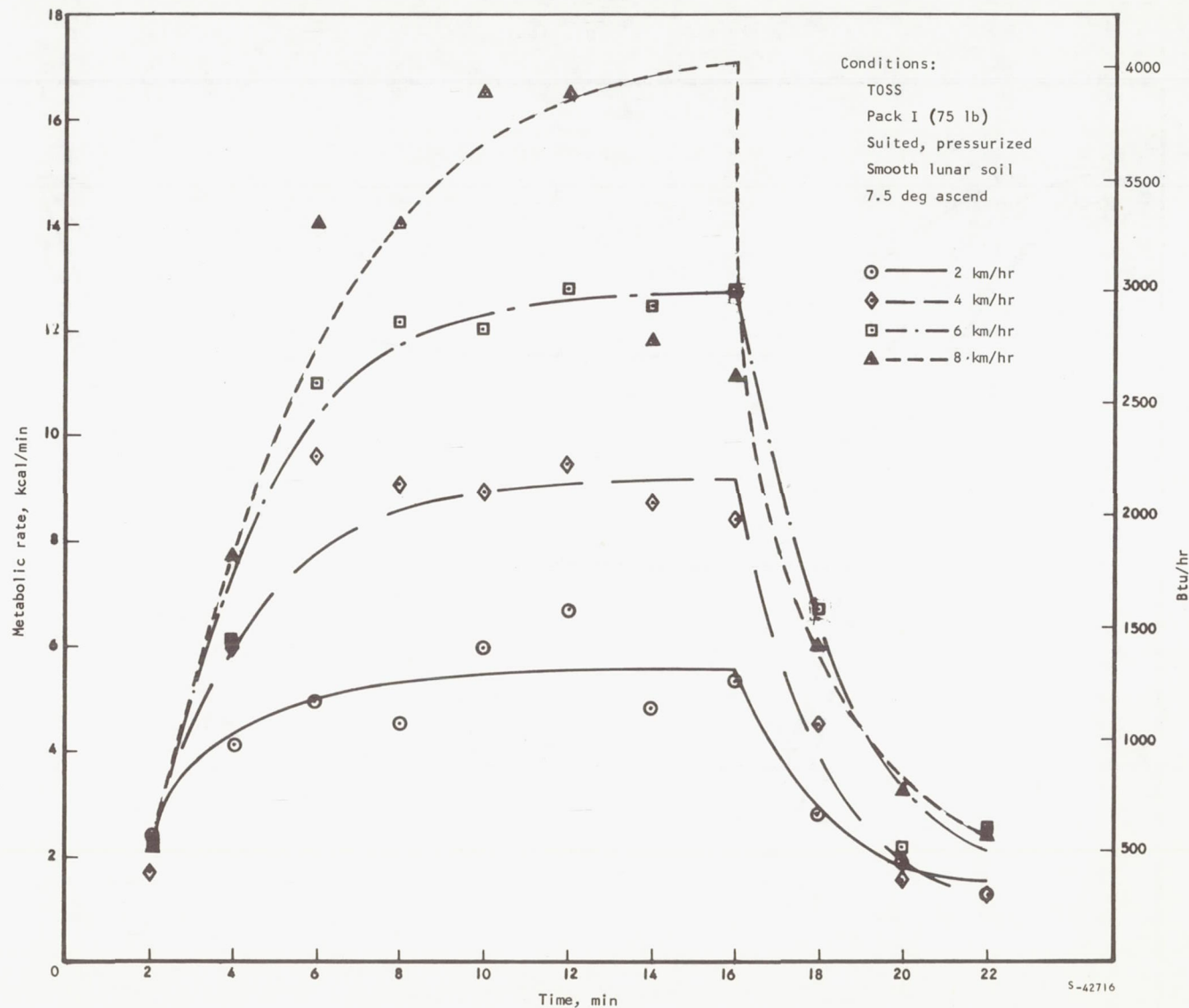


Figure A-37. TOSS, Smooth Lunar Soil, Ascending a 7.5-deg Slope

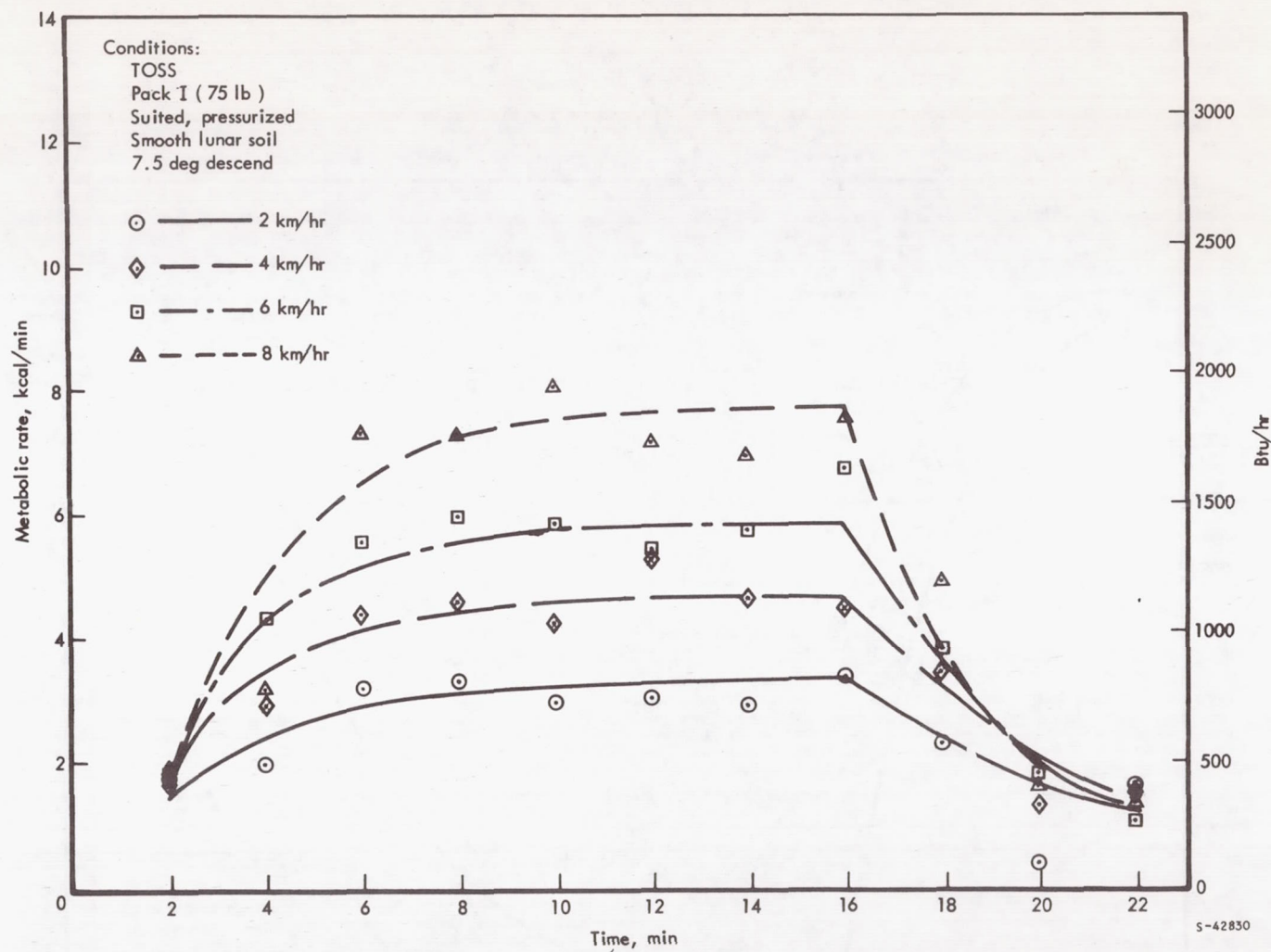


Figure A-38. TOSS, Smooth Lunar Soil, Descending a 7.5-deg Slope

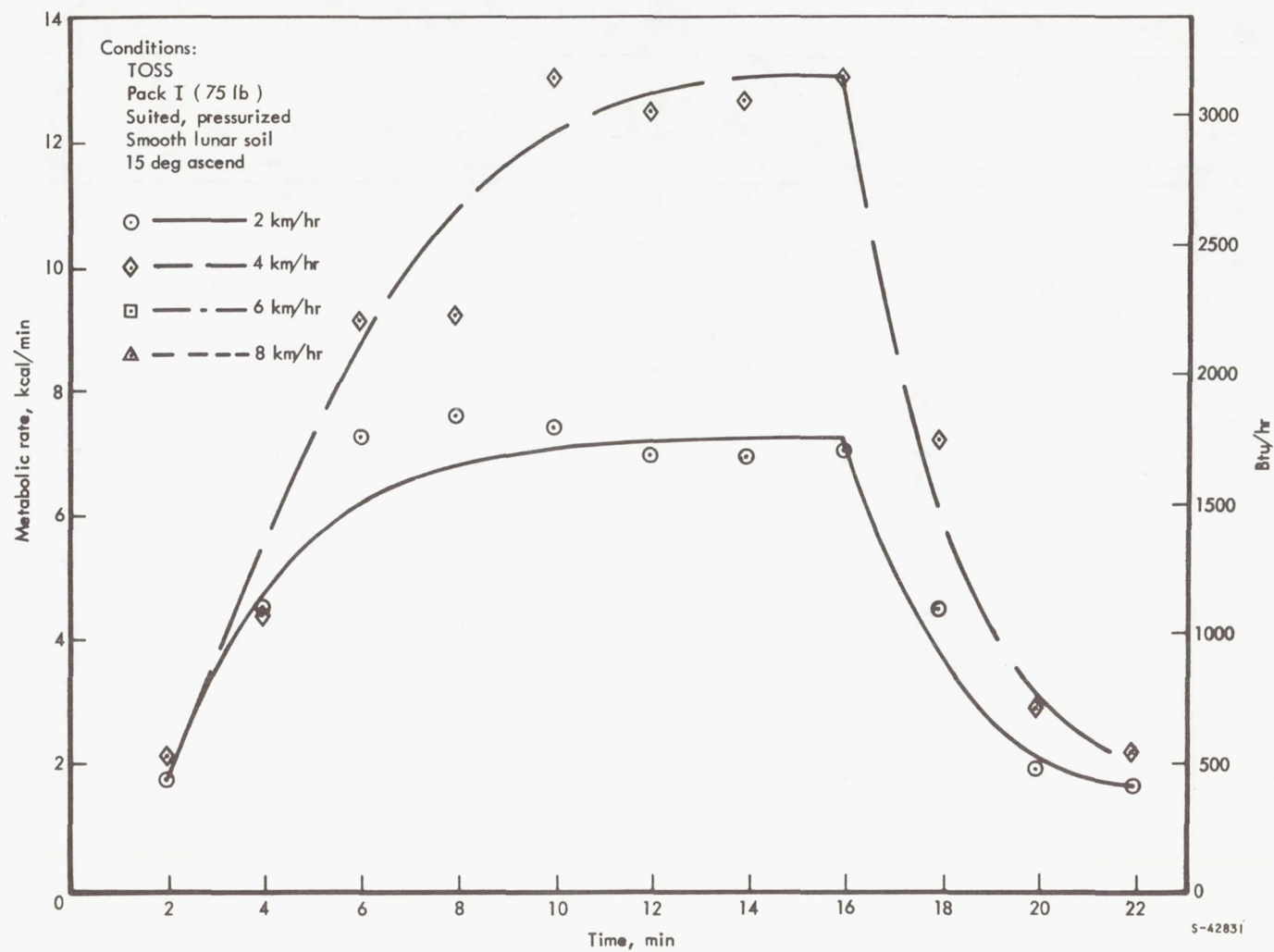


Figure A-39. TOSS, Smooth Lunar Soil, Ascending a 15-deg Slope

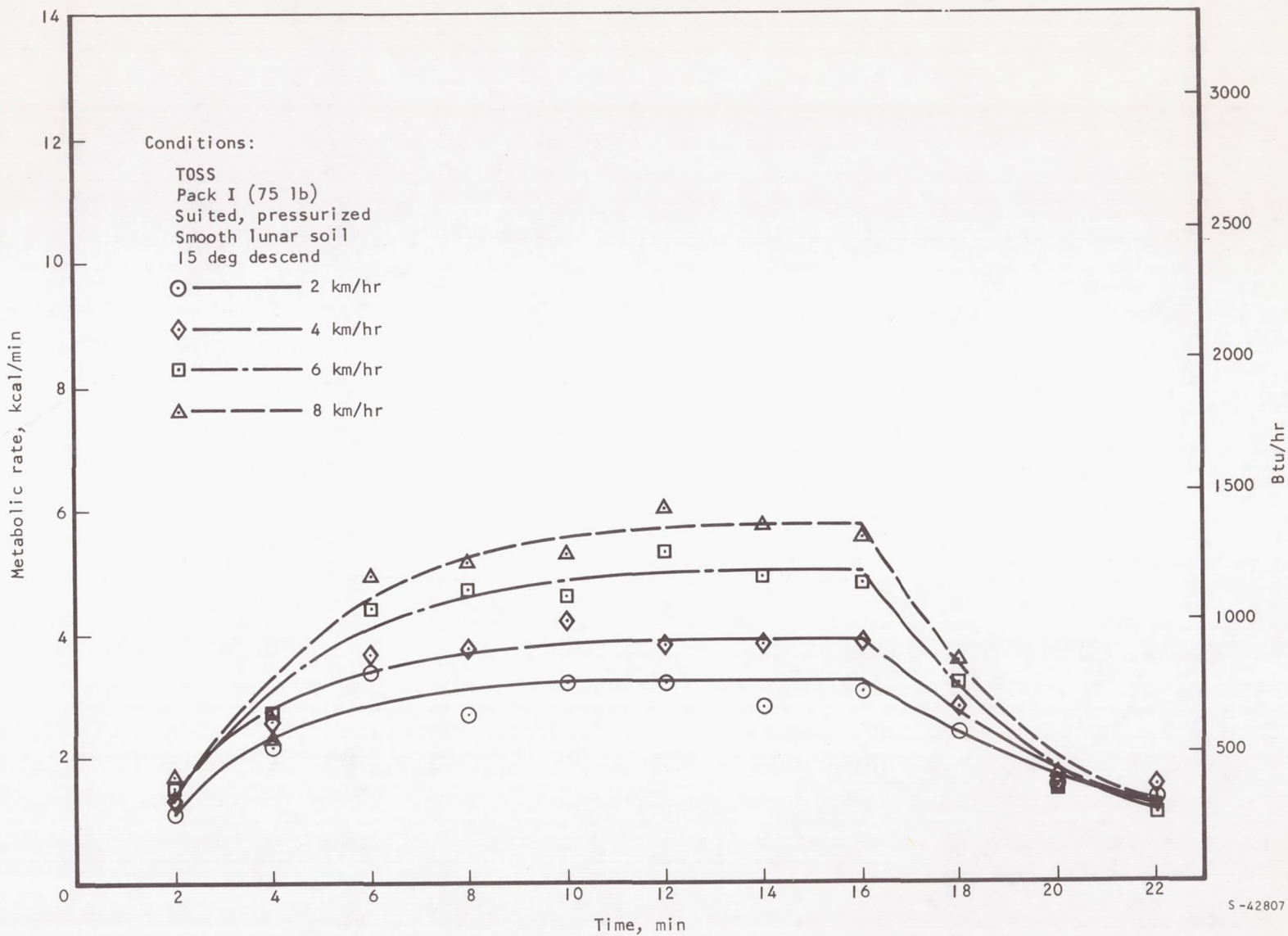


Figure A-40. TOSS, Smooth Lunar Soil, Descending a 30-deg Slope

Page Intentionally Left Blank

APPENDIX B

CRITIQUE OF LITERATURE COMPARING LOCOMOTION ON A TREADMILL TO LOCOMOTION ON A STATIONARY SURFACE

In studies involving measurement of the metabolic costs for given levels of physical activity, use of a motor-driven treadmill has almost completely replaced actual outdoor walking or running conditions. More convenient for such measurements, treadmill experiments can be conducted in a stationary, confined area or room with an easily controlled environment. The treadmill also permits more accurate measurements because of the constancy of the work load imposed on a subject. In addition, the test subjects are not required to carry the physiologic test equipment.

It is normally assumed that treadmill tests give the same results as if the experiment had been conducted on a stationary surface. However, there are differences in the conditions imposed by these situations. A subject on a motor-driven treadmill remains in place and the belt moves past him in a backward direction. When walking or running on a stationary surface, the subject moves forward over the surface. There are two work-producing machines in action when one walks on a motor-driven treadmill, the subject and the motor. There is always a possibility of interaction between the two machines. They may supplement each other, hinder each other, or have no effect on each other. Because of this possible interaction, investigators using treadmills in their studies occasionally ask the question: Does running or walking on a treadmill differ from walking or running on a stationary surface? If so, how and to what extent? (See References B-1 through B-6.) If the mechanics of the two modes do differ, it should be evident in either the metabolic costs or the gait of the subject or both.

Atzler and Herbst (Reference B-1) reported a comparison of treadmill walking with road walking. They concluded that the energy cost for treadmill walking is about 1.2 percent higher than for road walking. Durig (References B-2 and B-3) indicates that treadmill progression requires a higher energy expenditure than road walking, but Smith (Reference B-4) indicates that treadmill walking was found to be more economical. Daniels (Reference B-5) reports that the metabolic requirements are approximately 10 percent lower for treadmill walking than for road walking. Daniels suggests that some of the energy used in vertical rise may be derived from the motion of the treadmill. More recently, Ralston (Reference B-6) has found no significant differences between treadmill walking and floor walking in terms of the energy requirements. At first glance, it appears impossible to arrive at any conclusions based on the reported findings above. However, critical review of these reports does provide some insight. The parameters that could affect a comparative study of the mechanics of locomotion are discussed in succeeding paragraphs.

PARAMETERS

Training

Some instruction and practice in using the respiratory apparatus is necessary before the tests begin. The subject should practice locomotion on the treadmill, if for no other reason than to remove any possible anxiety.

Velocity

Velocity of locomotion on the treadmill is constant and can be accurately set to a fixed value; this is not easily accomplished for road walking. In particular, the constancy of motion is difficult to achieve. The overall velocity may be accurate, but road walking permits unwanted accelerations and decelerations.

Environmental Conditions

Laboratory conditions are, of course, easily controlled. Temperature, wind, and humidity affect metabolic rates and possibly gait characteristics.

Surfaces

The treadmill platform over which the belt slides is usually either a flat surface (slipway) or consists of a series of rollers. The rollers offer less friction to belt motion and thus result in a more constant belt speed; however, this advantage is offset by a less stable footing. Increases in metabolic rate on this type of treadmill, as opposed to the slipway treadmill, have been noted. The treadmill belt has been made of leather, fabric, and rubber. Road surfaces may be smooth, uneven or rough, and consist of dirt, gravel, black-top or concrete. Floor surfaces in a building could be made of wood, linoleum, plastic, tile, masonry, or concrete. These floors may be in various states of wear and have various coats of wax. The soles of the subjects shoes may vary between leather (slippery) and rubber tread (sure grip). The interface between the shoes and the surface is probably the most important factor. With less friction, more work is involved in locomotion. The metabolic costs of walking on different types of surfaces have been studied (References B-7 through B-10)

Clothing

The subject's clothes should not be restrictive and should be the same for treadmill or stationary surface travel.

ANALYSIS OF DATA

Durig (References B-2 and B-3) used a treadmill with rollers, which could account for his findings which show higher energy requirements for treadmill locomotion than for road walking. Atzler and Herbst (Reference B-1) found treadmill locomotion to be slightly higher than road walking, but they used only one subject and obtained two readings for each mode with one of the road readings much lower than the other.

Daniels (Reference B-5) compared indoor treadmill testing to outdoor road walking for one group of men and to outdoor walking on a cinder track for another group. The treadmill tests on the first group were run in a laboratory at 19°C (66°F). The men wore light underclothing and twill fatigue uniforms with leather combat boots. They walked at 3.5 mph on a fabric belt. The metabolic rates of the same group were measured on a different day, outdoors, with the subjects wearing the same clothing and walking along a blacktop road. The outdoor temperatures ranged from -4°C to +10°C (25°F to 50°F). No mention was made of wind conditions. In view of the relatively light clothing which these men wore, these outdoor temperatures ranged from cool to quite cool. It is likely that these men were initially in a negative heat balance state and their thermoregulatory systems would have brought into play heat conservation mechanisms and possibly heat generating mechanisms (shivering). Even after they had begun walking, their heat production would have been higher because of the increased heat loss. This alone could easily account for the 9-percent increase in metabolism found for this group. The second group of men wore the same type of clothing, and the indoor treadmill tests were the same. For the stationary surface tests, however, the subjects walked on a cinder running track. The outdoor temperatures for this group ranged from 18°C to 21°C (64°F to 70°F). For these tests there was no metabolic difference between indoor and outdoor temperatures. For some reason, Daniels indicated a mean metabolic difference of 10 percent, the track walking being higher, even though his own statistical analysis of the metabolic rate data showed that this difference was not significant (Table VI of Reference B-5). This is further indication that the colder temperatures influenced the first group.

Ralston (Reference B-6) found no significant differences between treadmill walking and walking on a wooden floor in the laboratory. His experiments seem very well controlled. All tests were conducted indoors at a constant temperature. His subjects wore light clothing and rubber-soled shoes. Two types of tests were conducted at two different velocities. In the first series of tests, the subject walked the floor for 10 min, then 10 min on the treadmill, and then another 10 min on the floor. The subject did not stop or break his stride in transferring from one surface to the other. In the second series of experiments, the progression was reversed, treadmill to floor to treadmill. Metabolic rates were measured during the final minutes during each phase of the 10-min tests.

The possibility of differences in gait between the two modes may exist. Daniels (Reference B-5) mentions that some of his subjects lean backward on the treadmill and attributes this to the tendency of the treadmill to rotate

the subjects about the transverse axis. Ralston indicated that the gait for each of his subjects was constant.

From the evaluation of the above papers, it seems most likely that no differences exist between treadmill and road walking as far as the metabolic expenditures are concerned. While differences in gait may exist, they are not prominent and do not show up in the cost of performing the physical activity. Further studies are needed along these lines.

APPENDIX C

PILOT STUDY: EFFECT OF STEP RATE ON METABOLIC COST OF LOCOMOTION ON AN INCLINED-PLANE TREADMILL AT 1/6 G

This appendix presents the data on a single subject who walked a treadmill at a constant velocity but at different step rates. This was the first of a series of tests designed to study the effect of step rate, stride length, and velocity on the metabolic cost of locomotion at constant speeds.

METHODS AND APPARATUS

Subgravity was simulated by the method developed by Hewes and Spady, which consists of an overhead trolley with a cable and sling suspension system. The system supports and positions a subject perpendicular to a walking surface (variable-speed treadmill) that is inclined 9 deg 47 min from vertical. Using this technique, 5/6 of the subject's body weight is carried by the cables, and 1/6 is directed perpendicular to the treadmill. A strain-gage load ring permits precise measurement of the weight component directed perpendicular to the treadmill. The torso slings are 8-in. wide and contain a foam plastic insert. This design provides comfortable and gentle sling support for the body load. Subjects report no respiratory impairment during rest or exercise with this arrangement.

An additional set of experiments was conducted to answer the question of possible respiratory impairment imposed by the chest strap arrangement. The method of suspending the subjects in these experiments was identical to the first series except for the chest support strap. The modified chest support strap consists of a 1/4-in.-thick, 16-in.-dia aluminum plate containing a 2-in. foam pad. (See Figures C-1 and C-2 for comparison.) This configuration permits the subject to be comfortably supported, while eliminating the back and chest restriction imposed by the previous sling configuration.

A Goddard Pulmonet spirometer was used to measure oxygen consumption in the experiment.

PROCEDURES

After positioning the subject in the sling, a weight measurement was made to make sure he then weighed 1/6 of his original weight (including tennis shoes, clothes, and helmet), and the test was started. The subject first rested until his O_2 consumption approached a steady-state, at which time the treadmill was started and set for 4 mph. After 4 min of continuous exercise was completed, the treadmill was stopped, and the subject was allowed to rest until his O_2 consumption curve again approached a steady-state. This procedure was repeated for four different stepping rates. The step rate was calibrated by having the subject pace himself with a metronome.

RESULTS

The results from the single test are shown in Figure C-3. The form of the curve is that of a typical efficiency curve, and it depicts the most efficient step rate as 98 steps/min to provide the lowest oxygen cost for this activity.

DISCUSSION

These data support the premise that locomotive rates can be optimized to provide low oxygen costs for a fixed activity. This idea may provide the basis for planning the astronaut's extravehicular lunar excursion to reduce the metabolic cost to the man and reduce his logistic requirements. These results are derived from a single test, and further testing will be needed to prove their reliability. Testing must also be accomplished at different locomotive rates per stepping rate to determine the most efficient locomotive rate as well as the step rate within locomotion. It is also imperative that testing be carried out in the state-of-the-art Apollo suits.



58131-2

Figure C-1. Sling Arrangement with Chest Support Plate (View A)

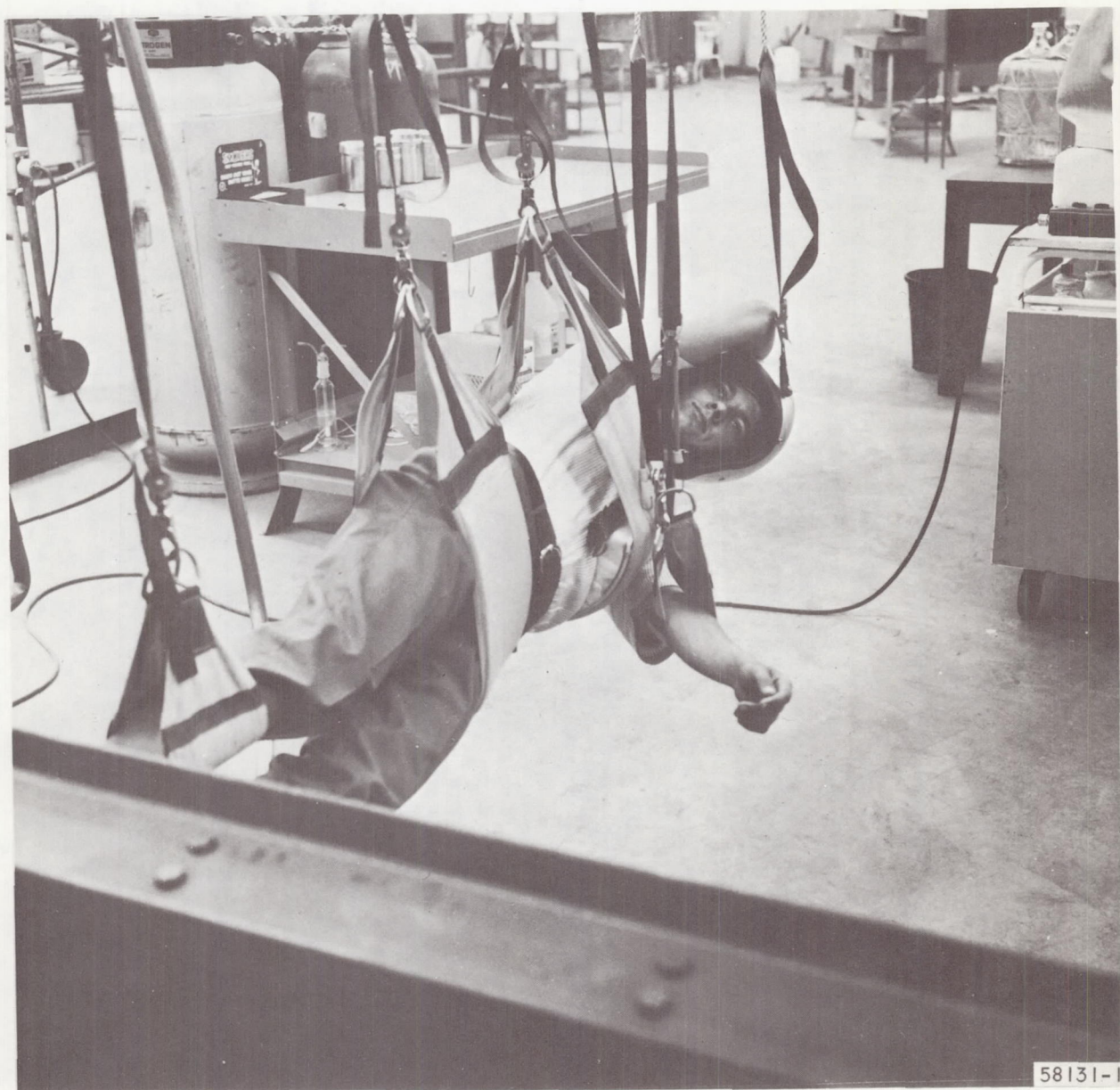
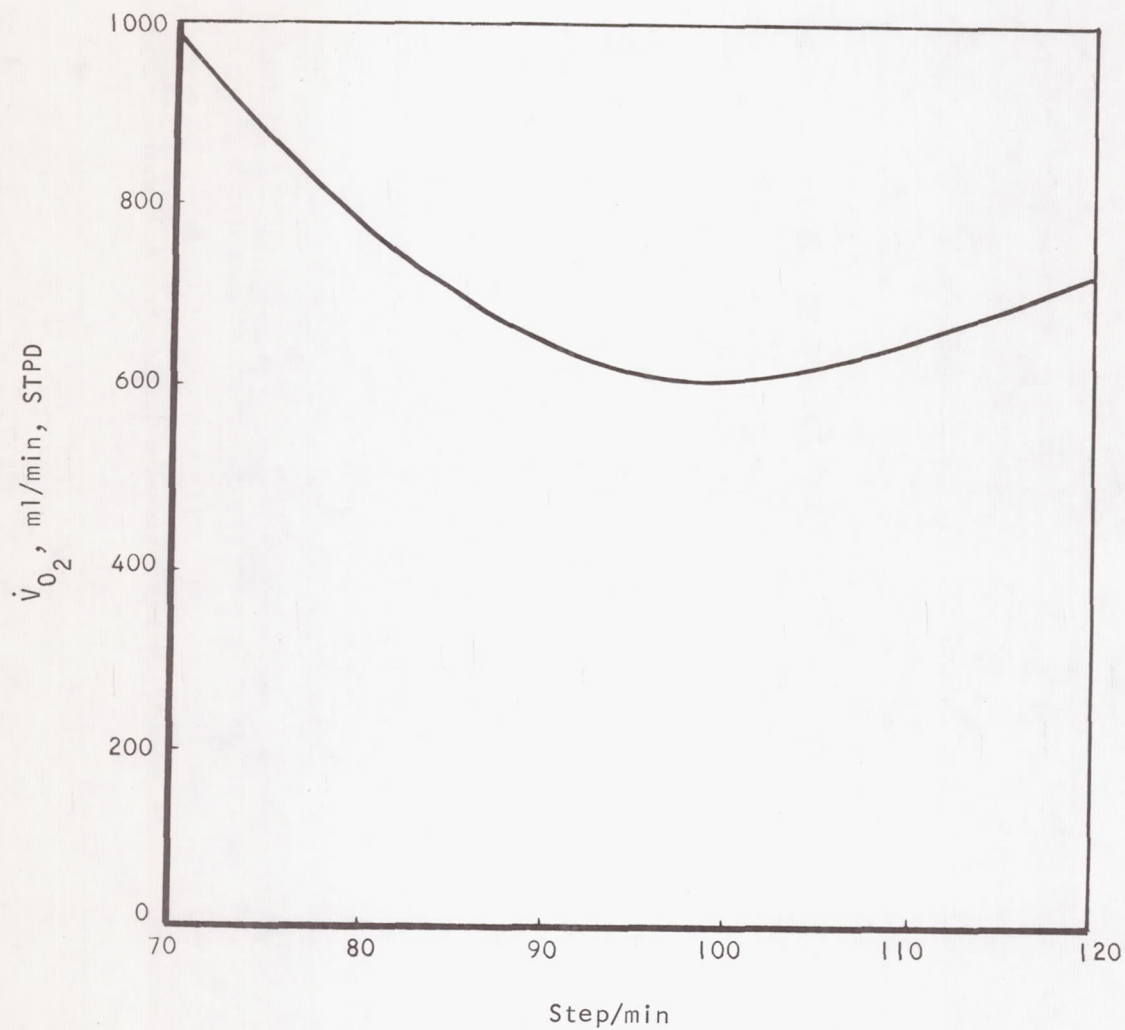


Figure C-2. Sling Arrangement with Chest Support Plate (View B)



A-23300

Figure C-3. Effect of Step Rate on Metabolic Cost, Treadmill Walking at 4 mph

Page Intentionally Left Blank

APPENDIX D

SYSTEM ERROR ANALYSIS

The underlying assumption in this analysis is that all errors occur randomly. Whether this is a valid assumption depends upon what is known about the instruments actually used to make the measurements. With the exception of the respirometer, which is calibrated against a piston pump, all the instruments are listed with plus and minus errors. Since the respirometer is a major contributor of error in the system, verification of its true behavior is quite essential. A careful analysis of the piston pump has been completed and appears in SAM Report TR-66-4.

The equations in this appendix are complex. In many cases the total system error could not be calculated without assuming values for specific parameters. Where this was required, the values chosen were representative of the values measured during the test runs. Errors appearing in the denominator are cleared by the following technique:

Assume the expression $X = A/B$ and let the error of A and B be given by a and b. The expression now becomes

$$X = \frac{A \pm aA}{B \pm bB}$$

$$X = \frac{A}{B} \frac{(1 \pm a)}{(1 \pm b)}$$

Multiplying both numerator and denominator by $1 \mp b$ yields the following:

$$X = \frac{A}{B} \frac{(1 \pm a)(1 \mp b)}{(1 \pm b)(1 \mp b)}$$

$$X = \frac{A}{B} \left(\frac{1 \pm a \mp b - ab}{1 \pm b \mp b - b^2} \right)$$

The error term, b, cancels out of the denominator leaving only $-b^2$. In the numerator all terms appear separately plus the combined term, $-ab$. As long as the error terms ab and b^2 are less than 1 percent of a or b, b^2 or ab are negligible with respect to the sum of a and 1. This decision permits writing the value of X as

$$X = \frac{A}{B} (1 \pm a \pm b)$$

If a and b are known to vary randomly, the root-sum-square method is justified. The error in X may then be written as

$$E_X = \pm \sqrt{a^2 + b^2} \frac{A}{B}$$

ERROR CALCULATIONS

The vapor pressure of water is

$$\log_{10} \frac{P_{CH_2O}}{P_{H_2O}} = \left[\frac{K_1 - (T \pm a)}{K_2 + (T \pm a)} \right] \left[\frac{K_3 + K_4 [K_1 - (T \pm a)] + K_5 [K_1 - (T \pm a)]^3}{1 + K_6 [K_1 - (T \pm a)]} \right]$$

<u>Symbol</u>	<u>Quantity</u>	<u>Value</u>
P_{CH_2O}	critical pressure	165806.29 mm Hg
P_{H_2O}	vapor pressure of water	unknown variable
T	temperature in the respirometer case	assumed to be 30°C
K_1	critical temperature minus 273.16°K	374.11°K
K_2	0°C	273.16°K
K_3	a specified constant	3.24378
K_4	a specified constant	5.86826×10^{-3}
K_5	a specified constant	1.17024×10^{-8}
K_6	a specified constant	2.187846×10^{-3}

First, let the left-hand side of the expression equal Z and solve for Z:

$$Z = \left[\frac{C_1 \mp a}{C_2 \pm a} \right] \left[\frac{K_3 + K_1 K_4 - K_4 T \mp K_4 a + K_5 C_1^3 \mp 3K_5 C_1^2 a}{1 + K_6 K_1 - K_6 T \mp K_6 a} \right]$$

The following substitutions will be made:

<u>Symbol</u>	<u>Substituted for</u>
C_1	$K_1 - T$
C_2	$K_2 + T$
C_3	$K_3 + K_1 K_4 - K_4 T + K_5 C_1^3$
C_4	$1 + K_6 K_1 - K_6 T$

$$Z = \frac{C_1}{C_2} \times \frac{C_3}{C_4} \left[\frac{1 \mp \frac{a}{C_1}}{a \pm \frac{a}{C_2}} \right] \left[\frac{1 \mp \frac{K_4 a}{C_3} \mp \frac{3K_5 C_1^2 a}{C_3}}{1 \mp \frac{K_6 a}{C_4}} \right]$$

Clearing the denominator yields

$$Z = \frac{C_1}{C_2} \times \frac{C_3}{C_4} \left[\left(1 \mp \frac{a}{C_1}\right) \left(1 \mp \frac{K_4 a}{C_3} \mp \frac{3K_5 C_1^2 a}{C_3}\right) \left(1 \mp \frac{a}{C_2}\right) \left(1 \pm \frac{K_6 a}{C_4}\right) \right]$$

The accuracy of T is $\pm 1^\circ\text{C}$; hence,

$$Z = \frac{C_1}{C_2} \times \frac{C_3}{C_4} \left[1 \mp 0.00292 \mp 0.00102 \mp 0.00073 \mp 0.00330 \pm 0.00125 \right]$$

Since the only error term is a,

$$Z = \frac{C_1}{C_2} \times \frac{C_3}{C_4} (1 \mp 0.0067)$$

The error in Z therefore is

$$E_Z = \mp 0.0067 Z$$

where Z equals 3.716

Solving for $P_{\text{H}_2\text{O}}$ yields

$$P_{\text{H}_2\text{O}} = \frac{P_{\text{CH}_2\text{O}}}{10^Z}$$

When $T = 30^\circ\text{C}$,

$$P_{\text{H}_2\text{O}} = 31.87 \text{ mm Hg}$$

When $T = 31^\circ\text{C}$,

$$P_{\text{H}_2\text{O}} = 33.76 \text{ mm Hg}$$

And when $T = 29^{\circ}\text{C}$,

$$P_{\text{H}_2\text{O}} = 30.10 \text{ mm Hg}$$

The average error in $P_{\text{H}_2\text{O}}$ is $\pm 1.84 \text{ mm Hg}$ and follows the direction of the error in T ; i.e., $T_{31} > T_{30}$ and $P_{\text{H}_2\text{O}(31)} > P_{\text{H}_2\text{O}(30)}$. The error in $P_{\text{H}_2\text{O}(30)}$ therefore is

$$E_{P_{\text{H}_2\text{O}}} = \pm 0.0577 P_{\text{H}_2\text{O}(30)}$$

$\dot{V}_E(\text{ATPS})$ to $\dot{V}_E(\text{BTPS})$:

$$\dot{V}_E(\text{BTPS}) = \dot{V}_E(\text{ATPS}) f_I$$

Here, ATPS refers to the environment in which the respired gases were measured (i.e., inside the pressurized respirometer case). The factor f_I is found from the expression

$$f_I = \left[\frac{P_B \pm b + P_S \pm c - (P_{\text{H}_2\text{O}} \pm 1.84)}{P_B \pm b - 47} \right] \left[\frac{K_7}{K_2 + (T \pm a)} \right]$$

<u>Symbol</u>	<u>Quantity</u>	<u>Value</u>
P_B	barometric pressure	assumed to be 760 mm Hg
P_S	pressure inside respirometer case	assumed to be 181 mm Hg above ambient
K_7	body temperature in $^{\circ}\text{K}$	310.16°K

The errors have the following values:

- b is the 0.33 percent full scale (140 mm Hg) barometer error plus a 0.2 mm Hg reading error and equals 0.66 mm Hg.
- c is the ± 1 percent full scale error of the suit pressure transducer (FS = 258 mm Hg) and equals 2.58 mm Hg.

$$f_I = \left[\frac{P_B + P_S - P_{\text{H}_2\text{O}} \pm b \pm c \mp 1.84}{P_A - 47 \pm b} \right] \left[\frac{K_7}{C_2 \pm a} \right]$$

The following substitutions will be made:

<u>Symbol</u>	<u>Substituted for</u>
C_5	$P_B + P_S - P_{H_2O}$
C_7	$P_B - 47$

Using these substitutions yields

$$f_I = \frac{C_5}{C_6} \times \frac{K_7}{C_2} \left[\frac{1 \pm \frac{b}{C_5} \pm \frac{c}{C_5} \mp \frac{1.84}{C_5}}{\left(1 \pm \frac{b}{C_6}\right) \left(1 \pm \frac{a}{C_2}\right)} \right]$$

Clearing the denominator of error terms yields

$$f_I = \frac{C_5}{C_6} \times \frac{K_7}{C_2} \left(1 \pm \frac{b}{C_5} \pm \frac{c}{C_5} \mp \frac{1.84}{C_5} \mp \frac{b}{C_6} \mp \frac{a}{C_2} \right)$$

$$f_I = \frac{C_5}{C_6} \times \frac{K_7}{C_2} (1 \pm 0.00073 \pm 0.00284 \mp 0.00202 \mp 0.00093 \mp 0.00330)$$

After noting that b/C_5 and b/C_6 are of opposite sign, and that $1.84/C_5$ and a/C_2 are of the same sign, f_I reduces to

$$f_I = \frac{C_5}{C_6} \times \frac{K_7}{C_2} (1 \mp 0.0002 \pm 0.00284 \mp 0.00532)$$

Applying the RSS method to the error terms gives

$$f_I = \frac{C_5}{C_6} \times \frac{K_7}{C_2} (1 \pm 0.0060)$$

The error in f_I is found to be

$$E_{f_I} = \pm 0.0060 f_I$$

where $f_I = 1.304$

Calculation of \dot{V}_E (BTPS) is

$$\dot{V}_E(\text{BTPS}) = \dot{V}_E(\text{ATPS}) (1 + d) f_I (1 \pm 0.0060)$$

From empirical measurements, the error, d , in the gas flow through the respiration meter was found to equal ± 2.8 percent.

Hence, $\dot{V}_E(\text{BTPS}) = \dot{V}_E^f (1 \pm 0.028 \pm 0.0060)$

$$\dot{V}_E(\text{BTPS}) = \dot{V}_E^f (1 \pm 0.0286)$$

The error in $\dot{V}_E(\text{BTPS})$ is given by

$$E_{\dot{V}_E(\text{BTPS})} = \pm 0.0286 \dot{V}_E(\text{BTPS}), \text{ where } \dot{V}_E(\text{BTPS}) = 1.304 \dot{V}_E(\text{ATPS})$$

$\dot{V}_E(\text{ATPS})$ to $\dot{V}_E(\text{STPD})$:

$$\dot{V}_E(\text{STPD}) = \dot{V}_E (1 \pm 0.02800) \left[\frac{P_B \pm b + P_S \pm c - (P_{H_2O} \pm 1.84)}{K_8} \right] \times \left[\frac{K_2}{K_2 + (T \pm a)} \right]$$

<u>Symbol</u>	<u>Quantity</u>	<u>Value</u>
K_8	standard atmospheric pressure	760 mm Hg

$$\dot{V}_E(\text{STPD}) = \dot{V}_E (1 \pm 0.02800) \left[\frac{C_5 \pm b \pm c \mp 1.84}{K_8} \right] \left[\frac{K_2}{C_2 \pm a} \right]$$

$$\dot{V}_E(\text{STPD}) = \frac{C_5}{K_8} \times \frac{K_2}{C_2} \dot{V}_E (1 \pm 0.02800) \left[\frac{1 \pm \frac{b}{C_5} \pm \frac{c}{C_5} \mp \frac{1.84}{C_5}}{1 \pm \frac{a}{C_2}} \right]$$

After clearing the denominator,

$$\dot{V}_E(\text{STPD}) = \frac{C_5}{K_8} \times \frac{K_2}{C_2} \dot{V}_E (1 \pm 0.02800 \pm \frac{b}{C_5} \pm \frac{c}{C_5} \mp \frac{1.84}{C_5} \mp \frac{a}{C_2})$$

Recognizing that $1.84/C_5$ and a/C_2 have the same sign,

$$\dot{V}_E(\text{STPD}) = \frac{C_5}{K_8} \times \frac{K_2}{C_2} \dot{V}_E (1 \pm 0.02800 \pm 0.00730 \pm 0.00284 \mp 0.00532)$$

The root-sum square of the error terms yields

$$\dot{V}_E(\text{STPD}) = \frac{C_5}{K_8} \times \frac{K_2}{C_2} \dot{V}_E (1 \pm 0.0287)$$

The error in $\dot{V}_E(\text{STPD})$ is given by

$$E_{\dot{V}_E(\text{STPD})} = \pm 0.0287 \dot{V}_E(\text{STPD}), \text{ where } \dot{V}_E(\text{STPD}) = 1.087 \dot{V}_E(\text{ATPS})$$

Calculation of $\dot{V}_I(\text{STPD})$:

$$\dot{V}_I(\text{STPD}) = \dot{V}_E(\text{STPD}) (1 \pm 0.02870) \left[\frac{1 - (F_{E_{O_2}} \pm e) - (F_{E_{CO_2}} \pm e)}{1 - (F_{I_{O_2}} \pm e) - (F_{I_{CO_2}} \pm e)} \right]$$

<u>Symbol</u>	<u>Quantity</u>	<u>Value</u>
$F_{I_{O_2}}$	fraction O_2 in inspired gas	0.230
$F_{E_{O_2}}$	fraction O_2 in expired gas	0.195
$F_{I_{CO_2}}$	fraction CO_2 in inspired gas	0.001
$F_{E_{CO_2}}$	fraction CO_2 in expired gas	0.033

The error term is ± 1 percent, determined by calibrating over the experimental range, and is not the same error because four separate instruments were used to measure the "F" quantities.

$$\dot{V}_I(\text{STPD}) = \dot{V}_E(\text{STPD}) (1 \pm 0.02870) \left[\frac{1 - F_{E_{O_2}} - F_{E_{CO_2}} \mp F_{E_{O_2}} e \mp F_{E_{CO_2}} e}{1 - F_{I_{O_2}} - F_{I_{CO_2}} \mp F_{I_{O_2}} e \mp F_{I_{CO_2}} e} \right]$$

After the following substitutions

<u>Symbol</u>	<u>Substituted for</u>
C_7	$1 - F_{E_{O_2}} - F_{E_{CO_2}}$
C_8	$1 - F_{I_{O_2}} - F_{I_{CO_2}}$

$$\dot{V}_I(\text{STPD}) = \dot{V}_E(\text{STPD}) \left(1 \pm 0.02870 \right) \frac{\left[1 \mp \frac{F_{E_{O_2}}^e}{C_7} \mp \frac{F_{E_{CO_2}}^e}{C_7} \right]}{\left[1 \mp \frac{F_{I_{O_2}}^e}{C_8} \mp \frac{F_{I_{CO_2}}^e}{C_8} \right]} \times \frac{C_7}{C_8}$$

Clearing the denominator,

$$\dot{V}_I(\text{STPD}) = \frac{C_7}{C_8} \dot{V}_E(\text{STPD}) \left(1 \pm 0.02870 \right) \left[1 \mp \frac{F_{E_{O_2}}^e}{C_7} \mp \frac{F_{E_{CO_2}}^e}{C_7} \pm \frac{F_{I_{O_2}}^e}{C_8} \pm \frac{F_{I_{CO_2}}^e}{C_8} \right]$$

When the fractional error terms are computed,

$$\dot{V}_I(\text{STPD}) = \frac{C_7}{C_8} \dot{V}_E(\text{STPD}) (1 \pm 0.02870 \mp 0.00250 \pm 0.00042 \pm 0.00299 \pm 0.00001)$$

Since all the error terms are independent of one another,

$$\dot{V}_I(\text{STPD}) = \frac{C_7}{C_8} \dot{V}_E(\text{STPD}) (1 \pm 0.0290)$$

The error in $\dot{V}_I(\text{STPD})$ will be given by

$$E_{\dot{V}_I(\text{STPD})} = \pm 0.0290 \dot{V}_I(\text{STPD}), \text{ where } \dot{V}_I(\text{STPD}) = 1.083 \dot{V}_E(\text{ATPS})$$

Calculation of $\dot{V}_{O_2}(\text{STPD})$:

$$\begin{aligned} \dot{V}_{O_2}(\text{STPD}) &= \dot{V}_I(\text{STPD}) \left(1 \pm 0.02870 \mp \frac{F_{E_{O_2}}^e}{C_7} \mp \frac{F_{E_{CO_2}}^e}{C_7} \pm \frac{F_{I_{O_2}}^e}{C_8} \pm \frac{F_{I_{CO_2}}^e}{C_8} \right) \\ &\quad \times F_{I_{O_2}} (1 \pm e) - \dot{V}_E(\text{STPD}) (1 \pm 0.02870) F_{E_{O_2}} (1 \pm e) \end{aligned}$$

Factoring out $\dot{V}_I F_{I_{O_2}}$ from both parts of the equation yields

$$\dot{V}_{O_2} = \dot{V}_I F_{I_{O_2}} \left[1 \pm 0.02870 \mp \frac{F_{E_{O_2}}^e}{C_7} \mp \frac{F_{E_{CO_2}}^e}{C_7} \pm \frac{F_{I_{CO_2}}^e}{C_8} \right. \\ \left. \pm F_{I_{O_2}}^e - \frac{\dot{V}_E F_{E_{O_2}}}{\dot{V}_I F_{I_{O_2}}} 0.02870 \pm \frac{\dot{V}_E F_{E_{O_2}}^e}{\dot{V}_I F_{I_{O_2}}} \right]$$

Several error terms in this expression are from common sources and can be combined as follows:

$$\dot{V}_{O_2} = \dot{V}_I F_{I_{O_2}} \left[\left(1 - \frac{\dot{V}_E F_{E_{O_2}}}{\dot{V}_I F_{I_{O_2}}} \right) \pm \left(0.02870 - \frac{\dot{V}_E F_{E_{O_2}}}{\dot{V}_I F_{I_{O_2}}} 0.02870 \right) \right. \\ \left. \mp \left(\frac{F_{E_{O_2}}^e}{C_7} + \frac{\dot{V}_E F_{E_{O_2}}^e}{\dot{V}_I F_{I_{O_2}}} \right) \mp \frac{F_{E_{CO_2}}^e}{C_8} \pm \left(\frac{F_{I_{CO_2}}^e}{C_8} + F_{I_{O_2}}^e \right) \right]$$

The error term, $\frac{F_{I_{CO_2}}^e}{C_8}$, contributes nothing to the total error and has been

dropped. After factoring out the term $1 - \frac{\dot{V}_E F_{E_{O_2}}}{\dot{V}_I F_{I_{O_2}}}$ and performing the arithmetic operations,

$$\dot{V}_{O_2} = \dot{V}_I F_{I_{O_2}} - \dot{V}_E F_{E_{CO_2}} (1 \pm 0.02870 \mp 0.06790 \mp 0.00261 \pm 0.08070)$$

$$\dot{V}_{O_2} = \dot{V}_I F_{I_{O_2}} - \dot{V}_E F_{E_{CO_2}} (1 \pm 0.1090) \text{ at STPD}$$

The error in \dot{V}_{O_2} is given by

$$E_{\dot{V}_{O_2}}(\text{STPD}) = \pm 0.109 \dot{V}_{O_2}(\text{STPD}), \text{ where } \dot{V}_{O_2}(\text{STPD}) = 0.04009 \dot{V}_E(\text{ATPS})$$

Note that total error has increased from a previous maximum of 2.9 percent (in the \dot{V}_I calculation) to 10.9 percent. This type of error magnification occurs whenever difference quantities are involved. As the two quantities approach the same value, the difference becomes swamped in the error bands; the situation cannot be eliminated in open-circuit systems. The compromise

position is sought where CO₂ build-up and response time are adequate while the flow rate is slowed down as much as possible, or if the gas flow rate is specified, the errors in the measurement devices should be reduced as much as possible.

Calculation of \dot{V}_{CO_2} (STPD):

$$\dot{V}_{CO_2} = \dot{V}_E (1 \pm 0.02870) F_{E_{CO_2}} (1 \pm e) - \dot{V}_I \left(1 \pm 0.02870 \mp \frac{F_{E_{O_2}}^e}{C_7} \mp \frac{F_{E_{CO_2}}^e}{C_7} \right. \\ \left. \pm \frac{F_{I_{O_2}}^e}{C_8} \pm \frac{F_{I_{CO_2}}^e}{C_8} \right) F_{I_{CO_2}} (1 \pm e)$$

After factoring out $\dot{V}_E F_{E_{CO_2}}$,

$$\dot{V}_{CO_2} = \dot{V}_E F_{E_{CO_2}} \left(1 \pm 0.02870 \pm 0.01 - \frac{\dot{V}_I F_{I_{CO_2}}}{\dot{V}_E F_{E_{CO_2}}} \mp \frac{\dot{V}_I F_{I_{CO_2}}}{\dot{V}_E F_{E_{CO_2}}} 0.02870 \right. \\ \left. \pm \frac{\dot{V}_I F_{I_{CO_2}}}{\dot{V}_E F_{E_{CO_2}}} \times \frac{F_{E_{O_2}}^e}{C_7} \pm \frac{\dot{V}_I F_{I_{CO_2}}}{\dot{V}_E F_{E_{CO_2}}} \times \frac{F_{E_{CO_2}}^e}{C_7} \mp \frac{\dot{V}_I F_{I_{CO_2}}}{\dot{V}_E F_{E_{CO_2}}} \times \frac{F_{I_{O_2}}^e}{C_8} \right. \\ \left. \mp \frac{\dot{V}_I F_{I_{CO_2}}}{\dot{V}_E F_{E_{CO_2}}} \frac{F_{I_{CO_2}}^e}{C_8} \mp \frac{\dot{V}_I F_{I_{CO_2}}}{\dot{V}_E F_{E_{CO_2}}} \right)$$

When like terms are collected, after eliminating those terms contributing nothing to the total error,

$$\dot{V}_{CO_2} = \dot{V}_E F_{E_{CO_2}} \left[1 - \frac{\dot{V}_I F_{I_{CO_2}}}{\dot{V}_E F_{E_{CO_2}}} \pm \left(0.02870 - \frac{\dot{V}_I F_{I_{CO_2}}}{\dot{V}_E F_{E_{CO_2}}} 0.02870 \right) \pm 0.01 \mp 0.00030 \right]$$

Factoring out the term $1 - \frac{\dot{V}_I F_{I_{CO_2}}}{\dot{V}_E F_{E_{CO_2}}}$ yields

$$\dot{V}_{CO_2} = \dot{V}_E F_{E_{CO_2}} - \dot{V}_I F_{I_{CO_2}} (1 \pm 0.02870 \pm 0.01030 \mp 0.00031)$$

$$\dot{V}_{CO_2} = \dot{V}_E F_{E_{CO_2}} - \dot{V}_I F_{I_{CO_2}} (1 \pm 0.0305) \text{ at STPD}$$

The error in \dot{V}_{CO_2} is given by

$$E_{\dot{V}_{CO_2}}(\text{STPD}) = \pm 0.0303 \dot{V}_{CO_2}(\text{STPD})$$

where $\dot{V}_{CO_2}(\text{STPD}) = 0.03448 \dot{V}_E(\text{ATPS})$

Unlike the \dot{V}_{O_2} calculation, the error term containing C_7 and C_8 contributes nothing to the total error. This arises because $F_{E_{CO_2}}$ is 33 times $F_{I_{CO_2}}$.

Calculation of R:

$$R = \frac{\dot{V}_{CO_2} (1 \pm 0.02870 \pm 0.01030 \mp 0.00031)}{\dot{V}_{O_2} (1 \pm 0.02870 \mp 0.06790 \mp 0.00261 \pm 0.08070)}$$

$$R = \frac{0.03448 \dot{V}_E(\text{ATPS})}{0.04009 \dot{V}_E(\text{ATPS})} \left[1 \pm (0.02870 - 0.02870) \pm (0.01030 + 0.00261) \right. \\ \left. \mp 0.00031 \pm 0.06790 \mp 0.08070 \right]$$

$$R = 0.86 \left[1 \pm 0.01291 \mp 0.00031 \pm 0.06790 \mp 0.08070 \right]$$

$$R = 0.86 (1 \pm 0.1060)$$

This calculation accounts for like error terms appearing in the numerator and denominator. To see this relationship, the numerator and denominator are written below indicating the origin of the error.

$$E_R = f \left[\frac{\pm E_{\dot{V}_E} \pm E_{F_{E_{CO_2}}} \mp E_{F_{I_{CO_2}}}}{\pm E_{\dot{V}_E} \mp E_{F_{E_{O_2}}} \mp E_{F_{I_{O_2}}}} \right]$$

The error in R is given by:

$$E_R = \pm 0.106 R$$

where $R = 0.86$

The error in R reflects primarily the contribution of the errors in \dot{V}_{O_2} . In fact, the error in R is less than that in \dot{V}_{O_2} because the \dot{V}_E error terms cancel out.

Calculation of metabolic rate:

$$MR = \dot{V}_{O_2} \left[1 \pm 0.02870 \mp 0.06790 \mp 0.00261 \pm 0.08070 \right] [k_8 + k_9 (R)]$$

<u>Symbol</u>	<u>Quantity</u>	<u>Value</u>
K_8	a specified constant	3.815
K_9	a specified constant	1.232

$$MR = \dot{V}_{O_2} \left[1 \pm 0.02870 \mp 0.06790 \mp 0.00261 \pm 0.08070 \right] \left[1 \pm \frac{k_9 R}{C_9} 0.01291 \mp \frac{k_9 R}{C_9} 0.00031 \pm \frac{k_9 R}{C_9} 0.06790 \mp \frac{k_9 R}{C_9} 0.08070 \right] C_9$$

The term C_9 has been substituted for $K_8 + K_9 R$. To clarify the origin of each term, the expression is written as

$$E_{MR} = f \left[\begin{array}{cccccccc} \dot{V}_E & \mp E_{FEO_2} & \mp E_{FECO_2} & \pm E_{FIO_2} & \pm E_{FECO_2} & \mp E_{FICO_2} & \pm E_{FEO_2} & \mp E_{FIO_2} \end{array} \right]$$

subtract
subtract

subtract

After combining like terms,

$$MR = \dot{V}_{O_2} C_9 \left[1 \pm 0.02870 \mp 0.05310 \pm 0.00019 \pm 0.0632 \mp 0.00007 \right]$$

$$MR = \dot{V}_{O_2} C_9 \left[1 \pm 0.0874 \right]$$

The error in MR is given by

$$E_{MR} = \pm 0.0874 MR$$

where $MR = 0.195 \dot{V}_E (\text{ATPS})$

Because \dot{V}_{O_2} and R both contain error terms from the same sources, which are of opposite sign, the error in MR is less than the error in either \dot{V}_{O_2} or R.

Applying the RSS method to the errors, where possible, leads to the following conclusions:

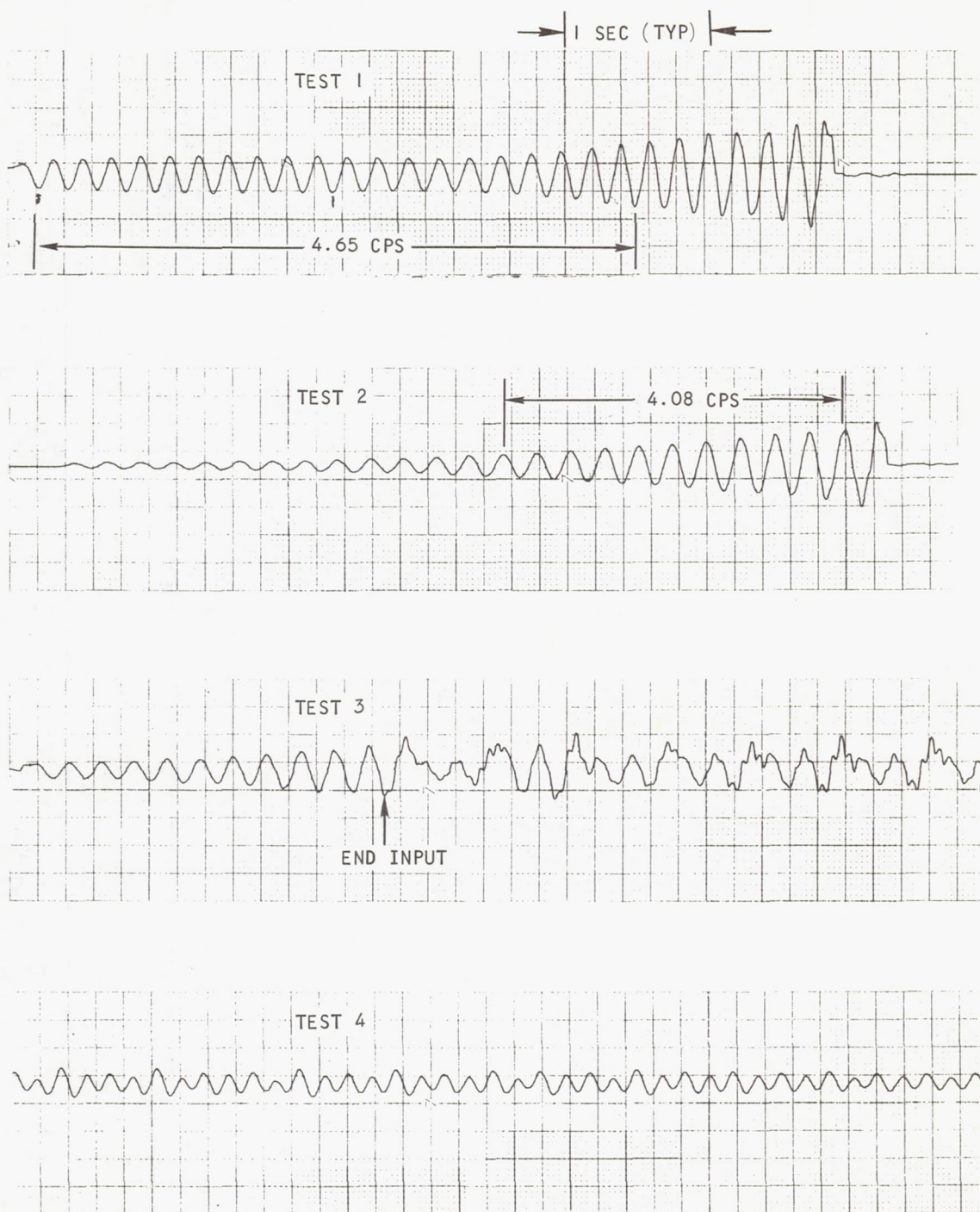
- (a) No single calculated parameter is in error by more than ± 11 percent.
- (b) Metabolic rate, which is a function of \dot{V}_{O_2} and R (in turn a function of \dot{V}_{O_2}) shows less than the maximum error due to subtraction of like error terms.
- (c) Since the error analysis was based on instrument errors and the magnitude of the values measured, it would be necessary to use instruments with very high accuracies (better than one percent) to reduce the calculated error bandwidth. It is doubtful that available instruments with the accuracies required to reduce the error band to less than five percent would provide the reliability or ruggedness required for these analyses.

Page Intentionally Left Blank

Page Intentionally Left Blank

APPENDIX E
LOAD CELL TRACES

This appendix reproduces load cell traces for test configurations through 19.



S-42285

Figure E-1. Load Cell Traces (Tests 1 Through 4)

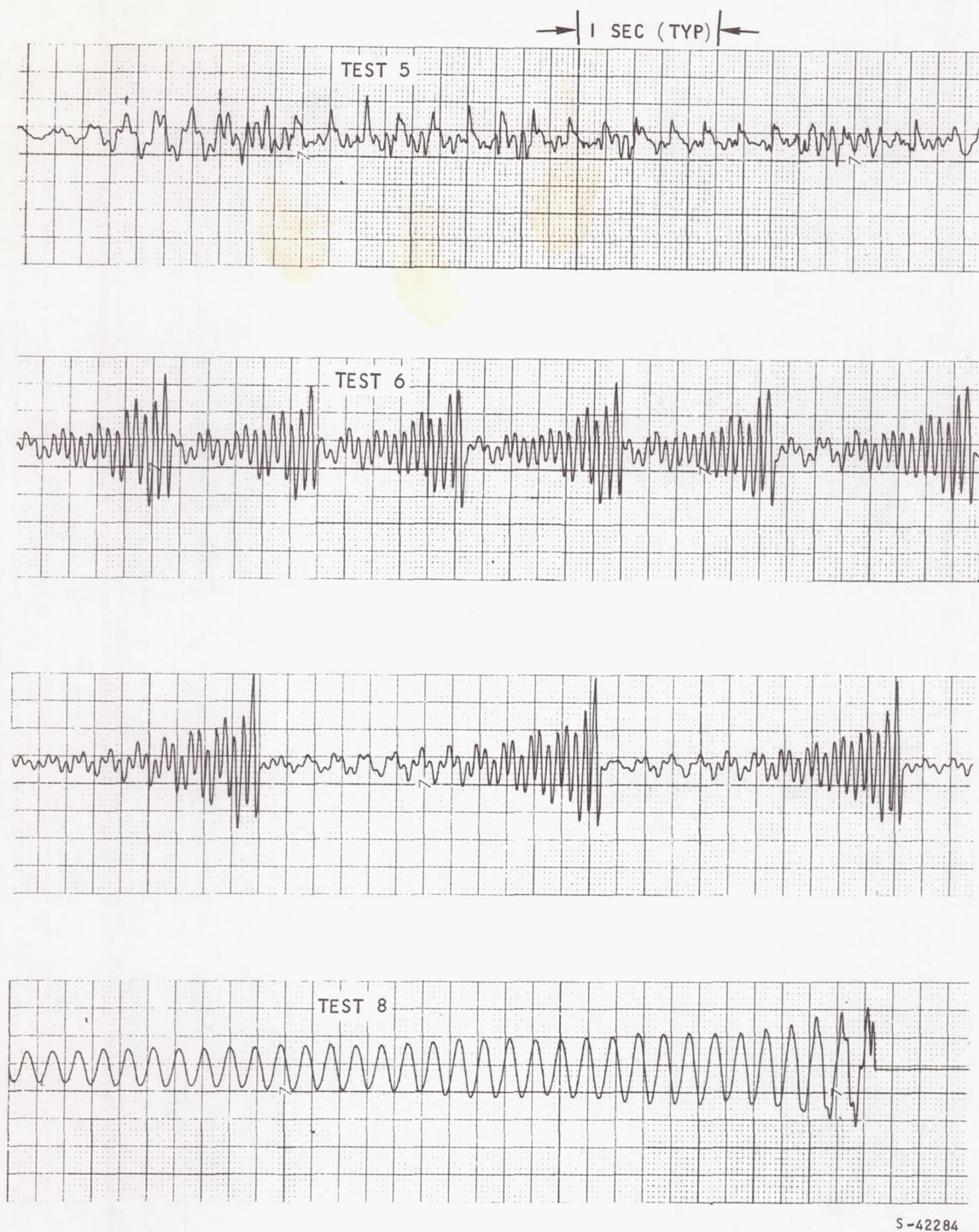


Figure E-2. Load Cell Traces (Tests 5 Through 8)

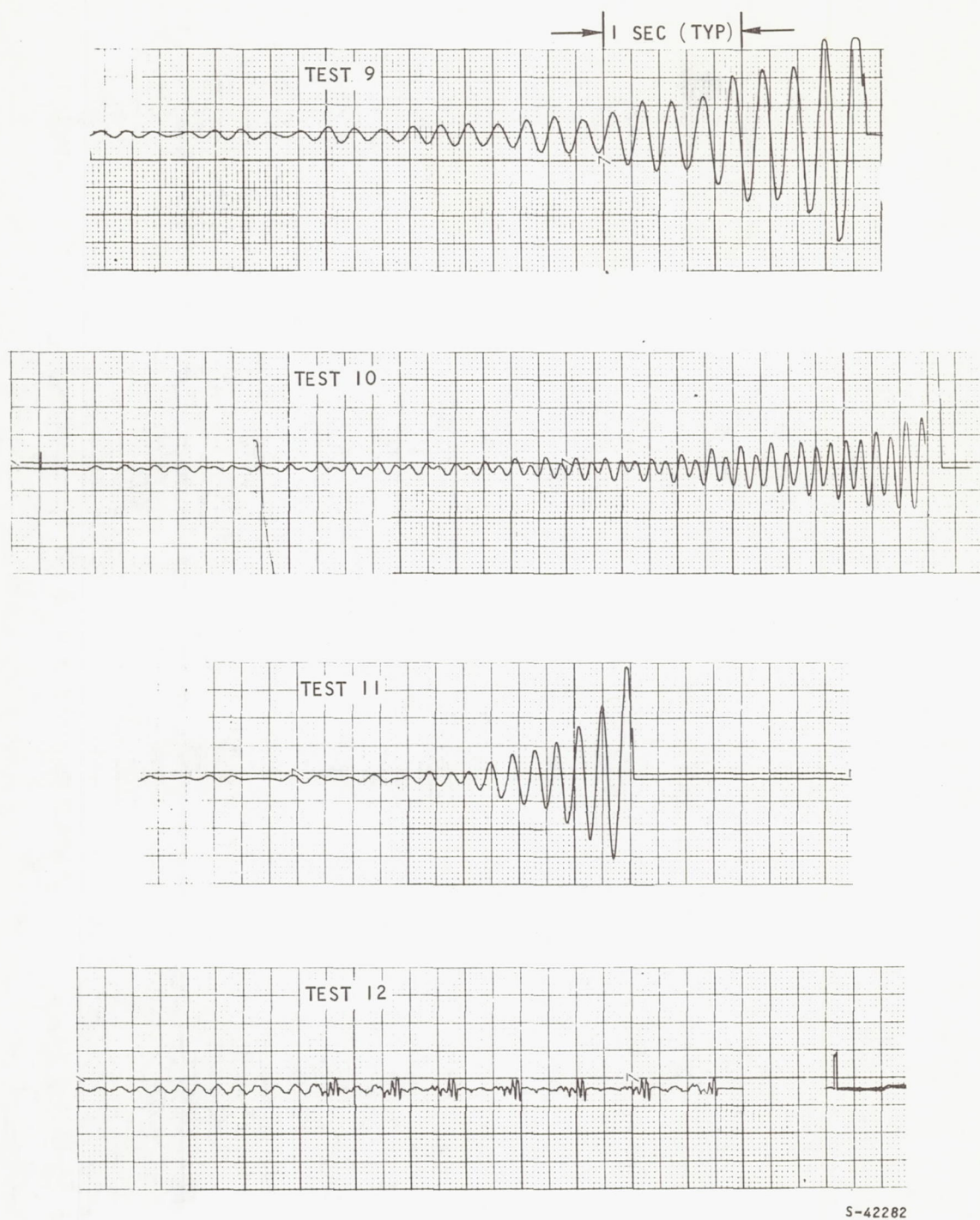
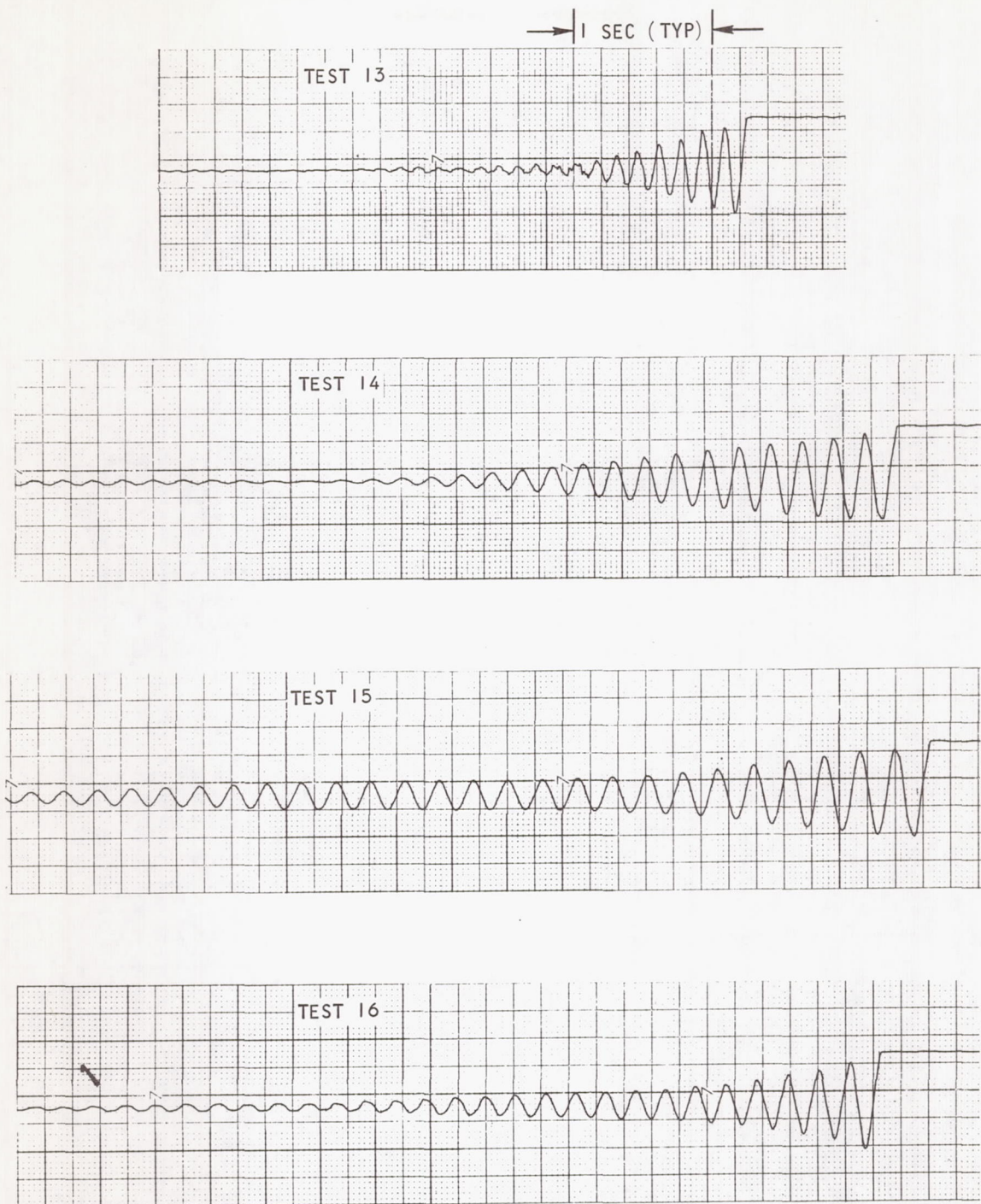


Figure E-3. Load Cell Traces (Tests 9 Through 12)



S-42283

Figure E-4. Load Cell Traces (Tests 13 Through 16)

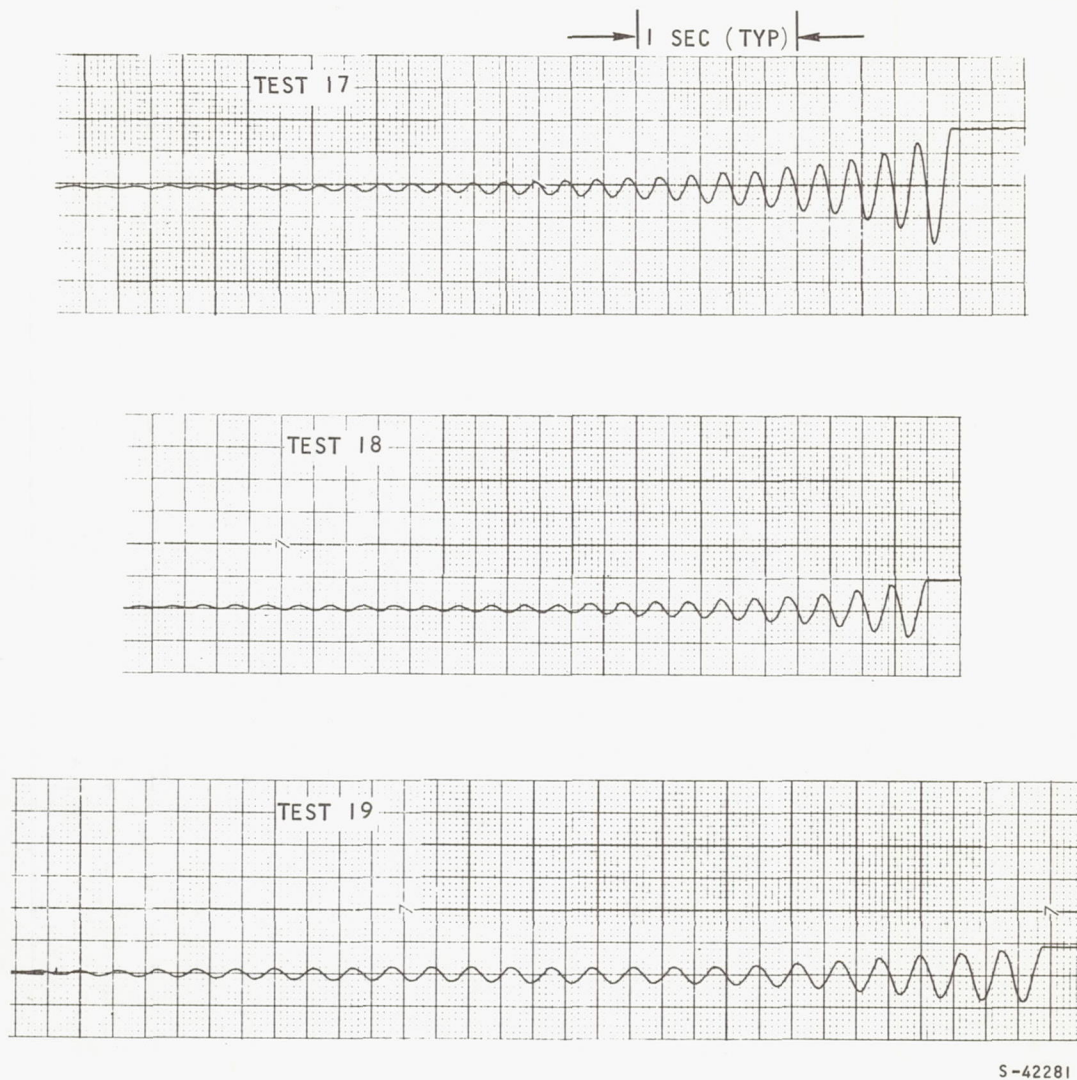


Figure E-5. Load Cell Traces (Tests 17, 18, and 19)

APPENDIX F

TIME CONSTANT FOR GAS ANALYSIS

The time required for gases sampled at the suit helmet to reach the analyzers (line washout time) and the time constants for the sensing mechanisms are presented graphically in Figure F-1 and tabulated in Table F-1.

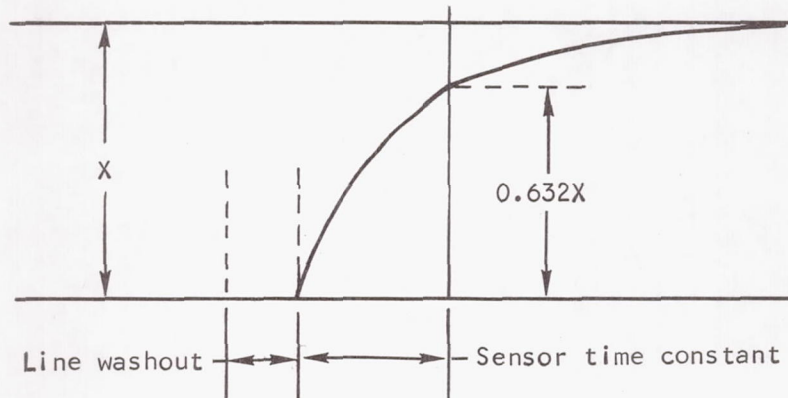


Figure F-1. Diagram of the Time Constant

TABLE F-1

TIME CONSTANT TABULATION

Gas	Gas sample (X) change, percent	Sensor time constant, sec	Line washout time, sec
O ₂ (Inspired)	0 to 40.2	13.3	8.4
O ₂ (Inspired)	40.2 to 0	14.1	8.1
O ₂ (Expired)	0 to 40.2	14.1	9.6
O ₂ (Expired)	40.2 to 0	13.5	10.5
CO ₂ (Expired)	0 to 8.9	5.1	8.4
CO ₂ (Expired)	8.9 to 0	6.0	12.9
CO ₂ (Inspired)	0 to 8.9	4.8	12.6
CO ₂ (Inspired)	8.9 to 0	6.6	12.0

Page Intentionally Left Blank

APPENDIX G

REFERENCES

- 3-1. Hewes, D. E.; and Spady, A. A.: Evaluation of a Gravity Simulation Technique for Studies of Man's Self-Locomotion in a Lunar Environment. NASA TN D-2176, 1964.
- 3-2. Anon.: Surveyor I Mission Report, Part II. Tech. Rep. 32-1023, Jet Propulsion Laboratory, Sept. 1966.
- 3-3. Anon.: Surveyor II Preliminary Science Results. Project Document 125, Jet Propulsion Laboratory, May 1967.
- 3-4. Batch, Joseph W.: Measurements and Recording of Joint Function. U. S. Armed Forces Medical Journal, vol. VI, no. 3, March 1955.
- 5-1. Spady, A. A.: A Kinematic Study of the Effects of Reduced Gravity on Self Locomotion. ASME 66-WA/BHF-6, Sept. 1967.
- 5-2. Wortz, E. C.: Effects of Reduced Gravity Environments on Human Performance. Aerospace Med. vol. 39, no. 8, 1968, pp.799-805.
- 5-3. Robertson, W. G.; and Wortz, E. C.: The Effects of Lunar Gravity on Metabolic Rates. Aerospace Med., vol. 39, no. 8, 1968, pp.799-805.
- 5-4. Wortz, E. C.; and Prescott, E. J.: The Effects of Subgravity Traction Simulation on the Energy Cost of Walking. Aerospace Med., vol. 37, no. 12, 1966.
- 5-5. Hogberg, P.: How Do Stride Length and Stride Frequency Influence the Energy Output During Running? Arbeitsphysiologie, Bd. 14, 1952, pp.437-444.
- 5-6. Sanborn, W.: A Pilot Study on the Effect of Step Rate on the Metabolic Cost of Locomotion on an Inclined Treadmill at 1/6 G. Rep. LS-66-1277, AiResearch Mfg. Co., 1966.
- 5-7. Benedict, F. G.; and Murchauser, H.: Energy Transformation During Horizontal Walking. Pub. No. 231, Carnegie Institution of Washington, 1915.
- 5-8. Fern, W. O.: Work Against Gravity and Work Due to Velocity Changes in Running. Amer. J. Physiol. 93, 1930, pp. 433-462.
- 5-9. Cavagna, G. A.; Saibene, F. P.; and Margaria, R.: External Work in Walking J. Appl. Physiol. 18(1), Jan. 1963, pp. 1-9.
- 5-10. Margaria, R; Cavagna, G. A.; and Saiki, H.: A Theoretical Approach to Human Locomotion at Reduced Gravity. Paper presented at the Seventh International Symposium on Space Technology and Science (Tokyo, Japan), 1967.

- 5-11. Kuehnegger, W.: A Study of Man's Physical Capabilities on the Moon. NASA CR-66118 and NASA CR-66119, 1966.
- 5-12. Roth, E. M.: Bioenergetic Considerations in the Design of Space Suits for Lunar Exploration. NASA SP-84, 1966.
- 5-13. Sanborn, W. G.; and Wortz, E. C.: Metabolic Rates During Lunar Gravity Simulation. Aerospace Med., vol. 38, no. 4, 1967.
- 5-14. Kuehnegger, W.: A Study of Man's Physical Capabilities on the Moon. Rep. 6, Northrop Space Laboratories (Contract NAS 1-4449).
- 5-15. Prescott, E. J.; and Wortz, E. C.: Metabolic Costs of Upper-Torso Exercises vs. Torque Maneuvers Under Reduced-Gravity Conditions. Aerospace Med., vol. 37, no. 10, 1966.
- 5-16. Streimer, I.; Springer, W. E.; and Tarditt, C. A.: An Investigation of the Output Characteristics of Workers During the Performance of a Specific Task in Reduced Traction Environments. Rep. D-290393, The Boeing Company, 1963.
- 5-17. Springer, W. E.; Stephens, T. L.; and Streimer, I.: The Metabolic Cost of Performing a Specific Exercise in a Low-Friction Environment. Aerospace Med., vol. 34, no. 486, 1963.
- 5-18. Passmore, R.; and Durin, J. V. G. A.: Human Energy Expenditure. Physiol. Rev. 25, 1955, pp. 801-840.
- 5-19. Wortz, E. C.; et al.: Full Pressure Suit Heat Balance Studies. Rep. LS-140, AiResearch Mfg. Co., 1965.
- 5-20. Harrington, T. J.; Edwards, D. K.; and Wortz, E. C.: Metabolic Rates in Pressurized Pressure Suits. Aerospace Med. 36, 1965, pp. 825-230.
- 5-21. Andrews, R. B.: Estimation of Values of Energy Expenditure Rate from Observed Values of Heart Rate. Human Factors 9, 1968, pp. 581-586.
- 5-22. Berggren, G.; et al.: Heart Rate and Body Temperature as Indices of Metabolic Rate During Work. Arbeitsphysiologie 14, 1950, pp. 255-260.
- 5-23. LeBlanc, J. A.: Use of Heart Rate as an Index of Work Output. J. Appl. Physiol. 10, 1957, pp. 275-280.
- 5-24. Malhotra, M. S.; et al. Pulse Count as a Measure of Energy Expenditure. J. Appl. Physiol. 18, 1963, p. 994.

- 5-25. Brouha, L.; Maxfield, M. E.; Smith, P. E.; and Stopps, G. J.: Discrepancy Between Heart Rate and Oxygen Consumption During Work in the Warm. *J. Appl. Physiol.* 18, 1963, pp. 1095-1098.
- 5-26. Braune, W.; and Fischer, O.: *Klass, Kgl. Acad. d. Wiss. Abth Math. Phys.* xvi, 1964, p. 153.
- 5-27. Fern, W. O.: Frictional and Kinetic Factors in the Work of Sprint Running. *Am. J. Physiol.*, vol. 92, 1930, pp. 583-611.
- 5-28. Fern, W. O.: Work Against Gravity and Work Due to Velocity Changes in Running. *Am. J. Physiol.*, vol 93, 1930, pp. 433-462.
- 5-29. Hewes, D. E.; Spady, A. A.; and Harris, R. L.: Comparative Measurements of Man's Walking and Running Gaits in Earth and Simulated Lunar Gravity. NASA TN D-3363, 1966.
- 5-30. Hewes, D. E.: Analysis of Self Locomotive Performance of Lunar Explorers Based on Experimental Reduced-Gravity Studies. NASA TN D-3934, 1967.
- 5-31. Klopsteg, P. E.; and Wilson, P. D.: *Human Limbs and Their Substitutes.* McGraw-Hill, 1954.
- 5-32. Roth, E. M.: Bioenergetic Considerations in the Design of Space Suits for Lunar Exploration. Rep. II, NASA-115, 1963.
- 5-33. Saunders, J. B. de C.M.; Inman, V. T.; and Everhart, H. D.: The Major Determinants in Normal and Pathological Gait. *J. Bonejoint Surg.*, 35-A (American), 1953, pp. 543-558.
- 5-34. Spady, A. A.: A Kinematic Study of the Effects of Reduced Gravity on Self-Locomotion. ASME 66-WA/BHF-6, Nov. 1966.
- 5-35. Spady, A. A.; and Harris, R. L.: Effects of Pressure Suits and Backpack Backpack Loads on Man's Self-Locomotion on Earth and Simulated Lunar Gravity. NASA TN D-4464, 1968.
- 5-36. Steindler, A.: *Mechanics of Normal and Pathological Locomotion in Man.* Charles C. Thomas, Baltimore, 1935.
- 5-37. Weber, W.; and Weber, E.: *Mechanik Menschlichen Gehwerkzeuge* Gottingen, Dieterich, 1936.
- B-1. Atzler, E.; and Herbst, R.: *Arbeitsphysiologische Studien III. Teil.* Pflugers Archiv. 215, 1922, p. 291.

- B-2. Durig, A.: Contribution to the Physiology of Humans Living at High Altitudes. Arch f.d. ges. Physiol. 113, 1906, p. 213.
- B-3. Durig, A.: Ueber dem Gaswechsel beim Gehen auf Horizontale Bahn. Vienna. K. Akad. der Wissenschaften. Math.-Naturw. Kl. Denkschriften 86, 1911, pp. 241-291.
- B-4. Smith, H. N.: Gaseous Exchanges in Physiological Requirements for Level and Grade Walking. Carnegie Institute, Wash., Pub. 309, 1922.
- B-5. Daniels, F.; Vanderbie, J.H.; and Winsman, F.R.: Energy Cost of Treadmill Walking Compared to Road Walking. Natick Q.M. Research and Development Laboratory. ASTIA AD 20049, Aug. 1953.
- B-6. Ralston, H. J.: Comparison of Energy Expenditure During Treadmill Walking and Floor Walking. J. Appl. Physiol. 15(6), Nov. 1950, p. 1156.
- B-7. Glasow, W.; and Müller, E. A.: Des Gehen auf Verscheidenen Boden. Arbeitsphysiol. 14, 195, p. 379.
- B-8. Müller, E. A.: Der Wirkungsgrad des Gehens. Arbeitsphysiol. 14, 1950, p. 236.
- B-9. Passmore, R.; and Durin, J. V. G. A.: Human Energy Expenditure. Physiol. Rev. 35, 1955, p. 801.
- B-10. Roth, E. M.: Bioenergetics of Space Suits for Human Exploration. NASA SP-84, 1966.